N. Waldau
P. Gattermann
H. Knoflacher
M. Schreckenberg

Editors

Pedestrian and Evacuation Dynamics 2005

Springer

Pedestrian and Evacuation Dynamics 2005

Nathalie Waldau · Peter Gattermann
Hermann Knoflacher · Michael Schreckenberg

Editors

Pedestrian and Evacuation Dynamics 2005

With 256 Figures, 111 in Color, and 42 Tables

Springer

Editors

Nathalie Waldau

Ingenieurbüro WALDAU
Sickenberggasse 13/3
1190 Wien, Austria
office@ibw-wien.at

Hermann Knoflacher

Institut für Verkehrsplanung
und Verkehrstechnik
Technische Universität Wien
Gußhausstraße 30/231
1040 Wien, Austria
hermann.knoflacher@ivv.tuwien.ac.at

Peter Gattermann

Österreichisches Institut
für Schul- und Sportstättenbau
Prinz-Eugen-Straße 12
1040 Wien, Austria
gattermann@oeiss.org

Michael Schreckenberg

Physik von Transport und Verkehr
Universität Duisburg-Essen
Lotharstraße 1
47048 Duisburg, Germany
schreckenberg@traffic.uni-duisburg.de

Opening Speech at the University

Dear State Secretary Mag. Eduard Mainoni,
Dear Prof. Dr. Hans Kaiser,
Ladies and Gentlemen, dear colleagues:

On behalf of the Organising Committee of the PED 2005 it is my pleasure to welcome you to Vienna.
I feel honored to have had the opportunity to contribute to the organizing efforts and to meet with all the renowned specialists assembled here.

I would like to acknowledge the support of our main sponsor, the Federal Ministry of Transport, Innovation and Technology, as well as our other sponsors, TraffGo HT and Arsenal Research.

I am especially pleased that Eduard Mainoni, the State Secretary of the Federal Ministry of Transport, Innovation and Technology could join us here today. He is leading the Project for the Austrian state-supported Program for Safety Research.

I hope all of you will have a very successful conference and a pleasant stay in our beautiful city. Thank you! «

Nathalie Waldau

Opening Speech HSTS Mag. Eduard Mainoni

Dear Prof. Dr. Hans Kaiser,
Distinguished Members of the Organisation Committee,
Invited speakers and distinguished guests
Ladies and Gentlemen!

It is a pleasure for me to welcome you at the Third International Conference on Pedestrian and Evacuation Dynamics at the Technical University of Vienna.

Most of all, I would like to warmly welcome all the researchers and practitioners from more than 17 countries who visit Vienna to participate in this conference. I hope all of you had a pleasurable journey and might already have had the opportunity to grasp some of the charm of this city.

This year's conference on Pedestrian and Evacuation Dynamics is the third one in a series of conferences. The first was held in Duisburg, Germany in 2001 and the second one in Greenwich, UK 2003. It is a pleasure for me to welcome you know in Vienna to PED 2005.
It is also a pleasure for me to welcome the two persons who have hosted the previous conferences: Prof. Michael Schreckenberg from the University of Duisburg-Essen and Prof. Ed Galea from the University of Greenwich.

You might know the famous quotation from Isaac Newton: "If I have seen further it is by standing on the shoulders of giants."
Even though the term giants might sound a bit exaggerating in this context, it shows nevertheless the very important function of continuity and tradition. Being able to accumulate and refine the knowledge on crowd dynamics and all aspects of evacuation and pedestrian movement is one of the major benefits of a series of conferences. And is certainly not an exaggeration, if one claims that this conference series on Pedestrian and Evacuation Dynamics plays a pivotal role in the advancement of these fields.

Of course, this advancement is fostered by the passion and commitment of researchers and practitioners alike. Without you, the participants of this conference, this would not be possible. You are probably interested in different aspects of pedestrians, crowds, egress, and evacuation processes.

Nevertheless, you came here to present your results, discuss them with your colleagues, and exchange views and knowledge. This is a clear sign for the vitality and the attractiveness of the field you are working in. Furthermore, each and every person can profit from this conference, since all of us are usually members of crowds.

This is obvious in large cities like Vienna. Public transportation systems are built for mass transport. Large gatherings of people are a characteristic feature of modern cities and therefore for modern societies.

Because of the importance of this subject, I am proud to say, that this years conference is held under the patronage of His Vice Chancellor Hubert Gorbach and is financially supported by the Federal Ministry of Transport, Innovation and Technology (15.000 € in total: ½ received in March/April 2005, rest after the conference).

As we are talking about security and research, let me say a few brief words about the Austrian Security Research Program, which is coordinated by the Federal Ministry of Transport, Innovation and Technology:

The Austrian Security Research Program KIRAS was recommended by RFTE (Austrian Council for Research and Technology Development) in July this year with a first budget of € 5 Millions for 2005. (2005-2013: 110 Mio. € in total)

In order to that Austria is the first EU-Member State, with a national Security Research Program, and it is part of the 7th EU-Framework-Program.

A call for expressions of interest will start by the end of the year. The FFG (Austrian Research Promotion agency) will act as project coordinator and as point of contact for applicants.

The main aims of the national program are:
» *Generation of the knowledge, which is needed for the reaching of the security-political goals of Austria*
» *Increase of objectively measurable security for the population and the security-feeling of the individual*
» *Achievement of security-relevant procedure and technology jumps*
» *Growth of the Austrian security economy*
» *Structure of Excellency within the field of the security research*

At the EU-level the Preparatory Action PASR (2. Call finished, Preparation of 3 Call in 2006) is continued.

At the moment the security research agenda and overall governance with the help of ESRAB (European Security Research Advisory Board), in consultation with Member States, with other security "user" DG´s and with EDA (European Defence Agency) is prepared. It should start 2007 and be supported with 1 Billion € per year.
Additional specific implementation rules (e.g. contract aspects, funding level, handling of classified information, participation) are established.

The main Security Research Event during the EU-Council Presidency will be the European Conference on Security Research in Vienna from the 20th to the 21st February 2006.

But let me come back now to today's conference on Pedestrian and Evacuation Dynamics:

I am strongly convinced that evacuation and crowd dynamics will play a vital role in shaping the future of our societies. And I hope that the results of your research and investigations will be directly transferred into improvements of public safety and convenience and will be used for the benefit of all of us. In the light of these considerations I am especially glad that this conference takes place in Vienna. Be assured that our Ministry will closely monitor the progress of your field.

Therefore, I wish all of you fruitful discussions and many new ideas and stimulation. Let me finally thank you again for coming here and good look for your conference. «

Preface

Due to an increasing number of reported catastrophes all over the world the safety especially of pedestrians today is a dramatically growing field of interest, both for practitioners as well as scientists from various disciplines. The questions arising mainly address the dynamics of evacuating people and possible optimisations of the process by changing the architecture and /or the procedure. This concerns not only the case of ships, stadiums or buildings, all with restricted geometries, but also the evacuation of complete geographical regions due to natural disasters. Furthermore, also 'simple' crowd motion in 'relaxed' situations poses new questions with respect to higher comfort and efficiency since the number of involved persons at large events is as high as never before.

In principle four different methods to tackle these problems exist: One is the analysis of well documented (mainly by video) crowded situations worldwide, another one is the performance of specially designed and elaborated experiments with a certain (normally not as large as necessary) number of participants confronted with a 'real' environment and a predefined task. The third is the investigation of animal behaviour in comparable but (down-)scaled environments where the shaping of the experiments can be easier controlled. The fourth one is to perform simulations based on as realistic as possible mathematical models which incorporate the correct physical movements of the individuals as well as their psychological and social behaviours.

The first three methods have evident disadvantages: Well-documented catastrophes are always singular and rare, experiments with test subjects are not able to reproduce the quantitative (number of persons) and qualitative (emotional and behavioural) tasks of real situations and, finally, animal behaviour can only be extrapolated to human behaviour with respect to a few aspects. In contrast, simulations can, in principle, overcome most of these problems. However, they depend crucially on the quality of the underlying models. This concerns the physical motion of humans, but much more the psychological and social particularities of the individuals under consideration. These can, at least in parts, be derived from the first three methods, nevertheless the properties have to be improved step by step towards a satisfactory performance of the simulations with respect to reality.

The focus of this conference held in Vienna, the third one in a series after Duisburg (2001) and Greenwich (2003), therefore was once more on modelling and simulation of evacuation dynamics, represented by 29 contributions. In addition, pedestrian data collection (8), pedestrian dynamics (5) and collective animal behaviour (4) completed the scope of the conference (amounting to a total of 46 scientific paper in this volume). The number and the quality of these contributions give evidence for the enormous progress made in this field since the last conference only two years ago.

Last but not least we would like to thank everyone who has helped make this conference a reality and success: the members of the technical committee, Katja Schechtner, Hubert Klüpfel, and Tobias Kretz, as well as the organizational staff: Christian Drexler, Tim Meyer-König, Martina Theissl, Yvonne Ginthör, Gabriel Wurzer, Thomas Reichart, Uemit Seren, and finally Florian Szeywerth for the website, poster and the design of the proceedings. «

Vienna, August 2006

Nathalie Waldau
Peter Gattermann
Hermann Knoflacher
Michael Schreckenberg

Contents

Pedestrian Performance Data

Pedestrian Dynamics

Evacuation Simulation

Ship Evacuation

Collective animal motion

List of participants

Antonini Gianluca, Ecole Polytechnique Federale de Lausanne, Signal Processing Institute, Lausanne, Switzerland, *gianluca.antonini@epfl.ch*

Atalla Mauro, United Technologies Research Center, E. Hartford, USA, *atallamj@utrc.utc.com*

Averill Jason, National Institute of Standards and Technology, Building and Fire Research Laboratory, Gaithersburg, USA, *jason.averill@nist.gov*

Bauer Dietmar, arsenal research, Human Centered Mobility Technologies, Vienna, Austria, *dietmar.bauer@arsenal.ac.at*

Berrou Jean Louis, The Maia Institute, Monaco, *jlberrou@maia-institute.org*

Bitzer Florian, Universität Stuttgart, Institut für Straßen- und Verkehrswesen, Stuttgart, Germany, *bitzer@isvs.uni-stuttgart.de*

Bohannon John, Science Magazine, Berlin, Germany, *john@johnbohannon.org*

Botschek Katharina, ILF Consulting Engineers ZT GmbH, Linz, Austria, *katharina.botschek@linz.ilf.com*

Breitenecker Felix, Vienna University of Technology, Institute for Analysis and Scientific Computation, Mathematical Modelling and Simulation, Vienna, Austria, *felix.breitenecker@tuwien.ac.at*

Brell-Cokcan Sigrid, II Architects int, Vienna, Austria, *brell-cokcan@2architects-int.com*

Casburn Ledah, Oregon State University, School of Electrical Engineering and Computer Science, Corvallis, USA, *lcasburn@eecs.oregonstate.edu*

Cavens Duncan, ETH Zürich, Institute for Spatial and Landscape Planning, Zürich, Switzerland, *cavens@nsl.ethz.ch*

Chen Yan Yan, Beijing University of Technology, Transportation Research Center, Beijing, China, *cdyan@bjut.edu.cn*

Chooramun Nitish, The University of Greenwich, Fire Safety Engineering Group, London, *nitishchooramun@yahoo.com*

Christensen Keith, Utah State University, Logan, USA, *keithc@cpd2.usu.edu*

Cokcan Baris, II Architects int, Vienna, Austria, *cokcan@2architects-int.com*

Covarrubias Alvaro, Metro de Santiago de Chile, Metro S.A., Santiago de Chile, Chile, *acovarrubias@metro-chile.cl*

Daamen Winnie, Delft University of Technology, Department of Transport and Planning, Delft, Netherlands, *w.daamen@ct.tudelft.nl*

Dammasch Kristina, Dr. Schniz GmbH, Munich, Germany, *kristina.dammasch@schniz.de*

Deere Steve, The University of Greenwich, Fire Safety Engineering Group, London, UK, *s.deere@gre.ac.uk*

Deneubourg Jean-Louis, Université Libre de Bruxelles, Center for Nonlinear Phenomena and Complex Systems, Bruxelles, Belgium, *jldeneub@ulb.ac.be*

Dorigo Marco, Université Libre de Bruxelles, Institut de Recherches Interdisciplinaires et de Développements en Intelligence Artificielle (IRIDIA), Bruxelles, Belgium, *mdorigo@ulb.ac.be*

Drexler Christian, Kersken + Kirchner GmbH, Munich, Germany, *ch.drexler@kk-fire.com*

El-Hakim Jean-Marc, Minden, Germany, *ingenieurbuero@el-hakim.de*

Fink, Matthias, Vienna University of Technology, Vienna, Austria, *mo.fink@gmx.net*

Galea Ed, The University of Greenwich, Fire Safety Engineering Group, London,UK, *e.r.galea@gre.ac.uk*

Gattermann Peter, Österreichisches Institut für Schul- und Sportstättenbau, Vienna, Austria, *gattermann@oeiss.org*

Geczek Georg, JCI Weltkongress AusrichtungsgesmbH, Vienna, Austria

Gerodimos Alex, Legion Limited, London, UK, *alex.gerodimos@legion.biz*

Hertling Steffen, Dr.Schniz GmbH, Munich, Germany, *steffen.hertling@schniz.de*

Illenberger Johannes, Technische Universität Berlin, Berlin, Germany, *johannes@illenberger.net*

Illera Christa, Vienna University of Technology, Institut für Raumgestaltung und Entwerfen, Vienna, Austria, *cillera@raumgestaltung.tuwien.ac.at*

Jiang Chuansheng, Beijing Municipal Institute of Labour Protection, Beijing, China, *jiang@citysafety.net*

Johansson Anders, Dresden University of Technology, Institute for Transport and Economics, Dresden, Germany, *johansson@vwitme011.vkw.tu-dresden.de*

John Alexander, Universität zu Köln, Köln, Germany, *aj@thp.uni-koeln.de*

Kaneda Toshiyuki, Nagoya Institute of Technology, Nagoya, Japan, *kaneda@archi.ace.nitech.ac.jp*

Kath Karin, Vienna University of Technology, Vienna, Austria

Kerridge John, Napier University, School of Computing, Edinburgh, UK, *j.kerridge@napier.ac.uk*

Kirchberger Hubert, Vienna University of Technology, Institute for Building Construction and Technology, Vienna, Austria, *hubert.kirchberger@tuwien.ac.at*

Klingenburg Volker, Triad Berlin Projektgesellschaft mbH, Berlin, Germany, *klingenburg@triad.de*

Klüpfel Hubert, TraffGo HT GmbH, Duisburg, Germany, *kluepfel@traffgo-ht.com*

Knoflacher Hermann, Vienna University of Technology, Institute for Transport Planning and Traffic Engineering, Vienna, Austria, *hermann.knoflacher@ivv.tuwien.ac.at*

Kobes Margrethe, Netherlands Institute for Fire Service and Disaster Management, Arnhem, Netherlands, *m.kobes@nibra.nl*

Koltchanov Vladimir, ATN Application de Techniques Nouvelles, Paris, France, *v.koltchanov@atn-france.com*

Kraft Markus, Hagen - Ingenieure für Brandschutz, Kleve, Germany, *kraft@hagen-ingenieure.de*

Kretz Tobias, University Duisburg-Essen, Physics of Transport and Traffic, Duisburg, Germany, *kretz@traffic.uni-duisburg.de*

Kruse Dirk, Dehne, Kruse & Partner Ingenieure für Brandschutz, Gifhorn, Germany, *kruse@kd-brandschutz.de*

Landman Ramon, Delft University of Technology, Delft, Netherlands, *c1005162@hotmail.com*

Legout Matthieu, ATN Application de Techniques Nouvelles, Paris, France, *m.legout@atn-france.com*

Mannion Kevin, Legion Limited, London, UK, *kevin.mannion@legion.biz*

Metoyer Ronald A., Oregon State University, Electrical Engineering and Computer Science, Corvallis, USA, *metoyer@cs.orst.edu*

Meyer-König Tim, TraffGo HT GmbH, Flensburg, Germany, *m-k@traffgo-ht.com*

Millonig Alexandra, arsenal research, Human Centered Mobility Technologies, Vienna, Austria, *alexandra.millonig@arsenal.ac.at*

Nakayama Akihiro, University of Ryukyus, Department of Physics and Earth Sciences, Okinawa, Japan, *nakayama@sci.u-ryukyu.ac.jp*

Namazi Alireza, Universität zu Köln, Institut für Theoretische Physik, Köln, Germany, *cdt@ut.ac.ir*

Neumann Christof, ILF Consulting Engineers ZT GmbH, Linz, Austria, *christof.neumann@linz.ilf.com*

Ortega Juan, Metro de Santiago de Chile, Metro S.A., Santiago de Chile, Chile, *jortega@metro-chile.cl*

Oswald Monika, Vienna University of Technology, Institute for Building Construction and Technology, Vienna, Austria, *monika.oswald@tuwien.ac.at*

Park Jin H., Korea Ocean Research and Development Institute, Korea Research Institute of Ships & Ocean Engineering, Daejeon, Republic of Korea, *jhpark@kriso.re.kr*

Pauls Jake, CPE Jake Pauls Consulting Services in Building Use and Safety, Maryland, USA, *bldguse@aol.com*

Phillips Donald, Polytechnic University, New York, USA, *dphillip@poly.edu*

Pietrzykowski Christopher, Otis Elevator Co., Vienna, Austria, *chris.pietrzykowski@otis.com*

Plaum Marcel, Fraport AG, Frankfurt am Main, Germany, *m.plaum@fraport.de*

Popkov Timofei, XJ Technologies, Saint Petersburg, Russian Federation, *tim@xjtek.com*

Qiao Jiangang, Beijing University of Technology, Transportation Research Center, Beijing, China, *qiaojg@emails.bjut.edu.cn*

Reichhart Thomas, Vienna University of Technology, Dept. of Computer-Aided Architecture (IEMAR), Vienna, Austria, *thomasreichhart@yahoo.de*

Revi Aromar, TARU Leading Edge, New Delhi, India, *arevi@taru.org*

Rivers Eric, Arup, Melbourne, Australia, *eric.rivers@arup.com*

Rogsch Christian, Universität Wuppertal, Neustadt, Germany, *info@rogsch.de*

Rupprecht Tobias, University of Wuppertal, Salzkotten, Germany, *rupprecht@gmxpro.de*

Saloma Caesar A., University of the Philippines, National Institute of Physics, Quezon City, Philippines, *csaloma@nip.upd.edu.ph*

Schadschneider Andreas, Universität zu Köln, Institut für Theoretische Physik, Köln, Germany, *as@thp.uni-koeln.de*

Schmid Alex, Savannah Simulations, Herrliberg, Switzerland, *info@savannah-simulations.ch*

Schneider Volker, I.S.T Integrierte Sicherheits-Technik GmbH, Frankfurt am Main, Germany, *volker.schneider@uni-konstanz.de*

Schreckenberg Michael, University Duisburg-Essen, Physics of Transport and Traffic, Duisburg, Germany, *schreckenberg@uni-duisburg.de*

Schultz Michael, Technical Universitity of Dresden, Institut of Aviation, Dresden, Germany, *schultz@ifl.tu-dresden.de*

Schwickert Lars, Fraport AG, Frankfurt am Main, Germany, *l.schwickert@fraport.de*

Seren Uemit, Vienna University of Technology, Dept. Of Computer-Aided Architecture (IEMAR), Vienna, Austria

Seyfried Armin, Forschungszentrum Jülich, Zentralinstitut für angewandte Mathematik, Jülich, Germany, *a.seyfried@fz-juelich.de*

Shi Jiangang, Beijing University of Technology, Transportation Research Center, Beijing, China, *gangfish@emails.bjut.edu.cn*

Streppel Gijs, Jos. L. Meyer GmbH, Sales and Design Department, Papenburg, Germany, *streppel@meyerwerft.de*

Sugiyama Yuki, Nagoya University, Department of Complex Systems Science, Nagoya, Japan, *sugiyama@phys.cs.is.nagoya-u.ac.jp*

Szeywerth Florian, Österreichisches Institut für Schul- und Sportstättenbau, Vienna, Austria, *szeywerth@oeiss.org*

Tabak Vincent, Eindhoven University of Technology, Design Systems group, Eindhoven, Netherlands, *v.tabak@bwk.tue.nl*

Tauböck Michèle, Vienna University of Technology   , Institute for Analysis and Scientific Computation, Mathematical Modelling and Simulation, Vienna, Austria, *shaby@osiris.tuwien.ac.at*

Tavoussi Kamyar, Vienna University of Technology, Institute of Architectural Science, Structural Design and Timber Engineering, Vienna, Austria, *tavoussi@iti.tuwien.ac.at*

Terekhov Alexander, XJTechnologies, Saint Petersburg, Russian Federation, *tim@xjtek.com*

Turner Alasdair, University College London, Architectural and Urban Computing, London, UK, *a.turner@ucl.ac.uk*

Veldhuijzen Van Zanten Diederick, TNO Human Factors, Soesterberg, Netherlands, *VeldhuijzenvanZanten@tm.tno.nl*

Waldau Nathalie, Ingenieurbüro Waldau, Vienna, Austria, *waldau@ibw-wien.at*

Walkow Karl-Friedrich, Technical University of Dresden, Dresden, Germany, *karl@walkow.de*

Wiesenhofer Siegfried, arsenal research, Human Centered Mobility Technologies, Vienna, Austria, *siegfried.wiesenhofer@arsenal.ac.at*

Wölki Marko, University Duisburg-Essen, Physics of Transport and Traffic, Germany, *woelki@traffic.uni-duisburg.de*

Wurzer Gabriel, Vienna University of Technology, Dept. of Computer-Aided Architecture (IEMAR), Vienna, Austria, *wurzer@iemar.tuwien.ac.at*

Xie Hui, The University of Greenwich, Fire Safety Engineering Group, London, UK, *xh01@gre.ac.uk*

Zhu Wei, Eindhoven University of Technology, Urban Planning Group, Eindhoven, Netherlands, *w.zhu@bwk.tue.nl*

Zimmermann Gerhard, University of Kaiserslautern, Kaiserslautern, Germany, *zimmermann@informatik.uni-kl.de* «

Federal Investigation of the Evacuation of the World Trade Center on September 11, 2001

J.D. Averill[1], D. Mileti[2], R. Peacock[1], E. Kuligowski[1], N. Groner[3], G. Proulx[4], P. Reneke[1], and H. Nelson[5]

This paper presents the findings of the NIST World Trade Center Investigation describing the occupant evacuation of WTC 1 and WTC 2 on September 11, 2001. The egress system, including stairwells and elevators, is described along with the evacuation procedures. The population in WTC 1 and WTC 2 on September 11, 2001 at 8:46 a.m. is enumerated and described, where the background of the population was relevant to the subsequent evacuation, including training, experience, mobility status, among others. The progress of the evacuation of both towers is described in a quasi-chronological manner. A decedent analysis explores where occupants were located when each tower was attacked. Multiple regression models were built to explore the sources of evacuation initiation delay (why people did not immediately start to leave the building), as well as stairwell evacuation time (how long the average occupant spent in the stairwells per floor). Issues identified as contributing to either slowing or aiding the evacuation process were explored. Egress simulations provided context for estimating how long WTC 1 and WTC 2 would have taken to evacuate with different populations, using three different models, and subject to different assumptions of damage to the building.

1.   Investigation Scope

The National Institute of Standards and Technology (NIST) announced its building and fire safety investigation of the World Trade Center (WTC) disaster on August 21, 2002. This WTC Investigation, led by NIST, was conducted under the authority of the National Construction Safety Team Act (Public Law [P.L.] 107 231).

The goals of the WTC Investigation were to: (1) investigate the building construction, the materials used, and the technical conditions that contributed to the outcome of the WTC disaster. (2) serve as the basis for:

» Improvements in the way buildings are designed, constructed, maintained, and used;
» Improved tools and guidance for industry and safety officials;
» Recommended revisions to current codes, standards, and practices; and
» Improved public safety.

[1]Natonal Institute of Standards and Technology, Gaithersburg, MD, USA
[2]University of Colorado – Boulder, Boulder, CO, USA
[3]John Jay College, New York City, NY, USA
[4]National Research Council Canada, Ottawa, ON, Canada
[5]Independent Consultant

The objectives of the NIST-led Investigation[1] of the WTC disaster were to: (1) determine why and how WTC 1 and WTC 2 collapsed following the initial impacts of the aircraft; (2) determine why the injuries and fatalities were so high or low depending on location, including all technical aspects of fire protection, occupant behavior, evacuation, and emergency response, (3) determine what procedures and practices were used in the design, construction, operation, and maintenance of WTC 1 and 2, and (4) identify, as specifically as possible, areas in current building and fire codes, standards, and practices that warrant revision.

The Investigation included eight interdependent projects that, in combination, met the objectives. A detailed description of each of these eight projects is available at http://wtc.nist.gov.

2.   Background

While most attention has properly focused on the nearly three thousand people who lost their lives at the World Trade Center site that day, five times that many people successfully evacuated from the WTC towers due to heroic efforts of occupants, as well as emergency responders. Understanding why many, yet not all, survived the World Trade Center attacks was one of the four objectives of this Investigation.
Success in evacuating a building in an emergency can be characterized by two quantities: the time people needed to evacuate and the time available for them to do so.
To the extent the first time exceeded the second, it follows that there will be casualties. When the second time exceeds the first, perhaps by some suitable margin, nearly all should be able to evacuate the building.

The Investigation Team examined the design of the building, the behavior of the people, and the evacuation process in detail to ascertain the parameters that factored prominently in the time needed for evacuation. In order to accomplish this objective, numerous sources of data were collected and analyzed, including: over 1,000 new interviews with survivors; a collection of over 700 published interviews with WTC survivors; 9-1-1 emergency calls; transcripts of emergency communication among building personnel and emergency responders; historical building design drawings, memoranda, and calculations; building modifications and upgrades; formal complaints filed with Occupational Safety and Health Administration (OSHA); and other relevant material.

3.   Interview Methodology

There were three forms of interviews with survivors: 803 telephone interviews, over 225 face-to-face interviews, and 6 focus groups.

---

[1] NIST is a nonregulatory agency of the U.S. Department of Commerce. NIST investigations are focused on fact finding, not fault finding. No part of any report resulting from a NIST investigation into a structural failure or from an investigation under the National Construction Safety Team Act may be used in any suit or action for damages arising out of any matter mentioned in such report (15 USC 281a, as amended by P.L. 107 231).

3.1. Telephone Interviews

The telephone interviewees were randomly selected using independent proportionate stratification from a list of occupants who had badges to enter WTC 1 or WTC 2 on September 11, 2001. In other words, each occupant of a particular tower had an equal probability of being selected. Roughly 400 occupants in each tower were interviewed in order to achieve a high level of statistical precision within each tower. Reported percentages from tower-specific survey data (n = 400) exhibited sampling errors no greater than 2.5 percentage points, and 95 percent confidence intervals of percentages are no greater than ± 5 percentage points. This level of precision was more than adequate for examining characteristics of occupants and egress attributes. The telephone interview results enabled a scientific projection of the population and distribution of occupants in WTC 1 and WTC 2, as well as causal modeling to explore fundamental egress issues such as sources of evacuation delay.

3.2. Face-to-face Interviews

The objective of the face-to-face interviews was to gather first-hand accounts and observations of the activities and events inside the buildings on the morning of September 11th. This approach identified unknown information, aided in the evaluation of technical hypotheses, and explored motivations for occupant behaviors, while allowing for comparisons to the telephone interview data. A typical face-to-face interview averaged approximately two hours. The methodology for the face-to-face interviews was a synthesis of two established methodologies, designed to assist survivors in providing comprehensive and accurate accounts of their evacuation, given the latency between experience and interview.

3.3. Focus Group Interviews

Six focus groups were conducted in order to elicit accurate group representations of specific events or themes and complement the findings of the telephone and face-to-face interviews. The focus groups were: (1) occupants located near the floors of impact; (2) floor wardens; (3) mobility challenged occupants; (4) persons with building responsibilities; (5) randomly-selected evacuees in WTC 1; and (6) randomly-selected evacuees in WTC 2.

4.   WTC 1 and WTC 2

The team documented the WTC egress system, including the location of the three primary stairwells, exit doors, core hallways, transfer corridors, wall construction, location and layout of the 100+ elevators in each tower, and emergency communication devices. WTC 1 and WTC 2 each consisted of 110 stories above the Concourse Level (or 109-stories above the plaza / Mezzanine Level) structure. There were also 6 basement levels

below the Concourse Level. Although the towers were similar, they were not identical. The height of WTC1 at the roof level was 1,368 ft (418 m) above the Concourse Level (6 ft taller than WTC 2), and WTC 1 additionally supported a 360 ft (110 m) tall antenna on the roof for television and radio transmission. Each tower had a square plan with the side dimension of 207 ft 2 in. (63.2 m). Each tower had a core service area of approximately 135 ft x 87 ft (41 m x 27 m), although the core space changed on tenant spaces throughout the towers. Placing all service systems within the core provided column-free floor space of roughly 31,000 sq ft (2,900 m^2) per floor outside the core. The long axis of the core in WTC 1 was oriented in the east-west direction while the long axis of the core in WTC 2 was oriented in the north-south direction.

Stairwells

WTC 1 and WTC 2 each had three primary stairwells designed for emergency egress, designated as A, B, and C. There were additional stairwells located in the basement levels (B1 – B5), convenience stairs for tenants leasing multiple floors, and mechanical room stairs. Stairwells A and C were 1.1 m (44 in.) wide and extended from floor 2 (plaza or Mezzanine Level) to floor 110 (lower mechanical space). Stairwell B was 56 in. (1.4 m) wide and ran from the subgrade 6 levels below ground to floor 107 including the Concourse (main lobby); there was no exit from Stairwell B onto the 2nd floor (plaza / Mezzanine Level).

The WTC 1 and WTC 2 stairwells were occasionally routed horizontally around equipment on mechanical floors, through what were called transfer hallways. Stairwell B required a horizontal transfer at floor 76. For all other floors, stairwell B maintained vertical alignment through the building. Stairwells A and C required several horizontal transfers, some longer than others, which ranged from several feet to over 100 ft (33 m).

Elevators

The World Trade Center complex contained more than 240 elevators, with 99 elevators serving the above-ground levels in each of the two main towers and an additional 7 elevators serving primarily the sub-grade basement levels. In the towers, the elevators were arranged to serve the buildings in three sections divided by skylobbies, which served to distribute passengers among express and local elevators.

5.   Occupant Characteristics

NIST estimates that there were 8,900 ± 750 people in WTC 1 at 8:46:30 a.m. on September 11, 2001. Similarly, NIST estimates that there were 8,540 ± 920 people inside WTC 2 at 8:46:30 a.m. New York City officially announced 2,749 fatalities at the World Trade Center, including emergency responders, airplane passengers and crew (not including

the 10 hijackers), and bystanders. NIST estimated that of the $17,400 \pm 1,180$ occupants inside WTC 1 and WTC 2 at 8:46:30 a.m., 2,163 – 2,180 perished. (No information could be found for 17 persons. The remaining individuals were emergency responders, airline passengers, or bystanders.) More than twice as many occupants were killed in WTC 1 as WTC 2, largely due to the fact that occupants in WTC 2 used the 16 minutes between the attacks on WTC 1 and WTC 2 to begin evacuating, including the use of elevators by some occupants in WTC 2.

The demographic characteristics of the evacuees were explored where the characteristics were relevant to the evacuation on September 11, 2001. Few differences in the characteristics of WTC 1 or WTC 2 were observed. Men outnumbered women roughly two to one. The average age was mid-forties. The mean length of employment at the WTC site was almost six years, while the median was 2 and 3 years for WTC 1 and 2, respectively. Sixteen percent of 2001 WTC evacuees were also present during the 1993 bombing, although many other occupants were also knowledgeable about the 1993 evacuation. Two-thirds of the occupants had participated in at least one fire drill during the 12 months immediately prior to September 11, 2001. Eighteen percent did not recall whether they had participated in a fire drill during that time period and eighteen percent reported that they did not participate in a fire drill during that time period.

6.   September 11, 2001 - Evacuation

6.1.

In WTC 1, all three stairwells and the elevators were destroyed in the impact region, extending as low as floor 92. No occupant evacuated from above the 91st floor, although some survived until the building collapsed after 102 minutes. Helicopter rescue from the roof was considered by an NYPD aviation unit but deemed not possible due to the heat and smoke from the building fire. Occupants of both towers delayed initiating their evacuation after WTC 1 was hit. In WTC 1, the median time to initiate evacuation was 3 minutes for occupants from the ground floor to floor 76, and 5 minutes for occupants near the impact region (floors 77 – 91). Occupants observed various types of impact indicators throughout the building, including wall, partition, and ceiling damage and fire and smoke conditions. The most severe damage was observed near the impact region, fatally trapping some occupants. Announcements in WTC 1 were not heard by the occupants, despite repeated attempts from the lobby fire command station to order an evacuation. Damage to critical communications hardware likely prevented announcement transmission. Evacuation rates reached a peak, steady-state in approximately 5 minutes, and remained roughly constant until the collapse of WTC 2, when the rate in WTC 1 slowed to about one-fifth of the peak, steady-state. WTC 1 collapsed at 10:28:22 a.m., resulting in approximately 1,500 occupant deaths, 111 of which were estimated to be below the 92nd floor. A rest station for mobility challenged occupants was established in WTC 1 somewhere between floors 12 and 20. Less than ten minutes prior to the collapse

of WTC 1, the occupants and helpers on the floor were ordered to evacuate, although it remains unclear whether all rest station residents survived.

6.2. WTC 2

The evacuation of WTC 2 was markedly different from the evacuation of WTC 1. There was a 16 minute period after WTC 1 was attacked, but before WTC 2 was attacked. During this time period, occupants were forced to decide whether to remain inside WTC 2, and if they decided to leave, they had to choose between using one of the three stairwells or using an elevator. Further complicating this decision process were multiple, conflicting announcements around 9:00 a.m., first instructing occupants to return to their offices, and then within one minute of impact, instructing them to begin an evacuation if conditions on their floor warranted that decision. Over 90 percent of WTC 2 survivors started to evacuate the building prior to its being attacked. Sixteen percent of the survivors used elevators to evacuate. Approximately 75 percent of the occupants who were above the 78th floor (the lowest floor of impact) descended to at least below the impact region prior to the attack on WTC 2. Over 40 percent of the survivors had left WTC 2 prior to 9:02:59 a.m. After WTC 2 was attacked, at least 18 individuals used Stairwell A, located in the northwest corner and furthest from the impact damage, to descend below the 78th floor to evacuate the building. Additional public address announcements were made after the airplane strike on WTC 2, although occupants who survived generally did not hear those announcements. After the initial peak in evacuation rate due to concurrent elevator and stairwell usage, the rate reached a steady-state similar to the rate observed in WTC 1 until approximately 20 minutes prior to collapse of WTC 2. The evacuation rate during the final 20 minutes dropped significantly, likely due to a decreased number of occupants remaining in the egress system below the 78th floor. NIST analysis indicated only eight occupants initially below the 78th floor were killed when WTC 2 collapsed at 9:58:59 a.m. Overall, NIST estimated that 626 occupants of WTC 2 perished.

7.   Causal Modeling

Using the statistical power of the telephone interview results, two models were constructed to explore the primary components of total evacuation time: evacuation initiation delay and stairwell traversal time. Each model explained between 49 percent and 56 percent of the variance in the ultimate dependent variable, which are high levels for human behavior studies.

7.1. Evacuation Initiation Delay

The first component of total evacuation time is the time delay prior to starting evacuation. This was defined as the time from the attack on WTC 1 until the occupant left the floor using a stairwell or elevator to leave the building. The factors that best predicted
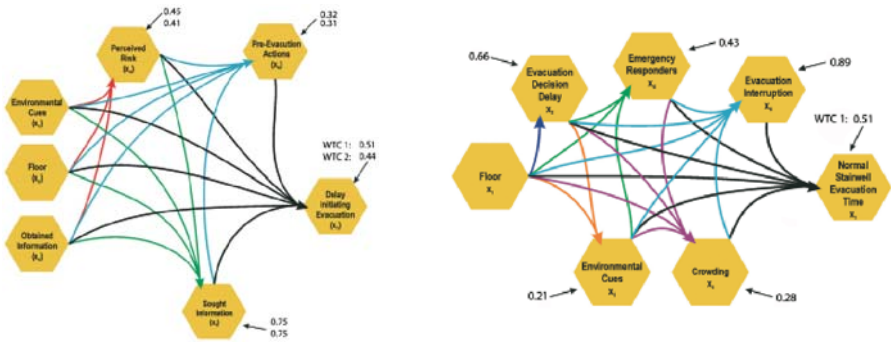
Figure 1: Causal models for (left) evacuation initiation delay (WTC 1 and WTC 2) and (right) normalized stairwell evacuation time (WTC 1).

evacuation initiation delay in WTC 1 were (1) which floor the respondent was on when WTC 1 was attacked, (2) whether occupants encountered environmental cues (smoke, fire, debris, etc.), and (3) seeking additional information (or milling) about the nature of the event. In WTC 2, the same process occurred as in WTC 1, except that perceived risk (sense of immediate danger) was a predictor of seeking additional information (along with floor and environmental cues).

7.2. Normalized Stairwell Evacuation Time

The second component of total evacuation time was the time spent in the stairwells. This analysis determined the factors and social processes that influenced the normalized stairwell evacuation time per flight of stairs for the people who evacuated out of WTC 1 on September 11, 2001. WTC 2 was excluded from this analysis because evacuees used stairs, elevators, and/or a combination of both for their evacuation and could not be separated for the analysis. Evacuation time was defined as the average number of seconds per flight of stairs that it took people from the time they entered a stairwell until they completed their evacuation out of the building. The model used to predict important factors in stairwell evacuation time again used variables that preliminary analyses and general evacuation theory suggested as salient.

The main process that led to increased normalized stairwell evacuation time in the evacuation of WTC 1 on September 11th was straightforward and clear. Floor (increased distance to safety) substantially increased the odds that people would encounter environmental cues. Floor also increased delay in starting evacuation (this relationship was elaborated upon in the first model), which, in turn, also increased the chances that people would encounter environmental cues. But it was encountering environmental cues that had a large and direct effect on increasing the amount of time that people spent, on average, to traverse their evacuation stairwell. In addition to this multi-step process with environmental cues as the key predicting variable, interrupting the process of evacua-

tion for any reason also increased the amount of time, on average, that people used to descend their evacuation stairwell.

8.   Egress Modeling

Multiple evacuation models were used to simulate different WTC tower evacuations, subject to a number of assumptions. The goal of the modeling was to frame an understanding of actual evacuation findings on September 11, 2001. Simulations demonstrated that a phased evacuation (also known as defend-in-place, whereupon occupants on the fire floor and the immediately surrounding floors descend to three floors below the fire floor) would have taken between 4 minutes to complete without delays in evacuation initiation and 11 mintues to complete with evacuation initation delays between 0 and 10 minutes. Total evacuation of a tower assuming a full occupant load without visitors (19,800) would have required as few as 92 – 112 minutes. With visitors (total population 25,500 people) total evacuation would have required as little as 114 – 142 minutes. The ranges reflect two different model outputs, each assuming two different delay times (no delay and a ten minutes distribution of delay times). An evacuation simulation for 8,800 people (approximately the number present in each tower on September 11, 2001) in the absence of any damage to the building, would have required at least 52 – 71 minutes, depending on the model or the delay times. Finally, the model output was 'calibrated' to approximate the gross evacuation rates observed in WTC 1 and WTC 2 on September 11, 2001. Once the model input necessary to approximate the observables was determined, additional occupants were added in order to estimate how many occupants might have been unable to evacuate on September 11, 2001 (given the damage to the building and observed delay times) if the buildings had had larger occupant loads. NIST estimated that approximately 14,000 occupants would have been unable to evacuate from WTC 1 and WTC 2 on September 11, 2001 had the starting building population been 19,800 in each building.

9.   Recommendations Related to Egress

Building evacuation should be improved to include system designs that facilitate safe and rapid egress, methods for ensuring clear and timely emergency communications to occupants, better occupant preparedness for evacuation during emergencies, and incorporation of appropriate egress technologies[2].

---

[2] This effort should include standards and guidelines for the development and evaluation of emergency evacuation plans, including best practices for both partial and full evacuation, and the development of contingency plans that account for expected conditions that may require adaptation, including the compromise of all or part of an egress path before or during evacuation, or conditions such as widespread power failure, earthquake, or security threat that restrict egress from the building. Evacuation planning should include the process from initial notification of the need to evacuate to the point the occupants arrive at a place where their safety is ensured. These standards and guidelines should be suitable for assessing the adequacy of evacuation plans submitted for approval and should require occupant training through the conduct of regular drills.

Recommendation: NIST recommends that public agencies, non-profit organizations concerned with building and fire safety, and building owners and managers should develop and carry out public education campaigns, jointly and on a nationwide scale, to improve building occupants' preparedness for evacuation in case of building emergencies. This effort should include better training and self-preparation of occupants, an effectively implemented system of floor wardens and building safety personnel, and needed improvements to standards. Occupant preparedness should include:

a. Improved training and drills for building occupants to ensure that they know evacuation procedures, are familiar with the egress route, and are sufficiently aware of what is necessary if evacuation is required with minimal notice (e.g., footwear consistent with the distance to be traveled, a flashlight/glow stick for pathway illumination, and dust masks).

b. Improved training and drills that routinely inform building occupants that roof rescue is not (or is) presently feasible as a standard evacuation option, that they should evacuate down the stairs in any full-building evacuation unless explicitly instructed otherwise by on-site incident commanders, and that elevators can be used if they are still in service and haven't been recalled or stopped.

c. Improved codes, laws, and regulations that do not restrict or impede building occupants during evacuation drills from familiarizing themselves with the detailed layout of alternate egress routes for a full building evacuation[3].

Recommendation: NIST recommends that tall buildings should be designed to accommodate timely full building evacuation of occupants due to building-specific or large-scale emergencies such as widespread power outages, major earthquakes, tornadoes, hurricanes without sufficient advanced warning, fires, accidental explosions, and terrorist attack. Building size, population, function, and iconic status should be taken into account in designing the egress system. Stairwell and exit capacity[4] should be adequate to accommodate counterflow due to emergency access by responders.

a. Improved egress analysis models, design methodology, and supporting data should be developed to achieve a target evacuation performance (e.g., time for full building evacuation[5]) for the design building population by considering the building and egress system designs and human factors such as occupant size, mobility status, stairwell tenability conditions, visibility, and congestion.

b. Mobility challenged occupants should be provided a means for self-evacuation in the event of a building emergency. Current strategies (and law) generally require the

---

[3] New York City Local Law 5 prohibits requiring occupants to practice stairwell evacuation during drills.

[4] Egress capacity should be based on an all-hazards approach that considers the number and width of stairs (and doors) as well as the possible use of scissor stairs credited as a single stair.

[5] Use of egress models is required to estimate the egress capacity for a range of different evacuation strategies, including full building evacuation. NIST found that the average surviving occupant in the WTC towers descended stairwells at about half the slowest speed previously measured for non-emergency evacuations.

mobility challenged to shelter-in-place and await assistance. New procedures, which provide redundancy in the event that the floor warden system or co-worker assistance fails, should consider full building evacuation, and may include use of fire-protected and structurally hardened elevators[6], motorized evacuation technology, and/or dedicated communication technologies for the mobility challenged.

c. If protected/hardened elevators are provided for emergency responders but become unusable during an emergency, due to a malfunction or a conventional threat whose magnitude exceeds the magnitude considered in design, sufficient stairwell capacity should be provided to ensure timely emergency responder access to buildings that are undergoing full evacuation. Such capacity could be provided either via dedicated stairways for fire service use or by building sufficient stairway capacity (i.e., number and width of stairways and/or use of scissor stairs credited as a single stair) to accommodate the evacuation of building occupants while allowing access to emergency responders with minimal hindrance from occupant counterflow.

d. The egress allowance in assembly use spaces should be limited in state and local laws and regulations to no more than a doubling of the stairway capacity for the provision of a horizontal exit on a floor, as is the case now in the national model codes[7]. The use of a horizontal exit creates an area of refuge with a 2 hour fire rated separation, at least one stair on each side, and sufficient space for the expected occupant load.

Recommendation: NIST recommends that egress systems should be designed: (1) to maximize remoteness of egress components (i.e., stairs, elevators, exits) without negatively impacting the average travel distance; (2) to maintain their functional integrity and survivability under foreseeable building-specific or large-scale emergencies; and (3) with consistent layouts, standard signage, and guidance so that systems become intuitive and obvious to building occupants during evacuations.

a. Within a safety-based design hierarchy that should be developed, highest priority should be assigned to maintain the functional integrity, survivability, and remoteness of egress components and active fire protection systems (sprinklers, standpipes, associated water supply, fire alarms, and smoke management systems). The design hierarchy should consider the many systems (e.g., stairs, elevators, active fire protection, mechanical, electrical, plumbing, and structural) and system components, as well as functional integrity, tenant access, emergency responder access, building configuration, security, and structural design.

---

[6] Elevators should be explicitly designed to provide protection against large, but conventional, building fires. Fire-protected elevators also should be structurally hardened to withstand the range of foreseeable building-specific or large-scale emergencies. While progress has been made in developing the requirements and technologies for fire-protected elevators, similar criteria and designs for structurally hardened elevators remain to be developed.

[7] The New York City Building Code permits a doubling of allowed stair capacity when one area of refuge is provided on a floor and a tripling of stair capacity for two or more areas of refuge on a floor. In the world of post-September 11, 2001, it is difficult to predict (1) if, and for how long, occupants will be willing to wait in a refuge area before entering an egress stairway, and (2) what the impact would be of such a large group of people moving down the stairs on the orderly evacuation of lower floors.

b. The design, functional integrity, and survivability of the egress and other life safety systems (e.g., stairwell and elevator shafts and active fire protection systems) should be enhanced by considering accidental structural loads such as those induced by overpressures (e.g., gas explosions), impacts, or major hurricanes and earthquakes, in addition to fire separation requirements. In selected buildings, structural loads due to other risks such as those due to terrorism may need to be considered. While NIST does not believe that buildings should be designed for aircraft impact, as the last line of defense for life safety, the stairwells and elevator shafts individually, or the core if these egress components are contained within the core, should have adequate structural integrity to withstand accidental structural loads and anticipated risks.

c. Stairwell remoteness requirements should be met by a physical separation of the stairwells that provide a barrier to both fire and accidental structural loads. Maximizing stairwell remoteness, without negatively impacting the average travel distance, would allow a stairwell to maintain its structural integrity independent of any other stairwell that is subject to accidental loads, even if the stairwells are located within the same structural barrier such as the core. The current "walking path" measurement allows stairwells to be physically next to each other, separated only by a fire barrier. Reducing the clustering of stairways that also contain standpipe water systems provide the fire service with increased options for formulating firefighting strategies. This should not preclude the use of scissor stairs as a means of increasing stair capacity—provided the scissor stair[8] is only credited as a single stair.

d. Egress systems should have consistent layouts with standard signage and guidance so that the systems become intuitive and obvious to all building occupants, including visitors, during evacuations. Particular consideration should be given to unexpected deviations in the stairwells (e.g., floors with transfer hallways).

Recommendation: NIST recommends that building owners, managers, and emergency responders develop a joint plan and take steps to ensure that accurate emergency information is communicated in a timely manner to enhance the situational awareness of building occupants and emergency responders affected by an event. This should be accomplished through better coordination of information among different emergency responder groups, efficient sharing of that information among building occupants and emergency responders, more robust design of emergency public address systems, improved emergency responder communication systems, and use of the Emergency Broadcast System (now known as the Integrated Public Alert and Warning System) and Community Emergency Alert Networks.

a. Situational awareness of building occupants and emergency responders in the form of information and event knowledge should be improved through better coordination of such information among emergency responder groups (9-1-1 dispatch, fire department or police department dispatch, emergency management dispatch, site security, and appropriate federal agencies), efficient sharing and communication of information between building occupants and emergency responders, and improved emergency responder communication systems (i.e., including effective communication within steel and

---

[8] Two separate stairways within the same enclosure and separated by a fire rated partition.

reinforced concrete buildings, capacity commensurate with the scale of operations, and interoperability among different communication systems).

b. The emergency communications systems in buildings should be designed with sufficient robustness and redundancy to continue providing public address announcements or instructions in foreseeable building-specific or large-scale emergencies, including widespread power outage, major earthquakes, tornadoes, hurricanes, fires, and accidental explosions. Consideration should be given to placement of building announcement speakers in stairways in addition to other standard locations.

c. The Integrated Public Alert and Warning System (IPAWS) should be activated and used, especially during large-scale emergencies, as a means to rapidly and widely communicate information to building occupants and emergency responders to enhance their situational awareness and assist with evacuation.

d. Local jurisdictions (cities and counties or boroughs) should seriously consider establishing a Community Emergency Alert Network (CEAN), within the framework of IPAWS, and make it available to the citizens and emergency responders of their jurisdiction to enhance situational awareness in emergencies.[9] The network should deliver important emergency alerts, information and real-time updates to all electronic communications systems or devices registered with the CEAN. These devices may include e-mail accounts, cell phones, text pagers, satellite phones,and wireless PDAs.

Recommendation: NIST recommends that the full range of current and next generation evacuation technologies should be evaluated for future use, including protected/hardened elevators, exterior escape devices, and stairwell navigation devices, which may allow all occupants an equal opportunity for evacuation and facilitate emergency response access. **«**

---

[9] Types of emergency communications could include life safety information, severe weather warnings, disaster notifications (including information on terrorist attacks), directions for self-protection, locations of nearest available shelters, precautionary evacuation information, identification of available evacuation routes, and accidents or obstructions associated with roadways and utilities.

Free speed distributions –
Based on empirical data in different traffic conditions

W. Daamen[1] and S.P. Hoogendoorn[1]

Free speeds are defined as the speeds pedestrians like to walk with when they are not hindered by other pedestrians.

Since pedestrians have different characteristics influencing their choices, free speeds will differ among individuals. These pedestrian characteristics are often not taken into account explicitly, which makes it necessary to describe free speeds as a stochastic variable with a distribution. Moreover, (free) speeds will be influenced by the characteristics of the walking infrastructure, such as grade, length, width, the type of pedestrian facility, and weather and other external conditions.

Free speeds and their distribution play an important role in many traffic flow models, but are also relevant in other applications.

The aim of this research is to derive free speed distributions for a number of traffic flow conditions. The data on which the distributions are estimated come from large-scale laboratory walking experiments. In these experiments different traffic conditions are simulated, such as unidirectional flows, opposite flows, and crossing flows.

Free speeds are highest in unidirectional flows (1.54 m/s), somewhat lower for opposite flows (1.41 m/s), and lowest for crossing flows (1.35 m/s). Reduction of this free speed is due to the interaction with other flows. For opposite flows, this interaction is reduced by lane formation (effect of self-organisation). For crossing flows however, this interaction cannot be reduced, since the flows have to interact during the crossing.

1. Introduction

Free speeds or desired speeds are defined as the speeds pedestrians like to walk with when they are not hindered by other pedestrians.

Since pedestrians have different characteristics influencing their choices, free speeds will differ among individuals. These pedestrian characteristics are often not taken into account explicitly, which makes it necessary to describe free speeds as a stochastic variable with a distribution. Moreover, (free) speeds will be influenced by the characteristics of the walking infrastructure, such as grade, length, width, the type of pedestrian facility, and weather and other external conditions.

Free speeds and their distribution play an important role in many traffic flow models, macroscopic as well as microscopic ones. In illustration: the free speed distribution is an important input for gas-kinetic models (1,2). Many microscopic simulation models draw the free speed of individual vehicles from free speed distributions.

Insights into free speeds are also important from the viewpoint of design. Walking times between origins and destinations in a facility can be derived, while transfer times can be derived for the design of public transport timetables. It is also interesting to see how free

---

[1] Delft University of Technology, Faculty of Civil Engineering and Geosciences, department of Transport & Planning

speed distributions change with varying conditions (type of infrastructure, weather) and with different types of travellers (men versus women, commuters versus tourists).

The aim of this research is to derive free speed distributions for a number of traffic flow conditions. The data on which the distributions are estimated come from large-scale laboratory walking experiments, in which different traffic conditions have been simulated.

This paper starts with an overview of free speeds found in literature (section 2). Then, a description is given of the laboratory experiments we performed. The data derived from these experiments are used to estimate free speed distributions. Section 4 describes in short the method to estimate free speed distributions. This method is illustrated by the graphs derived for the narrow bottleneck experiment. The free speed distributions for the other experiments are discussed in section 5 and compared to the literature referenced earlier. We end with conclusions and recommendations for future research.

2.   Free speeds in literature

Much literature has been found on pedestrian walking behaviour, especially on real-time observations of pedestrian traffic characteristics, such as (free) speed, flow, and density. This paper focuses on the findings on pedestrian free speeds. Table 1 shows pedestrian free speeds found in literature. Both the average free speed and the variance (if available) are shown, as well as the country where the study has been performed.

The speed of individuals appears to follow a normal distribution, with an estimated mean of 1.34 m/s and a standard deviation of 0.37 m/s. The standard deviation has been calculated as a mean of the free speeds in Table 1 using the co-efficient of variance. Weidmann (3) performed a literature study on pedestrian speeds in 1993. He found a mean speed of 1.34 m/s, with speeds varying between 0.97 m/s and 1.65 m/s (against 1.08 m/s and 1.6 m/s in Table 1). Under specific circumstances, the normal distribution can have a positive skewness. The median speed, considered to be more representative than the average speed, is found to be 1.2 m/s (4).

Basic traffic characteristics depend on individual pedestrian characteristics and external conditions. Influencing aspects are age, culture, gender, shy away distance, temperature, travel purpose, type of infrastructure, and walking direction. In Table 1 we see the influence of the countries in which the studies have been performed. Most studies have been performed in Northern America, Europe and Asian countries. Walking behaviour in Northern America and Europe appears to be similar, whereas walking behaviour in the Asian countries is significantly deviant. This is mainly caused by the body buffer zone space, including pedestrian size (Asian pedestrians are much smaller than in western countries) and culture (Asian pedestrians maintain smaller inter-pedestrian distances) (23).

The average speed in European studies appears to be 1.41 m/s, 1.35 m/s in studies in the United States, 1.44 m/s in an Australian study and in Asian studies 1.24 m/s.

Source	Mean speed (m/s)	Standard deviation (m/s)	Location
CROW (5)	1.4		the Netherlands
Daly et al. (6)	1.47		United Kingdom
FHWA (7)	1.2		United States
Fruin (4)	1.4	0.15	United States
Hankin and Wright (8)	1.6		United Kingdom
Henderson (9)	1.44	0.23	Australia
Hoel (10)	1.50	0.20	United States
Institute of Transportation Engineers (11)	1.2		United States
Knoflacher (12)	1.45		Austria
Koushki (13)	1.08		Saudi-Arabia
Lam et al. (14)	1.19	0.26	Hong Kong
Morrall et al. (15)	1.25		Sri Lanka
	1.4		Canada
Navin and Wheeler (16)	1.32		United States
O'Flaherty and Parkinson (17)	1.32	1.0	United Kingdom
Older (18)	1.30	0.3	United Kingdom
Pauls (19)	1.25		United States
Roddin (20)	1.6		United States
Sarkar and Janardhan (21)	1.46	0.63	India
Sleight (22)	1.37		United States
Tanariboon et al. (23)	1.23		Singapore
Tanariboon and Guyano (24)	1.22		Thailand
Tregenza (25)	1.31	0.30	United Kingdom
Virkler and Elayadath (26)	1.22		United States
Young (27)	1.38	0.27	United States
Estimated overall average	1.34	0.37	

Table 1: Free speeds observed in literature

3. Data collection on pedestrian walking behaviour using laboratory experiments

The Transport & Planning department of the Delft University of Technology has performed experimental research by organising controlled walking behaviour experiments. Main advantage of performing experiments is the control of the conditions – both with respect to the observed situation and the system of data collection, such as location of the camera, ambient and weather conditions. Another benefit is the flexibility to systematically vary the experimental variables to see effects of these variables on the behaviour of individual pedestrians and of the total pedestrian flow. It may be argued that the behaviour of pedestrians during the experiments will not be very different from their real-life walking behaviour since walking is mostly a skill-based task, thus requiring little or none conscious consideration. For further comparisons and more information see (28).

By performing walking experiments, we can determine the stimuli, the walkers' responses, and the relations between them that determine pedestrian behaviour. Apart from the methodological advantages, experiments allow observations of conditions that are not readily available or are very difficult to observe. The process variables are both the input and output variables that are deemed relevant, for details see (29).

Ten walking experiments were conducted in a large hallway. A digital camera was mounted at the ceiling of the hallway, at a height of 10 m, observing an area of approximately 14 m by 12 m. In each of these experiments approximately 75 pedestrians were involved, not only TU Delft students, but representative for the Dutch population. Results of five experiments are shown in this paper. These experiments concern unidirectional flows, opposite flows, crossing flows, and two experiments with a bottleneck. In the wide bottleneck experiment the bottleneck has a width of 2 meters, whereas the bottleneck has a width of 1 meter in the narrow bottleneck experiment. The width of the narrow bottleneck is such that pedestrians inside of the bottleneck are not able to pass each other. The flow in each experiment varied from very low to congestion in the narrow bottleneck experiment.

Hoogendoorn et al. (30) discuss the approach to extract individual pedestrian data from digital video footage, allowing pedestrian trajectories to be determined with high accuracy.
Figure 1 shows the view from above on the narrow bottleneck experiment. All pedestrians wear caps and white shirts to facilitate automated detection and tracking of the pedestrians. The bottleneck of 1 m wide is situated on the left, whereas pedestrians walk from right to left. The white circles indicate cones marking the observation area.

Figure 1: Overview of the narrow bottleneck experiment

4.   Free speed estimation method

The free speed of a pedestrian is defined by the walking speed of pedestrians when they are not hindered by others. The free speed will be influenced by characteristics of the pedestrian, the infrastructure, and ambient conditions such as weather.
Estimation of free speeds and free speed distributions is not as straightforward as it looks like. Pedestrians are either walking at their free speed or following another pedestrian. This suggests that only those pedestrians walking freely are considered to derive the free speed distribution. However, pedestrians having a relatively high free speed have a higher probability of being constrained than pedestrians with a relatively low free speed (31). This will lead to underestimation of the free speeds.

In (31) an overview of alternative free speed estimation approaches for car traffic is presented, among which the following:

1.   Estimation of the free speed by considering the speed at low volumes (32). A weakness of this model is that the composition of the flow in these non-peak periods may be different from that in peak periods. The free speed distribution will therefore be different.
2.   Extrapolation towards low intensities. The method allows using the relevant population, but is known to be liable to errors (31).
3.   Application of simulation models. This method involves the use of microscopic simulation models to establish relations between observable variables and the free speed distribution (33).
4.   Method based on Erlander's model. Erlander (34) developed an integral equation for traffic operations on two-lane roads with the free speed distribution as one of its components.

Since all methods mentioned above have severe disadvantages, Hoogendoorn (35) recently developed a new estimation approach referred to as the modified Kaplan-Meier approach. This approach is based on the concept of censored observations (36) using a non-parametric estimation approach to estimate the parameters of the free speed distribution. In section 4.1 the applied approach is described in short. Section 4.2 illustrates the approach showing the (intermediate) results of the free speed estimation for the narrow bottleneck experiment.

4.1. Description of the estimation method

Let us consider individual pedestrian data collected at a cross-section. For each pedestrian i that has passed the cross-section, we have determined its speed v_i and its headway t_i. The aim of the approach is to determine the distribution $F(v^0)$ of free speeds v^0 using the available data $\{t_i, v_i\}$.

Speed observations are marked as either censored (constrained) or uncensored (free flowing). Approaches based on censored data appear to be quite sensitive to the distinction between censored and uncensored measurements. The new approach uses a composite headway model (37) combined with a distribution free estimation approach (38) to establish the constrained and unconstrained headway distributions from the available (time) headway data, as well as the probability θ_i indicating the extent in which the observations are censored. To be able to use these partially censored data, the method of Kaplan and Meier (39) has been adapted. In this method the probabilities θ_i and the speeds v_i are used to determine the modified Kaplan-Meier distribution function $F(v^0)$.

4.2. Free speed estimation for the narrow bottleneck experiment

First, we determine a border value T^*, where all headway observations $T_p > T^*$ stem from freely walking pedestrians. To do this, Hoogendoorn (35) uses the empirical survival function. However, for the pedestrian laboratory experiments, we already calculated T^* when studying pedestrian behaviour at bottlenecks, see (40). In this paper, we will use the same value, that is, $T^* = 2.5$ s.

The next step is to estimate a composite headway distribution model. The mathematical formulation of this model is given by the following equation:

$$f(t) = \phi g(t) + (1 - \phi)h(t) \qquad (1)$$

where g(t) and h(t) respectively denote the headway probability density functions of the constrained headway and the free headway; ϕ denotes the fraction of followers. We will now calculate distributions for both the free flow headways $h_1(h)$ and the constrained headways $g_1(h)$, based on the histogram of the observed headways $f_{hist}(h)$. Figure 2 shows these estimated distributions as well as the histogram of the observed headways. As indicated before, the original method of Kaplan and Meier (39) requires explicit
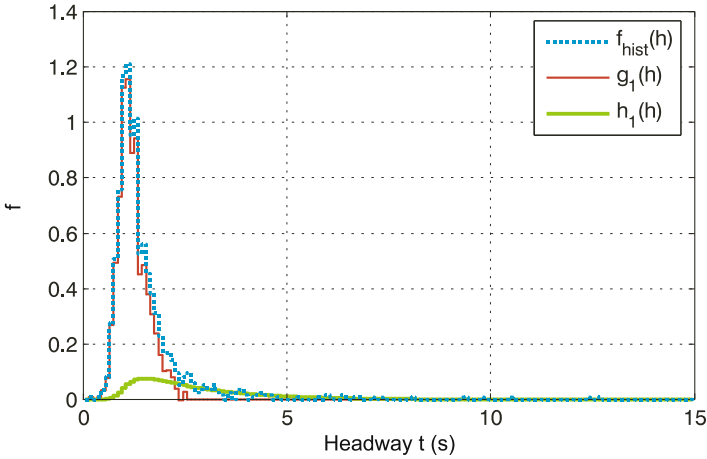
Figure 2: Distribution free headway estimation for the narrow bottleneck experiment

distinction between censored and uncensored data, implying that speed observations v_i need to be labeled either constrained or free flowing. In establishing an unbiased estimation, Hoogendoorn (35) uses the conditional probability $\theta(t_i)$ for observation i and labels this observation as 'censored' with probability $\theta(t_i)$ by drawing from a uniform distribution function. This probability distribution is shown in Figure 3.
Figure 4 shows the estimation results from application of the modified Kaplan – Meier
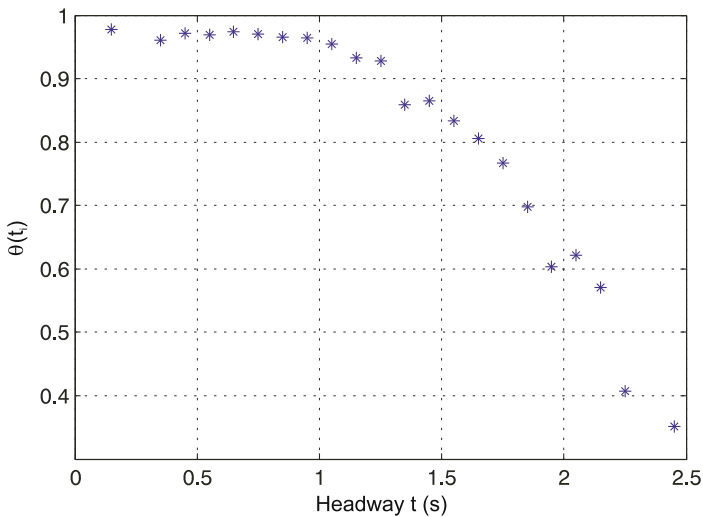
Figure 3: Conditional probability $\theta(t_i)$ that a pedestrian with headway t is constrained by the pedestrian in front

approach (35) for the calculation of free flow speeds. The figure shows the empirical distribution function of the speed F_n. The figure clearly shows that the modified Kaplan – Meier method yields higher estimates for the free speed compared to the other estimates. We have also computed the empirical speed distribution F^0_n by considering the speeds of pedestrians that walk in free flow conditions. More details on the estimation results are shown in Table 1.
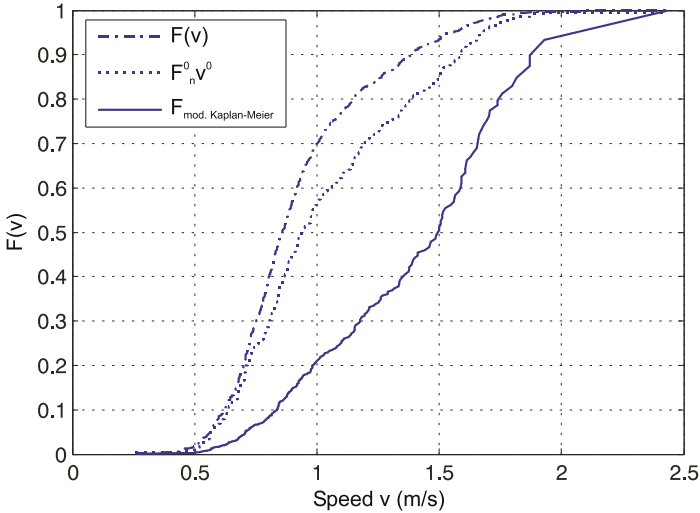
Figure 4: Estimation results for the narrow bottleneck

	Variable		Units	Value
Headways	Nr. of observations	n	-	1123
	Flow	q	peds/h	2281.3
	% Constrained peds	ϕ	-	80.3
	Arrival rate free peds	λ	1/s	0.57
	Exp. constr. headway	$E(\overline{x})$	s	1.18
	Var. constr. headway	$\sigma(\overline{x})$	s	0.35
Speeds	Expected speed	$E(\overline{v})$	m/s	0.93
	Speed variance	$\sigma(\overline{v})$	m/s	0.30
Free speeds	Expected free speed	$E(\overline{v}^0)$	m/s	1.42
	Free speed variance	$\sigma(\overline{v}^0)$	m/s	0.41

Table 2: Estimation results for the narrow bottleneck

5.   Free speed estimation for different flow directions

Let us now consider application of the approach for the other experiments. Table 3 shows the estimation results, also for the narrow bottleneck experiment shown in the previous section.

Experi-ments	Headways						Speeds		Freespeeds	
	n	q	ϕ	λ	$E(\overline{x})$	$\sigma(\overline{x})$	$E(\overline{v})$	$\sigma(\overline{v})$	$E(\overline{v}^0)$	$\sigma(\overline{v}^0)$
	(-)	(peds/h)	(-)	(1/s)	(s)	(s)	(m/s)	(m/s)	(m/s)	(m/s)
One-dir.	1167	638	0.17	0.26	1.31	0.47	1.49	0.18	1.54	0.19
Opposite	709	390	0.08	0.36	1.33	0.50	1.33	0.19	1.41	0.21
Crossing	532	170	0.05	0.08	1.43	0.63	1.33	0.24	1.35	0.25
Wide	1843	1627	0.41	0.58	1.19	0.44	1.22	0.29	1.43	0.32
Narrow	1123	2281	0.57	0.80	1.18	0.35	0.93	0.30	1.42	0.41

Table 3: Estimation results for different experiments

We can see that the estimated free speeds vary between the experiments, with a maximum of 1.54 m/s (unidirectional flow) and a minimum of 1.35 m/s (crossing flows). The free speeds are slightly higher than found in literature, which may be due to the fact that pedestrians voluntarily subscribed for the experiments, not including people having difficulties in walking in the population.
The estimated free speeds are significantly higher than the observed speeds, demonstrating the positive effects of the applied estimation method. This is especially the case in the two bottleneck experiments, where congestion occurred.
The variance in the free speeds also varies between the experiments. This effect is mainly caused by the occurrence of congestion, where speeds differ significantly from the speeds in more free flowing situations. Also, the experiments with opposite and crossing flows show a slightly higher variance. This is due to the higher complexity of the situation. Pedestrians do not react on pedestrians walking in the same direction, but also react on pedestrians walking in the opposite direction and pedestrians coming from the side. This will change the composition of the flow and makes adaptation of walking speed and direction more often necessary. Moreover, the time left to react is shorter due to the conflicting walking directions. Finally, walking speeds of pedestrians walking towards you or walking in from the sides are more difficult to estimate than speeds of pedestrians walking in a similar direction.

For the experiments with the opposite flows and with the crossing flows the data has been split into two: for each direction a separate data file has been created. The headways resulting from these two data sources have been combined and the final estimation

has integrated the two walking directions. However, differences might occur between the two walking directions. Therefore, Table 4 and Table 5 contain estimation results per walking direction for opposite flows and crossing flows respectively.

Experi-ments	Headways						Speeds		Free speeds	
	n	q	ϕ	λ	$E(\overline{x})$	$\sigma(\overline{x})$	$E(\overline{v})$	$\sigma(\overline{v})$	$E(\overline{v}^0)$	$\sigma(\overline{v}^0)$
	(-)	(peds/h)	(-)	(1/s)	(s)	(s)	(m/s)	(m/s)	(m/s)	(m/s)
Opposite	709	390	0.356	0.081	1.332	0.499	1.333	0.188	1.409	0.214
RightLeft	352	414	0.412	0.079	1.237	0.456	1.337	0.187	1.423	0.204
LeftRight	357	369	0.302	0.083	1.460	0.525	1.328	0.190	1.382	0.210

Table 4: Estimation results for opposite flows specified per walking direction

Experi-ments	Headways						Speeds		Free speeds	
	n	q	ϕ	λ	$E(\overline{x})$	$\sigma(\overline{x})$	$E(\overline{v})$	$\sigma(\overline{v})$	$E(\overline{v}^0)$	$\sigma(\overline{v}^0)$
	(-)	(peds/h)	(-)	(1/s)	(s)	(s)	(m/s)	(m/s)	(m/s)	(m/s)
Crossing	532	170	0.080	0.046	1.433	0.627	1.331	0.243	1.346	0.246
RightLeft	190	135	0.002	0.037	1.432	0.515	1.433	0.203	1.433	0.210
BottomUp	340	200	0.101	0.054	1.512	0.651	1.274	0.245	1.293	0.249

Table 5: Estimation results for crossing flows specified per walking direction

In both cases we see that the free speeds for the two flows differ: 3% in case of the opposite flows and nearly 10% for the crossing flows. This can be explained by the complexity of the situation: crossing flows always interact, while in opposite flows the lanes are formed by people walking mainly next to each other instead of 'through' each other. In both experiments, the leading (first present) flow was from right to left and in both experiments, this flow has the highest free speeds. Also, the variance in free speeds is lowest for this dominant flow.

6.   Conclusions

In this paper a new (unified) approach is applied to estimate free speed distributions for pedestrian traffic. This approach is based on the method of censored observations, which proves to be significantly more accurate than other existent methods, such as esti-mation of the free speed by considering the speed at low volumes, extrapolation towards low intensities, and application of simulation models.

Free speed distributions have been estimated on data derived from laboratory expe-riments, in which unidirectional flows, opposite flows, and crossing flows have been

simulated. Free speeds were highest for the unidirectional flow without congestion. Speeds were lower in the experiments with opposite flows, and lowest for the experiment with crossing flows. This is due to the interaction between the flows: in opposite flows the self-organisation causes lane formation, where lanes along each other, but do hardly interfere. Crossing flows interfere by nature, causing pedestrians to react more often to other pedestrians. In studying the characteristics of the walking directions for the opposite and the crossing flows, it appears that one walking direction is dominant, while the other direction adapts its speed. **«**

References

1.   D. Helbing: *A Fluid Dynamic Model for the Movement of Pedestrians*, Complex Systems 6, pp. 391-415 (1992).

2.   S.P. Hoogendoorn and P.H.L. Bovy: *Gas-kinetic Modelling and Simulation of Pedestrian Flows*, Transportation Research Record 1710, pp. 28-36 (2000).

3.   U. Weidmann: *Transporttechnik der Fußgänger*, Report Schriftenreihe Ivt-Berichte 90, ETH Zürich, (in German) (1993).

4.   J.J. Fruin: *Pedestrian Planning and Design*, Metropolitan association of urban designers and environmental planners, New York (1971).

5.   CROW, ASVV: *Recommendations for Traffic Provisions in Built-up Areas*, Report 15, CROW (1998).

6.   P.N. Daly, F. McGrath, and T.J. Annesley: *Pedestrian Speed/Flow Relationships for Underground Stations*, Traffic Engineering and Control 32 (2), pp.75–78 (1991).

7.   FHWA, *Manual on Uniform Traffic Control Devices*, US Department of Transportation (1988).

8.   B.D. Hankin and R.A. Wright: *Passenger Flow in Subways*, Operational Research Quarterly 9 (2), pp. 81–88 (1958).

9.   L.F. Henderson: *The Statistics of Crowd Fluids*, Nature 229, pp. 381–383 (1971).

10.   L.A. Hoel, *Pedestrian Travel Rates in Central Business Districts*, Traffic Engineering 38, pp. 10–13 (1968).

11.   Institute of Transportation Engineers, *Transportation and Traffic Engineering Handbook*, Prentice Hall Inc., New Jersey (1969).

12.   H. Knoflacher: *Fußgeher und Fahrradverkehr: Planungsprinzipien*, Böhlau Verlag, Vienna, (in German) (1995).

13.   P.M. Koushki: *Walking Characteristics in Central Riyadh*, Saudi Arabia, Journal of Transportation Engineering 114 (6), pp. 735–744 (1988).

14.   H.K. Lam, J.F. Morrall, and H. Ho: *Pedestrian flow characteristics in Hong Kong*, Transportation Research Record 1487, pp. 56–62 (1995).

15.   J.F. Morrall, L.L. Ratnayake, and P.N. Seneviratne: *Comparison of Central Business District Pedestrian Characteristics in Canada and Sri Lanka*, Transportation Research Record 1294, pp. 57–61 (1991).

16.   F.P.D. Navin and R.J. Wheeler: *Pedestrian Flow Characteristics*, Traffic Engineering 39, pp. 30–36 (1969).

17.   C.A. O'Flaherty and M.H. Parkinson: *Movement on a City Centre Footway*, Traffic Engineering and Control 13, pp. 434–438 (1972).

18.   S.J. Older: *Movement of Pedestrians on Footways in Shopping Streets*, Traffic Engineering and Control 10 (4), pp. 160–163 (1968).

19.   J. Pauls: *Calculating Evacuation Times for tall Buildings*, Fire Safety Journal 12, pp. 213–236 (1987).

20.   M. Roddin: *A Manual to Determine Benefits of Separating Pedestrians and Vehicles*, Report 240, Transportation Research Board (1981).

21.   A.K. Sarkar and K.S.V.S. Janardhan: *A Study on Pedestrian Flow Characteristics*, In: Cd-rom with Proceedings, Transportation Research Board, Washington (1997).

22.   R.B. Sleight: *The Pedestrian: Human Factors in Highway Traffic Safety Research*, Wiley-Interscience (1972).

23.   Y. Tanariboon, S.S. Hwa, and C.H. Chor: *Pedestrian Characteristics Study in Singapore*, Journal of Transportation Engineering, ASCE 112(3), pp. 229–235 (1986).

24.   Y. Tanariboon and J.A. Guyano: *Analysis of Pedestrian Movements in Bangkok*, Transportation Research Record 1294, pp. 52–56 (1991).

25.   P.R. Tregenza: *The Design of Interior Circulation,* Van Nostrand Reinhold Company, New York (1976).

26.   M.R. Virkler and S. Elayadath: *Pedestrian Speed-flow-Density Relationships*, Transportation Research Record 1438, pp. 51–58 (1994).

27.   S.B. Young: *Evaluation of Pedestrian Walking Speeds in Airport Terminals*, Transportation Research Record 1674, pp. 20–26 (1999).

28.   W. Daamen: *Modelling Passenger Flows in Public Transport Facilities*, PhD Thesis, Delft University of Technology, Delft (2004).

29.   W. Daamen and S.P. Hoogendoorn: *Experimental Research of Pedestrian Walking Behaviour*, Transportation Research Record 1828, pp. 20-30 (2003).

30.   S.P. Hoogendoorn and W. Daamen: *Extracting Microscopic Pedestrian Characteristics from Video Data*, In Cdrom with Proceedings, Transportation Research Board, Washington (2002).

31.   H. Botma: *The Free Speed Distribution of Drivers: Estimation Approaches*, In: P. Bovy (Ed.), Five years 'Crossroads of theory and practice', Delft University Press, Delft, pp. 1-22 (1999).

32.   Highway Research Board, *Highway Capacity Manual 2000*, Special Report (2000).

33.   C.J. Hoban: *Overtaking Lanes on two-lane Rural Highways*, PhD thesis, Monash University (1980).

34.   S. Erlander: *A Mathematical Model for Traffic on a two-lane Road with some Empirical Results*, Transportation Research 5, pp. 149-175 (1971).

35.   S.P. Hoogendoorn: *Unified Approach to Estimating Free Speed Distributions*, Transportation Research Part B 39, pp. 709-727 (2005).
36.   W. Nelson: *Applied Life Time Analysis*, Wiley, New York (1982).
37.   D. Buckley: *A Semi-Poisson Model of Traffic Flow*, Transportation Science 2 (2), pp. 107-132 (1968).
38.   P. Wasielewski: *Car-Following Headways on Freeways Interpreted by the Semi-Poisson Headway Distribution Model*, Transportation Science 13 (1978).
39.   E. Kaplan and P. Meier: *Non-Parametric Estimation for Incomplete Observations*, Journal of the American Statistical Association 53, pp. 457-481 (1958).
40.   S.P. Hoogendoorn and W. Daamen: *Pedestrian Behaviour at Bottlenecks*, Transportation Science 39 (2), pp. 147-159 (2005).

Collecting Pedestrian Trajectory Data In Real-time

J. Kerridge[1], S. Keller[2], T. Chamberlain[1], and Neil Sumpter[3]

The ability to collect pedestrian flow data, without the need for subsequent post-processing and analysis to extract measurements such as density and flow rate is a goal, which up to now, has proved infeasible on a large scale for a number of reasons, such as the cost of processing the data, the ability of the people observing the scene or subsequent video tapes and the effects of variation in the lighting conditions of the area being observed. A system using low cost infrared sensors is described that can be used to track the movement of pedestrians within their field of view and the resulting data stream is then used to generate density, flow-rate and speed data and instantaneous counts every two seconds. This data is displayed and also saved in a file. In addition, the path taken by each pedestrian can also be written to file for post-processing. The processing system associated with the sensors has been designed to be scalable from the outset and we describe how this been achieved to ensure that the it can be used in a variety of application environments.

1. Introduction and Motivation

The analysis of pedestrian movement is hampered by the difficulty of obtaining accurate data in a timely and cost effective manner that does not perturb the area being observed. A number of approaches are available to analysts but these all have their limitations. The most common techniques involve the use of a number of human observers counting the pedestrians and observing an area with a video camera and then analyzing the resulting videotapes in the laboratory. Both techniques are expensive because the former uses a lot of people to observe the space and the latter because it takes a long time to analyse videotape, typically one hour of tape requires one week of analysis. Both techniques are prone to human error because observers cannot be expected to accurately record movements in a complex area and analyzing videotape is tiring, especially when the same piece of video tape is reviewed several times to obtain all the information from it. In both cases, the resulting data has to be transformed into some form of computer readable format to obtain the required analyses, which in itself is error prone.

The research presented in this paper builds on previously reported work (1), which demonstrated it was possible to construct a system based upon low-cost infrared sensors (2) (provided by the UK manufacturer IRISYS Ltd (3)) to track the movement of pedestrians in a corridor. This used a linear array of three sensors with adjacent edges of their fields of view touching each other. Since this previous work was reported, the authors have switched over to using the manufacturer's higher frame-rate that is obtainable from the sensor. This has given an effective 10-times increase in performance compared with previous work, moving from 3 frames-per-second (fps) to over 30fps. This means we can extract pedestrian trajectories more accurately, and has enabled us to overcome many of the problems we previously had with detecting pedestrians at the edge of the field of view of the sensor. The output from the sensor is provided on

a serial data stream containing one or more distinct types of data. In particular, for the purposes of this research it has been modified by the manufacturer to output the [x, y] location of each pedestrian in the field of view of the sensor. The developed system permits processing of this stream of target locations to extract density, flow-rate, speeds and counts of the number of people entering and exiting from each edge of the observed area at a sample rate set by the user. In the experiments reported in this paper the under-lying data is sampled every 2 seconds. The output from the system is in the form of a display showing the trajectories of every pedestrian in the observed area together with a display showing the derived statistics. Data is also saved to files thereby enabling more sophisticated subsequent analysis. The main advantage of this approach is that the base data is collected directly from the sensors and can be stored immediately in a form that allows analysis of the data, hence the claim that the data is available in real-time and without any intervention from a human operator or technician. Once the data has been saved at a small granularity it is then relatively easy to transform the data into other time scales such as 1 or 5 minute series. In addition to the statistics that are saved in files the system also stores the entire base data derived from the sensors and also the tracks of each pedestrian as they traverse the observed area. This will permit detailed analysis of the trajectories taken by all pedestrians as they move through the observed space. This will give not only edge counts but also the distribution over time of where people enter the observed space and subsequently exit from it. Hence changes in movement patterns in the space can be determined as a function of time of day.

2.   Background

Hoogendoorn (4) describes a method of tracking pedestrians using visible spectrum camera technology but comments that the initial detection of the pedestrian is difficult. There are many models (see (5) for the more commonly used models) that assume know-ledge of pedestrian movement data, such as walking speed, but have not undertaken any real study of the distribution of such parameters. PEDFLOW (6) is a notable exception in that it has collected data from several locations for many different scenarios. The data was collected using video cameras and analyzed by technicians. The resulting parame-ter distributions give values for factors such as walking speed, inter-person space and distance at which people modify their trajectory to miss an obstruction either static or moving (another person). It also analysed the effect of people walking in various sizes of group because it had been observed that groups radically affect the general movement. The limitation of the PEDFLOW approach is that the analysis technique requires the pedestrians' head and feet to be observable at all times (7). In crowded situations this is not always possible. There are a number of different approaches to measuring Levels of Service, the most common of which are Fruin (8), Hankin and Wright(9), Predte-chenskii and Milinski (10) most of which report studies undertaken more than 30 years ago. In general these studies were looking to define flow rate / density relationships for people moving in the same direction. There is a paucity of data pertaining to the more normal, non-commuter, flows where people move in several directions resulting

in counter-flows, rather than moving in the same direction or where lanes form and are maintained for some time. Landis (11) proposes a different way of evaluating pedestrian level of service by taking into account the effect of sidewalk width, volume and speed of traffic, number of driveways, presence of parked cars and other similar factors thereby developing a proxy for pedestrian level of service that does not require the measurement of detailed pedestrian movements

Thompson (12) suggests that data needs to be collected for a variety of situations, specifically to provide base microscopic movement data for evacuation models; however, the same type of microscopic data is also required for more typical use of a pedestrian space. We suggest that the technology developed as part of this research could be used to obtain such data for a variety of different situations both for normal and evacuation situations, as well as for analyzing existing situations.

The rest of the paper is organized as follows: in the next section we briefly describe the operating parameters of the sensor and the data it produces. The following section then describes the data processing system and how it was designed to scale to a wide variety of sizes and types of pedestrian spaces. We then describe a series of experiments used to evaluate the operation of a single sensor and finally draw some conclusions and identify the further work required to build a system capable of observing a larger space.

3.   Operation of Sensor

The sensor comprises a 16x16 array of pyroelectric ceramic detectors (2) to measure changes in temperature. Most infrared imaging systems measure absolute temperature, or use an internal chopper to measure the temperature difference between the scene and a known reference; this adds complexity to a pyroelectric detector. The detectors we have been using only measure temperature differences, and rely on the pedestrian to be both moving and also being at a different temperature from the background. This has the disadvantage that a few pedestrians are difficult to discriminate because their temperature is close to ambient (ideally a difference of at least 2 degrees Celsius is required). However, it does have the advantage that the background disappears from the image, leaving pedestrians as clear targets (13). The sensor contains an integrated digital signal processor that fits an ellipse to the pedestrians in the field of view of the sensor, and tracks robustly the motion characteristics of the pedestrian over time. The center of the tracked ellipse is then returned as a floating-point number in the range 0.0 to 16.0, thereby locating the pedestrian or target, with sub-pixel accuracy. In normal operation the sensor is mounted vertically at around 3 metres above the space to be observed and covers a space between 3 and 4 meters square. The manufacturer provides variants with alternate sensor optics that enable counters to be mounted at up to 10 metres above ground. In normal operation the manufacturer's product is set-up to count the number of people crossing user defined datum lines. For set-up purposes, a grey-scale representation of the thermal data is passed across the serial connection, in order to assist the placement of these datum lines. For the purposes of this research, the manufacturer has provided detectors that have been configured to output just the target pedestrian locati-

ons, in order to reduce the serial data being passed along the connection.

The detector outputs serial data, with no flow control, equivalent to a frame rate of 30 frames per second. If there are more than 10 people in the area being observed then the serial data link is unable to maintain the data rate required. In this case the sensor omits a frame of data as required to ensure that a complete frame is transferred, once any part of it has been transmitted. The processing system reading the data stream only receives complete packets of data with a variable size time gap between each frame.

4.   Data Processing System

The data processing system is subdivided into three basic components connected by an Ethernet. This design philosophy has been adopted so that we can build an inherently scalable system that can process the data from any number of sensors. In addition, a further component can be added to record video images that can be used to determine the effectiveness of the sensor system in extracting data from complex scenes. In normal operation this video collection system need not be used. Figure 1 shows the basic structure of the system.
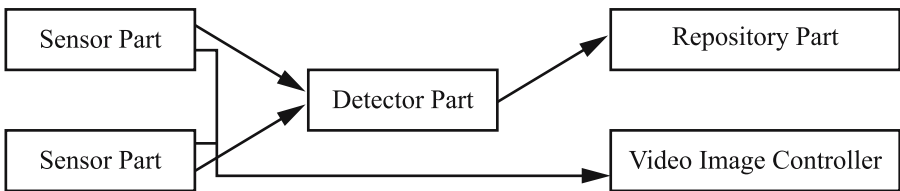
Figure 1: Processing System Structure

The processing system has been designed to be scalable from the outset by employing parallel processing techniques. Each of the components shown in Figure 1 can be executed on a separate processor connected by means of an Ethernet. Each Sensor Part is capable of processing the data stream from one or more sensors up to a limit of four sensors depending upon the number of people that are likely to be observed by each sensor. The system is written in Java to enable easy portability to a large number of platforms and the management of the parallelism is achieved using a package JCSPNet(14) that utilizes Hoare's Communicating Sequential Process concepts (15). A detailed description of the operation of the Sensor Part of the system can be found in (16). The JCSPNet package allows processes to communicate with each other in a secure manner regardless of the particular location of the processes be they on one or more processes. The communication is handled transparently.

4.1.   Sensor Processing

A Sensor Process comprises a set of process that inputs a serial data stream from a sensor and outputs Data Frames containing information about each pedestrian that has been

identified within the field of view of the sensor. A stream of serial data bytes is received from the sensor as soon as it has analysed a frame of data. The sensor processor inputs this data stream and extracts data values. A Data Frame is created that contains data about each person in the field of view of the sensor. The data comprises an identifier for each target, its X and Y co-ordinates and a status value. The sensor process is also able to determine if no person is currently in the field of view. This can be used to control the collection of any video images that may be being collected for validation puposes.

Experiments (16) have shown that a 1Ghz Pentium 3 processor with 256 Mbytes of memory can handle up to four sensors with sufficient spare capacity to not cause any processing problems.

4.2. Detector Process

There is one Detector Process for each sensor in the system, and the components of a Detector Process are shown within the dashed line of Figure 2. Data Frames from the corresponding Sensor Process are received by the Process Target Data (PTD) process, which carries out the majority of the processing of pedestrian data within the system.

The primary data structure within the processing system is called a Person Block. A Person Block is used to record the complete trajectory taken by an individual person as they move through the observed space. In particular, as a person moves from the field of view of one sensor to an adjacent one, the trajectory data held in a Person Block is passed from one PTD to another. The bi-directional arrows labeled with 'Person Blocks' in Figure 2 show this data transfer. When a person leaves an observed space the complete trajectory taken, contained in the Person Block, is written to file. This data can then be processed subsequently to obtain more detailed information about movements within the space. The mechanism used to transfer pedestrian data between adjacent sensors to build up a complete trajectory was described in (1).

The PTD process also outputs data that can be used to construct a display of the trajectory taken by a person through the space observed by the sensor(s). The trajectory path is formed by connecting successive [x, y] co-ordinates. When a person leaves a sensor's field of view the trajectory is removed from the display.

The other process shown within the Detector Process, SC, Statistics Collector undertakes the capture of statistical data from the PTD process, which is then manipulated and communicated to further processes that display and save the statistical data for further analysis. The SC process collects data from the PTD process at a fixed interval, say every 2 seconds, which provides a snapshot of activity within the sensor.

4.3. Target Data Processing

The PTD process receives Data Frames from the sensor to which it is directly connected, allocates a timestamp and then extracts data concerning all the targets (pedestrians) currently in the field of view. Each target is allocated its own Target Identifier by the sensor, which remains the same while the sensor is tracking that target. As soon as the
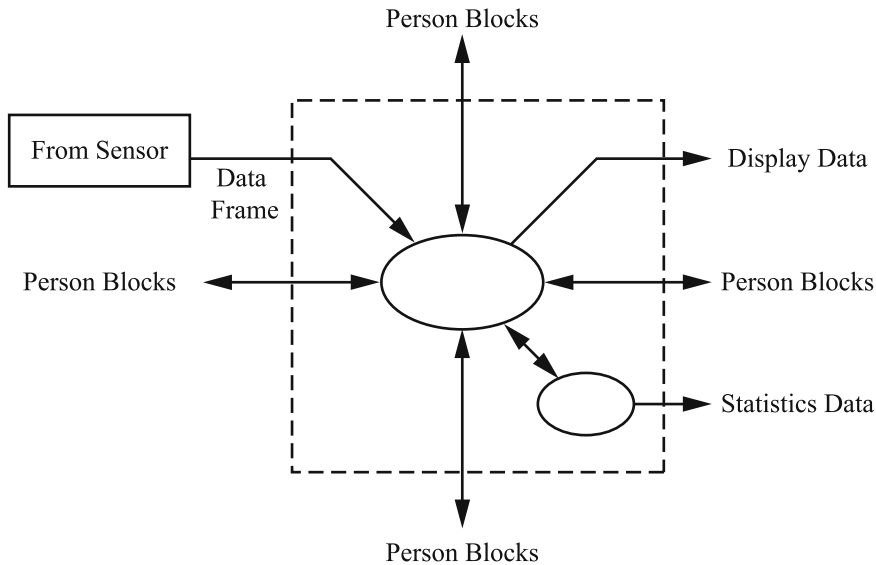
Figure 2: Detector Process Structure

target leaves the field of view of the sensor does not reuse the identifier again until either the sensor is switched off or it has looped through the full range of values (32767). Adjacent sensors will allocate a different Target Id to the same Person as they move from one sensor to another. A mechanism to match targets as they cross sensor boundaries (see (1)) is required. Hence we need to create a unique Person Identifier (PID), which remains with the person as they move through the observed area. The PID is created when a new person arrives at the edge of the observed area.

PTD extracts the data for each target from the Data Frame and uses this to update the trajectory maintained within the Person Block for this pedestrian. The same data is used to update the Display. The PTD process also calculates the total distance traveled by the person both within this sensor's field of view and within the whole observed space. A simple application of Pythagoras' theorem enables the distance traveled between the current and previous position of this person. Similarly, the time spent both in this sensor's field of view and overall is also maintained as this allows the calculation of various speeds, both overall and within the current sensor.

Figure 3 shows a human readable version of the person block showing the movement of a person's path through the experimental area discussed later in the Experimental Evaluation section (highlighted in Figure 5). The person entered the area by the bottom edge at [7.00, 0.00] at time 1088420712917, derived from the computer's system clock. The person then moved diagonally towards the doorway and left the area at location [15.33, 7.95] at time 1088420714840. The distance traveled is 2.3m in 1.923 seconds.

PersonID:	Detector	Edge	Number			
	0	2	0			
	Detector	X	Y	Time (ms)		
EntryPoint:	0	7.00	0.00	1088420712917		
Exit Point	0	15.33	7.95	1088420714840		
	Total	Local				
Distance (m)	2.30	2.30				Elapsed
Time (sec)	1.92	1.92				Time
Target	Detector	Mode	X	Y		msecs
158	0	259	7.00	0.00		0
...						
158	0	261	7.09	0.12		161
...						
158	0	261	11.07	3.10		1142
158	0	261	11.91	3.92		1272
…						
158	0	261	14.48	7.21		1793
...						
158	0	261	15.33	7.95		1923

Figure 3: A Person Block Showing the Trajectory Taken by a Person Moving to the East Edge from Bottom Edge of the Area Shown in Figure 5

4.4. Statistics Collection

The SC process requests data from PTD, which responds with some basic data from which the required statistics can be calculated. The rate at which data is obtained from the PTD is user determined. PTD maintains a count of the number of people that have entered or exited each edge of the sensor's field of view during the last data collection period. The number of people currently in the field of view is also returned. In addition, for each person, the local and total times and distances traveled by that person are returned.

Fundamental measurements concerning the length and width of the sensor's field of view are required parameters of the SC process. These values are required to calculate the density, speeds and flow rates. The summary statistics, together with the counts of people entering and exiting each edge of the sensor are then output as the Statistics Data.

Time secs	People	(LoS) Density p/m2	Mean Speed m/sec	Max Speed m/sec	Min Speed m/sec	Flow p/m/m	Output Counts				Input Counts			
							N	E	S	W	N	E	S	W
34	3	0.40	0.29	0.50	0.14	6.93	0	0	0	0	2	0	1	0
36	5	0.67	0.35	0.52	0.26	14.12	0	0	0	0	1	0	1	0
38	4	0.53	0.39	0.44	0.34	12.45	0	2	0	0	0	0	1	0
40	2	0.27	0.38	0.43	0.34	6.16	0	2	0	0	0	0	0	0
42	0	0.00	NaN	0.00	0.00	NaN	0	2	0	0	0	0	0	0

Figure 4: Formatted Statistical Output During Pedestrian Movement Shown in Figure 5

(Fruin LoS (p/m2) 0.31 <= B < 0.43; 0.43 <= C < 0.72; 0.72 <= D < 1.08; 1.08 <= E < 2.17)

The data is output in a format that can be easily manipulated by spreadsheet and database programs. An example is shown in Figure 4, which shows that the relative time interval between data collections is also saved. Depending upon the form required this low-level 2-second data could be summed to provide 1 and 5 minute counts. However the basic data has been collected at a much finer granularity, enabling more sophisticated analysis, such as exploring platoon effects as people are released at a signal controlled cross walk.

In Figure 4 we see that part of the statistical output pertaining to the movement of 3 people from the top edge of the observed area and a further 3 people from the bottom edge and all are moving towards the east edge (see Figure 5). The data is gathered every two seconds as can be observed in the Time column. The People column gives the number of people in the field of view at the end of the two-second period. The count columns show the number of people entering and leaving on each edge during each two-second period. As can be seen each of the entrants from the bottom edge (South) entered during a different two-second period, whereas those entering from the top (North) edge did so in two such periods. They exited two at a time during three consecutive two-second periods on the East edge.

4.5. Repository

The Repository Part (see Figure 1) is ideally located on a separate processor and saves all the data that is written to file. It also is used for the display process.

5.   Evaluation

5.1. Controlled Environment

A controlled experimental evaluation was undertaken in corridor 3.25m wide, with a 1.4m wide doorway to the eastern edge. One sensor was mounted 3.0m above the ground on the centerline of the doorway. The sensor observed 0.3m into the doorway. People were asked to undertake specific movements within this area. The doorway is the entrance to a café and thus during the experimental period other pedestrians were walking through the area. Initial experiments suggest that in conflicted flow the sensor was able to distinguish the movement of up to 8 people within the observed area, but that this became progressively less accurate as the number of people increased. The effective area of the space is 6.75m², which takes into account the shy away distance from the wall with the doorway but not the effect of the doorway width. This equates to a Fruin Level of Service just into LoS E and for 6 people to LoS D. During the experiment only LoS C was observed (see Figure 4). This suggests that the sensor is suited to observing areas of a more open nature rather than for those of very high commuter activity as occurs in LoS F areas.

Figure 5 shows a screen shot during the movements described previously. The trajectories of five of the six people can be seen. The elapsed time since the start of the experiment is shown above the display used to indicate the number of people entering and exiting from each edge of the sensor. The grayed area to the left of the numeric data shows the density, mean, max and min speeds and the flow rate, which can be seen in the context of the previous periods in Figure 4 where the equivalent row has been highlighted. The background color for the density value changes depending upon the equivalent LoS, as indicated in Figure 5.

In these experiments the sensor, detector and repository parts were all running on a single processor running Windows XP, at 1.6GHz with 256Mbytes memory. The video images were recorded on a separate machine running Windows XP at 4GHz with 512Mbytes memory. The experiments overall took some fifteen minutes to undertake. During this time the files sizes amounted to 591Kbytes for the trajectory information but this was in human readable format rather than in binary. The statistics data amounted to 8.47 Kbytes. Thus the amount of data recorded is minute compared to the file storage available on modern computer systems. A USB camera was used to collect the video images and the resultant file was 8.1Mbytes. The processor was running at about 85% during the data collection, however, this could be improved with hardware specific coding.

5.2. Open Environment

The system was set up in an open area as part of a poster presentation of this work[17]. A total of 1386 people entered and exited the survey area, shown in Figure 6, of which about 10% were probably going to the rest rooms but some of those will be people who
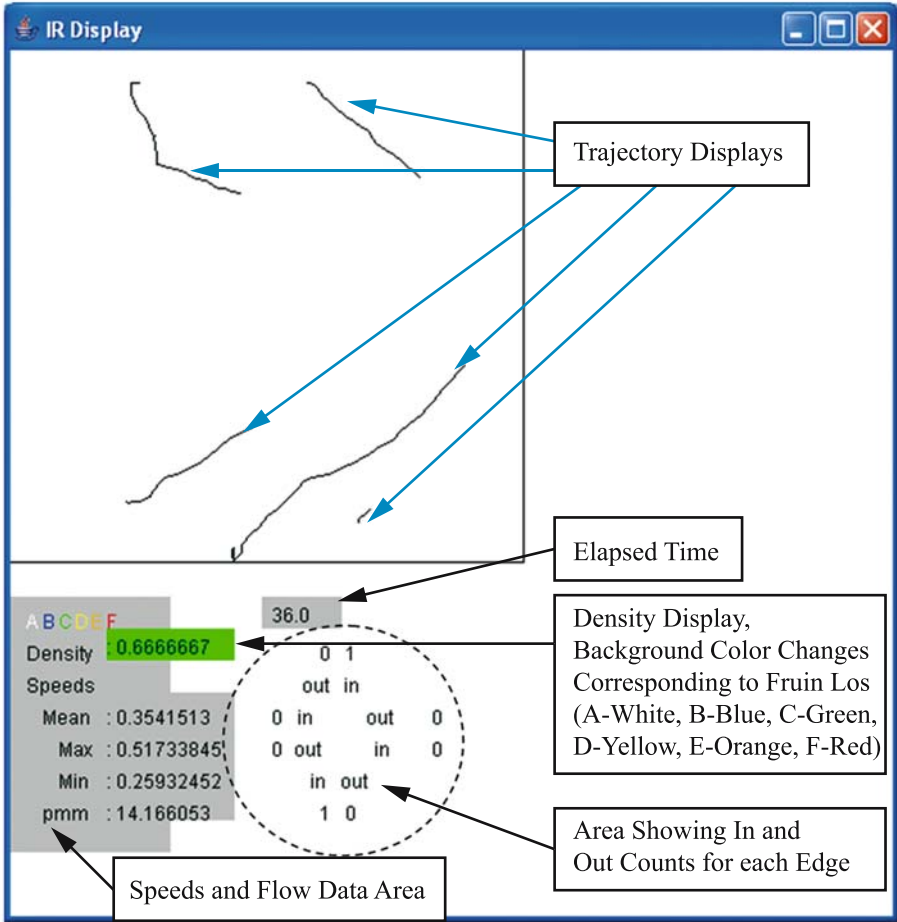
Figure 5: Shot During the Movement of Six People Towards Eastern Edge

were forced to go round the people that congregated to watch the trajectories as they were displayed in real time on the laptop. Most of the time there were people standing in the irregualr area indicated and thus they also caused an obstruction. The data was collected over 2.75 hours. The mean speed of people through the area was 0.75m/sec. When people were in the survey area the flow rate was 4.89 people/m/m (low). The mean density, when people were in the survey area was 0.11 people/m^2, again very low but people tended to arrive round a pillar (dark circle) in ones or twos. The maximum number of people observed at one time was 4, equivalent to a density of 0.35 people/m2. This happened during 6 of the 4900 2-second periods used during the survey (there were more than 3400 such 2-second periods with no people and 1120 with 1 person). We can

also see that the majority of people arrived from the entrance around the pillar. The figures will be distorted as a number of people "dallied and played" in the survey area so their friends could observe unnatural trajectories.
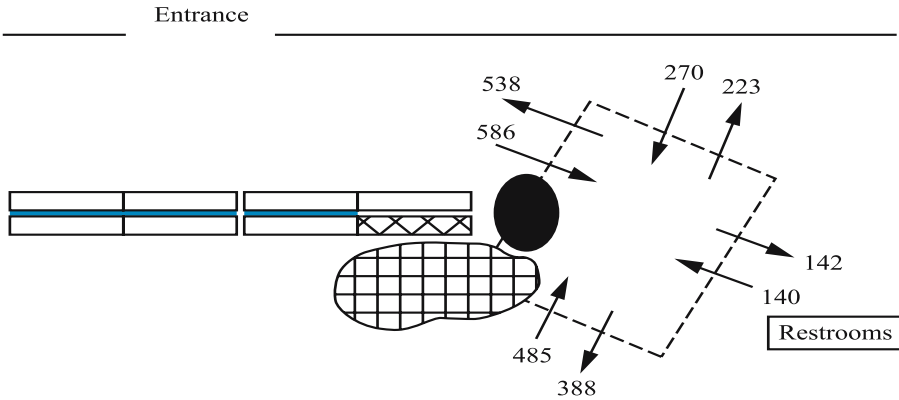
Figure 6: Layout of a Poster Presentation of System

6.   Conclusions and Further Work

The techniques described in this paper have demonstrated that it is possible, using low-cost infrared sensors, to collect individual pedestrian's trajectories through an observed space. In addition to collecting the trajectory it is also possible to calculate, display and save parameters such as density, flow, speeds and entry and exit edge counts at as fine granularity as is likely to be required. In the experiments reported here we used two-second granularity. The trajectories are stored in a form that permits further analysis without additional processing to determine the location of the pedestrians in the space. More importantly, the processing can be undertaken using commodity-processing components. The system is however limited to spaces that have ceilings or that have street furniture, such as lighting poles, to which the sensors can be attached.

The next phase of research will be to integrate a number of sensors monitoring a larger space and to investigate the use of embedded systems for the sensor part and the use of wireless connections between the sensor parts and the detector part to permit easier installation of the system in a real environment. This will mean that it will be possible to monitor pedestrian movements in shopping malls, transport concourses at rail stations and airports. **«**

References

1. J. Kerridge, A. Armitage, D. Binnie, L. Lei, and N. Sumpter: *Monitoring the Movement of Pedestrians Using Low-Cost Infrared Detectors: Initial Findings*, Transportation Research Record, pp. 11-18 (2004).
2. M.V. Mansi, S.G. Porter, J.L. Galloway, and N. Sumpter N: *Very Low Cost Infrared Array Based Detection and Imaging Systems* (SPIE) Aerosense 2001, Orlando, Florida USA, pp. 17-19 (2001).
3. Irisys Ltd, http://www.irisys.co.uk the web site describing current sensors and giving data sheets, accessed on 22/6/2004.
4. S.P. Hoogendoorn, W. Daamen, and P.H.L. Bovy: *Extracting Microscopic Pedestrian Characteristics from Video Data*, Transportation Research Board 2003 Annual Meeting, CD-ROM, Paper No 477, National Academies, Washington USA (2003).
5. E.R. Galea (Ed): *Proceedings of the International Conference on Pedestrian and Evacuation Dynamics*, CMS Press, University of Greenwich, London (2003).
6. A. Willis, N. Gjersoe, C. Harvard, J. Kerridge, and R. Kukla: *Human Movement Behaviour in Urban Spaces: Implications for the Design and Modelling of Effective Pedestrian Environments*, Environment & Planning B, in press (2004).
7. A. Willis, R. Kukla, J. Kerridge, and J. Hine: *Laying the foundations: The Use of Video Footage to Explore Pedestrian Dynamics in PEDFLOW*, In: Proceedings of the International Conference on Pedestrian and Evacuation Dynamics, M. Schreckenberg et al (Eds), Springer, Berlin, pp. 181-186 (2001).
8. J.J. Fruin: *Pedestrian Planning and Design*, Metropolitan Association of Urban Designers and Environmental Planners, New York (1971).
9. B.D. Hankin and R.A. Wright: *Passenger Flows in Subways*, Operational research Quarterly, Vol 9, pp. 81-88 (1958).
10. V.M. Predtechenskii and A.I. Milinskii: *Planning for Foot Traffic Flow in Buildings*, Amerind Publishing Co, New Delhi, India (1969).
11. B.W. Landis et al: *Modeling the Roadside Walking Environment Pedestrian Level of Service*, Transportation Research Record 1773, pp. 82 – 88.
12. P. Thompson: Simulex: *Simulated People Have Needs Too*, available at http://www.iesve.com/downloads/simulexdata.pdf accessed on 12/7/2004.
13. A. Armitage, T.D. Binnie, J. Kerridge, and L. Lei: *Measuring Pedestrian Trajectories with Low Cost Infrared Detectors: Preliminary Results*, In: Proceedings of the International Conference on Pedestrian and Evacuation Dynamics, E.R. Galea (Ed), CMS Press, University of Greenwich, London (2003).
14. Quickstone Ltd, JCSPNet documentation, http://www.quickstone.com/xcsp/jcsp-networkedition/ , accessed on 12/9/2004.
15. C.A.R. Hoare, *Communicating Sequential Processes*, Prentice-Hall 1985, available from http://www.usingcsp.com/cspbook.pdf accessed on 12/9/2004.

16. S. Clayton and J. Kerridge: *Active Serial Port: A Component for JCSPNet Embedded Systems*, to appear in Communicating Process Architectures 2004, I. East, J. Martin, P. Welch, D. Duce, and M. Green (Eds.), IOS Press (2004).

17. J. Kerridge, S. Keller, and N. Sumpter: *Collecting, Processing and Calculating Pedestrian Flow Data in Real-Time*, Transportation Research Board Annual Meeting, Washington, pp. 05-0191 (2005).

Full-Scale Evacuation Experiments
in a smoke filled Rail Carriage – a detailed study
of passenger behaviour under reduced visibility

M. Oswald[1], C. Lebeda[1], U. Schneider[1], and H. Kirchberger[1]

The paper investigates the evacuation of passengers from commuter trains with a focus on reduced visibility due to smoke. Fire situations in trains, where smoke can obscure the vision and have a debilitating effect on the passengers and the close geometry of the compartment allows the occupants almost no space to move away from the hazard area, require the incorporation of efficient mechanisms to assist in a rapid egress. Due to those risks two full-scale evacuation experiments were conducted in a newly released commuter train presently used by the Austrian Federal Railways, in which participants were partially subjected to non-toxic smoke. The findings of the trials have highlighted a number of issues as for example possible design revisions, improvements of the signage system and modifications of the acoustic announcement system.

1. Introduction

A successful evacuation requiring the rapid egress of passengers from a train is dependent on a variety of conditions. The main influencing parameters are:

» vehicle design (e. g. arrangement of the seats, different floor levels, elevation above ground, width and number of doors)
» crew procedures (e. g. approach to the evacuation, passenger information)
» human behaviour (e. g. attitude of the passengers, willingness to support other passengers)
» condition of the train (e. g. overturned and/or smoke filled carriage)
» location of the train stop (e. g. in a station, in a tunnel, someplace on the track)

Under severe conditions, e. g. fire/smoke, the circumstances of the evacuation will be further aggravated through the loss of visibility and the development of unendurable environmental conditions (e. g. heat, toxic gases …). Thus there is an obvious physical requirement to ensure that the rail vehicle design and crew procedures are adequate to allow safe and fast egress under controlled circumstances. Furthermore the perceptions of the passengers throughout the evacuation have to be taken into account to be able to improve the measures taken in a rail carriage.

This paper investigates the evacuation of passengers from a newly released commuter train in Austria. The train used in the experiments consisted of three rail carriages with two railcars on either end of the train and one trailer vehicle in between the two railcars. The vehicle design includes a raised floor level connected by three steps with the lower

---

[1] Vienna University of Technology
Institute for Building Construction and Technology
Center of Materials and Testing, Fire Safety Science
Adolf-Blamauergasse 1-3, A 1030 Vienna

exit level of the railcars. The three compartments of the train are connected by two double leaf sliding doors, which remain open under normal conditions but are closed automatically in the case of fire.

Two full scale evacuation experiments were conducted, in which the participants of one rail carriage were subjected to non-toxic smoke. One trial involved evacuating the whole train through the doors on one side of each rail carriage. The other trial resulted in passengers evacuating from the smoke subjected carriage at one end of the train to the adjacent rail carriage. The trials were conducted under non-competitive conditions, 192 participants took part in both trials. All seats in the rail carriages were occupied; the load factor of the aisles was 1 person/m^2. The participants were briefed beforehand that they were going to participate in an evacuation exercise involving non toxic smoke. They were informed that there would be two evacuation trials and that they should take special interest in the emergency instructions provided by the train operator throughout the evacuation process.

After each trial questionnaires were handed out to the participants to gain insight into the evacuation efficiency. These questionnaires included questions about the carriage design, the crew procedures, the visibility of the signage, the audibility of announcements, cooperativeness among the passengers etc… The trials were also recorded by video for the purpose of a detailed analysis of passengers' movement and behaviour throughout the experiments.

The main outcomes of the experiments and subsequent analysis of the data are:

» Insights in possible improvements concerning the information process before and during the evacuation on behalf of the passengers.
» Aspects of human behaviour, personal perceptions of every participant, communication and cooperativeness among the participants.
» Revision of the train design on behalf of the observations and perceptions of the participants and the observers.

The evacuation experiments were conducted as part of the licensing procedure for the commuter train by the federal ministry for transport, innovation, and technology. The main task of the two trials was to analyse the influence of the raised floor level (elevated by 3 steps) and the raised passage (elevated by 1 step) within the train on the movement of passengers [1]. A second goal was to gain perceptions concerning the handling of the double leaf sliding doors between the compartments of the train. This kind of fire door, which remains open under normal conditions but is closed automatically in case of fire, was incorporated in a commuter train for the first time in Austria. The findings of the trials have highlighted a number of issues which will be examined further in the future as part of a research project which deals with fire safety in trains emphasizing fire and evacuation simulation in railway carriages.

2. Test Procedure

2.1. Description of the train

The evacuation experiments were accomplished with a commuter train of the series E-Talent type ETW, which consists of three rail carriages with two railcars on either end of the train and one trailer vehicle in between the two railcars (see figure 1):

1. carriage type T1: railcar 1
2. carriage type M1: trailer vehicle
3. carriage type T2: railcar 2
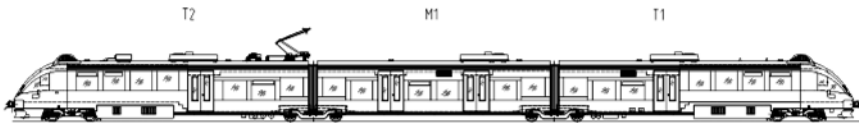
Figure 1: Commuter train of the series E-Talent type ETW [2]

The commuter train type ETW is designed for the transport of 233 passengers, of which 151 passengers are seated and 82 persons are standing. This represents a load factor of 100 %. The train is approximately 52 m long and 2.9 m wide and has 8 exit doors, of which 4 doors are located on each side of the carriages. The exit doors are double leaf swivelling-sliding doors of the dimensions 1.3 m by 2.0 m.

In each exit area near the doors an illuminated passenger information display is located underneath the ceiling which provides up-to-date information in an emergency (see figure 2).

Figure 2: Illuminated passenger information display underneath the ceiling situated in the exit area of each door

For the case of fire, smoke detectors are installed in the venting system and in the passenger compartments. As soon as a fire is detected by the smoke detectors, the train operator activates the „fire emergency train movement", which causes closing of the internal sliding doors and announcement of the "Fire Alarm" by voice message and by the illuminated passenger information display.

The vehicle design of the railcars (carriage type T1 and T2) includes a raised floor level connected by three steps with the lower exit level and a passage that is raised by one step from the lower exit level of the carriage. The trailer vehicle (carriage type M1) is designed with a passage that is raised by one step from the lower exit level and connects the carriage M1 with the railcars T1 and T2. The different levels of the carriages are shown in figure 3.
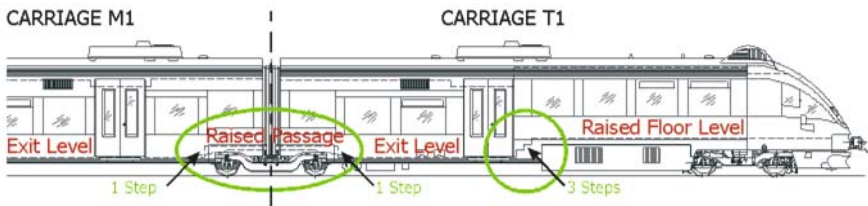
Figure 3: Level design of the commuter train type ETW

The train contains a toilet that is situated on the exit level in the carriage T1. The three compartments of the train are separated by two double leaf sliding doors, which remain open under normal conditions but are closed automatically in the case of fire. The sliding doors have dimensions of 0.7 m by 2.0 m.

2.2. Description of the environmental factors

The evacuation trials were conducted on the premises of the Austrian National Railways (ÖBB) in Vienna Floridsdorf. Throughout the experiments the train remained stationery although the experiments simulated a situation in which it would have been moving. This approach to the trials was selected for reasons of security and the participants were informed about the fact that the movement of the train was only an assumption.

For the experiments the participants had to overcome a height of about 65 cm from the exit level inside the train to the surrounding terrain. The evacuation of the carriages took place only on one side of the train. This was a conservative approach to the evacuation experiment taking into account that under certain circumstances the evacuation can only be performed on the side away from the other track (e.g. oncoming traffic on the other side of the train with non warning and the danger of evacuating passengers being run down).

For the experiments under reduced visibility a fire was supposed, which would lead to heavy smoke production and major view restriction for the evacuation. Furthermore it

was assumed that the fire could not be suppressed by the existing means of fire extinguishing. For the trials involving smoke a non-toxic chemical mist was used, that was produced by two portable smoke generators.

2.3. Description of the participants

Physical data of the participants
The participants were obtained by a personnel services' agency for temporary staffing. The physical data of the participants were determined by inquiries in questionnaires. For this purpose the following specifications were requested:

» Indication of the starting number
» Indication of the gender
» Indication of the body size
» Indication of the body weight
» Indication of the age

Gender	male [-]	94
	female [-]	97
Size	average size [m]	1.74
	maximal size [m]	1.97
	minimal size [m]	1.46
Weight	average weight [kg]	67.01
	maximal weight [kg]	136.00
	minimal weight [kg]	43.00
Age	average age [a]	25.65
	maximal age [a]	58.00
	minimal age [a]	16.00

Table 1: Physical data of the participants

A detailed summary of the values mentioned with their maximum, average and minimum is shown in table 1.
The analysis of the age data shows that the participants formed a rather young group of passengers, which is not representable for an average person distribution in a train at any

rate. Nevertheless such a person allocation can be found on morning train connections to school, university etc.

Distribution of the participants

Both experiments involved a partial occupation of the entire train. All seats were occupied and for the aisles 1 person per m² free standing surface was determined. Thus 192 persons took part in the two evacuation trials, of whom 151 passengers were seated and 41 persons were standing. This represented a load factor of 100 % for the seats and 50% for the aisles.

Each participant received a starting number, which specified where every single person was located at the beginning of the evacuation trial. Additionally the passengers in the „smoke filled" carriages (T1, T2) were equipped with different coloured caps in order to be able to identify the movement of the participants form one carriage to the other. Passengers in the carriage T1 were provided with blue caps and in the carriage T2 with red caps.

Inside the train 11 observers were placed, which were provided with signal coloured jackets and had the authority to stop the trial at any time there was risk of injury to any of the participants. In the case of non-emergency these observers where instructed not to take part or intervene actively in the evacuation process. Safety officers were also positioned externally by each exit to watch over the exit process of the carriages.

A train operator was placed in the driver's cab, which was next to the smoke filled carriage: for trial 1 the driver was seated in the driver's cab of the railcar 1; for trial 2 in the driver's cab of the railcar 2.

The participants were loaded from one side of the train, which corresponded to the evacuation side of the trials.

Due to the fact that the experiments would take place in a newly released commuter train, which was not yet it use, the participants were completely unfamiliar with the train design and layout.

Instructions for the participants

Given that the experiments involved human volunteers in a potentially dangerous environment subjected to reduced visibility by the influence of non toxic smoke, two risk assessments were carried out by the staff of the fire brigade and the safety officers.

Furthermore the participants were briefed beforehand that they were going to participate in an evacuation exercise involving non toxic smoke. They were informed that there would be two evacuation trials and that they should take special interest in the announcements given by the train operator throughout the evacuation process. All participants had to be in a good state of health and not suffer from any movement disabilities. Within the scope of a short introduction for the evacuation procedure the following information was given to the participants:

1. Thank you for your cooperation. By your participation you make an important contribution for the further improvement of the security in rail-mounted vehicles in the case of fire.
2. The „smoke" produced by the smoke generator is not health-endangering for humans.
3. Persons with claustrophobia or with troubles of the respiratory system (e.g. asthma) should not choose a place in carriage T1 or T2, where the smoke generators are situated.
4. When stepping out of the train the participants should descend carefully, they should not jump down. If necessary the participants should sit down at the exit and slip out of the train to the ground level.
5. The evacuation experiments are non-competitive; the first one out of the train doesn't win anything.
6. The train may be left only by the doors; window panes may not be broken in the course of the evacuation.
7. The necessity to operate the fire extinguishers does not exist.
8. Persons wearing yellow signal jackets or fire-brigade uniforms are contact persons for the participants.
9. In the event of any concerns (e.g. fear, distress etc.) participants are asked to sit down immediately and call one of the contact persons for attention and help.
10. In case of any difficulties, participants are given the opportunity to withdraw from the exercise at any time.
11. The signal for the beginning of the evacuation process is an appropriate announcement through the public address system given by the train operator.
12. The signal for the break off of the trial is a steady tone of the train horn and/or the sounding of a continuing whistle blast. In this case please pause and don't push forward. Please obey the instructions provided by the contact persons.
13. For the handling of the questionnaires we kindly ask for your constructive cooperation. The evaluation of the questionnaires is anonymized.

In the course of the briefing the participants asked whether the emergency door release, the intercom and the emergency brake may be operated in the context of the evacuation trial. This was affirmed.

2.4. Documentation and evaluation of the experiments

Each participant received a questionnaire, which had to be filled out and delivered following each trial. Furthermore each observer inside and outside the train had to answer a special questionnaire, which asked for observations concerning the reaction and communication of the passengers, the approach to the evacuation, the attitude of the passengers with regard to willingness to support other passengers etc.
The evacuations were recorded by internal and external cameras.

Range and uncertainties

With interrogations as in questionnaires it must be accepted that the determined values have a certain range of variations and uncertainties.
Such a range can be affected by most diverse factors. Reasons for uncertainties in the results can be:

» False answers given by the participant unconsciously affected by misinterpretation of the question.
» False answers given by the participant consciously caused by lack of interest and/or coincidental marking of answers.

Due to the high number of participants (192) one can assume that a representative result is achieved by the questionnaires.

2.5.   Description of the evacuation set up

Two full scale evacuation experiments were conducted, in which the participants of one rail carriage were subjected to non-toxic smoke. Trial 1 involved evacuating the whole train through the doors on one side of each rail carriage. Trial 2 resulted in passengers evacuating from the smoke subjected carriage T2 at one end of the train to the adjacent rail carriage M1. The trials were conducted under non-competitive conditions.
In order to simulate the reduced visibility in a train as a consequence of a fire, non-toxic smoke was generated throughout the experiment. For trial 1 two smoke generators were set up in the toilet area in the carriage T1, for trial 2 they were installed within the range of the entrance of the carriage T2. The devices of the smoke generators were set up in such a way that they caused no handicap for the evacuating participants.
The smoke production was started with the beginning of the trials, which was announced by the train operator. The production was kept steady throughout the evacuation experiment.

Setup for Trial 1 and Trial 2

In the following the planned operational sequence of trial 1 and trail 2 is described.
After all participants have taken their intended places in the train, the production of the „smoke" by operating the smoke generator starts. As soon as the smoke detectors announce the fire to the driver's cab, the train operator activates the „fire emergency train movement", which also starts the passenger information display informing the passengers about the "Fire Alarm" and asking them to "Obey the instructions of the crew".
The basic assumption for trial 1 is that the train drives at full speed at the time of the fire detection. Furthermore it is assumed that a time period of 2 minutes will be necessary before the train comes to full rest at an appropriate place and the emergency instructions for the evacuation will start. After the expiration of these 2 minutes the train operator

will inform the participants that the train has stopped and the passengers can leave the train through the doors on the right side of the train. The end of trial 1 will be reached as soon as the last person leaves the train.

The basic assumption for trial 2 is that the train drives at a certain speed in a tunnel at the time of the fire detection. Furthermore it is assumed that it takes a time period of 15 minutes before the train leaves the tunnel and comes to full rest at an appropriate place where the evacuation of the train can start. Right after the fire detection the train operator will instruct the passengers to leave the smoke filled carriages and move on to the adjacent compartment. After the expiration of the 15 minutes the emergency instructions for the evacuation will start informing the passengers to leave the train through the doors on the right side of the train. The end of trial 2 will be reached as soon as the last person leaves the train.

The train operator will leave the driver's cab after setting the necessary actions and measures according to regulations.

3. Results and Discussion

For a correct understanding of the following results one has to bear in mind that the train remained stationery throughout the experiments although the trials simulated a situation in which it would have been moving. This approach to the trials was selected for reasons of security and the participants were informed about the fact that the movement of the train was only an assumption.

3.1. Progress and observations

Trial 1

As the chronology of the evacuation trial 1 shows, the participants in carriage T1 didn't wait for the voice message of the train operator to inform them to start the evacuation of the train. As soon as the smoke production began and the announcement of the "Fire Alarm" on the passenger information display was visible, passengers, who were placed near the smoke generator, got up and tried to open door 1 by activating the emergency door release. This course of action showed that the participants had forgotten about the basic assumption of a moving train. By trying to open the door while the train was still "driving" they tried to get off the moving vehicle. One can assume that this would maybe not have happened if the train was really moving.

It was interesting to see that the passengers in carriage T1 at door 1 had difficulty in opening the door because they didn't understand the opening mechanism of the double leaf swivelling-sliding door. Because of the missing instructions how to open the door the participants took more than 30 seconds to find out how to get out of the carriage T1. Under severe conditions a time loss of 30 seconds can aggravate the evacuation process through the development of disastrous unendurable environmental conditions (e. g. heat, toxic gases …). Thus there is an obvious physical requirement to ensure that

the rail vehicle design and crew procedures are adequate to allow the safe and fast egress under controlled circumstances. Though the passengers in carriage T2 and M1 had no problems to open the doors of the train, it is obvious that improvements have to be made concerning the information given about the opening mechanism of the doors. This conclusion is further confirmed by the evaluation of the questionnaires.

On exiting the carriages the participants displayed a combination of jumping and one-big-step-climbing manoeuvres. The strategy adopted appeared to depend on the size and gender of the participants. The age may also have an important influence, but because the whole passenger group was rather young with an average age of 25 years the influence of age could not be observed.

The video documentation showed that female passengers with a smaller body height tended to use the side handrails and climbed carefully out of the carriage by taking one big step; whereas the taller male and female participants adopted the strategy to jump out of the train without the use of the side handrails.

Once the flow of people through the doors began it was interesting to watch that only one person at a time exited a door. The passengers adopted a staggered strategy to leave the train one by one in which one person left the carriage for example through the left side of the door and the next person followed closely at the right side of the door and so forth. Although the doors are 1.3 m wide almost each participant adopted this staggered strategy to leave the train. The behaviour of the participants during the trial as observed by the safety staff was described as co-operative or non-competitive.

Trial 2

The video documentation and the results of the questionnaires show that throughout the whole evacuation trial 2 the participants were uncertain about how to react to the fire in carriage T2 and how to evacuate. Some of the participants in carriage T2, who stood next to the internal sliding door, moved very fast from the smoke affected carriage T2 to the adjacent carriage M1. Other participants, who were situated in the raised floor area next to the smoke generator, remained seated for more than 7 minutes though the visibility at that time was reduced to such an extend that the passengers could not see their feet, nor could they see the person in front of them clearly. In moving through the smoke participants relied on their sense of touch, feeling the side partitions and handrails with their hands and tapping the steps of the raised floor area cautiously with their feet. The progress in the raised floor area of the smoke filled carriage T2 was slow creating a small congestion in this area. Responsible for the slow progress was that most of the participants in the raised floor area started to leave at a very late stage of the evacuation process when visibility was reduced to less than 30 cm at face level in parts of the carriage T2.

Because the participants didn't know whether all persons should evacuate to the adjacent compartment or just the passengers from the smoke filled carriage T2 to the next compartment M1, most of the participants in the smoke free carriages stayed at their places at the beginning of the trial. But as most of the participants of carriage T2 moved to the compartment M1, it became more and more crowded on the aisles and people star-

ted queuing. People at the end of carriage M1 asked other participants to move forward. Therefore after about 5 minutes a lengthwise evacuation movement started, where the participants moved slowly and in a stagnant way towards carriage T1. Progress along the centre pathway of the train was orderly but slow.

Seated participants tended to remain at their places in the smoke free carriages. Later when more and more smoke poured from carriage T2 to carriage M1, also the seated passengers of carriage M1 left their seats and started to move towards carriage T1. Delays were caused as the seated passengers filed into the queue and congestion occurred around the internal sliding door from carriage M1 to carriage T1 as only one single passenger at a time could master the door.

Although the passengers were informed that it was supposed that the train would drive at a certain speed in a tunnel and that it would take a time period of 15 minutes before the train would leave the tunnel and come to full rest at an appropriate place where the evacuation of the train could start, one of the passengers opened door 4 to let fresh air in and improve the visibility in carriage T2. This person took a leading position and warned the other passengers to keep away from the open door. This participant also asked the remaining passengers in carriage T2 to leave the compartment and to move on to carriage M1 in the 10th minute of trial 2.

3.2. Results of the Questionnaires

In the following the main outcomes of the questionnaires and subsequent analysis of the data are highlighted.

Since the investigation in this paper was concerned with evacuation experiments, which can never reflect the reality completely, first of all some fundamental differences between the trials and real fire incidents have to be stated:

1. In general an evacuation experiment can only resemble the severe conditions of a real incident. Because of the briefing the participants were better prepared for what to expect during the evacuation than passengers can ever be in actual train accidents. Human behaviour as observed in fire related evacuation conditions [8, 9] was only partially observed during the trials. The participants tended to react more calmly and their course of action was more composed than in reality.

2. The age distribution of the participants points at a clear overhang of young persons, this leads to the fact that the average age of the participants is approximately 25 years, whereby the oldest person had the age of 58 years and the youngest test participant was 16 years old. This rather young group of participants is not representable for an average person distribution in a train at any rate.

3. The rather young group of passengers leads to fast evacuation times and high flow rate capacities, which will definitely be slower respectively lower with an older group of participants considering e. g the rather high exit height of step down from the carriage onto the track level. An average person distribution in a train does not only include older persons but also mobility impaired passengers, which were also not represented in the trials.

4. Likewise it is probable that passengers, who are in an accident, suffer from crash related injuries and incident related shock. However the evacuation experiments investigated in this paper were not concerned with a train crash. It was assumed that the primary incident, which required the fast egress of the passengers, was a fire causing obscured vision and reduced visibility.

5. The smoke used in the trials did not contain fire irritant and toxic gases, it only reduced the visibility conditions. The effects of a real fire causing not only smoke but also heat, irritant and narcotic gases were not reflected in the trials. As investigated by Jin [3, 4, 5] actual fire gases would also reduce the travel speed of the passengers and cause slower evacuation times.

6. The behaviour of the participants in the trials was cooperative and non-competitive. According to investigation conducted by Muir et al [6, 7] it is likely that, had the trials been undertaken in competitive mode, the evacuation times would have been longer. As observed in the trials the participants showed a steady and controlled behaviour in the cooperative evacuations.

Taking all those factors into account one can assume that the measured evacuation times have to be longer under severe conditions of a real fire incident. Nevertheless the answers and suggestions made by the participants have highlighted a number of possible improvements for the investigated commuter train, which will be discussed in the following:

Acoustic communication systems:

»   The participants indicated in the questionnaires that they would prefer acoustic announcement to visual communication relating to the influence of visibility for the efficiency of the signage.

»   In general the participants stated that the information provided through the voice message by the train operator was clearly audible throughout the trials. But most of the participants asked for more detailed information before and during the evacuation process. Especially in the second trial, that took more than 16 minutes, the participants complained about the little information that was given to them by the train operator. They asked for more instructions and accompanying announcements concerning the status of the evacuation process and the condition of the train. This information should be conveyed to the passengers by voice message in certain temporal succession, so that no uncertainty or suspense could arise among the passengers.

Exit doors:

»   Because of the swivelling-sliding mechanism of the external doors, which have to be opened manually after the emergency release is used, some of the participants had troubles to open door 1 during trial 1. The mechanism is such that the door

has to be pushed outwards first and afterwards moved laterally. This was not recognised by the participants in carriage T1 until several attempts had been made to open it. At door 1 it took almost 30 seconds until five passengers managed in common to open the exit door. They thought they would have to pull the emergency release and open the door right at the same time. Therefore they needed at least two persons to open the swivelling-sliding doors.

» In any emergency situation the knowledge of emergency procedures and systems can make the crucial difference between a successful or unsuccessful outcome. As the remarks in the questionnaires show it is essential that signage systems indicate clearly and simply the location and use of emergency equipment in this special case the mechanism of the exit doors and the emergency door release.

» As a result of the above described incident a part of the participants asked for a clear indication of the manual opening device and operation procedure of the external doors in form of pictograms combined with written instructions.

Exit height:

» Most of the passengers complained about the exit height of 64 to 67 cm from the carriage level to the rail track level. As stated in the questionnaires the participants felt strongly constrained by this height of step down. Although the group of participants was rather young and the video documentation showed that there was no obvious problem for one of the participants to get out of the train, more than 50 % of the participants were irritated by the exit height and the possibility of injury as a potential result of evacuation process.

» Therefore the participants proposed more detailed and precise announcements especially asking for references to the exit height.

Internal sliding doors:

» For the internal sliding doors, which separate the three compartments of the train, passengers also identified the need for design modifications. A small number of participants mentioned, that the grip of the internal doors was too small and situated to low, therefore the handling of the door was handicapped by the seats which were situated next to the door.

» Others stated that the sliding doors could be opened only by pulling with the full body weight. Therefore some of the participants, who were not able to open the door immediately, thought that the internal doors were locked.

» As a result of the trials the participants asked for design modifications concerning the grip size and clear indication of the manual opening device and operation procedure of the sliding doors in form of pointed arrows combined with written instructions, with reference to the closed status in the case of fire.

Signage systems:

» Participants of the smoke subjected carriages claimed that the visibility in the cabin was very poor, so that they couldn't see their own feet not to mention the existing signage. As the outcomes of trial 2 showed clearly the evacuation process tends to slow down with reduced visibility, resulting from the ingress of smoke.

» Regarding the illuminated passenger information display the prevailing opinion of the participants was that they excited just little as far as no attention with a fully occupied train. Therefore additional written announcements would be essential according to comments of some passengers.

» Passengers also stated that during smoke formation the illuminated passenger information display as well as the yellow markings of the internal and the steps itself were not visible. Therefore the stairs were sensed as dangerous by several participants. Furthermore the steps appeared too high for some passengers. It was required to light up the edges of the steps, so that they would be recognizable in spite of the obstructions of vision.

» A small number of passengers in the smoke subjected carriage required luminescent and/or blinking markings on the floor. Some participants mentioned that emergency lighting, similar to that found on aircrafts, should be considered for the carriages.

Crew members:

» Except for the train operator no other crew members were present in the train at the time of the evacuation experiments. In this type of commuter train crew members are generally not incorporated into the evacuation procedures. But as trial 2 showed in cases where no crew members are present some passengers tend to adopt the role of an authority figure, which takes care of the other passengers and attempts to manage the evacuation process [10]. As the outcomes of the questionnaires stated a small part of the passengers did not mind the authoritarian behaviour of this person but were grateful for help and support. But most of the participants stated that they didn't need any kind of help from other persons in the train and knew perfectly well what to do throughout the evacuation.

4.   Conclusions

As a result of the observations of the participants' behaviour and the evaluation of the questionnaires design modifications were taken into account and the development of specific evacuation procedures were incorporated into the emergency plan:

» Design modification were made concerning the grip size of the internal sliding doors, which means bigger and handier grips were attached.

» The signage systems for the internal and external doors were improved by using

pictograms with clearly indicated information about the opening mechanism of the doors.

» The acoustic announcement system was reconsidered providing more detailed information that would be given in closer sequence and adjusted to the specific emergency situation.

By the taken measures a significant improvement for the safety of the investigated commuter train and therefore for the survivability of the future passengers was achieved and an already safe form of transport was made even safer by design. **«**

References

1. Technische Universität Wien, Institut für Baustofflehre, Bauphysik und Brandschutz: *Evakuierungsversuch TW 4023, ÖBB "E-Talent" Zug 4023-005*, Versuchbericht, (unpublished) (Juli 2004).

2. Technische Universität Wien, Institut für Baustofflehre, Bauphysik und Brandschutz: B*randschutztechnisches Gutachten Rh 4023 und Rh 4024, ÖBB „E-Talent"*, (unpublished) (Jänner 2004).

3. T. Jin: *Studies on Human Behaviour and Tenability in Fire Smoke*, Proceedings of the 5th International Symposium IAFFS, Melbourne Australia, pp. 3-21 (1997).

4. T. Jin and T. Yamada: *Irritating Effects from Fire Smoke on Visibility*, Fire Science and Technology, Vol. 5, No. 1, pp. 79-90 (1985).

5. T. Jin: *Visibility Through Fire Smoke*, Report of the Fire Institute of Japan No. 42, (Sept. 1976).

6. H. Muir, C. Marrison, and A. Evans: A*ircraft Evacuation: The Effect of Passenger Motivation and Cabin Configuration Adjacent to the Exit*, CAA Paper 89019, ISBN 0860394069, CAA London (1989).

7. H. Muir and A. Cobbett: *Influence of Cabin Crew Behaviour in Emergency Evacuations at Floor Level Exits*, Report prepared for CAA/FAA, CAA Paper 95006 Part A, ISBN 0860396495, CAA London (1996).

8. S. Gwynne, E.R. Galea, M. Owen, and P.J. Lawrence: *An Investigation of the Aspects of Occupant Behaviour Required for Evacuation Modelling,* Journal of Applied Fire Science Vol. 8 (1), pp. 19-59, ISSN 1044-4300 (1998/1999).

9. S. Gwynne, E.R. Galea, M. Owen, and P.J. Lawrence: *Escape as a Social Response*, Report published by the Society of Fire Protection Engineers, USA (1999).

10. E.R. Galea and S. Gwynne: *Evacuating an Overturned Smoke Filled Rail Carriage*, Paper No. 00/IM/55, Centre for Numerical Modelling and Process Analysis, University of Greenwich, ISBN 1899991565, London (2000).

Minimum Stair Width for Evacuation, Overtaking Movement and Counterflow – Technical Bases and Suggestions for the Past, Present and Future

J.L. Pauls[1], J.J. Fruin[2], and J.M. Zupan[3]

Traditional lane models such as the 560 mm (22-in.) unit of exit width are examined as historical artifacts and, when studied empirically, as flawed bases for minimum stair width determination. Criticisms of this lane model were presented separately by the authors as early as about 1970 and improved bases for minimum width determination were also presented. Currently, even the improved bases for minimum stair width—based on the authors' early work—need to be updated for stair user demographics and other factors that have changed in recent decades. Three types of crowd flow are considered; coherent flow, overtaking movement, and counterflow. All of these occurred in the evacuations of the World Trade Center in 1993 and 2001. Partly as a result of the latter incident, counterflow has recently received particular attention in some US standards and building code-change deliberations that led to a minor increase—from 1120 mm to 1422 mm (44 in. to 56 in.) in minimum, nominal exit stair width requirements for certain occupancy conditions. Completing an examination of past, current and future criteria for setting minimum stair width, the authors provide suggestions for studies that will help provide significantly improved bases for such widths in the future.

1.   Objectives and Issues

The purpose or objective of this collaboration—of three North American pioneers in modern pedestrian studies(1-3)—is to develop recommendations for long overdue empirical study that will lead to a more substantial reconsideration of traditional lane models such as the 560 mm (22-in.) unit of exit width. This model, although largely eliminated from national building code requirements in North America over the last two decades, still is the most widely used basis for regulating minimum exit (escape) stair width for building evacuation. To what extent was a minimum width of 1120 mm (44 in.) ever appropriate for coherent crowd flow, for overtaking movement, and for counterflow? What factors were ignored or misunderstood in setting this minimum? What factors have changed over time that make this a more dubious minimum today, especially within a US context where there are significant changes in people's body size and fitness? What are the implications for modeling pedestrian movement on stairs? What are the implications for building or facility design and construction? What are the implications for research?

---

[1] Consulting Services in Building Use & Safety, USA

[2] PED Associates, USA

[3] Regional Plan Association, USA

2.   Traditional Bases and Justifications for the Lane Model

A 560 mm (22-in.) lane model for pedestrian movement, at least within the context of US requirements for means of egress (escape), apparently has its origins in the early part of the 20th century. This was related to the creation, in 1905, of the first US model building code—the National Building Code, by the National Board of Fire Underwriters, and, in 1913, of the National Fire Protection Association, NFPA, Committee on Safety to Life which developed the Building Exits Code, now the Life Safety Code.

As part of a review by Pauls (4), the views about exit width presented in two committee reports—from the US, 1935, and from Britain, 1952 (5, 6)—were critically discussed. While both reports concluded that there was not definitive empirical evidence for a lane model for egress flow, the building codes (regulations) that followed for a few decades after these reports maintained a traditional lane or unit-width model (22 in. or 560 mm in the US and 21 in. or 550 mm in Britain). Reflecting the overwhelming influence of tradition, the US report asserted, "In the opinion of many who have studied the matter, 22 inches can be taken as the width of a file of people in motion. Its origin is said to be in experience gained in the Army. A stairway width of 44 inches will permit 2 files of people to move freely down the stairs at the same time." No scientific reference was provided for these assertions.

Notably, the British report, considering both the US work from 1935 and subsequent French work, stated: "The tests do not give any reliable evidence on the effect of small differences in width, say 6 in. increments," and "Before this question can be definitively settled it will be necessary to get experimental conditions where reasonably consistent results can be obtained for each particular width." As one example of the weight given to the traditional lane model—even after the 1952 report, the NFPA Building Exits Code, 1963 edition, stated:

> "Measurement of exit width in terms of units representing the width occupied by one person, rather than measurement in feet and inches is an important concept of the Building Exits Code. Measurement in feet may in some cases involve additional expense in building construction without corresponding increase in safety. For example, a 44-in. stairway comfortably accommodates two files of people; adding 4 in. to make a 4-ft. stairway does not increase the capacity of the stairway. However, it has been shown by count of stairway flows that adding 12 in. to a 44-in. stairway does increase the flow of people, in effect permitting an intermediate staggered file."

The NFPA Building Exits Code did not provide a specific citation to the study having this conclusion which, according to the work of Pauls among others, is partly correct and mostly incorrect; both a 100 mm (4-in.) width increase and a 305 mm (12-in.) width increase result in higher flows—in proportion to effective width or, respectively, about

13 percent and 38 percent (3, 7). Here it should be noted that flow capacity varies direct-ly—and linearly— with effective width (the nominal width less 300 mm or 12 in.), not with the nominal width.

3.   Research from the 1960s and 1970s in North America

Both the nature of the lane model and its dimensions were challenged by researchers who, for perhaps the first time, examined and documented—in detail—crowd move-ment in the contexts of urban-scale movement (including mass transportation systems) and intra-building egress in evacuation drills. The work of Fruin and of Pushkarev and Zupan in the New York City area, circa 1970, has been especially influential in traffic engineering (1, 2). Fruin recommended a minimum 1524 mm (60-in.) nominal stair width based on a 560 mm (22-in) shoulder width and body sway of 100 mm (4 in.) to each side. For building design and regulation contexts, there was extensive documen-tation in Canada by Pauls of, first, high-rise building evacuation drills and, later, crowd movement at large events like the Olympic Games, mostly in the 1970s. Pauls' studies, both in tall office buildings and in large buildings with assembly occupancies, covered extensively used stairs in the nominal width range of 914 mm to 2235 mm (36 to 88 in.), a range of widths and use conditions allowing Pauls to develop the Effective Width Model which was included in a chapter of the SFPE Handbook of Fire Protection Engi-neering in 1988 (7).

Especially notable for its intensive focus on one particular stair width was Pauls' field study, in 1978, of aisle stair use in the Edmonton Commonwealth Stadium which, as well as leading to some detailed data analysis (of particularly intensive film and video documentation), resulted in the unique documentary film, The Stair Event (8-9). Notab-ly, that study was done with intensively used stairs having a nominal width effectively about 1422 mm (56 in.) by virtue of the fact that the clear width between seats, on either side of the aisle, was approximately1200 mm (48 in.).

During the 1980s, as a result of Pauls' aisle stair study and a widely used report by the US-based Board for the Coordination of the Model Codes (BCMC) in 1985, this 1200 mm (48-in.) clear width became the standard minimum requirement for aisle stair width regulated by US model building codes and standards, beginning with the BOCA Nati-onal Building Code in 1987 and the NFPA Life Safety Code in 1988. Notably, a center handrail (with gaps every three to five seat rows) is usually provided for such aisle stairs as the preferred option to providing handrails on each side. Thus two lanes of nearly 600 mm (24 in.) clear width—actually about 590 mm (23 in.)—were created on each such subdivided aisle stair which are used for coherent egress flow, overtaking movement and counterflow. In addition to its use in the Edmonton stadium, there has been extensive use of this aisle stair width in new aisle stairs constructed in the USA since approximately 1990. The widespread existence and extensive use of such stair widths offer significant research possibilities on the minimum stair width issue (as discussed below).

Empirically based recommendations from the authors, for minimum stair width, were in the range of 1370 mm to 1525 mm (54 in. to 60 in.)—significantly greater than the traditional 1120 mm (44 in.) minimum nominal width enshrined in building codes. Notably, the authors took careful account of lateral body sway in their work; lateral body sway had not been taken into account in the development and use of the traditional unit exit width approach using the 560 mm (22-in.) lane width. Other ergonomics-oriented authors, Panero and Templer, have also opined on significantly wider minimum widths—1422 mm (56 in.)—and preferred widths—about 1753 mm (69 in.) based on two 95th percentile men side-by-side, in their books in 1979 and 1992 respectively (10, 11). For all the foregoing dimensions, the nominal width is used (e.g., wall-to-wall clearance in those cases where a stair flight is bounded by walls on each side). Handrails (and everything below handrail height) are typically permitted, by US building code requirements, to project up to about 100 mm (4 in.) into required minimum, nominal stair width.

4.   Current Situation regarding Minimum Stair Width Rules

Not until the World Trade Center (WTC) disaster in 2001 was there a major push to reconsider minimum exit stair width requirements in building codes and safety standards, especially given some limited but influential photographic evidence as well as research survey data indicating a major problem with counter flow of evacuees and firefighters. Preliminary evidence on evacuee speed and flow during the 2001 evacuation of the WTC also has raised questions about appropriate stair geometry. Although there are three major studies currently being done on the evacuation of the World Trade Center, most of the currently published work is that of the US National Institute of Standards and Technology (NIST) which has posted all of its 10,000 pages of comprehensive findings and presentations (heavily focused on structural collapse) on a special web site, http://wtc.nist.gov. The two other studies—which are more focused on human behavior and evacuation issues—are being done by Columbia University and by a three-university consortium in the UK. Information on at least two of these studies is found in other papers given at the PED2005 conference.

All of this background, but most explicitly the need for emergency responder counter-flow, led committees of the National Fire Protection Association (NFPA) to introduce a wider 56-inch, 1425 mm minimum exit stair width requirement to NFPA codes and standards for certain high-occupancy contexts (2,000 occupants per stair). This was in response to proposals to NFPA from Pauls, first in 2001 and then more successfully in 2003, for incorporation in the Life Safety Code (NFPA 101) and Building Construction and Safety Code (NFPA 5000), both ANSI documents being finalized during 2005. Not yet well addressed are clear indications, from public health data, of significant increases in body mass and size as well as significant reductions in fitness for the US population. Increased body mass/size and reduced fitness—resulting in slower speed on stairs—influence lateral body sway, for example, which also affects needed stair width. All of

these factors underline the urgent need for new empirical studies and improved modeling, preferably of an international and cross-cultural nature, of pedestrian movement on stairs in a variety of contexts. Detailed recommendations are offered below on planning, conducting and applying such studies which have major implications for evacuation and pedestrian dynamics plus the design and operation of buildings in which evacuation is anticipated.

Summing up the current situation, where are we now with the three-decade old recommendations coming especially from the work and analyses of Fruin and Pauls, the two North American investigators of human movement who have thought the most about minimum stair width in relation to coherent crowd movement, overtaking movement and counterflow? Given traditional requirements and the demographics of North American adults—studied about three decades ago, we can assume a base clear width of about 560 mm (22 in.). To this we need to add an allowance for body projections and lateral sway of 100 mm (4 in.) to each side. This results in a nominal minimum stair width—with two channels or lanes—of 1320 mm (52 in.) to 1520 mm (60 in.). Where one selects a width within this 200 mm (8-in.) range depends on whether the 100 mm (4 in.) of body sway toward the center of the stair is ignored (assuming side-by-side individuals are swaying laterally in the same direction or in phase, and thus not interfering) or is fully accounted for (assuming side-by-side individuals are swaying toward each other, out of phase).

A width in the middle of the range—specifically 1400 mm (56 in.) has been the recommendation from Pauls' work, while the wider option—1520 mm (60 in.) has been advanced by Fruin. Incidentally, the 1400 mm (56-in.) width, with handrails approximately 1200 mm (48 in.) apart allows an adult—with a 5th percentile female to 95th percentile male stature—in the middle of the stair to simultaneously grasp handrails on each side. While not adopted generally for minimum exit stair width, Pauls' recommended minimum has had relatively wide acceptance in US model building codes and standards for two contexts. The first accepted of these contexts is aisle stairs in assembly seating facilities. The second is exit stairs where an occupied wheelchair will have to be carried—by three persons—on the stair (as opposed to using a one-person-operated, gravity-powered, stair descent, evacuation device transporting the person otherwise unable to use stairs). As this paper is being prepared a third context, for the 1400 mm (56 in.) nominal minimum width, is being adopted for NFPA model codes and standards for new exit stairs used by more than 2,000 persons per stair. Otherwise, the minimum nominal stair width required by model building codes and safety standards in North America is 1120 mm (44 in.).

Again, the foregoing recommendations date from three decades ago and relate to demographics that are significantly different from those becoming increasingly pervasive in the USA due to increased body mass and reduced fitness generally. Development of new minimum stair width recommendations should not be based merely on anthropometric

changes over the last three decades (or, for that matter, even projections of such changes over the coming decades when buildings constructed today will still be in use). More basic (re)examination, taking into account public health and ergonomics, is warranted. This is addressed in the next section.

5.   Research Suggestions and Future Design Requirements

The underlying assumption behind the following recommendations is that information about people's use of stairs, in relation to establishing justified criteria for minimum stair width, should be based on field observations of actual stair use. The authors' early work from a few decades ago demonstrates the value of this approach as contrasted to a literature-based approach or use of computer models—both of which may be flawed by out-of-date or otherwise incorrect information or methods.

Moreover, while this paper is based on predominantly North American experience, it is recommended that more than one cultural or demographic context be examined. One way to do this, which will have other advantages (listed in Section 5.1), is to conduct detailed field studies of crowd movement on aisle stairs of large buildings used for public assembly; i.e., arenas and stadia. Thus, even though the contexts for most urgent application might be exit stairs in multistory buildings (dealt with in Section 5.2), with office or residential occupancy, the best study possibilities appear to occur with assembly occupancy aisle stairs. Effectively, much of the following set of recommendations is for a second, albeit more sophisticated iteration of the studies headed by Pauls in the 1970s, especially in the context of the Edmonton Commonwealth Stadium which led to the documentary film, The Stair Event (8, 9).

5.1. Why Study Stair Use in Assembly Aisle Stairs?

Among the reasons for conducting new research within the context of assembly aisle stairs are the following.
1.   The buildings, containing an abundance of such stairs, are found in virtually all countries.
2.   Such buildings typically have very limited use and are thus available frequently and for long periods without disrupting their normal use for spectator events. This provides two documentation options: observations during normal events with thousands of spectators and observations during other times, including observations with experimental modifications to the stairs and with controlled tests of counterflow and overtaking movement for example.
3.   The stairs, especially for outdoor facilities, have relatively good lighting which will facilitate detailed photographic and video documentation.
4.   The stairs can be observed and documented from numerous vantage points, including especially overhead ones (for example, from lighting catwalks and towers), that are needed to best document critical aspects of people's movement.

5.   Camera positions can be set up at great distance from the observed activity thus satisfying two important criteria. First, the camera activity will be unobtrusive to those using the stairs. Secondly, there will be minimal problems with parallax as long-focal length lenses can be used at distances of up to 200 metres (700 ft.), a very good approximation of infinity. This was, for example, a much-used setup for the study leading to the film, The Stair Event, as high-quality (Beaulieu) Super-8 film cameras were used with high-quality (Hasselblad) lenses, of up to 500 mm focal length, so that a person's image nearly filled a frame—shot in vertical format—at a distance of 200 metres! At the left side of Figure 1 is a single frame from one of the research films; it depicts aisle stair ascent by a girl with a stature of about 1500 mm (60 in.). There is a central handrail, the aisle stair has a width of 1200 mm (48 in.) measured at the treads; and this is effectively similar to a non-aisle stair with a nominal width of about 1400 mm (56 in.). At the right side of Figure 1 is the camera setup on the other side of the stadium about 200 metres (700 feet) distant from the girl on the aisle stair.
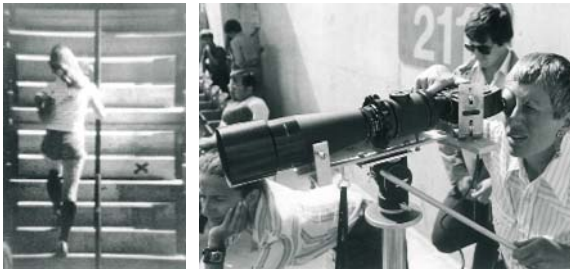
Figure 1: Film documentation 200 metres (700 ft.) distant from aisle stair

Such facilities often have a variety of aisle stair widths, although for newer facilities in the US, there will be a preponderance of aisle stairs with a clear width of 1200 mm (48 in.) which, fortunately, is the single width warranting the most intensive study given current understanding of minimum width and recent code requirement practice.

6.   Current aisle facilities, depending to some extent on the country, seat deck pitch, and the age of the facilities, have various approaches to provision of handrails. Outside the US and with older facilities generally, many aisles have no handrails at all. Within the US, especially with facilities built in the last decade or so, all of some aisle stairs will have handrails, usually installed at the centerline of the aisle, with gaps every three to five rows. Some facilities have handrails at the side of aisle stairs, with gaps at each row. For experimental purposes—with aisles not already equipped with handrails, temporary handrails could be installed at, or near, the sides of aisles to test effectiveness of various clear stair widths.

7. Such facilities typically have various seat deck slopes which leads to different step geometries including, especially in the US, the 180 mm (7-in.) maximum rise by 280 mm (11-in) minimum run/going geometry that is a commonly required for enclosed exit stairs in multistory buildings. In chapter 3 of his book, Pedestrian Planning and Design, Fruin (1) first reported—quantitatively—that better step geometries would be associated with higher speeds, especially in descent. His data cover only two rise-run/going step geometries: 180 mm (7 in.) by 285 mm (11.25 in.) and 150 mm (6 in.) by 305 mm (12 in.) with the former being on an indoor stair and the latter on an outdoor stair. Subsequent studies by Templer (12) and Roys and Wright (13, 14), among others, have provided information on usability and safety differences among various step geometries but there remains a relative dearth of studies that specifically address the benefits—to crowd egress flow—of various step geometries. Thus studies in the context of aisle stairs, with their range of step geometries in otherwise comparable conditions, can be useful.

5.2. The Case for Studies of Stair Use in Tall Building Exit Stairways

The fact that tall building stairs are, geometrically, different from typical aisle stairs underlines the need to conduct systematic studies there as well. For example, there might be particular step geometries that are more typical in office buildings—older ones especially—than are found in aisle stairs. Also, there are important differences in provision of walls, enclosing the stairs, and provision of landings—one, two or four per building floor so that crowd movement on exit stairs consists of a combination of steps and level walkways with the latter providing, on the one hand, places of lower energy expenditure or even rest while, on the other hand, they require frequent transitions from one type of gait to another that is very different biomechanically and in terms of safety. Indeed, the mere fact that there are such frequent transitions—onto and from steps—significantly affects safety as well as the degree of attention people need to pay to their own movement while coping with the movement of others nearby.

Thus, even given this incomplete discussion of differences, there are very good reasons for research to be done within the context of typical tall buildings. However, enclosed stairs with frequent landings pose difficult challenges in terms of detailed documentation. Cameras cannot be placed so distant and fewer options are available for type of view. Some of these difficulties can be partly mitigated if mirrors are used—for example on soffits and ceilings—to provide greater flexibility with camera placement while doubling (or tripling) distances between cameras and observed action to reduce parallax. Lighting will be a problem in actual exit stairs and, given the need to document evacuation movement under emergency lighting and lights-out, photoluminescent marking conditions, infrared cameras may be needed.

Generally, to provide data also from actual evacuations, use should be made of permanently installed cameras so that some key data are available from real-world conditions as opposed to tests. At a minimum, such cameras should be set up at the discharge levels of exits, directed toward the final stair flights.

5.3. Other Study Contexts

Only brief of mention will be made of two other options for studying crowd movement. One is transit system stairways—where there are no problems getting extensive usage. The second, where setting up crowd usage may be a challenge, is laboratory settings. This offers better precision and instrumentation possibilities.

5.4. What Data Should Be Collected?

Regardless of the crowd movement context, standard measures of pedestrian movement—speed, flow and density—should be determined for each observation. Other data to be collected include the following.

1. Traditionally, body width (as it affects width of circulation facilities) has been measured at shoulders. A more meaningful dimension may be body width at a person's elbows. In any event, measurements should be made of the maximum lateral dimension of people's bodies (with clothing) at both elbows and shoulders to establish which governs and for what kind of movement conditions.
2. Regarding the space required by special stair users—notably emergency responders who might need to ascend stairs carrying bulky firefighter turnout gear and other equipment, data need to be collected on the resulting counterflow with descending evacuees.
3. Other special users and use conditions, as part of evacuation flow, include persons with mobility disabilities using walking aids such as crutches or canes, persons being carried in wheelchairs (either by two persons or by three persons), and persons being transported on one of the several commercially available evacuation chairs or gravity-powered stair descent devices.
4. A potentially important factor is whether the predominant evacuation flow is downward—the usual case for high-rise buildings—or upward, as would be the case for underground facilities. How does the width required change as a function of predominant travel direction?
5. Regarding precision for all such measurements, it is suggested that (with better quality digital documentation methods now available) measurement to the closest 10 mm (0.4 in.) should be the goal. This is approximately a factor of ten better than achieved in studies done some three decades ago by Pauls, based on relatively poor video resolution then available. With higher-resolution motion picture film (of Super-8 format and low-grain, 40 ISO speed) used for the Edmonton Commonwealth Stadium study in 1978, the subsequent analysis achieved a precision of about 40 mm or 1.5 in. (10), for example to code individual foot placement

across the stair width. Precision with video was only slightly better than Pauls achieved with video nearly a decade earlier.

6. In general, the analysis of Edmonton records (performed under contract for Pauls) could be one starting point for future studies although modern human movement study technologies should permit less dependence on manual data take off from visual records. For example, data acquisition technologies such as employed in the recent stair use studies at the UK Building Research Establishment laboratory by Mike Roys and Michael Wright should also be exploited where possible (13, 14) as should other studies of human movement being performed in other laboratories. (No literature research of such general human movement study methods has been performed for this paper; however it should be one of the first steps taken in a subsequent study.)

7. The extent of lateral body sway should be assessed in an absolute sense (relative to a fixed line) and relative to the person's average walking line taken as the center point between ones feet or ones center of gravity projected vertically to the walking surface. How lateral body sway varies as a function of anthropometrics, walking speed, gender, and other factors should be investigated. An important factor also to assessed, relative to body sway, is the lateral spacing of ones feet. Use or nonuse of a handrail (or of handrails) should also be assessed as it might affect lateral body sway.

8. The lateral clearance between people, when side by side, should be measured for the three conditions—coherent flow, overtaking movement and counterflow. For coherent flow, the extent to which adjacent persons are using the same weight-bearing foot—and thus swaying—in phase or in unison should be investigated. This may be a prime reason that people marching with military precision might be able to achieve high flow with relatively small inter-person spacing and with lane widths as small as the traditionally assumed 560 mm (22 in.).

Ultimately, the suggested studies should provide useful data and models that can help describe the dynamic space requirements for crowd movement on stairs taking into account user demographics, nature of the movement, and stairway geometry. These data and models should then be employed to help set minimum stair width criteria that can be implemented in model codes and standards for building design. A goal here should be to develop models that can address changing demographics—for example, even larger and less fit people than is currently typical in the US. The movement models should also be used to improve the quality of evacuation and crowd movement models generally, in terms of both the analysis or simulation and the graphic output.

6.   Concluding Remarks

Moving beyond the current, tradition-based criteria for minimum exit stair width will require substantial research to address adequately coherent flow, overtaking movement and counterflow plus to take into account changing demographics. The demographic

changes, especially in the US, have led to larger, heavier people with fitness levels lower than was the case when the authors first began documenting pedestrian movement a few decades ago.

The traditional 1120 mm (44-in.) nominal minimum width for exit stairs was flawed, and known to be flawed a few decades ago. Even with knowledge available around 1970, it was clear to the authors that a minimum nominal width of between 1400 mm (56 in.) and 1520 mm (60 in.) should be used for design of stairs where two-abreast movement could occur reliably. Preferred widths, facilitating more efficient crowd movement were approximately 1730 mm to 1750 mm (68 in. to 69 in.) measured nominally, or about 1520 mm (60 in.) measured as the clear width between handrails on each side. Indeed the 1520 mm (60 in.) clear width between handrails has been the maximum permitted clear distance between stair handrails if all of the stair width is to be credited for egress capacity in US model building codes, based on Pauls' analyses of adult anthropometrics and of field data (3, 15). With this width, everyone on the stair is within reach of one handrail. Moreover, according to the Effective Width Model developed by Pauls, based on field studies of tall building evacuation and crowd movement in large assembly facilities (3, 7, 15), this preferred 1730 mm (68-in.) nominal width has an effectiveness for evacuation flow that is 75 percent greater than the traditional 1120 mm (44-in.) nominal stair width even though its nominal width is only 55 percent greater.

But the foregoing recommendations are based on observations made a few decades ago. Today, user demographics have changed significantly. Moreover, some of the applications are very tall buildings where a total evacuation by stairs will be a lengthy, arduous experience—even more so now with typical occupants having lower fitness levels than was the case a few decades ago. New research must be done. Also, with the much improved video documentation methods available now, much higher quality data can be collected. We cannot afford to ignore both the research needs and the research opportunities. For these reasons, several suggestions have been made for conducting such new research. Given that these recommendations come from three senior pedestrian movement researchers, we should not be surprised that today's younger, highly skilled and (we hope) more motivated researchers will accept the challenge. After all, new, better founded criteria for minimum exit stair width will affect the design of buildings that will still be in use long after the authors—and, indeed, even today's younger researchers—have passed on.

The life safety implications of getting critical features for building evacuation designed correctly are too great to ignore. Thus we hope that our account of how we got to where we are today and our suggestions about preparing sensibly for the future will find an audience among pedestrian researchers and building safety policy makers among others.

Moreover, to all responsible for developing the increasingly sophisticated and sometimes visually compelling models of pedestrian movement, we request that human move-

ment be better represented in your models. If body sway, for example, is as important in crowd movement as we believe it to be—especially for larger, heavier, slower-moving people—then pedestrian and evacuation models should take it into account and depict it realistically.

7.   Postscript

Within hours of this paper being finalized, the US National Bureau of Standards and Technology, NIST, released its draft final reports, totaling some 10,000 pages (accessible at http://wtc.nist.gov/pubs/reports_june05.htm) with 30 recommendations including recommendations 4, 16-20 on evacuation of tall buildings. These recommendations, for code changes and (indirectly) future research, along with findings reported especially on project 8 (Emergency Response Operations), clearly identify counterflow—of emergency responders and evacuees—as a phenomenon to be addressed in relation to exit stair width. Most important, NIST recommendation 4 calls for tall building design facilitating full evacuation of occupants within time limits set by the capability of the building to withstand burnout without collapse. Thus stair width and effectiveness of crowd movement now have renewed importance. **«**

References

1.   J. Fruin: *Pedestrian Planning and Design*, Metropolitan Association of Urban Designers and Environmental Planners, Inc., New York (1971).
2.   B. Pushkarev and J. Zupan: *Urban Space for Pedestrians*, Regional Plan Association, MIT Press (1975).
3.   J. Pauls: *Building Evacuation: Research Findings and Recommendations*, In: D. Canter (Ed.) Fires and Human Behaviour, John Wiley and Sons, pp. 251-275 (1980).
4.   J. Pauls: *Development of Knowledge about Means of Egress*, Fire Technology, 20, 2, pp. 28-40 (1984).
5.   Design and Construction of Building Exits, National Bureau of Standards, US Department of Commerce, Gaithersburg, Maryland (1935).
6.   Fire Grading of Buildings, Part III, Personal Safety, Post War Building Studies, No. 29, Her Majesty's Stationery Office, London (1952).
7.   J. Pauls: *Movement of People*, The SFPE Handbook of Fire Protection Engineering, National Fire Protection Association, Quincy, MA, Section 1, Chapter 15, pp. 246-268 (1988).
8.   J. Pauls: *The Stair Event,* 18-minute documentary film, National Research Council of Canada, Ottawa (1979).
9.   J. Pauls: *The Stair Event: Some lessons for design*, In: Proceedings of Conference, People and the Man-Made Environment, University of Sydney, Australia, pp. 99-109 (1980).

10.   W. Rhodes et al.: *Studies of Stair Ecology in Public Assembly Facilities: Handrails, Speed, Density, Flow, Distribution and Foot Placement*, Report for National Research Council of Canada, Ottawa (1980).
11.   J. Panero and M. Zelnik: *Human Dimension & Interior Space: A Source Book of Design reference Standards*, Whitney Library of Design, New York (1979).
12.   J. Templer: *The Staircase: Studies of Hazards, Falls, and Safer Design*, MIT Press, Cambridge, MA (1992).
13.   M. Roys and M. Wright: *Minor Variations in Gait and their Effect on Stair Safety*, Contemporary Ergonomics 2005, Taylor and Francis, pp. 427-431 (2005).
14.   M. Wright and M. Roys: *Effect of Changing Stair Dimensions on Safety*, Contemporary Ergonomics 2005, Taylor and Francis 469-474 (2005).
15.   J. Pauls: *The Movement of People in Buildings and Design Solutions for Means of Egress*, Fire Technology, 20 1, pp. 27-47 (1984).

Study on information guiding based on human psych-physiological responses in China

J. Qiao[1,2], J. Shi[1], J. Rong[1], and F. Ren[1]

In order to deal with the event pedestrian crowd evacuation quickly in places of public assembly, to remove hidden trouble of safety in public site, the psych-physiological responses in the movement of evacuation are surveyed, using dynamic eye tracking instrument (iView X) in the related simulating scenarios, then the outputs including image files and data files are analyzed in computer. The results are useful for discussing if the location of information guideposts and boards sound reasonable and the notability of them. As a result, some principles on guiding fitting for oriental human psych-physiological reaction, and a new study method in the traffic safety field is attempted in China in the same time.

1.   Introduction

The walking space of traffic consists of pedestrian and environment with the society development and the increase of living standard, more and more people participate in assembly and sports event. The trip of people increase, thereupon the swiftness, comfortableness and safety of people's trip have been put on discussion. According to a five-year comprehensive research on traffic safety in Indiana University of U.S.A., the result demonstrated that 90.3% of accidents have something to do with human factor [1]. Previous traffic safety experts and scholars have given much research to road and vehicle; therefore safety devices reduced traffic accidents to some extent. But there is few research concerning psychological and physiological activities, and even fewer dealing with psychological and physiological events especially to people's congregation and evacuation in large events. According to the material investigated, people such as Ho et al studied the role of interfering thing (clutter) during vehicle steering in 2001 [2]. Namely the search situation of the traffic signs on the detected road, first presenting a traffic sign for the people tried, then give him a scene, while requiring him to search for this goal sign, the result revealed that the error rate during the day when there is more interference is much higher than that with fewer interference. The pedestrian maybe congested in the large event and there are many pedestrian accidents in stadium or religious festivals in different countries in history. Among these accidents, many of them are caused by lack of information, so it is necessary to study information guidance in pedestrian space.

In September 1991, an extremely serious accident happened at the lantern exhibition in Yingze park of Shanxi province, 105 people died and 99 people were injured. And the main cause is also indefinite setting of guidance signs.

The size of safety guidance information signs in the large event stadium is set up empirically; this poses many negative effects to bring its function into play. As figure 1a) to 1d) shows. The setting of traffic signs and traffic management strategies little reach to

---

[1] Transportation Research Center, Beijing University of Technology
[2] College of Mechanical Engineering, North University of China
Qiao Jiangang, Ph.D. Candidate, qiaojg@emails.bjut.edu.cn

people's demand including psychological and physiological feeling to carry on humanization consideration, it is apt to pose potential safety hazard in pedestrian traffic. So the related research should be carried on aiming at information guidance and pedestrian safety.

2.   Experiment design

2.1.   Experiment object

Regarding traffic safety as goal, proceeding from people's physiology and psychological theoretical foundation, aiding by the advanced dynamic eyes instrument, this paper is intended to analyze the rationality of the setting of safe sign and advertisement board in public, putting forward a humanized system setting principle of traffic guidance.

2.2.   Experiment principle

As we all know from knowledge of psychology and physiology, people will behave such phenomena as perspiring, rising of blood pressure, accelerating of heart rhythm and eyes opening wide whiling meeting nervous or urgent accidents. The change of pupil is a key index of eye movement, it to some extent reflects people's psychological activity situation. The change of the pupil is 1.3~8 mm under normal conditions. Investigation revealed that the diameter of pupil would diminish with the increase of people's fatigue degree. Pupil can be caused to enlarge when people is cast into psychological anxiety. Blinking is a kind of contact movement by upper and lower eyes, and at that time, eyeballs are hidden behind temporarily. Tecca's research shows that the average blinking frequency is 15-20 times each minute when people are at relaxed state [4]. The blinking situation can be recorded by eye instrument during the process of the quizzee's eye movement.

2.3.   Experiment instruments

MeyeTrack dynamic eye instrument is a Hi-Tech product produced by a German company named SMI (Senso Motoric Instruments). Dynamic eyes instrument carry out its detection by virtue of the principle of reflecting light of eye's cornea and pupil, which is characteristic of being accurate detection, light, stable working performance and easy and simple to operate. And it can write down the change of eyes, the orbit of eye's fixation point, watching times, time of focusing, location of attention, etc. additionally it can record the factual detection situation, carrying on a playback analysis, increasing the success rate of data detection. Camera, vidicon and stopwatches are used as supplementary instrument.

Figure 1: Unreasonable safety signs; a) unobvious signs b) too low signs and much more interference c) too complicated signs d) no safety signs

2.4. Measurement

In order to gain accurate measure result, we carried on an elementary test to find out the system error of instruments, through designing, revising the testing plan, and experimental procedures are confirmed as the following.

1. Measure time: for the authenticity and practicability of measure result, we choose the situation duration at a fine day and the peak time of pedestrian.
2. Selection of locations: to select public places where there has higher potential accident probability such as subway station and stadium. To those places where accidents may happen, the measures of imitating accident scenes are adopted to replay it again.
3. Quizzee: 45 people were chosen to be examined from the age range from 15 to 55 years old. Because the people within this age range participates in activity with more trip.
4. The installation of instrument: equipping with the quizzee with dynamic eyes instrument and using "five points method" to locate and adjust. In the places where there has dense crowd, it is inconvenient to use dynamic eyes instrument to measure, so alternatives should be taken, namely using camera to record all the scenes first and then go back to the laboratory to carry on later treatment.

5.   Testing: quizzees were tested by dynamic eye instrument for 10 minutes, the time of some unusual accident can be recorded by stopwatch. Arithmetic mean was calculated from the result measured, table 1 is a result which recorded the quizzee's blinking situation in 100 seconds whose serial number is 03.

Detection time (s)	Amount of blinking (Times)	Time of closing eyes (s)	Detection time (s)	Amount of blinking (times)	Time of closing eyes (s)
0-10	4	0.38	50-60	8	1.16
10-20	11	1.40	60-70	8	1.10
20-30	9	1.36	70-80	12	1.82
30-40	12	1.94	80-90	7	1.08
40-50	7	1.02	90-100	6	0.92
Average	8.4 times/10s		50.4 times/min		

Table 1: Measure result on the amount of blinking

3.   Data processing and analyzing

The data gained by dynamic eye instrument can be analyzed with the special-purpose software (iVan) in virtue of the supplementary calculation of computer. The relationship between safety guidance system and psychological and physiological reaction is obtained under urgent conditions. Based on the data mentioned above, the relationship between the amount of blinking and time can be obtained as figure 2.
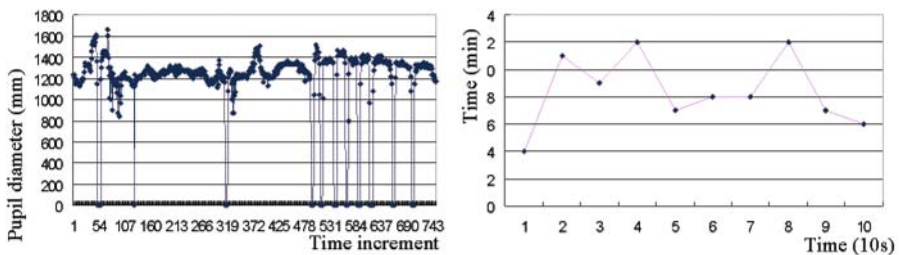
a) Relation chart between pupil diameter and blinking

b) Relation chart between amount of blinking and time

Figure 2: The relation between the amount of blinking and time by 03 quizzee

Under a quiet and relaxed state, the average blinking frequency is 15 to 20 times per minute, from table 2. The average blinking frequency reaches to 50.4 times per minute at that moment, which is caused by anxiety of people, from figure 2a). We found out that the amount of blinking is more at the beginning, the people is looking for the exit at the beginning and then he found it, and the amount of blinking decrease slowly, anxiety in his heart was removed. When people reached the exit, but because there is so much people there and the setting of sign is undistinguished and with more interference, the result shows that the people will be nervous and the amount of blinking is increased subsequently. Judging from the figure 2b) qualitatively, the figure is characteristic of being bimodal. The first peak is the amount of blinking when looking for the exit, the width is its duration, and the second peak is the amount of blinking when interference appear, the width denotes the lasting time of interence. The more nervous his psychological condition, the higher and the wider the peak is. Judging from the figure quantitatively, because there is no stimulus at first, the amount of blinking is 24 times per minute. When there are urgent accidents, the amount of blinking is 60-70 times per minute, and after finding exit, the amount of blinking is lowered to 42 times per minute. When congestion appears, the amount of blinking increases to 72 times per minute again, until coming out thoroughly, the amount of blinking is lowered to 36 times per minute. So we think that the sign should be set up where can be seen at first glance, and should be in succession to exit.

And then come to see the diameter change of pupil, figure 3 shows the variation of pupil detection result of the No. 03 quizzee in the first 15 seconds. In order to be intuitionistic, two directions, V (vertical direction) and H (horizontal direction), are discussed separately. Figure 3a) denotes the trend change diagram of pupil diameter detection result from V direction. Table 3 denotes the change of pupil diameter from H direction's detection.

Serial number	1	2	3	4	5	6	7	8
Time (ms)	1399	2199	5199	7319	7879	9479	10839	12259
Diameter of pupil (mm)	17.05	11.08	16.12	13.60	16.42	13.06	15.51	13.62
Change of pupil (mm)	5.97	5.04	2.82	2.52	3.36	2.45	1.89	1.32

Table 2: Diameter value of pupil and time by detection

The relation graph between pupil change of H direction and time as followed in virtue of data from table 2.
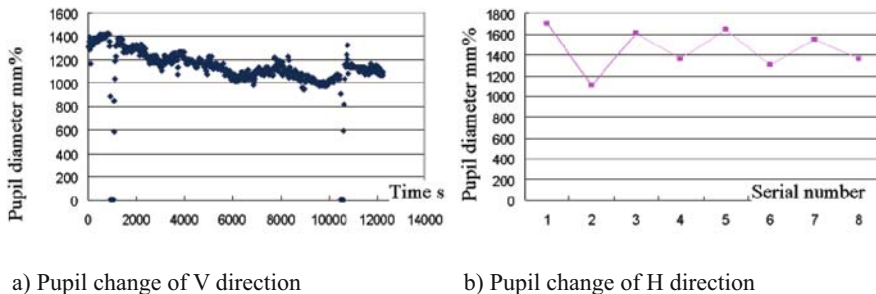

a) Pupil change of V direction   b) Pupil change of H direction

Figure 3: Relation between diameter change of pupil and time of No. 03 quizzee

The change range of pupil is 1.3~8 mm in normal cases. Pupils will become larger when being nervous. Because the first intuition of people is to flee for life, he will look at near place first and then turning to the distant places searching for the exit, so it is extremely suitable to set security guidance signs at the near places, people can confirm the route direction for flee as soon as possible, thus reducing the loss of accidents. From figure 3a), we know that the pupil is the biggest when accidents happen one second or so, and interferences at this moment will increase the time to look for the exit. Several seconds later, exit was found, anxiety was eliminated, and then the graph drop slowly at linear form. The enlargement of pupil at 8s is caused by the crowded state, so something noticeable should be eliminated such as interference objects like advertisement board. In contrast, those signs that determine the security of people should be more striking. Figure 3b) denotes a relatively intuitionistic change graph after the trend graph of H direction is processed, which can be seen that the change of pupil diameter presents a damping oscillation with the variation of time. The pupil changes was enlarged to 5.97mm at the beginning, and then dwindled to 2.52mm, but after another 8 second, it was enlarged to 3.36mm again. Finally, pupil diameter was 1.89mm when anxiety was removed. So the setting of the safety signs should be obvious and successive until to the entrance, interferences should be diminished and soft light should be increased in order to eliminate the anxiety of pedestrians.

4.   Conclusion

Through analyzing people's psychological and physiological condition, it is found that the rational setting of the traffic information signs is a paramount guarantee for security of pedestrian in large event. Through investigations and experience analysis, based on actual condition in China, the setting principles of safety signs are suggested as followed:

1. The safety signs should be set up at the upper level of the very front of people's eyesight, the best situation is that safety signs can be seen from every position in the stadium.
2. Interferences such as advertisement board should be eliminated around safety signs.
3. Safety signs should be established successively until to the exit.
4. The size of safety signs should be large in order to be obvious.
5. The color used should be the traditional white background with green character using the reflective traffic paint, and the light should be soft

After studying these setting principles, it is to make pedestrians find the safety signs within the shortest time in emergency and to reach the exit as soon as possible, thus reducing the number of casualties. Simultaneously, a new research method in the field of traffic safety is put forward. **«**

References

1. R. Futian: *Psychology of Traffic Engineering*, Beijing University of Technology Publishing House, 1993.3, pp. 201-204 (1993).
2. G. Ho, C.T. Scialfa, J.K. Caird, and T. Graw: *Visual Search Traffic signs: The effects of Clutter, Lminace, and Aging*, Human Factors, 43 (3), pp. 194-207 (2001).
3. Y. Guoli: *Application of Eye Move Analysis Method*, In: Psychological Research, 2004.4, Tianjin education publishing houses, pp. 340-355 (2004).
4. J.J. Tecce: *Psychology, Physiology and Experimental*. In: McGraw-Hill Yearbook of Science and Technology, New York: McGraw-Hill, pp. 375-377 (1992).

Research on pedestrian crowd characteristics and behaviours in peak-time on Chinese campus

J. Shi[1], Y. Chen[1], j. Rong[1], and F. Ren[1]

The Level of Service (LOS) is an important and necessary in evaluation on pedestrian crowd characters. It is necessary to obtain the parameters for evaluation on the facilities by analyzing the pedestrian crowd characteristics. In China, there are many crowded sites, and the authorities of government take seriously on traffic sites considering the public use, along with economic development. In crowded sites, both making analysis on pedestrian crowd traffic characteristics and to verify the LOS of the related sites, are important in practice.

In this article, in peak-time on Chinese campus, some sites may assemble pedestrian crowd, information of pedestrian crowd are surveyed, which are obtained from digital files of video cameras. By observation and measurement, the traffic environments and pedestrian traffic parameters including speed, density and volume, can be obtained. Then the relationships between parameters and the distributions of the parameters are analyzed, which is the basement of calculating the LOS of the spots and facilities and modelling. Subsequently, pedestrian crowd traffic characteristics in different sites could be supervised easily. Furthermore, pedestrian crowd behaviours and characteristics would be analyzed in details with more attention. As a result, it is used for reference on management in daily work and the same to decision-making on evacuation of pedestrian crowd in emergency.

1.   Introduction

University campus is a location where exists pedestrian crowd and there appears pedestrian peak volume in certain place several times daily. In crowded locations, the pedestrian LOS (level of service) is low and it would induce hidden trouble, which is a potential threaten to public safety. So it is necessary to analyze the crowded pedestrian characteristic in the related spot on campus.

The people on campus, which consist of many students, mostly are young men and they often are the majority in event. The ingress and egress on campus are similar to those events, such as hunting job agora, sports match and other business and cultural activities. Therefore, it is useful for the management, operation, and suggestion in work to study the pedestrian crowd characteristics on campus. It also can be reference for big event. In China, it is lacking that research on pedestrian in big event before. With the development of Olympic Games and World Expo being held, pedestrian design and management are taken more serious, which prompt the research on pedestrian crowd.

The frequency of pedestrian crowd peak is high on campus is easy to survey repeatedly and the pedestrian characteristic is similar to that in big event. So the study is helpful to the combination of the research results before and actual situation and it will promote the related research.

[1]Transportation Research Center, Beijing University of Technology
Shi Jiangang, Ph.D. Candidate, gangfish@emails.bjut.edu.cn

2.   Background

In this paper, teaching building, library lobby, entrance and related route of dinning room, and the way on campus in Beijing University of Technology are surveyed, for there may congregate pedestrian crowd in some periods such as in long break in the morning, the time when class is over before noon and library is closing. When students walk to change classroom for different lessons, for lunch to dinning room, to return dormitory, they in and out of building ingress and egress pedestrian. In bottleneck of walk route, pedestrian should queue for egress in someplace and it bring crowd group, for the supply is lower than the pedestrian demand. So pedestrian crowd in different spots should be surveyed and measured, the analysis of pedestrian characteristic will be the reference of research on pedestrian behaviours in event for the management and operation.

The videos are mainly by monitor cameras (See figure 1). The dimensions of spots are measured in locale. The pedestrian characteristics are measured by manual work and the data is processed using computer. Cameras are set up on high position and they work 24 hours a day. Once somebody walks in the view range of camera, the movement will be recorded and saved in video files. They are the original materials in measurement. It is important that pedestrian in the videos is their movement truly for the camera can never disturb or influence their own behaviours. Because nobody will look at the cameras with curiosity and students walk as normal, the characteristic measured will embody the real situations without survey disturb.
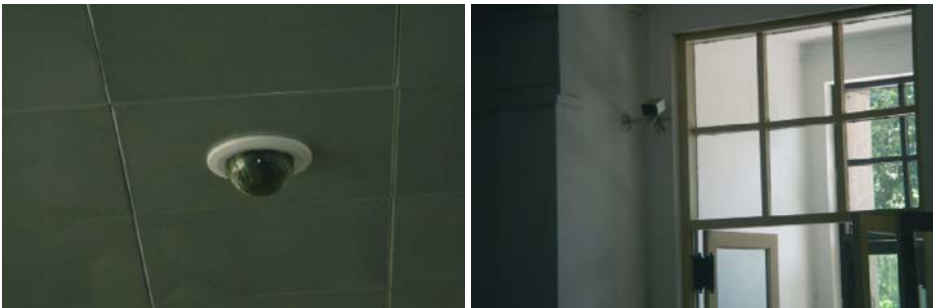

Figure 1: Cameras in monitoring system on campus

In long break in morning, students should change their classrooms for different lessons, so they come and go among teaching buildings, laboratory buildings and reading rooms, thus congregate in entrance, stairs and the way on campus. When it is going to noon, students walk from buildings to dinning rooms, they congregate in the paths and entrances. When library is being closed, students leave altogether but they should walk through detect gate one by one, there will appear shockwave. Pedestrian crowd characteristic in the spots mentioned above are different, so the surveys proceed respectively. The surveys will be described and the figure 2 shows the main spots in north zone of campus. The photos of survey spots are in figure 3 as follow.

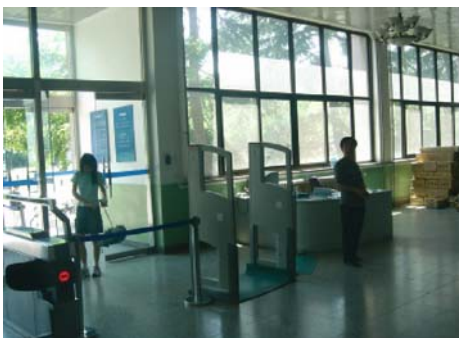**Figure 2**: The main survey spots in north zone of campus of BJUT

Figure 3: Photos of survey spots

a) Main stairs in No.1 T-building   b) South exit of No.1 T-building
c) Detect gate of library   d) Crossing in North zone

Figure 3: Photos of survey spots

      e) Exit of No.5 dinning room   f) Stairs of No.7 dinning room

3.   Pedestrian characteristic analysis

3.1.   Stairs and south entrance of No.1 teaching building

There are many classrooms for lessons in No.1 teaching building, which are used in high frequency. When class is over for morning long break or lunch, students will congregate on stairs and in the entrance area. For the go and come pedestrian flows, there also are conflicts in walking. Each spot, two periods including long break and after class finish for lunch, are surveyed. The width of stairs is 2m, and the south entrance consists of three doors side by side, with 1.4m width and 0.4 spacing. The inner doors are always open and the outer doors will be open by pushing (See figure 2(a) and 2(b)). The results of analysis are showed in figure 4, figure 5 and figure 6.
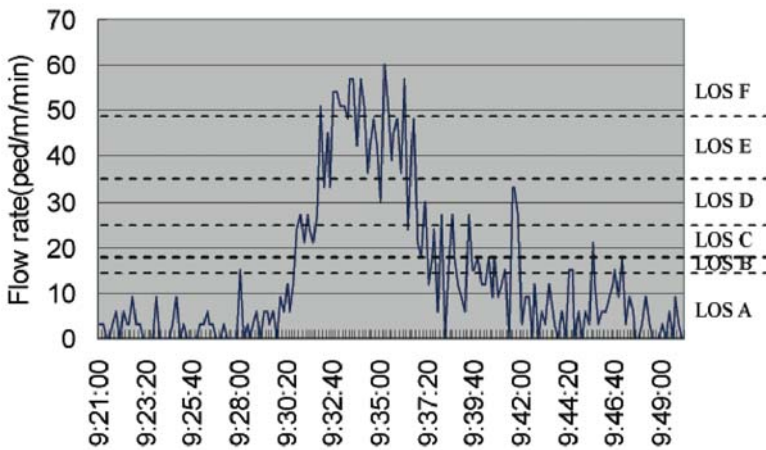

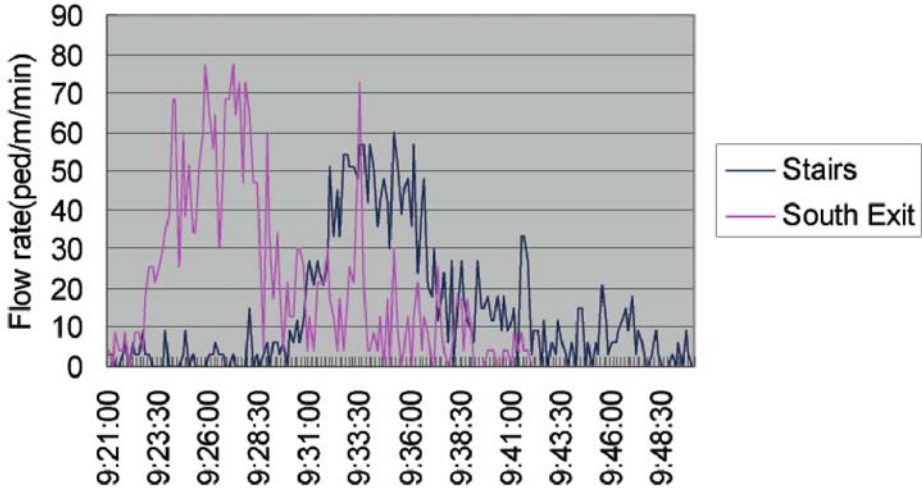**Figure 4**: Pedestrian flow on stairs and the LOS analysis

Figure 5: The contrast of pedestrian flow of stairs and that of south entrance
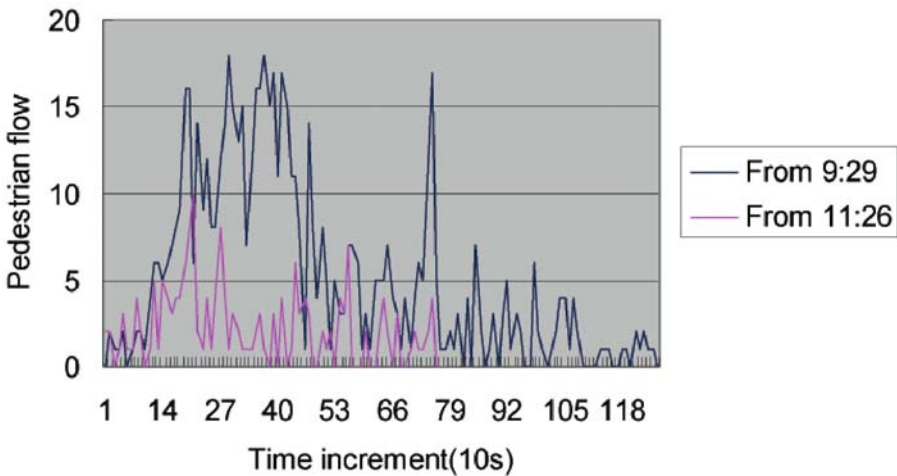

Figure 6: Contrast of pedestrian flow in different period of south entrance

The distribution of pedestrian flow on stairs is normal and it dropped to LOS F in short periods (See figure 4). That of south entrance is asymmetry distribution with higher maximum flow (See figure 5). There are two reasons: one is that the capacity of plane is larger than stairs, and another is that the flow fluctuates through the door, pedestrian queue and accumulate in block occasionally, which makes flow change suddenly and form a flow peak. For the stairs has continuous space, the pedestrian flow in there runs more stably and smoothly than it in the entrance area.

To contrast the pedestrian flow in different periods, the two flows in stairs are similar but the flows in south entrance fluctuates sharply (See figure 6). The reason results in the function of buildings and the location. For the stairs is a certain way after class but the later is an alternative one. Pedestrian demand, flow and the behaviours in the two periods are different obviously. In the morning long term break, students make transfer from classrooms or study spots and they choose the route through because most of study spots to the south of No.1 teaching building. But near noon, they walk ahead to dinning rooms and dormitories to the north, so the flow decrease rapidly. So when do planning on buildings, including the use of building, capacity and layout, it need to think the management according to pedestrian demand seriously.

3.2. Library

A detect gate with 1m width is set between the entrance and the lobby of library (See figure 3(c)). When the library is being closed, students in different reading rooms would leave in succession and gather in the lobby, then walk through the detect gate to get out. In this area, because in the lobby the arrival flow from rooms is higher than departure flow, for students should walk through the gate one by one, a shockwave forms in the lobby on the upstream of the gate. A video file of one night is used in the survey, and the period is 9min long from 21:44 to 21:53, the accumulation and evacuation course are recorded and the flow consists of 363 pedestrians. The data histograms and analysis are showed in figure 7 to figure 9.
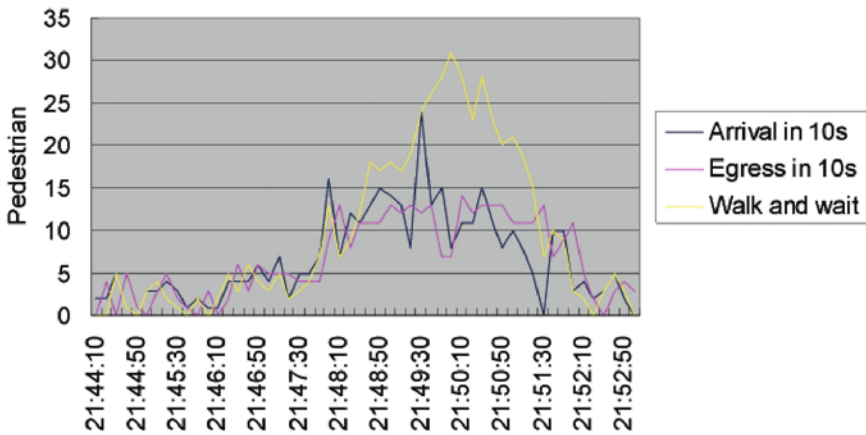

Figure 7: Pedestrian arrival and evacuation in every 10s and the number of pedestrian walking in lobby with 10s interval
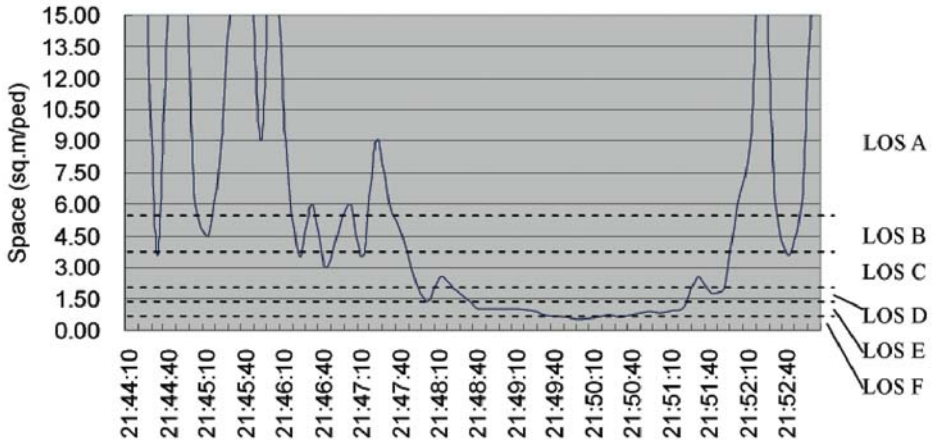
Figure 8: Average occupied space of pedestrian in library lobby
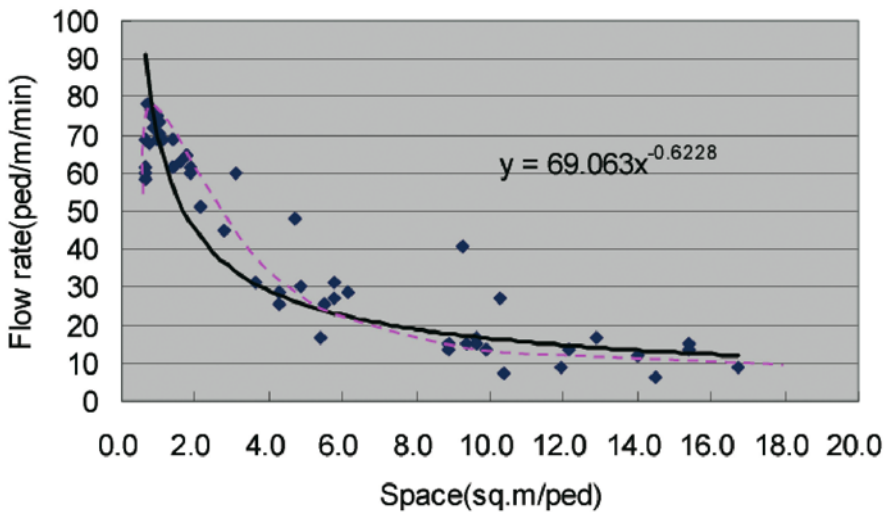

$$y = 69.063x^{-0.6228}$$

Figure 9: Relationship between space and flow rate

At 21:49:50, the detect gate alarmed and the pedestrian flow had been paused for a short time. Then a small scale shockwave appeared. It can be seen directly in the figure that in the related periods the accumulation upstream pedestrian increased and the LOS fall down for the capacity of the gate run to zero and reached to normal after a while. To discuss the relationship between space and flow rate, in figure 9, the dots are sample measured, the black continuous line is the regression curve with equation and the pink dash line is the trend curve. The later curve is consistent to the former research results.

The X-coordinate of intersection of two curves is LOS F threshold, which shows that pedestrian flow is influenced and disturbed easily and the movement is going to unstable.

3.3. Crossing in north zone of campus

The crossing in north zone is an important spot on campus, for it is the junction of teaching area and living area (See figure 2 and figure 3(d)). To the northeast of crossing there is a kiosk for papers and magazines sale (in the left of photo) and many campus associations propagandize on roadside (in the right of photo). In crossing, the space is open and the density of crowd is lower than in building when there are many pedestrians after class. The direction of pedestrian is at will and there is not forcing flow. But in crossing the cross of different direction pedestrian and the activity on roadside, some factors will influence the movement of pedestrian. Figure 10 shows some sample dots measured from video, which is the relationship between speed and flow rate there.
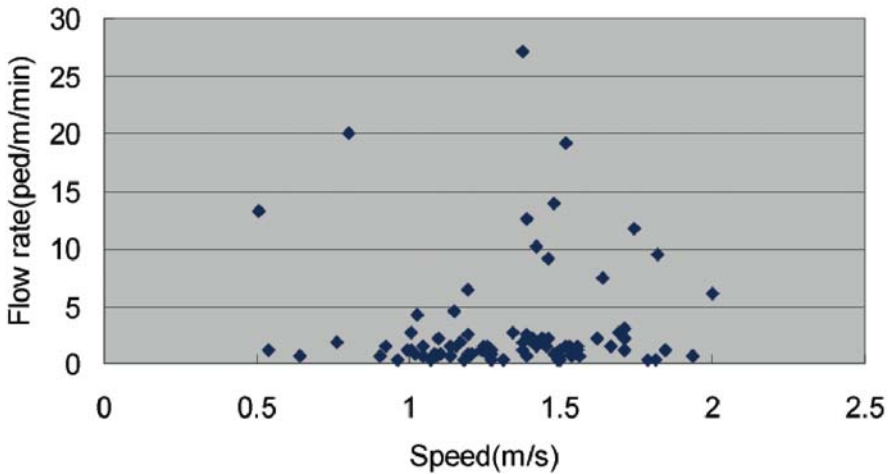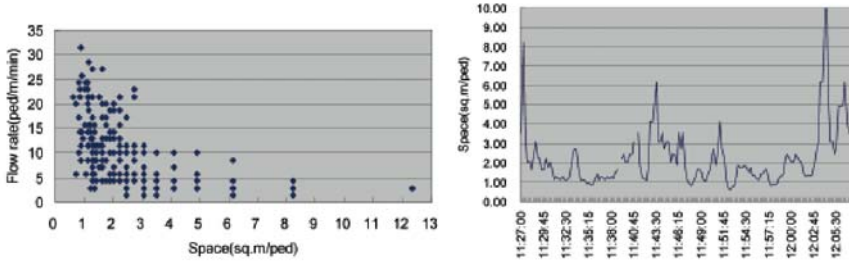

Figure 10: Relationship between speed and flow rate in crossing of north zone

3.4. Entrance area of dinning room

The entrance of No.5 dinning room and stair path of No.7 dinning room (See figure 3(e) and 3(f)) are surveyed and the pedestrian flow distribution and the relationships between characteristics are measured. The width of entrance of No.5 dinning room is 2.8m and the length of survey area is 2.2m. The stairs of No.7 dinning room surveyed consists of 13 stages, which is 0.14m high, 0.30m long in walking direction and 1.6m width between balustrades.

The pedestrian LOS in different periods in the entrance area of No.5 dinning room are above E class and most of them are above D class (See figure 11(b)). The speed of pe-

a) Relationship between space and flow rate   b) Space diversification with time

Figure 11: Pedestrian characteristic analysis of No.5 dinning room
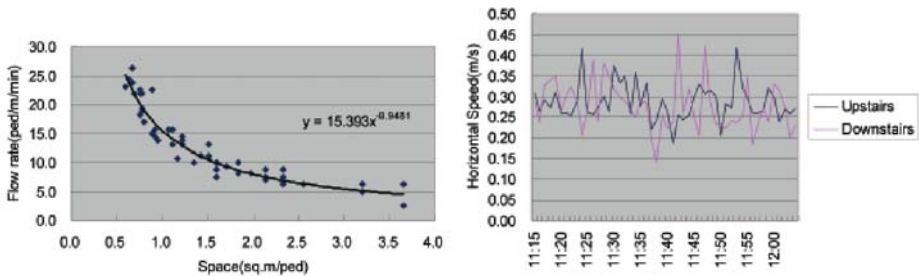
a) Relationship between space and flow rate   b) Speeds of upstairs and downstairs

Figure 12: Pedestrian characteristic analysis of No.7 dinning room

destrian upstairs and downstairs fluctuate with a median 0.30m/s, which is located LOS F class reference to the criteria in HCM2000. But there are not in high density and crowded pedestrian flow, so it illustrates that the speed in this type area is lower than others. Furthermore, the difference between upstairs speed and downstairs speed is little.

4.   Pedestrian crowd behaviours

In general, the pedestrian behaviours on campus are described after surveys in different spots. The pedestrian characteristics can also be known in sense.

4.1. Pedestrian movement tactic and direction

(1) On stairs when the pedestrian flow is not high enough, two directions pedestrians, downstairs and upstairs, would become troops and each group occupy one or two lanes, for sometimes a group may separate by another group in opposite direction. In the survey of No.1 teaching building, in the survey period, the pedestrian flow downstairs is much more than that upstairs, and the space time between adjacent flow tides is small.

When the pedestrians going upstairs want to move on, they took two tactics. (a) They keep waiting until the density of stairs is lower or they have accumulated in large group with more people over the group going downstairs which made them in dominance. (b) Some impatient pedestrians shove up along the balustrade, sometime they sandwich sideways for less friction. It decreases the waiting time but the speed is very low and it is very uncomfortable. Different tactics and directions result from individual psychological characteristics and the behaviour result in the judgement and decision-making in the special situation then.

(2) Kiosk on roadside is a spot which may attract some pedestrians staying and browsing. There is space between kiosk and tree, which is on the short way between the crossing and entrance of dinning room. Some pedestrian slow down and some pedestrians would stay or make a halt becoming surround crowd. At first, pedestrian who make no interest to the kiosk would walk through the area directly beside the standing students, or make a circumambulation through the area. While the stayed crowd enlarge (from crowd 1 to crowd 2), there are more frictions on the route and the body touch is inevitable if they continue walking through, pedestrian in upstream will change their direction and move tactic. They walk towards east and turn to north when near the entrance. Like a triangle, route 1 is the bevel edge and route 2 consists of two right edges. The later is a chosen result from the convenience and friction resistance (See figure 13).
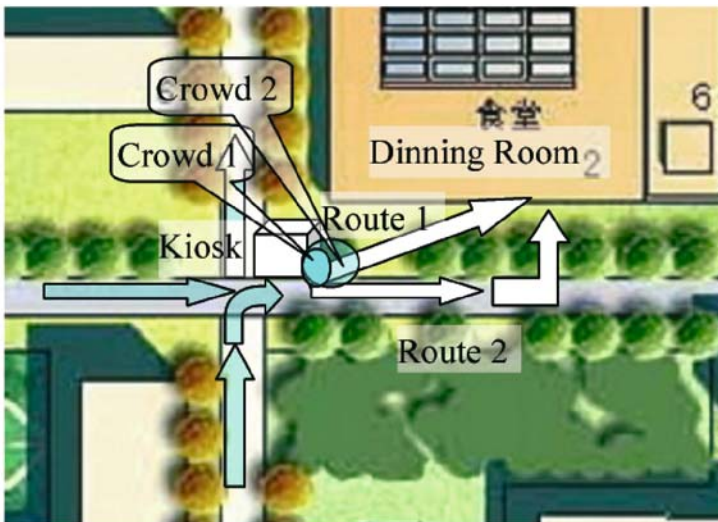
Figure 13: Walk route changes by the influence of kiosk

(3) Pedestrian on roadway on campus, often take little restrict in the walk environment in low density, and the trajectory is a fluctuate line with a straight direction. For the main destination is a guiding, the breadth of walk wave is small when pedestrian near a linear subject of reference, but pedestrian in middle of roadway will probably walk in an in-straight trajectory, for adjust or sway in landscape orientation. On the roadway in high

density, pedestrian sway breadth is limited by each other, and the trajectory is a sway line with small breadth.

4.2. Pedestrian party and crowd troop

In high density or flow, pedestrians will become crowd troop. In some environment, there is no more space for the faster to overpass the slower, so the later pedestrian must follow the former in sway trajectories.

Some pedestrians walk in party, and when the party meet or walk together with a large crowded group, the interaction of pedestrians in the party become feeble since the party will merge into a larger crowd group, only if the small party walk different from the group strongly. Space among members in the party is equal or similar to the space among the troop. Parties merge into troops and they can be managed as a whole group. The self-organize phenomenon is a good factor to utilize the facilities in high efficiency in order. Pedestrians under similar status, background, motive and direction would possess less private space, if they know each other. The parties are thought as a troop more easily and the will be prompted when private space decreased.

4.3. Environment influence and pedestrian response

Environment will influence pedestrians and individuals in crowd troop will appear respective response. The ratio influenced by environment in crowd may produce different effect on the whole movement. (a) The minority walk tactic change influenced by environment and they disengage from crowd troop. The whole troop movement will appear fluctuation and shock and adjust to normal state. (b) The majority change walk tactic or movement, the rest consist a new group. In general, the first condition will do more harmful influence, and the second condition is mainly result from guiding signs.

In the case of crossing survey, the stay time in front of kiosk are measured and made statistic analysis simply. The maximum is 150s, the minimum is 5.5s, the mean is 48.3s and standard deviation is 41.2. The results narrate that individual characteristics are very different when there exist an environment influence. More sample and detail analysis should be used to explain the environment influence.

5. Motivation for future research

More detailed work should be done to find out more useful data in detail from video files. In the article pedestrian characteristics and their locomotive behaviours are analyzed and some relationships between traffic parameters are obtained with regression method in some spots on campus. But it is need to enlarge the number of sample to increase the accuracy of measurement with more observation and survey, such as the distribution of speeds in different spots. The relationships between pedestrian characteristics, motives and behaviours should be analyzed more deeply, which are useful to improve management, operation and design.

To estimate pedestrian state in a certain facility, pedestrian satisfy level can be a criteria and the classify method can refer to customer surplus in economic theory. For with the increase of density, individual private space will decrease with respective expected. The decrease of LOS of facilities may not results in individual satisfy level synchronously in the same grade. It means different LOSes in different facilities are maybe in same satisfy level. The sense of user is an important factor in management. It should be based on a lot of questionnaires.

6.   Conclusion

Pedestrian demand fluctuated in different spots on campus and pedestrian crowd congregate in high density in some spots and periods. The total number and the period are under controlled by the whole arrangement on curriculum schedule. Resulting from walk motive, direction and space, individual characteristics of students are similar in troop movement. Individual deviation in group is little, which is benefit to the order of crowd troop, pedestrian public safety and the use efficiency of facilities.

The principle of "more haste, less speed" should be enshrined, especially in pedestrian crowd. A troop move together is to decrease the individual deviation, and it is to decrease the conflict among pedestrians. Thus, less unnecessary adjustment of movement will promote the walk efficiency and exclude the outer and inner disturb. The crowd troop will be more stable. As a result, to keep the order of pedestrian crowd is a priority in management and operation, which is also an essential work. **«**

References

1.   R. Futian, L. Xiaoming, R. Jian, et al.: *Traffic Engineering*, People's Communication Publishing House, Beijing China (2003).
2.   Transportation Research Board, Highway Capacity Handbook 2000, National Research Council, Washington D.C. (2000).
3.   M.R. Virkler and S. Elayadath: *Pedestrian Density Characteristics and Shockwaves*, In: Proceedings of the Second International Symposium on Highway Capacity, R. Akcelik (Ed.), Volume 2, pp. 671-684 (1994).
4.   S.P. Hoogendoorn: *Walker Behavior Modeling by Differential Games*, Delft University of Technology, Work paper, 2002.
5.   S.P. Hoogendoorn and P.H.L. Bovy: *Normative Pedestrian Behavior Theory and Modeling*, 15th International Symposium on Transportation and Traffic Theory, Sydney (2002).
6.   S.B. Young: *Evaluation of Pedestrian Walking Speeds in Airport Terminals*, The 78th Annual Meeting of the Transportation Research Board (1999).
7.   J.S. Milazzo II, N.M. Rouphail, et al.: *Quality of Service for Uninterrupted Pedestrian Facilities in the 2000 Highway Capacity Manual*, The 78th Annual Meeting of the Transportation Research Board (1999).
8.   S.P. Hoogendoorn: *Microscopic Simulation of Pedestrian Flows*, The 82th Annual Meeting of the Transportation Research Board (2003).

Behaviour on tunnel fire

L.C. Boer[1] and D.W. Veldhuijzen van Zanten[2]

Motorists drive through tunnels at high speeds. In consequence, they see the tunnel in a flash and have no idea how the tunnel looks like when they have to walk in the tunnel, for example, when evacuation is required. The authorities responsible for evacuation (and escape signs) are experts who fail to see the tunnel the way the general public does because they know too much. TNO studied how the nonexpert (the general public) reacts to signs when instructed to evacuate. The results showed that escape ways are ignored, and should be improved, for example, by making escape doors look like exits rather than access doors to technical rooms. One of the keys to improvement is a better signal-to-noise ratio, the signal being the evacuation signs—the noise all other visual stimuli including cars with flashing alarm lights. In a follow-up study, TNO investigated how motorists react to an unannounced disaster. Seven different groups of 50 cars each participated. They got stuck behind a „burning" heavy-goods vehicle that blocked the roadway. The study showed that motorists decided that the problem was a normal traffic jam, and so ignored the threat, waiting for the congestion to dissolve. This shows the need for an adequate „wake-up message" in order to start an evacuation.

How do motorists react to a fire in a tunnel? Recent disasters have shown underuse of safety provisions like emergency doors. The Dutch Civil Engineering Division of the Department of Public Works and Water Management, Centre for Tunnel Safety, commissioned TNO to carry out studies to record the behaviour of motorists in tunnel fires. There are all kind of rumours and stories about how people react, and it would be a pity to spend money on solving a problem that on closer inspection was just a tall story. Objective data help identifying the real problems.

The first question addressed in this paper is: How do motorists see the evacuation provisions of the tunnel (do they see the evacuation provisions of the tunnel at all)? The second question addressed in this paper is: How do motorists react on a truck on fire in a tunnel (do they react)? We begin with the question, then come back to the second question.

1.   Do Motorists See the Evacuation Provisions of the Tunnel?

Cars drive through tunnels at speeds of 80 km/h or more. In consequence, motorists see little of the tunnel and its evacuation provisions. They look forward, not sideways, and the signs on the wall flash by. Figure 1a is an artist's impression of the perspective while driving through a tunnel. The tunnel is narrow, and the walls seem to rush past. The perspective is completely different when one walks the tunnel as a pedestrian. All of a sudden, the tunnel is huge, much longer than imagined, and all kind of details on the walls and the roadway become visible. Figure 1 illustrates the difference.
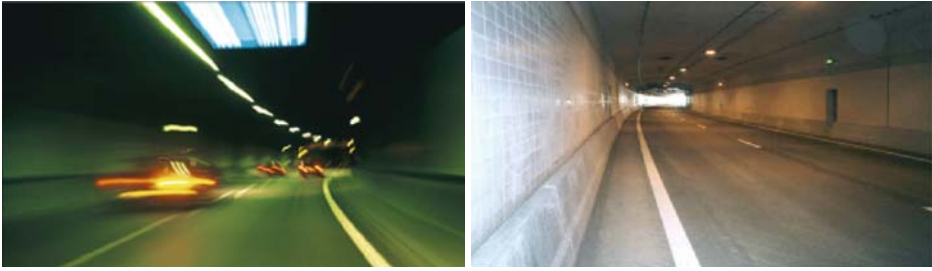

[1,2] TNO, box 23, NL 3769 ZG

Figure 1：Artist's impression of the motorist's perspective while driving through at a speed (left; source: www.tunnelveiligheid.nl) and the perspective of the evacuee at pedestrian speed.

People may use the tunnel daily as motorists, but still have little idea of how the tunnel looks like from the pedestrian perspective, walking at a speed of 5 km/h. They simply don't know the tunnel! TNO asked motorists who used the tunnel frequently, sometimes 10 times a week, whether there were emergency exits. Thirty percent did not mention the exits; when prodded, still 13% were completely unaware about the emergency exits. We asked those who were aware about the emergency exits which side of the tunnel had these exits. Only 54% had the correct answer (Krul & Boer, 2002) which is not much considering that guessing would produce 50% correct answers. We conclude that motorists don't know the tunnel from the pedestrian's perspective!

Then, we brought individual motorists actually over to the tunnel, 1-km long, and let them leave the car with the instruction „find refuge". They were left to their own devices; there were no additional instructions, and no other persons present. Many (24%) ignored the emergency exits completely, and evacuated over the roadway back, 500m. Being in the tunnel as a pedestrian was apparently not enough to make use of the emergency exits.

Did the test participants see the doors? Well, if they did, they did not see them as doors they could use. Apparently, the marking of the doors as emergency exits is poor. In another investigation, we let people find the escape way of a ship's interior. Missing the door was the most frequent error made. With a corridor nearby, 1 out of every 3 participants ignored the emergency door, despite its markings. These participants preferred the corridor nearby (Boer, 2001). Figure 2 shows the emergency exits of two tunnels in The Netherlands, both marked with an illuminated double-sided sign (running manikin, arrow, and door symbol).

The marking at the emergency door seems adequate; moreover, it satisfies the regulations. Adequate—that is, in the eyes of those who operate the tunnel, and the people who inspect the tunnel. These experts know perfectly well that there are doors for emergency situations, and that these particular doors are for emergency. They know also about the subsequent escape footpath that continues all the way into the open air. In fact, they

Figure 2: Marking of emergency exits with illuminated signs above the door (situation 2001 and 2004, left to right).

don't need any sign at all. For them, the signs are an extra service. But our studies show that the public needs more than these signs. We conclude that the emergency exits of Figure 2 are marked inadequately, and need improvement.

Improving the marking is not simply a matter of „crying more loudly". At first sight, this seems to be the solution with, for example, blinking or flashing lights. For human beings, however, the ratio of visual signal to visual noise is critical. The visual signal is the escape sign; the visual noise is the remainder of the visual surrounding. A flashing sign can be very conspicuous (e.g., on a quiet night) or very inconspicuous (e.g., in a disco surrounded by multitudes of flashing lights). Note that in an emergency the tunnel can be filled with cars with flashing alarm lights.

A better solution is to reduce the visual noise; in the examples shown in Figure 2 by removing the letters „2D" from the door, or reducing their size, or placing them away from the door (the other door in Figure 2 carries the letters „1N"). To be sure, the experts know that these letters mean „the second door of the D, or 4th tube", and „the first door of the North tube". The public, however, doesn't know what to make of these letters, and interprets them as „staff only", „not for us" or something similar. Moreover, people looking for refuge are psychologically tense and anxious, and are easily chased away. In another study, we observed that a sign „crew only" was enough to put out many test participants (Boer, 1993).

2.   Do Motorists React on a Truck on Fire in a Tunnel?

Self-rescue is very important because rescue workers need, say, 15 minutes to arrive on the scene. During this period, motorists are left to their own devices. Quick action is recommended because the situation for escape is best during the initial period. The question of the investigation was: how do motorists react to the unannounced emergency „truck on fire".

Specific questions were how long it would take motorists to get out of their cars, and their willingness to let go of the car. Group effects make the behaviour unstable; the initiative of one single motorist can start a complete evacuation. Therefore, the test was done 7 times, with new participants each time.

We will describe this study in some detail. Elaborated versions are available from the author (Boer, 2002).

2.1. Methods

Participants

Participants were recruited for pay with the suggestion that driving behaviour in tunnels was studied. Seven groups of 45-50 motorists participated (total 328). At the test location, they received (and subsequently signed) an instructions form that repeated the aim "to study driving behaviour" and added "you will drive through the tunnel a couple of times; please drive as you would normally do; things can happen on a ride but they are all fake and without real danger; however, react as if they were real; our first ride is to get to know the tunnel; drive carefully, no overtaking".

Test Location

The scene of the tests was the Benelux tunnel, tube D; Tube D was closed for normal traffic. The tunnel is 1 km long, runs underneath the port's main waterway, and is part of the motorway circle around Rotterdam. About 40 000 000 vehicles use the tunnel every year (10 M/tube). The speed limit is 100 km/h. The studies were done in winter evenings—no daylight and temperatures close to freezing.

All doors were sliding doors, ½m above the road, with two steps in front of them. A (horizontal) force of 8 kg was required to set the door into motion, a force of 5 kg to keep the door moving. Doors self closed if released.

Figure 3 shows the tube and the emergency doors every 100m (to the motorist's right hand side), and numbered 1-12. The doors in the middle of the tunnel, 6 and 7, were 50m apart. A pump installation at the deepest point blocked the escape path between doors 6 and 7. The signs in the escape footpath always pointed "upwards"; that is, at doors 1-6 they pointed South; at doors 7-12 they pointed North. The signs were illuminated from the inside and showed a running manikin; an arrow, and a rectangle—see Figure 2a. During the studies, there was a steady airflow of ½ m/s in the direction of driving (North).

Materials

A truck was available with a smoke generator in its load compartment. Containers with "gas smell" were also available. Loudspeakers in the tunnel could make public announcements.
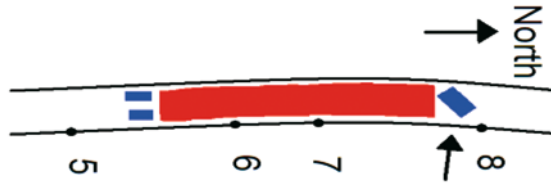
Figure 3: Test location: Benelux tunnel. (The side arrow shows to the location of the „burning"
truck.)

Procedure

On arrival at the test location, participants were parked over two lanes on the road 500
m before the tunnel. They read the instruction form and their questions, if any, were an-
swered. Two test assistants, posing as ordinary participants, closed off the "formation"
at the rear end. At a go-signal, the formation departed. The truck, until then parked 300
m down the tunnel, started driving at a 30 km/h speed on the left lane, its alarm lights
flashing. The first participants saw the truck shortly after entering the tunnel.

Some 320 m further down the tunnel, the truck came across the road and stopped, blo-
cking both lanes. This was some 25 m before emergency door 8, and 75 m after door 7
(see Figure 3). Smoke developed during the move across the road and continued until
the end of the test. Meanwhile, one of the assistants evaporated gas smell from the back
of the queue.

Five to six minutes after the stop of the truck, the loudspeakers announced "attention,
attention, there is explosion danger; I repeat, there is explosion danger". Two minutes la-
ter, there was a second announcement "please leave the tunnel, please leave the tunnel".
The announcement was repeated at 30 s intervals until the tunnel was empty.

At the end of the test, participants were escorted back to their cars. They were debriefed
about the purpose of the test; asked (by a show of hands) whether they had experienced
the test as "thrilling". Then, they boarded their cars and left the tunnel.

2.2. Results

Observations

In 6 out of the 7 tests, motorists remained in their car without taking action until the
announcement of explosion danger, 5-6 minutes later.

In only 1 of the 7 tests, a few motorists left their car immediately, even while the rear of
the queue was still closing in. Others followed the example (herd behaviour). Motorists
disappeared behind the emergency doors, but some of them began to use the door (and
the steps in front) as an observation post. Others followed this example. Two to three mi-
nutes later, the evacuation was stagnant. Motorists came back from the escape footpath,
apparently curious to see what happened. Then, the first announcement came.

In all 7 tests, this announcement was sufficient to (re)start the evacuation; motorists left their cars, sometimes in a hurry, and disappeared through the emergency doors. The second announcement came 2 minutes later, sometimes in an already empty tunnel.

Figure 4: One of the tests of Study 2. (Pictures taken 1'31" and 4'49" after the stop of the truck in front; test participants don't leave.).

One test showed extreme passivity among the motorists in front. The head of the queue was gradually engulfed in smoke (due to an airflow problem), but motorists remained seated in their cars, and failed to react to the first announcement (as all others in this and the other 6 tests did) even while their colleagues further down the queue left the tunnel. Two minutes later the second announcement "please leave the tunnel" made these motorists in front to leave their cars and go through the emergency doors. Figure 4 shows some pictures.

Miscellaneous observations were
a)   No participants went past the fire to the nearest emergency door.
b)   Some participants used the telephones in the tunnel. In one test, this lengthened the evacuation period.
c)   A few participants stopped their evacuation to return to their car to make some adjustment, than resumed evacuation. In one test, this lengthened the evacuation period.
d)   Congestion at an emergency door was observed once because many participants arrived from both sides simultaneously.

Debriefing remarks

During debriefing, 13% of the participants admitted (show of hands) to have experienced the test as "somewhat thrilling"—a few even felt "threatened". Incidental comments to the test assistants revealed some indignation about the instruction „the first ride is familiarisation" whereas it was the one and only test ride. [TNO explained that this was done deliberately.] Questioned why they did not react to the incident, a reply heard more than once was "no-one else did anything".

3.   Discussion

Passivity prevailed. In a queue (backup), motorists failed to react to a situation of possible danger, and remained seated in their cars. This tendency to stick to the original role (the motorist's role) is also reported elsewhere (Canter, 1980). Passivity could be quite remarkable (Figure 4). A simple announcement "explosion danger" was sufficient to start the process of evacuation.

Spontaneous evacuation occurred just once, but came to a spontaneous standstill some minutes later, with motorists loitering on the road or around the emergency doors to see what would happen—curiosity. The announcement "explosion danger" restarted the process of evacuation.

The practical conclusion is that motorists need a signal for starting the evacuation; on itself, an incident is not enough to start an evacuation. The tunnel operator has great responsibilities because he is the one to start the evacuation.

Group behaviour (herd effect) was important in evacuation; where one sheep goes, another follows. Group behaviour made the simple announcement "please leave the tunnel" very effective; one or two motorists obeying the order, and going through the emergency door made others follow.

The negative side of the herd effect was reinforcement of passivity. When all motorists around you remain seated "no-one else does anything", and your tendency will be to remain seated as well. Another negative effect of group behaviour was when motorists started using the elevated emergency doorway as observation posts. Soon, groups were formed on the road around the emergency doors, and the evacuation came to a standstill.

When smoke takes away vision, group behaviour is also gone; there is no following of others if you don't see any others. This explains why the motorists at the smoke-engulfed front of the queue stayed in their cars; they were unable to see the motorists behind them leaving their cars.

Telephones in the tunnel are a mixed blessing. Overuse of telephones, congested lines, and extra mental load for the operator is likely. Moreover motorists may delay their evacuation because they are busy trying to make calls. An operator announcement is recommended: "the alarm has been raised—please no telephoning".

The behavioural studies demonstrated that talkers are not yet doers. Behavioural studies identify the real problems whereas questionnaires (or other opinion methods) run the risk of identifying both real and imaginary problems. Solving a real problem such as motorist passivity is worth the effort; solving an imaginary problem is a waste of resources. An example of an imaginary problem is walking past the fire (because the nearest emergency door is beyond the fire). Such risky behaviour was anticipated, but never observed. Another example of an imaginary problem is difficulty opening the emergency door (which is heavy and needs a special opening receipt). Problems opening the door were anticipated, but never observed in the current studies. The tunnel authorities can save the effort to „remedy" such imaginary problems, and concentrate the efforts on remedying some real problems. **«**

References

1. L.C. Boer: *Wayfinding during Emergencies*, TIEMS 2001 Conference, Oslo, June 19-22 (2001).
2. L.C. Boer: *Behaviour of Motorists when Escaping from a Tunnel*, Report TM-02-C34. Soesterberg, The Netherlands: TNO Human Factors, (in Dutch) (2002).
3. D. Canter (Ed): *Fires and Human Behaviour*, New York: Wiley (1980).
4. A.J. Krul and L.C. Boer: *Knowledge of Emergency Provisions in Road Tunnels,* Report TM-02-C08, Soesterberg, The Netherlands: TNO Human Factors, (in Dutch) (2002).

Earthquake – the importance of earthquake-resistant design in case of emergency evacuations

B. Çokcan[1], S. Brell-Çokcan[2], and K. Tavoussi Tafreshi[3]

1.   Introduction

Strong earthquakes can occur at irregular intervals, often separated from each other by long intervals. This is why the danger of earthquakes in many of the threatened countries is very often underestimated and regarded as a rather theoretical item. We should also remember: The existing earthquake maps in these countries are not accurate; Bam (Iran) and Kobe (Japan) were not listed among the most endangered zones on the hazard maps.

The amount of damage caused by earthquakes could increase in the future. This will not be due to a rise in the number and severity of quakes but rather to the increase in world population, linked to the growing number of crowded metropolitan areas and the increasing value of property and material in these areas. More than three-quarter of the mega cities in the world (cities with a population of more than 10 million) are located in endangered zones.

The most efficient way to avoid a disaster caused by earthquakes is employing earthquake-resistant design in seismically active regions.

2.   Earthquake-resistant design

2.1. The question of cost

The possibility of influencing a project's quality and cost is greatest at the early design stage, later this possibility decreases dramatically. Initial decisions on a project's structural concepts can do much to determine its ultimate seismic resistance, for better or worse. Even if no lives are lost, poorly performing buildings and their contents can suffer major damage, which can be devastating to occupants, e.g., tenants or businesses forced to vacate or to suspend operations.

It is possible to limit the most typical kinds of earthquake damage at very little additional expense. In short, owners' decisions to go for the lowest fee when negotiating design contracts may result in small initial savings, but can prove very costly later in the event of a destructive earthquake.

---

[1]II Architects int; Vienna University of Technology, Institute of Architectural Science/ Structural Design and Timber Engineering

[2]II Architects int; Vienna University of Technology, Institute of Architectural Science/ Digital Architecture and Planning

[3]Vienna University of Technology, Institute of Architectural Science/ Structural Design and Timber Engineering

Several studies have tried to estimate these costs through the use of representative case study buildings. These studies found that incorporating seismic resistance features into new buildings increases construction costs by about 1 to 2 percent, see table 1.

Building type	Estimated increase in construction costs (percent)
Low-rise residential	0,7
High-rise residential	3,3
Office	1,3
Industrial	0,5
Commercial	1,7
Average	1,6

Table 1: Costs of Seismic-Resistant Features in New Buildings [1].

2.2. Urban Strategies

Reducing the catastrophic effects of an earthquake depends primarily on political and economical decisions, which also very strongly affect the planning of urban strategies.
The areas that are required for urban development should be examined for the potential threat posed by the forces of nature.
At each location the expected damage to buildings and facilities caused by an earthquake depends on local ground conditions.
Therefore micro zoning of all earthquake-endangered regions, with measurements and data regarding the expected periodical ground accelerations and soil shifts (answer spectra) for different soil types, is essential.
As a further aspect of micro-zoning development plans should be drawn up for the respective regions. These plans should define the construction strategies and, above all, building heights, in order to minimize the resonance effect of seismic waves.
This procedure is a matter of course in most earthquake-endangered regions, but there are deficiencies in the practical enforcement of building regulations and zoning plans, which are hardly ever observed.
In the earthquake in Mexico in 1985 it was observed that the 20-storey buildings at the town center were put under the most stress because these buildings exhibited the same vibration response as the soil type in the area.

Many reinforced concrete buildings ranging between 7-10 floors in height in the district of Avcilar were seriously damaged or caused to collapse by the earthquake in Gölcük (Turkey) in 1999 because these buildings had an acceleration response similar to the ground type. The zoning plans for these districts were drawn up according to these soil conditions (soft soil) and they only permitted buildings of up to four floors in height.

To devise urban strategies, the planning authorities should base their planning on a number of different development scenarios for the area. The expected population, the location of industry and the degree of national importance must be taken into account. Before developing these districts the service facilities should be considered. To ensure that the emergency and disaster protection services function, an appropriate program must be drawn up.

2.3. Measures to be taken by architects and structural engineers

Different buildings affected by the same earthquake respond differently. The effects of the earthquake on a building depend on the specific characteristics of the structural system used in the building. One important building characteristic is the fundamental period of vibration of a building (measured in seconds). The fundamental period of a building depends on the stiffness of its structural system, its mass, and its total height. Seismic waves with periods similar to those of the building will cause resonance, and thus amplify the intensity of the earthquake forces that the building must resist. Structural systems using concrete or masonry shear walls are stiff and result in buildings with short periods, whereas more flexible moment-frame systems have longer periods. In general, a large portion of the earthquake energy is contained in short-period waves. Therefore, short-period buildings with stiff structural systems are designed to cope with greater forces than long-period, flexible, buildings. This concept is also applicable to the amount of force that individual structural elements and their components must resist. Stiff elements must be made stronger because they will attempt to resist larger earthquake forces than flexible elements within the same structural system. Shape or configuration is another important characteristic affecting a building's response. The shaking of a simple rectangular building by an earthquake results in a fairly uniform distribution of the forces throughout the building. In more complex T - or L-shaped buildings, forces concentrate at the inside corners of these shapes. Similar problems arise where the floor or roof levels of adjacent parts of a building are offset vertically (split levels), or when the first story is taller or „softer" than the other stories. Special design rules must be applied to irregularly shaped buildings because they can suffer greater damage than regularly shaped buildings.

The first goal of the earthquake-resistant design is to protect lives. In the past, most building-related deaths and injuries occurred due to the failure of the primary structural systems. But the standard of the earthquake-resistant construction for primary structural components has continued to rise. If new buildings follow the building design regulations their structural safety can, essentially, be taken for granted. For older buildings seismic re-fitting is probably necessary.

The second goal is to avoid and/or reduce damage to property. Many injuries, and a great deal of the total economic loss in an earthquake, stem from or are related to damage to non-structural components. The term „non-structural building components" refers to those elements of a building that are not part of the structural system that carries vertical and horizontal loads. Non-structural building components include architectural elements

such as suspended ceilings, parapets, partitions and cladding; mechanical elements such as HVAC ducts, equipment and associated piping; electrical elements such as lights and switchgear; fire sprinklers; and other integral parts of the completed building. Damage to non-structural components is a frequent cause of earthquake-related fires.

Another aspect is the psychological one the less damage that occurs to buildings, the more calm and considered the behavior of the people living in them. In such cases the evacuation can generally take place without any significant difficulties.

In a multi-storey building, the roof level and the upper story's are subject to greater motion during an earthquake. This is why the position of the non-structural components in relation to the base of the building is most important.

The earthquake forces acting on each non-structural component depend on the component's mass. For example, exterior claddings, such as pre-cast concrete panels are very heavy and require specially detailed connections to take the vertical loads. The fixing must also be sufficient to resist lateral out-of-plane loads. The fixings used for such elements must also be designed to accommodate thermal, wind and seismic in-plane lateral movements of the structural elements to which they are attached. In older buildings, cladding systems may be heavy, not particularly well anchored, they may not have been designed to cope with movement or may have worn or defective connections. If these elements fail during an earthquake they can be form a hazard to pedestrians around the building perimeter, especially at building exits. Parapets are also a cause for concern because their failure is dangerous for pedestrians around the building perimeter, especially at building exits. Parapets that are not properly anchored or braced may become loose and fall on pedestrians below, see figures 1-3. [2]

Figure 1: A building that did not suffer structural damage but the complete failure of the outer walls meant a risk of injury to pedestrians [3]

Figure 2: Failure of pendant light fixtures in a school library [4]

Figure 3: Damage to suspended ceiling and recessed ceiling lights [4]

Figure 4: Earthquake-damaged bookshelves [2]

2.4. Measures to be taken by tenants

Earthquake safety involves more than minimizing the damage to buildings. Earthquake vibrations may cause light fixtures and bookshelves to fall, and make other large items topple or move across the floor. Heavy crates or boxes stacked high, such as those in warehouses or discount stores, can fall on tenants, employees, or customers. This means that, to reduce the risk of injuries and the danger of blocked gangways and exits, the contents of the buildings should be properly secured, see figure 4. [2]

Heavy equipment and furniture should be fastened to the floor or to stable walls. Heavy objects should be stored on low shelves or in areas that pose fewer hazards. All beds ought to be in „safe areas," where someone can ride out an earthquake without injury. Falling window glass is a serious hazard. If a bed must be located under a window, safety film ought to be fitted. For further instructions see [4].

3. Behavior during a quake

Earthquakes occur suddenly and last only a relatively short time. Organized evacuations are possible only once the earthquake is over. The correct way to behave during an earthquake is something that should be learned by everyone. In Japan people do not panic during an earthquake because they have been educated in the appropriate behavior during and after a seismic shock.

The Japanese government spends approximately 3 billion dollars each year to ensure a functioning disasters protection program. A large part of this money is spent on the preparation and the development of evacuation possibilities. The law calls for people to be informed about how to prepare for the eventuality of an earthquake and how to behave when an earthquake actually happens. Earthquake drill in schools and offices in endangered areas is just as normal as fire alarm drill. Bells ring, sirens howl and thousands of schools children put a cushion over the head and creep under the tables or meet at pre-determined evacuation places. [7]

Each town and village has developed its own disaster control plan and many people form civil defense groups in order to avoid panic during or after an earthquake.

In Turkey it can happen that people jump out of windows because they have not been well trained in how to deal with seismic shock and because they have no confidence in the buildings.

In well-designed, earthquake resistant buildings it is advisable not to run outside the buildings during an earthquake. In such buildings total structural failure is unlikely. The greatest risk of injury during an earthquake is from non-structural hazards. During an earthquake one should stay away from heavy furniture, appliances, large panes of glass, shelves holding heavy objects, and stone claddings (such as to a fireplace). These items tend to fall or break and can cause injuries. Usually, a hallway (if it is not crowded with objects) is one of the safest places. Kitchens and garages tend to be the most dangerous. Also, the safest place in each room should be known, as it is difficult to move from one place to another during a severe earthquake.

All the possible ways of leaving houses and workplaces in emergency situations should be known. For further instructions see [5].

Figure 5: Children taking part in an earthquake exercise [7]

4.   After the quake: evacuation?

Following an initial earthquake, aftershocks can occur, possibly causing additional da-
mage (or even the first damage) to the building. If an earthquake could have caused
damage to a facility and the structural integrity of the building is therefore in doubt, buil-
ding occupants should be evacuated along pre-established evacuation routes, (provided
these routes are accessible and clear of obstacles), to a safe refuge before conducting
a preliminary damage assessment. Non-structural damage does not necessarily require
evacuation.
An inspection of the building should be carried out if the amount of ground motion was
great enough to cause books to fall off shelves.
A fundamental assumption in the evaluation process is that, in order to declare a struc-
ture safe, it must be capable of withstanding (at least) a repetition of the earthquake
that caused the initial damage without collapsing and without any additional risk from
falling (or other) hazards. It should be emphasized, however, that this is a minimum
requirement and that this engineering assessment is a difficult one to make.
Typically, damage to the structural system will show through non-structural finishes.
For example, cracks in stucco or plaster finishes can be assumed to be equal in size to
the cracks in the structural system hidden below the finish, for example brickwork walls,
concrete block walls or concrete walls. For further reading see [6].

A rapid assessment of damaged public and private buildings and infrastructure that ex-
amines the danger of collapse due to aftershocks is of great importance for the rescue
work, for evacuation or to plan the further use of the building. Buildings should be
classified in the following categories:

» "Still habitable"
» "No longer habitable"
» "May be entered for the clearance of the personal things at short notice"
» "Entry prohibited" [8].

Also the efficiency of so-called „life-line" systems must be checked (e.g. the load-car-
rying capacity of bridges, efficiency of the service facilities).
In this way the damage caused by aftershocks can be reduced and at the same time unne-
cessary evacuations can be avoided, thus reducing the length of the period until „normal
life" can be renewed.
As experience from abroad shows, rapid and efficient reaction by the authorities after
the earthquake is extremely important to calm the disturbed and frightened population.
The rapid evaluation of the stability of damaged buildings and service facilities is a
complicated task, which can be undertaken only by specially trained and experienced
civil engineers. Because of the large amount of damage adequate numbers of staff and
the appropriate organization are necessary. In order to meet this need, specialists should
be trained in advance in how to evaluate building stability [8].

Fires caused by earthquakes are a serious reason to evacuate. Particularly in cities with a natural gas supply this problem arises frequently. Gas lines and connections are subject to great stress by earth tremors. Gas can escape uncontrolled from these damaged gas lines, greatly increasing the danger of explosion.

Before the earthquake in Alaska in 1964 certain preventive measures affecting the utility systems had already been taken. The most important electrical generators were equipped with an earthquake-sensitive switch-off mechanism, while the main gas lines were automatically closed by a sudden decrease of pressure in damaged pipes. The result was that significantly fewer fires broke out after this earthquake [7].
However, at the Kobe earthquake in 1995 many lives were lost due to fire (350 fires). 100 hectares of residential area were burned down in few days. Many residential areas had to be evacuated due to the danger of further fire.

5.   Reconstruction

It is almost impossible to make all buildings earthquake-proof. Many of the earthquakes that occurred in the 20th century have shown us that, especially in the proximity of large cities, following an earthquake reconstruction measures are essential.
Following the catastrophic effects of an earthquake rapid reconstruction is of great importance. This goal can only be achieved, if a detailed and well-organized reconstruction plan has been prepared in advance.
To facilitate rapid reconstruction the following points should be dealt with before a disaster occurs:

» A legal base must be established for the conception, co-ordination, priority-setting and financing of the reconstruction.
» Creation of additional regulations for the assessment of facilities that have an unusually high danger potential. (Damage to or destruction of nuclear power stations, chemical plants etc. can cause additional disasters such as contaminated water supply, contamination of the earth, air pollution).
» The „lifelines" that are of essential importance during a catastrophe must be identified in advance. These include buildings, facilities and services that provide the necessary infrastructure required for survival. The minimum functions necessary to cope with the effects of earthquakes of different severity must be defined. („Lifelines" include, for example, hospitals, police stations, communication centers, transport routes etc.) All such facilities should be examined during construction for their resistance to earthquakes and should be particularly well equipped to deal with any possible catastrophes. Erzincan earthquake in 1993 – during this earthquake two of the three hospitals in the city collapsed and one was severely damaged.
» Earthquake insurance of the building should be required by law. This point is crucial for financing the reconstruction. Funds can be accumulated over a number

of years, making it possible to redevelop the areas affected, with or without small amounts of outside financing. A further possibility is outside financing by means of loans from the World Bank. After the earthquake in Erzincan, Turkey it was possible to rebuild the city thanks to World Bank financing (150 million USD).

» Disaster drill and evacuation training programs for the inhabitants
» Training of the local disaster organizations – a catastrophe can impose excessive strain on the local disaster emergency organizations. In this case additional local, national, if necessary even international level assistance is needed.

5.1. Looking after the Injured and Homelesses

The devastating earthquake in Kobe in 1995 killed 6,500 people, injured 40,000 and left 350,000 people homeless as well as causing more than 200 billion dollars of damage to property. The earthquake of Gölcük, Turkey resulted in 125,000 injured and an estimated 1 million homeless people.

These figures indicate the magnitude of the task of looking after people following an earthquake.

In order to care for people injured during an emergency and to look after those made homeless special organization is necessary.

In order to meet the spatial needs it is important that several large public buildings be defined as meeting places.

These defined buildings should be identified in annual disaster drills organized by civil defense organizations.

The routes or roads leading to these meeting places should be defined and signposted by a permanent system.

Lifeline facilities must be preserved to provide services and transfer injured people to hospitals. A properly functioning infrastructure can save many lives in an emergency.

5.2. Temporary Housing [9]

In the second stage „temporary rehabilitation" is a transition period that can range in length from several weeks to several months. The main concern is to establish a temporary social infrastructure to provide a minimum standard living environment. The major problem of this phase is the provision of temporary shelter that can be occupied until the completion of permanent housing.

Three alternative approaches to temporary housing can be listed. These are:

» Temporary settlement outside the disaster area: Victims of the disaster are sent to other districts until the completion of reconstruction activities. They are settled either in public buildings or at camping facilities specifically established for this purpose. Although this approach seems to initially solve the problem of shelter, it is not popular due to the disruption it causes to peoples' social and economic relations.

» Communal settlement within the disaster area: Victims are settled at camping facilities erected in the vicinity of disaster. This approach is recommended, as it is easier to administer and has a high cost-effectiveness factor. In addition to its advantages some problems must mentioned:

» Single private shelters are preferable to communal dormitories. Communal service facilities such as kitchens, bathrooms, etc. can be used in the short term.

» Temporary settlements are rarely left, even after the completion of normal residential buildings. There are many examples, such as Cholomo, where camps turn into permanent settlements.

» Temporary settlements have a three-stage development. In the first stage victims are ready to settle wherever they are sent. The second stage is the re-organization phase of the community and the formation of new social relations. In the third stage ownership patterns develop together with the extension of the original shelter accommodation [9]. «

References

[1]   S. Weber: *Cost Impact of the NEHRP Recommended Provisions on the Design and Construction of Buildings*, National Institute of Standards and Technology (1985).

[2]   Build to Resist Earthquakes, Applied Technology Council, http://www.atcouncil. org/pdfs

[3]   Earthquake Tips, Los Angeles Fire Department, http://www.lafd.org/eqtips.htm

[4]   A Homeowner's Guide to Earthquake Retrofit, Institute for business and home-safety, http://www.ibhs.org/publications/downloads

[5]   Putting Down Roots in a Earthquake Country, Earthquake Country Web Portal; http://www.earthquakecountry.info/roots

[6]   Post Earthquake Damage Evaluation, A Guide Book for Arkansas Schools; Arkansas Center for Earthquake Education and Technology Transfer, http://quake. ualr.edu/schools/guide/append1b.htm

[7]   B. Walker: *Erdbeben*, Time Life Bücher Amsterdam; ISBN 9-06-182-481-8

[8]   SGEB Swiss Society for Eartquake Engineering and Structural Dynamics; *Handlungsbedarf von Behörden, Hochschulen, Industrie und Privaten zur Erdbebensicherung der Bauwerke in der Schweiz*; Zürich (1998).

[9]   Chamber of Architects Turkey; *Urban Settlements and Natural Disasters*, ISBN 975-395-311-9 Ankara 1999 Yildiz Sey; Temporary Housing After Disasters (1999).

Decision Loads and Route Qualities for Pedestrians – Key Requirements for the Design of Pedestrian Navigation Services

A. Millonig[1] and K. Schechtner[2]

Based on studies about human orientation behaviour, the contribution presents a synopsis of main requirements for pedestrian navigation systems, focussing on the key qualities for designing pedestrian wayfinding systems and the consideration of landmarks as spatial information in portable pedestrian navigation services (e.g. in smart phones, PDA's, etc.). Mobile navigation services can enable pedestrians to achieve precise spatial information; yet the actual systems are not responsive to individual preferences of route characteristics.

In contrast to car drivers, pedestrians are characterized by several specific attributes: they are sensitive in terms of distance, acclivity and climatic conditions; they need salient landmarks for orientation and try to minimize the extent of mental work during the navigational process. Therefore, pedestrian navigation services have to offer a wider range of route qualities: e.g. convenience, attractiveness or safety.

To provide efficient navigational information for pedestrians, the consideration of three main route qualities is required: topography (physical quality), topology/attractiveness (psychological quality) and complexity (mental quality). Additionally, the definition of specific route characteristics is of great importance for the simulation of pedestrian flows to imitate route choice behaviour.

We give an outline of the most important design qualities for the development of route networks suitable for pedestrians' needs.

1. Introduction

Transport Telematic Systems so far have been mainly focusing on systems to enhance travel and transport by road bound vehicles or by public transport. They offer the possibility to plan highly complex interactions between different transport modes. The major fields of interest are positioning technologies and navigation systems. Navigation services for individual drivers are available as so called in-vehicle technologies and VMS (Variable message signs). Usually they provide the user with information about the "shortest" or "fastest" route leading to a desired destination.

There are two basic findings supported by the work done in research and implementation projects: first that different methods of positioning technologies should be combined in different layers to get as accurate information as possible in the most effective way, and secondly that the HMI (Human Machine Interface) design is a key element in the acceptance and usage rates.

[1]alexandra.millonig@arsenal.ac.at

[2]arsenal research, Human Centered Mobility Technologies, katja.schechtner@arsenal.ac.at
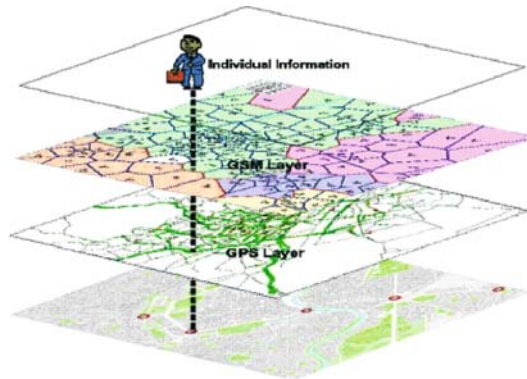
Figure 1: Information Layers (arsenal research).

Research shows that drivers perceive familiar routes as shorter and quicker, even when the navigation software calculates different routes. Therefore the users only change familiar routes when the benefit in time or cost is substantial and when the information about it is offensively presented and absolutely clear.

The same is true for pedestrians, but the challenge to precisely inform the users according to their needs is even higher.

In recent times technological progress has led to the development of portable navigation services (e.g. mobile systems applied to smart phones or PDA's), which allow pedestrians to gain navigational aid at any unfamiliar place. Still mainly common concepts for car navigation services are used to assess routes and to communicate spatial information to users on foot.

However, pedestrian's movements occur under different terms and conditions than the way drivers reach their destination. People travelling by car are bound to road networks and formal restrictions like one-way streets, speed limitations, etc. Pedestrians possess greater freedom in movement; they can walk in any directions they like and have access to places, where vehicles are excluded[1]. Another aspect concerns the fact, that car drivers own the opportunity to control their environment and are provided with a constant level of comfort (protection against climate impacts, dust, pollution, noise, etc.), while on the other hand walking people are exposed to a great variety of environmental impacts. Mobile navigation systems for pedestrians have to take these constraints into account and must consider individual preferences concerning specific route qualities to provide individually "optimal" routes.

In fact, the "shortest" route to a desired destination is not chosen in many cases. People often prefer the "most beautiful" or the "safest" route[2]. Studies on environmental preference and route choice behaviour confirm that pedestrians prefer certain routes owing to their environmental qualities, such as relative quietness and greenery[3].

Pedestrians are very sensitive in terms of different route attributes. But the definition of an "optimal" route network for pedestrians is hard to put into practise, as several

findings reveal differences in people's route choice behaviour[4, 5, 6]. These differences are on the one hand caused by several route characteristics and on the other hand by individual preferences. In this contribution the main characteristics influencing the perceived quality of a specific route are discussed.

2. Effects on Route Choice Behaviour

To identify the quality of a specific route, several attributes of the implied paths have to be taken into account, as the following examples show:

» Convenience: This issue is composed by many different factors. Convenience may be influenced by distance, acclivity, "Level of Service" (LOS) (frequency of pedestrians and broadness of the path) or environmental conditions like weather, noise or pollution.

» Safety: This issue includes aspects of traffic safety as well as spaces evoking fear in people passing through (e.g. dark underpasses or parks, disreputable quarters etc.)

» Attractiveness: People rather feel up to walk longer distances, if the surroundings are appealing.

» Simplicity: Given the choice between a short, complex route and an easier, but longer route, most pedestrians would choose the longer route[4]. The simplicity of a route depends on the number of decision points to be traversed and the number of salient landmarks along the route.

» Availability of facilities: A route where several attractive facilities can be found will be preferred to routes offering fewer facilities (e.g. shops, sights, rest areas, etc.).

» Availability of landmarks: Landmarks are vitally important in human navigation as they are used for the mental structuring of the environment and help to find the right way to a specific destination[7]. Routes with many salient landmarks can be followed and remembered easier and are considered a higher quality than routes with fewer landmarks.

Due to the numerous attributes influencing the quality of a route for pedestrian's needs, the proposition of the "shortest" route is insufficient and mainly required, if the individual is in a hurry. Depending on individual preferences and the actual purpose of the route, additional qualities are demanded, e.g. the "most beautiful", the "safest" or the "simplest" route.

3. Dimensions of Route Qualities

The different attributes affecting the perceived quality of a route partly interact among each other and can be combined to three main, interdependent route qualities concerning the topography, the topology/attractiveness and the complexity of a route.

Topography (physical quality)	Topology/Attractiveness (psychological quality)	Complexity (mental quality)
» Distance	» Attractiveness	» Number and complexity of decision points
» Acclivity	» Availability of facilities	» Availability of landmarks
» Level of Service	» Safety	
» Protection from negative external effects		

Table 1: Dimensions of Route Qualities.

3.1. Influence of Topography on Route Quality

The term topography refers to a wide range of physical route characteristics. Physical qualities can raise or diminish the effort needed to walk along the route. The main components of physical route quality include distance, acclivity, LOS and protection from negative external effects.

Distance

The length of a given route is a crucial factor when estimating the route quality. The distance to be covered is one of the critical factors which determine, if a destination is reached by walking or if other modes of transport are chosen. Under normal circumstances, a pedestrian will select the shortest path among several different potential routes to reach a desired destination.

The willingness to walk a certain distance varies individually. Young children and elder People naturally have difficulties to walk long distances; similarly disabled persons have fewer difficulties to reach their destination if the distance is rather short.

However, the effort to cover a longer distance can be alleviated, e.g. by appropriation of seating facilities.

Acclivity

Although people naturally try to avoid detouring, in some cases longer routes are preferred if the shortest path is too steep. Differences in level are also crucial factors of route qualities, as they may cause the exclusion of specific persons from some areas (e.g. if places can only be reached by crossing stairs, people in wheelchairs have no chance to arrive without help).

The installation of ascension facilities is very important to ease physical exhaustion and can improve the quality of a route to a great extend.

Level of Service

One of the key requirements for route quality is the provision of adequate space for the people using routes. The Level of Service (LOS) is an internationally recognized standard for the capacity of pedestrian spaces, which is defined by the broadness of the actual path and the amount of people passing. Level A describes the highest quality level, providing an average pedestrian area occupancy of at least 3.25 m² per person. Under these circumstances, standing and free circulation through the area is possible without disturbing others. On the contrary, the lowest quality level is defined by level F: the average pedestrian area occupancy amounts to less than 0.46 m² per person and practically all persons within the area are standing in direct physical contact with those surrounding them. This density is extremely discomforting, as no movement is possible within the crowd[8].

LOS A   LOS B   LOS C   LOS D   LOS E   LOS F
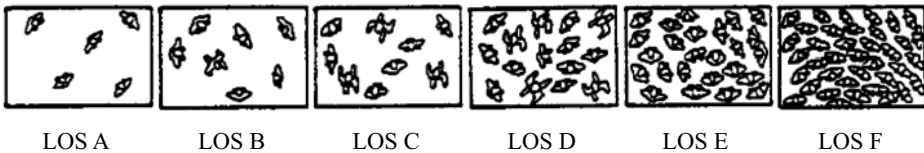
Figure 2: Density of pedestrians defined by Level of Service.

Simulation models currently take this aspect into account. However, actual concepts assume that all persons behave equally. But the individual sense of discomfort varies and is determined by several factors (e.g. age, sex, cultural background, etc.); hence in future individual influencing factors have to be considered in the context of agent-based-modelling.

In urban surroundings due to limited space many pedestrian areas can not fulfil the highest quality level. Nevertheless, a low level of service creates great discomfort; therefore the achievement of the highest possible quality should be realised to improve the quality of pedestrian route networks.

Protection from negative external effects

People afoot are usually very sensitive to external effects like adverse weather conditions, noise and pollution[9]. They prefer routes providing protection from rain, snow, intense insolation, traffic noise and pollution. Planting can improve the route quality very effectively, e.g. by shading, reducing wind and keeping off the rain.

3.2. Influence of Topology/Attractiveness on Route Quality

Topology and attractiveness refer to psychological characteristics of route quality. The structuring of an environment can strongly influence the perceived comfort of a route. People usually prefer routes arousing a general feeling of well-being. Of course also physical characteristics may cause discomfort and have a bearing on the psychological perception of route quality. Apart from that, the main factors influencing the psychological qualities of a route are attractiveness, availability of facilities and safety.

Attractiveness

As already mentioned, many pedestrians forbear from walking the shortest route, choosing a "more beautiful" path instead. Highly structured environments providing a great amount of visual clues lead to the tendency to accept longer distances, while poorly structured environments have a boring affect and force people to become aware of the physical effort they have to make[8]. Despite that, salient objects (landmarks) can easily be found and remembered and help people to find the right way; thus the fear of getting lost decreases and a higher level of comfort is perceived.

Availability of facilities

Depending on the intended purpose of a trip, pedestrians demand the existence of specific facilities along their route. Generally, routes providing resting facilities are considered having a higher level of quality than routes without seating or similar amenities [10]. Additionally, several purposes of moving around require visiting specific places or services (e.g. certain shops on a shopping tour or places of interest for tourists). Frequently, people combine several aims; so some tasks are dispatched "en route" while walking to a specific destination. These supplementary intentions are taken into account when choosing a route – the probability of a route to be chosen increases with the amount of opportunities along the way.

Safety

Safety is a very crucial factor of route quality. Feelings of discomfort and insecurity can force people to avoid specific areas of a city. Although the feeling of safety usually has little in common with the actual crime rate[11, 12], route choice behaviour is strongly influenced by the fear of "dangerous" district and pedestrians prefer to give them a wide berth. Additionally traffic safety is an important factor of route quality, e.g. children are taught to use the safest path to reach school to minimize the risk of getting injured in an accident. Many pedestrians are well aware of their vulnerability and feel uncomfortably when being forced to choose routes with heavy traffic (e.g. under time pressure). Actions being taken to enhance the safety of pedestrian ways can increase the number of people choosing to walk there.

Nevertheless, some efforts to improve the safety of foot traffic are not successful. Pedestrian underpasses for example may protect people from serious traffic accidents, but contain other disadvantages like the necessity of overcoming the differences in level or a psychological founded unpleasant feeling.

3.3. Influence of Complexity on Route Quality

People walking afoot try to minimize the extent of mental work during the navigational process. Hence, routes offering a minimum amount of decision points are preferred, even if an alternative route is shorter. An adequate number of salient landmarks along the route can also help to reduce the required mental effort to reach a destination. So the main influencing factors of mental route qualities are the number and complexity of decision points along the way and the availability of landmarks.

Number and complexity of decision points

The less information has to be remembered, the smaller is the risk of forgetting or overlooking important facts within the description of a specific way. Consequently the simplest path offers a high quality, as both mental efforts and the fear of getting lost are diminished. The simplicity of a route and hence the danger of losing one's way are determined by the number of decision points to be passed and the complexity of the traversed intersections (i.e. the number of streets on an intersection) [13].

Availability of landmarks

The importance of landmarks in human navigation is revealed in several studies[14, 15]. Landmarks are stationary, distinct and salient objects or places, which serve as cues for structuring and building a mental representation of the surrounding area. The saliency of a landmark is a crucial characteristic: objects or places which are remarkable can easily be recognized and remembered and help to simplify the navigational task, as visual clues are mentally less stressing than the need to remember distances, directions or street names.

Figure 3: Landmarks can be situated along (local landmarks) or distant from the route (global landmarks) or they can be a remarkable part of the route itself.

Any object can be perceived as a landmark, if it is unique enough in comparison to the adjacent items. Routes providing salient landmarks at critical points are therefore easier to be followed than routes with few or less conspicuous landmarks.

Landmarks do not only serve as mental clues for remembering or recognizing the correct route to a specific destination, they also have great influence on the perceived psychological quality of a route. The presence of a sufficient amount of reliable landmarks minimizes the fear of getting lost and offers the possibility of paying attention to other concerns than wayfinding.

Considering the importance of landmarks and their positive effect on the solution of navigational tasks, it is obvious that future research has to concentrate on efforts to identify and include salient landmarks in route instructions for pedestrians.

4.   Conclusion

Pedestrians show different preferences when choosing a particular route to a specific destination. The main dimensions of route qualities regard physical (e.g. distance, Level of Service, etc.), psychological (e.g. attractiveness, safety, etc.) and mental (e.g. complexity, availability of landmarks, etc.) qualities. Some attributes have influence on different types of route qualities. The estimation of different aspects of route qualities has to be focussed on in future studies.

As research has shown that landmarks are vital elements in pedestrian navigational strategies, some of the major challenges lie in the concept of Landmark Orientation itself and in the recognition of visually salient objects and their inclusion in guiding tools, as well as in the automation of the analysis process of the motion behaviour.

The research process about quality criteria for Landmarks is on a very early stage. The reliability of the chosen landmarks has to be determined by a quality measurement system to avoid ambiguous landmarks misleading the user. A system for qualifying landmarks has to be established to speed up future projects, data mining methods to provide a mechanism to automatically extract objects with a relative uniqueness in a given environment have been researched by Elias[16], but are so far only working in outdoor surroundings.

This paper summarizes the main dimensions of route qualities and their interaction with each other as a starting point for future research as a basis for further development of simulation tools for pedestrian flows in non emergency situations. **«**

References

1. B. Corona and S. Winter: *Datasets for Pedestrian Navigation Services*, Ange-wandte Geographische Informationsverarbeitung, Proceedings of the AGIT Symposium, J. Strobl, T. Blaschke, and G. Griesebner (Eds.), Salzburg, Austria, pp. 84-89 (2001).

2. C. Thomas: *Zu Fuss einkaufen*, final report of project (2003), http://www. fuss-verkehr.ch/presse/zufuss_schlussbericht.pdf (last access June 2005).

3. S. Blivice: *Pedestrian Route Choice: a Study of Walking to Work in Munich*, Ph.D. Diss. University of Michigan (1974), quoted by M.R. Hill, Walking, Crossing Streets, and Choosing Pedestrian Routes, Lincoln, NE: University of Lincoln (1984).

4. J. M. Wiener, A. Schnee, and H. A. Mallot: *Navigation Strategies in Regionalized Environments*, Technical Report TR-121, Max-Planck-Institut für biologische Kybernetik, Universität Tübingen (2004).

5. A. Millonig: *Menschliches Orientierungsverhalten – Eine Gegenüberstellung von Landmarkenbasierten und Zeichenbasierten Fußgängerleitsystemen*, Diploma Thesis, Dept. f. Raumentwicklung, Infrastruktur- und Umweltplanung, Vienna University of Technology, Vienna, Austria (2005).

6. K. Shriver: *Influence of Environmental Design on Pedestrian Travel Behavior in Four Austin Neighbourhoods*, Transportation Research Record 1578, pp. 64-75 (1997).

7. M. Sorrows and S. Hirtle: *The Nature of Landmarks for Real and Electronic Spaces*, In: Spatial Information Theory, International Conference COSIT '99, Proceedings, C. Freksa and D.M. Mark (Eds.), Springer, Heidelberg, pp. 37-50 (1999).

8. J.J. Fruin: *Pedestrian Planning and Design*, Metropolitan Association of Urban Designers and Environmental Planners, New York, (1971).

9. S. Sarkar: *Qualitative Evaluation of Comfort Needs in Urban Walkways in Major Activity Centers*, Transportation Quarterly 57 (4), pp. 39-59 (2003).

10. H. Knoflacher: *Fußgeher- und Fahrradverkehr* – Planungsprinzipien, Böhlau, Wien (1995).

11. C.A. Lawton: *Gender Differences in Wayfinding Strategies and Anxiety about Wayfinding: A Cross-cultural Comparison, Sex Roles*, A Journal of Research 47 (9), pp. 389-401 (2002).

12. S. Matei, S.J. Ball-Rokeach, and J.L. Qiu: *Fear and Misperception of Los Angeles Urban Space: A Spatial-Statistical Study of Communication-Shaped Mental Maps*, Communication Research 28, pp. 429 – 463 (2001).

13. E. Grum: *Danger of getting lost: Optimize a Path to Minimize Risk*, Proceedings, CORP 2005, Vienna (2005).

14. P.-E. Michon and M. Denis: *When and Why Are Visual Landmarks Used in Giving Directions? Spatial Information Theory*, Proceedings of the International Conference COSIT 2001, Heidelberg: Springer, pp. 292-305 (2001).

15.   A. Tom and M. Denis: *Referring to Landmark or Street Information in Route Directions: What Difference Does It Make?* Spatial Information Theory, Lecture Notes in Computer Science, Vol. 2825, W. Kuhn, M. Worboys, and S. Timpf (Eds.), Heidelberg: Springer, pp. 384-397 (2003).

16.   Elias, B.: *Determination of Landmarks and Reliability Criteria for Landmarks*, Technical Paper, ICA Commission on Map Generalization, Fifth Workshop on Progress in Automated Map Generalization, IGN, Paris (2003).

Cyclone and Storm Surge,
Pedestrian Evacuation and Emergency Response in India

A. Revi and A.K. Singh

1. The Importance of Pedestrian Evacuation in India

India is one of the more vulnerable and disaster risk prone regions of the world (IFRC, 2005, Parasuraman & Unnikrishnan, 2000). Much of the population (72 percent) live in rural areas in about 0.6 million settlements while the rest live in 5,161 urban centres (Census, 2001). Road quality to many rural settlements is indifferent and in a large number of states is very poor. A moderate number of villages are inaccessible during the monsoon or following the onset of natural hazard event such as flood, cyclone and storm surge.

Public transportation is unreliable and infrequent. The car ownership in rural India is very low under 8.5 million, with another 0.7 million buses and 3.2 million trucks for a population of over 1.1 billion (GoI, 2002). Therefore, the primary modes of vehicular transport are bicycles (over 100 million), motorcycles and scooters (45 million) and animal-drawn vehicles (15 million). Women and children typically do not drive vehicles and hence their access to motorised transport in an emergency is often less than desirable. Hence, the most pragmatic form for primary evacuation for much of the Indian population is on foot especially in more remote and inaccessible areas.

Nevertheless, part-pedestrian and part-motorized evacuation is becoming more common, especially in large State initiated evacuations in response to natural hazards (flood, cyclone and surge strike, and more recently a post-Tsunami alert) (GoAP, 2000).

2. Regional Pedestrian Evacuation

Much of the emphasis of pedestrian evacuation and its modeling in OECD countries has been on local evacuation from buildings, facilities and transportation systems (Schreckenberg and Sharma, 2002). Regional pedestrian evacuation simulation and planning has been rarely undertaken, and if so most have assumed the availability of some form of mechanized transport (USDEA, 1991).

In India however, the availability of mechanized transport for evacuation can rarely be taken for granted especially during extreme events. These include the Bhopal Union Carbide chemical accident (1984); Orissa (1989) supercyclone and regional flooding

and the Mumbai (2005) rain storm and regional flooding events (TARU, 2000, Chohan, 2004, Revi, 2005) where pedestrian evacuation was the dominant form of egress from hazard prone locations.

Hence, regional pedestrian evacuation planning and simulation is an important and legitimate class of problems in India. Large-scale evacuation of up to 0.2 million people have been facilitated by the various levels of government in India (GoAP, 2000). Because of this large scale, regional pedestrian evacuation needs to be situated in the context of overall disaster risk reduction rather than solely disaster event management.

This shift in perception and hence action is necessary as the pedestrian is often seen as the most vulnerable link during motorized evacuation and hence mitigation and response chain. In operational conditions in India, where road networks are thin, physical access to roads and rail networks are poor and hazards (cyclone, surge, flooding) often damage or disrupt networks during an event – the pedestrian, in spite of being slow may also be the most resilient element in the entire system.

3.   Cyclone and Storm Surge Risk and Impact in Gujarat

The following section presents a long-range profile of the risk due to cyclonic winds and storm surge for the western Indian state of Gujarat using probabilistic analysis based on historical cyclone and extra-tropical storm tracks over the 1872-2002 period (IMD, 1979, IMD, 1996, FNMOD, 2000, GSDMA/TARU, 2005).

Cyclones and storm surge are among the most severe natural hazards in South Asia, especially if they impact densely populated coastal, delta and estuarine areas (GoG, 1982, TARU, 1998, TARU, 2000, Parasuraman & Unnikrishnan, 2000). The key observed impacts are:

» Moderate to high number of deaths due to storm surge, cyclone associated rainstorms and flooding and possible river and coastal embankment failure apart from some deaths due to wind-induced building collapses.
» High cattle and livestock deaths following storm surge inundation or flooding especially if human and cattle evacuation is incomplete.
» Damage to roads, bridges and railway lines if located within the core damage zone.
» Damage and precautionary shutdowns of power and telecommunication infrastructure depending on anticipated event intensity, leading to an interruption of critical services during and after an event
» Damage to houses, industrial buildings and other buildings due to high wind and the hydrodynamic action of surge.

3.1. Challenges of Preparing for Effective Cyclone & Storm Surge Evacuation

» *Early warning is often late and especially for cyclone and storm surge not precise and comprehensible locally in terms of possible strike location, potential event magnitude, and impact.*

» *Most formal metrological warning systems are not understood or credible as far as lay people are concerned.*

» *The real gap often lies in the 'social distance' between the warning agency and the community or population at risk, which inhibits the communication of a warning locally.*

» *People (especially the poor) are reluctant to leave their livelihood assets behind during evacuation, even if faced with exceptional use of force. They prefer to say behind rather than loose assets that may ensure continuity of post-event livelihood.*

» *Post-event failure of infrastructure and services which are often outside the control or knowledge of emergency management agency, leading to communication and logistical failures after an event.*

Hence, most evacuations in India are:

» *Partially spontaneous rather than planned as a determinate techno-social system. This limits the potential for analytical modeling of system and evacuation behavior.*

» *Therefore, a mix of probabilistic and scenario-based GIS models combined with full-scale simulation drills are after a moderately effective means of preparedness for possible required future evacuation.*

Source: WMO, 1999, Holland, 2000, TARU analysis, 2005

The Gujarat Hazard Risk and Vulnerability Atlas (GSDMA/TARU, 2005) focuses considerable attention on quantifying cyclone and storm surge hazard risk vulnerability to assist the process of evacuation planning and composite risk mitigation. Cyclone and storm surge hazard risk for Gujarat was simulated digitally from historical cyclonic and extra-tropical storms tracks for the region for a 130-year period. Estimated wind fields for 150 historical storms were computed to determine probabilistic hazard risks estimated based on 3-second peak gust wind speeds at 10 m elevation over, 25, 50, 100 and 200-year return periods using an appropriate extreme value distribution (GSDMA/TARU, 2005). Following this, key zones in the State were identified based on their exposure to various cyclonic wind intensities and storm surges inundation levels as presented in Fig. 1 (Chittibabu, 1997)

Based on this analysis and the vulnerability of buildings, population, infrastructure and economic activity in the State, estimates were made of the impact of cyclone and storm
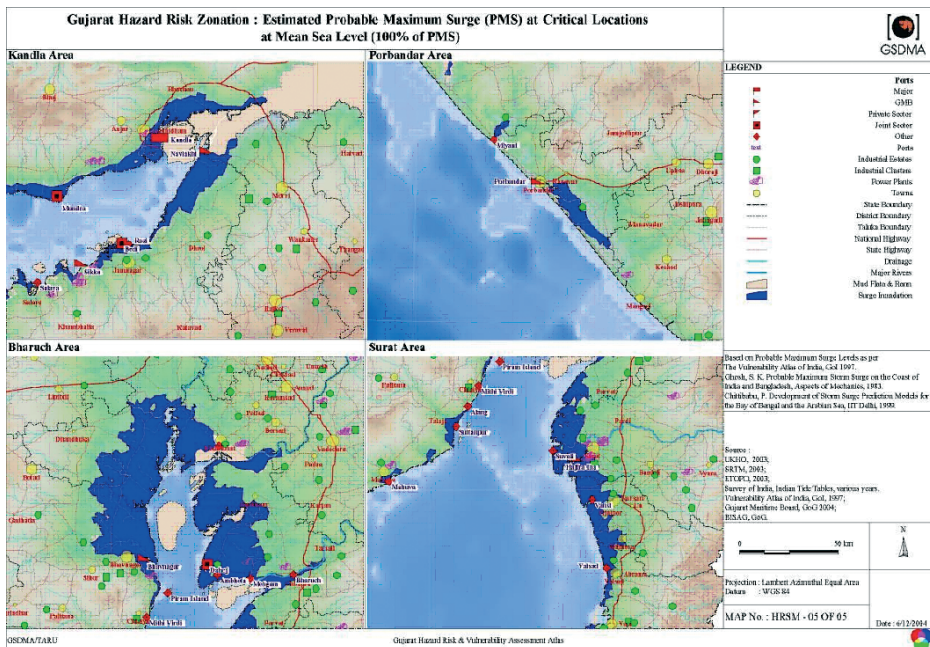
Figure 1: Potential Areas affected by storm surge in Gujarat

surge risk over a 50 and 100-year return period as presented in Fig. 2. The bulk of the analyzed risk is to capital stock (roughly 80 percent), about 12 percent due to the estimated value of loss of life and only 8 percent of the risk to the value of economic output.
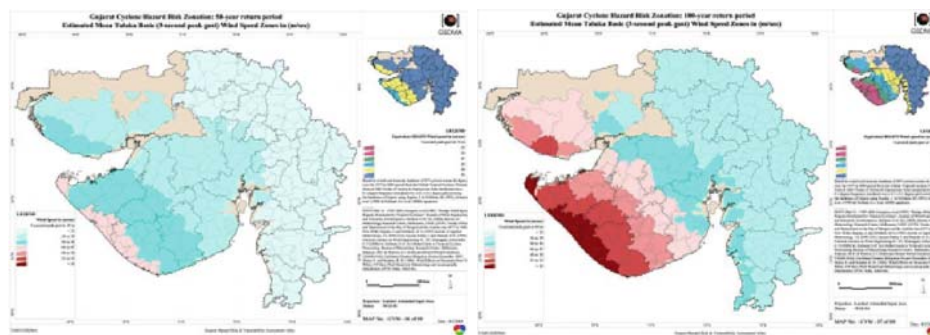

Figure 2: Gujarat: Cyclonic Winds Risk (50 and 100-year return period)

3.2. Critical Evacuation Zones

Based on an analysis of areas and zones at risk, critical cyclone and surge evacuation zones especially those in which large industrial or critical infrastructure concentrations are located were identified. A significant proportion of Gujarat's population lives within 25 km of the coastline and a large number of major industrial installations and critical infrastructure are located along the coastline or within the coastal plain (GoG, 1987, GoG, 1989). Hence, mitigation of strategic risk due to storm surge and cyclonic wind impact on housing and critical infrastructure is a serious challenge.

The Gujarat Hazard Risk and Vulnerability Atlas also presents a detailed GIS network of the state road systems. This includes major roads and bridges as presented in Fig. 3. This is expected to form the backbone of a hybrid coastal pedestrian and motorized evacuation system.
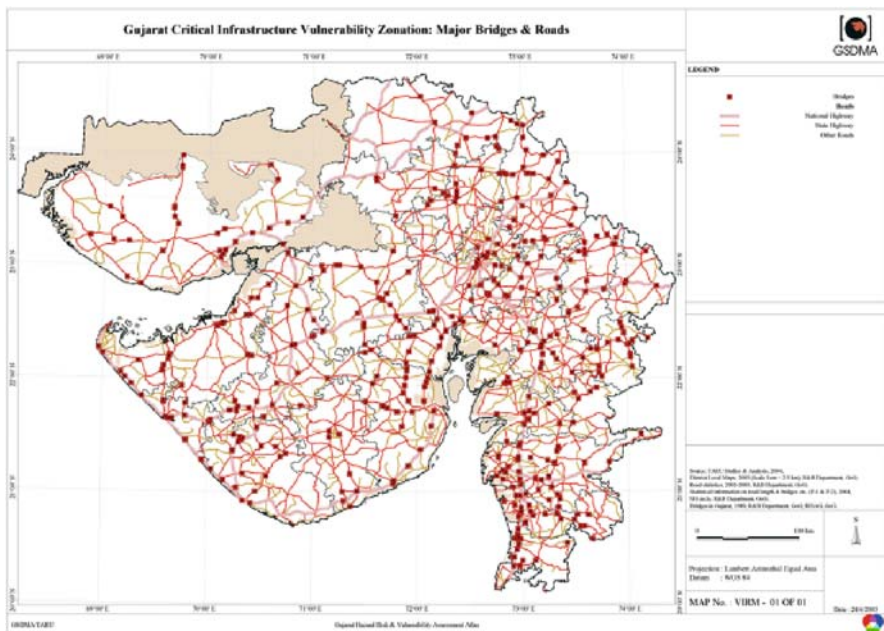
Figure 3: Gujarat Critical Infrastructure Vulnerability Zonation: Major Bridges & Roads

3.3. Hazira: an Area-specific Mitigation Assessment

Based on the regional analysis, an area-specific mitigation assessment exercise was undertaken in early 2005 for one of India largest industrial concentrations at Hazira in South Gujarat (TARU, 2005). This industrial zone has industrial investments of over $ 12 billon, which is expected to double over the next five years. This includes a LNG terminal, a 5 million tonne steel plant, multiple gas-based thermal power plants, a large petrochemical complex and pumping and processing infrastructure for one of India's most important gas pipelines as presented in Fig. 4.
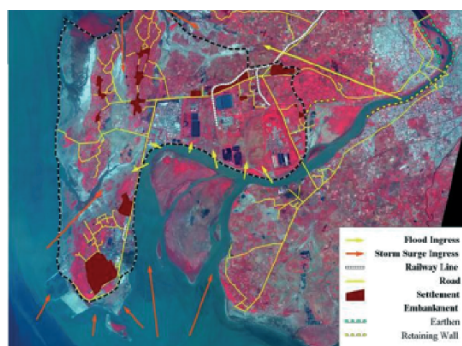
Figure 4: Location of Industrial Installations   **Figure 5**: Infrastructure & old settlements

Hazira lies at the mouth of the estuary of the Tapi river, which has a high tidal range of over 5 m. An important feature of the region is a history of settlement relocation to areas above the peak flood or surge line as presented in Fig. 5. A series of benchmarking activities were undertaken to determine historical peak flood levels and identify potential evacuation corridors and strategic risks, particularly to vulnerable populations of migrant workers those who were too indigent to live at higher locations. Residents of roadside ribbon development and migrant workers living in informal slum settlements were found to be most vulnerable.

A series of regional storm surge scenarios were developed for the Surat-Hazira region in Fig 6. This detailed storm surge simulation exercise estimated the peak mean surge (PMS) at mean sea level. Four scenarios are presented ranging from 25 to 100 percent of the PMS. This simulation presents counter intuitive results including the inundation of some of the critical industrial facilities and main evacuation corridors. The traditional settlements which were historically relocated to higher ground are almost untouched both by flood and surge inundation.

Further, ground truthing of specific major surge pathways are undertaken and surge ingress lines defined to examine whether structural mitigation measures (e.g., saline
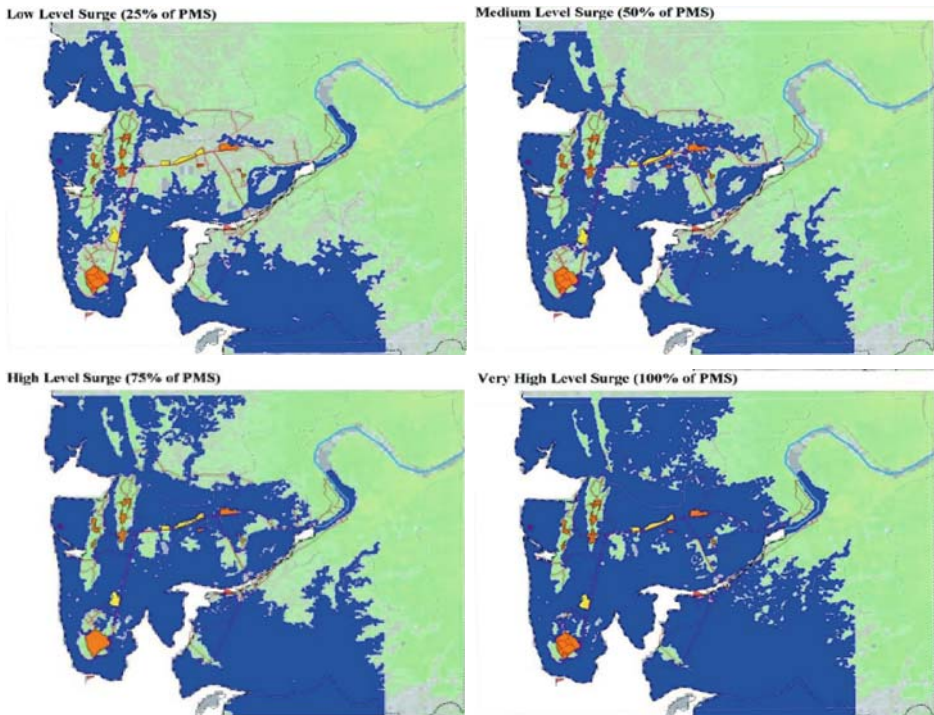
Figure 6: Hazira: Inundation due to 25%, 50%, 75% & 100% Peak Mean Surge at MSL

embankments) could be introduced, apart from biological measures such as mangrove regeneration and shelterbelt plantation.

3.4. Cyclone Storm Surge Refuge and Shelter Analysis

Detailed settlement level analysis of building types and potential damage for private and public buildings has been undertaken in various assessment exercises to assist in settlement-level mitigation and evacuation planning (TARU 1988, 1999). Potential buildings which would serve as refuges due to their siting above peak inundation levels and their material of construction are identified along with measures to retrofit and strengthen them. This however, is rarely adequate to provide shelter to the entire population of this densely populated area. Following the identification of public land that could be available for the construction of new community storm surge and cyclone shelters, a more detailed simulation analysis of potential locations has been undertaken for the Hazira area as presented in Fig. 7.

The estimated evacuation zones given an appropriate location in selected settlements (with a design a maximum walking time of 30 minutes) is presented in Fig. 8a assuming
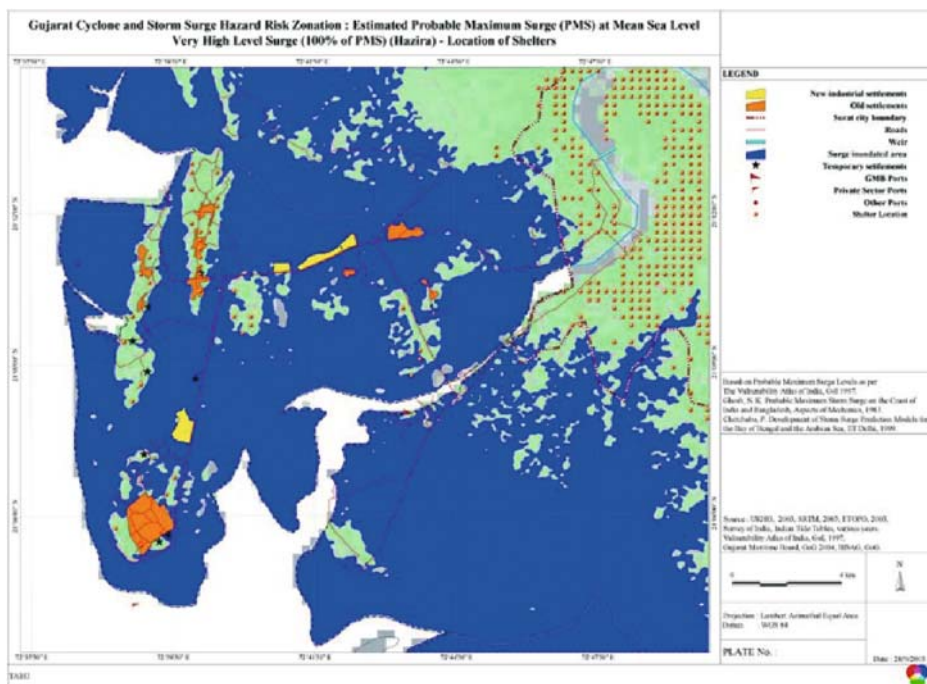
Figure 7: Hazira: Possible Surge Shelter Locations

a mean pedestrian evacuation velocity of 5 km per hour for adults. A similar analysis for older people at a mean velocity of 4 km per hour and for children at 2 km per hour were also undertaken (Fig. 8b and 8c).
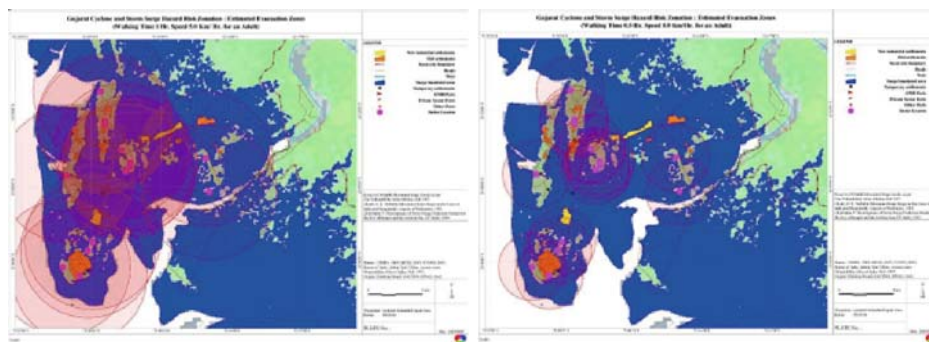

Figure 8a: Estimated Evacuation Zones (Walking Time 1 & 0.5 hrs & 5.0 km/hr Walking Speed
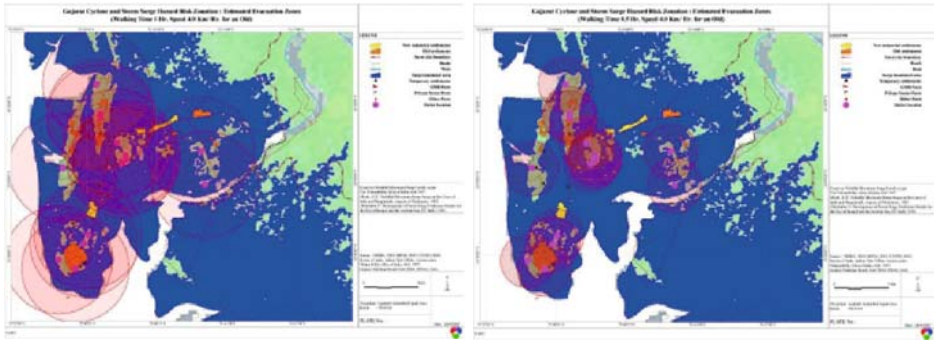
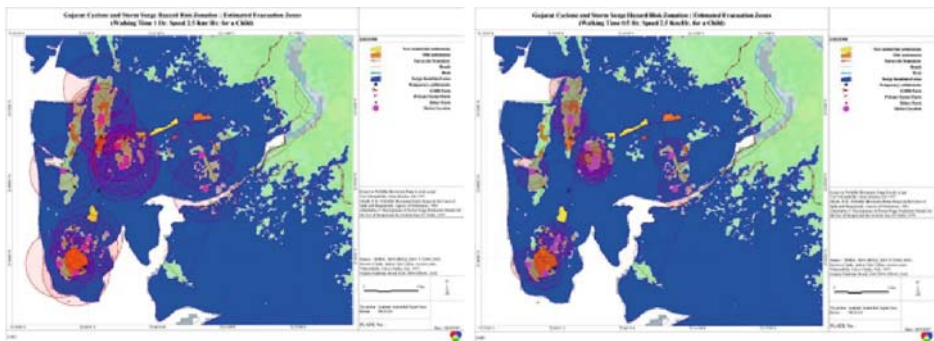**Figure 8b:** Possible Shelter Locations (Walking Time 1 & 0.5 hrs & 4.0 km/hr Walking Speed)

Figure 8c: Possible Shelter Locations (Walking Time 1 & 0.5 hrs & 2.5 km/hr Walking Speed)

This analysis shows that the effectiveness a pedestrian evacuation system based on designated community cyclone and storm shelters is significantly constrained by the demographic structure of the evacuee population. This will need to be taken into account while designing regional evacuation systems.

3.5. Key Drivers and Constraints to Successful Evacuation

Given the constraints of a large population of over 0.2 million at risk at Hazira, a series of key drivers and constraints to successful mitigation and evacuation system were identified (TARU, 2005):

» Rationalisation of landuse and coastal ecosystem conservation within the constraints of potential hazard exposure
» Relocation of populations and settlements at risk and provision of adequate structural flood and surge defense

» Upgradation of critical infrastructure and evacuation corridors to take the projected traffic flows in the extreme case given the realistic model composition of traffic flows
» Segregation of critical transportation corridors, gas and other pipelines

Based on this, a series of lifeline infrastructure upgrading interventions were identified:

» The provision of two additional hazard high capacity evacuation corridors via a land and sea route
» Upgradation of critical lifeline infrastructure (roads, bridges, power lines and water pipelines) to hazard resistant infrastructure
» Regulation and hazard assessment of the local pressurized gas distribution network.
» Rationalisation of bulk goods transport to a rail rather than a multiple road corridors along with segregation to reduce impact
» Establishment of a network of nodal points or refuge locations with disaster resistant buildings and lifeline infrastructure
» Establishment of a network of nodal points or refuge locations with disaster resistant buildings and lifeline infrastructure as staging points for pedestrian evacuation.
» Establishment of a network of surge and flood shelters within the identified radius of pedestrian evacuation, as motorized evacuation may be seriously constrained during a storm surge event.

4.   Conclusion: Ten Commandments of Successful Evacuation

Based on the operational experience of cyclone and storm surge evacuation in India, the following ten key interventions are suggested to improve cyclone and storm surge induced evacuation:

1. Ensuring reliable cyclone track, storm and surge intensity and strike location forecasts
2. Identification of areas potentially at risk to surge inundation, regional and local flooding and appropriate mitigation or relocation measures
3. Choice of an appropriate mix of pedestrian and motorized evacuation, sequencing and staging keeping in mind local demographic structure and constraints
4. Identification of appropriate and accessible shelter locations and designing them to function effectively at all times
5. Ensuring appropriate road access, quality and appropriate walk time of different population and age groups to shelters
6. Ensuring adequate post-warning local response time following an evacuation alert to enable systematic evacuation

7. Building local community warning and evacuation management capacity to mobilize effective pedestrian evacuation and staging
8. Undertaking full-scale simulation and response drills at appropriate intervals typically, before the cyclone season
9. Ensuring the availability of post-evacuation basic services: water, sanitation, food and medical aid are crucial to effective evacuation management
10. Recourse to regional evacuation should only be taken when all other mitigation options are exhausted.

While each of these interventions may not have an impact on evacuation management on their own, the entire suite are expected to enable a significant impact on current practice. Therefore a new set of modeling tools and methods would need to be developed to respond to the need for planning and hybrid regional evacuation management decision support. «

References

1. Census of India, Provisional Population Totals India New Delhi (2001).
2. P. Chittibabu: *Development of Storm Surge Prediction Models for the Bay of Bengal and the Arabian Sea*, IIT, Delhi (1997).
3. T.R. Chouhan and others: *Bhopal The Inside Story*, Other India Press, Goa (2004).
4. GoAP, Andhra Pradesh Cyclone Contingency Plan of Action, Hyderabad (2000).
5. GoG, Planning Atlas of Gujarat, Resource Profile, Directorate of Economics & Statistics, Gandhinagar (1987).
6. GoG, Gujarat State Gazetteer. Government of Gujarat, Gandhinagar (1989).
7. GoG, Government of Gujarat Memorandum to Central Team on Cyclone and Unseasonal Rains (November 1982).
8. GoI, Handbook of Transport Statistics in India New Delhi (2002).
9. GSDMA/TARU, Gujarat Hazard & Vulnerability Atlas, Gandhinagar (2006).
10. G.H. Holland (Ed.): *Global Guide to Tropical Cyclone Forecasting*. Bureau of Meteorology Research Centre. Melbourne (2000).
11. IFRC, *World Disasters Report 2005*, Geneva.
12. India Metrological Department, *Tracks of Storms and Depressions in the Bay of Bengal and the Arabian Sea 1877 to 1970*, New Delhi (1979).
13. India Metrological Department, *Tracks of Storms and Depressions in the Bay of Bengal and the Arabian Sea 1971 to 1990*, New Delhi (1996).
14. M. Schreckenberg and S.D. Sharma (Eds.): *Pedestrian and Evacuation Dynamics*, Springer Berlin (2002).
15. S. Parasuraman and P.V. Unnikrishnan: *India Disasters Report*, Oxford New Delhi.

16.   A. Revi: *Lessons from the Deluge: Priorities for Multi-Hazard Risk Mitigation in Mumbai*, Economic and Political Weekly, Mumbai, Vol XL No. 36, September 3-9, 2005 (2005).

17.   TARU: *Damage Assessment of Cyclone Affected Areas of Kachchh and Saurashtra in Gujarat,* New Delhi (1998).

18.   TARU: *Assessment of damage to Buildings and Lifeline Infrastructure in Districts of Orissa Affected by Cyclonic Storm,* 05B-99 New Delhi (2000).

19.   TARU: *Disaster Management* Plan Blueprint for the Hazira Area Development Committee Gandhinagar (2005).

20.   U.S. Navy Fleet Numerical Meteorology and Oceanography Detachment (FN-MOD), Global Tropical Cyclone Climatic (GTCC) Atlas Version 1.0, Asheville (2000).

21.   US Department of Energy, *Regional Evacuation Modeling*: A State-of-the-Art Review Oak Ridge (1991).

22.   WMO, *Tropical Cyclone Operational Plan for the Bay* of *Bengal and the Arabian Sea*, Report No. TCP-21, Geneva (1999).

Experimental Study and Theoretical Analysis of Signage Legibility Distances as a Function of Observation Angle

H. Xie[1], L. Filippidis[1], E.R. Galea[1], S. Gwynne[1], D. BlackShields[1], and P.J. Lawrence[1]

Signage systems are widely used in buildings to provide information for wayfinding, thereby assisting in navigation during normal circulation of pedestrians and, more importantly, exiting information during emergencies. An important consideration in determining the effectiveness of signs is establishing the region from which the sign is visible to occupants, the so-called Visibility Catchment Area (VCA). This paper attempts to factor into the determination of the VCA of signs, the observation angle of the observer using both experimental and theoretical analysis.

1.   Introduction

Signage within complex building spaces is intended to provide occupants with information relating to wayfinding. A successful signage system can reduce the apparent complexity of an enclosure thereby improving wayfinding under both general circulation and emergency conditions. While inefficient signage may contribute to loss of commercial earnings in general circulation situations, it can have more serious consequences in emergency situations. It has been known for many years[1,2] that in emergency situations occupant unfamiliarity with exit routes can significantly contribute to the resulting casualties[3-7]. To ensure reliable recognition and comprehension of signage information, safety signs are required to conform to certain design criteria specified in various national and international standards and guideline documents.

These documents usually contain basic requirements relating to the size of the sign, the size of the premises and the intended use of the premises[8,9]. As an example consider the NFPA Life Safety Code Handbook[8]. This suggests that reflective signs that have a lettering height of 15.2 cm are legible for up to a distance of 30m. To extend the visibility of a sign the letter height can be increased, with a linear relationship existing between lettering height and visibility distance. These design criteria are generally based on data collected from standard eyesight tests, which involve participants viewing a sign of given size viewed with an observation angle of zero degrees (i.e. the sign is viewed straight on). This enables the determination of maximum viewing distances as a function of the letter height. However, in reality occupants may approach a sign from a multitude of angles (i.e. non zero observation angles), which in turn will influence the ability of the individual to resolve the sign. This influence on sign legibility has been virtually ignored to date.

Fire Safety Engineering Group
University of Greenwich
London SE10 9LS, UK
http://fseg.gre.ac.uk

Evacuation and pedestrian circulation models[10] have also generally ignored the interaction of occupants with the wayfinding system; the implicit assumption in most of these techniques is that the occupants "know" the route. While this may be appropriate in many situations, it is clearly a simplification of reality. In order to produce realistic representation of evacuation and circulation in arbitrarily complex structures, it is necessary to represent the interaction between occupants and signage systems.

Recently the representation of the interaction between modelled agents and signage systems has been introduced into the buildingEXODUS evacuation model through the concept of the Visibility Catchment Area (VCA)[11,12]. The VCA of a sign is defined as the region from where it is physically possible to visually receive and discern information from the sign. Within this model, the maximum viewing distance or the VCA termination distance, is currently arbitrarily set as the distance specified in regulations[8].

In this paper we examine, through theoretical analysis and experimental study, the relationship between sign lettering size, observation angle and maximum viewing distance. Through this work we establish new maximum viewing distances as a function of observation angle. These results are then incorporated within the VCA concept and several demonstration applications of the new model are presented. It is important to note that this work does not include recognition of signage pictograms. Recognition of pictograms is expected to occur at greater distances than the legibility distance of text. Thus, the legibility distance represents a conservative or lower limit of the maximum recognition distance.

2.   The Evacuation model

2.1. buildingEXODUS

The core software used in this paper is the buildingEXODUS V4.0 evacuation model. The basis of the model has frequently been described in other publications[13,14] and so will only be briefly described here. EXODUS is a suite of software tools designed to simulate the evacuation of large numbers of people from complex enclosures. The version of the software used to simulate evacuation from the built environment is known as buildingEXODUS. The software takes into consideration people-people, people-fire and people-structure interactions. The model tracks the trajectory of each individual as they make their way out of the enclosure, or are overcome by fire hazards such as heat, smoke and toxic gases. The software has been written in C++ using Object Orientated techniques utilising rule base technology to control the simulation. Thus, the behaviour and movement of each individual is determined by a set of heuristics or rules. For additional flexibility these rules have been categorised into five interacting submodels, the OCCUPANT, MOVEMENT, BEHAVIOUR, TOXICITY and HAZARD submodels. These submodels operate on a region of space defined by the GEOMETRY of the enclosure.

2.2. VCA Concept

buildingEXODUS V4.0 currently includes a method of representing the visibility of particular objects through the application of the VCA concept. The VCA of an object is defined as the region of space from where it is possible to visually receive information from that object; i.e. from where the information of the object is legible. The VCA of a sign attempts to address only the physical aspect of visibility, leaving the psychological and physiological aspects of sign recognition to the behaviour component of the model.

The algorithm uses a line of sight search method to determine the locations within the geometry that have visual access to the sign. Geometrically the VCA of a sign is assumed to correspond to the visibility polygon15 spanning outwards from a point. The calculation of the VCA considers the location of the sign, the size of the lettering on the sign, its height above the floor, the position and size of any obstructions and the observer height.

For simplicity the current algorithm used to determine the VCA makes use of the central point of the lower edge of the sign and a point in space at a height equal to that of the average occupant, which is a user defined parameter. In this work the default average occupant height is arbitrarily taken as 1.75m. Another feature which will influence the size and shape of the VCA is the observation angle. The observation angle is defined as the angle subtended by the observers line of sight to a normal line bisecting the surface of the sign. An observation angle of 0° means that the observer is viewing the sign straight on. There will be a maximum observation angle beyond which it will no longer be possible to resolve the sign and hence it will not be possible to detect the sign. Due to lack of data, in the current implementation[12], the extent to which the observation angle of the observer impacts the shape of the VCA is arbitrarily set to 85°.

3.   A theoretical representation for the angular extent of the VCA

In the previous section, the method of representing the VCA of a sign implemented within the software was described. However, this method only approximates the VCA due to the assumption that the level of visibility afforded to the individual viewing a sign (i.e. the maximum distance from which a sign can be seen) was independent of the observation angle. This was primarily imposed on the approach due to the lack of reliable data linking observation angle with maximum viewing distance. Using this approach, the VCA for a sign would include a region of space defined by a near semi-circle, with a centre point located at the centre of the sign and a radius determined by the maximum viewing distance as defined by regulation. This region is represented in Figure 1 by the dashed semi-circular line.

It was suggested[12] that the size and shape of the VCA will be further influenced by the ability of an observer to resolve the angular separation of the sign. This is defined as the apparent angular separation of the ends of the sign as measured by a distant observer (i.e. angle φ in Figure 1). The angular separation of the sign will be dependent on the size of the sign (or more correctly the size of the letters on the sign), the distance of the observer from the centre of the sign and the observation angle. The observation angle is defined as the angle subtended by the observers line of sight to a normal line bisecting the surface of the sign (i.e. θ in Figure 1). An observation angle of 90º (i.e. viewing the sign side on) results in an angular separation (φ) of 0º, effectively making the sign invisible to the observer, while an observation angle of 0º (i.e. viewing the sign straight on) provides the maximum angular separation at fixed observation distance.

Clearly, there will be a minimum angular separation (φ_{min}) beyond which it will no longer be possible to resolve the sign and hence there will be a maximum observation angle beyond which it will be impossible to detect the sign. In this work, the minimum angular separation (φ_{min}) which can be resolved by the human eye is taken as a constant. For a sign of fixed size with an observer at a fixed distance from the centre of the sign, as the observation angle (θ) increases, the angular separation (φ) of the sign decreases until a maximum observation angle is reached beyond which it is no longer possible to resolve the angular separation of the sign (i.e. $\varphi < \varphi_{min}$). Thus for a sign of given sign size, in order to resolve the angular separation of the sign, as the observation angle increases, the maximum viewing distance must decrease. Similarly, for a given viewing distance there will be a maximum observation angle beyond which the sign cannot be resolved. As the size of the sign increases, both the maximum viewing distance and the maximum observation angle increases.
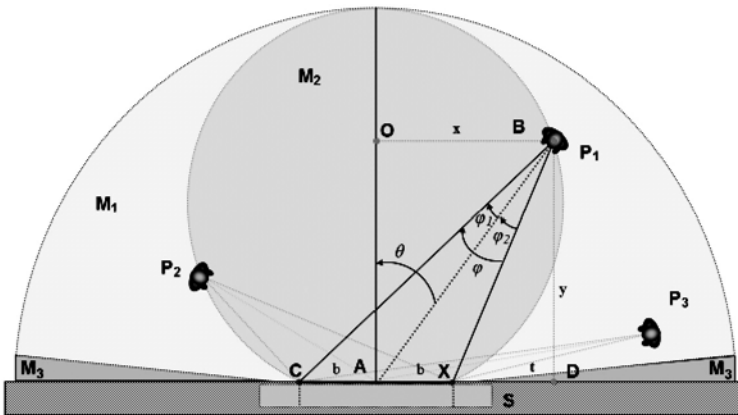

Figure 3: The geometric relationship between the observer and the sign.

Thus for an observer to be able to resolve a sign (i.e. make out the individual elements in the sign) at the maximum observation distance, the observation angle should be such that the angular separation of the individual elements making up the sign are greater than or equal to φ_{min}.

To estimate φ_{min} we use the maximum viewing distance for viewing signs with an observation angle of 0° (i.e. straight on) as specified in the NFPA Life Safety Code Handbook. For signs with lettering of 15.2 cm height, the maximum viewing distance is 30m [8]. This produces a φ_{min} of 0.29°.

Thus, in order to resolve the information on a sign at the maximum viewing distance, the observation angle should be such that the angular separation of the elements in the sign is greater than or equal to φ_{min} or 0.29°. This problem can be described geometrically by considering the relative positions of the observer, the sign and the observation angle. Depicted in Figure 1 are the positions of a sign (S) and an observer (P_1). Angle φ represents the angular separation of an element of sign S from observer P_1. In order for the observer to be able to read the lettering on the sign the distance from the sign must be such that the angle φ is greater than or equal to φ_{min} or 0.29°. Therefore as the observation angle increases, the maximum distance AB must decrease in order to maintain the angular separation of the sign to φ_{min}. By determining the length of the line AB within the constraints of the angular resolution of the eye the visibility catchment area of the sign can then be defined.

Known values	Description
φ	Angular separation of the sign; $\varphi = \varphi_1 + \varphi_2$
θ	Observation angle in relation to the normal line bisecting the surface of the sign
CX	Size of an element that an individual uses to resolve the sign (i.e. sign lettering)
b	b is set to half of the size of the recognisable element (CX)

Table 1: Variables used in formulation

The most efficient method of determining whether the sign is visible from a particular location within the geometry, given the considerations described above, would be to determine the geometrical shape that is formed by the maximum viewable distance from the sign. Considering the configuration of Figure 1, the known variables are listed in

Table 1. It can be shown that the geometrical shape of the visible region of the sign is given by the following formulation:

$$\left(\frac{b}{\sin(\varphi)} \right)^2 = x^2 + \left(y - \frac{b}{\tan(\varphi)} \right)^2$$

(1)

This has the equivalent form of a circle with centre at point $(0, b/\tan(\varphi))$ and radius $b/\sin(\varphi)$. This circle defines the VCA of sign S that is formed of text elements of dimension CX (see Figure 1) assuming a constant angular separation of φ_{min} degrees (i.e. 0.29° derived from the NFPA regulation). In this instance, we assume in this calculation that the human ability to resolve vertical components of the sign (i.e. the height of the text) is equivalent to their ability to resolve horizontal components.

Figure 1 depicts the catchment area of sign S generated using the original algorithm (area M_1) – which effectively ignores the dependence of VCA on observation angle. This image is overlapped by the catchment area of the formulation derived above, labelled as M_2 in the same figure. The restrictions imposed upon the VCA produced by the formulation are clearly evident, as is its circular appearance.

It has been shown theoretically that if the ability of a observer to resolve a sign is based on the assumption that the eye can resolve angular separations down to a constant minimum value (irrespective of observation angle), then the maximum viewing distance will decrease as the observation angle increases. This is an important result as the regulations implicitly assume that viewing distance is independent of observation angle. Furthermore, instead of the VCA being defined by a semi-circular region, as is implicitly assumed in regulation, from the above analysis we note that the VCA has a circular appearance with diameter approximately equivalent to the radius of the previously assumed semi-circular VCA.

In the next section, this theoretical finding is examined through a series of experimental trials designed specifically to examine this aspect of signage visibility.

4.   Experimental method

The purpose of the trials was to test the theory presented in the previous section that the distance from which a sign can be perceived is dependent upon the angle at which it is approached. The experimental trials have been designed specifically to examine the distances from which individual participants are able to recognise the text (or some portion of it) within the sign for given observation angles.

The trials were completed by 48 volunteers, consisting of 29 males and 19 females, each of whom experienced the same number (15) of experimental conditions. The or-

der in which these conditions were experienced was varied in a systematic manner in order to minimise the influence of uncontrolled variables, e.g. learning. The vision of approximately 55% of the sample required constant correction in the form of spectacles or contact lenses, which were used during the trials. A detailed analysis of the results according to a number of variables (e.g. prior eye workload, text size, and use of visual correction) was produced; however the presentation of this material is beyond the scope of this paper.

The experiment was performed in a corridor 39 metres in length with consistent artificial illumination along its length. Three standard signs were used during these trials: two plastic signs and one photo luminescent sign. These signs varied in the letter size of the text, the case of the text and the background colour of the signs. The text within these signs differed in the height and the width of text, and the thickness of script that formed the text. Although the three signs used were of standard designs, it was felt that a variety of text types and signage designs were required in order to strengthen the credibility of the results produced.

Given the restricted nature of the corridor, the sign used in each trial was placed on a pivoting platform. Thus the observation angle was changed by varying the orientation of the sign to the observer rather than the observer to the sign. In this way each participant commenced the trial in the same location and approached the sign along the same path, irrespective of the observation angle. Five different observation angles were experienced by each participant: 0º, 30º, 60º, 70º and 80º. For each observation angle the observer would approach the sign until the lettering on the sign was legible. Therefore, each participant was equally exposed to 15 trial conditions (3 signs × 5 angles) in total.

5.   The experimental results

The average viewing distance for each of the three signs at the five observation angles are shown in Table 2 for each of the categories. The results presented in Table 2 clearly demonstrate a relationship between the observation angle and the distance from which the text in the sign could be resolved: for all of the signs as the angle of observation is increased, the maximum viewing distance at which the text in the sign could be resolved decreased. From the experimental results it is apparent that the relationship between maximum viewing distance and observation angle is nonlinear and consistent for each of the three types of sign.

	Mean viewing distance at each observation angle (m)				
	0°	30°	60°	70°	80°
Sign 1	23.38	21.09	14.82	10.12	5.10
Sign 2	33.11	30.79	21.23	13.64	6.34
Sign 3	19.84	18.98	12.65	9.04	4.60

Table 2: Mean viewing distances of three signs at 5 different observation angles.

To further examine the relationship between observation angle and viewing distance the data is plotted using polar co-ordinates, with θ (the rotational ordinate) representing the observational angle and r (the radial measurement) representing the distance at which the text in the sign could be resolved. In Figure 2(a) the results are presented in this form for each of the signs examined and are reflected on the vertical axis. The validity of this action is based on the assumption that the observational angle is independent of the direction of the approach to the sign (i.e. whether they approach from the left or the right side). A solid curve passes through the average of the data-sets collected. It is apparent that although the size of the curve produced in each of these graphs is different, their general shape is similar: a circle is approximated by the curve connecting the averages of the five experimental conditions examined for each of the signs.
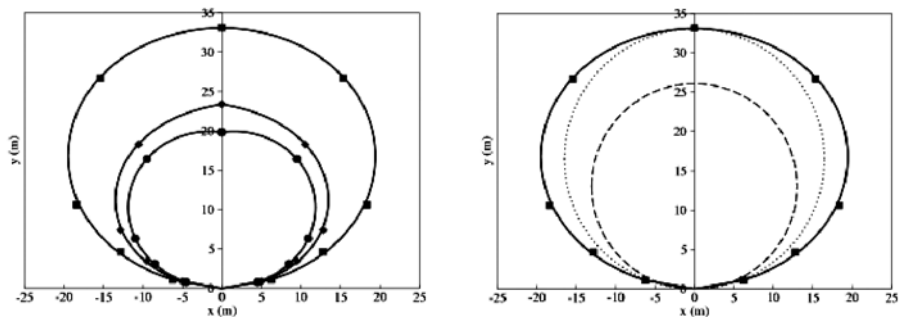
Figure 2: (a) The reflection of the original experimental data of Sign 1 (♦), Sign 2 (■) and Sign 3 (●), across the vertical axis, and (b) the comparison of the experimental VCA of Sign 1 (solid curve) and two VCAs of the same sign based on the theoretical model discussed in Section 4 using the maximum viewing distances suggested by BS 5499[9] (dotted curve) and the NFPA Life Safety Code Handbook[8] (dashed curve) respectively. In both cases, the safety factor of 2 is excluded.

The curves generated from the experimental data represent a slightly flattened circle; moreover, from Figure 2(b) this closely approximates the theoretical findings discussed in Section 3 and clearly contradicts the implicit assumption used within building regulations that the maximum distance from which a sign can be resolved is independent of the observation angle.

In the first edition of BS 5499[9] the following formulation is provided relating the viewing distance (D) to the height of text (h)

$$D=250h \tag{2}$$

As mentioned previously, this formulation is based on the result of eye sight tests that people with normal (or corrected to normal) vision can reliably resolve a detail that

subtends an angle of 1 minute. This formulation also includes a small additional margin of extra difficulty in resolving some complex letters and a safety factor of 2.0 in order to guarantee a conservative estimate of the distance from which the sign can be resolved. Finally the coefficient is rounded off to two significant figures[16]. For instance, given the height of the text on Sign 2, the results produced by the formulation is

$$D=250 \text{x} 0.066 = 16.5 m,$$

which is approximately half of the measured average viewing distance (33.11m) for Sign 2 with observation angle of 0°. Given the incorporated safety factor of 2.0 and the other correctional factors mentioned, this approximates the findings of our experimental trials. The value describing the angular resolution of the eye demonstrated in this experiment is therefore consistent with the advice provided in the regulatory documentation. Alternatively, it should be noted that the NFPA Life Safety Code Handbook[8] suggests a viewing distance of 30m for the exit lettering with a height of 15.2 cm. Again if the safety factor is taken into consideration, it approximates the relationship between sign size and average maximum viewing distance produced during the experimental trials, but it is a little more conservative compared to BS 5499[9] standard (see Figure 2(b)).

It can be shown that the maximum viewing distances recorded during the trials approximate the values assumed in the NFPA and BS 5499 formulation, adding some credibility to the experimental conditions.

The results of the experiment indicate that the VCA of a sign approximates a circle. This confirms the initial hypothesis that a sign can be seen by an observer from a circular area located at a tangent to the surface of the sign. This is due to the constant nature of the angular resolution of the human eye and the non-linear relationship between the observational angle and maximum distance from which the sign can be resolved. Within buildingEXODUS the theoretical model describing the non-linear relationship between observation angle and maximum viewing distance has been implemented. This produces conservative results as it generates a circular VCA with the same maximum radius as the flattened circle generated from the experiment (VCA circle from theory lies within the flattened VCA circle produced by experiment).

6. Implementation of proposed algorithm into the evacuation software

The algorithm described in Section 3 has been implemented in prototype form within buildingEXODUS. Here we demonstrate the performance of the algorithm using an example, which assumes a complex compartment with many internal obstacles. The geometry used in this example is the supermarket layout used in previous analysis of the VCA[12]. The geometry will only be briefly described in this section as a fuller account can be found in previous publications[12]. The supermarket contains an array of internal shelving components, tills and a café in the southern part of the geometry. Four main

exit points (exits 3, 4, 5, 6) are located at the south side of the building. Four emergency exits (exits 1, 2, 7, 8) are available: two on the east side and two on the west side. The total free area of the supermarket has been calculated within the model to be approximately 2927 m² after the shelving and other furnishings have been taken into account. Signage is provided by exit signs located above each of the exits (main and emergency) and by two sets of four connected signs at the cross aisles.

The majority of the shelving extends to a height of 2.5m. However, there are some shelves with a height of 1.8m and the tills and tables in the café area have a height of 1.2m. The emergency exit signage is positioned at a height of 2.2m above the floor. All the remaining features are at ceiling height, thus preventing any visibility access past them. The height of the shelving and furnishings is taken into account when calculating the VCA of each exit. The width of each door is assumed to be 2.5m. The signs are assumed to have lettering of 15.2cm corresponding to a visibility cut off distance of 30m as suggested by the NFPA Code[8] and the observer is assumed to have the default height of 1.75m.
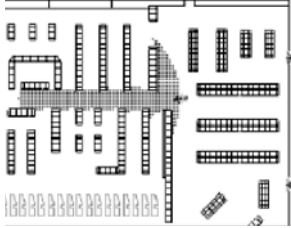
	Existing VCA method	Prototype VCA method
VCA of sign S6		
Area covered	196.75m²	142.75m²
Percent coverage	6.72%	4.88%

Table 3:   VCA comparison of sign S6 between the existing and prototype methods

The VCA of the signage system is determined using both methods. Using the existing method, the combined VCA of all the signs is 2006.25m², while using the prototype algorithm produces a combined VCA of 1896.0m²; thus, the existing method over estimates the VCA by some 6% (or 110m²). Presented in Table 3 is an example of the difference between the VCA produced by both methods for an interior sign S6.

In a simple example, the differences between the VCA produced by the two techniques was shown to be significant (see a comparison between area M_1 and area M_2 in Figure 1). However, these differences are somewhat diminished as the complexity of the compartment is increased through the introduction of internal obstacles. This is due to the presence of the obstacles intercepting and preventing the propagation of the VCA. In

this way, the presence of the obstacles masks some of the over estimation produced by earlier method.

We note that the average Total Evacuation Time was 1 min 23 secs using the existing technique and 1 min 21 secs using the new algorithm. The average individual evacuation time was 34.2 seconds and 33.8 second for the old and new approach respectively. The average congestion experienced by an individual was 10.9 and 9.9 seconds while the average distance travelled was 28.7 m and 29.5 m for the old and new approach respectively.

As is to be expected, the reduction in VCA generated by the new algorithm has resulted in a greater number of occupants utilising the normally used (or main) exits – i.e. exits 3-6. On average there are some 17 additional people utilising the main exits when the new algorithm is used to determine the VCA. As a result there is a slight increase in the average distance travelled, generated by a larger section of the population not utilising the nearer emergency exits. In this case, the slight decrease in the number of occupants using the emergency exits has resulted in a slight decrease in the levels of congestion experienced (at the emergency exits) which in turn has resulted in a slight decrease in both the average overall evacuation time and the average personal evacuation time. Thus the differences in the key results produced by the incorporation of the new technique of calculating the VCA in this example are small and self consistent.

7.   Conclusion

In this paper we have demonstrated both theoretically and through experimental trials that the maximum viewing distance is dependent on the viewing angle and that as the viewing angle increases, the maximum viewing distance decreases in a non-linear manner. This is the result of the angular separation of the sign (or more precisely the angular separation of the lettering on the sign) decreasing as the angle of observation increases at fixed observation distance and the human eye possessing a lower limit to its angular resolving abilities. Furthermore, when the viewing angle is taken into consideration, the VCA associated with the sign describes an area defined by a flattened circle which is tangent to the surface of the sign with minor radius equal to the previously defined semi-circle or half of that if the safety factor is considered.

These results are valuable in their own right as they more accurately define the visibility limits of signs. In addition, the method of determining the VCA of signs has been implemented with the buildingEXODUS evacuation model providing a more accurate way of determining the visibility of signs in complex geometries. The impact that the new developments may exert when combined with the other factors evident during a simulated evacuation have been shown to be sensitive to the complexity of the geometry and the scenario modelled. While the overall differences in the key evacuation indicators (e.g. average total evacuation time and average personal evacuation time) resulting from

the introduction of the new developments may on occasion be small, it is essential to correctly represent these subtleties if the model is to correctly represent reality.

8.   Acknowledgements

References

1.   J. Sime: *Escape Behaviour In Fire: ,Panic' Or Affiliation?,* PhD Thesis, Department of Psychology, University Of Surrey (1984).
2.   S. Gwynne, E.R. Galea, M. Owen, and P.J. Lawrence: *Escape as a Social Response*, Published by the Society of Fire Protection Engineers (1999).
3.   P.M. Weinspach, J. Gundlach, H.G. Klingelhofer, R. Ries, and U. Schneider: *Analysis of the Fire on April 11th, 1996, Recommendations and Consequences for Dusseldorf Rhein-Ruhr-Airport*, Staatskanzlei Nordrhein-Westfalen, Mannesmannufer 1 A, 40190 Düsseldorf, Germany (1997).
4.   Report of the Tribunal of Inquiry on the Fire at the Stardust, Artane, Dublin, 14th Feb 1981 (1981).
5.   R.L. Best: *Reconstruction of a Tragedy: The Beverly Hills Supper Club Fire*, Southgate, Kentucky, May 28, NFPA (1977).
6.   Summerland Fire Commission Report, Douglas: Isle of Man Fire Report (1974).
7.   W. Grosshandler: *The Station Nightclub Fire, Federal Advisory Committee*, Building and Fire Research Laboratory, National Institute of Standards and Technology, December 3, 2003, http://wtc.nist.gov/media/Final_RI_Station_Nightclub_Status_12-3.pdf.
8.   NFPA, *Life Safety Code Handbook*, National Fire Protection Association, Quincy, MA (1997).
9.   BS5499-1:1990, *Fire Safety Sings, Notices and Graphic Symbols. Specification for fire safety signs*, ISBN 0 580 18830 2, UK (1990).
10.   S. Gwynne, E.R. Galea, M. Owen, P.J. Lawrence, and L. Filippidis: *Review of Modelling Methodologies Used in the Simulation of Evacuation*, Journal of Building and the Environment, 34, pp. 441-749 (1999).
11.   L. Filippidis, S. Gwynne, E.R. Galea, and P.J. Lawrence: *Simulating the Interaction of Pedestrians with Wayfinding Systems*, Proceedings of the 2nd International Conference on Pedestrian and Evacuation Dynamics, E.R.Galea (Ed.), CMS Press, Greenwich, London, ISBN 1904521088, pp. 39-50 (2003).
12.   L. Filippidis, E.R. Galea, S. Gwynne, and P.J. Lawrence: *Representing the Influence of Signage on Evacuation Behaviour with Evacuation Models*, to appear in the Journal of Fire Protection Engineering, Sage Publications (2005).

13. E.R. Galea, S. Gwynne, P.J. Lawrence, L. Filippidis, and D. Blackshields: *buildingEXODUS V4.0 User Guide and Technical Manual*, University of Greenwich, London (2004).
14. S. Gwynne, E.R. Galea, P.J. Lawrence, and L. Filippidis: *Modelling Occupant Interaction with Fire Conditions Using the buildingEXODUS Evacuation Model*, Fire Safety Journal, 36, pp. 327-357 (2001).
15. D. Avis, G.T. Toussaint: *An Optimal Algorithm for Determining the Visibility of a Polygon from an Edge*, IEEE Trans. On Computers, C-30, No.12, pp. 910-914 (1981).
16. J. Creak: *Viewing Distances, Means of Escape* (1997).

Exploring Pedestrian Shopping Decision Processes – an Application of Gene Expression Programming

W. Zhu[1] and H. Timmermans[2]

Abstract: Random utility theory and discrete choice models have been widely used to explore mechanisms underlying pedestrian shopping behavior. However, these models tend to be mis-specified due to unrealistic assumption of utility maximising behavior. The bounded rationality theory may be more suitable for building models representing real shopping decision process, but existing statistical models are not able to extract information hidden in the decision process proposed by the theory. We therefore developed GEPAT, a computer program using Gene Expression Programming to solve this problem with its two most significant features. The first feature is that it has an extendable multi-gene-section chromosome structure which allows several inter-related target functions to be estimated simultaneously. The second feature is that it uses processors, representing mental operators, as building blocks to implement simple information processing and facilitate constructing and testing complex schemes of the problem by linking the processors properly. The overall workflow of GEPAT, its advantages, disadvantages and potentials are discussed.

1.   Introduction

Modeling pedestrian shopping behavior in shopping streets or city centres, as a decision support tool for city planners, retailers and real estate developers, has a long tradition. By hypothesizing both external factors such as retail floor space and distance and internal factors such as age and income to influence the decision-making process, researchers can test their effectiveness on behavioral outcomes and manipulate them in prediction for various theoretical or practical purposes. From the earlier gravity-based approaches (e.g., Hagishima et al. 1987, Berry et al. 1988) representing aggregate pedestrian movement patterns to the later discrete choice approaches modeling individual decision mechanisms (e.g. Borgers and Timmermans 1985, Oppewal and Timmermans 1997, Arentze and Timmermans 2001) and agent-based models simulating interactive group behaviors (e.g. Haklay and O'Sullivan 2001, Kerridge et al. 2001), we witnessed an ever-continuing endeavour in exploring the roots of behavioral phenomena. Among these models the discrete choice family, built on the random utility theory (RU), has received most attention and is widely used in explaining behavioral reasons such as why the pedestrian chose one store rather than another. The wide usage is largely due to its behavioral perspective and mathematical elegance which make it easy to manipulate. However, some fundamental questions still remain if a model reflecting real behavioral mechanism is our ultimate pursuit.

---

[1]Ph.D. candidate, Urban Planning Group, Vertigo 08.16, Eindhoven University of Technology, P.O.Box 513, Den Dolesh 2, 5600 MB Eindhoven, The Netherlands. Phone: 0031-040-2472861, Fax: 0031-040-2438488, E-mail: w.zhu@tue.nl

[2]Professor, Urban Planning Group, Eindhoven University of Technology. E-mail: h.j.p.timmermans@bwk.tue.nl

1.1. Theoretical question

Although random utility theory may be applicable in many situations, it is not very suited to explain pedestrian shopping behavior. Three major assumptions are questionable. First, the pedestrian is assumed to be omniscient, knowing every choice option (store) in the shopping environment. This is hardly true even for a local resident. Second, the pedestrian is assumed to have full information about the shopping environment. Third, a pedestrian is assumed to choose the store that brings maximum utility. Utility maximization has deep roots in classical economics but still lacks sound support in the context of shopping behavior. Such a fully rational man hardly exists in reality. Instead, a normal person's rationality and ability are more likely limited, or say, bounded. An alternative theory more suited for choice and decision problems is the bounded rationality theory (BR) proposed by Herbert A. Simon in 1947.

The base idea underlying the notion of BR is that people have ecological rationality, making good (enough) decisions by exploring the structure of the environment (Todd and Gigerenzer 2003). For a normal person, three principle steps are necessary to complete a decision process: first, recognition processes that largely obviate the need for further information search; second, heuristics that guide search and determine when it should end; and third, simple rules that make use of the information found. This theoretical proposition looks more human and was proved reasonable by many psychologists and experimental economists. Payne et al (1993) argued with experimental results that "When faced with more complex choice problems involving many alternatives, people often adopt simplifying (heuristic) strategies that are much more selective in the use of information." Further, "When faced with two alternatives, subjects use compensatory types of decision strategies. When faced with more complex (multialternative) decision tasks, subjects prefer noncompensatory strategies." This evidence suggests that human decision processes are wisely undertaken within the physical boundaries to reach the good enough choice in a fast and frugal way. This notion is also highly transferable to the real shopping situation when the pedestrian is more like a "satisficer" rather than a "maximizer", who always utilizes information within a limited spatial extent and chooses the store sufficing his expectation. Therefore, BR provides a theoretically better founded basis for modeling pedestrian shopping behavior.

1.2. Methodological question

A simpler decision process is not necessarily a simpler methodology. Even although BR has been proposed 30 years earlier than RU, models derived on this theory have been developed relatively slowly and unsystematically compared with the full-fledged discrete choice models. This could be largely due to the unobservable nature of the decision process which BR aims to articulate. The RU models are easier to fit because they are based on statistical theory, and utility maximizing provides an explicit model specification that can be estimated using decision outcomes and covarying factors. In contrast, BR models need more precise inputs most of which, unfortunately, are comple-

tely hidden from the researcher. Gathering data about the outcomes of decision making is typically insufficient to determine the underlying mechanisms (Todd and Gigerenzer 2003). For example, "to use enough information" and "to make good enough decision" both imply some thresholds or cutoffs as judgment standard. They are the things the respondent can feel, but they are hard to express. Kau and Hill (1972) and Bettman (1974) built models for consumer goods choice behavior, which incorporated cutoffs assumed to be probabilistically distributed. Grether and Wilder (1984) introduced information search costs into the utility function. But the model was only tested on experimental data. The recently appearing synthetic RU models incorporating cutoffs or costs (Swait 2001, Vroomen et al. 2004) can be seen as some kind of compromise between the two theories. However, these models still cannot escape the unappealing utility maximizing assumption. Without any data input from the hidden information, RU models or other traditional statistical models cannot estimate the right parameters.

The other aspect hindering BR modeling is the decision processor as a coherent system whose working mechanisms are hidden, too. In reality, problem solving very likely involves processing information through a sequence of mental operators (Newell and Simon 1972, Payne et al, 1993). According to Todd and Gigerenzer (2003), "To study particular heuristics in detail, it is crucial to develop computational models that specify the precise steps of information gathering and processing involved in generating a decision." Translating these statements into technical solutions, the BR model should include several inter-linked mental operators each of which completes certain task using a specific function. These functions might be interdependent, using the outputs of each other as their input variables. Estimating such model is sometimes referred to the co-evolutionary estimation procedure where not only the parameters in each function but the optimal combination of the functions are derived. Though RU models and traditional statistical models could be incorporated in this procedure, they have limited flexibility to explore possible hidden solutions because both the specification of functions and their relationship have to be strictly pre-defined or at least some organization rules are assumed (e.g. Krygsman et al, 2003).

1.3. Genetic algorithm, a possible solution

The better solution may exist in the alternative model family, computational models, among which the Genetic Algorithm (GA) provides a suitable and promising frame for BR modeling. Totally different from relying on mathematical and statistical manipulation, GA is built on the basis of evolution theory and biological process. "The fitter is the better" is directly utilized in GA to find the target function fittest to the population. Generally, this process starts from a GA program randomly generating an initial set of functions composed of numbers, variables and mathematical operators. Then the outcome of each function is compared with the target variable and a kind of fitness value is derived as the index of strength of the model. This fitness value determines the probability of the model surviving to give offspring which, after mutation, recombination, crossing over with other offspring just like the real DNA does, is evaluated again. This

process iterates until the preset number of iterations or other criteria are met. Though the algorithm is non-deterministic, non-theory-driven and purely established on trial and error, it is practically proved to be very powerful in finding good, even perfect solutions, especially when the underlying mechanism is unknown and the environment is varying. Probably it is truly close to the way our world is built. This characteristic finds BR modeling a suitable position to extract those hidden information from an almost blank, assumption-free solution space. Previous examples of the application of genetic algorithms in BR modeling include Geisendorf (2000), whereas Kitazawa and Batty (2004) have used it in the context of pedestrian movement, although their approach is quite different from the one presented in this paper.

Existing GA techniques are designed to get a solution with a single function, such as Automatic Problem Solver. They are not enough for shopping decision process modeling whose operators need several target functions to be estimated simultaneously. The other major requirement they cannot provide is that the tool should be flexible enough for researchers to test different schemes of the decision process and identify the best one.

Aiming to fulfill these two requirements and build a platform for exploring pedestrian shopping decision process, we developed GEPAT (Gene Expression Programming as an Adaptive Toolbox), a computer program using the Gene Expression Programming technique which is similar to its counterparts of the GA family. The core technique in this program is largely based on Candida Ferreira's paper (2001). In the next section, we will introduce GEPAT, how is it designed, and how it works. In the third section we will discuss advantages, disadvantages and potentials of GEPAT and conclude this paper.

2.   The program: GEPAT

GEPAT has two most significant features. The first is that it can get the simultaneous solution for several inter-related functions. The second is it can be used to model complex systems easily through organizing simple building blocks.

2.1.   Get simultaneous solutions

In Gene Expression Programming (GEP), a target mathematical function is derived from a code sequence which is composed of numbers, variables and mathematical operators. It is this code that be transformed, mated with other codes to give offspring. Usually, the structure of the code is similar to Figure 1. It is an analogy to the biological chromosome, though not completely the same. The fundamental element of this structure is the condon where operators and operands are randomly generated and stored. Several numbers of codons compose the gene, the basic element creating functions after being translated. Both the length (the number of codons) and the number of the genes can be extended to include more information and create more complex functions. Among the genes, a space for the link function is designated for them to work together. All of these

elements compose the chromosome. After the evolutionary process, the best chromosome with the highest fitness value is preserved which returns the target function.
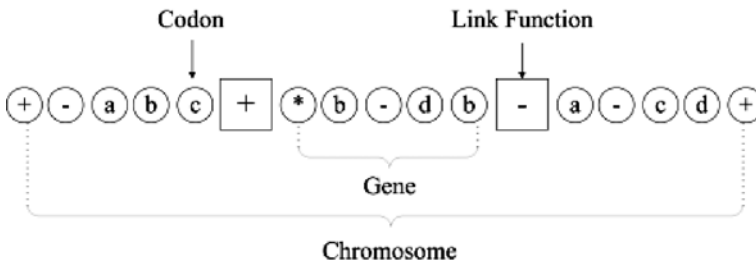

Figure 1: Structure of a chromosome in GEP

This structure is not suitable for BR modeling when several functions need to be estimated simultaneously. Fortunately, there is almost no limit to such a structure. We can extend it as complex as we wish. In GEPAT, an additional element, gene-section, is included (Figure 2). The gene-section is just the chromosome in GEP and the chromosme here is the composition of gene-sections. Each gene-section is an individual function block, physically connected from head to tail with other gene-sections by some abstract cohension.
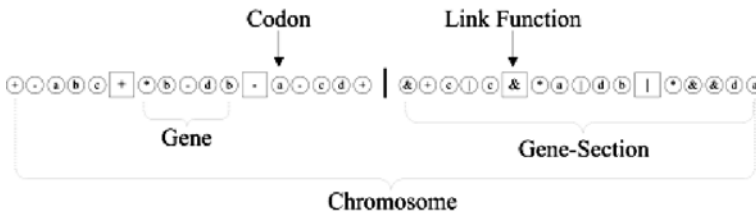
Figure 2: Structure of a chromosome in GEPAT

This structure brings more flexibilities. First, each gene-section can have its own length according to the complexity of the target function we wish to get from it. Second, each gene-section can be assigned a specific type of function according to the nature of the task we want it to solve. In Figure 2 for example, two gene-sections are assigned with different operators. The gene-section to the left is an arithmetic function and the gene-section to the right is a logical function. Third, each gene-section can have its own data source or communicate with each other with predictions and byproducts of the function. This is the most important feature for modeling decision processes where information flows are frequently exchanged among mental operators. With this structure, simultaneous solutions for parallel functions are viable. It is also reasonable to believe this structure can make good cooperation among gene-sections just as the normal GA

program does, because they are built on the same mechanism. In this mechanism, no rules are pre-set; the functions are constructed, tested, refined and referenced from each other simultaneously rather than sequentially towards the only ultimate purpose, fitting best to the data.

2.2. Test different problem schemes

Identifying the mechanisms underlying the pedestrian shopping decision process is far from easy. It is not only because this information is hidden, but also many mechanisms can generate the same outcomes in common situations (Todd and Gigerenzer 2003). Hence researchers have to test every possible mechanism and judge which one is appropriate. GEPAT is designed to facilitate these tests by providing the researcher with building blocks each of which performs simple information processing, simulating the working of mental operators. They are called processor. Each processor has input and output interfaces to receive information from and send information to other processors. By properly organizing these processors, the researcher can construct many complex problems. In the following, some main processors for shopping decision process modeling are introduced.

Satisficer

As one of the most important concepts in BR, "satisficing" behavior implies some thresholds as judgement standards to stop further information search and accept the option. The satisficer has two input interfaces: one includes the choice option for judgement returned from other processors; the other includes all available options whose qualifications (whether they survive the thresholds) are predicted by some logical function of a gene-section. Then the single option is referenced to its qulification in the option sets. If it survives, the satisfied option will be passed to other processors. If not, the satisficer returns none.

Maximizer

Though the shopping decision process is not a single utility maximizing process, maximizing behavior may still exist, either intentionally or unintentionally in the context of limited information. The maximizer represents the simple information process, picking the option with the maximum (or minimum) value returned by some function. For example, before the pedestrian performing the satisficing judgement, there must firstly be one option comes to his mind. We could assume that when the pedestrian perceives the shopping environment and one store catches his attention, he unintentionally accepts the dominant impact, such as floor space, window arrangement, advertisement, and distance, emitted from the store among nearby stores. If the maximum option, after passed to the satisficer, doesn't survive, the second maximum one will be passed. This processor could repeat until a satisfied one is found or some conditions stop it.

Memorizer and updater

Pedestrian's memory must be incorporated into the modeling of the decision process. Both post experience and impression on the shopping environment learned on the spot can make the pedestrian better informed or cause him to adjust the decision strategy. The memorizer is used to recall stored information when needed. For example, if the memorizer tells the pedestrian there are many unsatisfied judgements related to previous stores, the pedestrian would better lower his expectation level in the following decision process to save the cost of too much search. In contrast, if there is a lot of satisfied experience in the memory, the pedestrian would better raise his expectation level so that he could receive more benefit from the next satisfied search. The updater usually cooperates with the memorizer to update stored information. The updating process could be conditional, say, only updates satisfied experiences. Moreover, the quantity to be updated could also be selected by the researcher. It can be a pre-set constant or an input from a gene-section which could generate variant quantities based on different stages of the shopping process.

Auxilliary processors

The auxiliary processors all have their specific functionalities in shopping decision process modeling.

Decider: It is a judgement processor that outputs different information according to different requirements.
Collector: It collects pieces of information and send them out as a whole when needed.
Nickeler: Though not happening often, the pedestrian may encounter situations hard to make a decision. When he decides by throwing a nickel, the nickeler processor is activated.
Evaluator: After fitted to the data, each chromosome is evaluated by the evaluator processor. It evaluates the chromosome with the fittness value and records the best performed chromosome in this generation.

2.3. How does it work?

Figure 3 illustrates an example workflow of GEPAT. It starts from the data source transferring data to the receivers. Note that there could be multiple data sources. If the model needs memorized information, the data is first transferred to the memorizer, then to the gene-sections. If it is the first time to run the model, an initial generation of chromosomes must be randomly generated. Only after this process, the data can find their right positions in the gene-sections. The translation process is wrapped in the gene-section, which returns the value of the function represented by the gene-section once the code and the data are ready. Usually, each gene-section corresponds to a processor about whose decision mechanisms we care most. In this example, gene-section1 corresponds

to a maximizer so that in the end we could get a function telling how the pedestrian trades off factors and chooses the option. The gene-section2 corresponds to a satisficer. It could extract some judgement thresholds by using logical functions. After the information being transferred and modified in other processors, the evaluator evaluates each chromosome. If this is not the end of the iteration, the chromosomes are modified by gene operations according their fitness values. If the iteration ends, GEPAT outputs the results including the best chromosomes and their corresponding functions. Manipulating GEPAT is no more difficult than drawing such a flowchart. Each building block is represented by a visual element. By linking them and setting parameters properly, we can test many complex schemes of pedestrian shopping decision process.
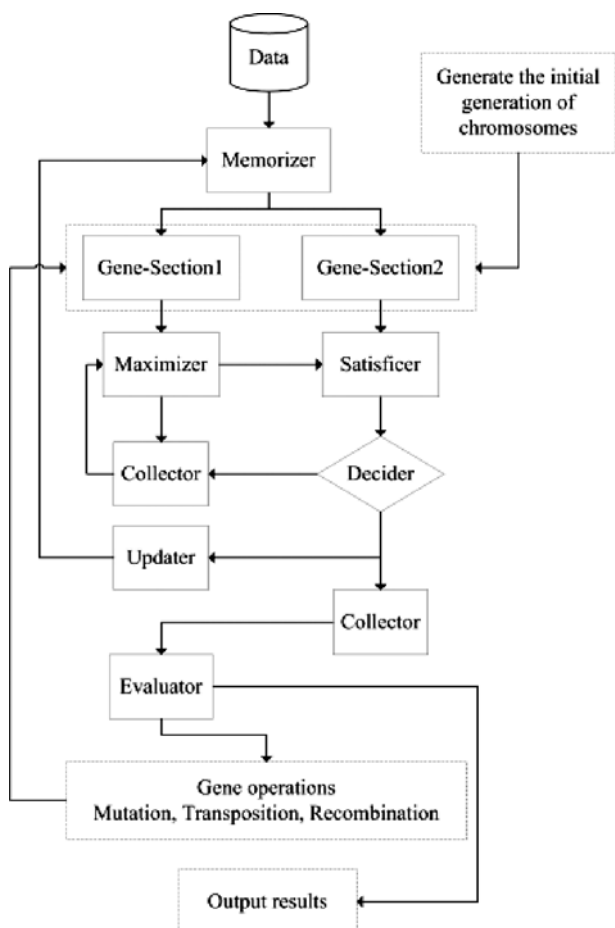
Figure 3: Workflow of GEPAT

3.   Discussion and conclusion

Except the above two methodological potentials of GEPAT as tool for solving complex, multi-functional problems, an advantage is that the researcher does not need a strong prior theory nor has to make rigorous assumptions about the function specification of the model. Unlike traditional statistical modeling, the forms of functions evolve rather than are defined. This implies large possibilities of finding unexpected model specifications which could give the researcher new perspectives to look into a problem. However, such advantage causes the most negative effect to GEPAT and similar GA programs: they are extremely resource-intensive. The non-deterministic process usually requires a large chromosome population and large number of generations (iterations), especially for complex problems, to evolve into a single good solution. Neither can it guarantee the best solution from each test. It requires a certain numbers of experiments, time, patience and more powerful computation platforms than a PC.

There is no perfect tool; the question is how we can make best use of a tool. GEPAT is designed to solve decision problems, but its functionalities could be extended. Building blocks specific for other kinds of problems can be designed and added to the program. If it is thought to go too far beyond the traditional way of modeling, it can be designed to receive self-defined functions and make gene-sections as parameter finders. If we trust its ability and have enough hardware and time, it can be designed to find the best combination of building blocks automatically.

Still in development, GEPAT has been partly operational on simple problems. We believe that GEPAT will be a useful tool to explore pedestrian shopping behavior within the more realistic bounded rationality framework and to support decision making of related professionals more effectively. **«**

References

1.   T.A. Arentze and H.J.P. Timmermans: *Deriving Performance Indicators from Models of Multipurpose* Shopping Behavior, Journal of Retailing and Consumer Services 8, pp. 325 (2001).
2.   B.J.L. Berry, B.J. Epstein, A. Ghosh, et al: *Market Centers and Retail Location: Theory and Applications*, Prentice-Hall, (1988).
3.   J.R. Bettman: *A Threshold Model of Attribute Satisfaction Decisions*, Journal of Consumer Research 1, pp. 30 (1974).
4.   A. Borgers and H.J.P. Timmermans: *City Centre Entry Points, Store Location Patterns and Pedestrian Route Choice Behavior: a Microlevel Simulation Model*, Socio-Economic Planning Science 20, pp. 25 (1985).
5.   C. Ferreira: *Gene Expression Programming: A New Adaptive Algorithm for Solving Problems*, Complex Systems 13, pp. 87 (2001).

6.   S. Geisendorf: *Modeling Bounded Rationality by Genetic Algorithms: Strengh and Limitations*, Paper for the 24th International Conference of Agricultural Economists, Berlin (2000).

7.   D. Grether and L. Wilder: *An Analysis of Conjunctive Choice: Theory and Experiments*, Journal of Consumer Research 10, pp. 373 (1984).

8.   S. Hagishima, K. Mitsuyoshi, and S. Kurose: *Estimation of Pedestrian Shopping Trips in a Neighborhood by using a Spatial Interaction Model*, Environment and Planning A 19, pp.1139 (1987).

9.   M. Haklay, and D. O'Sullivan: *'So go downtown': Simulating Pedestrian Movement in Town Centers*, Environment and Planning B 28, pp. 343 (2001).

10.   P. Kau and L. Hill: *A Threshold Model of Purchasing Decisions*, Journal of Marketing Research 9, pp. 264 (1972)

11.   J. Kerridge, J. Hine, and M. Wigan: *Agent-Based Modeling of Pedestrian Movements: The Questions that Need to be Asked and Answered*, Enviroment and Planning B 28, pp.327 (2001).

12.   K. Kitazawa and M. Batty: *Pedestrian Behaviour Modelling: An Application to Retail Movements using a Genetic Algorithm*, Paper for the 7th International Conference on Design and Decision Support Systems, Eindhoven (2004).

13.   S. Krygsman, T. Arentze and H. Timmermans: *Capturing Interdependencies in Tour Mode and Activity Choice: A Co-Evolutionary Logit Modelling Approach*, Paper for the 10th International Conference on Travel Behaviour Research, Lucerne (2003).

14.   A. Newell and H.A. Simon: *Human Problem Solving*, Prentice-Hall (1972).

15.   H. Oppewal and H.J.P. Timmermans: *Modelling the Effects of Shopping Centre Size and Store Variety on Consumer Choice Behavior*, Environment and Planning A 29, pp. 1073 (1997).

16.   J.W. Payne, J.R. Bettman, and E.J. Johnson: *The Adaptive Decision Maker*, Cambridge University Press (1993).

17.   J. Swait: *A Non-Compensatory Choice Model Incorporating Attribute Cutoffs*, Transportation Research B 35, pp. 903 (2001).

18.   P.M. Todd and G. Gigerenzer: *Bounding Rationality to the World*, Journal of Economic Psychology 24, pp. 143 (2003).

19.   B. Vroomen, P.H. Franses, and E. Nierop: *Modeling Consideration Sets and Brand Choice using Artificial Neural Networks*, European Journal of Operational Research 154, pp. 206 (2004).

A Discrete choice framework for acceleration and direction change behaviors in walking pedestrians

G. Antonini[1] and M. Bierlaire[1]

The walking process is interpreted as a sequence of decisions about where to put the next step. A dynamic and individual-based spatial discretization is used to represent the physical space. A behavioral framework for pedestrian dynamics based on discrete choice models is given. Direction change behaviors and acceleration behaviors are taken into account, both in a constrained and unconstrained formulation. The unconstrained direction changes (keep direction, toward destination) and acceleration (free flow acceleration) behaviors are the same as those introduced in our previous work. In this paper we focus on the definition of the constrained counterparts. A leader follower behavior is interpreted as a constrained acceleration while collision avoidance behavior as a constrained direction change. The spatial correlation structure in the choice set deriving from a simultaneous choice of speed regimes and radial directions is taken into account specifying a cross nested logit model (CNL). Quantitative results are presented, obtained by maximum likelihood estimation on a real data set with more than 10 thousands observed positions, manually tracked from video sequences.

1.   Introduction

Modeling pedestrian behavior is becoming always more important. Several approaches have been adopted by researchers from different fields, such as transportation science, architecture and land use, artificial intelligence and computer graphics, among others. For a detailed review of the state of the art on pedestrian behavior modeling we remind the interested reader to [1].

This paper focuses on the walking behavior of individuals at the operational level, extending the discrete choice set up already defined in our previous work. Here we extend the framework keeping the same spatial discretization and choice set definitions, which are quickly reviewed in the next section. The main contribution of this work is a more detailed analysis of acceleration and change direction models. Inspiration is taken from previous works in transport engineering ([2],[3] among others) and those methodologies are extended and adapted to the pedestrian case. A constrained acceleration model (leader follower) and a constrained direction change model (collision avoidance) are specified and fitted to the DCM framework. Quantitative analysis is performed by maximum likelihood estimation, using real human trajectory datasets, manually tracked from video sequences. The paper is structured as follows. In section 2 we define the modeling elements, in section 3 we describe the behavioral model, in section 4 we present

Signal Processing Institute
Operations Research Group ROSO
Ecole Polytechnique Federale de Lausanne
CH-1015 Lausanne, Switzerland

the datasets used for the estimation process and in section 5 we present the results. We conclude with final remarks and future works.

2.   Modeling elements

In our approach the walking process is considered as a sequence of choices on the next step position. The time resolution of such decision making process is of the order of 1 second. Assuming the final destination being exogenous to the model, we are interested in modeling the short range behavior of pedestrians, as a response to their kinematic state and to the presence of other pedestrians. In this context, we define the following modeling elements.

The space model

A dynamic and individual-based spatial representation is used, which depends on the current speed and direction of the individuals. The adaptive discretization is obtained assuming three speed regimes (accelerated, decelerated and constant current speed) and eleven radial directions, as shown in Figure 1.
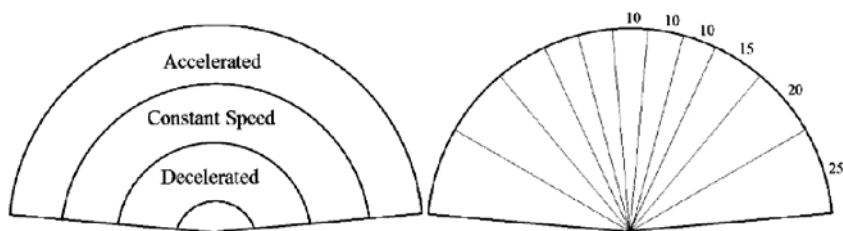
Figure 1: Choice set

Behaviors

As already said, individuals walk on a 2D plane. Basically, any kind of behavior influencing their movement will result in two kind of observations: changes in directions and changes in speed, i.e. accelerations. In this spirit, we define the general conceptual framework for pedestrian walking behavior, illustrated in Figure 2.

The leafs of the tree show the behavioral patterns we want to capture. In the following, we give a short qualitative description.

» keep direction: Pedestrian trajectories in normal conditions[1] are characterized by a certain regularity. People do not change direction often over time, up to a certain level of density. With the keep direction behavior we identify the tendency of individuals to keep, when is possible, their current direction

---

[1] With the term normal conditions we mean non-evacuation and non-panic situations.
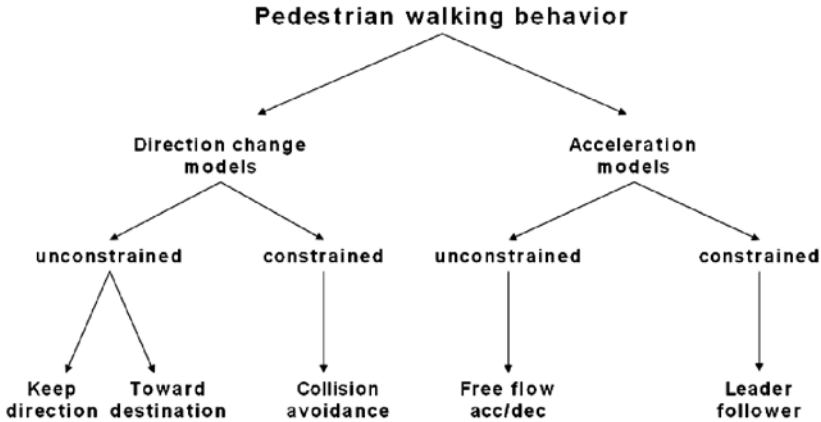
Figure 2: Conceptual framework for pedestrian walking behavior.

» toward destination: We assume the final destination of an individual as an exogenous variable in the model, being fixed at the strategical decision level. Being pedestrian movements 2D displacements, we assume that both the difference in direction and the distance from the final destination influence individuals. With the toward destination behavior we identify the tendency of pedestrians to move, when is possible, directly toward their final destinations.

These first two behaviors can be interpreted and located in a more general context. First of all, they are unconstrained models for direction changes, i.e. they do not depend on the presence of other individuals. Referring to the hierarchical decision process described above, individuals choose their final destinations at a strategic level while a route choice and/or intermediate destination choice happen at the tactical level. Such higher level choices are reflected naturally on the short term behavior, captured at the operational level by the keep direction and toward destination behavioral patterns.

» free flow acceleration/deceleration: We refer here to the free flow, unconstrained, acceleration behavior. The main assumption is that the acctractiveness for an acceleration (deceleration) depends on the current individual speed module. Indeed, someone who is already walking fast has less incentive for further accelerations with respect to someone who is walking slowly. This model for accelerations is conceptually related to the idea of a maximum physical speed. Such a value is unobserved and individual dependent, being related to socio-economics characteristics such as age, gender, weight etc. ... In our model we use the maximum observed speed module in the data and for simplicity we assume it as homogeneous over the population

» leader follower: A common phenomenon observed in highly crowded situations is the lane formation. People behave identifying leaders in their surrounding

environment and choose to follow them as an optimal solution to better attain their goals. Individuals satisfying at the leader conditions represent the potential leaders. We allow for more potential leaders for each radial direction. A leader choice process is assumed, leading to one leader for each direction, constraining the acceleration (deceleration) behavior of the decision maker

» collision avoidance: Individuals change direction in order to avoid possible collisions with other individuals. As for the leader follower, potential colliders are defined on the base of certain collider conditions. An implicit collider choice process is assumed, leading to one collider for each direction, influencing the direction change behavior of the decision maker

3.   The pedestrian behavior model

Three speed regimes and 11 radial directions give rise to a choice set composed by 33 alternatives, each of them represented by its central point.

Systematic utilities

The systematic utilities of the full model are reported in equation 1:

$$
\begin{aligned}
V_{vdn} = {} & \beta_{dir} dir_{dn} & + \\
& \beta_{acc} I_{v,acc} (v_n/v_{max})^{\lambda_{acc}} & + \\
& \beta_{dec} I_{v,dec} (v_n/v_{max})^{\lambda_{dec}} & + \\
& \beta_{ddest} ddest_{vdn} & + \\
& \beta_{ddir} ddir_{dn} & + \\
& I_{v,acc} I^L_{acc} \alpha^L_{acc} D^{\rho^L_{acc}}_{L_L} \Delta v^{\gamma^L_{acc}}_{L_L} \Delta \theta^{\delta^L_{acc}}_{L_L} & + \\
& I_{v,dec} I^L_{dec} \alpha^L_{dec} D^{\rho^L_{dec}}_{L_L} \Delta v^{\gamma^L_{dec}}_{L_L} \Delta \theta^{\delta^L_{dec}}_{L_L} & + \\
& I_{d,d_n} I_C \alpha_C e^{-\rho_C D_C} \Delta v^{\gamma_C}_C \Delta \theta^{\delta_C}_C &
\end{aligned}
$$

$$(1)$$

where all the β parameters as well as λ_{acc}, λ_{dec}, α^L_{acc}, ρ^L_{acc}, γ^L_{acc}, δ^L_{acc}, α^L_{dec}, ρ^L_{dec}, γ^L_{dec}, δ^L_{dec}, α_C, ρ_C, γ_C, δ_C are unknown and have to be estimated. Note that this specification is the result of an intensive modeling process, where many different specifications have been tested. For the keep direction and free flow acceleration behaviors (the first 3 terms in equation 1) we keep the same specification as defined in [1]. For the toward destination behavior (the 4th and 5th terms in 1) the distance of an alternative from the destination has been added (the βddestddestvdn term), with no conceptual changes with respect to its previous specification. In the following, the new elements introduced in this work are described.

» **Leader follower**

The leader follower behavior has been inspired by car following models, used in transport engineering since the early work of [4]. In such models, a subject car follows a leader one, reacting to its actions under different criteria. Here we adapt this idea to the case of pedestrians, using a sensitivity-stimulus framework (see [2]).

The leader follower behavior is modeled as a constrained acceleration (deceleration) term. The indicator function $I_{v,acc}$ in equation 1 is 1 if $v = v_{acc}$, that is, if the alternative corresponds to an acceleration and 0 otherwise. $I_{v,dec}$ is similarly defined. We consider several potential leaders in the surrounding of the current decision maker (see Figure 3(b)). An individual k is defined as a potential leader if she satisfies at the leader conditions. We can informally define potential leaders as those individuals inside the region of interest, not so far from the decision maker and having movement directions not so different from the radial cone where they lies. We formalise such ideas by means of the indicator function I_g^k:

$$I_g^k = \begin{cases} 1, \text{if } d_l \leq d_k \leq d_r \\ \quad \text{if } 0 < D_k \leq D_{th} \\ \quad \text{if } 0 < |\Delta\theta_k| \leq \Delta\theta_{th} \\ 0, \text{otherwise.} \end{cases}$$

where d_l and d_r represent the bounding left and right directions of the choice set defining the region of interest (see Figure 3(b)) while d_k is the direction identifying the pedestrian k position. D_k is the distance between pedestrian k and the decision maker, $\Delta\theta_k = \theta_k - \theta_d$ is the difference between the movement direction of pedestrian k (θ_k) and the angle characterizing direction d, i.e. the direction identifying the radial cone where individual k lies (θ_d). The two thresholds D_{th} and $\Delta\theta_{th}$ are fixed at the values $D_{th} = 5D_{max}$, where D_{max} is the radius of the choice set, and $\Delta\theta_{th} = 10$. We assume an implicit leader choice process executed by the decision maker herself and modelled choosing as leader for direction d that pedestrian satisfying at the leader conditions, and which is at distance $D_L = \min_{k \in K}(D_k)$, as illustrated if Figure 3(b), where K is the number of potential leaders in the radial cone characterized by direction d. The corresponding indicator function is I_g^L, where g = {acc, dec} indicates accelerations and decelerations, based on the sign of the leader's relative speed Δv_L defined as:

$$\Delta v_L = |v_L - v_n|$$

(2)

where v_L and v_n are the leader's speed module and the decision maker's speed module, respectively. The acceleration of the decision maker as a response to the presence of the leader individual is given by:

$$acceleration = sensitivity \times stimulus \tag{3}$$

The sensitivity term of the model is a non linear function of the leader distance D_L, defined as follows:

$$sensitivity = f(D_L) = \alpha_g^L D_L^{\rho_g^L} \tag{4}$$

with D_L defined above. The parameters α_g^L and ρ_g^L have to be estimated. The decision maker reacts to stimuli coming from the chosen leader. We model the stimulus as a function of the leader's relative speed Δv_L and the leader's relative direction $\Delta\theta_L$ as follows:

$$stimulus = f(\Delta v_L, \Delta\theta_L) = \Delta v_L^{\gamma_g^L} \Delta\theta_L^{\delta_g^L} \tag{5}$$

where the parameters γ_g^L and δ_g^L have to be estimated. A leader acceleration (deceleration) induces a decision maker acceleration (deceleration). A substantially different movement direction in the leader reduces the influence of the latter on the decision maker herself. The use for such functional forms finds its justification in the numerous previous works on car following models.

(a)   (b)
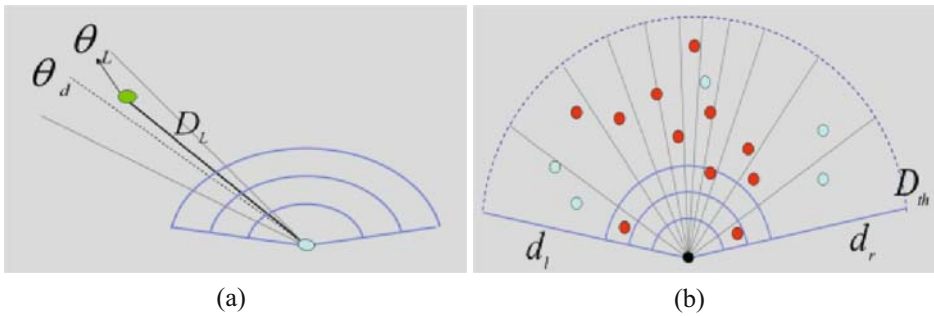
Figure 3: The elements defining the leaders. More than one potential leader is allowed for each radial cone. That one at the minimum distance from the decision maker is chosen as leader

» **Collision avoidance**

Based on the dynamic characteristics of other individuals the decision maker changes her own direction, attempting to avoid collisions with other pedestrians. We keep for this model a sensitivity/stimulus formulation. Following the approach used for the leader follower model, we assume different potential colliders for each of the 11 directions. Using a similar notation as before, a pedestrian k represents a potential collider if she satisfies at the collider condictions, as defined by the following indicator function:

$$
I_C^k = \begin{cases} 1, \text{if } d_l \leq d_k \leq d_r \\ \quad \text{if } 0 < D_k \leq D'_{th} \\ \quad \text{if } \dfrac{\pi}{2} \leq |\Delta\theta_k| \leq \pi \\ 0, otherwise. \end{cases}
$$

where d_l, d_r and d_k are the same as those defined for the leader follower model. D_k is now the distance between individual k and the center of the alternative, $\Delta\theta_k = \theta_k - \theta_{dn}$ is the difference between the movement direction of pedestrian k, θ_k, and the movement direction of the decision maker, θ_{dn}. The value of the distance threshold is now fixed to $D_{th} = 10 d_{max}$. We use a larger value for such a threshold compared to the leader follower model, assuming the collision avoidance behavior being a longer range interaction, happening also at a lower density level. We assume an implicit collider choice process, executed by the decision maker and modeled choosing as collider for direction d that potential collider having $\Delta\theta_C = \max_{k \in K} |\Delta\theta_k|$, where K is the number of potential colliders in the radial cone characterized by direction d. The related indicator function is I_C. The scenario for the potential colliders is similar to the leader follower model and is reported in figures 4(a) and 4(b).We assume a sensitivity function being a function of the distance D_C between the collider position and the center of the alternative, defnded as follows:

$$
sensitivity = f(D_C) = \alpha_C e^{\rho_C D_C}
\tag{6}
$$

where the parameters α_C and ρ_C have to be estimated. We choose the exponential form to keep the same functional form as that used in [1]. The decision maker reacts to stimuli coming from the collider. We model the stimulus as a function of two variables:

$$
stimulus = f(\Delta v_C, \Delta\theta_C) = \Delta v_C^{\gamma_c} \Delta\theta_C^{\delta_C}
\tag{7}
$$

with $\Delta\theta_C$ defined above and Δv_C defined as follows:

$$\Delta v_C = |v_C| + |v_n|$$

(8)

with v_C and vn the collider and decision maker speed modules respectively. The parameters γ_c and δ_c have to be estimated. Individuals walking against the decision maker at higher speeds and in more frontal directions generate stronger reactions, weighted by the sensitivity function.
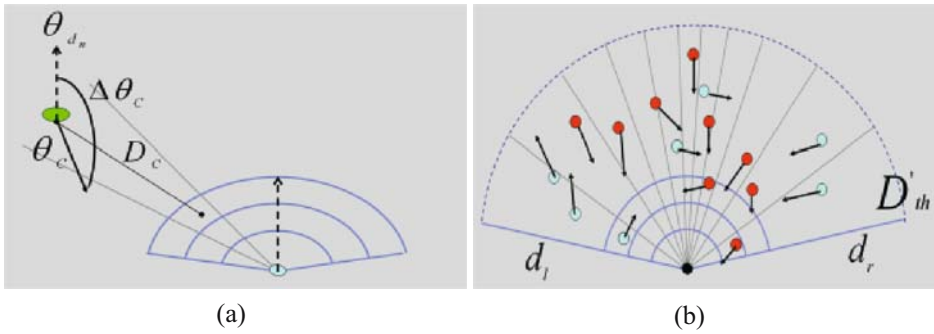

(a)   (b)

Figure 4: The elements defining the colliders. More than one potential collider is allowed for each radial cone. That one forming the maximum angle *DeltaTheta*$_C$ is chosen as collider

The random term

We keep the same cross nested logit specification used in our previous work. Such a model allows for flexible correlation structures in the choice set, keeping a closed form solution. The probability of choosing alternative *i* within the choice set *C* for a given choice maker is:

$$P(i\,|\,C) = \frac{\sum_m (\alpha_{im} y_i)^{\mu_m} (\sum_j (\alpha_{jm} y_j)^{\mu_m})^{\frac{\mu}{\mu_m}-1}}{\sum_m (\sum_{j\in C} (\alpha_{jm} y_j)^{\mu_m})^{\frac{\mu}{\mu_m}}}$$

(9)

where $\alpha_{jm} \geq 0\ \forall j,m;\ \mu > 0;\ \mu_m > 0\ \forall m;\ \mu \leq \mu_m\ \forall m$. The systematic utility function enters this formula as $y_i = e^{V_i}$. We assume a correlation structure depending on the speed and direction and we identify five nests: accelerated, constant speed, decelerated, central direction and not central direction. Given the lack of any a priori information, we fix the degrees of membership to the different nests (α_{jm}) to the constant value 0.5 (see [5]).

4.   Data

The datasets used to estimate the model consists of pedestrian trajectories manually tracked from video sequences. We have pooled together two different datasets, collected separately in Switzerland and Japan.

The swiss dataset: This part of the dataset consists of 36 pedestrian trajectories, manually tracked from a digital video sequence. The scene has been recorded out of the Lausanne metro station in 2002. For a detailed description of this dataset we refer the reader to [1].

The japanese dataset: This dataset has been collected in Sendai, Japan, on August 2000 (see [6]). The video sequence has been recorded from the 6th floor of the JTB parking building (around 19 meter height), situated at a large pedestrian crossing point. Two main pedestrian flows cross the street, giving rise to a large number of interactions. In this context, 190 pedestrian trajectories have been manually tracked, with a time step of 1 second. The collected data contain the pedestrian identifier, the time step and the image coordinates. The mapping between the image plane and the walking plane is approximated by a 2D-affine transformation, whose parameters are learnt by linear regression.

5.   Results

Table 1 reports the estimation results for the CNL specification. We have estimated the unknown parameters of the model using the Biogeme package ([7]). It is a freeware package for the estimation of a wide range of random utility models.
The negative signs for the β_{ddir} and β_{ddist} indicate that a cost is perceived for those alternatives farther from the final destination, both in distance and direction. The β_{dir} estimated value reflects the tendency of individuals to avoid frequent direction changes. People decide their final destinations at a strategic level, their routes and paths at a tactical level ([8]). These decisions are reflected on a short time horizon and are coherent with negative signs for the β_{ddir}, β_{ddist} and β_{dir} coefficients. This conclusion is also accordant with other previous studies on the idea that individuals move through spaces along paths that minimize the angular displacements (see [9] for more details). β_{acc} and β_{dec} signs confirm the idea that changes in speed reduce the utility of the corresponding alternatives, indicating a preference of pedestrians for constant speed values. A positive sign for the elasticity parameter λ_{acc} reflects the fact that the attractiveness for accelerations is a non linear function of the current speed value, as already shown in [1]. The elasticity for decelerations, λ_{dec}, has not been estimated significantly different from zero. This first part of the estimated parameters correspond to the unconstrained behaviors, depending only on the decision maker movements.
The α^L_{acc}, ρ^L_{acc}, γ^L_{acc} and δ^L_{acc} describe the leader follower behavior in case of an accelerated leader. The presence of such an accelerated leader increases the utility of the accelerated

alternatives ($\alpha^L_{acc} > 0$). The negative sign for ρ^L_{acc} reflects the fact that the distance of the leader is negatively correlated with the induced acceleration, as expected. Increments in the absolute value of the leader relative speed induce greater accelerations, as indicated by $\gamma^L_{acc} > 0$. The leader relative direction coefficient, δ^L_{acc}, has not been estimated signifi-

Variable name	Coefficient estimate	t test 0	t test 1
β_{ddir}	-0.061	-19.066	
β_{ddist}	-1.614	-1.9749	
β_{dir}	-0.027	-11.342	
β_{acc}	-19.822	-5.847	
β_{dec}	-2.069	-2.651	
λ_{acc}	0.969	26.880	
α^L_{acc}	4.883	3.368	
ρ^L_{acc}	-0.657	-3.034	
γ^L_{acc}	0.869	9.877	
α^L_{dec}	4.061	6.278	
ρ^L_{dec}	-0.481	-4.280	
γ^L_{dec}	0.524	9.089	
δ^L_{dec}	-0.892	-1.642	
α_C	-0.0058	-4.639	
ρ_C	-0.313	6.748	
γ_C	0.781	3.318	
μ_{const}	1.597	32.413	12.119
$\mu_{not\_central}$	1.487	15.765	5.160
μ_2	0.591	-	-8.565
Sample size = 10783			
Number of estimated parameters = 19			
Init log-likelihood = -78558.3			
Final log-likelihood = -22572.7			
Likelihood ratio test = 30260.3			
$\bar{\rho}2 = 0.4007$			

Table 1: CNL estimation results

cantly different from 0. Similar interpretation for the decelerated leader parameters α^L_{dec}, ρ^L_{dec}, γ^L_{dec} and δ^L_{dec}. We keep δ^L_{dec} in the model, even if it is not significant (t-test = 1.642). Its negative sign might be explained as a lower influence of those leaders having movement directions quite different from the radial cones where they are, as expected. The α_C, ρ_C, γ_C and δ_C describe the constrained direction change behavior, i.e. collision avoidance. The negative sign for α_C indicates a lower utility for those directions where there is a collider, as expected. Colliders farther from the alternatives have a lower negative influence on the utilities ($\rho_C < 0$). Higher values for the collider relative speed, indicating early possible collisions, decrease the utility values ($\gamma_C > 0$). The value of δ_C is not estimated. It has been fixed arbitrarily to 1.

Two over five nest coefficients have been estimated significantly different from 1. μ_{const} and $\mu_{not\_central}$ capture the correlation between the alternatives in the constant speed and the not central direction nests, respectively. Finally, two different scale parameters have been used to capture the heterogeneity in the two different datasets. We have fixed to 1 the scale related to the Japanese data and the scale related to the Swiss sample ($\mu2$) has been estimated. Its value is significantly different from 1, as reported in Table 1.

6.   Summary

We have presented here a development of our previous work on pedestrian modeling. A discrete choice framework is used, interpreting the walking process as a sequence of choices, step by step. In this paper we have generalized the approach, identifying direction changes and accelerations behaviors for a short time range pedestrian model. Both such behaviors have unconstrained and constrained formulations. The first refer to decisions taken by individuals based on their kinematic state and on decisions taken at a strategical and/or tactical levels (destination choice, route choice). The seconds refer to constrained accelerations (decelerations) induced by individuals perceived as leaders, who are defined on the base of certain leader conditions. Similarly, constrained direction change behaviors are described in terms of collision avoidance patterns, induced by the presence of colliders, defined on the base of certain collider conditions. The model shows a good explanatory power with respect to the datasets used for estimation. The heterogeneity in the data has been captured by two different scale parameters. Correlations between alternatives are captured by means of a CNL formulation.

Interesting extensions to our approach would include the use of controlled experimental conditions, allowing for the use of socio-economic variables, such as age, sex, weight etc. ... The influence of the spatial layout should also be included, being the model a pure human-to-human interaction model. **«**

Acknowledgments

References

1.   G. Antonini, M. Bierlaire, and M. Weber: *Discrete Choice Models of Pedestrian Behavior*, Under review for publication on Transportation Research (2004).
2.   T. Toledo: *Integrated Driving Behavior Modeling*. PhD thesis, Massachusetts Institute of Technology (2003).
3.   K.I.Ahmed: *Modeling drivers' acceleration and lane changing behaviors*, PhD thesis, Massachusetts Institute of Technology (1999).
4.   R. Reuschel: *Fahrzeugbewegungen in der Kolonne*, Österreichisches Ingenieur Archiv, 4, pp. 193–215 (1950).
5.   M. Bierlaire: *A Theoretical Analysis of the Cross-Nested Logit Model*. Accepted for publication in Annals of Operations Researchs.
6.   K. Teknomo, Y. Takeyama, and H. Inamura: *Review on Microscopic Pedestrian Simulation Model*, In: Proceedings Japan Society of Civil Engineering Conference (2000).
7.   M. Bierlaire: *An Introduction to BIOGEME Version 0.6*, www.roso.epfl.ch/biogeme, February 2003 (2003).
8.   S.P. Hoogendoorn, P.H.L. Bovy, and W. Daamen: *Microscopic Pedestrian Wayfinding and Dynamics Modelling*, In: M. Schreckenberg and S.D. Sharma (Eds.), Proceedings of the International Conference on Pedestrian and Evacuation Dynamics, pp. 123–154. Springer (2002).
9.   A. Turner: *Angular Analysis*, In: Proceedings 3rd International Symposium on Space Syntax, pp. 30.1–30.11 (2001).

Calibration and validation of the Legion simulation model using empirical data

J.L. Berrou[1], J. Beecham[1], P. Quaglia[1], M.A. Kagarlis[1], and A. Gerodimos[2]

A frequently encountered difficulty in the field of pedestrian modelling and crowd dynamics is the scarcity of systematic empirical data. This paper attempts to narrow this gap by discussing the collection and analysis of large amounts of empirical data from around the world, which is used to first calibrate and then validate the microscopic pedestrian interaction model that lies at the heart of the commercial simulation software package 'Legion'.

We briefly review the model which represents pedestrians as learning-adaptive agents with individual preferences and objectives. Next we describe our method of extracting microscopic (individual) and macroscopic (crowd) data from video recordings of real-life pedestrian crowds, filmed at selected locations. The former supply demographic profiles of pedestrian attributes used as inputs, and help calibrate the model parameters by probing context dependencies of the dynamics. The latter yield collective observables and patterns, used to benchmark simulation outputs.

We present examples of measurements and corresponding simulations, which demonstrate the breadth and quantitative agreement of the model with the data. Examples include sports spectators queuing as a result of operational procedures; commuters queuing at a bottleneck created by limited vertical circulation capacity; and train passengers boarding, and alighting from, densely populated carriages.

1. Introduction

Pedestrian simulation models are increasingly used by consulting engineers, asset owners and operators to help design safer, efficient and visitor-friendly places such as mass transportation terminals, sport stadiums and plazas. A number of theoretical models have been proposed with some having been further implemented as commercial software. An emerging trend is the migration from macroscopic fluid-flow crowd models, onto discrete space automata models and microscopic multi-agent models in continuous space.

Multi-agent models should by definition outperform all other types on many fronts including:

» simulating cross-flows and counter-flows in normal operations
» modelling merging flows in evacuation situations
» predicting flow values and travel time in bottlenecks
» understanding the distribution (as opposed to the mean) of
   individual travel times

---

[1]The MAIA Institute, 41 Avenue Hector Otto, 98000 Monaco
[2]Legion Limited, 22-26 Albert Embankment, London, SE1 7TJ, UK

» being used to produce plausible 3D Virtual Reality rendering
» mapping space utilisation, density and speed as a function of time with superior accuracy and granularity
» arriving at more realistic estimates of size and shape of queues at congestion points.

These advantages are, in theory, within the reach of a well-implemented model in which agents make their own decisions in continuous space; in practical terms, though, the ability to develop an appropriate abstraction of pedestrian movement, identify and calibrate the right parameters and, crucially, validate simulation outputs is hindered by the relative absence of empirical measurements, particularly so in high densities[14]. Constrained by resources and time as well as objective technical difficulties, modellers are often forced to resort to "recycling" published and believed-to-be-obsolete data[5]. They may also rely on organised experiments which shed some light on particular issues but often cover small and not sufficiently diverse population samples and contexts.

Specifically, a common vulnerability of all fluid-flow and discrete space models and most agent models is their inability to predict flow values when the crowd density exceeds its critical value and the flow begins to drop from its peak. The common reason for this failure is an implicitly or explicitly assumed flow-density relationship based on a combination of real-life observations up to 1.5-2.0 p/m^2 and conjecture beyond that point. However, in terms of real-life situations much greater densities are readily observed in congestion points like: checkpoints; entrances to narrow passages and vertical circulation elements; or in carriage and lift boarding and alighting scenarios.

The Legion measurements discussed in this paper address these very issues, concentrating on values of flow beyond critical density. Through a series of examples we show that the Legion model replicates the whole distribution of flow and density fluctuations in the congestion points.

2.   Brief overview of the Legion Model

The multi-agent pedestrian model at the heart of the Legion simulator has been developed at the Maia Institute since 2000. It replaces an earlier version developed by G.K. Still[3].

Each pedestrian is modelled as a two-dimensional "entity" with a circular body, which moves in 2D continuous space, in 0.6s time steps. The model can handle multiple floors, with special objects to enable the modelling of circulation elements such as stairs, escalators, ramps, moving walkways and lifts (elevators).

Each entity moves towards its current target by selecting a step which seeks to minimise a perceived objective cost function. Details of the model are outside the scope of this

paper but the interested reader may refer to Kagarlis[1] and Kagarlis et al.[2]. This cost is a weighted sum of the following three components:

» Inconvenience: Work to move, in excess of the amount which is necessary to reach one's destination
» Frustration: Energetic cost equivalent of violating the speed preference time expenditure,
» (Spatial) Discomfort: Energetic cost equivalent of violating the preferred clearance from neighbours and obstacles (a sum of functions of distances to predicted positions of perceived closest neighbours, and other functions of distances to local obstacles).

Entities try to minimise their perceived composite cost. Their perception of the neighbourhood is imperfect, because their vision is bounded by angle and distance, and they must often predict the future position of their neighbours. As they move, entities learn from recent experience and adapt the weights of inconvenience, frustration and discomfort to the local circumstances (available space, local geometry, density, speed of companions and others). They distinguish their companions, who travel in the same general direction, from other entities who are in cross flows. Finally, entities communicate with immediate neighbours to either prevent or resolve blockages.

The entity parameters are drawn from entity population profiles which may vary with:

» Types of pedestrian–commuters, sport spectators, tourists
» Region–Continental Europe, UK, USA, Far East
» Context–indoor, outdoor, walkways, escalators, platforms, stairs up and down.

These parameters include:

» The physical radius of each entity, drawn from the distribution of sizes as published by Pheasant[4].
» The preferred free speed, drawn from our measured distributions of the preferred speeds of real pedestrians in similar locations and contexts. Throughout a simulation each entity has a context-dependent free speed but conserves its preferred speed rank, while the whole population speed distribution matches measured speed distributions in the various venue contexts.
» Personal space[5,6] (oriented in the direction of movement) surrounding each entity. The size of this space is also drawn from a distribution measured on real people, but for simplicity its shape at rest is similar for all entities. This shape also depends on an entity's relative speed[2].

3.   Measurement objectives and approach

In this section we consider the motivation for collecting empirical data, some of the methods available to researchers, and our preferred approach, which is prompted by the need to obtain very accurate data even under mitigating circumstances.

Objectives

The decision to collect measurements has been largely motivated by the absence of sufficient qualitative and quantitative data for carrying out three main activities:

Model abstraction: the process of developing a realistic pedestrian-interaction model from observations of real pedestrians and their decision-making processes.

Model calibration: the process of extracting, from observations of real pedestrians, the values (or the distributions of values) of the entity parameters which produce realistic behaviour for single pedestrians. Associated with this process is an iterative approach that eliminates unwanted parameters and introduces others as appropriate to increase the realism of the model.

Model validation: the process of verifying that the collective behaviour of modelled crowds correctly replicates the behaviour of real crowds, once the individual parameters have been set. The task of validating a model intensifies as the model becomes capable of representing more features of crowd behaviour. We not only verify that the simulator replicates the range of the fluctuations of real crowds' flow, speed and density at capacity but are also concerned with qualitative issues such as the size and shape of emergent queues at bottlenecks. This significantly complicates the measurement requirements.

Approach

Real pedestrian observations can be carried out under controlled experiment conditions[7,8,9]. Since the obstacle-geometry and the circulation scenarios can be altered at will, these observations are particularly useful for understanding pedestrian movement "laws". A further advantage is the possibility of using automated tracking hardware and software which facilitate greatly the automatic extraction of data from the experiment.

However, these controlled experiments can probe only part of the variety of phenomena generated by real pedestrians, environments and scenarios. They must be complemented by a very large collection of empirical observations and measurements of real crowds in real environments.

To capture a broad spectrum of authentic pedestrian and crowd behaviours, we use unannounced experiments in which unobtrusive video equipment is fitted overnight and

discreetly controlled by a few operators. Video recording has become our preferred method because the advent of cheap digital recording equipment and software to process and visualize video on personal computers has made extensive coverage possible without jeopardising the quality of the extracted data.

Other researchers[7,10,11] have reported their use of automatic methods to detect and track pedestrians on video files. The performance of these methods can be excellent at low densities or when participants can be equipped with devices to facilitate their classification. But the state-of-the-art in pedestrian automatic recognition and tracking technology does not yet permit the proper and speedy tracking of a crowd of unaware pedestrians in cluttered environments like metro stations or stadium concourses where low ceilings often force the use of surveillance-type cameras, set at unhelpful angles and in poor light conditions. These constraints, coupled with the need to obtain high-quality data, give rise to a time-consuming process involving different kinds of expertise, human intervention and various software tools. We outline the process in the following section.

4.   Measurement process overview

Filming equipment

We use mainly miniature PAL surveillance cameras, connected either via video cable or 2.4GHz radio link to remote Digital Video Recorders, recording either on video tapes in DV format (720x576 pixels, interlaced, 25 fps) or on SD memory cards in ASF format (320x240 pixels, 12.5 or 25fps). This permits to position and conceal the surveillance cameras at good viewpoints, while keeping the recorders at more accessible and discreet locations. Up to 32 such systems can be deployed in parallel, allowing extensive coverage of pedestrian movements across multiple floor buildings, or through whole metro stations or sport stadiums. Each DV tape recorder can record continuously for up to 90 minutes; the SD card recorders can record up to about 5 hours in LP mode (12.5 fps) on a 512 MB card.

Measurement database

The video sequences are subsequently catalogued in a database, which also stores the type of equipment used and the details of the filmed events (scenarios and timings of events, annotated plans, CAD plans and photos of the venue). The sequences are transferred into AVI format and compressed for archival on a digital storage medium. The database is fully searchable and is used to store and link all relevant outputs throughout the process.

Since January 2000, we have started collecting video recordings of various situations involving large numbers of people, focusing on heavily populated train and metro stations, sport spectators in and around sport arenas, evacuation drills, and other large

crowd gatherings like street parties and F1 Grand prix. Our pedestrian film collection currently holds over 900 hours of video footage, consisting of about 1,530 different video sequences. About one third of that footage has been extracted and transferred on around 1,800 video files. Of these, 1,300 have been subjected to the tracking process described below, and the current total number of marks lies somewhere between 6 and 7 millions.

Tracking pedestrians

Because of the suboptimal light and angle conditions and the limited resolution of the equipment used, manual tracking is the only option for producing accurate outputs. We have therefore developed an in-house "video annotator" software tool called ZEUS, to enable an operator to quickly but manually mark pedestrians on video files. The marks form a track for each pedestrian, and all the tracks on a video file are recorded into a corresponding project file. The operator can document each pedestrian track to identify and classify individuals according to gender, age, type of luggage carried, impairment, destination, activity, or any other recognisable criterion we may want to study. The ZEUS marks and the annotations in a project can be replayed with the movie, in order to correct mistakes or address other anomalies: for instance, on occasions we have to "interpolate" missing marks.

The way pedestrians are marked on a given video sequence depends on the type of measurements to extract from the movie:

» For speed measurements projects, each pedestrian is given a name and description (gender, age, type of luggage if any, group if not single, etc.). The marks are often painted on the feet when and where these touch the ground (or the steps of a stairway). Head marks are used when the camera height is sufficient to neglect the error induced by stature differences between pedestrians.

» For flow measurements, one or more flow lines are drawn across the video, and each directed flow through that line is painted as a "dummy pedestrian track", by laying a mark on the line whenever a crossing in the flow direction occurs. The time series is then processed to give flow values.

» For personal space estimation, and for measurements used for validation, each pedestrian head is marked at regular intervals, usually every 0.2s. This allows us to decimate the time interval being analysed to obtain three "interlaced" space/time files at 0.6s sampling time, for direct comparison with model predictions.

» To measure elapsed time, like when people pass control points, read information, or use various services, each pedestrian is marked just twice: at the beginning and at the end of the event.

Extracting real-world coordinates

With unannounced experiments inside large public buildings, it is very seldom possible to position the camera high above the crowd, and facing straight down. Most of the time, low ceilings force the choice of poor camera positions and dictate the use of very wide angle lenses, which have considerable barrel distortion. It is then necessary to correct for the lens distortion and for the perspective deformation, in order to derive the 2D coordinates of the pedestrian on the ground (or 3D if the ground is not flat) from the pixel coordinates of his/her marks in the video frame. We have developed proprietary methods and software tools to perform these operations, but their descriptions are outside the scope of this paper.

Analysis

The histories of pedestrian coordinates on the ground can then be analysed, and compared to the ones predicted by the simulator. This is done using a variety of in-house software modules developed using the ROOT[12] data analysis framework from CERN. These modules include:

» Pre-processing tools to:
  » Verify the integrity and the quality of the "ZEUS marks" histories;
  » Visualize the raw data in various formats;
  » Filter for unimpeded pedestrians (for preferred speed measurements);
  » Filter pedestrian by category (gender, age, etc. …).

» Speed Calibration tools to:
  » Estimate individual speeds from head marks or feet marks on flat ground;
  » Estimate individual speeds from feet marks in stairs;
  » Calculate histograms and fit empirical speed distribution functions.

» Personal Space Calibration tools to:
  » Identify the closest neighbours of each individual;
  » Filter out the individuals that do not have enough neighbours;
  » Estimate the personal space shape and size, taking into account each pedestrian speed vector.

» Validation Analysis modules to estimate:
  » Flows on selected flow lines;
  » "Space Density" in predefined areas;
  » "Entity Density" as perceived by each pedestrian;
  » Average speed and speed dispersion in predefined areas;
  » Speed changes statistics for a selected pedestrian along his path;

>>   Speed synchronisation between neighbours;

>>   Space utilisation, density and speed maps.

Most Validation analysis tools can be used on real measurement result files as well as on simulation result files, to enable direct comparison of our model predictions and the observed reality.

5.   Examples of calibration measurements

New York Metro Commuters – preferred speeds in Grand Central station

In December 2004 in collaboration with New York City Transit (NYCT), we carried out an extensive measurement study at Grand Central Metro Station, New York. The study involved the installation of 23 cameras at various sites to yield around 360 hours' of video footage. One of our cameras was set up to film the rush-hour commuters at their desired free speed, in a 6m-wide passageway, as shown in Figure 1. Two of the 18 hours of video from that camera were processed, which gave foot marks for 5,562 pedestrians, over a distance of around 4 m. The density in that passage was always very low, well within Level of service A, and only very few pedestrians were not walking at their preferred unimpeded speed.
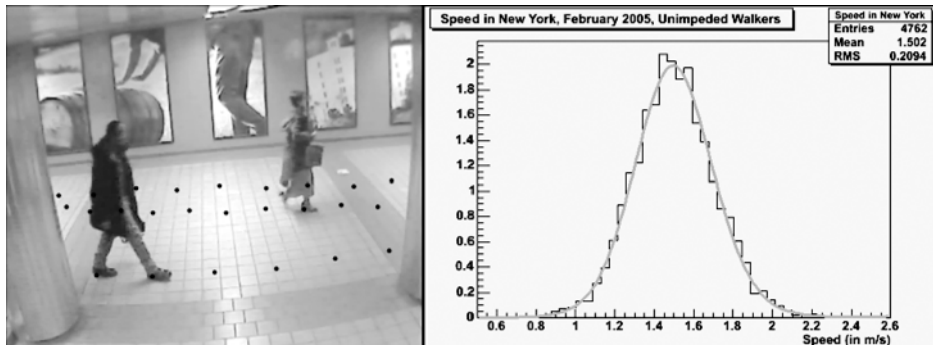
Figure 1: Speed measurements in Grand Central Station, New York

The marks were laid where (and when) feet touched ground. The time accuracy was around 1/50th of a second and the position accuracy around 3 cm. Figure 1 (left) shows 3 pedestrian tracks overlaid on the picture (2 of them correspond to the pedestrians on the picture). All the marks were processed to obtain the corresponding pedestrian coordinates on the ground. The 5,562 pedestrian tracks were subsequently filtered to remove the ones with missing steps or distorted paths. The remaining 4,762 tracks were processed to estimate individual speeds averaged between the first and the last foot mark of each track. Over this length, the time error and the position error have about equal

influence on the individual speed measurement error, which results close to 1%. The graph of Figure 1 gives the resulting preferred speed histogram, and the corresponding fitted distribution function used for New York commuters in the Legion simulator.

Table 1 compiles the free speed statistics published by Fruin[5], together with some of our own measurements and other published data. The New York commuters of 2004 are faster compared to the measurements reported by Fruin[5]. Importantly, their average speed is commensurate with the speeds measured nowadays in other large cities.

Source	Location	type of pe-destrians	sample size	Speed Avge m/s	Speed Stdev m/s
Fruin[5] p40	New York (PABT+PENN)	Commuters	1000	1.35	
MAIA	New York Grand Central	Commuters	4762	1.50	0.21
MAIA	London Clapham Junction	Commuters	1043	1.55	0.23
MAIA	Hong Kong Port (open air)	Commuters	588	1.47	0.21
MAIA	Hong Kong Tsim Tsa Tsui	Commuters	485	1.32	0.22
MAIA	Hong Kong Tsim Tsa Tsui	Week Enders	1560	1.25	0.22
MAIA	Monaco Train station	Commuters	2524	1.40	0.19
MAIA	Leeds outside stadium	Football Egress	6777	1.43	0.20
Tanaboriboon[13]	Singapore Sidewalks		519	1.23	0.20

Table 1: A sample of measured preferred speed statistics

London and Hong Kong Commuters – preferred speeds in stairs

To measure preferred speed distributions in stairs, we mark the feet when they touch each step, and we derive the horizontal component of the speed for each individual over at least a dozen steps. Figure 2 gives two examples of our measured distributions of unimpeded (horizontal) speeds in stairs.
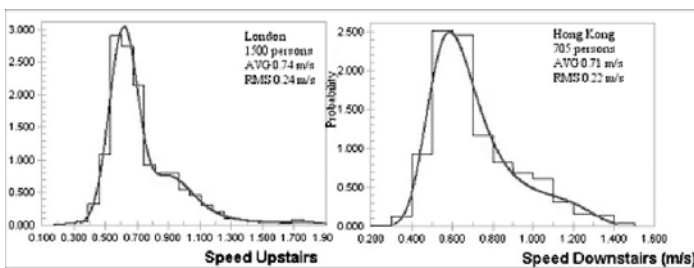
Figure 2: London Upstairs speeds and Hong Kong Downstairs speeds

Observe that our London commuter sample climbed stairs slightly faster than the Hong Kong sample descended (steeper) stairs.

6.   Examples of validation measurements

Monaco Grand prix spectators - queuing at train station after the event
In 2000, 2001, and 2002, we filmed the Monaco Grand Prix spectators as they were entering the train station after the event. To prevent crowding accidents on the platforms, the police sets up a series of barriers to control the inflow in the station.
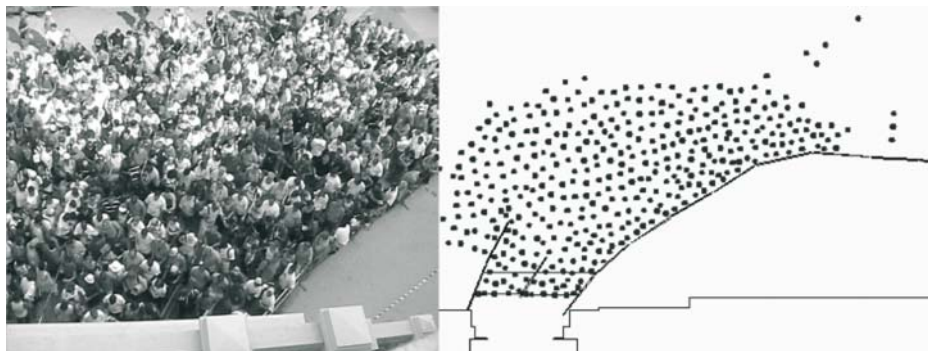
Figure 3: Monaco GP 2000 spectators "Queue 5" at the train station

In 2000, we filmed the arrival and evacuation of 8 successive queues of spectators in the last "corral", just before the entrance of the station. Queues 4 to 8 were painted and analysed to estimate arrival rate and preferred speed into the corral, exit flow, and density in various areas. The data from Queue 4 were also processed to estimate the GP spectators "personal space" parameters. We subsequently simulated Queues 4 to 8, where the corral shape for each queue, the arrival rate in the corral, and the desired speeds corresponded to our measurements. The simulated flows and densities matched well the real ones, well within the real fluctuations from queue to queue. These fluctuations were mainly a result of differences in queue size and in corral shape, as Queue 5 produced a serious "hot spot" where density exceeded 7 p/m², which prompted the police to modify the corral shape to prevent this from re-occurring in subsequent queues.
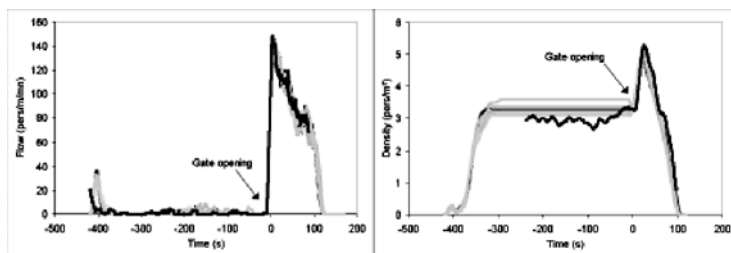
Figure 4: Flow through door and density near station entrance for MC2000 queue 5 : thick black curve : Real, thin curves: 5 Simulations

In 2002, the corrals were redesigned in order to reduce the inflow into the station and the corral density in the exit phase. Ten successive queues were filmed and measured. Two of these queues were simulated, using the correspondent measured arrival profile, but keeping the pedestrian parameters as calibrated from the 2000 measurements.
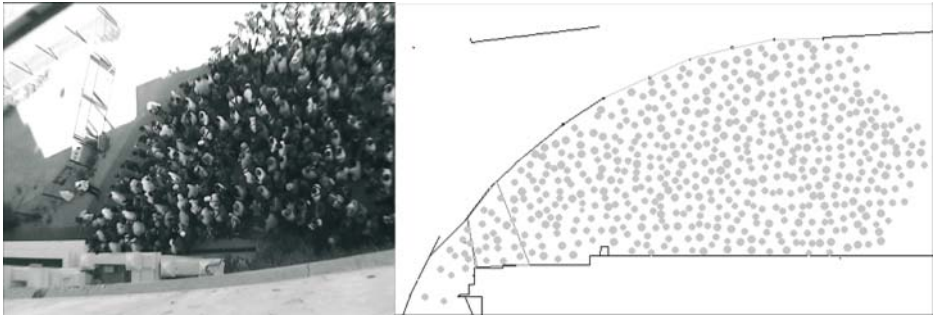
Figure 5: Monaco GP 2002 spectators "Queue 1" entering the train station

Figure 5 shows a film snapshot of Queue 1 starting to get in the station, and the corresponding snapshot of a simulation. The new design reduced the width of the queue apex from 3.44m (station door width) for 2000 to 2.5m for 2002. Figure 6 gives the real and 5 simulated densities and flows for that queue. Again, simulated values are in very close agreement with the real ones. In particular, both real and simulated densities stabilise between 2 and 3 p/m² in the waiting crowd, and oscillate between 4 and 3 when the crowd moves forward, as density waves build up in the corral.
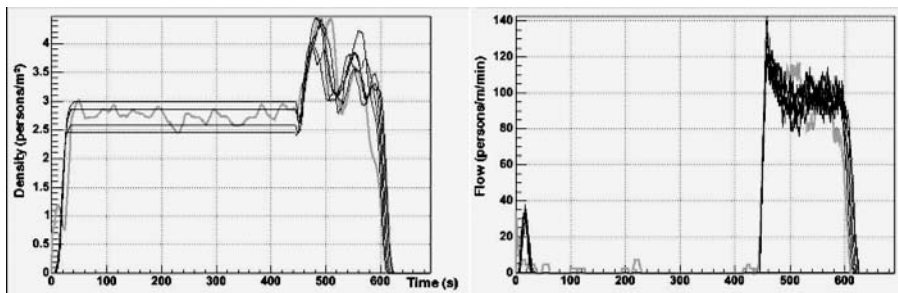
Figure 6: Density and Flow through corral entrance for GP2002 Queue 1
        Thick grey curve : Real, thin curves: 5 Simulations

London Metro Passengers- Carriage Boarding and Alighting times

In November 2002 in collaboration with London Underground Limited (LUL) we carried out a week-long measurement campaign focussing on commuters boarding and alighting metro carriages in many stations on various lines. One of them was Canary Wharf which is a modern Jubilee Line station with Platform Edge Doors (PEDs) and high ceilings convenient for filming. We filmed during the AM (heavy alighting) and PM peak (heavy boarding). 156 trains were filmed using two cameras: a distant one to capture 3 doors and the escalators on the platform; and one positioned close to a door for timing accurately each passenger through it. Figure 7 shows a close-up snapshot of video footage and a corresponding simulation for the same number of boarders, alighters and stayers.
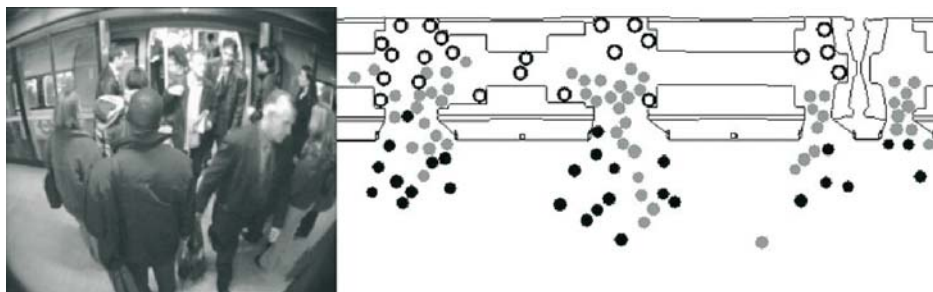
Figure 7: Boarding and Alighting Canary Wharf Train and simulation: grey entities board, black
alight, white stay on train

Figure 8 shows the good agreement between the simulated and the real ranges of individual boarding and alighting times.
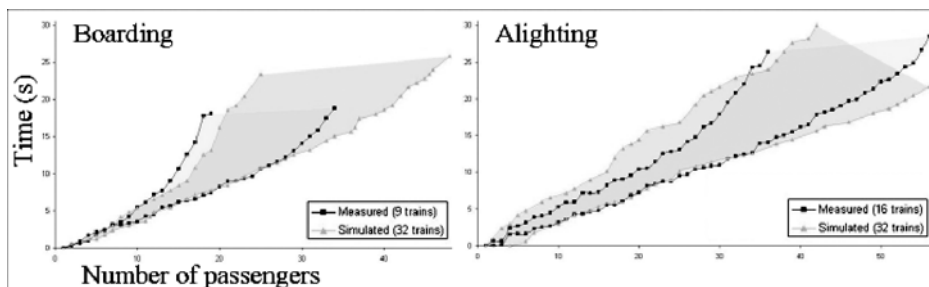
Figure 8: Density and Flow through corral entrance for GP2002 Queue 1
Thick grey curve : Real, thin curves: 5 Simulations

London Metro Commuters –
stair and escalator flows and boarding queues

Vertical circulation is very often a bottleneck in public venues. When congestion builds up at the entrance of an escalator or a stair on a platform, the extent and the density of the resulting queues are key information to design platform and concourse widths.

In February 2004, in collaboration with LUL we carried out a measurement programme at Earl's Court station over a period of two days while station refurbishment was taking place. The resulting traffic on stairs was substantially higher than normal, making it ideal for flow measurements over a broad range of densities.

Figure 9 shows a picture of people going down a staircase from the District line Platform to the Picadilly line in station, together with a scatter plot of flow versus density for the real and simulated flows through these stairs. The flow is measured on the upper stair; the density is measured just ahead of the stair ingress.
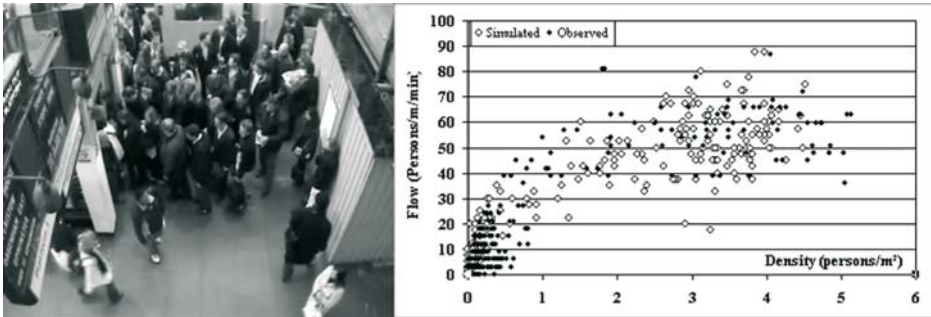
Figure 9: Stairs boarding queue at Earl's Court Metro station and flow in stairs versus density in boarding area

Figure 10 shows a picture of real escalator queues as filmed on Canary Wharf platform, and a snapshot of the Legion Simulator for a similar ingress geometry.
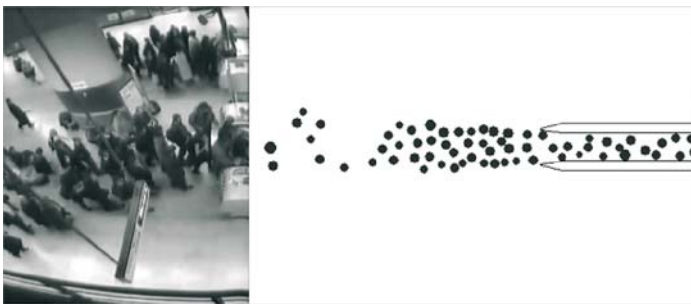
Figure 10: Real and Simulated escalator boarding queues

The simulator not only outputs the right flow distribution at capacity, ranging between 100 and 145 people per minute (average 125p/m), but also the correct queue shape and density in the boarding area.

7.   Conclusions

The measurements discussed in this paper cover a broad range of contexts and values of flow, crucially including much needed data beyond critical density. Through examples we show that the Legion model replicates the whole distribution of flow and density fluctuations in the congestion points examined. What is more, our measurements suggest that there is no basis for assuming that a straightforward flow-density relationship exists. Data shows that strong context-dependencies need to be factored into any attempt to model crowd patterns.

We conclude that pedestrian simulation models that focus on the quality of interactions between and among intelligent individuals and their environment are much better positioned to attain a broad range of validity compared to models premised upon an assumed flow-density relationship. This, as illustrated in this paper, comes at the expense of substantial measurement and validation effort. **«**

References

1.   M.A. Kagarlis: *Method of Simulating Movement of an Autonomous Entity Through an Environment*, US Patent Application 20040059548 (2002).
2.   M.A. Kagarlis, et al: *An Overview of the Legion Intelligent–Agent Pedestrian Simulation Model*, in preparation (2005).
3.   G.K. Still: *Crowd dynamics*, PhD Thesis (2000).
4.   S. Pheasant: *Bodyspace, Anthropometry, Ergonomics and the Design of Work*, second edition, pp. 178-213 (1998).
5.   J.J. Fruin: *Pedestrian Planning and Design*, Revised edition (1987).
6.   E.T. Hall: *The Hidden Dimension*.
7.   S.P. Hoogendoorn, W. Daamen, and P.H.L. Bovy: *Extracting Microscopic Pedestrian Characteristics from Video Data*, TRB2003 Annual Meeting (2003).
8.   S.P. Hoogendoorn, W. Daamen, and P.H.L. Bovy: *Microscopic Pedestrian Traffic Data Collection and Analysis by Walking Experiments: Behaviour at Bottlenecks*, In: E.R. Galea (Ed.), Proceedings of the 2nd International Conference on Pedestrian and Evacuation Dynamics, University of Greenwich, CMS Press, pp. 89-100 (2003).
9.   W. Daamen and S.P. Hoogendoorn: *Qualitative Results from Pedestrian Laboratory Experiments*, In: E.R. Galea (Ed.), Proceedings of the 2nd International Conference on Pedestrian and Evacuation Dynamics, University of Greenwich, CMS Press, pp. 121-132 (2003)

10.   A. Willis, R. Kukla, J. Kerridge, and J. Hine: *Laying the Foundations: The Use of Video Footage to Explore Pedestrian Dynamics in PEDFLOW*, In: M. Schreckenberg and S.D Sharma (Eds.), Proceedings of the International Conference on Pedestrian and Evacuation Dynamics, Springer Berlin, pp. 181-186 (2001).
11.   G. Antonini, S. Venegas, J.P. Thiran, and M. Bierlaire: *A Discrete Choice Pedestrian Behaviour Model for Pedestrian Detection in Visual Tracking Systems*, ACIVS 2004 (2004).
12.   http://root.cern.ch/
13.   Y. Tanaboriboon, S.S. Hwa, and C.H. Chor: *Pedestrian Characteristics Study in Singapore*, Journal of Transportation Engineering, vol 112, n°3 (1986).
14.   J. Pauls: *Evacuation and Other Movement in Buildings: Some High-Rise Evacuation Models, General Pedestrian Movement Models and Human Performance Data Needs*, In: E.R. Galea (Ed.), Proceedings of the 2nd International Conference on Pedestrian and Evacuation Dynamics, University of Greenwich, CMS Press, pp. 75-88, (2003).

Evacuation Simulation for Road Tunnels –
Findings from the use of microscopic methodology
for escape route analyses

K. Botschek[1], B. Kohl[1],and M. Steiner[2]

When designing complex buildings and tunnels featuring special characteristics, it is necessary to study the evacuation scenario in case of an incident in addition to the empirical figures gained from practice and expertise, in order to optimise the respective structures.

1. Evacuation Simulation for Bindermichl Tunnel

1.1. Enclosure and Lowering of A7 Motorway in the Bindermichl Area in Linz

The requirements set by the inner city location necessitated a complex design with a challenging arrangement of lanes and ascending and descending ramps inside the tunnel. The resulting, continuously changing tunnel cross-sections and the multitude of tunnel portals adversely affected the performance of the designed longitudinal ventilation system.
Every day up to 100,000 vehicles are using this motorway section.
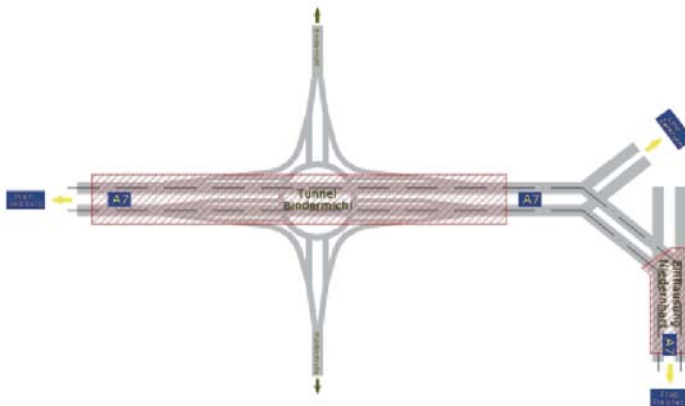
Figure 1: System Sketch of Motorway Section

As the complexity of such a tunnel system can not fully be covered by the existing guidelines on safety installations, a detailed investigation of escape routes and escape times in case of a fire was performed.

---

[1]ILF Consulting Engineers
[2]Asfinag

1.2.   General Project Data

The project comprises the following works:

»   Twin-tube motorway tunnel in the Bindermichl area with a length of 1,084 m
»   Twin-tube motorway enclosure in the Niedernhart area with a length of 508 m
»   Conversion of Muldenstrasse junction into a traffic circle with a total of 6 access and exit lanes entering and leaving the tunnel respectively

The northern part of the Bindermichl tunnel has a longitudinal gradient of approx. 4 %, while the ramps to the Muldenstrasse traffic circle have longitudinal gradients of up to 5 %. These considerable gradients create especially difficult ventilation conditions in case of a fire (chimney effect).

Due to the high traffic volume and the complex tunnel situation, the cross-passages and the emergency staircases are envisaged to be provided at maximum distances of 130 m (operation phase with one-way traffic), but during the construction phase (completion of the western tube), in which the eastern tube is operated in a two-way mode and the second tube has not yet been completed, the cross-passages may not yet be used as escape routes and the distance between the emergency exits comes to 500 m.

1.3.   Decisive Simulation Elements

Simulation Software

The „buildingExodus V4.0" simulation software [1] is a valuable tool for a dynamic simulation of evacuation processes. It focuses on the computation and simulation of large streams of people in pre-defined geometric structures.
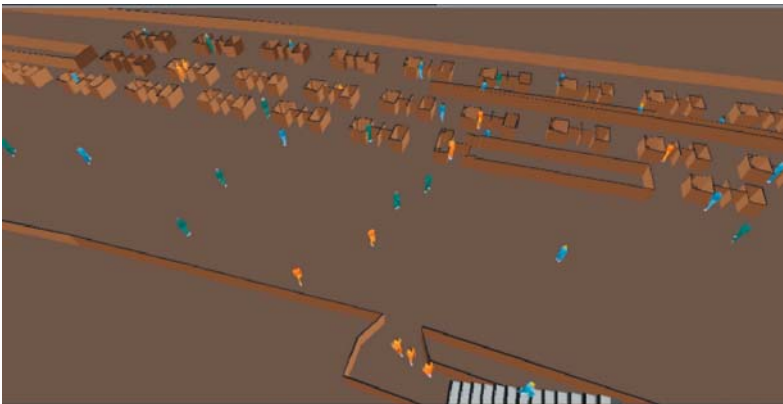
Figure 2: Tunnel users during evacuation simulation with buildingExodus

The following figure illustrates the individual process steps to be taken for an evacuation simulation:
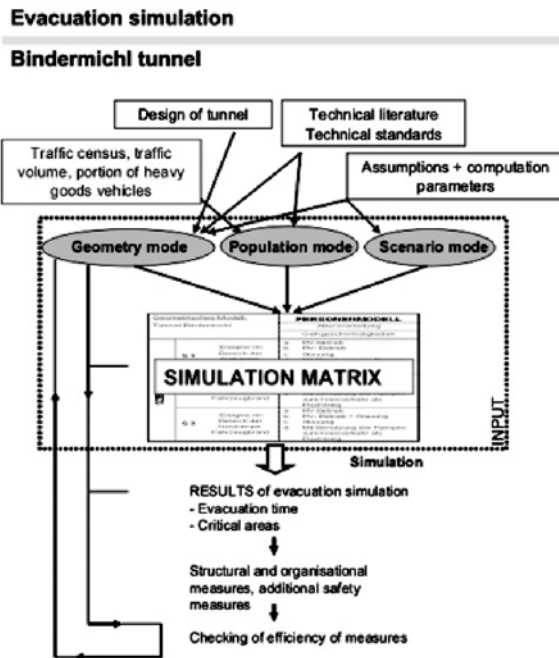
Figure 3: Simulation sequence and interaction of input data

Microscopic methodology

In order to calculate the evacuation time, the program covers the people-people, the people-structure and the people-environment interaction. For this computation, every person is seen as an individual, whose behaviour and movement is determined by heuristic rules. The respective rules are allocated to 5 different submodels (occupant, behaviour, movement, toxicity, hazard). These submodels work on the basis of a defined grid, which maps out the geometry of the structure under investigation. This uniform 2-dimensional grid is made up of nodes, to which individuals may be assigned. Between the nodes, arcs are defined, allowing individuals to travel from node to node. The movement trajectories of the individuals are largely determined by a potential map, which is developed depending on the distance to the nearest exit. Apart from the potential for the distance to the exit, additional attributes (type, concentration of smoke, etc.) are assigned to every node. These characteristics further influence the behaviour and movement of people seeking to escape a potentially hazardous situation.

Total evacuation time

The total evacuation time is determined by the following components:

Total evacuation time
Composition

Recognition of danger

Coordination of response in control center

Decision for tunnel evacuation

Instruction for tunnel evacuation

- -

Leaving of vehicles

Leaving of danger zone

Moving into safe area

Queuing in front of emergency exit (door capacity)

Escaping to safe area

empirical values

values in accordance with scenarios of the evacuation simulation

Figure 4: Simulation sequence and interaction of input data

1.4. Determination of Investigation Scenarios

The fire scenarios were designed in such a way that the event occurs immediately in front of one of the emergency exits, blocking this exit in question for tunnel evacuation and as a result creating a longer escape way.

In addition, several, rather adverse boundary conditions were chosen (peak traffic volume, high vehicle occupancy, reduced escape speed due to increased gradient, long detection time, long reaction time, etc.).

1.5. Consideration of Smoke Build-up

As, in case of a fire, smoke spreads inside the tunnel, the visibility is impaired as is the escape behaviour of the people heading to the emergency exits. The spreading of smoke leads to orientation and breathing problems. In the evacuation simulation these problems are considered by reducing the walking speed of the people seeking to escape the hazard scenario.

1.6. Sensitivity Analyses

Detailed Investigations for Construction Period

Numerous emergency exits will be leading into the adjacent tunnel tube, but are not available while constructing the Western tube from December 2004 to December 2005.

As a result, the spacing between the emergency exits increases to 506 m during construction. In the light of this scenario, investigations were performed to determine how the integration of operational facilities into a temporary escape route could help improve evacuation times.

Based on the simulation results, steps were taken to adjust the staircase in the operation centre in a way for it to be used as temporary emergency exit. This way, a tunnel evacuation within an adequate period of time will also be possible during construction.

Detailed Investigations for Western Tube

The Austrian design guidelines for ventilation systems in tunnels stipulate that in case of a fire the existing air flow of the ventilation system may not be changed. In the case of the western tube of the Bindermichl Tunnel, which is operated in a one-way mode, this stipulation leads to a longitudinal air flow in a southerly direction. Yet as a result of the unfavourable conditions encountered (longitudinal gradient, open ramps. meteorology, location of fire, etc.), this requirement can in some cases not be met. A strong thermal buoyancy may induce the smoke to change direction after a certain time, sweeping over the vehicles behind the source of fire.

It was the task of the evacuation simulation to investigate, whether the emergency exit situation in the western tube created conditions offering enough time to evacuate the tunnel before smoke would spread over the vehicles trapped inside the tunnel.

1.7. Findings

Despite the great variety of unfavourable assumptions, which are unlikely to occur in this combination, an evacuation of the tunnel in the required period of time is still possible.

The details of this computation allow significant conclusions to be drawn for the following tunnel design components:

» Decisive escape routes and escape route elements
» Additional safety measures
» Temporary escape route design during construction
» Impact of unfavourable boundary conditions on evacuation time
» Interfaces to alarm and rescue planning

2.   General Applicability of Evacuation Simulation for Risk Analyses for Road Tunnels

In general there is a wide field of application for evacuation simulations in road tunnels; a simulation model may for example be used to assess the extent of damage in the framework of quantitative risk analyses. A risk is calculated considering the occurrence

frequency of events of damage and the resulting extent of damage. As the extent of damage incurred by infrequent events, like a major vehicle fire, can not be assessed based upon statistics, the evacuation simulation is used to evaluate the extent of damage caused by effects of fire in varying tunnel configurations. The use of an evacuation simulation in combination with a ventilation model, which allows the development of the fire and the spreading of the smoke to be simulated in an integrated model, makes it possible to represent the time factor, which is of such significance for the rescue chances. With the help of the evacuation simulation model, the impact of heat, smoke and toxic gas can be considered with respect to both the speed of movement and the toxic effects exerted on individual persons [1]. For the modelling of various types of tunnels, the following influencing factors can be brought into play:

- » Size of fire
- » Spacing of emergency exits
- » Traffic volume
- » Type of ventilation
- » Traffic routing (one way or two-way tunnel)

By determining the evacuation times, the impact of toxic gas on individual persons can be concluded and as a result the extent of damage for defined scenarios may be assessed.

This method may be used for a good relative comparison and – if further data are added – it may also be applied for an absolute evaluation.

In order to develop a sufficiently accurate model, which illustrates the concentration and spreading of smoke inside a tunnel, a detailed ventilation computation, which considers the parameters which are of relevance for the flow patterns inside a tunnel, is to be performed. «

References

1.   E.R. Galea, S. Gwynne, P.J. Lawrence, L. Filippidis, D. Blackshields: *buildingEXODUS, User Guide and Technical Manual*, Fire Safety Engineering Group, University of Greenwich, London (2004).

A Data-Driven Model of Pedestrian Movement

L. Casburn[1], M. Srinivasan[1], R.A. Metoyer[1], and M.J. Quinn[1]

We present a method for simulating individual pedestrian motion based on empirical data. Our model keeps track of the pedestrian's position and body configuration (pose) and uses motion capture data to produce plausible motion. While our ultimate goal is creating 3D animations of crowds, our initial efforts focus on 2D simulations. In this paper, we present a 2D model for an able-bodied male. Using our approach, we could also capture data and build models for a heterogeneous population, including children, the elderly, pedestrians in wheelchairs, and people on crutches. We demonstrate the realism of our model with a small-scale test case and a larger crowd evacuation simulation.

1.   Introduction

The goal of our research is to demonstrate the feasibility of using pedestrian simulation for emergency planning, emergency response decisions, and training with respect to transportation facilities, sports arenas, and high-rise office buildings. In addition, we hypothesize that faithful computer models of pedestrian motion will be useful to architects designing new facilities. In particular, such a system will help them gain confidence that they have provided for the rapid egress of diverse populations in emergency situations. In order to be effective, training devices must be realistic enough that the users are able to "suspend disbelief." Realistic motion of individual pedestrians is a necessary condition for the suspension of disbelief. Several existing models produce pedestrian motion that is not realistic at the level of the individual pedestrian. For example, pedestrians may exhibit abnormally high velocities or unnatural direction changes. We argue that in order to build accurate models of how people move, we should observe real 3D human motion and build models from these observations. We hypothesize that the more realistic the motion is, the more accurate the results of the simulation will be.

In this paper, we describe a new model of 2D pedestrian motion. We begin by collecting 3D motion capture data from a human subject. We maintain a 3D kinematic model of each pedestrian throughout the simulation. Every "pose" (configuration of joints) adopted by a pedestrian is consistent with the motion capture data we have collected. Likewise, every pedestrian movement generated by the model is consistent with the motion capture data. At any moment in the simulation, a pedestrian has the capability to reach a variety of different spatial points at some future time. The behavior of the pedestrian is reflected by its particular choice of these spatial points. Hence we call our approach the capability-behavior model of pedestrian motion.

---

[1]School of Electrical Engineering and Computer Science,
Oregon State University, Corvallis, Oregon, USA

2.   Related Work

Many other microsimulation models of pedestrian motion exist. For an excellent survey of these models, see Helbing et al. [3]. One way to categorize microsimulation models is to divide them into cellular automata models, agent-based (or AI-based) models, and behavioral force models.

The principal advantage of cellular automata models is that they execute very fast on computers. However, because cellular automata models divide space into cells, motion is discrete, undermining our goal of creating training simulators that will encourage participants to suspend disbelief.

Behavioral force models accurately predict a variety of phenomena that occur when crowd densities are high. However, they have a couple of issues which make them problematic for us. First, pedestrians inside dense clusters exhibit an unnatural "jitter." Also, our experience with this model has been that there is no single set of parameters that works in every instance. Instead, the parameters must be carefully tuned in order to fit the scenario being modeled. Finally, it is unclear how this force-based approach would be able to model pedestrians with restricted motion abilities. For example, a person in a wheel chair cannot instantaneously shift sideways.

Agent-based models allow each pedestrian to have a unique behavior. Hence modeling a heterogeneous population is much easier with an agent-based model. Agent-based models have shown good success when pedestrian densities are low to moderate. They have the liability that the computational demands for simulating an agent can be high. We categorize our capability-behavior model as an agent-based model.

Human motion generation has been a key problem in computer graphics for a number of years. Most recently, research in motion graph techniques has led to algorithms for generating natural human motion that satisfies some user constraints, such as trajectory tracking [1, 6, 7, 8]. Another important area of computer animation and simulation is level of detail generation. Creating multiple levels of detail allows for efficiency optimizations when accuracy can be traded off for speed. Most closely related to our work is that of Brogan et al., in which they have built capability models that describe what motions a physical simulation is capable of achieving [2]. In our case, we want to build capability models based solely on motion capture data, because we believe such models will result in more realistic motion patterns than current approaches.

3.   Motion Capture

Our goal in this paper is to create a 2D motion model that encodes the capabilities of a walking human. This model should take into account not only the physical characteristics of the person (size, weight, disabilities, etc), but also the current state of the person when making movement decisions. For example, is the person standing still or in the middle of a walking stride? To do so, we will build our model from real human motion data recorded with motion capture technology.

Motion capture technology has been used in biomechanics and entertainment for many

years as a means of recording human motion. There are several different motion capture technologies. Magnetic and optical systems are the two most commonly used approaches in computer graphics and entertainment.

For this work, we used a Vicon 612 optical motion capture system [10]. An optical motion capture system consists of three main components: markers, sensors, and a workstation.

Figure 1: Highly reflective optical markers placed on a motion capture subject.

The markers consist of highly reflective spheres, 5 mm in diameter, that are placed at strategic locations on the subject to be recorded (Figure 1). The sensors consist of several high speed infrared cameras. Each camera is placed on the perimeter of an area around the subject of interest and aimed toward the center of the activity. The intersection of the camera view frustums forms the capture region. As the subject moves within the capture region, the camera images are recorded on the workstation.

The Vicon system processes the recorded data to produce 3D locations for each marker. As long as a marker is visible in the images of any two cameras, the 3D location of that marker can be computed. This 3D location information for each marker is called the raw marker data.

To generate animated motion, or in our case, models of human motion, we convert the data to a more usable form. Using the Vicon software suite, the raw marker positions are converted to joint angles according to a kinematic model of the subject.
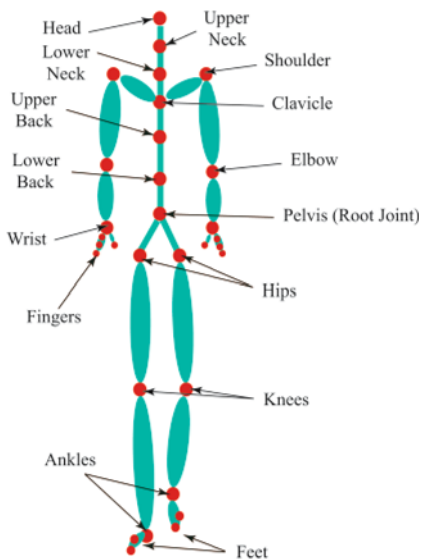
Figure 2: Our kinematic human model consists of 30 joints, each with three degrees of freedom.

For all of our experiments, we used the Vicon 612 3D optical motion capture system with 6 cameras and captured the data at a rate of 60Hz. The raw marker information was converted to joint angles for a kinematic subject model consisting of 30 joints (Figure 2).

4.   Motion Graphs and Mobility Maps

Once the joint angles are computed for each frame of motion, we further process the data to build a data structure known as a motion graph. Motion graphs have recently been used in the computer animation field to generate synthetic human motion by drawing upon a library of previously recorded human motion. In the following sections we will give a brief overview of motion graphs. For a more detailed description, see [1, 6, 7, 8].

Using our Vicon optical motion capture system, we capture the 3D motion of subjects performing various tasks relevant to pedestrians: walking straight at various rates, turning at various radii, coming to a stop, starting from a stop, and turning in place. We then build a graph that encodes natural transitions between these sequences of motion.

The recorded motion segments are first combined into a single large collection of poses, where a pose is defined as the set of angles for each degree of freedom, as well as the root body position and orientation for a single frame of motion. Each frame, therefore, consists of 96 floating point values, representing the three Euler angle values for each of the 30 joints and the 6 degrees of freedom of the root body. In our experiments, the root body is centered at the pelvis (Figure 2).

We define a distance metric that measures the similarity of two poses, and we use this metric to develop a pose transition cost. The pose transition cost function determines the cost to move from one pose to another. If a pose is likely to follow another pose in natural motion sequences, the cost is low. We build a fully connected graph, where each node in the graph is a pose from the original motion data, and each arc in the graph is the cost to transition between the poses connected by the arc. The graph is then pruned to remove all transitions that are above a threshold value (i.e., the unrealistic transitions). We call the resulting graph a motion graph.

The motion graph encodes natural transitions, such as transitions from poses that come from walking in a straight line to poses that come from turning. Current motion graph techniques typically search this graph for an optimal path that adheres to some constraint, such as following a 2D trajectory or reaching a desired point on the 2D floor plane. The result is a sequence of poses that meets the constraints while maintaining smooth transitions. These search-based approaches result in compelling motion for the given trajectory but are fairly expensive. Since we would like to generate motion at interactive rates, search based approaches are not sufficient.
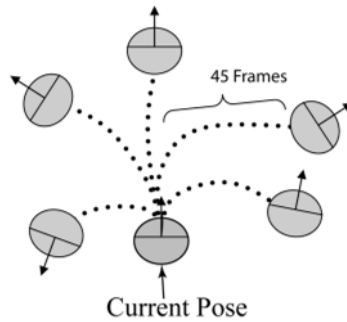
Figure 3: Illustration of movement options from a single pose in the mobility map. Each pose reachable from the current pose in 45 frames is called a movement option and is stored along with the sequence to reach it, the final position, and the final orientation with respect to the current pose.

For this reason, we further process the motion graph to produce a data structure that sacrifices memory space for speed. For each pose in the graph, we compute the shortest path between it and every other pose in the path. We call this the "all pairs shortest path" (APSP) graph. For each pose in the APSP graph, we collect all nodes that can be reached in some small time horizon (1.5 Seconds = 45 frames). For each reachable node, we store the final pose as well as the sequence of intermediate poses that lead to that pose and the relative change in position and orientations (Figure 3).

This last step results in what we call a mobility map. The mobility map can be viewed

as an oracle that the simulated pedestrian can consult to understand its capabilities given its current state. The mobility map can tell the pedestrian all locations it can reach, how it will be oriented, and the sequences of poses to get it there. For a more detailed description of mobility maps, see [9].

Using mobility maps, one can produce compelling 3D motion at interactive rates for up to 500 characters. However, the pedestrians sometimes suffer from a wandering behavior. Wandering occurs when a pedestrian cannot achieve a spatial request because the database of motions simply does not contain enough of the right kind of data. In other words, there is no smooth sequence of poses that quickly brings the pedestrian from its current location and pose to the desired location. This smoothness constraint is very important when generating 3D motion, because viewers are very good at noticing small discontinuities in synthetic human motion.

In this paper, we modify the mobility map approach by taking advantage of the fact that we are not creating 3D animations. Rather, we are concerned with developing 2D human motion models. This goal allows us to relax the 3D motion smoothness constraint. In doing so, we can increase the controllability of the pedestrian by clustering similar poses and building a more coarse-grained mobility map from the clustered poses. The result is a clustered mobility map, where each pose is replaced by a cluster of poses with a larger number of movement options. Since a single mobility map can be shared by all 'similar' pedestrians (e.g., all able-bodied male pedestrians, ages 30-35) in the scene, space usage scales linearly with the number of pedestrian types, and not with the number of pedestrians.

5.   Clustered Mobility Maps

A simulated pedestrian is capable of reaching a number of spatial locations, which we call mobility points, within a time step of 1.5 seconds. We set the time step to 1.5 seconds because this is long enough to provide the pedestrian with a reasonable number of mobility points, but short enough to keep the memory requirements reasonable. The nature of the motion is determined by the current body posture or pose. For instance, if a pedestrian is standing in a pose with two feet on the floor it is likely that it will continue to stand or begin to walk at a low velocity. If the pedestrian is in a pose with one foot on the floor, the pedestrian may be in a position to move more quickly because it is in the middle of a walking stride.

Similar poses should also exhibit similar dynamics. Motion sequences starting from a pose with a left heel down and right toe pushing on the floor, for example, should share the same characteristics as motion sequences generated from a different pose that also has its left heel down and right toe on the floor. Therefore, we group similar poses together into a single cluster. In order to identify groupings of similar poses, we use a subtractive clustering algorithm described by Kim et al.[5]. For determining clusters for basic able-bodied locomotion, the upper body degrees of freedom contribute very little information and therefore are ignored. We consider only the degrees of freedom from the waist down.

Once the poses have been clustered, we can combine the individual original mobility maps for each pose in a cluster into a single mobility map for the cluster. The cluster shares the movement options from all the poses within it, thus giving a simulated pedestrian more mobility and greater ability to react to movement requests. In the following section, we will describe how we use this new clustered mobility map to drive the 2D simulation.

6.   Capability-Behavior Model

At run-time, we use the clustered mobility map to animate the motion of each 2D pedestrian. We assume that the pedestrian simulator makes target requests for each pedestrian. We define a target to be a position a pedestrian wants to reach, such as the location of the nearest exit. Pedestrians exit the building by moving toward the targets. At any point in time, a pedestrian is in a particular pose of a cluster and will have movement options dictated by the mobility map of that cluster.
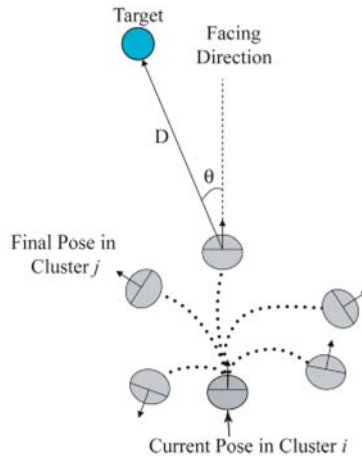
Figure 4: The new clustered mobility map is combined with a cost function to rank each option. The cost of a movement option depends on the distance from the target and the deviation between the facing direction and the target direction.

Given a target request, the movement options are first ranked based on a cost function:

$$C_i = \omega_D D + \omega_\theta \theta - \omega_S S + \sum \omega_P P \qquad (1)$$

The cost function is similar to that presented by Srinivasan et al. [9], where D measures the Euclidian distance from a mobility point to the target and θ is the deviation angle (Figure 4). The deviation angle is the angle between the facing direction a pedestrian has upon taking a movement option and the vector from the mobility point to the target. We modify the function to include a term, S, which encourages faster movement, and another term, P, which incorporates interference from neighboring pedestrians. S represents the displacement from the current position when taking a movement option. Options that move the pedestrian farther in 1.5 seconds will have a lower cost.
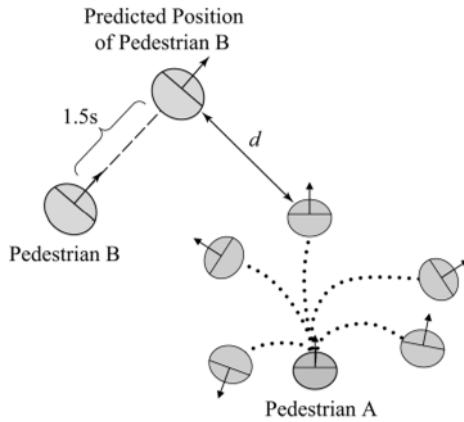
Figure 5: Illustration of pedestrian interference factors. To determine the cost due to nearby pedestrians, we consider the distance from the mobility point to the predicted position of the nearby pedestrian.

The last term in the cost function measures the influence of neighboring pedestrians (Figure 5). We represent this influence with a function similar to that used by Helbing and Molnar in the social forces model [4]. The closer the mobility point is to another pedestrian the higher the cost. If, however, the pedestrian is moving at a slower velocity, it will be more comfortable selecting a move that is close to another pedestrian. We represent the cost with a decreasing exponential function:

$$P = a * e^{-d/(b*v)} \qquad (2)$$

where d is the distance between the pedestrian at the mobility point and the predicted position of the other pedestrian. To compute the predicted position of other pedestrians, we assume constant velocity over the time step. The velocity of the pedestrian at the mobility point is represented by v, while a and b are constants with values 10.5 and 0.09,

respectively. These values were determined through trial-and-error and used throughout all of our experiments. The total pedestrian influence for that movement option is the summation of the influence from each of the neighboring pedestrians.

Variables ω_d, ω_θ, ω_S, and ω_P are weighting terms for the distance, deviation angle, speed, and pedestrian interference terms, respectively. Pedestrians that are behind the mobility point are not considered to be interfering, therefore $\omega_P = 0.0$, otherwise $\omega_P = 1$. We use a grid spatial subdivision scheme to determine nearby pedestrians efficiently.

We rank the movement options according to their cost and store them in a priority queue. The first option in the priority queue has the least cost. Our algorithm iteratively extracts the options from the queue until one is found that does not intersect with walls or nearby obstacles. We implemented a quadtree subdivision scheme to efficiently determine nearby walls and obstacles for intersection tests. This movement option is chosen as the desired option; it is used to animate the pedestrian motion for the next 1.5 seconds (45 frames). If the algorithm cannot find a suitable option, we allow our pedestrian to linearly interpolate its position and orientation, for four frames, toward its goal. This allows the pedestrian to move into a position or face away from the obstacle so that at least one movement option can become feasible. In our experiments, the simulated pedestrians resort to the interpolation option only 2% of the time.

In summary, the cost function leads the simulation to prefer movement options that quickly move the pedestrian closer to the target, orient the pedestrian toward the target, and have the least amount of interference with other pedestrians.

7.   Results

These experiments demonstrate that the capability-behavior model can create realistic-looking crowd motion. Even when moving in a straight line, simulated pedestrians have a bit of side-to-side motion characteristic of actual pedestrian movement. Pedestrians spread out and avoid collisions when moving through an area where there is plenty of room. At bottlenecks, they bunch up without intersecting. Simulated pedestrians within crowds stand quietly, without any of the "jitter" characteristic of the social forces model (Figure 6). The capability-behavior model parameters are identical for all the examples we have presented; no "tuning" of parameters to fit the particular situation was required.

Figure 7 illustrates the use of the capability-behavior model to simulate the orderly evacuation of a nearly-full auditorium, along with several adjacent offices. This example demonstrates the ability of our current simulator to move pedestrians in a more complicated setting. Two simplifying assumptions reduce the realism of this simulation. First, every pedestrian begins moving at the same time. Second, every pedestrian has the goal of leaving the building through the nearest exit. In this simulation the total egress time was 316 seconds.

To date, we have only collected motion capture data for a single person. About 20 minutes of samples resulted in a total of 33,404 different poses. The clustering algorithm collected these poses into 670 clusters. In the experiments reported in this paper, the mo-

vements of every simulated pedestrian are drawn from the same set of mobility maps. Even with this limitation, we believe the resulting crowd movements are plausible. Collecting additional motion capture data will enable us to create a greater diversity of simulated pedestrians, adding to the overall realism of the results produced by the system.
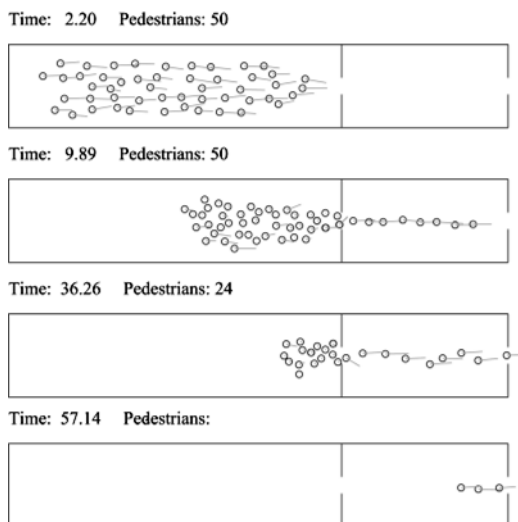

Figure 6: Snapshots of the doorway experiment at simulated times (sec) of 2.2, 9.89, 36.26, and 57.14. The pedestrians must approach the door, move through the door, and proceed to the second door.

8.   Future Work

There are several avenues of research remaining for future work. First, we plan to capture motion of pedestrians with varying capabilities to begin building a diverse database of 2D motion models. We hope to capture individuals with crutches, canes, in wheelchairs, and of varying ages (children and elderly), for both males and females.

Ultimately, we intend to create models that can be used in real-time simulators. We are currently investigating statistical techniques for improving the efficiency of our approach in terms of memory requirements and CPU time. We hope to eliminate the need to store and search all movement options and replace them with movement option distributions that encode the capabilities of a pedestrian from a given pose with statistical measures.

Finally, we are investigating the addition of higher level behaviors, such as route choices, grouping, and collision negotiation and avoidance, into our overall pedestrian simulation system. These behaviors will be designed to sit on top of the presented motion model.

The behaviors will be included in the cost function and will therefore lead to the choice of movement options appropriate for the desired behavior.

Time: 5.49   Pedestrians: 746
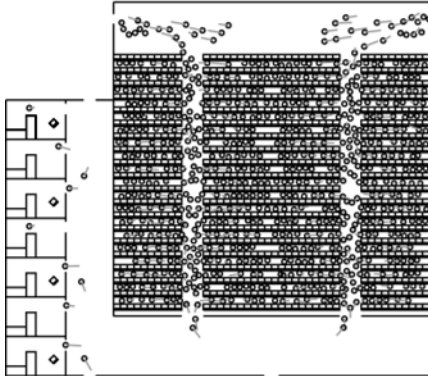
Time: 71.43   Pedestrians: 552
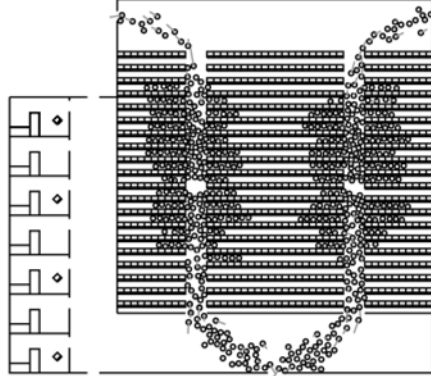
Time: 181.31   Pedestrians: 222
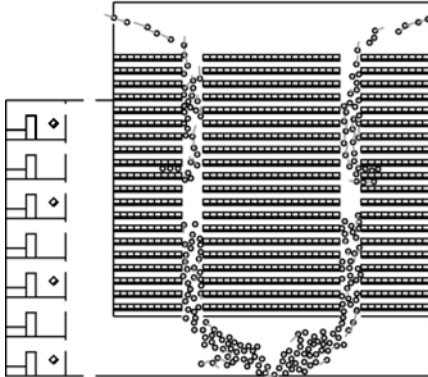
Time: 307.67   Pedestrians: 9
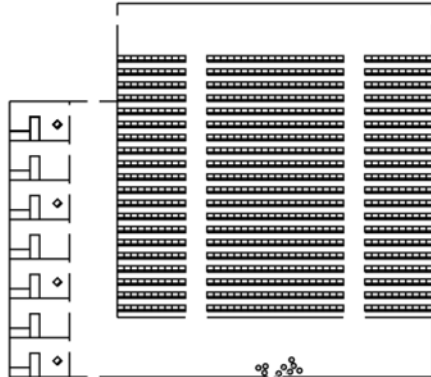
Figure 7: Four snapshots of a simulation of 750 persons evacuating an auditorium and adjacent offices.

9.   Acknowledgments

References

1.   O. Arikan and D. A. Forsyth: *Interactive Motion Generation from Examples*, ACM Transactions on Graphics 21, pp. 483–490 (2002).
2.   D. Brogan and J. Hodgins: *Simulation Level of Detail for Multiagent Control*, In: Proceedings of the First International Joint Conference on Autonomous Agents and Multiagent Systems, ACM Press, pp. 199–206 (2002).
3.   D. Helbing, I.J. Farkas, P. Molnar, and T, Vicsek: *Simulation of Pedestrian Crowds in Normal and Evacuation Situations*, In: M. Schreckenberg and S.D. Sharma (Eds.), Proceedings of the International Conference on Pedestrian and Evacuation Dynamics, Springer, Berlin, pp.21-58 (2002).
4.   D. Helbing and P. Molnar: *Social Force Model for Pedestrian Dynamics*, Physical Review, 51(5), pp. 4282-4286 (1995).
5.   T. Kim, S.I. Park, and S.Y. Shin: *Rhythmic-Motion Synthesis Based on Motion-Beat Analysis*, ACM Transactions on Graphics, 22, pp. 392-401 (2003).
6.   L. Kovar, M. Gleicher, and F. Pighin: *Motion Graphs*, ACM Transactions on Graphics, 21, pp. 473–482 (2002).
7.   J. Lee, J. Chai, P.S.A. Reitsma, J.K. Hodgins, and N.S. Pollard: *Interactive Control of Avatars Animated with Human Motion Data*, ACM Transactions on Graphics, 21, pp. 491–500 (2002).
8.   R. Metoyer: *Building Behaviors with Examples*, Ph.D. Thesis (2002).
9.   M. Srinivasan, R. Metoyer, and E. Mortensen: *Controllable Real-Time Locomotion using Mobility Maps*, In: Proceedings of Graphics Interface, Victoria, B.C, pp. 51-59 (2005).
10.   Vicon, *Vicon 612 optical motion capture system*, http://www.vicon.com (2004).

Distributed intelligence in pedestrian simulations

D. Cavens[1], C. Gloor[2], J. Illenberger[3], E. Lange[4], K. Nagel[3], and W.A. Schmid[1]

In order to accurately simulate pedestrian behaviour in complex situations, one is required to model both the physical environment and the strategic decision-making of individuals. We present a method for integrating both of these model requirements, by distributing the computational complexity across discrete modules. These modules communicate with each other via XML messages. The approach also provides considerable flexibility for changing and evolving the model. The model is explained using an example of simulating hikers in the Swiss Alps.

1.   Introduction and Motivation

An important question in pedestrian simulation systems is the determination of the direction in which the pedestrians are heading. For the investigation of simple geometrical structures, it is sufficient to give the pedestrians pre-computed and fixed directions, which translate to a desired velocity vector for each pedestrian which is constant in time. Somewhat more advanced are evacuation simulations, which are solved either by using potentials or by using simple rules that combine searching and herd behaviour.

As one moves towards more complex spatial environments and social situations, a correspondingly more complex approach is required to modelling agents' desired direction. This is required for models that simulate, for example, how pedestrians explore a museum or a department store, or how they move around in a crowded urban park at lunchtime. In these situations, agents, like the individuals they represent, need to be able to adapt their desired directions in response to their surrounding environment and the activities of other agents.

In general, a mobility simulation consists of at least two components: the simulation of the agents' interactions with the physical world, and the simulation of the agents' strategic or mental decision-making [1]. The first component, what we call the physical simulation, deals with how a pedestrian adapts its movement to accommodate obstacles and physical constraints in its immediate environment (i.e. strategies to avoid a group of other pedestrians that are between the agent and its destination.) The second component, the agents' decision-making, models the agents' goals and strategies at a broader and temporal scale (i.e. the selection of an agent's destination from a set of similar alternatives.) while there is some overlap between the two components, for the purposes of this paper the agents interaction While both of these components, plus their interplay, are important to making a realistic pedestrian simulation, there has been comparatively little research into how to make the two components work together [2].

---

[1]ETH Zürich, Switzerland
[2]Gloor Consulting, Switzerland
[3]Technical University of Berlin, Germany
[4]University of Sheffield, United Kingdom

While the primary purpose of the work presented here seeks to integrate the modelling of pedestrians' physical movements with their strategic decision-making, it was also triggered by a research project that simulates the reaction of hikers to changes in the landscape. This created additional demands on the described system, requiring that the system be able to model and simulate the following aspects:

» Large scale: The study area is typically used for extensive day hikes. This implies an area of at least 25 km x 25 km, and requires the simulation of several thousand pedestrians per day.

» Sophisticated mental models: The evaluation of a landscape (both aesthetically and from a functional perspective) by recreational users is a process that is not well understood. This implies the use of a flexible method in which very different mental models can be tested.

» Distributed Computation: Since variability of experiences over the course of a day seems to have a strong influence on hiker satisfaction, a computational method that automatically evaluates sequences of views is needed. Since this is a time-consuming computation, this implies the use of distributed computing where several view analyzers can run on different computers.

We present an approach that satisfies these goals.

2.   Overview of the Approach

Our method consists of dividing the simulation into distinct modules. These modules interact with each other via network messages. Each module has a distinct role in the overall simulation system, but can be classified into the following broad categories:

» Mental modules simulate the processes that go on in peoples' heads. These modules determine how an agent can best fulfil its goals and expectations, based on their experience on previous simulation runs. These modules also receive events from the other modules, in order to refine their knowledge of the area being simulated.

» The physical simulation (in this case a pedestrian simulation) executes the plans of all involved agents simultaneously. The module is responsible for modelling how the agents react to their physical environment such as slow-downs due to congestion or path characteristics. While the mobility simulation is running, it constantly emits messages (called events) stating the status of each agent. Most of these events are simply status messages (containing the agent's location), but some messages contain additional information about the agent's surrounding environment.

» There are secondary analyzer modules that read the event stream, compute secondary information, and re-insert that secondary information into the same event stream.

»   There are additional control modules that coordinate communication between the other modules and keep track of the overall state of the simulation.

The simulation is designed to run over many iterations, during which the agents „learn" about their environment. Initially, the agents are assigned characteristics and non-spatially specific goals, but have no knowledge of the physical characteristics of the simulated area. These characteristics and goals are generated externally to the simulation and fed to the Agent Database.
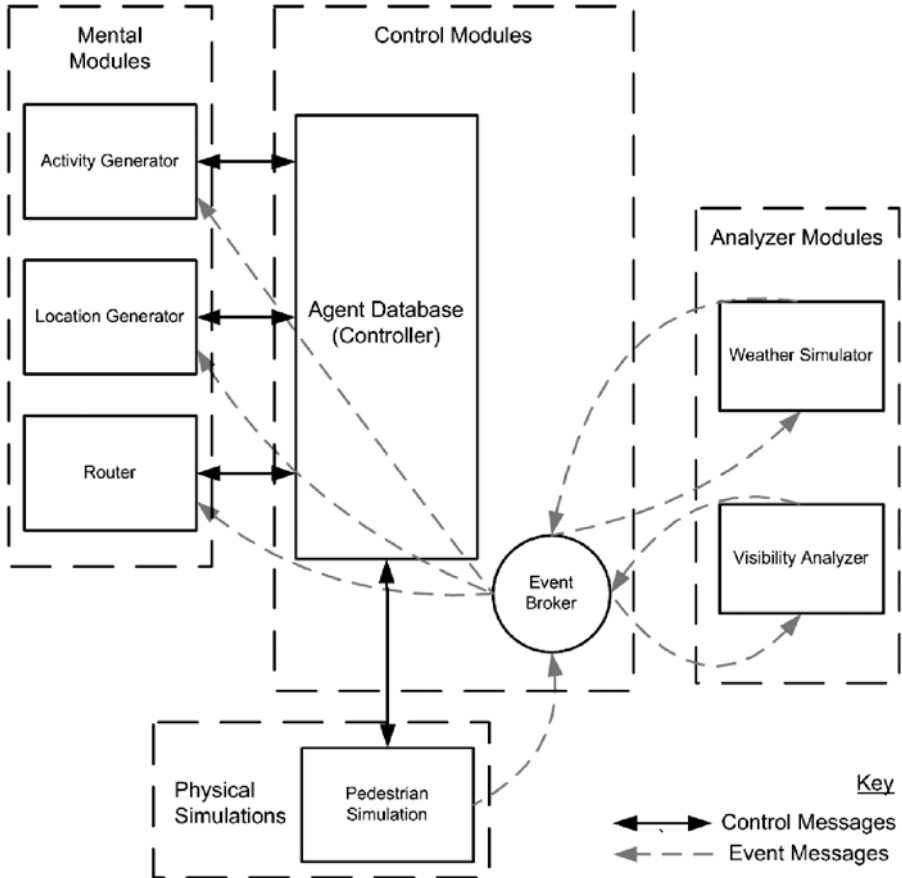
Figure 1: Overview of the Simulation System. Each Module can be implemented as a separate executable if required.

At the beginning of each simulation run (in this case representing a single day), the Agent Database, with the assistance of the mental modules, generates for each agent a plan that the simulation system expects is the most likely to fulfil the particular agent's goals and expectations. Once all plans have been elaborated, the Agent Database submits these plans to the physical simulations which simultaneously execute them.

During the model run, the physical simulations broadcast events to the rest of the simulation. These events include information about the location of the agents and any experiential information that is available (i.e. indicating that the agent has encountered a steep hill, or is in a congested area.) The mental and analyzer modules listen to events being broadcast by the physical simulation. This information is used by the mental modules to refine their knowledge of the physical environment and generate better plans in subsequent model runs. For example, they might note that an agent sees nothing but trees while the agent is interested in sunshine. On subsequent model runs, the agent will search for a different hiking path that provides more open areas.

At the end of a simulation run, the control module determines if the agents have achieved their goals and expectations using the current plan. If not, the mental modules are asked for a new plan. In order to ensure that agents are able to discover new locations, a degree of randomness is used to determine the agents' choices (the random factor decreases over many simulation runs.)

3.   Modules

In order to further elucidate the major concepts, the following are descriptions of key modules in the simulation system. More complete descriptions are available in [3] and [2].

3.1. Agent Database / Controller Module

The Agent Database fulfils two major functions within the simulation system: it maintains the master list of agents in the simulation and co-ordinates the rest of the modules.

As part of the system initialization, the agent database loads in a synthetic population of agents. This population, defined in an externally generated XML file, describes each agent's individual characteristics. This includes the agents' physical constraints (such as fitness levels) as well as their goals and expectations. At this stage, the goals and expectations are non-spatial: they are simply a list of activities (in the case of the Hiking simulator, these include hiking, eating at a restaurant, etc.) and their desired durations.

Before each simulation run, the Agent Database determines if the agent has a plan that meets its expectations. If not, the Agent Database requests that the Mental Modules (Activity Generator, Location Generator and Router) provide suggested routes that po-

tentially fulfil the agent's goals. In these transactions, the Agent Database acts as an "ignorant" broker: it contains very little knowledge about the simulated environment or agent logic.

At the end of this elaboration process, the Agent Database contains a plan for each agent has a plan that represents the overall system's current best solution to the agent's goals and expectations. (Over the course of many simulation runs, this solution will generally improve as the agents have the opportunity to explore the simulated landscape and discover more appropriate solutions.)

A simplified representation of an agent's plan is contained in figure 2.

Once the Agent Database has received elaborated plans for each agent, they are submitted to the Physical Simulation for execution. At this point, the Agent Database assumes more of a "controller" role, primarily ensuring that the various modules are able to keep up with each other. It does this by throttling the entire simulation (by requesting that the physical simulation wait after each time step) if some of the modules not able to process events and/or requests quickly enough.

```xml
<plan agent ="1" plan_id="1" >
      <activity id="1-1" type="enter_simulation" time="324000">
            <location id="1-1-1" type="parking_lot" x="512432.2" y="508343.5" />
      </activity>
      <activity id="1-2" type="hike" suggested_duration="3600"  >
            <waypoint id="1-2-1" type="node" node_id="1246" x="512438.5 y="5078334.3" />
            <waypoint id="1-2-2" type="node" node_id="1247" x="512436.0 y="507820.9" />
            (…)
      <location id="1-2-1" type="hike_waypoint" x="512450.0 y="508012.3" />
      <waypoint id="1-2-12" type="node" node_id="1281" x="512470.5 y="507950.3" />
      <waypoint id="1-2-13" type="node" node_id="1284" x="512322.5 y="507912.8" />
      (…)
      </activity>
      <activity id="1-3" type="eat" duration="1800" >
            <location id="1-3-1" type="restaurant" x="514432.0" y="505323.0" />
      </activity>
</plan>
```

Figure 2: Simplified XML Plan. The simulation system dynamically generates a new plan for each agent every day. The plan is used by the Physical Simulation Module to direct the agent's movements over the course of a simulation run.

3.2.   Physical Simulations – Pedestrian Simulation Module

The Pedestrian Simulation Module models how the agents interact with the physical environment. This includes interactions with other agents (such as avoiding collisions) and interactions with the physical world (i.e. slowing down when climbing up steep hills.)

Because of the need for realistic arbitrary movement, the pedestrian simulation module uses a hybrid approach adopted from Mauron [4]: the module uses a continuous representation of geographic space, but also uses a network representation of available paths as a guide for the agents' movements. This means that agents are free to move anywhere in the model, but are more likely to walk along existing paths and trails.

The pedestrian model uses a force-based approach, with strong forces along the path trajectories and weak forces toward the middle of the path which encourage agents to follow the trails. Additional forces are generated by neighbouring agents and inanimate objects near the agent. The force model was calibrated based on video data of pedestrian movement and provides very realistic movement patterns.

A continuous space implementation requires, in general, considerably more computational resources than a network-based approach, particular for areas as large as our study area (over 600 km^2). However, the particular nature of hiking areas means that the study area is very sparsely populated with agents at any given time, and they tend to congregate within a much smaller subset of the total area available to them. In order to reduce the computational demand, the pedestrian simulation module takes advantage of these features and uses lazy-initialization and caching techniques to ensure that only a small proportion of the total area is loaded into memory at any given time[3]. As a result, the physical simulation module can easily fit within the resources available on standard desktop PCs.

From the perspective of the Pedestrian Simulation Module, the agent's plan consists of a
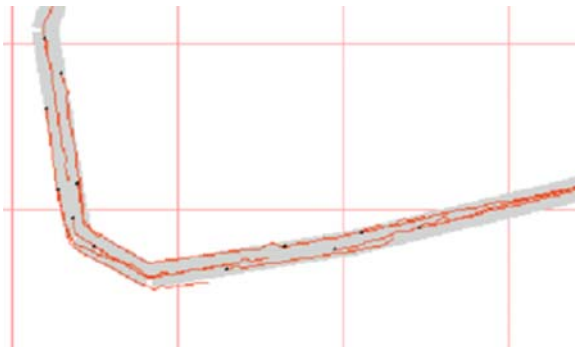
Figure 3: Hybrid Continuous Space Model: Traces of Simulated Pedestrians following a path while avoiding each other.

series of waypoints that it needs to traverse over the course of a simulated day. The plan also indicates where and when the agent should enter the simulation, and if it should wait at any given waypoint (such as at a bench for a rest). Once the simulation module has received all of the agent plans, it simultaneously executes these plans for all agents in the simulation.

While the simulation is being executed, the module broadcasts messages describing the agents' interactions with the physical world to the event stream. These messages include:

» the location and orientation of each agent,
» if the agent has encountered congestion,
» information about the steepness of the terrain, and
» trail condition information.

The physical simulation uses additional GIS data, provided as a series of raster layers, to provide information such as the steepness and trail conditions. These two particular kinds of information are also used by the simulation, in conjunction with the agent's particular characteristics (such as agent fitness), to determine the agents' velocity. This is calibrated based on hiker data collected in other recreational areas[5].

3.3. Mental Modules

As described in section 2, part of the role of the mental modules is in elaborating plans. More importantly, however, is the mental module's key roles in observing and interpreting the agents' environment. The Mental Modules are where all agent learning takes place: the modules receive events from the physical simulations, which describe the agents' experiences, and use them to inform their suggested agent plans.

Each mental module is responsible for a different spatial and temporal scale in the plan-generating phase:

» The activity generator generates an ordered chain of activities based on the agent's goals and expectations.
» The location generator assigns specific locations to this activity chain, including key points in the middle of mobile activities such as hiking.
» The router generates specific routes between the locations specified by the location generator.

The three mental modules share a lot of similarities (they are implemented as closely related software classes). Each:

» maintains an internal representation of all possible agent choices at their respective spatial scales (for the router and location generators these representations are akin to a geographic map of nodes and links, while the location generator's is simply a list of possible permutations, in keeping with its non-spatial nature.)

» listens to the event stream generated by the physical simulation and summarizes this information into distinct "experiences". These experiences are stored based on the spatial and temporal scale of the module (i.e. per activity pair in the case of the activity generator, per location pair by the location generator and per node-pair for the router).

» Contains an evaluator function that scores these previous experiences based on a particular agent's expectations (i.e. while a hike may be too steep for another hiker, it might be exactly what another hiker is seeking.)
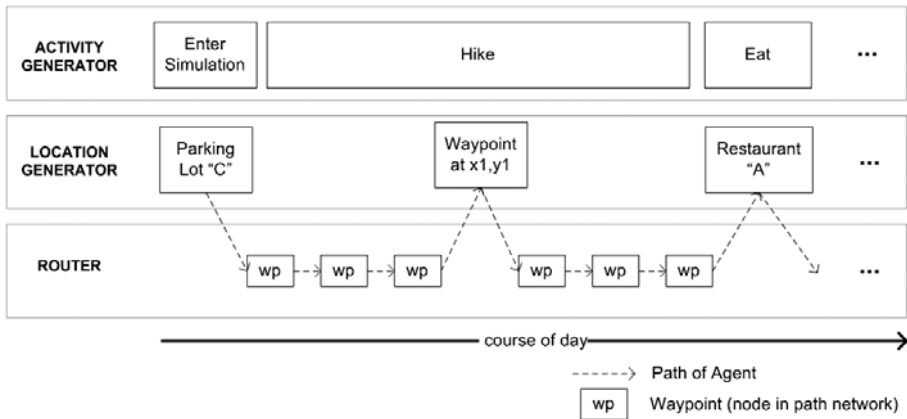
Figure 4: Schematic representation of each Mental Module's contribution to the plan generation process. As the Agent Database queries the Modules from top to bottom, the agent's plan gains increasing resolution.

In the current implementation, only the location generator and router have been fully implemented: as an interim measure the activity generator uses some simple heuristic rules to create plausible activity chains.

Example Mental Module: Router

The router operates at the smallest spatial scale- it suggests routes between locations provided by the location generator. In order to do so, the router is preloaded with an internal network of nodes and links which represent the available paths within the simulated area. During a simulation run, every time an event is received indicating that an agent has passed a node (and therefore entered a link), the router begins collecting the events and stores them until a subsequent event indicates that the agent has left the link. These events, which indicate landscape features (such as the quality of a view, type of landscape or terrain difficulty) or human factors (congestion, trail closed etc.) are then summarized by the router and stored, along with the time the agent entered the link and how long it took for the agent to walk the link. Over time, as other agents walk the same route, their experiences are also associated with that particular link.

When asked to elaborate an agent's plan, the router parses the given plan, and extracts all of the location pairs. For each of these pairs, it computes the best available route along the path network according to the agent's individual characteristics. It computes this by first converting each link's set of experiences to a numerical value using a generalized cost function calibrated to the agent's goals and expectations (as the precise implementation of this function is part of ongoing research, details are to follow in a forthcoming publication.) An optimal path between the two locations is then computed using a modified Djikstra's algorithm[6]. Although our standard implementation uses the typical Djikstra algorithm, its heritage as a shortest path algorithm means that it is unsuited for modelling recreational activity: as at least part of the attraction for recreational users is the "getting there", a more complex algorithm is required and is currently under development.

3.4. Analyzer Modules

One particular strength of the described modelling framework is the ability to create new modules that model external factors and/or interpret the agents' environment in different ways. One does this by creating new analyzer modules that listen to the event stream (broadcast either by the physical simulations or by other analyzer modules). The analyzer modules can then insert additional information as events into the event stream, where they can be interpreted by the various Mental Modules, if appropriate. While the mental modules do need to be modified to be able to react to any additional information provided by the Analyzer Module, the overall simulation approach means that only minor changes need to be made (i.e. in the Evaluator and Summarizing functions of a single Mental Module). Two analyzer modules have already been implemented: a weather simulator, and a Visibility / Visual Quality Model.

Figure 6: The visibility analyzer module calculates what can be seen by each agent in the simulation. Using positional data generated by the physical simulation, the module uses 3D rendering techniques to render false colour images and depth maps of the agent's field of view. These images are analyzed and information about what is seen is broadcast back to the event stream.

Example Analyzer Module: Visibility / Visual Quality Module

The visibility module is an example of a secondary analyzer module: it listens to the main event stream, and based on the current agent locations, it calculates what is visible to that particular agent. It then broadcasts this visibility to the main event stream, where it can be "heard" and interpreted by one of the mental modules. The visibility module uses a 3D representation of the landscape being modelled to calculate what can be seen from any location in the model [7]. Depending on the needs of the questions asked of the simulation, the visibility calculations information can be pre-computed or done in real-time as the simulation is running (useful if the visibility of other agents is important.) As interpreting the results of the visibility calculations are rather computationally intensive, a further Analyzer Module was developed that interprets what an agent sees and returns an aggregated visual quality score. This means that the mental modules need not be further complicated by this interpretation. Like any other analyzer module, the Visual Quality Module can be inserted almost transparently into the event stream.

4.   Communication and Coordination

As the individual modules are implemented in most cases as separate executables, communication and co-ordination between the modules is a crucial part of the overall system design. The modules communicate with each other via TCP network messages, which are formatted as XML. There are two major message types in the system:

» Control messages: these messages are used for communication between the control modules and the mental modules or physical simulations. They consist of XML "requests" from the control modules and "responses" from the other modules.

» Event messages: these messages are used to broadcast information about agents' current location and state to the entire simulation system. The events are sent by the physical simulation and analyzer to the Event Broker module, which re-

broadcasts them to all interested modules. The events indicate when an agent has started a specific activity (such as hiking), reached a specific location (such as a path intersection), encountered congestion, etc.

A key issue is timing: in order to keep all modules synchronized during a model run, messages are sent to identify which modules are ready to receive additional input. We use a variation of the Time Warp algorithm [8], whereby modules inform the control module at which temporal resolution they are operating (some modules, such as the physical simulation might need to react every 10 seconds "real-time", whereas others, such as the weather simulator, might only need to re-compute every 15 minutes) and if they are ready for the simulation to proceed.

One of the advantages of using XML messages over TCP is that it is relatively trivial to distribute the various modules across multiple computing nodes. While this requires some configuration changes in the control modules, and perhaps in the modules being distributed, those modules receiving messages generally do not need to be modified to accommodate this. The current implementation has the visibility analyzer distributed transparently across multiple hosts, as it requires a fair amount of computing resources.

Another advantage of this approach is that the modular nature allows one to test different implementation approaches for different modules without needing to rewrite the entire system.

4.1. Within-Simulation Replanning

One example of using the modular structure to test different approaches was the implementation of replanning during the simulation run. In the typical implementation, during a model run the mental modules only observe the event stream. They use this data to make decisions for the next model run. However, with a simple modification to the mental modules, the system was modified to accommodate changing the agents' plans in the middle of a simulation run. As the mental modules realized that an agent's plan was not appropriate for the day's weather (modelled by the weather simulator), it sends a revised plan to the control module, which forwards it to the pedestrian simulation.

5.   Outlook

While at first glance the system might seem rather over-complicated, the modular structure now in place allows for it to be easily extended and tweaked without extensive rewriting of software code. A particular strength of the framework is that modelling the agents' physical interaction is completely separate from modelling the agents' mental processes, which is an area which requires extensive research before the simulation of pedestrian behaviour will be entirely plausible.

Although the current implementation is still some steps away from a real-world applicability in the tourism industry, our prototype nevertheless demonstrates that all these features can indeed be implemented into a computational system. Future work will include to make the system more robust, and to include better behavioural models.

6.   Acknowledgements

References

1.   J. Ferber: *Mutli-agent Systems, An Introduction to Distributed Artificial Intelligence*, Addison-Wesley (1999).
2.   C. Gloor: *Distributed Intelligence in Real World Mobility Simulations*, In: Unpublished Doctoral Thesis, Department of Computer Science, ETH Zürich (2005).
3.   C. Gloor et al.: *A Pedestrian Simulation for Very Large Scale Applications*, In: A. Koch and P. Mandl (Eds.), Multi-Agenten-Systeme in der Geographie, Institut für Geographie und Regionalforschung der Universität Klagenfurt (2003).
4.   L. Mauron: *Pedestrian Simulation Methods*, In: Unpublished Diploma Thesis, Department of Computer Science, ETH Zürich (2002).
5.   J.W. van Wagtendonk and J.M. Benedict: *Travel Time Variation on Backcountry Trails*, Journal of Leisure Research 12, pp. 99-104 (1980).
6.   E.W. Dijkstra: *A Note on Two Problems in Connexion with Graphs*, Numerische Mathematik 1: pp. 269–271 (1959).
7.   D. Cavens et al.: *Integrating Visual Quality Modeling within an Agent-Based Hiking Simulation for the Swiss Alps*, In: The Second International Conference on Monitoring and Management of Visitor Flows in Recreational and Protected Areas, Rovaniemi, Finland (2004).
8.   D.R. Jefferson: *Virtual Time*, ACM Transactions on Programming Languages and Systems 7(3), pp. 404-25 (1985).

Design of Escape Routes by Simulating Evacuation Dynamics in Conjunction with a Probabilistic Safety Concept

M. Dehne[1] and D. Kruse[1,2]

Shopping centers and event halls established today are to be brought only with difficulty in harmony with the demands of the building code regulations and directives concerning the escape routes. Engineering methods like simulation-models for evacuation dynamics for the calculation of the evacuation time supply an indispensable instrument to find a compromise between a safe enough and coevally economical building. With simulation models it can be proved computational for example that in case of fire persons can leave a building quickly enough and without dubious congestions so that they are not endangered by smoke and fire gases. The difficult is that it is impossible to estimate the achieved safety level of a simulation because of the absence of a probabilistic safety concept. The question is: "How safe is safe enough"? In this article a global probabilistic safety concept is presented which in case of evacuation (for example in case of fire) starts from an extraordinary unfrequent event. The essential safety depends on the authoritative side conditions, varying by usefulness of a building, for the endangering of persons.

1.   Parameters influencing the safety level when using simulation models

Fire safety engineering methods like simulation-models for evacuation are a valuable instrument to verify the evacuation concept of complex buildings. Evacuation models help to detect mistakes in the safety concept and they help to decide on necessary measures to evacuate buildings within an available time.

The available time to escape could be calculated for example by CFD analysis. Occupants have to escape from a building as long as there is still a smoke free layer in the escape routes.

The necessary time for escape t_{escape} needs to be smaller than the available time for escape $t_{available}$.

$$t_{escape} < t_{available}$$

A requirement for the application of engineering methods like simulation-models for evacuation dynamics is to obtain the customary safety level as it is defined through the number of fire casualties and the fire damage per year.

Very often these methods are used without any safety concept. Three important influences are neglected completely:

---

[1]Dehne, Kruse & Partner Fire Safety Engineers
[2]Fraunhofer Institut für Holzforschung Wilhelm-Klauditz-Institut WKI;
Dehne, Kruse & Partner Fire Safety Engineers

» Variance of the model parameters
» Probability for failure of fire safety measures
» Uncertainty of the used models

The parameter used by the respective models can be classified into stress variables (e.g. fire load, occupancy) and into resistance variables (e.g. critical temperature, least visibility). Both are subject to statistical distribution [1].

The safety level is sufficient if the collapse of a building structure or the death of people due to smoke gas appears within the planned design life with an acceptable low probability (target reliability).

Failure happens if one of the possible limit states is exceeded. In general terms the state of a construction can be described as follows:

$Z = R - S$ with

Z   Safety distance (Sicherheitsabstand)
R   variable describing the resistance (resistance-Variable)
S   variable describing the action (stress-Variable)

The limit state is reached if Z equals zero, failure occurs if Z is below zero. Normally the mean values of these variables are used. This can lead to a higher number of failure due to an infringement of limit states as shown in figure 1 [1].
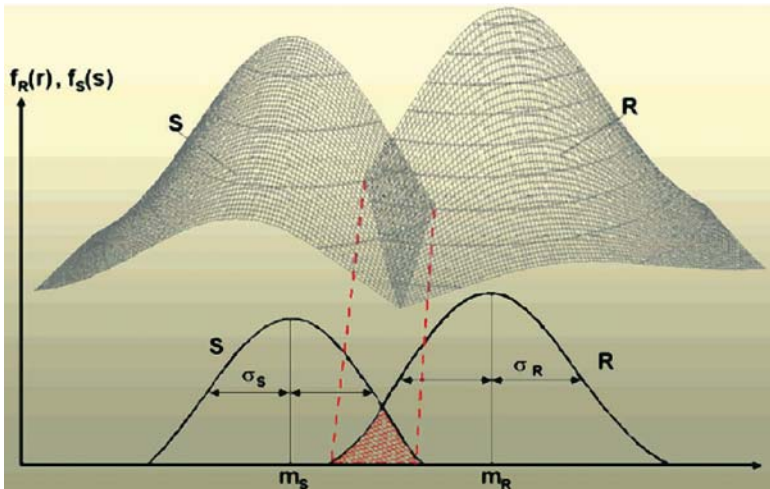
Figure 1: Graphical display of the limit state equation $Z = R - S$

Statistical analysis of fires showed that the reliability of system technology and preventive fire safety measure does not reach 100%. They rather show an individual differently failure probability. Instead most designers assume that the corresponding measure is absolutely able to function whenever requested. This assumption can be dangerous. For example it might happen that a fire alarm signal or a voice communication system fails. This has a direct influence on the reaction time of the occupants.

Since it is necessary to idealize in some cases a deviation is inevitable between calculated fire effect and experimental arbitrated temperature load or smoke layer. Likewise there are differences between the calculated component resistance and the resistance of components against the thermal attack measured in furnace experiments. The same goes for the simulation of evacuation dynamics.

Deviations between calculation and escape practice are quite normal. In order to be able to make an assessment about the safety level achieved in each individual case, the above described parameters (Variance of the model parameters, probability for failure of fire safety measures, uncertainty of the used models) have to be taken into account.
In the following contribution an approach for a probabilistic safety concept is given which can be used in combination with a simulation-model for evacuation dynamics.

2.   Probabilistic Safety Concept

The probabilistic safety concept for preventive fire protection measures assumes an extending fire as an extraordinary action. The necessary safety for occupants is derived from the determinant boundary conditions varying from the utilization of a building.
The safety concept can be adapted to different utilizations and used in combination with different fire models as well as the simulation of simulation of evacuation dynamics. The design calculation can be done alternatively with design values based on theory of probability or semi-probalistic with partial safety factors respectively additive safety elements.
The interaction of different fire safety measures as well as their interaction with the course of the fire can be considered in a system analysis following the Second Order Reliability Method (SORM) [1].

Structural fire protection measures as well as preventive and active fire protection measures are integrated by means of corresponding models and through the heat release rate into the determination of the fire effects. Since their deviation and failure probabilities are considered in the system analysis or the safety concept too, it is possible to compare the effectiveness of single fire protection measures and to find optimal combinations of different measures in respect to the boundary conditions of the building. As an objective comparison standard for the effectiveness of the measures serves the conditional failure probability in the case of fire p_{fBA} [1].

In a first step the safety level for the design of a structure, for the configuration of the smoke extraction systems or the determination of the necessary width of escape routes is established using a target reliability pf according to traditional design. One possibility to determine the target reliability in dependency of the individual boundary conditions and the risk is the Life-Quality-Index method according to Rackwitz [2]. Normally the target reliability is 10^{-6}/year.

Through evaluation of fire statistics it is possible to determine the fire spread probability p_{BA} (the probability wether a starting fire develops into a fully developed fire) in dependence of the utilization of the building and the existing fire compartment area.

The conditional failure probability in the case of fire can be calculated using the target reliability pf and the probability of a fire spread pBA

zul $p_{fBA} = p_f / p_{BA}$ for the corresponding design situation [1].

This has to be compared with the existing conditional failure probability in the case of fire vorh p_{fBA} which can be determined by a system reliability analysis.

A time-dependent calculation is necessary because the failure probability of a component under thermal attack changes due to the influences of the fire on the boundary conditions. To do this all the possible fire scenarios sorted according to function and failure of the existing fire protection infrastructure and according to the fundamental parameters affecting the fire e.g. fire load and ventilation have to be recorded in an event tree (fig. 2).
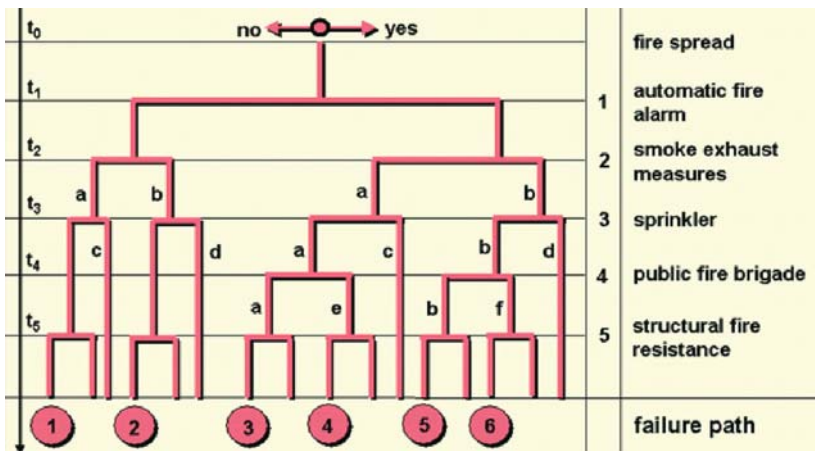
Figure 2: Event analysis for the determination of the failure path

Different fire courses (a to f in fig. 3) which are described by the temporal course of the heat release rate need to be assigned to each single event path (fig. 3).
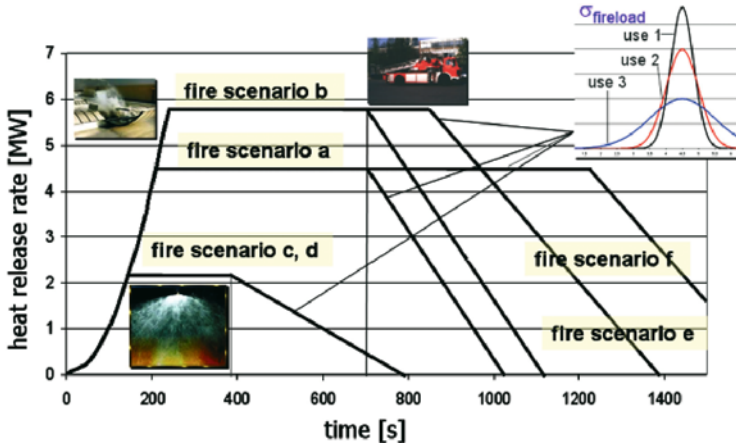
Figure 3: Fire spread (qualitative) in dependency on the active and preventive measures

Further details of the system reliability analysis like the determination of the stochastic model of the deviating parameters and the analysis of the failure of certain measures by fault trees can not be given here. For further information refer to [1].
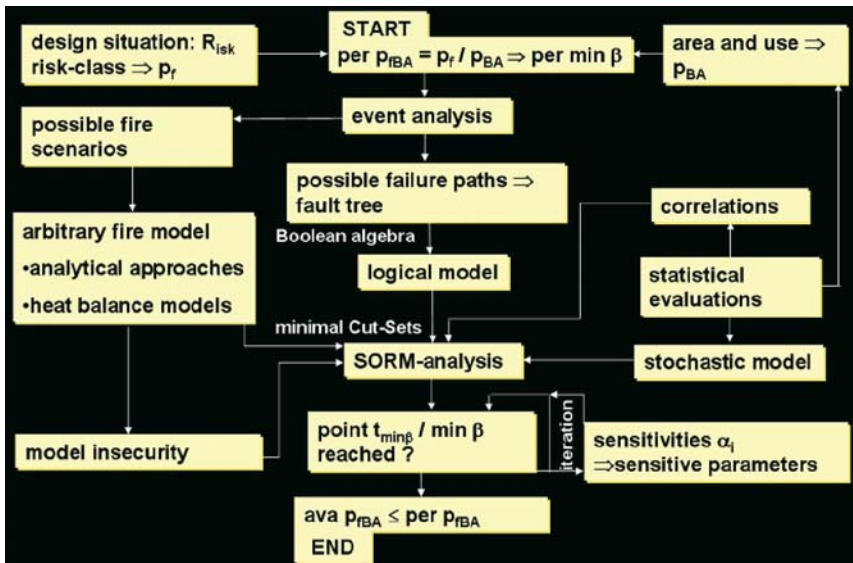Figure 4 summarizes the steps of a probabilistic design in a flow chart.

Figure 4: Flow chart for the probabilistic design

After a first run of the time-dependent system reliability analysis (Second Order Reliability Method SORM) the calculated minimal conditional failure probability vorh p_{fBA} at the time $t_{min\beta}$ is compared with the beforehand fixed limiting value zul p_{fBA} (see fig. 5). Normally a difference Δp_{fBA} will turn out. This difference has to be reduced by a change of the design parameter until at the time $t_{min\beta}$ it is valid: vorh p_{fBA} = zul p_{fBA}
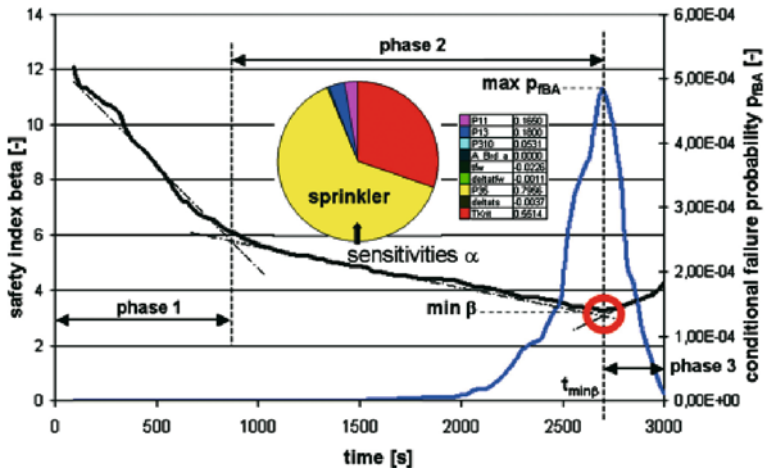
Figure 5: Comparison of vorh p_{fBA} resp. vorh min β with the limiting value zul p_{fBA} resp. zul min β

The design will normally be done semi-probabilistic with partial safety factors or with additive safety elements which are derived by the described methods. The derivation has to take the utilization into account since especially the probability of a fire spread and the deviation of the fire load strongly depend on the utilization.

3.   Example: Shopping-mall

A shopping mall shall serve as an example how specific fire protection problems can be solved by modern engineering methods. It will be shown that the customary safety level can be achieved by a combination of these methods with a probabilistic safety concept. In this special case it shall be verified by appropriate engineering methods that the protection aim of a safe escape of the occupants can be achieved.

According to § 14 3 of the German Muster-Verkaufsstättenverordnung [3] in every storey of a mall an exit width of 0,3 m must be existing per 100 m² sales area.

Stores up to 100 m² sales area must have an exit of at least 1,0 m width. Stores of more than 100 m² up to 500 m² must have at least two separate exits with at least 1,0 m width each and stores with an sales area bigger than 500 m² need to have 2 separate exits with at least 2,0 m width each.

In the respective mall the exit width for every shop complies with the regulations. The requirement of the exit width in the respective storeys is reneged in the basement and the first floor. The necessary exit width is reduced hereby approx. 20%.

To prove that the occupants are able to escape the building safely in case of danger the evacuation time needed was calculated under adverse conditions. The result was compared to the available escape time derived from a flue gas simulation. The occupants have to evacuate the mall as long as there is a layer of low smoke in the shopping street which serves in some cases as primary resp. secondary escape route.

The evaluation of the potentially existent danger due to flue gases is done through quantitative safety criterias for personal protection. If people are exposed for 30 minutes the following limits have to be observed according to [4]:

» CO-Concentration ≤ 100 ppm,
» Visual range ≈ 15 - 20 m.

The calculation with the CFD-model FDS [5] showed that the safety criterias in the layer of low smoke are complied with (fig. 6).
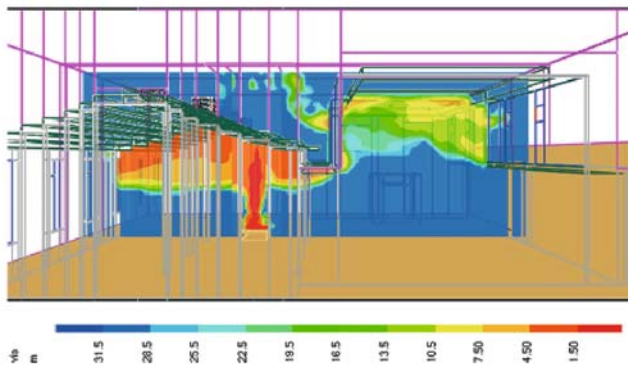
Figure 6: Visibility in the longitudinal section of the mall at the time t = 1800 s

In the next step it had to be shown through a calculation of the evacuation time needed that the occupants could evacuate the building within the 30 minutes. For the simulation of the evacuation dynamics software „buildingExodus V4.0" of the Fire Safety Engineering Group, University of Greenwich was used [6].

The entire mall including park deck and the residential and office use of the higher floors was divided into cells according to figure 7. The cells represent the areas were theoretical occupants can be.

Figure 7: Arrangement of cells in the basements for the evacuation simulation

Occupants will use the escalators of a mall as an escape route indeed because they are the most familiar route within a mall. In the simulation the escalator were not taken into account because it had to be proven that the occupants even under maximum occupancy could leave the building adequately fast using only the systematic horizontal and vertical escape routes.

The maximum occupancy was in this case determined according to [7]. Hereafter the maximum occupancy of modern malls of approx. 0,3 persons per m² of sales area can be assumed. The boundary conditions regarding both physically and mentally characteristics of the 9675 occupants were defined. A positive aspect of a mall is that a vast majority of the occupants is able to escape on their own.

Since it is possible to define physical and mental flexibility of single persons in the software a representative sample of the population was generated including disabled as well as elderly people and infants. Conservative a proportion of 2% disabled people were considered in the simulation.

The speed of non-disabled people without luggage reaches a maximum of approx. 1,5 m/s. Disabled people were assigned a maximum speed of 0,5 m/s.

Figure 8: Illustration of the occupancy in the basement

The evacuation analysis was done following a conservative approach. It can be described as follows:

»   Fire in a shop in the basement. To cover the risk of the people by flue gases a fire on the lowest level from which the flue gas can reach the plenum of the mall has to be presumed. Due to the long flow path from the basement to the ceiling, there is a high heat emission of the flue gases. This corresponds to a significant reduction in propulsion. Furthermore the amount of smoke is at a maximum because of the longest possible path for a mixture with air. Under such conditions a maximum flue gas layer will arise under the ceiling. For the flue gas simulation a fire in the same shop was assumed.

»   The people in the shop had to evacuate through the back emergency exit because it was assumed that the front sector of the shop was not passable because of the fire.

The building has a fire detection system with fire alarm and smoke detectors. Furthermore a voice communication system is available to warn the occupants in the case of danger and to declare an evacuation of the building. Because of the smoke detectors and the presence of occupants during the opening hours the delay between the burst of fire and the acoustical announcement of the evacuation instruction averages 2 minutes.

To compensate the above described uncertainties of the fire protection design an additional safety element Δt is introduced. It is added to the time needed $t_{Räumung}$ for the evacuation of the building. This additional safety element is determined through a system reliability analysis according to chapter 2 with a failure probability of 10^{-6} per year. In this special case the safety element was calculated to $\Delta t = 5$ min.

 The time span for the evacuation (reaction time + running time) of the respective building averages for an occupancy of 9675 persons to 23:32 minutes (mean value of 10 simulations). Figure 9 shows the number of evacuated persons per time as a result of one of the 10 simulations.
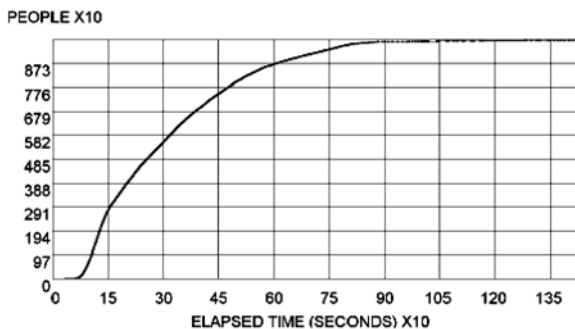
PEOPLE X10

Figure 9: Number of evacuated people over the time

The shape of the curve shows clearly the higher amount of time for the evacuation of the disabled persons. After 15 minutes the majority of occupants has left the building. At this time the slope of the curve is significantly reduced. The number of people evacuated per unit of time is reduced due to the decreased mobility of the disabled persons.

The calculated value includes the reaction time and the running time. To obtain the time span for the evacuation from the burst of fire $t_{\text{Räumung}}$ the time until the detection and the announcement of the evacuation instruction has to be added. As described above this value can be assumed to equal 2 minutes because of the smoke detectors.

The overall evacuation time from the burst of fire results for this respective building to 25:32 minutes.

$t_{\text{Räumung}}$ = 25:32 minutes

Considering the safety element Δt the time for evacuation is:

$t_{\text{Räumung}}$ + Δt = 30:32 minutes

A CFD-Simulation showed that the shopping street of the respective mall can serve as an escape route for at least 30 minutes because the criteria of a 2,5 m smokeless layer thickness is fulfilled at least for 30 minutes.

It is very likely that the shopping street will be passable even after 30 minutes because after 10 minutes the CFD-Simulation reaches nearly stationary conditions regarding the smokeless layer.

4.   Conclusion

This contribution shows the necessity to use modern engineering methods like simulation-models for evacuation only in combination with a safety concept. Then it is possible to adhere natural deviating parameters like e.g. the number of persons. Also one has to bear in mind that systematical existing fire protection measures are not to 100 % reliable but might fail with a certain probability. Furthermore all models bear a certain uncertainty which has to be taken into consideration for the fire protection design.
For this purpose a probabilistic safety concept was presented. It determines the true existing failure probability under consideration of all the uncertainties by a system reliability analysis with accepted methods (Second Order Reliability Method SORM). The true existing failure probability can be compared with a target reliability. The approach was shown by an example. «

References

1. M. Dehne: *Probabilistisches Sicherheitskonzept für die brandschutztechnische Bemessung*, Dissertation, Institut für Baustoffe, Massivbau und Brandschutz, Technische Universität Braunschweig, Braunschweig (2003).
2. R. Rackwitz and H. Streicher: *Optimization and Target Reliabilities*, JCSS Workshop on Reliability Based Code Calibration, Zürich (2003).
3. ARGEBAU, *Muster-Verordnung über den Bau und Betrieb von Verkaufsstätten Muster-Verkaufsstättenverordnung (MVkVO)*, Fassung September 1995 (1995).
4. D. Hosser: *vfdb-Leitfaden Ingenieurmethoden des Brandschutzes*, erarbeitet vom vfdb-Referat 4 Ingenieurmethoden des Brandschutzes (2005).
5. K.B. McGrattan: *Fire Dynamics Simulator (Version 3) – User´s Guide*, National Institute of Standards and Technology, Gaithersburg (2002).
6. E.R. Galea, *buildingEXODUS V4.0 User Guide and Technical Manual*, Fire Safety Engineering Group, University of Greenwich, London (2004).
7. National Fire Protection Agency Staff: *NFPA Life Safety Code 2000*, February 2000 (2000).

The 2001 World Trade Centre Evacuation

E.R. Galea[1], P. Lawrence[1], S. Blake[1], A.J.P. Dixon[1], and H. Westeng[1]

The WTC evacuation of 11 September 2001 provides an unrepeatable opportunity to pro-be into and understand the very nature of evacuation dynamics and with this improved understanding, contribute to the design of safer, more evacuation efficient, yet highly functional, high rise buildings. Following 9/11 the Fire Safety Engineering Group (FSEG) of the University of Greenwich embarked on a study of survivor experiences from the WTC Twin Towers evacuation. The experiences were collected from published accounts appearing in the print and electronic mass media and are stored in a relational data base specifically developed for this purpose. Using these accounts and other available sources of information FSEG also undertook a series of numerical simulations of the WTC North Tower. This paper represents an overview of the results from both studies.

1.   Introduction

The 9/11 evacuation of the World Trade Centre (WTC) towers is of fundamental importance to the future design of high-rise buildings. The attack on the WTC towers brought home to the world the importance of providing adequate and robust means of evacuation in high-rise buildings. It was also one of the largest full-scale evacuations of people in modern times. As such it is of great importance to our understanding of the complex interaction between structure, procedures, environment and human behaviour; and how these factors interact to determine evacuation performance.

Following 9/11, the Fire Safety Engineering Group (FSEG) of the University of Greenwich embarked on a series of studies centred on the evacuation of the WTC. These include a study of printed accounts from survivors of the WTC evacuation[1-4]; numerical simulation studies of the evacuation of WTC Tower 1[5] and project HEED, a study to collect and analyse data from face to face interviews with survivors of the WTC evacuation[6]. This paper reports on a selection of the published findings from the first two studies.

2.   The Event

While the events of 11 September 2001 are well known, it is worth recounting the main facts. WTC1 was hit by American Airlines Flight 11 at 08:46 a.m. The impact was nearly centred on the north face of the building which was hit between the 94th and 98th floors. WTC2 was hit by United Airlines Flight 175 at 09:03 a.m. The impact was at a skewed angle toward the southeast corner of the south face of the building which was hit between the 78th and 84th floors. WTC2 collapsed at 09:59 and WTC1 collapsed at 10:37. There are various estimates for the number of people in the building and the

number of fatalities. Denis Couchon of US newspaper USA Today estimates that there were between 10,000 and 14,000 people in the buildings at the time of the impact[7], while NIST, in their interim study estimate that there were 17,400 +/- 1,200 people in the buildings[8]. Couchon estimates that 1,432 building occupants perished in WTC1 and 599 in WTC2[9], while NIST estimate that 1,560 and 599 building occupants in WTC1 and WTC2 respectively perished[8].

3.   The Database of Human Experience

Following the WTC disaster, the Building Disaster Assessment Group (BDAG) of the UK Office of the Deputy Prime Minister, funded FSEG to gather, collate, categorise, electronically store and finally analyse data concerning human behaviour during the WTC evacuation. Reports were gathered from the literature published in the public domain. Material sources ranged from survivor accounts printed in newspapers and newspaper web sites, interviews in the electronic media, survivor web sites and books. Over 250 separate accounts were gathered that described occupant behaviour. Information appearing in print newspapers represents 70% of the accounts while information from websites (news and personal) represents 16% of the accounts. The remainder of the accounts have appeared in books, journals and the electronic media. These accounts provided information concerning 120 people from WTC1 (north tower or WTC1) and 119 from WTC2 (south tower or WTC2) and 21 of unknown origin[1,4].

The collected accounts were entered into a specially developed database. Each individual experience described within the account was stored and assigned specific behavioural references. This is similar to traditional qualitative analysis tools that allow users to categorise portions of textual accounts during the input process. The rationale for the database was that all information was centred on an experience. Each experience was assigned a main category and a sub-category that described the nature of the experience. A distinguishing feature of the database is that it is not only able to store experiences but also the location of the experience and a time reference for the experience.

The database contains reference to a total of 3291 experiences from 260 people (1869 accounts from WTC1, 1411 from WTC2 and 11 from unknown locations). Gender information was available for 240 people, 164 of which were male and 76 female. The quality of this data varied enormously. While some accounts were several pages long, others were only a couple of paragraphs in length. Of more importance, some accounts provide important detailed information such as a detailed description of events, locations at which events took place and reference to key time markers. The reports mainly came from occupants that begun their evacuation in the upper floors of either tower. Within the database, 73 (61 %) and 91 (76 %) of the occupants from WTC1 and WTC2 respectively were initially located on or above the 78th sky lobby. It is likely that this bias originates from the medias natural desire to focus on accounts that described the most extreme conditions during the disaster.

3.1. Data Analysis

The database has been used to study a number of issues concerning the evacuation of the WTC. These can be broadly separated into two categories, pre-evacuation and evacuation. The pre-evacuation category is intended to cover behaviours prior to the physical act of attempting to evacuate, while the evacuation category is intended to cover those actions and behaviours during the physical act of evacuation.

The study has provided useful insight into the following issues: occupant response times in high rise buildings; nature of occupant pre-evacuation activities; the use of telephones and other electronic devices for communications by the occupants during the evacuation; retrieval of items by occupants prior to evacuation; occupant assessment of the incident; occupant travel speeds on stairs during the evacuation; occupant interaction with firefighters during the evacuation process; usage of elevators for evacuation; group formation, cohesion, leadership and behaviour; response of fire wardens and fatigue issues. Due to space limitations, only a summary of the findings concerning occupant pre-evacuation times will be presented here, interested readers are directed to the BDAG report[1] for a full account.
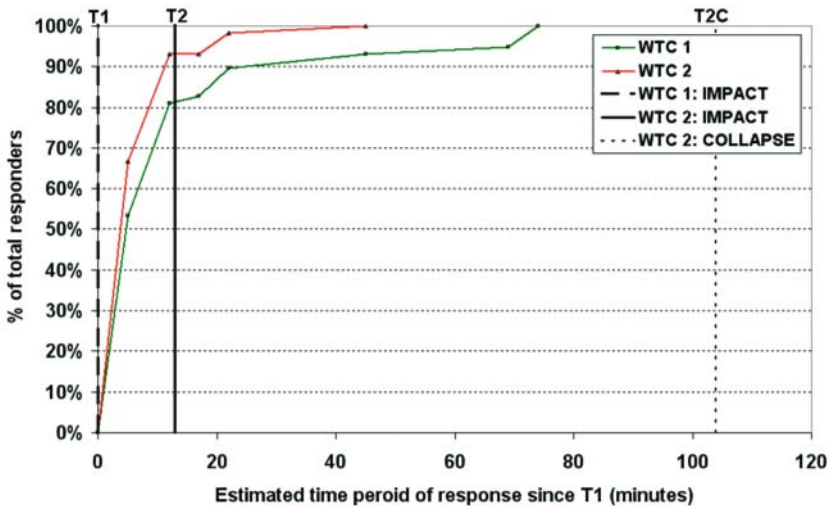
Figure 1: Percentage cumulative frequency distribution of occupant response

Of the 115 people who provided information on which a pre-evacuation time (also referred to as response time) could be estimated, 60% responded within an estimated 5 minutes of the assault on WTC1 and some 13% took longer than an estimated 17 minutes to respond (see Figure 1). Occupants in WTC2 responded quicker to the assault

than occupants in WTC1 - the first tower to be attacked. This occurred in WTC2 despite instructions issued over the PA system in WTC2 instructing occupants that there was no need to evacuate WTC2. It is important to note that even under the extreme conditions of the terrorist attack on the WTC, occupant pre-evacuation times can be quite long. A lack of data prohibited a meaningful analysis of pre-evacuation time and proximity to the incident. While it is difficult to generalise due to the lack of data, the rapid response times of occupants in WTC2 relative to WTC1 may have contributed to the smaller death toll experienced in WTC2.

4.   Simulating the evacuation of WTC 1

The modelling of the evacuation of WTC1 was performed using the buildingEXODUS simulation software, developed by the Fire Safety Engineering Group at the University of Greenwich. The basis of the model has frequently been described in other publications[10] and so will only be briefly described here. EXODUS is a suite of software tools designed to simulate circulation and evacuation of large numbers of people from complex enclosures. The EXODUS software takes into consideration people-people, people-structure and people-fire interactions. The model tracks the trajectory of each individual as they move around the geometry. In evacuation applications involving fire, the model can also predict when occupants will be affected by fire hazards such as heat, smoke and toxic gases. The software has been written in C++ using Object Orientated techniques utilising rule base technology to control the simulation. Thus, the behaviour and movement of each individual is determined by a set of heuristics or rules. For additional flexibility these rules have been categorised into five interacting submodels, the OCCUPANT, MOVEMENT, BEHAVIOUR, TOXICITY and HAZARD submodels. These submodels operate on a region of space defined by the GEOMETRY of the enclosure. The version of EXODUS used to simulate evacuation from the built environment is known as buildingEXODUS.

4.1.   The Model

Within buildingEXODUS it is necessary to specify the geometry of the building, the number, nature and distribution of the population and finally the nature of the evacuation scenario that will be investigated. Here we define each of these items.

The Geometry

In attempting to simulate the events of 11 September 2001, the geometry of WTC1 was approximated within the buildingEXODUS software. The model assumes that there is no significant damage to the building below the impact floors and that the elevators are not available to assist in the evacuation. The geometry is an approximation to the actual building as many details concerning its layout, while available were not provided to the authors despite a number of requests for such information. The broad structure of the

building geometry represented within the software included the number and width of staircases, number of floors, number of unoccupied floors, layout of staircase geometry, widths of main doors, etc. However, none of these sources provided an exact representation of the layout of each of the floors and so the model was kept as simple as possible.

WTC1 consisted of 110 floors above ground with a roof height of 417 m. The core area accommodated three exit stairs, 99 elevators and 16 escalators. Two of the stairs, Stair A and Stair C, were both 1.1 m (44 inches) wide. They both had exits out onto the Mezzanine Level and ran all the way up to the 110th floor. The third stair, Stair B, had a width of 1.4 m (56 inches). This went all the way from the Lobby and up to the 108th floor. The stairs did not run in continuous vertical shafts from the top to the bottom of the structure. Instead the plan location of the stairs shifted at some levels.

The layout of the non-core space on each floor varied from floor to floor and was dependent on tenant preference. Some floors had large open plan areas while others where more subdivided. Details of these layouts were not available for this study. As details of these open plan areas were not available and in order to reduce model memory requirements and execution time, most of the free space area outside the core area was not included within the model. Instead a 4 m wide area around the perimeter was modelled to represent the available space on each floor. This space provided sufficient to distribute the entire building population around the core in such a manner that allowed them to more freely without artificially incurred congestion related delays. Limited sensitivity analysis was conducted on the idealised and complete model representations. This suggested that this approach would not have a significant impact on model predictions as the majority of the delays experience by occupants occurred as they attempted to enter the staircases. The time crossing the open floors was insignificant.

As already described, there were a number of transfer corridors within the building effectively requiring occupants to leave a staircase, travel along a 'short' protected corridor before re-entering the staircase. While the exact details relating to the length of these transfer corridors was not available they have been represented within the model based on information available from the internet. As a result, the total travel distance represented within the model may not precisely represent the actual travel distance within the building. However, as the total stair length is more than 900 m, these small discrepancies are not expected to have a large impact on the final results.

The Population

Within the model the population was distributed only on the rented floors. In total three different sized populations consisting of 5,000, 7,000 and 25,000 people were considered. Here we will consider the 7,000 population. From press accounts it is thought that 1,432 people in WTC1 died, this included essentially everyone that was above the 91st floor (i.e. floors 92-110) and a few people on the lower levels[9,11] resulting in 5568 sur-

vivors able to evacuate from WTC1. These people were distributed evenly amongst the remaining 77 floors producing an average number of 72 people per occupied floor and a total of 5,544 people within the entire simulation (referred to as Population 1). Another population distribution (referred to as Population 2) was based on the assumption that a total of 304 people were killed on the impact floors and that a total of 6,696 people were able to evacuate, 5,544 below the impact floors and 1,152 people above the impact floors. This overestimates the suspected potential survivors above the impact floors by 205 however, at the time of this analysis this was not known. The survivors above the impact zone were also uniformly distributed. The number of people per floor was spread randomly across the open floor space in the geometry.

From the study of the media accounts, it was further decided that 30% of the population would be in the youngest age group, 50% in the middle age group and 20% in the older age group. The gender distribution was set at 65% males and 35% females based on information from the media accounts[1,4]. The default maximum travel speed settings available within buildingEXODUS, which are functions of age and gender were also adopted for these simulations. The response time distribution used within the simulations (see Table 1) was based on media account data. Individuals were assigned random response times based on the response time band in which they were assigned. It should be noted that the response time data from the study was based on the analysis of accounts from 58 people. It is acknowledged that this is a small sample and may not be representative of the entire building; however it was consider the best data relating to the incident available at the time of the analysis.

Response time Range	% of population
0 – 8 minutes	77
8 – 63 minutes	19
63 – 64 minutes	4

Table 1: Response time distribution used within the WTC simulations

Scenarios

For each population, a number of scenarios were investigated. These included cases in which; each population was assumed to react instantaneously (i.e. zero response time), each population assumed the response time distribution shown in Table 1, a single staircase remained in tact above the impact zone and rescue personnel were inserted into the building. In this paper we will briefly consider a subset of these cases as outlined in Table 2.

Accurate information regarding the number of rescue service personnel that may have entered WTC1 during the evacuation was not available at the time of the analysis. For the scenarios involving rescue services it was decided to investigate the impact of 300 rescue workers being sent into the building on the overall evacuation times. In the case presented here the rescue workers were sent into the building via Staircase B. From media accounts it was found that the fire fighters started their rescue attempt at approximately 09:00. It was therefore decided to insert the fire fighters into the simulation 14 minutes into the simulation. The procedures used by the fire fighters were not known at the time of this analysis and so they were represented as 30 teams of 10 people. The first fire fighter was generated after 14 minutes and the last after 58 minutes. The fire fighters were given an itinerary task instructing them to go to the 91st floor. The fire fighter travel speed up the stairs was arbitrarily reduced by 60% from the default value (effectively 0.38 m/s). This was intended to represent the fact that the fire fighters would be carrying a considerable amount of equipment and that fatigue would likely set in during the ascent. In addition, the buildingEXODUS parameter "DRIVE" was set arbitrarily high for each fire fighter. Within buildingEXODUS this means that whenever they were involved in a conflict with other people (of lower drive) they would always win the conflict. In effect, this would mean that building occupants would stand aside and let the fire fighter pass each time they vied for space on the stairs.

Scenario	Population	Response Time	State of Stairs	Rescue Services
1a	1	survey based	severed	absent
1b	1	survey based	severed	present
2a	2	survey based	single surviving	absent

Table 2: Summary of Scenarios considered in this paper.

Other buildingEXODUS specific behavioural settings that were set included enabling the staircase packing parameter. This means that the stairs can be occupied to their full capacity if necessary. Finally, occupants on each floor were attracted to their closest entrance into the core region. From there they would select their nearest staircase entrance.

5.   Model Predictions

All the cases presented in this paper were executed using a 2.66 GHz Pentium PC with 4 GB RAM. The run time for a single simulation of the 5,544 population was approximately 8 minutes 30 seconds.

5.1.   Scenario 1a: 5,544 survivors, survey based response times, staircase severed above 91st floor, no fire fighters.

This scenario is an attempt to reproduce the primary events of the actual incident. The population size and distribution matches the best estimates available at the time and the response time distribution is derived from the media accounts. This simulation involved 5,544 people who were able to evacuate the structure from the 91st floor and below. The average total evacuation time for this simulation is 1 hour 21 minutes. Stair C is the last to finish and the average spread in stair finish times is 1.3 minutes.
The average evacuation flow rate for this scenario is 68 survivors/minute.

If we compare this with the actual incident then it is estimated that 5,544 people managed to evacuate WTC1 some time before the building collapsed which was 1 hour 42 minutes 5 seconds after it was attacked. If we assume that the last person managed to evacuate the building just prior to building collapse, then this is equivalent to an average flow rate of 54 survivors/minute. The results produced from this simulation appear to be in good agreement with the available information. However, it should be noted that there were no fire fighters present in the simulation and hence no potential obstructions on the stairs.

An informative personal parameter that is determined by buildingEXODUS for each individual is the Cumulative Wait Time (CWT). This is a measure of the total amount of time that a person wastes in congestion. For this application, this includes the time queuing to get into the staircase and the time queuing on the stairs. Another useful parameter is the Personal Evacuation Time (PET). This is a measure of the time each individual requires to evacuate. The ratio of the two is a measure of the evacuation inefficiency incurred by the individual. A large value suggests that the individuals' personal evacuation was highly inefficient, spending most of the evacuation caught in congestion. An average value for this ratio can be determined for each floor of the building providing a view of the relative evacuation efficiency for each floor. Furthermore, the average floor evacuation efficiency can be determined for each staircase used by the occupants from that floor. This then gives a view of the relative evacuation efficiency for each floor as a function of the exit route (i.e. staircase) used (see for example Figure 2).
If these graphs are plotted for this case we note that the higher up the building a person starts their evacuation, the more inefficient the evacuation becomes relative to their personal evacuation time; i.e. the more of their personal evacuation time will be wasted in congestion. Were this trend to continue without abating, it would suggest that an eventual height would be attained above which the time spent in congestion by occupants would overwhelm the travel time (plus response time) making evacuation by stairs extremely undesirable, if not untenable. This is not the case in these scenarios, and we find a maximum of 13% of an occupants PET is lost in congestion across all the floors on Stairs A and C and a maximum of 35% is lost to congestion on the upper floors for Stair B (see Figure 2).
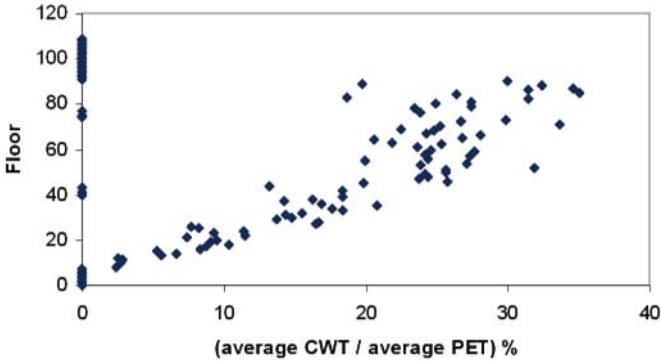
Figure 2: Evacuation efficiency per floor for Staircase B for Scenario 1a

These results also suggest that Stair B, which is the largest of the three stairs, was the most heavily used stair. This is indeed the situation with 44% of the occupants making use of Stair B. For this particular simulation, it is thought that the majority of this congestion is incurred at the stair entrance on each floor. This is supported by the observation that Stair B was heavily used, yet the evacuation time for Stair B was always quicker than the other stairs. As the average maximum inefficiency level is small (less than 15%) for Stairs A and C, this suggests that, for the number of people represented in this scenario combined with the imposed response time distribution, the building provides sufficient staircase and exit capacity. Furthermore, the primary factors driving this scenario are the response time distribution coupled with the size of the population and the travel speeds attained by the individuals. In reviewing these results it should be recalled that all of these factors are somewhat uncertain.

For the population and response time distributions used in this simulation, the model predictions suggest that the occupants did not experience high levels of congestion on the stairs. If this is the case, it is suggested that it is unlikely that the presence of fire fighters entering the building to undertake search and rescue operations would have had a significant detrimental impact on the evacuation times. This case is examined in the next scenario.

5.2. Scenario 1b: 5,544 survivors, survey based response times, staircase severed above 91st floor, fire fighters inserted.

This scenario is an attempt to gauge the impact that the fire fighters may have had on the overall evacuation efficiency. In the case considered here, the fire fighters are all inserted at the base of Stair B. It was noted in the previous case (Scenario 1a) that Stair B was the heaviest utilised staircase and it was not the last stair to finish. This simulation

involved 5,544 people who were able to evacuate the structure from the 91st floor and below. The average evacuation time produced for this simulation was approximately 1 hour 22 minutes. This is only one minute longer than the result for the equivalent case without fire fighters present.

As expected, introducing the fire fighters into the evacuation simulation did not have a significant effect on the total evacuation time for the simulation. However, if we consider the average floor evacuation inefficiency curve for Stair B we note that this has increased from a maximum of 35% in Scenario 1a to a maximum of approximately 45% in Scenario 1b (see Figure 3a). Thus on average the people using Stair B were hindered by the passage of the fire fighters as on average, their time spent in congestion has increased as a fraction of their total evacuation time. Those who experience the greatest effect are the occupants starting from the highest floors. The impact of the fire fighters can also been seen in the arrivals graphs for this scenario (see Figure 3b). In the mid portion of the evacuation sequence there is a dip in the arrival rate of occupants but after the passage of the fire fighters the arrival rate returns to normal. In addition, the entire evacuation sequence is extended slightly due to the earlier dip in arrival rates. It is also worth noting that in the previous case (Scenario 1a), Stair B was always the first to finish. However, in Scenario 1b, Stair B is almost always the last stair to finish. The average finish time for Stair B has increased from an average of 1 hour 20 minutes to an average of 1 hour 22 minutes.

The primary factors driving this scenario are similar to those of the previous case, namely the response time distribution coupled with the size of the population and the travel
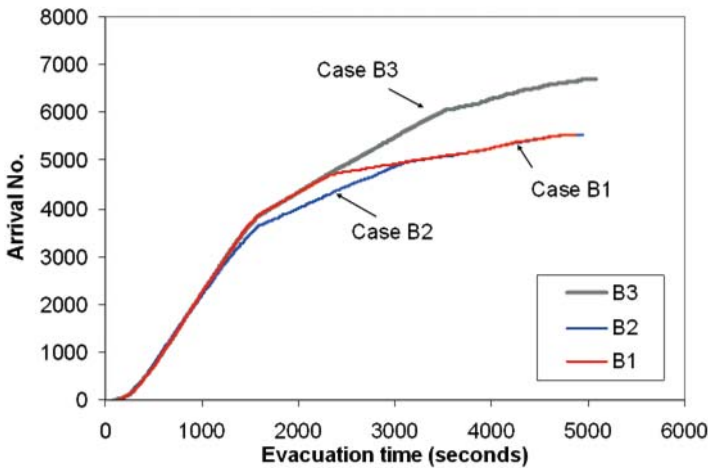
Figure 3: Arrival curves for Scenarios 1a (Case B1), 1b (Case B2) and 2a (Case B3)

speeds attained by the individuals. In addition, the nature of the fire fighter insertion and fire fighter physical capabilities, will also dictate the overall outcome of this scenario. In reviewing these results it should be recalled that all of these factors are somewhat uncertain.

5.3. Scenario 2a: 6,696 people, survey based response times, single surviving staircase above 91st floor, no fire fighters.

In this scenario we attempt to assess whether it was possible for the surviving building occupants trapped above the impact floors to have successfully evacuated prior to building collapse had a single staircase remained in tact throughout the impact zone. This model is based on Scenario 1a and so all the assumptions and caveats which applied to that simulation equally apply here.

In the work presented here, Stair B is selected as the surviving staircase. As in Scenario 1a, the population size and distribution matches the best estimates available at the time and the response time distribution is derived from media accounts. This simulation involved 5,544 people who were able to evacuate the structure from the 91st floor and below, but in addition, a further 1152 people are included above the 91st floor. These people are given the same response time distribution as the people below the impact zone. It is accepted that this assumption has little justification as the media accounts do not include response time data for those trapped above the impact floors. It is plausible that these people would have reacted with greater haste than those below the impact floors for which we have response time data. Equally, some may have undertaken other actions such as attempt to evacuate via the roof prior to attempting to descend via the stairs. As no other reliable response time data was available it was decided to use the media account data.

The average evacuation time produced for this simulation was approximately 1 hour 24 minutes. This is approximately 3 minutes longer than the time for Scenario 1a. This modest increase in evacuation time is somewhat unexpected but can be explained by the evacuation dynamics. As noted in Scenario 1a, due to the numbers of people involved, their physical distribution and the applied response time distribution, all three stairs are not utilised to their full capacity at any one time, and certainly not in the early and later stages of the evacuation. In the early stages of the evacuation this allows the early responders above the 91st floor to make good progress down the stairs. In the later stages of the evacuation this enables the long responders above the 91st floor to utilize the spare stair capacity.

This can be seen more clearly by studying the evacuation efficiency plot for Stair B and the arrivals graph for this scenario (see Figure 3). The presence of the additional people in this scenario is felt all the way down to approximately the 60th floor as above the 60th floor we note the average floor evacuation inefficiency increases slightly. The occupants

below the 60th floor are effectively able to evacuate as if these additional occupants were not present. Comparing the arrivals curve for this scenario with that of Scenario 1a (see Figure 3) we note that this is indeed the case as the two curves follow each other precisely up to approximately 2,300 seconds. After this time, the arrivals curve for Scenario 1a begins to flatten, reducing its slope (and hence exit flow rate) as there are insufficient people remaining within the structure to maintain the exiting rate. However, in Scenario 2a there are additional people available to maintain the flow rate and so the curve continues with its original trajectory.

This analysis suggests that had a single stair survived the impact above the 91st floor, survivors above the impact zone would have been able to escape the building prior to its collapse. It should also be noted that this analysis assumed a greater number of potential survivors above the impact floors than is likely to have been the case. However, this reinforces the conjecture that the survivors would have been able to escape prior to building collapse had an exit route been available.

6.   Conclusions

This work has been an attempt to explore the WTC evacuation resulting from the terrorist attack of 11 September 2001. The first part of this paper considered an analysis survivor accounts appearing in the public domain, primarily press accounts. One of the key outputs from this research is information relating to occupant response time. Of the 115 people who provided information on which a response time could be estimated, 60% responded within 5 minutes of the assault on WTC1. In WTC2, it is estimated that over 90% of people who provided response time information, responded within 5 minutes of WTC1 being hit. Information of this type is essential for fire engineering analysis of high rise buildings and was of pivotal importance in the evacuation simulation studies of WTC1.

While the modelling work is preliminary in nature, early results suggest that buildingE-XODUS is capable of reproducing the broad trends in this disaster. The model predicts the total evacuation time of the building for 5,544 survivors to be approximately 1 hour 21 minutes but this result depends on the precise nature of the model assumptions. This time compares favourably with the observation that the building collapsed after some 1 hour 42 minutes and supports the view that everyone that was able to escape from WTC1 on the day of the incident did get out. The model results also suggest that the insertion of the fire fighters into the building had minimal detrimental impact on the overall evacuation of the building.

The model was also used to explore a scenario in which at least one stair remained intact through the impact zone. The model suggests that had Stair B remained in tact throughout the building an additional 1,152 survivors trapped above the impact floor could have escaped prolonging the evacuation by approximately a further 3 minutes.

These results suggest that had at least one staircase survived from top to bottom, it is possible that everyone that survived the initial trauma of the impact could have managed to safely escape. This underlines the importance of staircase dispersal within buildings. It is essential to make it less likely to lose all means of escape in the event of plausible catastrophic incidents, and that staircases are sufficiently hardened to withstand plausible threats.

There are also some factors that at present cannot be easily and reliably represented within evacuation models such as fatigue. On descending 110 floors the average person will tire and slow down; they may even stop for a rest. While it is possible to artificially include a representation of fatigue within the simulation, it is desirable that a fatigue model is developed capable of predicting the onset and implications of fatigue on evacuation performance.

The issues left unresolved in both the survivor accounts and the computer simulation are being tackled by a larger and more ambitious project. The project, called HEED – High Rise Evacuation Evaluation Database – funded by the UK EPSRC (project GR/S74201/01) and involving the Universities of Greenwich, Ulster and Liverpool, with the support of; the Fire Department of New York, New York City Department of Buildings, New York City Department of Health and Mental Hygiene, and John Jay College of Criminal Justice New York, aims to conduct face-to-face interviews with survivors of the WTC twin towers evacuation and to perform more thorough computer simulations of the evacuation[6]. Unlike previous studies into the WTC, project HEED will utilise a combination of free-flow and semi-structured interview techniques during the face-to-face interviews allowing participants to relate their experiences in their own words while maximising the information elicited.

Analysis of the type presented in this paper are providing us with insight into both building and occupant performance under extreme conditions. It is hoped that calculations of this type will assist in building safer buildings, and develop procedures for existing buildings that will assist in maximising chances of survival in extreme events. **«**

References

1. E.R. Galea and S. Blake: *Collection and Analysis of Human Behaviour Data Appearing in the Mass Media Relating to the Evacuation of the World Trade Centre Towers of 11 September 2001*, Report prepared for the Building Disaster Assessment Group (BDAG) of the Office of the Deputy Prime Minister, London; ISBN 1 85112 765 8, Reference number 04LGFG02767(6), December 2004 (2004).
2. E.R. Galea and A.J.P. Dixon: *Collection and Analysis of Emergency Services Data Relating to the Evacuation of the World Trade Centre Towers of 11 September 2001*, Report prepared for the Building Disaster Assessment Group (BDAG) of the Office of the Deputy Prime Minister, London; ISBN 1 85112 766 6, Reference no. 04LGFG02767(7), December 2004 (2004).

3.   http://www.odpm.gov.uk/stellent/groups/odpm_fire/documents/page/odpm_fire_029625.hcsp

4.   S. Blake, E.R. Galea, H. Westeng, and A.J.P. Dixon: *An Analysis of Human Behaviour during the WTC Disaster of 11 September 2001 Based on Published Survivor Accounts*, In: Proceedings of the 3rd International Symposium on Human Behaviour in Fire, 1-3 September 2004, Belfast, UK, pp. 181-192 (2004).

5.   E.R. Galea, P.J. Lawrence, S. Blake, S. Gwynne, and H.Westeng: *A Preliminary Investigation of the Evacuation of the WTC North Tower using Computer Simulation*, In: Proceedings of the 3rd International Symposium on Human Behaviour in Fire, 1-3 September 2004, Belfast, UK, pp. 167-180 (2004).

6.   http://www.wtc-evacuation.com.

7.   D. Cauchon: Not found or not existing, 40 names to leave WTC death toll, USA Today 29/10/03 (2003).

8.   National Institute of Standards and Technology, Special Publication 1000-5, June 2004, CODEN: NSPUE2 (2004).

9.   D. Cauchon, *For Many on Sept 11, Survival Was no Accident*, USA Today 19/12/01 (2001).

10. S. Gwynne, E.R. Galea, P. Lawrence, and L. Filippidis: *Modelling Occupant Interaction with Fire Conditions using the buildingEXODUS Evacuation Model,* Fire Safety Journal 36, pp. 327-357 (2001).

Dynamic Navigation Field –
a local and on-demand family of algorithms for wayfinding

M. Gilman[1], H. Moldovan[1], and M. Tencer[1]

Simulation of pedestrian navigation in dynamic and complex real environments is a critic and hard problem. In this paper we will introduce a family of case-based reasoning algorithms for wayfinding called Dynamic Navigation Field or DNF that transforms global information into local knowledge according to the requirements of the surrounding environment. In DNF the case memory is composed by a set of navigation fields generated locally and on-demand with efficient storing and retrieval performance.

1.   Introduction

One of the most critic tasks involved in the pedestrian traffic simulation is the navigation in highly dynamic and geometrically complex real environments. In the heart of this task we find the wayfinding or path planning problem which takes two locations and finds a path connecting them.

Generation of "pedestrian-like" trajectories in transfer centers, large buildings and stadiums is a complex task and imposes restrictions on the set of trajectories to be generated. For a given path some directions are more likely to be followed than others by pedestrians. As an example we can mention the directions in large corridors where they are mostly parallel to walls.

Several and different approaches have been applied to solve this problem. The traditional AI approach is to use a goal-directed search heuristic in the solutions space of the navigation area. Unfortunately, this approach is not well suited for most of the real cases where pedestrian simulation is required due to the frequent environmental changes in these situations.

In the past, we combined the well-known A* algorithm with a mechanism for generating directions. When recalculation of paths and directions was frequently needed, the overall performance of the simulations was strongly degraded.

Case-based reasoning methods [1] offer an alternative approach where previously found solutions can be reused for solving new problems. Multistrategy Adaptive Path Planning [2] is an example of this approach where a hierarchical spatial model is used for generating paths for a given plan. Found paths are stored in the case memory, thus new plans can then be solved by retrieving and adapting previously stored paths.

By means of the case memory, knowledge can be shared by different agents. Sharing information or knowledge is a very interesting and promising approach to reduce the algorithmic complexity in path planning problems. An important drawback of these methods is that storing, retrieval and adaptation could be very time consuming and rapidly become into a bottleneck of the global performance of the system.

[1]Urbix, (CI) FADU – University of Buenos Aires – www.urbix.com.ar
Subsuelo Pabellón III. Ciudad Universitaria. – (1428) Buenos Aires – Argentina

2.   Deliberation and Reactivity

Simulation of pedestrian navigation is a complex task that requires the integration of multiple approaches. We found the field of Behavior-Based Robotics (see [3] for a review of the field) to be a good source of inspiration. Both fields share some problems such as wayfinding or path planning in complex real environments.

According to R. C. Arkin, a deliberative system "is best suited for integrating world knowledge and user intent to arrive at a plan prior to its execution"; on the other hand, a reactive system "is well suited to deal with the immediacy of sensory data". In general, we can consider deliberative systems for heavy planning tasks and reactive systems for fast executions.

At Urbix we have developed a behavior-based mechanism for solving the navigation problem. Inspired in AuRA [4], we developed a layered architecture for navigation. On top of this architecture there is a deliberative planner that generates plans which are then executed by the bottom reactive layer. Thus, we generate high quality plans executed by an efficient and flexible mechanism.

3.   The DNF Family of Algorithms

The Dynamic Navigation Field or DNF is a family of case-based reasoning algorithms for wayfinding that uses global knowledge to find local solutions.

We will start introducing some definitions and notation to properly define DNF. For simplicity we will consider a 2D navigation space and we will use the term "agent" to generalize the term "pedestrian" when possible.

We define a cell as a tuple $\langle p, r \rangle$ where $p \in \mathfrak{R}^2$ is the cell's position and $r \in \mathfrak{R}$ is the cell's radius. For any cell c we will use c_p and c_r to denote each component. The influence area of a cell c is the area inside the circle defined by $c : c_{\inf} = \{x \in \mathfrak{R}^2 : |x - c_p| \leq c_r\}$. Any point $q \in c_{\inf}$ is said to be covered by c.

Most of urban real environments such as transfer centers or large buildings have a set of boundaries (such as walls). Given a set of boundaries B, two points p and q are said to be visible in B or $p \leftrightarrow_B q$ if there is no boundary intersecting the line segment determined by p and q. Given a point q, a set of cells C, a set of boundaries B and $k \in N$, we define the influence set of q as the nearest k cells of C visible in B. Assuming that cells and boundaries are implicitly known, for simplification purposes the influence set will be denoted by q^k. If $k=1$ the influence set is composed by a unique cell (if such a cell exists) called the star cell and denoted by $q*$.

We define a navigation field or NF as a tuple $\langle trg, C, B, D, \Phi, \Omega \rangle$ where trg is a target cell, C is a set of source cells, B is a set of boundaries, D is a set of directions, Φ a function that assigns a direction of D to each cell of C and Ω a function that assigns a weight to each direction of D. For each direction vector d, we will use the following notation: $d_c = \Phi^{-1}(d), d_p = \Phi^{-1}(d)_p$ and $d_w = \Omega(d)$.

As every case-based reasoning algorithm, DNF manages keys, cases and the case memory. In DNF a key is a cell, a case is a set of directions from a source point to a target point
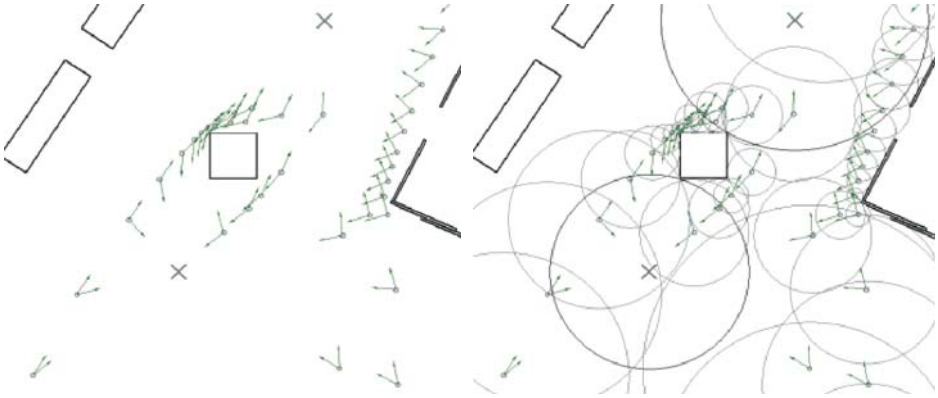
Figure 1: Two Navigation Fields for a particular environment. Target cells are shown with crosses, source cells with circles and boundaries with lines. Cells are shown with (right) and without (left) radiuses. More cells were generated near the boundaries to provide more accurate information in those areas.

and the case memory is composed by a set of navigation fields generated locally and on-demand with efficient storing and retrieval performance. This is probably the most interesting property of this family of algorithms. By contrast to other approaches based on the generation of fields, DNF produces vector fields dynamically and on-demand. No superfluous or useless information is generated in advanced. This is a very important issue considering that in many real cases of pedestrian dynamics, most of the generated trajectories are similar, leading to a sparse use of the navigation space. Moreover, DNF can manage different levels of "knowledge granularity": the more knowledge is needed the more knowledge is produced.

Figure 1 shows two NFs for two different target cells (crosses). For each source cell (circles) one direction for each NF is shown. It can be appreciated that near boundaries more cells are generated as more accurate knowledge is required in those areas.

As part of the reactive layer of our pedestrian navigation architecture, we implemented a microscopic algorithm that considers pedestrian flow as made of discrete self-driven particles. The model uses molecular dynamics concepts and takes into account forces (contact, desired and social) as described by Dirk Helbing [5, 6].

DNF was conceived as the mechanism responsible for finding the direction of the desired force. It can be decomposed into three different layers: bottom, middle and upper layers.

Bottom layer manages global knowledge. A graph representing the navigation area is used for this purpose. This layer is responsible for global searches in the graph and most of the heavy work such as pathfinding and visibility checks.

```
getDirection(Point src, Point trg): Direction
Parameters:
        int k: size of influence set

1)      Set<Cell> src_Inf ← influenceSet(src, k);
2)      if (src_Inf=Ø) {
3)         Cell src* ← generateCell(src);
4)         src_Inf ← {src*};
5)         storeCell(src_Inf);
6)      }
7)      Cell trg*;
8)      Set<Cell> trg_Inf ← influenceSet(trg, 1);
9)      if (trg_Inf=Ø) {
10)        trg* ← generateCell(src);
11)        trg_Inf ← {trg*};
12)        storeCell(trg_Inf);
13)     } else {
14)        trg* ← trg_Inf.first();
15)     }
16)     Set<Direction> case ← Ø;
17)     for each (Cell s in src_Inf) {
18)        Direction sdir ← getDirection(s, trg*);
19)        if (sdir=null) {
20)                sdir ← generateDirection(s, trg*);
21)                storeDir(s, trg*, sdir);
22)        }
23)        case ← case ∪ sdir;
24)     }
25)     Set<Direction> adaptedCase ← adaptDirections(src*, trg*, case);
26)     return selectDirection(adaptedCase);
```

Figure 2: getDirection method of a DNF algorithm.

Middle layer is responsible for managing local knowledge generated on top of the bottom layer. Navigation fields are generated and stored in this layer. The core of the middle layer is composed by the getDirection method shown in Figure 2 which is responsible for connecting all layers. It receives a source and a target point as inputs and returns the direction to be followed from the source in order to reach the target. The particular implementations of the sub-methods used in this method determine each DNF algorithm.
Lines 1-6 of Figure 2 generate cells for the source point by building the influence set of size k. If there is no cell, a cell is generated and stored for future reuse. Lines 7-15 generate a cell for the target point by retrieving or by generating and storing the star cell of the point. Lines 16-24 retrieve all the cases for the current cells. All the directions for all pair of source and target cells are retrieved or generated and stored. Line 25 adapts the cases and finally line 26 selects one adapted case and returns it.
The middle layer uses a double hierarchical index mechanism: cases are indexed by

source and target cells which are themselves indexed by position. This makes storage and retrieval of cases very efficient.

Finally, the upper layer is the user layer. How to use a DNF algorithm for navigation? The main loop of a navigation mechanism should periodically call the getDirection method for each agent with the current and target position as inputs. Different strategies can be applied to decide the proper instance for this call. Then each agent should adjust its current direction to the new obtained direction.

In this paper we will focus on the middle and bottom layers. We will now introduce some decisions or criterions we adopted for the implementation of a particular DNF algorithm.

3.1. Key Generation, Storage and Retrieval

As we already mentioned, a double hierarchical index mechanism is used: cases are indexed by source and target cells which are themselves indexed by position. In order to optimize cells storage and retrieval a neighborhood based on an R-tree spatial index (see [7] for a description) is used. Cells are stored in the neighborhood by their position.

For a point q, the influence set q^k can be obtained by first retrieving the m nearest cells of q, with $m \geq k$. The cells not covering q are filtered out and among the remaining cells the (at most) k nearest visible are returned.

The upper bound m was introduced to reduce the search space. For a position near to a boundary, nearest cells are typically located at all sides of the boundary and therefore not visible from the position. If there were a big number of cells in this situation and we did not use an upper bound, we would be exploring a big number of cells before arriving to the conclusion that none of them is visible. A side effect of this mechanism is that when the number of explored cells m decreases, the probability of getting an empty influence set is increased and therefore the number of generated cells is also increased.

Checking the visibility condition is a very time consuming operation. Getting the influence set is a frequent operation and therefore a mechanism for avoiding checking the visibility has been introduced. The following invariant called the boundary free or BF invariant must be satisfied: for every cell c there is no boundary inside or intersecting c_{inf}. On the right side of Figure 1 it can be appreciated how cells preserve the BF invariant.

If BF is preserved, q^k can now be calculated with the following simple algorithm: get the m nearest cells to q $(m \geq k)$ and return the (at most) k nearest cells covering q. Demonstrating that this and the algorithm introduced before in this section are equivalent is straight forward under the assumption that BF is satisfied: suppose that a cell c is returned by this algorithm but not $(q \leftrightarrow_b c_p)$, then there must be a boundary b between q and c and therefore $\text{dist}(b,c_p) \leq \text{dist}(q,c_p)$. Given that c covers q, $\text{dist}(q,c_p) \leq c_r$ and therefore $\text{dist}(b,c_p) \leq c_r$ which is a clear contradiction with the BF assumption.

In order to satisfy BF, a cell's radius must be at most the minimum distance from the cell to any existing boundary. We use an upper bound for radiuses. This decision not only contributes to improve cells generation performance, but mainly to increase the relevance of the retrieved cases. If the cell's radius is unbounded, the influence set of a

position could contain very far cells. Although during the adaptation phase the impact of these cells could be diminished, they constitute a source of noise.

Figure 3 shows an example where a set of cells A, B, C and D are stored in the neighborhood represented by the grid. No cell covers a boundary because radiuses are calculated to satisfy the *BF* invariant.
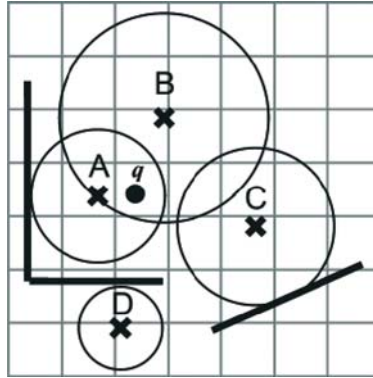

Figure 3: Cells A, B, C and D are stored in a neighborhood (represented by the grid). Cells' radiuses are calculated to satisfy the boundary free invariant. The influence set of size 2 of *q* is {A, B}.

3.2. Case Generation, Storage and Retrieval

Although the case memory conceptually was defined as a set of navigation fields, storage and retrieval of directions can be easily implemented by using a double key map, where the first key is a source cell and the second a target cell.

Given a set of source cells and a target cell, a case is built by retrieving a direction for each pair of source and target. In this paper we will introduce a method for generating directions which does not pretend to mimic humans' mechanisms for wayfinding but which has shown to reproduce macroscopic behavior satisfactorily.

As in [2] we use a graph representing the spatial model of the navigation area. Nodes are points representing different areas and links are valid connections between them. Links do not only provide structural information but also geometric information: a link cannot intersect a boundary. This is a sort of *BF* invariant for the graph. Links also have associated weights which can represent any measurable information: from the simple length of the link to additional domain information such as luminosity or density. In our particular algorithm we have simply used the Euclidean distance for the weighting function Ω.

Given a set of boundaries B, a node n and a path P we define the furthest visible point of n in P denoted by $fvp_{n,P}$ as the furthest point from n in P visible in B. The "furthest point"

is defined by the distance function determined by the following procedure: stretch out the path P and take the Euclidean distance from n to $fvp_{n,P}$.

Given a source cell src and a target cell trg a direction from the former to the latter is generated in the following way: let n_{src} and n_{trg} be the nearest visible nodes of the graph to src_p and trg_p respectively. Let P be the shortest path in the graph connecting n_{src} and n_{trg}. Find the $fvp_{src,P}$ and build the new direction as $(fvp_{src,P} - src_p) / |fvp_{src,P} - src_p|$.

Similar mechanisms to those applied for the cells are used here: a neighborhood with an underlying R-tree is used for indexing the nodes and the nearest visible node is selected among the m nearest nodes, with $m \geq 1$. If there is no path connecting both nodes or there is no nearest visible node from the source, a direction can not be generated.

The A* algorithm is used to find shortest paths in the graph. The weight of the new direction is generated by constructing the artificial path $P' = (src_p, fvp_{src,P}, ..., n_{trg}, trg_p)$ and then taking $\Omega(P')$, with $(fvp_{src,P}, ..., n_{trg})$ the subpath of P. Figure 4 shows an example of this procedure.
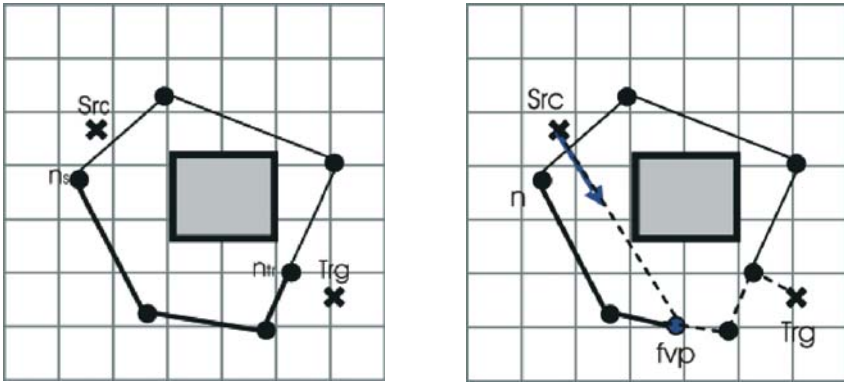
Figure 4: A graph is used to represent the navigation area. A direction must be generated to reach trg from src. On the left side the darkest path was selected to build the new direction. On the right side, the new direction in blue was built with the fvp_{src} and by constructing the artificial dashed path.

3.3. Case Adaptation

Let us consider the situation depicted in Figure 5. In order to reach p from q, we first find $q^k = \{A, B\}$. Both cells A and B offer to q a partial solution to the wayfinding problem. A final solution can be obtained by properly adapting the knowledge of both cells. We could be tempted to apply a weighted mean of the directions of the case but this mechanism could fail in many situations. Simple averaging of directions could led and agent to collide with a boundary.

The problem arises from the interpolation of directions belonging to different paths.

Figure 5: In order to reach p from q a new direction (the dashed direction) is built on the basis of the directions of the influence set {A, B}

To avoid this problem, we first classify the directions by using a bucket elimination algorithm (see [8] for details) using a distance function for classification. Each bucket is associated to a path from the source to the target. As this process belongs to the middle layer, we cannot make use of any global knowledge from the bottom layer. Therefore, the distance function between directions should not use information coming from the graph. We used the scalar product as distance function and a threshold to measure similarity.

Once the classification is concluded, all directions of the same bucket are collapsed. The resultant direction for the i-th bucket $\overset{\mu}{\vec{d}}_i$ is given by:

$$\overset{\rho}{d}_i = \frac{\sum\limits_{d \in Bucket_i} w_d.d}{\sum\limits_{d \in Bucket_i} w_d^2}$$

with $w_d = e^{\frac{(d_p - q)^2}{\sigma^2}}$, meanwhile the weight of the direction is given by:

$$\overset{\rho}{d}_{iw} = \frac{\sum\limits_{d \in Bucket_i} w_d.d_w}{\sum\limits_{d \in Bucket_i} w_d^2}$$

Therefore, each bucket is adapted by weighting each direction according to the distance to the source point q and the parameter σ. The closer is q to a cell, the stronger its contribution.

3.4. Case Selection

Once the case is adapted, selecting one direction is an easy procedure. Only one direction must be selected among the directions of the case. We randomly select one direction with the distribution given by the weights. The probability of selecting direction d_i is $d_{i_w} / \sum_j (d_{j_w})^2$.

4.   Results

In this section we will present some results we obtained for the DNF algorithm described before. The simulations and the shown results were generated with Smartcrowd; a pedestrian simulation software developed by Urbix.

The problem was taken from a football stadium simulation (see [12] for details) and simplified for this work. In our case, two opposite pedestrian flows are simulated: one southward (S) and the other northward (N). In order to isolate the influence of DNF over the simulations' performance we decided to use low flow rates (about 20 ped/min.) and the desired velocities were generated with a normal distribution with mean 1.35 and a standard deviation of 0.3 m/s. The upper bound for cells' radiuses was fixed at 4 meters and the σ^2 used for the resultant direction was set to 0.5. For the influence set we used an upper bound $m=10$.

Figure 6 shows the evolution of a simulation for an influence set of size $k=1$. In the upper row we can observe pedestrians' trajectories meanwhile in the lower row the genera-

| 30 sec | 90 sec | 180 sec |
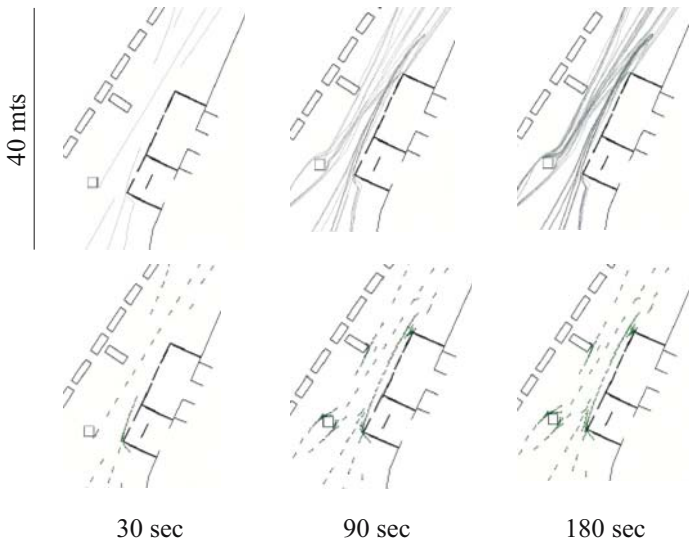
Figure 6: Evolution of a simulation for $k=1$. Trajectories (upper row) and navigation fields (lower row) are shown for different simulation times.

k=3   k=5
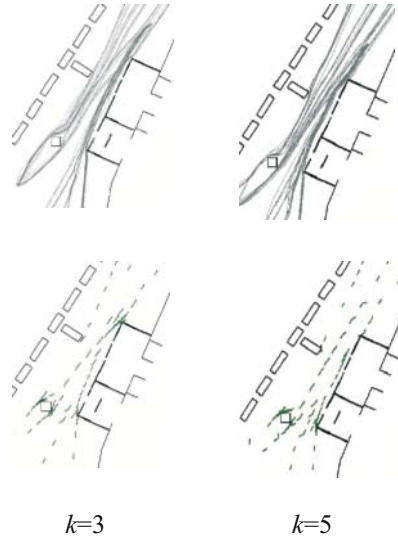
Figure 7: Trajectories (upper row) and navigation fields (lower row) for different k=3 and k=5 at simulation time 180 sec.

ted navigation fields. Figure 7 shows the same results for $k=3$ and $k=5$ at simulation time 180 sec. It can be easily appreciated that the three algorithms generate similar solutions. The generated trajectories and cells distributions are qualitatively similar.

For a quantitative comparison we have measured the transit time (time taken by a pedestrian to reach the target from the source) for the different algorithms and flows of the simulation. Table 1 resumes the results and as can be observed means and deviations are very similar.

Flow	k=1	k=3	k=5
S	(42.25, 10.26)	(43.61, 11.27)	(43.05, 11.18)
N	(41.42, 10.50)	(42.16, 10.57)	(41.41, 10.81)

Table 1: Mean and standard deviation of the transit time for the different algorithms and flows.

For further comparison, we compared the density maps for the different simulations. Densities were calculated by averaging the number of pedestrians along each simulation in a 1m×1m grid. Densities were then normalized and the difference map was built by subtracting cell by cell. Figure 8 shows the difference between the density maps of $k=5$ and $k=1$. Most of the differences are negligible. Minor differences observed in the upper right corner shows small changes in the generated trajectories. Differenced of the same magnitude are observe when comparing simulations produced by the same algorithm
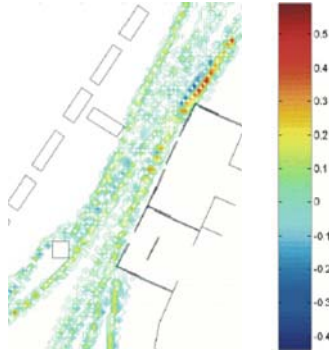
Figure 8: Difference of density maps for $k=5$ and $k=1$. Color bar indicates percentual diffe-
rences in ped/m/sec.
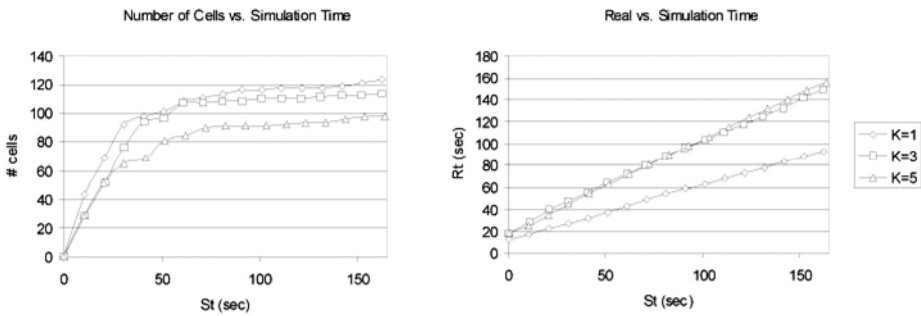
Figure 9: Comparing performance. On the left side number of cells along the simulations and on
the right side real vs. simulation time

due to the expected noise. These results strongly support our claim that all algorithms
are macroscopically undistinguishable.

We will now compare the obtained performances. On the left side of Figure 9 we can
observe the number of generated cells along each simulation. As we already mentioned,
for smaller k we get a greater number of cells. It is interesting to notice that in all simu-
lations, 80 percent of the cells is generated during the first 50 seconds. This means that
after generating a critical number of cases, the algorithms can reuse most of the cases or
knowledge previously generated. As we stated before, this is a very important property
considering that in many real cases of pedestrian dynamics, most of the generated tra-
jectories are similar.

By comparing the real vs. simulation time, on the right side of Figure 9 we observe
that $k=1$ outperforms the other algorithms. We detected that the main reason for the
performance gain of $k=1$ comes from the lack of cases adaptation of this algorithm.
Meanwhile $k=3$ and $k=5$ behave similarly. In this case we noticed that, despite of the

fact that different values of k were used, the mean size of the influence set was 1.38 for $k=3$ and 1.46 for $k=5$. This is possible because the influence set has at most k cells but the actual number depends on the surrounding conditions. Therefore, after retrieving the influence set, both algorithms had similar work. Once again this is evidencing that the adaptation of cases in case-based reasoning algorithms is a hard task and one of the bottlenecks of such systems.

In general, DNF has shown to behave macroscopically well. Nevertheless, we have detected some unusual situations where DNF does not provide a proper microscopic solution. For instance, near corners and depending on the cells distribution, some agents could be lead to the walls. A different problem is caused by the dependency of DNF on the initial flow: as cells are generated with the first agent in the area, this agent determines the knowledge to be used by other agents.

Nevertheless, these problems have relative impact on the overall macroscopic performance of the simulation. As we already mentioned, DNF is part of the reactive layer of our navigation mechanism and is used to determine the direction of the desired force. Other mechanisms, such as local collision avoidance, are complemented with DNF to obtain a pedestrian like emergent behavior. Therefore, the aforementioned problems are smoothed or attenuated.

5.   Conclusions

In this work we have described a family of case-based algorithms for wayfinding called DNF. Its main contribution is the introduction of a method for the dynamic generation of navigation fields. Different layers work together to transforms global information into local knowledge that fits the requirements of the surrounding environment. Thus, no resources are misused in the generation of useless or superfluous knowledge. Adaptation of cases does not constitute a bottleneck in DNF. Moreover, we have shown that using pure local knowledge without adaptation is macroscopically as good as using more global knowledge but with a direct performance gain for our simulation capabilities. **«**

References

1.   J. Kolodner: *Case-Based Reasoning*, Morgan Kaufmann (1993).
2.   A.K. Goel et al.: *Multistrategy Adaptive Path Planning*, IEEE Expert: Intelligent Systems and Their Applications 9, pp. 57-65 (1994).
3.   R.C. Arkin: *Behavior-Based Robotics*, The MIT Press (1998).
4.   R.C. Arkin and T. Balch: *AuRA: Principles and Practice in Review*, In: Journal of Experimental & Theoretical Artificial Intelligence 9, pp. 175-189 (1997).
5.   D. Helbing and P. Molnár: *Social Force Model for Pedestrian Dynamics*, In: Physical Review 51, pp. 4282-4286 (1995).
6.   D. Helbing, I. Farkas, and T. Vicsek: *Simulating Dynamical Features of Escape Panic*, In: Nature 407, pp. 487-490 (2000).

7. A. Guttman: *A Dynamic Index Structure for Spatial Searching*, Proceedings 1984 ACM-SIGMOD Conference on Management of Data, pp.47-57 (1985).
8. R. Dechter: *Bucket Elimination: A Unifying Framework for Reasoning*, In: Artificial Intelligence 113, pp. 41-85 (1999).
9. H. Moldovan, M. Gilman, P. Knoblauch and S. Woloj: *Football Stadium Simulation*, in these Proceedings (2006).

Microscopic calibration and validation of pedestrian models – Cross-comparison of models using experimental data

S.P. Hoogendoorn[1], W. Daamen[1], and R. Landman[1]

Calibration of microscopic simulation models is complex due to amongst other things the large number of model parameters, and the lack of suitable data. Rather than a qualitative test to determine whether model predictions are plausible on an aggregate (macroscopic) level, this contribution focuses on statistical calibration of model parameter from individual pedestrian trajectory data. To this end, a new generic approach is presented enables parameter estimation for microscopic models in general and in particular for walker models. The application results provide new insight into the behavior of individual pedestrians, the inter-pedestrian differences, as well as the resulting pedestrian flow characteristics. By comparing different models of increasing complexity, it is investigated which of the model amendments are significant from a statistical point of view and which are not. It is shown that besides anisotropy, finite reaction times play an important role in correctly describing microscopic walking behavior.

1.   Introduction

Estimating the parameters of microscopic pedestrian models is a complex task. This is in part caused by the relative large number of parameters (which can often not be observed directly), the lack of suitable data, as well as the lack of suitable calibration techniques.

In most cases, calibration of microscopic pedestrian models is performed by comparing aggregate model outcomes (flows, speeds, densities, etc.), predicted macroscopic relations (e.g. speed density curves), or emerging spatio-temporal patterns (dynamic lane formation) with macroscopic empirical data (if available) or expert opinion (does the model act as expected). In doing so, it has been shown that a number of pedestrian flow models are able to predict macroscopic flow conditions with reasonable accuracy.

There are many reasons why such a coarse approach to model calibration will not yield the desired results. For example, inter-pedestrian differences expressed by the variability in model parameters cannot be determined using macroscopic data. Furthermore, it is unclear if microscopic models are able to describe individual walking behavior accurately, or if they mainly provide a reasonable 'average' macroscopic prediction. This being the case, there is no way to assess whether the behavioral assumptions underlying a microscopic model are valid or not. If the underlying assumptions are not valid, it is doubtful whether the microscopic model is sufficiently generic and able to predict pedestrian behavior in other situations than the model was calibrated for.

---

[1]Transport & Planning Department, Delft University of Technology

This contribution focuses on the calibration of microscopic models using pedestrian trajectory data. A continuous time microscopic walker model is used and generalized to include different aspects of walking that are deemed important. It is emphasized that this is not a benchmarking study in the sense that all microscopic pedestrian models are cross-compared. We also do not consider route choice behavior.

In particular, we focus on the microscopic walker model NOMAD [1], which is similar to the well-known social-forces model [2]. We determine which of the model parameters are important in prediction microscopic pedestrian behavior, as well as considering their statistical properties. In doing so, we will study two potentially important aspects of walking behavior, namely anisotropy and finite reaction times. Lastly, since we establish model parameters for individual pedestrians, we will show inter-pedestrian differences in walking behavior.

2.   Considered walking models

In this contribution, we focus on a simplified version of the NOMAD model [1], which is similar to the original social-forces model [2]. This section presents the basic model and the amendments that are considered for further analysis. It is noted that many extensions to both the NOMAD model and the social-forces model have been proposed. For the purpose of this paper, it is however not necessary to consider these. The approach can however be directly applied to other models as well.

2.1. Basic model

The basic model predicts the two-dimensional acceleration vector $\vec{a}_p(t)$ as a function of the free velocity $\vec{v}_p^0$, the current speed $\vec{v}_p(t)$, and distance $d_{pq}(t)$ between pedestrians p and q as follows:

$$\vec{a}_p(t) = \vec{f}_p(\vec{v}_p(t), \vec{r}_p - \vec{r}_q, ...) = \frac{\vec{v}_p^0 - \vec{v}_p(t)}{T_p} - A_p \sum_{q \in Q_p} \vec{u}_{pq}(t) e^{-\frac{d_{pq}(t)}{R_p}}$$

(1)

where Q_p denotes the set of pedestrians that influence pedestrian p, and where

$$d_{pq}(t) = \| \vec{r}_q(t) - \vec{r}_p(t) \| \quad \text{and} \quad \vec{u}_{pq}(t) = \frac{\vec{r}_q(t) - \vec{r}_p(t)}{d_{pq}(t)}$$

(2)

The basic model has four pedestrian specific parameters, namely the free speed $V_p^0 = \| \vec{v}_p^0 \|$, the acceleration time T_p, the interaction constant A_p and the interaction distance R_p that are to be estimated from data. Note that the desired walking direction $e_p^0 = \vec{v}_p^0 / V_p^0$ determined by pedestrian route choice and is assumed known.

2.2. Instantaneous model including anisotropy

Anisotropy implies that pedestrians will only – or at least mainly – react to pedestrians in front of them. NOMAD has been amended to include anisotropy as follows [1]:

$$\vec{a}_p(t) = \frac{\vec{v}_p^0 - \vec{v}_p(t)}{T_p} - A_p \sum_{q \in Q_p} \vec{u}_{pq}(t) e^{-\frac{d_{pq}^*(t)}{R_p}} 1_{\vec{u}_{pq}(t) \cdot \vec{v}_p(t) > 0} \tag{3}$$

with

$$d_{pq}^*(t) = \frac{\vec{u}_{pq}(t) \cdot \vec{v}_p(t)}{\| \vec{v}_p(t) \|} + \eta_p \frac{\vec{w}_{pq}(t) \cdot \vec{v}_p(t)}{\| \vec{v}_p(t) \|} \tag{4}$$

Here, $\eta_p > 1$ is a pedestrian specific factor that describes differences in pedestrian reaction to stimuli directly in front and stimuli from the sides of the pedestrians, which is to be estimated from the available microscopic data. The indicator function $1_{\vec{u}_{pq} \cdot \vec{v}_p > 0}$ is one if pedestrian q is in front ($\vec{u}_{pq} \cdot \vec{v}_p > 0$) if p and zero otherwise ($\vec{u}_{pq} \cdot \vec{v}_p \le 0$). This implies full anisotropy in the sense that a pedestrian does not take notice of any pedestrians behind him or her.

2.3. Model including finite reaction time

Unlike most car-following models, walker models do generally not include a finite reaction time. To determine if the reaction time can be neglected or not, we consider the following retarded or delayed model:

$$\vec{a}_p(t + \tau_p) = \frac{\vec{v}_p^0 - \vec{v}_p(t)}{T_p} - A_p \sum_{q \in Q_p} \vec{u}_{pq}(t) e^{-\frac{d_{pq}^*(t)}{R_p}} 1_{\vec{u}_{pq}(t) \cdot \vec{v}_p(t) > 0} \tag{5}$$

where $\tau_p > 0$ is the pedestrian-specific reaction time (or rather, the perception-response time) to be estimated from the microscopic data. In this model, pedestrians are assumed to have a delayed response to the observations they make at time instant t. We expect that the reaction times will be between 0.1 s and 0.8 s.

3. Approach to model estimation

This section discusses estimation of the unknown parameters for general continuous-time microscopic pedestrian models. The approach will be applied in the subsequent sections to estimate parameters for individual pedestrians. Besides cross-comparison of model performance, the parameter estimates provide new insights into walking behavior and inter-pedestrian differences in this behavior.

The parameters to be estimated are the free speed V_p^0, the acceleration time T_p, the interaction factor A_p, and the interaction distance R_p. The reaction time τ_p is determined by considering all plausible reaction time values – i.e. between 0.1 s and 0.8 s – and afterwards determining which value yields the best performance. For the anisotropy factor η_p, different values have been considered and cross-compared to test which yields good model performance, after which one fixed value was chosen.

The available observations are trajectories (the location $\vec{r}_p$ as a function of time instant t_k, for $k = 1,\dots,n$; see Fig. 1) of all pedestrians p. From these data, all relevant quantities can be derived either directly or by applying finite differences, such as velocities $\vec{v}_p(t_k)$, accelerations $\vec{a}_p(t_k)$, distances between pedestrians, etc. For the data considered in the remainder, observations are present each 0.1 s (i.e. $t_k = 0.1k$).

3.1. Maximum likelihood estimation

Most continuous time microscopic walker models, including those considered in this contribution can be expressed in the following form:

$$\vec{a}_p(t + \tau_p) = \vec{f}_p(\vec{v}_p(t), \vec{r}_p(t) - \vec{r}_q(t),\dots \,|\, \theta_p) + \vec{\varepsilon}_p \tag{6}$$

The error vector $\vec{\varepsilon}_p$ is introduced to reflect errors in the modeling, similar to the error term used in multivariate linear regression. Note that the error vectors $\vec{\varepsilon}_p$ are generally serially correlated (i.e. $\vec{\varepsilon}_p(t)$ and $\vec{\varepsilon}_p(t-1)$ have a large positive correlation). For now, we assume that the error term is normally distributed with mean zero and standard deviation σ_p (pedestrian specific).

Since we can determine all relevant variables (positions, distances, speeds, relative speeds) directly from available experimental data, we can use Eq. (6) to determine a prediction for the retarded acceleration directly from the data. The prediction $\vec{a}_p(t_k + \tau_p \,|\, \theta_p)$ is clearly dependent on the model parameters θ_p to be estimated and can be compared with the observed acceleration $\vec{a}_p^{obs}(t_k + \tau_p)$. According to the model, the difference between the prediction and the observation follows the normal distribution with mean 0 and standard deviation σ_p.

The likelihood L_k of a single prediction step, say from time t_k to time t_{k+1}, is related directly to the probability density $g(\varepsilon)$ of the normal distribution. More specifically:

$$L_k(\theta_p, \sigma_p) = \frac{1}{\sigma_p \sqrt{2\pi}} e^{-\frac{\left(\vec{a}_p^{obs}(t_k + \tau_p) - \vec{a}_p(t_k + \tau_p)\right)^2}{2\sigma_p^2}} \quad \text{subject to}$$

$$\vec{a}_p(t_k + \tau_p \mid \theta_p) = \vec{f}_p(\vec{v}_p^{obs}(t), \vec{r}_p^{obs}(t) - \vec{r}_p^{obs}(t), \ldots \mid \theta_p) \tag{7}$$

Considering an entire sample of subsequent acceleration observations and neglecting correlation between subsequent samples (serial correlation), the likelihood of the observation given the model parameters becomes:

$$L = L(\theta_p, \sigma_p) = \prod_{k=1}^{n} \frac{1}{\sigma_p \sqrt{2\pi}} e^{-\frac{\left(\vec{a}_p^{obs}(t_k + \tau_p) - \vec{a}_p(t_k + \tau_p \mid \theta_p)\right)^2}{2\sigma_p^2}} \tag{8}$$

where n denotes the number of time-instants t_k for which an observation is available. Implying that the log-likelihood equals:

$$\tilde{L}(\theta_p, \sigma_p) = -\frac{n}{2}\ln\left(2\pi\sigma_p^2\right) - \frac{1}{2\sigma_p^2}\sum_{k=1}^{n}\left(\vec{a}_p^{obs}(t_k + \tau_p) - \vec{a}_p(t_k + \tau_p \mid \theta_p)\right)^2 \tag{9}$$

Maximum-Likelihood estimation involves finding the parameters that maximize the (log-) likelihood. A necessary condition for the optimum allows determination of the standard deviation:

$$\frac{\partial \tilde{L}}{\partial \sigma_p^2} = 0 \quad \Rightarrow \quad \hat{\sigma}_p^2 = \frac{1}{n}\sum_{k=1}^{n}\left(\vec{a}_p^{obs}(t_k + \tau) - \vec{a}_p(t_k + \tau_p \mid \theta_p)\right)^2 \tag{10}$$

From Eq. (10) we see that the ML estimate for the variance of the error term is given by the MSE of the predictions and the observations. For the remaining parameters, the ML estimates can be determined by numerical optimization, i.e.

$$\hat{\theta}_p = \arg\max \tilde{L}(\theta_p, \hat{\sigma}_p) \tag{11}$$

with

$$\tilde{L}(\theta_p, \hat{\sigma}_p) = -\frac{n}{2}\ln\left(\frac{2\pi}{n}\sum_{k=1}^{n}\left(\vec{a}_p^{obs}(t_k + \tau) - \vec{a}_p(t_k + \tau_p \mid \theta_p)\right)^2\right) - \frac{n}{2} \tag{12}$$

This expression shows that maximization of the log-likelihood is equivalent to minimization of the mean squared error (MSE).

3.2. Covariance estimates

To approximate the covariance matrix of the estimated parameters, we can use the so-called Cramér-Rao lower bound (Casella and Berger,1990), stating that:

$$\text{var}(\hat{\theta}_p) \geq -E(\nabla^2 \tilde{L})$$

(13)

Since ML is asymptotically efficient, we can show that the asymptotic variance of the parameters is given by the right-hand side of Eq. (13); see [4]. In the remainder, this approximation is used to determine an estimate for the covariance of the estimates.

The Cramér-Rao bound provides important insights into the statistical properties of the models by providing estimates for the model standard error and the statistical correlation between the parameter estimates. The standard-errors can be used to determine whether the model parameters are not equal to zero in a statistical sense. The correlation matrix provides additional insight into the statistical properties of the estimates, for instance by explaining large standard errors cause by large correlation between estimates.

In the remainder, we will use the so-called likelihood-ratio test to test whether the one model is better than the other. To this end, we will use the zero-acceleration model as a reference model, i.e. $\vec{a}_p(t) = \vec{\varepsilon}_p$. For this model we can determine the (null) log-likelihood:

$$\tilde{L}_0 = -\frac{n}{2}\ln\left(\frac{2\pi}{n}\sum_{k=1}^{n}\vec{a}_p^{obs}(t_k)^2\right) - \frac{n}{2}$$

(14)

The likelihood-ratio (LR) test involves testing the statistic:

$$2(\tilde{L}(\hat{\theta}_p,\hat{\sigma}_p) - \tilde{L}_0)$$

(15)

which follows the χ^2 distribution with m degrees of freedom, where m denotes the number of parameters of the model. The likelihood-ratio test is passed with 95% confidence if:

$$2\left(\tilde{L}(\hat{\theta}_p,\hat{\sigma}_p) - \tilde{L}_0\right) > \chi^2(0.95,m)$$

(16)

We emphasize that the log-likelihood test accounts for the number of parameters via the degrees of freedom, thereby enabling comparing simple and complex models.

3.3. Inter-pedestrian parameter correlation

Besides the correlation in the parameter estimates determined via the Cramér-Rao bound, inter-pedestrians differences can be determined. In the ensuing, this is achieved by computing the mean, variance and inter-personal correlation of the individual parameter estimates for the different pedestrians. These statistics provide insight into the behavioral differences between pedestrians, and the inter-pedestrian correlation between the parameter estimates.

4.   Experimental data used for model calibration

The trajectory data used in the ensuing of this contribution have been collected from walking experiments performed in 2003. These walking experiments were conducted in a large hallway of the Faculty of Civil Engineering and Geosciences. The group of pedestrians participating consisted of people of different ages and genders. Using a digital camera mounted at the ceiling of the hallway and dedicated software to process the digital footage into pedestrian trajectories, all trajectories of the pedestrians participating in the experiments were determined.

For the remainder of this contribution, data from the narrow bottleneck experiment are used. Fig. 1 shows a couple of trajectories. The narrow bottleneck experiment was characterized by a high pedestrian demand trying to pass through a narrow bottleneck of 1 m width. Since the demand was larger than the bottleneck capacity, the bottleneck became oversaturated resulting in congestion. For a detailed description of the experiment, the data and their characteristics, we refer to [3].
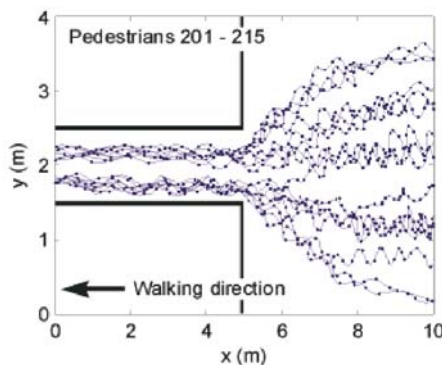
Figure 1: Example pedestrian trajectories for the narrow bottleneck.

5.   Estimation results

To get a general impression of the model performance as well as a better understanding of the important behavioral processes underlying walking behavior, this section presents the results of cross-comparing the model predictions with the naïve zero-acceleration reference model. The parameters of the models have been estimated from the experimental data discussed in the preceding section. The performance of the models is cross-compared based on the overall relative increase in the log-likelihood compared to the null-log likelihood, and the percentage of models that passed the likelihood ratio test.

Tab. 1 below shows an overview of the estimation results. The table clearly shows that the differences between model performances are considerable. Especially the difference between the instantaneous models and the retarded models is relatively large (improvement of the log-likelihood of 6.4% and 7.7% for the respective instantaneous models, compared to 19.7% in case of the retarded anisotropic model).

Model type	% Improvement log-likelihood	% of models passing likelihood ratio test
Basic model	6.4%	71%
Anisotropic model	7.7%	76%
Retarded anisotropic model	19.7%	83%

Table 1: Overview of estimation results for selection of models.

5.1. Basic model

Let us first consider the basic model, without anisotropy and without a reaction delay (Eq. (1)). In this case, the model passed the LR test in 71% of all cases. For the remaining 29%, the basic model did show a higher log-likelihood than the null-model (i.e. smaller RMSE), but the improvement was not large enough to pass the LR test.

Tab. 2 shows an overview of the statistics of the parameter estimates. The estimates are plausible in terms of their magnitude. The table shows that the inter-pedestrian differences are most prominently reflected by the differences in the acceleration times T_p and the interaction distance R_p, as can be concluded from the CoV (Coefficient of Correlation) values of 0.32 and 0.50 respectively. Furthermore, it turns out that the inter-pedestrian correlations between the parameter estimates are generally small, except for the positive correlation between free speed and interaction distance (0.49).

Parameter	Mean	Standard deviation	CoV	Correlation amongst personal parameter estimates			
				V_p^0	T_p	A_p	R_p
V_p^0 (m/s)	1.34	0.21	0.16	1	-0.20	0.02	0.49
T_p (s)	1.09	0.35	0.32		1	0.10	-0.36
A_p (m/s2)	11.96	0.23	0.02			1	-0.16
R_p (m)	0.16	0.08	0.50				1

Table 2: Statistics of parameter estimates for non-anisotropic model.

5.2. Anisotropic model

As concluded before, the anisotropic model with instantaneous reaction outperforms the basic model, although the improvement is rather limited. The LR test shows that the model improves significantly with respect to the naïve zero-acceleration model in case of 76% of all pedestrians considered.

Tab. 3 shows an overview of the parameter estimates for all individual estimates which passed the likelihood ratio test, as well as the correlation between the individual estimates. The results show that especially the acceleration time T_p has a relatively large standard deviation (judging from the CoV values), implying that the inter-pedestrian differences in acceleration times are large. This holds equally for the interaction distance R_p.

The correlation between the parameters reveals a considerable relation between the free speed and the interaction distance (positive correlation of 0.62), implying that on average, pedestrians having a large free speed V_p^0 have a large acceleration distance R_p. An interpretation of this (statistical) result might be that pedestrian with a high free speed have the tendency to better anticipate on pedestrians further away from them. However, the explanatory performance of the model is still limited, and care should be taken in interpreting the estimation results.

Other high correlations are found between the acceleration time T_p and the interaction factor A_p (negative correlation of 0.54), and between the interaction factor A_p and the interaction distance R_p (positive correlation of 0.46).

Parameter	Mean	Standard deviation	CoV	Correlation amongst personal parameter estimates			
				V_p^0	T_p	A_p	R_p
V_p^0 (m/s)	1.32	0.22	0.17	1	-0.23	0.28	0.62
T_p (s)	0.96	0.24	0.25		1	-0.54	-0.32
A_p (m/s2)	11.46	0.56	0.05			1	0.46
R_p (m)	0.33	0.09	0.27				1

Table 3: Statistics of parameter estimates for anisotropic model.

If we compare the estimates of the basic model with the estimates of the anisotropic model, we see that the estimates are similar, except for the interaction distance R_p. In the anistropic model, the interaction distance R_p is on average twice as large as in the non-anistropic model. Regarding the inter-pedestrian parameter differences, it turns out that the variability in the acceleration time T_p reduces substantially.

5.3. Retarded anisotropic model

The statistical analysis clearly reveals the importance of the finite reaction time in walking behavior modeling, as shown from the improvements of the model performances as indicated by Tab. 1: besides the fact that 83% of the considered cases passes the LR test, we can also see that the log-likelihood improvement over the naïve zero-acceleration model of 19.7% is much higher than for the non-retarded models (respectively 6.4% and 7.7% respectively).

Tab. 4 provides an overview of the average parameter values, their standard deviation and the inter-pedestrian correlation between the parameter estimates. The table shows that in particular the standard deviations - and thus the inter-pedestrian differences - of the acceleration times Tp and of the interaction distances are relatively large. Also note the medium inter-pedestrian differences in the reaction time (mean of 0.28 s and a standard deviation of 0.07 s).

As for the instantaneous models, from Tab. 4 we again observe that the free speed V_p^0 and the interaction distance R_p are positively correlated (0.57). It also turns out that the reaction time τ_p and the interaction factor A_p are negatively correlated, implying that the reaction time and the interaction factor are to a certain extent mutually exclusive.

Parameter	Mean	Standard deviation	CoV	Correlation amongst parameter estimates				
				V_p^0	T_p	A_p	R_p	τ_p
V_p^0 (m/s)	1.34	0.23	0.17	1	0.23	0.39	0.57	-0.02
T_p (s)	0.74	0.23	0.31		1	-0.23	-0.06	0.44
A_p (m/s2)	11.33	0.64	0.06			1	0.36	-0.46
R_p (m)	0.35	0.11	0.31				1	-0.17
τ_p (s)	0.28	0.07	0.25					1

Table 4: Statistics of parameter estimates for the retarded anisotropic model.

To gain more insight into the distributions of the parameter estimates, Fig. 2 shows histograms of the estimates, from which inter-pedestrian differences can be observed clearly. Also the shape of the parameter distributions becomes apparent. that all parameter distributions appear to be skewed rather than symmetric. This holds especially for the interaction factor A_p, which has a large right tail (few estimates with a very large value of A_p).
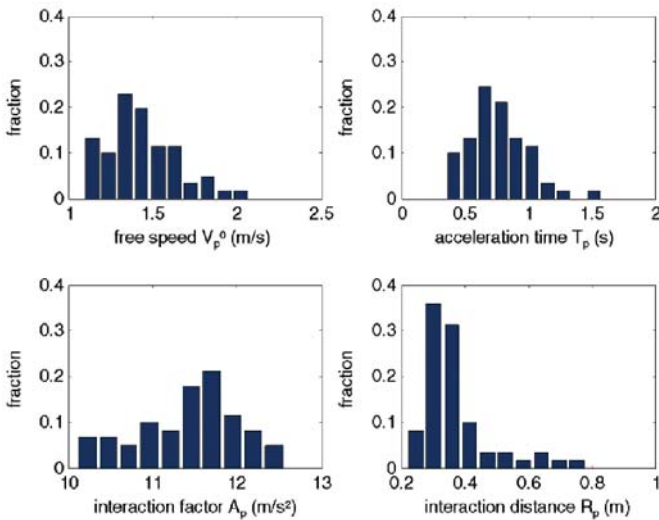
Figure 2: Parameter distributions for 82 pedestrians using an anisotropy factor of 8.

Fig. 3 shows the distribution of the reaction time estimates. Again the distribution appears to be skewed. The median reaction time equals 0.3 s; few pedestrians have a reaction time which is larger than the median of 0.3 s.

Let us finally note that the parameter estimates determined by applying the approach to data from other experiments are consistent.
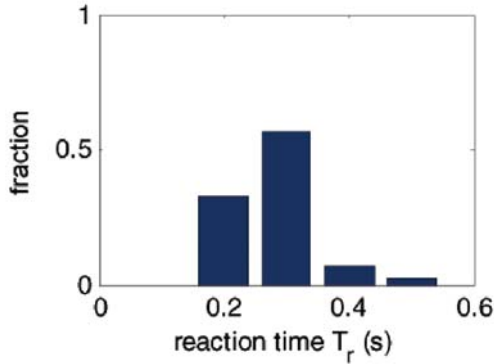
Figure 3: Distribution of the reaction time estimates.

6.   Conclusion and recommendation

In this contribution, a generic approach for calibration of microscopic models was put forward. Using trajectory data, the approach enables estimation of the personal parameters (i.e. specific for each pedestrian). The approach provides insight into the statistical properties of the estimates, as well as the performance of the models to which the calibration approach is applied.

In applying the approach to data collected during walking experiments, inferences could be made regarding the behavioral processes that are to be included in the modeling to ensure a realistic description of walking. In turns out that besides anisotropy, finite reaction times play an important role in correctly describing microscopic walking behavior as is reflected by the considerable increase in model performance of the retarded models compared to the instantaneous model. Furthermore, the inter-pedestrian differences in walking behavior have been shown.

Future research will entail studying the macroscopic properties of the microscopically calibrated pedestrian models. This research should reveal how the finite reaction time and the inter-pedestrian differences affect the dynamic flow properties. **«**

References

1. S.P. Hoogendoorn and P.H.L. Bovy: *Simulation of Pedestrian Flows by Optimal Control and Differential Games*, Optimal Control Applications & Methods 24, pp. 153-172 (2003).
2. D. Helbing, I.J. Farkas, and T. Vicsek: *Simulating Dynamical Features of Escape Panic*, In: Nature 407, pp. 487-490 (2000).
3. S.P. Hoogendoorn and W. Daamen: *Pedestrian Behavior at Bottleneck*, Transportation Science 39(2), pp. 147-159 (2005).
4. G. Casella and R.L. Berger: *Statistical Inference*, Duxbury Press, Belmont, California (1990).

Pedestrian flow optimization with a genetic algorithm based on Boolean grids

A. Johansson[1] and D. Helbing[1]

When a large group of pedestrians is to be evacuated out of a building, one of the most dangerous locations is at the doors. In emergency situations when pedestrians panic or fear for their lives, they tend to force their ways out, even if the exits are jammed, which creates a clogging phenomenon that is much more pronounced during an evacuation than under normal conditions. It has been shown that it is possible to increase the outflow by suitably placing a pillar or some other type of obstacle in front of the exit, which reduces the inter-pedestrian pressure in front of the door, decreases the magnitude of clogging and therefore makes the overall outflow higher and more regular. To investigate how the architectural infrastructure in the vicinity of a door, or other bottleneck, shall be constructed to maximize the pedestrian outflow under evacuation conditions, we present a method based on a Genetic Algorithm.

1.   Representation

In the past, studies regarding pedestrian flow optimization by variation of geometrical designs have been performed by Bolay (1998), Helbing et al (2001) and Escobar and De La Rosa (2003). However, they were all based on handcrafted solutions, which were then tuned. To give more freedom to the evolution of the infrastructure, we choose a representation similar to the one of Deb and Goel, 2001, which uses a Boolean grid where 0 means no obstacle and 1 means an elementary obstacle. To create an initial population of obstacle grids, $X_{i,j}^{\alpha}$, we use the following scheme:

1. Initialization:

Initiate

$$X_{i,j}^{\alpha} = \begin{cases} 1 \text{ with prob. } p_1 \\ 0 \text{ otherwise} \end{cases}$$

with $i \in [1, n]$ and $j \in [1, m]$

2. Clustering:

Choose i and j at random n*m*c number of times, where c is a clustering parameter. Then perform the nonlinear updating rule below, where the constant d denotes the size of the neighborhood taken into consideration.

---

[1]Institute for Transport and Economics,
Dresden University of Technology,
Andreas-Schubert Str. 23, 01062 Dresden, Germany

$$s_{i,j} = \sum_{k,l} X_{k,l}$$

for $k \in [\text{i-d, i+d}]$ and $l \in [\text{j-d, j+d}]$

$$p_1 = \frac{1}{2} + \frac{\arctan(k[2s_{i,j} - (2d+1)^2])}{\pi}$$

Then set $X_{i,j}^{\alpha} = 1$ with probability p_1, in the same manner as in the Initialization rule.

The use of *arctan* in the update rule is the key to force the clustering of the matrix elements and create smooth clusters of elementary obstacles. To avoid unwanted noise (small islands of only a few elements), numerical experiments indicate that the cluste-ring constant should be chosen $c \approx \frac{\sqrt{n*m}}{2}$. See figure 1 for a hint how the clustering works.
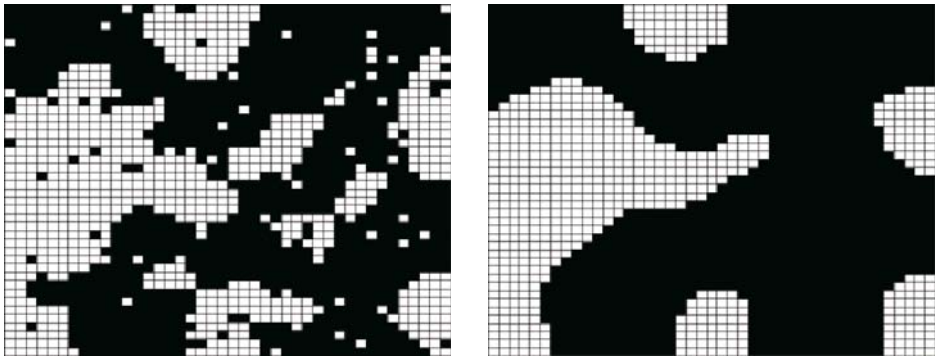
Figure 1: Clustering. Left: A matrix of elementary obstacles. Right: The same matrix after appli-cation of the clustering algorithm described in the text.

2.   Genetic Algorithm

Having defined a method for creating obstacle grids, we implement a simple Genetic Algorithm to improve these grids for evacuation scenarios, as mentioned in section 1. A population of N obstacle matrices is used, and our Genetic Algorithm uses the following scheme:

1. Generate N matrices according to the initialization rule, specified in Section 1.

2. Choose four geometrical setups at random and perform a simulation for 600s each, e.g. with the Social-Force Model (Helbing, 2001; Helbing et al 2005).

3. Assign a fitness value to each of the four geometrical setups according to the outflow rate of pedestrians. Keep the two setups with the best fitness, X^α and X^β, and update the two worst ones according to the following rule with pseudo random numbers $p_\alpha = rnd[0,1]$ equally distributed between 0 and 1:

$$X_{i,j} = \begin{cases} X_{i,j}^\alpha \text{ with prob. } p_\alpha \\ X_{i,j}^\beta \text{ otherwise} \end{cases}$$

$\forall i, j$

Then smoothen the outcome by the clustering rule described in Section 1.

2.1. Characterization of solutions

To get an idea what has really been improved by adding the obstacles, we make measurements of flow as a function of the distance to the exit and average both over the first 45s of simulated time as well as 900s of simulated time. The reason for the shortness of the first interval is that we want to capture the transient phase, so the drops in flow are more easily distinguishable. Figure 2 shows these relations both for the case with no obstacles and for the solution with highest throughput. Due to the nonlinear nature of the interactions, it is apparently better to create a smaller bottleneck before a bigger one, so that the transition between the parts with different capacity is not that sharp. It becomes obvious that the weakest link does not set a strict upper limit for the flow, but rather the weakest link may be improved by changing the infrastructure preceding it.
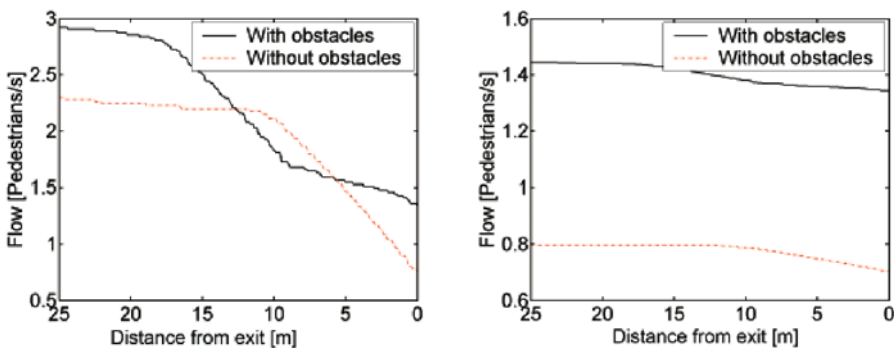
Figure 2: Evaluation of the flows, during the first 45 seconds of our simulation (left) and during the first 900s of the same simulation (right). Note that with obstacles, the minimum flow close to the exit can be significantly increased.

3.   Results

Fig. 3 shows an optimized configuration in comparison with a corridor without any obstacles as a reference, where the outflow is around 0.50 pedestrians per second. Three of the best outcomes, each from a class with different characteristics, are shown in figure 4. By implementing the best evolved solution, the outflow may be increased by up to a factor of four times. Note, however, that this does not mean that the throughput will always be four times higher by adding these obstacles. It shall rather be seen as an upper limit, how much the throughput may be increased under certain conditions.
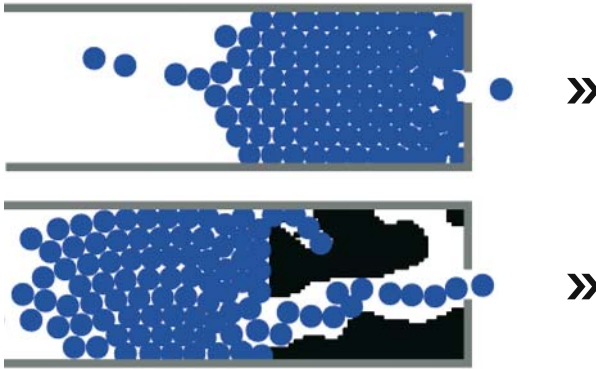
Figure 3: Snapshots from the simulations. Top: Case without any obstacles. Bottom: Improved geometrical solution, where the useless channel in the upper area has obviously no negative effect on the flow.
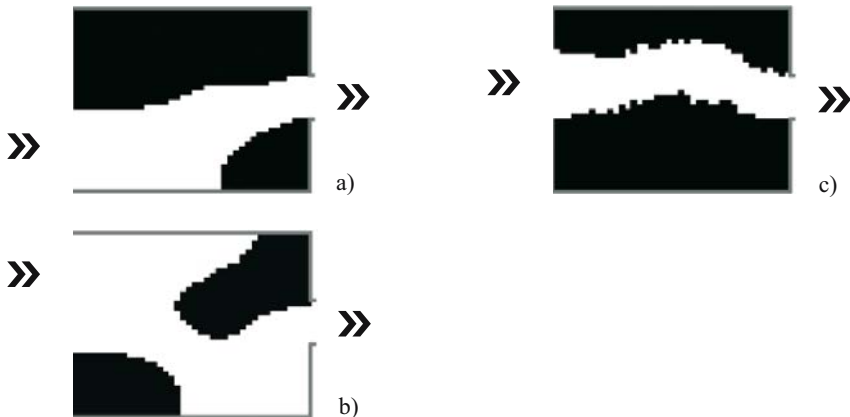
Figure 4: Representatives of different classes of top-ranked solutions. a) Funnel-shape (fitness 1.99). b) Compartment structure (fitness 0.83). c) Zig-zag shape (fitness 1.78).

From the various resulting improved solutions, we conclude that the following design elements are potentially favourable:

» asymmetry, as the evolving obstacles at the left side are usually different from the obstacles on the right side.
» funnel shape decrease of the walkable width for positions closer to the bottleneck.
» compartment structure similar to the funnel shape, but with an increase in the walkable width after one bottleneck before another, which creates an area of lower density compared to the rest of the crowd.
» zig-zag shape i.e. a series of turns in different directions.

4.   Conclusion

In previous publications, it has been pointed out that suitably planned obstacles can surprisingly increase pedestrian flows. For example, an asymmetrically placed pillar in front of an exit may speed up the evacuation of crowd from a large room. This design contains the favourable elements 1 and 2 in the above list. A particular zig-zag-shaped design has been recently suggested to improve the safety of egress routes in sports stadia (Helbing et al. 2005).

The applicability of design solutions obtained with a Genetic Algorithm based on Boolean grids goes beyond outflow maximization through doors. Rather it gives an insight into how interfaces may be improved between areas with different capacities.

Our future work will focus on the further improvement of automated, simulation-based design optimization of pedestrian facilities. In particular, we want to test multi-goal functions considering not only flows, but also other performance measures. Moreover we will search for algorithms that avoid designs with unused channels as in Fig. 3b.

Acknowledgements

References

1.   K. Bolay: *Nichtlineare Phänomene in einem Fluid-Dynamischen Verkehrsmodell*, Master Thesis, University of Stuttgart (1998).
2.   R. Escobar and A. de la Rosa: *Architectural Design for the Survival Optimization of Panicking Fleeing Victims*, Presented at 7th European Conference on Artificial Life (ECAL 2003), Dortmund, Germany, September 14-17 (2003).

3.   D. Helbing, P. Molnár, I. Farkas, and K. Bolay: *Self-Organizing Pedestrian Movement*, Environment and Planning B, pp. 361-383 (2001).
4.   D. Helbing, L. Buzna, A. Johansson, and T. Werner: *Self-Organized Pedestrian Crowd Dynamics: Simulations, Experiments, and Design Solutions*, Transportation Science, 39(1), pp. 1-24 (2005).
5.   K. Deb and T. Goel: *A Hybrid Multi-Objective Evolutionary Approach to Engineering Shape Design*, In: Proceedings of the First International Conference on Evolutionary Multi-Criterion Optimization (EMO-2001), 7–9 March, Zurich, Switzerland, pp. 385–399 (2001).
6.   D. Helbing: *A Mathematical Model for the Behavior of Pedestrians*, In: Behavioral Science 36, pp. 298-310 (1991).
7.   D. Helbing, I. Farkas, and T. Vicsek: *Simulating Dynamical Features of Escape Panic*, In: Nature 407, pp. 487-490 (2000).
8.   D. Helbing, I. J. Farkás, P. Molnár, and T. Vicsek: *Simulation of pedestrian crowds in normal and evacuation situations*, In: M. Schreckenberg and S.D. Sharma (Eds.), Proceedings of the International Conference on Pedestrian and Evacuation Dynamics, Springer Berlin, pp. 21-58 (2002).

Developing a Pedestrian Agent Model for Analyzing an Overpass accident

T. Kaneda[1]

Recent softwares have enabled us to apply pedestrian dynamics models into analyses on pedestrian accidents. The author had already developed a pedestrian dynamics model, called ASPF, based on the cell space model, that is evolved from Cellular-Automata (CA). After a couple of years' efforts for continuous revision, we analyze the causes on an accident of Asagiri Pedestrian Overpass in 2001 even though retrospectively. In this paper, the typical existing models for pedestrian dynamics are reviewed, especially explaining on the class of cell space models. Next, ASPF (Agent Simulator of Pedestrian Flows) are explained, in that each pedestrian moves according to several behavioural rules on the cell-grid space of 40 cm side each. Based on not only the fundamental findings from the existing spatial researches but also these from the accident report, ASPF ver.2 is 'tuned up' carefully. ASPF ver.2 is to assess measures for managing pedestrian flows by focusing on the domino risk (density 3 to 5) that shows a symptom for the accident rather than a reconstruction of the real accident itself that had occurred at extremely high density (more than 10). The simulation results show that a two-way flow, combined with standing spectators (stoppers) can trigger an accident even on an overpass that satisfies present design standards. Moreover, we have confirmed that even simple traffic regulations such as partitions can be an effective measure to prevent a pedestrian accident.

1. Introduction

Recent softwares have enabled us to apply pedestrian dynamics models into analyses of pedestrian accidents. The author had already developed a pedestrian dynamics model, called ASPF, based on the cell space model, that is evolved from Cellular-Automata (CA). After a couple of years' efforts for continuous revision, we analyze the causes on an accident of Asagiri Pedesrtian Overpass in 2001, even though retrospectively.

This paper addresses our development project of a pedestrian agent simulation model, ASPF. In section 2, after a bottom-up approach is described, the cell space models on which our pedestrian model is based and which belong to a class of the models are reviewed with typical existing models for pedestrian dynamics. ASPF (Agent Simulator of Pedestrian Flows) is also explained, in that each pedestrian moves according to behavioural rules on the cell-grid space of 40 cm side each. In section 3, the development circumstances, the outline of ASPF ver.2 that tried an accident analysis, the results of the simulation analysis and consideration are described in due order. Based on not only the fundamental findings from the existing spatial researches but also these from the accident report, the rule configuration of ASPF ver.2 has been 'tuned up' carefully. ASPF ver.2 is to assess measures for managing pedestrian flows by focusing on the domino risk (density 3 to 5) that shows a symptom for the accident rather than a reconstruction of the real accident situation itself that had occurred at extremely high density (more

[1]Nagoya Institute of Technology,
Gokiso, Showa, Nagoya 466-8555, JAPAN,
kaneda.toshiyuki@nitech.ac.jp

than 10). The simulation results show that a two-way flow, combined with standing spectators can trigger an accident even on an overpass that satisfies present design standards. Moreover, we have confirmed that even simple traffic regulations such as partitions can be an effective measure to prevent a pedestrian accident. Instead of conclusion, our recent revise works of ASPF and future works are to be stated.

2.   Existing Researches and Our Approach

2.1. Bottom-up approach

Pedestrian agent modelling appears to be under developed when compared to vehicle modelling, partly because the micro behaviours of pedestrians are so richly varied. The author, who has an interest in the practical application of modelling from the viewpoint of urban planning, can perceive a bottom-up modelling approach – loading higher-order functions for a pedestrian agent on the cell space in order – as this process is developed, it would be cross checked against survey data and observation gained through research.

Firstly, to explain this bottom-up approach, the broad body of existing research has been divided into four categories (Fig. 1). The first category is the actual survey, observation and measurement of pedestrian behaviour and pedestrian flow[1–7]. In this category, a wide variety of case studies have been accumulated; taking fundamental data through to practical application, from micro to macro, from the every day's behaviours to panic behaviours.

The second category is research on models of pedestrian dynamics demonstrating the emergence of macro phenomena in pedestrian flow from the accumulation of micro-motives of pedestrians' behaviours[9–21]. This category includes the physical phenomenon analogy model, the CA model and the cell space model evolved from CA. However, in many cases, pedestrians just make straightforward movements and avoid others.

The bottom-up approach means the development of a model that loads such higher-order functions as route selection, trip planning and the scheduling of a visiting order into this second category of pedestrian model; all of which must be checked against data taken from survey research.

The third category is research on elemental models of these functions[22–25]. Much of this research has been studied in OR, transportation planning or the artificial intelligence fields.

The fourth and final category is research to study integrated models for application incorporating all these models by using platforms such as GIS[26–29].
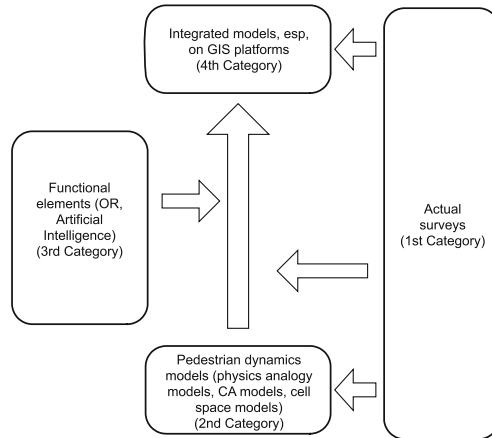
Figure 1：Existing Studies and the bottom-up approach

2.2. From CA model to cell space model

The key characteristic that distinguishes pedestrian behaviour from the physical pheno-menon analogy describing the dynamic movement of gas, liquid and granules is avo-idance behaviour; humans unlike particles naturally move out of each others way. By considering this characteristic, models called pedestrian dynamics were created; very different models to the physical phenomenon models.

In the theoretical model by Helbing, an acceleration vector of a pedestrian is expressed by the sum of social force and the individual term, and the social force is also expressed by the sum of the accelerating force, border repulsive force, interaction with other pe-destrians and time term sums[12]. Helbing sought this idea in the concept of "field" in social science. In this connection, Burstedde's model uses the same concept of field used in the cell space model that will be mentioned later. In this model, the selection proba-bility for each forward movement cell is in proportion to the product of two potentials in that place; the static field and the dynamic field. In particular, the dynamic field is interpreted in a way that treats the other pedestrians' walking history as a pheromone[10]. Now, the CA model and its extended type – the cell space agent model, or more simply the cell space model – are described starting with a brief explanation of the difference between the two.

Firstly, as an example of a simple two-dimensional CA, the life game is examined. This CA has three characteristics: (1) update structure – the state of cells in a term are all up-dated according to information from the previous term; (2) neighbourhood – the use of the state of the neighbouring cells as information to prescribe the cell's update; and (3) two value status – the state of cells is a two value status of light ON or light OFF.

When pedestrian behaviour is expressed using this CA, after assuming that a pedestrian is positioned on a light ON cell, a concept of movement is introduced, expressed by (4) light ON and OFF – as a cell turns its light OFF, another cell turns its light ON. In

this case, (5) the upper limit of occupancy – the maximum number of pedestrians that can occupy one cell is assumed to be one. In the case of a one-way flow, this model can express pedestrian behaviour and for a one-dimensional CA, rule 184 of Wolfram[21] is applied.

In comparison, when dealing with a multi-directional flow or a long movement with one step, such conditions as update structure, neighbourhood, two value states or upper limit of occupancy need to be eased. In particular, when the update structure is changed, one of the following rules needs to be applied:

» after updating all cells relating to movement by using information from the previous term in parallel, solve the conflict for cells that have surpassed the upper limit of occupancy;
» apply an order to every pedestrian and move them in turn.

The former is called a parallel update and the latter a sequential update. The sequential update has a path dependency – a calculation result differs according to an applied order – therefore, some researchers prefer parallel updates and some prefer sequential updates, especially with random sequential updates (RSU), when random numbers are used to establish an order of precedence.

When using these methods, especially in a sequential update, the expression form of a cell space is given as a walking space model, but in a narrow sense this is beyond the definition of CA and it is common to call it an agent model. In this paper this is called a cell space model and is an extension of the CA model. Table.1 shows recent research using this cell space model. All the research is designed to enable the emergence of pedestrian flow macro phenomenon from the accumulation of pedestrian agents' micro behaviour; however, while the two models on the left side are included mainly for theoretical interest, the three models on the right side show the characteristics of model development reproducing macro phenomenon observed by survey research. Particularly, our ASPF ver.2 on the far right also aims at measurement evaluation by comparing to numerical survey data.

When modelling cell spaces, discrete approximation is also important; in the mutual comparison of Table 1, the space scale of a cell is nearly 40 cm including unspecified ones. On the other hand, variations in time scale can be seen, but this variation appears to be related to the distance within which avoidance behaviour starts. Each of the algorithms in the three models on the right side in Table.1 has a different characteristic and they can be classified in the following ways:

» The model of Burstedde et al. – has a short measurement for both time slice and the avoidance behavior distance, with a focus on high density flows.
» The model of Blue and Adler – has a short time slice and a long avoidance behaviour distance with a focus on low density flows.
» The model of the author et al. – has a middle measurement for both and focuses on the changing processes from low to high density flows.

	Models	Muramatsu et.al (1999)	Fukui, Ishibashi (1999)	Burstedde et.al (2001)	Blue, Adler (2001)	ASPF ver.1 (2002) and ver.2 (2004)
Time and Space Scales	Cell Size	No description	No description	40 cm side each	45.7 cm side each	40 cm side each (ver.2)
	Time Slice	No description	No description	approx. 0.3 sec	No description (1 sec)	0.5 sec
	Cell Occupancy Limit	One person	One person	One person	No description (one person)	Two with a surrounding density of two or more, one with other case (ver.2)
	Behavioral Rules, (Number on the rules in bracket)	To move to one of three adjacent cells (forward, right or left), according to the situation of the adjacent three cells	(Diagonal Stepping Mode) To move forward one in a case that the forward interval is one or more (Wolfram's no.184 rule). To avoid to a cell diagonally forward, if possible, in a case of the existance of the other on the adjacent forward cell. Otherwise, to stop	To move to one of the adjacent eight cells, according to these cells. The probability is proportional to M (dynamic potential) and S (static potential). Potential concepts are analogous to the recent physics	To choose the maximum interval lane from forward three lanes, and move forward on it. In cases of same length of interval, use randomness. Adjacent two confronters exchange their position by using randomness.	Basic behaviors (6), Avoiding others (4), Slowdown (8), High density walking (3), Flow cognition (1), Cornering (ver.2)
Simulation Algorithm	Maximum Speed/ Distribution of the maximum Speed	One	One	One	Four 5%, Three 90%, Two 5%	Three
	Maximum interval to avoid/Symmetry	One / Symmetric	One / Symmetric	Two / Symmetric	Eight / Symmetric	Three / asymmetric (a flow cognition rule)
	Updating & Conflict Resolution Methods	SU (Sequential Updating)	No description	PU (Parallel Updating), then conflict resolution by using random numbers	Two times PU at the avoidance and advance	RSU (Random Sequential Updating)
Main Findings of the Study		(1) Emergence of jam in confrontation flows, (2) Calculation of relation between flow coefficient and speed, (3) Case study on characteristics of avoidance behaviours	(1) Proposal of side stepping model and diagonal stepping model, (2) Phase transition from straightforward to stable diagonal in cases of confrontation flows on DSM, (3) Calculation of a density - speed realtion	(1) Representation of refugees' flows in indoor space, (2) Emergence of stable 'lanes' in confrontation flows	(1) Calculation of relations among flow-phases, ratios of confrontation and exchange probabilities, (2) Estimation of an exchange probability, based on cross-check of actual measurement, (3) Calculation of relations of density-frequency of avoidance	(1) Emergence of stratification in confrontation flows (ver.1), (2) Cross-check graphs of density-speed to actual surveys (ver.2), (3) Simulation of an accident situation (under density 4), based on the descriptions of the office ex post facto inspection (ver.2), (4) Calculation of effects of crowd control measures (ver.2)

Table 1:   Comparison among agent models with cell spaces[17,11,9,8,15,25]

3.   Agent Simulation of Pedestrian Flows (ASPF) Ver.2

3.1   Development of ASPF

The author's laboratory had been dealing with the modelling of pedestrians' shopping-around behaviours for some years and early in the summer of 2001, we started to study the modelling of more basic pedestrian flow with the aim of trying out the performance of an agent simulation software[1]; in recent years the usefulness of the software has been significantly improving.

In July while designing a model, a tragic pedestrian accident occured at Akashi City Firework Festival; articles of the event and speculation of the causes were given in the press. These articles became the basis for ASPF ver.1 of the software program which was published in December; the program examined high density pedestrian flow in an L-shaped corridor and was modelled on the Asagiri Station Pedestrian Overpass[15]. In January 2002, Akashi City published an accident report – ex-post facto inspection --[1] revealing further detailed information, which was then used to review and improve ASPF ver.1, reconstructed the situations of the accident and led the revision into ASPF ver.2. The simulation analysis of this program was published in February 2004[20].

3.2.   Simulation setting for an accident analysis

In the following section, an outline of the ASPF ver.2 model is given.

The main components of this agent model are the walking behaviour rules as shown in Fig. 2.

With a threshold density of 2 persons/m^2, at a low density time the following rules are applied: 6 basic behaviour rules, 8 slow-down rules, 4 avoidance rules and 1 flow pattern cognition rule. At a high density time, one of the 3 high density flow rules is applied. The priority order is a simple numerical order.

For walking on a L-shaped corridor, in addition to a cornering rule, a rule for shortening a route while cornering at a low density time was devised (Fig. 3).

One step was set at 0.5 seconds, 1 cell at 40 cm each and the maximum number of occupants per cell was 2 persons with a surrounding density of 2 or more and 1 person with any other density.

In the measurement of the relationship between the density and flow speed, a graph sloping to the right and closely resembling the survey research data, was obtained (Fig.4). The accident report concluded that the accident had occurred when the density on the overpass reached 13 to 15. On the other hand, typical domino accidents— in Japan, most of that people injured had occurred on the stairs, even that can occur on flat ground—can happen at density 3 to 5. So, in our simulation analysis under ordinary cases, not panic cases, a walking behaviour model in an L-shaped flat space was used where the difference between the stairs were eliminated and at the same time, a density of 4 − congestion giving rise to a possible domino accident − was focused on as the risk level.

It is also important to consider the flow coefficient. The Asagiri Pedestrian Overpass

---

[1] KK-MAS by Kozo Keikaku Engineering Inc., Japan[16]

was designed with an evacuation plan standard of 1.5 person/m • sec, which is far higher than the usual design standard of 0.33 person/m • sec[5,7]. However, both values assume a one-way flow. The flow coefficient value estimated by the author et al from the report was 0.48 at the peak time; a much lower value than the maximum capacity, but the accident still happened. The accident report states contributory factors to the accident were: 1) two counter flows meeting and becoming tangled up; and 2) fireworks spectators blocking the area around the south part of the pedestrian overpass.

In the simulation analysis on the south side of the L-shaped corridor (overpass: 17 cells wide, stairs: 9 cells wide), standing spectators (stoppers) in several rows of 2 to 5 cells were set up to give a trial calculation for these influences on the increase of density. The accident report also stated that effective crowd control measures were not carried out; the simulation analysis examined the effect of placing a partition in the center to control the crowd (Fig.5).
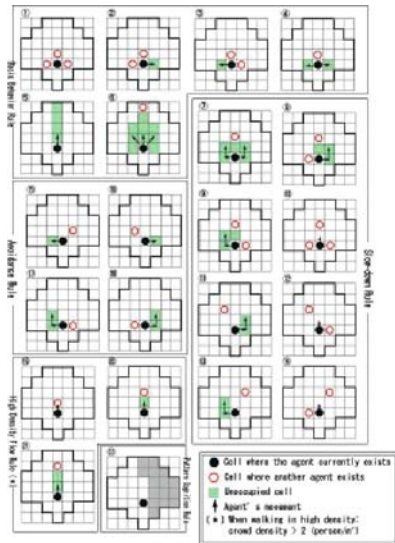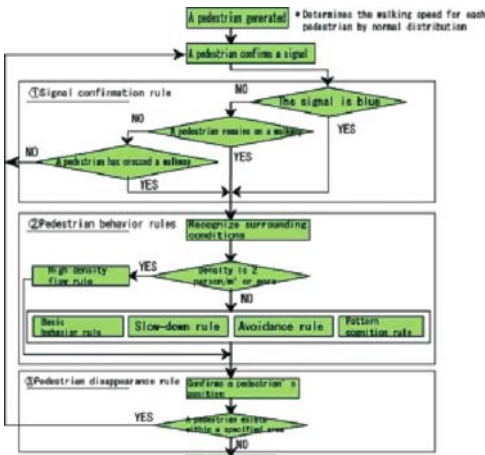
Figure 2: Algorithm of Pedestrian Agent in ASPF ver.2

Figure3: Behavioural rules of ASPF ver.2
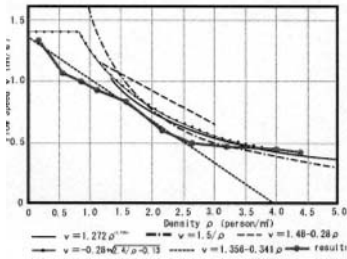
Figure 4: Benchmarking test of agent flows
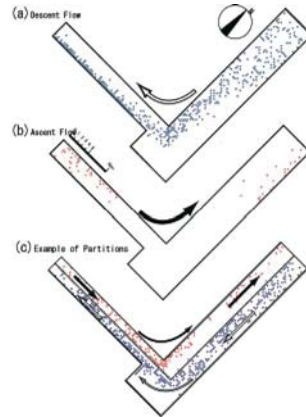
Figure 5: L-shaped model and density
distributions

3.3. Results and implications

The simulation result showed that when there were no standing spectators, even with two counter flows, as long as the sum of both flow coefficients was less than 1.5, the density never exceeded the risk level, but when the number of rows of stoppers (standing spectators) was 3 or more, the density increased and exceeded the risk level (Fig.6) .

The simulation also showed that the introduction of a simple partition controlled the crowd density, but when the stair width was divided into two parts – each half was 1.8 m; below 2.1 m – this minimum width resulted in a bearing experiment to examine an arch action. In conclusion it was found that the introduction of a one-way flow and a prohibition on standing are the best safety precautions.

Here we will briefly mention about simulation analysis. Computer simulation is known as a tool for 'forward reasoning', which draws conclusions from assumptions. Howe-ver, recent improvements in operational capability have allowed 'backward reasoning' to narrow the possible assumptions for a given conclusion, by examining a variety of different conclusions through changing assumptions in the simulation. Generally, in an ex post facto inspection it is considered difficult to gather all the data items necessary for determining the cause. In such a case, a simulation is carried out by using any avai-lable data in conjunction with a working hypothesis; this allows a reconstruction of the accident situation and the exploration of a logical coherent cause and effect explanation. This type of simulation analysis is used within this paper and it would appear that the analysis made in this section is significant, as by using a model including information from detailed and consistent accident reports, the accident process was reconstructed, accident data was confirmed to be accurate and moreover it was possible to attempt den-sity calculations and numerical evaluations for the implementation of counter measu-res.

When conducting this type of analysis, it is important to collect many facts and several models to prove or disprove any hypothesis, and closely scrutinize their relationships. In the case of pedestrian flow, the testimonies of pedestrians relating their experiences are also necessary.
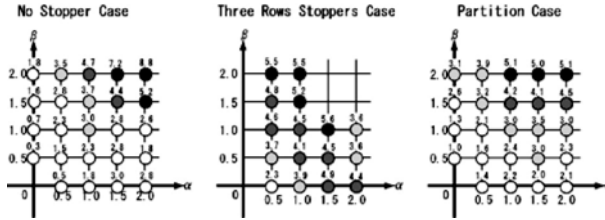
Figure 6: Simulation Results

4.   Concluding Remarks—Further Development

This paper explained ASPF ver.2 by which we analyzed a pedestrian accident as an instance of the class of cell space model. ASPF ver.2 has a structural restriction of the cell space mainly caused by the grid shape, when simulating pedestrian's cornering behavior etc. Fortunately, the software that we use as the platform for developing our ASPF models provides us a modeling environment to make agents' walking in a free direction. Then the authors have also revised ASPF further -- while the simulator moves each pedestrian agent on XY continuous coordinates space, but inside of each agent, he/she has own relative cell space according to the walking direction and the same behavioral rules as ASPF ver.2's. By using this ASPF ver.3, we tried a crowd analysis on an 'scramble' intersection with straight and diagonal crosswalks (Table.2).

If a free direction walk of an agent can be expressed, simulation of the cornering behavior on a L-shaped corridor will be considered to become still minuter. Therefore, we are going to introduce a direction correction function (Helmsman function[29]) that corrects the direction to a given walking target (waypoint) periodically even when an agent receives other agents' interference, and to tackle the accident analysis in the same L-shaped corridor space model as this paper's analysis again and again. **«**

	Main revises
ASPF, ver.1 (Dec. 2001)[15]	» Was developed as a prototype agent model with 18 rules on a cell space » Had verified an emergence of stratification in confrontation flows » Had tried to simulate an accident process on a L-shaped corridor space
ASP, ver.2 (Feb. 2001)[20]	» Was revised to 22 rules, based on examination of factal findings » Had simulated the accident process by introducing conering rules » Had assessed partition effects for crowd control
ASPF, ver.3 (Dec. 2004)[14]	» Has been implemented proper crusing speed of each agent » Has enabled agent's free-direction walking on relative coordinates system » Has compared with observation at ‚scramble' crosswalk
ASPF, ver.4 (Dec. 2005)	» To be examined and revised the high-density rules through benchmarking tests » To be introduced Helmsman function instead of the cornering rules » To be re-simulated the accident process on L-shaped corridor

Table 2:   Version up summary

References

1.   Akashi City Summer Festival Accident Investigation Committee, *Accident Investigation Report on the Firework Festival at the 32nd Akashi City Summer Festival*, (in Japanese) (2002).

2.   M. Arakawa and T. Kaneda: *Analyses on Redundancy of Shop Around Behaviour in Nagoya CBD*, Journal of Architecture, Planning and Environmental Engineering 556 pp. 227-233 (in Japanese) (2002).

3.   J. Fruin: *Pedestrian Planning and Design*, Elevator World Inc. (1971).

4.   L.F. Henderson: *The Statistics of Crowd Fluids*, In: Nature 229, pp. 381-383 (1971).

5.   Japan Road Association: *Three-Dimensional Crossing Technical Standards* (in Japanese) (1979).

6.   Architectural Institute of Japan: *Compilation Data for Architectural Design* (Human Being), Maruzen Co., Ltd. (in Japanese) (2003).

7.   Institute for Fire Safety & Disaster Preparedness: *Comprehensive List for Local Disaster Preparations Data* (Local Evacuation) (in Japanese) (1987).

8. V.J. Blue and J.L. Adler: *Cellular Automata Microsimulation for Modelling Bi-Directional Pedestrian Walkways*, Transportation Research B, 35, pp. 293-312 (2001).

9. C. Burstedde et al.: *Cellular Automaton Approach to Pedestrian Dynamics-Applications*, In: M. Schreckenberg and S.D. Sharma (Eds.), Proceedings of the International Conference on Pedestrian and Evacuation Dynamics, Springer Berlin, pp. 87-98 (2001).

10. C. Burstedde, K. Klauck, A. Schadschneider, and J. Zittarz: *Simulation of Pedestrian Dynamics using a Two Dimensional Cellular Automaton*, In: Physica A, 295, pp. 507/525 (2001).

11. M. Fukui and Y. Ishibashi: *Self-Organized Phase Transitions in Cellular Automaton Models for Pedestrians*, In: Journal of the Physical Society of Japan 65(8), pp. 2861-2863 (1999).

12. D. Helbing: *A Mathematical Model for the Behaviour of Pedestrians*, In: Behavioural Science 36, pp. 298-310 (1991).

13. D. Helbing, I. J. Farkas, P. Molnar, and T. Vicsek: *Simulation of Pedestrian Crowds in Normal and Evacuation Situations*, In: M. Schreckenberg and S.D. Sharma (Eds.), Proceedings of the International Conference on Pedestrian and Evacuation Dynamics, Springer Berlin, pp. 21-58 (2001).

14. T. Kaneda and D.Okayama: *A Pedestrian Agent Model Using Relative Coordinates System*, In: T. Terano et al. (Eds.), Proceedings of The Fourth International Workshop on Agent- Based Approaches in Economics and Social Complex Systems (AESCS'05) (in printing) (2005).

15. T. Kaneda and H. Yano, et al.: *A Study on Pedestrian Flow by Using an Agent Model - A Simulation Analysis on the Asagiri Overpass Accident, 2001*, In: T. Terano, H. Deguchi, K. Takadama (Eds.), Meeting the Challenge of Social Problems via Agent-Based Simulation, Springer, pp. 185-196 (2003).

16. Kozo Keikaku Engineering Inc., http://www2.kke.co.jp/mas

17. M. Muramatsu, T. Irie, and T. Nagatani: *Jamming Transition in Pedestrian Counter Flow*, In: Physica A 267, pp. 487-498 (1999).

18. A. Schadschneidar: *Cellular Automaton Approach to Pedestrian Dynamics-Theory*, In: M. Schreckenberg and S.D. Sharma (Eds.), Proceedings of the International Conference on Pedestrian and Evacuation Dynamics, Springer Berlin, pp. 75-86 (2001).

19. Y. Sugiyama, A. Nakayama, and K. Hasebe: *2-Dimentional Optimal Velcity Models for Granular Flow and Pedestrian Dynamics*, In: M. Schreckenberg and S.D. Sharma (Eds.), Proceedings of the International Conference on Pedestrian and Evacuation Dynamics, Springer Berlin, pp. 155-160 (2001).

20. T. Suzuki and T. Kaneda: *A Simulation Analysis on Pedestrian Flow Management with an Agent-Based Approach - A Reconstruction of the Pedestrian Overpass Accident in Akashi City*, In: T. Terano, H. Kita, T. Kaneda and K. Arai (Eds.), Proceedings of The Third International Workshop on Agent- Based Approaches in Economics and Social Complex Systems (AESCS'04), pp. 269-276 (2004).

21.   S. Wolfram: *Statistical Mechanics of Cellular Automata*, Reviews of Modern Physics 55(3), pp. 601-644 (1983).
22.   A. Borgers and H.A. Timmermans: *A Model of Pedestrian Route Choice and Demand for Retail Facilities within Inner-City Shopping Areas*, Geographical Analysis 18, pp. 115-128 (1986).
23.   G.G. Lovas: *Modelling and Simulation of Pedestrian Traffic Flow*, Transportation Research B 28B, pp. 429-443 (1994).
24.   S.P. Hoogendoorn, P.H.L. Bovy, and W. Daamen: *Microscopic Pedestrian Way-finding and Dynamics Modelling*, In: M. Schreckenberg and S.D. Sharma (Eds.), Proceedings of the International Conference on Pedestrian and Evacuation Dynamics, Springer Berlin, pp. 123-154 (2001).
25.   T. Kaneda, S. Takahashi, and Y. Yokoi: *A Pedestrian Simulator on Shop-Around Behaviour for Town Management Gaming*, On the Edge of the Millennium: A New Foundation for Gaming Simulation Elena Musci, (Ed.) B.A.Graphis, pp.158-163 (2001).
26.   M. O'Kelly: *A Model of the Demand for Retail Facilities*, *Incorporating Multistop, Multipurpose Trips*, In: Geographical Analysis 13(2), pp. 134-148 (1981).
27.   M. Batty, J. DeSyllas and E. Duxbury: *The Discrete Dynamics of Small-Scale Spatial Events: Agent-Based Models of Mobility in Carnivals and Street Parades*, Working Paper 56, Centre for Advanced Spatial Analysis, University College London (2002).
28.   T. Schelhorn et al.: STREETS: *An Agent-Based Pedestrian Model*, Working Paper 9, Centre for Advanced Spatial Analysis, University College London (1999).
29.   M. Haklay, M. Thurstain-Goodwin, D. O'Sullivan, and T. Schelhorn, *" So Go Downtown": Simulating Pedestrian Movement in Town Centres*, Environment and Planning B 28, pp. 343-359 (2001).

The simulation of crowd dynamics at very large events – Calibration, empirical data, and validation

H. Klüpfel[1]

In this article, we show three examples for the application of pedestrian flow simulation and analysis: the Haj to Makkah, the World Youth Day 2005 in Cologne, and the egress (non-emergency) from a football stadium. The former two are among the largest events in the world – concerning the number of participants. Various circumstances are specific for religious events. The persons might perform rituals and therefore the patterns of movement or gathering are governed by rules that go beyond simple necessity or comfort. Furthermore, the persons are usually very much attracted by the (idealistic) aim of their pilgrimage. For the Haj to Makkah, the Jamarat Bridge, where the symbolic stoning of the devil takes place, is the most interesting part concerning crowd dynamics. The same holds for the final service at the World Youth Day 2005 in Cologne, celebrated by the Pope. The paper is divided into five parts: The first section is concerned with model building and the second with the calibration of parameters by empirical data. The following two sections are dealing with simulation results and their verification. The final section summarizes the results, provides recommendations and concludes with the most important implications for the field of crowd dynamics simulation.

1. Model Building

Empirical data is used for model building on the one hand and for verification of results on the other hand. Straightforward approaches of model building are so called empirical models. They use empirical results like the relation between flow and density directly. Examples are the approaches of Pauls [4] and Predtetschenski [11]. These models are usually macroscopic, i.e., they describe the homogenous flow of persons. Adapting the nomenclature of Figure 1, they would be called global queuing models. When individual persons are distinguished, one speaks of microscopic models. Individual means in this context that persons can have different abilities and characteristics which are rep-
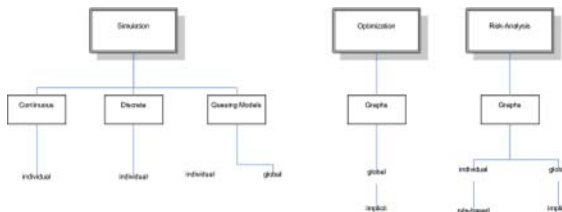
Figure 1: Classification of models.

TraffGo HT GmbH, Office Duisburg, Falkstraße 73—77, 47057 Duisburg, Germany; kluepfel@traffgo-ht.com

resented directly (individually) in the model. This is usually combined with a detailed (microscopic) representation of space – either continuously or discrete. However, it is not the major intention of this paper to classify models. Rather, practical examples and empirical observations are used to highlight the applicability of the different modeling approaches.

2.   Empirical Data and Calibration of Parameters

All the empirical observations shown in this paper relate to large scale events. Two of them are religious events, the Haj to Makkah and the World Youth Day in Cologne. The third is the egress from a football stadium after the match (non emergency). The former two are very large events with several hundred thousand pilgrims. In the later case, the stadium has a capacity of 80,000 persons. There is another distinction – of course – between the Haj and the World Youth Day concerning the operation and the staffs' training. The Haj takes place every year at the same place, the World Youth Day neither takes place every year, nor does it always take place at the same location. This is a major difference, especially concerning the location and the experience of the officials.

2.1. Identification of Key Parameters

Different models are of course based on different assumptions. Often, these assumptions are implicit. This means, that they are not explicitly stated but can be concluded from, e.g., the parameters used in the model. However, even experiments or observations are not free of assumption. In the context of such measurements, a distinction is usually made between independent and dependent variables. The former are varied freely and the latter are determined by the former. An example would be age and walking speed. Age would in this context be the independent and walking speed the dependant variable. Another example is the connection between group size and average walking speeds shown in Table 1. The data has been measured on the pedestrian bridge at the World Exhibition (Expo) 2000 in Hannover (Germany).

Group size	# Groups	Walking Speed / (m/s)
1	95	1,38
2	149	1,28
3	59	1,24
4	17	1,24
5	10	1,22
6	2	1,10
total	332	1,30

Table 1: Dependence of walking speed on group size.

From the connection between age and walking speed it can be seen that there is no one to one correspondence between independent variables and model parameters. In a simulation model, independent as well as dependent variables can be parameters. One can either define age as a parameter – whereas it is never a dependant variable – that has to be specified by the user. For further details see [6].

Or one can "directly" use walking speed as a parameter. Since the relation between age and walking speed is pre-determined, these two approaches are analogous.
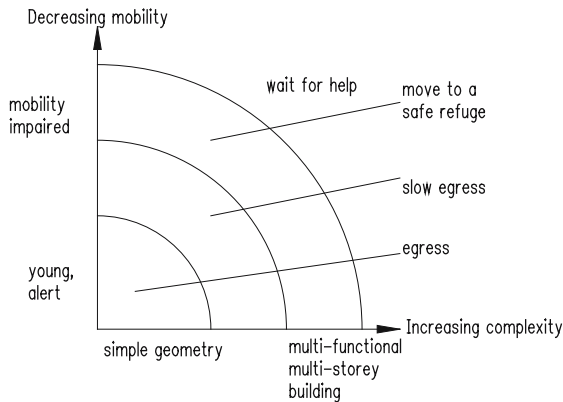
Figure 2: Different strategies for egress depending on the individual movement ability and the complexity of the surroundings.

However, for other parameters, the case is more complicated. Physiological variables can usually be accessed directly. Therefore, their distribution within a given population is usually known or can be derived via relations to other known variables. However, for psychological (or even sociological) parameters, like orientation capability, decision making abilities or group binding, this is not the case. Therefore, these are typically calibration parameters. The general question arises, whether they should be included in a model as parameters at all. Figure 2 shows different individual strategies for egress. They could be connected to the orientation capability shown in Table 2. This schematic relation between geometrical complexity, individual movement ability and egress strategy is neither functional nor quantitative. Therefore, it is not suited in this form for implementation in a simulation model. In stochastic models, however, parameters that represent probabilities can be used. One such parameter is for example an orientation frequency, which specifies the frequency of abrupt stops due to the need for orientation. The range of this parameter is per definition restricted to the interval from 0 to 1.

2.2. Quantification of Parameters

When quantifying parameters of phenomenological models, some of the parameters are per definition calibration parameters. This means they cannot be measured directly, but are calibrated by adapting simulation results to measureable quantities.

Name	Empirical quantity	Measurement
Free walking speed	Same	Video footage
Orientation capability	Decision time (?)	Video footage
Age	Same	Statistical tables
Gender	Same	Statistical tables
Further person parameters	Same	Statistical tables
Route choice	Strategy	Questionnaire
Motion impairment	speed reduction	Video footage
	lateral deviation	

Table 2: Relation between model parameters and empirical quantities.

It is usually not possible to determine the parameters for a population directly. Therefore, standard populations, e.g. a average populations, must be defined. One approach is to use census data. The column "measurement" in Table 2 indicates how each quantity can be "measured" respectively determined. The parameter "route choice" is illustrated in Figure 2. Many additional parameters can be defined, of course.

3. Simulation Results

Simulation results are the only way to verify (or falsify, if one prefers the Popperian concept) a model as a whole. Of course, there is no first principles approach to pedestrian movement. The term "ball bearing models" might partly result from this misunderstanding, either because the application range of a model based on first principles (i.e. non-phenomenological) has not been clearly stated or the fact that every model is based on simplifications is misunderstood.

Term	Definition
Validation	Validation and Verification are used synonymously.
Simulation	The systematic application of a (mathematical) model to obtain quantitative statements (i.e. numbers) that correspond to real world phenomena.
Validity	A number is valid, if it actually describes what it is intended to describe.
Reliability	A quantity is reliable, if repeated measurements (with the same boundary conditions) provide the same results.

Objectivity	The fact that the same results can be obtained by several persons (if the same assumptions are made).
Calibration	The adjustment of a parameter to obtain correct simulation results.
Dependent Variables	are those quantities that are actually measured. Measurement is not restricted to empirical observations but comprises also simulation results.
Independent Variables	are those that can be tuned by the user
Parameter	Parameters are independent variables in models.

Table 3: Glossary.

3.1. Haj

The empirical data concerning the Haj is manifold [1]. Since it takes place every year, much information has been collected concerning the pilgrims' movement.

Figure 3: Proposed new design for the Jamarat Bridge [16].

Currently, a major restructuring of the Mina area is under-way. The situation is different for the WYD however, where there is basically no quantitative data available. For the first case the data is used to calibrate the model and then simulations are performed to support the planning for the improvement of the structures. By comparing the performance of different procedures, operation guidelines can be formulated. Further empirical data will be available in the future. Therefore, the impact of the changes can be scrutinized and compared to the simulated predictions. The proposed bridge is shown in Figure 4. In the scenario considered here, there are 100,000 persons distributed equally on the bridge. The persons are indicated by the small red dots. This is an extreme case which is rather a worst case test. It does not imply that such a situation will occur regu-
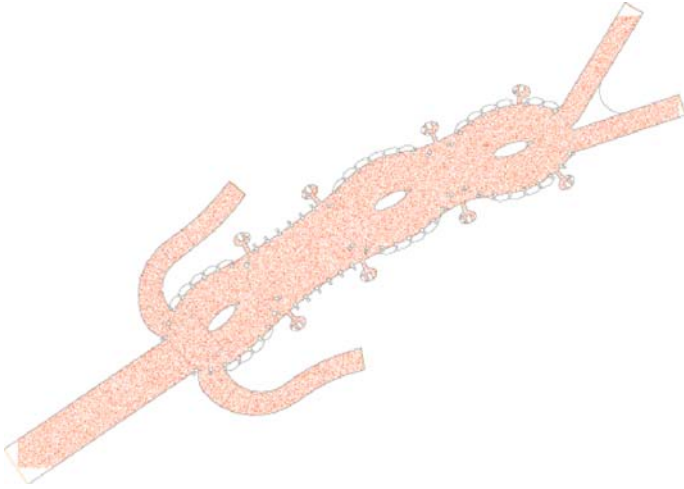
Figure 4: One level of the proposed new Jamarat Bridge.

larly in this environment. As can be seen from Figure 5, the simulation results (in this case the position of the persons after 10 minutes) depend on the assumptions made. The major influence in this case is the route choice of the persons. In the simulation, this route choice is modeled via a so called potential. Other authors call this "distance metric" [2] or static field [3]. However, the method is always based on using the distance to the exit or some intermediate goal to determine the direction of motion.

Of course this method can be refined by defining groups of persons and areas within the geometry where the potential is adapted to certain further assumptions (e.g., doors potential spreads through preferably).

The term potential is quite intuitive in this context, since the distance metric is similar to an electrostatic potential with a single source for a simple geometry.

There are additional boundary conditions, e.g. the walls which basically have a potential of minus infinity, i.e. cannot be penetrated. These boundary conditions do not compare to any boundary conditions used in electrostatics, however. The important point is that these assumptions concerning the route choice often determine the simulation results. The route-choice is normally not a result of the simulation, but is a pre-defined simulation parameter. Even if a complex method is applied (i.e. definition of several groups, guiding via a route choice graph, and additional limitations or boundary conditions for the determination of the walking direction which corresponds to the potential), all these have to be set by the user of the simulation.

This argumentation becomes quite clear, when one takes into account the fact that otherwise an artificial intelligence approach is necessary. The decisions made by the agents would then require a mental representation of the geometry every agent can access. Furthermore, there would have to be rules which model the decision making process of the individual. Whether these rules are deterministic or stochastic does not matter. At the
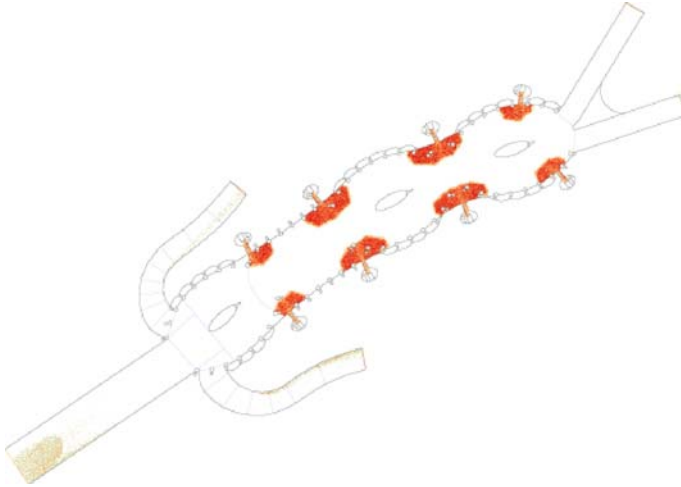
Figure 5: Situation after 10 minutes.

end of the day, parameters must be defined, which describe the different strategies of the agents. The decision, how to tune these parameters would again be the task of the user. Another argument for the importance of the user's settings is the analogy between a simulation and an evacuation trial or real evacuation. It is not only the evacuees themselves who autonomously decide which route to take. Of course, the staff members, the signage and other parts of the evacuation system influence the movement behavior and route choice. In this sense, a model simplifies and quantifies these influences. Since there are no first-principle rules, every model for crowd movement is phenomenological. This means, that its intended use is to correctly reproduce phenomena but not to describe the agents' behavior on a microscopic level.

3.2. World Youth Day

The World Youth Day took place in August in Cologne, Germany. The final event was a service with Pope Benedict XVI. It took place on a large ground (around 92 ha) with a stage in the centre. The geometry is shown in Figure 6.

Altogether around 700 to 800 thousand pilgrims were expected. Apart from the requirements to the roads and public transportation systems, the footpaths play of course also an eminent role in the mobility concept.

Two cases must be distinguished, when analyzing the geometry and operational performance: a normal case of getting to and back from the area and the emergency case, when part of the site has to be evacuated. In the former case, a time frame of 8 to 10 hours was considered. Since the final service was held in the late afternoon, the mobility concept is also based on a considerable part of the pilgrims staying at the place overnight. The major bottleneck is not the movement of pedestrians anyway, but the capacity of the

Figure 6: The area where the World Youth Day 2005 was held.

transportation system. A completely different scenario is emergency evacuation.
Since the size of the area is about 2km in East-West and about 1.6 km in North-South direction, a complete evacuation is in most cases neither sensible nor necessary. One point that is omitted in the presentation here is – due to lack of space and since it was performed by others – a quantitative risk analysis. The scenarios taken into account for the evacuation simulation were mainly accidents with trucks or a fire in an infrastruc-
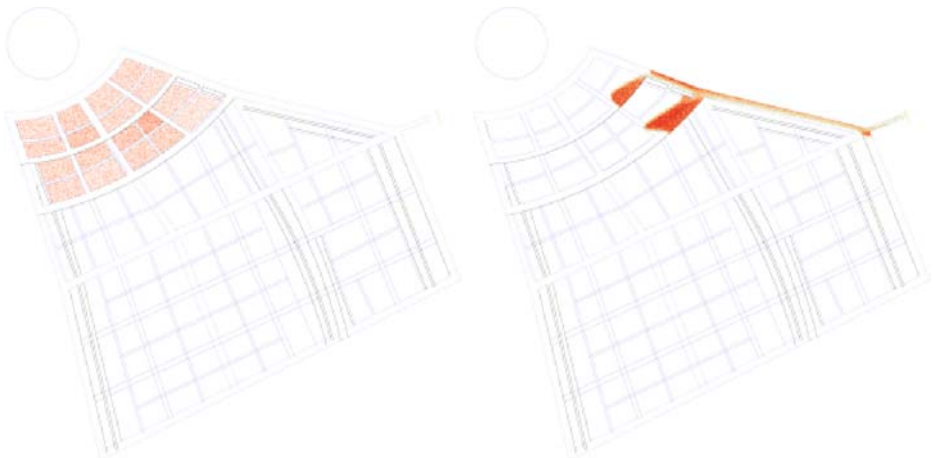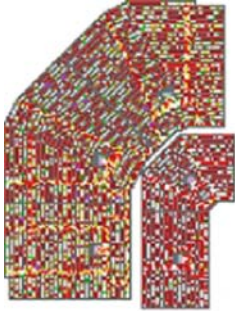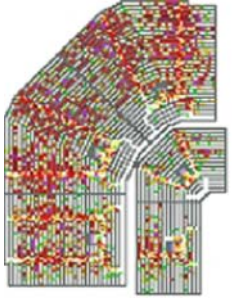
Figure 7: Simulation of the (fast) egress from four zones at the world youth day. The left part shows the initial population distribution and the right part the situation after 30 minutes.

ture unit. In these cases, the strategy is to evacuate the field affected directly and the neighboring field (fields are the rectangular or nearly quadratic areas in Figure 6 that form the smallest building blocks). The neighboring field was then the one where first aid facilities would be installed.

4.   Verification of the Results

Concerning quantitative verification, movement patterns provide a valuable tool to investigate the reliability of simulation results. In the following table, data from video footage is compared to simulation results. The most prominent aspect is the egress from the seating rows. The lower rows are emptied first. The difference at t=2 min is due to the shorter reaction time of the agents. Similar to reality, in the simulation the lower blocks are emptied earlier.

Reality	Simulation
t = 2 min: Only few spectators have started moving.	t = 20 s: Some of the agents have moved.
t = 5 min: Most of the spectators have reacted. Congestion forms on the stairs and in the seating rows.	t = 3 min: Most of the agents have reacted.

Reality	Simulation
t = 7 min: All spectators move.	t = 6 min: The lower blocks are already empty.
t = 10 min: Congestion remains only on the stairs.	t = 10 min: Different from reality the blocks 85, 86, and 89 are already empty.
t = 13 min: Blocks 85, 86, and 89 are empty.	t = 13 min: Apart from block 87, all blocks are empty.

Especially concerning the geometry, simulations can provide valuable hints on the creation, duration, and location of congestion.

5.   Recommendations and Conclusion

In this paper, three different events with very high numbers of pedestrians were presented. The simulation results are strongly determined by the choice of parameters, especially route choice strategies. An important aspect in the egress from football stadiums is the v-like shapes that are formed since the egress from the lower seating rows is faster. Recommendations can be derived from the observations and simulation results shown in two different ways: On the one hand, general recommendations, applicable for all large crowd events. On the other hand, there are specific recommendations that apply only for the specific event. The later takes into account the specific geometry and character of the event.

Acknowledgements

References

1.   S. AlGadhi, H. Mahmassani, and R. Herman: *A Speed-Concentration Relation for Bi-Directional Crowd Movements with Strong Interaction*, In: M. Schreckenberg and S.D. Sharma (Eds.), Proceedings of the Internaltional Conference on Pedestrian and Evacuation Dynamics, Springer, Berlin, pp. 3–20 (2002).
2.   P. Thompson, J. Wu, and E. Marchant: *Modeling Evacuation in Multi-Storey Buildings with 'Simulex'*, In: Fire Engineers Journal 56 (185), pp. 6–11 (1996).
3.   C. Burstedde, K. Klauck, A. Schadschneider, and J. Zittartz: *Simulation of Pedestrian Dynamics using a 2-Dimensional Cellular Automaton*, In: Physica A 295, pp. 507–525 (2001).
4.   J. Pauls: *Movement of People* [2nd edition], Chapter 3-13, pp. 3-263 - 3-285, In: DiNenno [10] (1995).
5.   U. Weidmann: *Transporttechnik der Fußgänger, Transporttechnische Eigenschaften des Fußgängerverkehrs*, Literaturauswertung, Schriftenreihe des IVT 90, ETH Zürich, January 1992 (1992).
6.   H. Klüpfel: *A Cellular Automaton Model for Crowd Movement and Egress Simulation*, Dissertation, Universität Duisburg (2003).
7.   RiMEA-Projekt: *Richtlinie für Mikroskopische Entfluchtungsanalysen*, www.rimea.de
8.   J. Fruin: *Pedestrian Planning and Design*, New York, Metropolitan Association of Urban Designers and Environmental Planners (1971).
9.   Transportation Research Board: *Highway Capacity Manual*, Washington, D.C., Transportation Research Board (1994).

10. P. DiNenno (Ed.): *SFPE Handbook of Fire Protection Engineering* (2nd edition), National Fire Protection Association (1995).

11. W. Predtetschenski and A. Milinski: *Personenströme in Gebäuden – Berechnungsmethoden für die Modellierung*, Köln-Braunsfeld: Müller (1971).

12. K. Ando, H. Ota, and T. Oki: *Forecasting the Flow of People*, In: Railway Research Review 45, pp. 8–14. (in Japanese) (1998).

13. J. Westphal: *Untersuchungen von Fußgängerbewegungen auf Bahnhöfen mit starkem Nahverkehr*, Institut für Verkehrswesen, Eisenbahnbau und –betrieb, Technische Universität Hannover, Dissertation (1971).

14. Statistisches Bundesamt (Ed.): *Datenreport 1999 – Zahlen und Fakten über die Bundesrepublik Deutschland*, Bonn (2000).

15. F. Mehl: *Bauaufsichtliche Akzeptanz von Ingenieurmethoden im baulichen Brandschutz – Anwendungsbereiche, Grenzen*, Promat Fachbeitrag, Ratingen, www.promat.de (2003).

16. Haj & Umra: Volume 59, Issue 2, April 2004, Ministry of Haj, Riyadh, Saudi-Arabia (2004).

Moore and more and symmetry

T. Kretz and M. Schreckenberg[1]

In any spatially discrete model of pedestrian motion which uses a regular lattice as basis, there is the question of how the symmetry between the different directions of motion can be restored as far as possible but with limited computational eort. This question is equivalent to the question „How important is the orientation of the axis of discretization for the result of the simulation?" An optimization in terms of symmetry can be combined with the implementation of higher and heterogeniously distributed walking speeds by representing different walking speeds via different amounts of cells an agent may move during one round. Therefore all different possible neighborhoods for speeds up to v = 10 (cells per round) will be examined for the amount of deviation from radial symmetry. Simple criteria will be stated which will allow to find an optimal neighborhood for each speed. It will be shown that following these criteria even the best mixture of steps in Moore and von Neumann neighborhoods is unable to reproduce the optimal neighborhood for a speed as low as 4.

1. Introduction

In a model which is spatially and temporally discrete the speed of an agent (as the model of a person in a simulation will be called) is the number of cells which he moves during one round. As the real-world interpretation of the size of a cell is fixed by the scale of the discretization, the real-time interpretation of one round fixes the real-world interpretation of such a dimensionless speed.

Subsequent steps within one of the neighborhoods of Fig. 1, leave an agent to be either $\sqrt{2}$ times as slow or as fast moving into the diagonal direction than moving horizontally or vertically. To some extent the situation can be improved by a mixture of von Neumann and Moore neighborhoods. If for example an agent would be allowed to do a total of five steps during one round, of which three are in von Neumann and two in Moore neighborhood, a larger total neighborhood of cells which can be reached during one
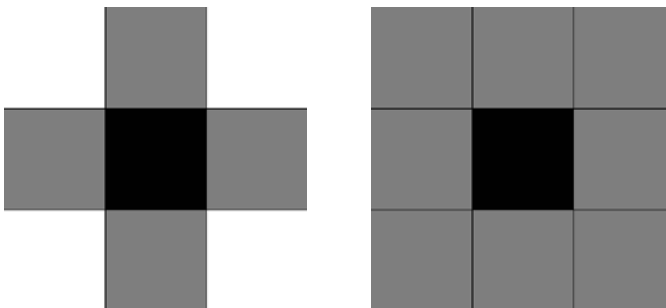
Figure 1: von Neumann- and Moore-neighborhood (*v=1*)

Physik von Transport und Verkehr, Universität Duisburg-Essen, 47057 Duisburg, Germany

round would result. The question is: Is there an optimal total neighborhood for a given speed? And can it be composed of von Neumann and Moore neighborhoods? In vertical and horizontal direction there is no doubt about the neighborhood: For a speed $v = v_m$ the neighborhood contains the cell of the agent and vm cells in each horizontal or vertical direction. For any other direction there are cells for which it is not obvious if they should be part of the neighborhood. At the very beginning for $v = 1$ there is the question if one should use the von Neumann or Moore neigborhood. (See Fig. 1).

Definition: Complete neighborhoods are four-fold symmetrical neighborhoods where all cells which belong to the neighborhood are closer to the center cell than those which do not.

Example: There are three complete neighborhoods for each $v = 2$ and $v = 3$. (See Figs. 2 and 3.)
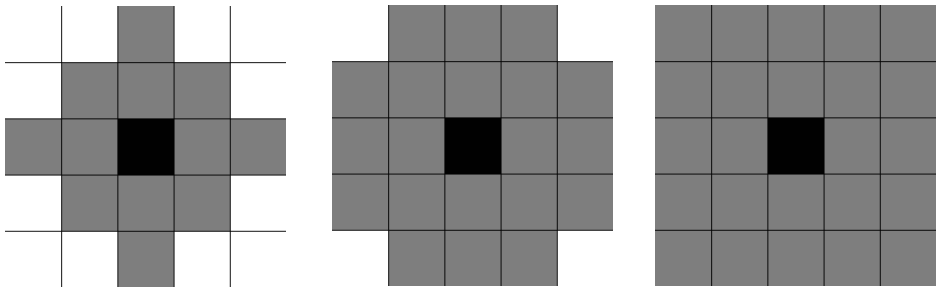
Figure 2: Complete neighborhoods for $v=2$
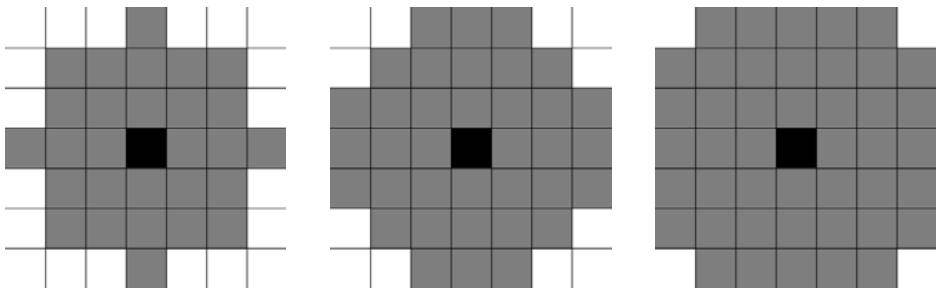
Figure 3: Complete neighborhoods for $v=3$

Obviously one can limit the search for an optimal neighborhood to complete neighborhoods.

The question is, which complete neighborhood represents the corresponding speed (which is number of cells in horizontal and vertical direction) best. However there might

exist other alternatives, the criteria chosen here are such that discretization eects concerning the axis of discretization of the original plan are minimized. Therefore at first for each complete neighborhood the speed v(ɸ) into each direction has to be written down. Then the direction-averaged speed is calculated:

$$\langle v \rangle = v_{av} = \frac{1}{2\pi} \int_\phi v(\phi) d\phi$$

(1)

After that the squared deviation of speeds into each direction from this average is calculated.

$$\Delta v = \sqrt{\frac{1}{2\pi} \int_\phi (v(\phi) - v_{av})^2 d\phi}$$

(2)

The criteria for an optimal neighborhood are then

» The direction averaged speed should be close to the corresponding integer.
» The deviation from this average into dierent directions should be small.

Complete neighborhoods up to $v = 10$: The neighborhoods are named by the maximum squared distance of a cell from the center, implying that neighborhood Y includes all cells of neighborhood $X \le Y$. For reasons of clarity in the following table the numbers are only shown in the second octant.

100	101	104	109	116			
81	82	85	90	97	106	117	
64	65	68	73	80	89	100	113
49	50	53	58	68	74	85	98
36	37	40	45	52	61	72	
25	26	29	34	41	50		
16	17	20	25	32			
9	10	13	18				
4	5	8					
1	2						
0							

NB: Of neighborhoods in the previous table only the neighborhoods 1, 2, 4, 5, 8, 10, 13, 17, 20, 29, 34, 40, 45, 58, 80 and 97 can be composed of the corresponding number of subsequent steps within von Neumann and Moore neighborhoods. (Take N von Neumann and $M = v - N$ Moore steps and check how the largest possible neighborhood looks like.)

1.1. v(φ) – the variation of speed with the direction of motion

Since all complete neighborhoods have a fourfold axe-symmetry it is sufficient to cal-
culate v(φ) for $0 \le \phi < \pi/4$.

v(φ) is continuously composed from dierent functions resulting from different ranges
of φ. The structure of those ranges depends on the shape of the edge of the neighborhood
(See Fig. 4).

Definitions:

δx_i horizontal distance (in cells) of a border cell to the origin (the black cell in Fig. 4);
with *i* starting with 0 at φ = 0 (see the numbering in the black circles in Fig. 4)

δy_i vertical distance of a border cell to the origin; with *i* starting with 0 at φ = 0

D a large distance

ΔX $D\cos(\phi)$

ΔY $D\sin(\phi)$

N total (minimal) number of steps to reach a cell in distance D into direction
$$\arctan\left(\frac{\delta y_i}{\delta x_i}\right) \le \phi_i < \arctan\left(\frac{\delta y_{i+1}}{\delta x_{i+1}}\right)$$

n number of steps into direction $(0/0) \rightarrow (\delta x_i/\delta y_i)$

$N\text{-}n$ number of steps into direction $(0/0) \rightarrow (\delta x_{i+1}/\delta y_{i+1})$
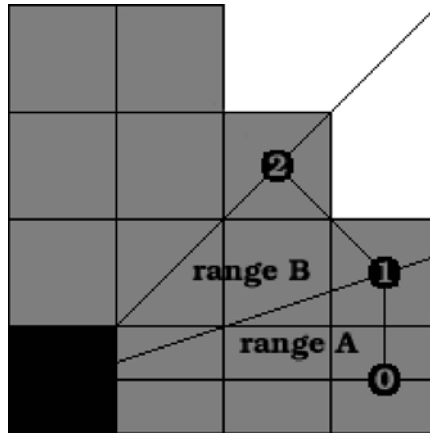
Figure 4: Example for calculating *v(φ)* for one of the *v=3* neighborhoods

To reach the point $(\Delta X/\Delta Y)$ an agent has to do n times a $(\delta x_i/\delta y_i)$ step and $(N - n)$ times a $(\delta x_{i+1}/\delta y_{i+1})$ step.
Such that

$$n\delta x_i + (N - n)\delta x_{i+1} = \Delta X \tag{3}$$
$$n\delta y_i + (N - n)\delta y_{+1} = \Delta Y \tag{4}$$

Solving this for N leads to

$$N = \frac{\Delta Y - r\Delta X}{\delta y_{i+1} - r\delta x_{i+1}} \tag{5}$$

where

$$r = \frac{\delta y_{i+1} - \delta y_i}{\delta x_{i+1} - \delta x_i} \tag{6}$$

In the intervall $[0,\pi/4]$ r can only take the values ∞ (range A in Fig. 4) and -1 (range B) which in the latter case in equation (5) has to be understood as limit. r is the local gradient of the border of the neighborhood.
Since speed is distance (in cells) over number of rounds to move that distance, one has

$$v(\phi) = \frac{D}{N} = \frac{\delta y_{i+1} - r\delta x_{i+1}}{\sin\phi - r\cos\phi} \tag{7}$$

See Fig. 5 for the speed's dependence on the direction of motion of all three complete v = 2 neighborhoods.
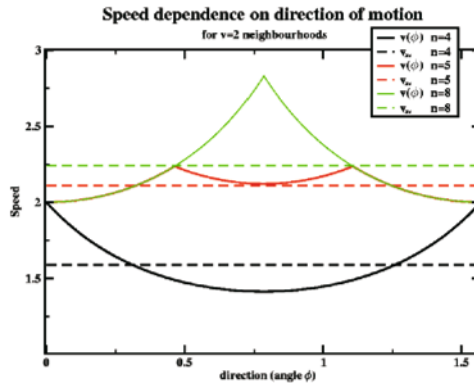
Figure 5: Example for the $v(\phi)$ dependence. ($v = 2$ neighborhoods 4, 5 and 8)

1.2. The integrals for the average speeds and the deviations

For ranges with the same gradient of the border as in range A (vertical, see Fig. 4) to get the average one has to integrate:

$$I_i^A = \int_{\phi=\phi_i}^{\phi_{i+1}} \frac{1}{\cos\phi}\,d\phi = \ln\left(\frac{\tan\left(\frac{\phi_{i+1}}{2}+\frac{\pi}{4}\right)}{\tan\left(\frac{\phi_i}{2}+\frac{\pi}{4}\right)}\right)$$

$$(8)$$

$$= \ln\left(\frac{\sqrt{1+\tan^2\phi_{i+1}}+\tan\phi_{i+1}}{\sqrt{1+\tan^2\phi_i}+\tan\phi_i}\right)$$

$$(9)$$

and for a range like range B (diagonal):

$$I_i^B = \int_{\phi=\phi_i}^{\phi_{i+1}} \frac{1}{\sin\phi+\cos\phi}\,d\phi = \frac{1}{\sqrt{2}}\ln\frac{\tan\left(\frac{\phi_{i+1}}{2}+\frac{\pi}{8}\right)}{\tan\left(\frac{\phi_i}{2}+\frac{\pi}{8}\right)}$$

$$(10)$$

$$= \frac{1}{\sqrt{2}}\ln\left(\frac{(\sqrt{2(1+\tan^2\phi_{i+1})}-1+\tan\phi_{i+1})(1+\tan\phi_i)}{(1+\tan\phi_{i+1})(\sqrt{2(1+\tan^2\phi_i)}-1+\tan\phi_i)}\right)$$

$$(11)$$

NB: To get the average speed in that range additionally one would have to normalize the integrals.

The average for the whole first octant is the sum

$$v_{av} = \frac{4}{\pi}\sum_i I_i^X(\phi_i,\phi_{i+1})$$

$$(12)$$

For the deviation integrals

$$\int_{\phi=\phi_i}^{\phi_{i+1}} (v(\phi)-v_{av})^2\,d\phi$$

$$(13)$$

the additionally needed integrals are

$$\int_{\phi=\phi_i}^{\phi_{i+1}} \frac{1}{\cos\phi^2}\,d\phi = \tan\phi_{i+1} - \tan\phi_i$$

$$(14)$$

and

$$\int_{\phi=\phi_i}^{\phi_{i+1}} \frac{1}{(\sin\phi + \cos\phi)^2}\,d\phi = \frac{1}{2}\left(\tan\left(\phi_{i+1} - \frac{\pi}{4}\right) - \tan\left(\phi_i - \frac{\pi}{4}\right)\right)$$

(15)

$$= \frac{1}{2}\left(\frac{1 + \tan\phi_{i+1}}{1 - \tan\phi_{i+1}} - \frac{1 + \tan\phi_i}{1 - \tan\phi_i}\right)$$

(16)

1.3. Results

However all integrals are simple and analytic, the analytic results do not provide too much insight and in the following only the numerical results are given. The following average speeds and deviations were calculated:

neighb. $(d^2{}_{max})$	average speed	relative deviation	neighb. $(d^2{}_{max})$	average speed	relative deviation
1	0.79	0.105	2	1.12	0.105
4	1.59	0.105	5	2.11	0.033
8	2.24	0.105	9	2.52	0.080
10	2.98	0.033	13	3.28	0.067
16	3.47	0.055	17	3.82	0.054
18	3.91	0.043	20	4.22	0.033
25	4.57	0.064	26	4.85	0.039
29	5.11	0.024	32	5.17	0.028
34	5.40	0.054	36	5.52	0.043
37	5.75	0.034	40	5.97	0.033
41	6.13	0.026	45	6.33	0.033
49	6.43	0.030	50	6.67	0.035
52	6.86	0.039	53	7.05	0.019
58	7.22	0.024	61	7.35	0.034
64	7.44	0.030	65	7.77	0.029
68	7.94	0.019	72	7.98	0.021
73	8.13	0.024	74	8.29	0.023
80	8.44	0.033	81	8.52	0.028
82	8.66	0.026	85	8.92	0.023
89	9.06	0.025	90	9.20	0.015
97	9.34	0.025	98	9.37	0.026

neighb. (d^2_{max})	average speed	relative deviation	neighb. (d^2_{max})	average speed	relative deviation
100	9.57	0.030	101	9.70	0.025
104	9.83	0.021	106	9.96	0.019
109	10.09	0.014	113	10.18	0.019
116	10.31	0.023	117	10.43	0.024

Table 1:   Average speeds and relative deviations (by angle) for all complete neighborhoods up to v=10

However there are ambiguities, these information point to this choice of neighborhoods (of which only the ones for speeds 1,2,3,5 and 6 can be composed out of the corresponding number of subsequent von Neumann or Moore steps):

speed	neighborhood (d^2_{max})
1	2
2	5
3	10
4	18
5	29
6	40
7	53
8	72
9	89
10	109

resulting in this quarter of speed neighborhoods (an agent with maximum speed v_m can reach all cells with a number $\leq v_m$):

10	10	10	10							
9	9	9	10	10	10					
8	8	8	9	9	9	10				
7	7	7	8	8	9	9	10			
6	6	6	7	7	8	8	9	10		
5	5	5	6	7	7	8	9	9	10	
4	4	5	5	6	7	7	8	9	10	
3	3	4	4	5	6	7	8	9	10	10
2	2	3	4	5	5	6	7	8	9	10
1	1	2	3	4	5	6	7	8	9	10
0	1	2	3	4	5	6	7	8	9	10

2.   A model of pedestrian motion

As it is not in the main scope of this paper, the model which makes use of the ideas above will now be presented only in short:

Space becomes discretized into quadratic cells with 40 cm as length of an edge. Each cell may be occupied by at most one agent.

Before the beginning of the main part of the simulation, the individual parameters { as the maximum speed { are spread over all agents.

Then the agents are assigned (deterministically or randomly) to their starting position.

Round by round the agents repeat the following steps until all agents have left the scenario via an exit:

» All agents in parallel choose one of the cells (destination) within the neighborhood assigned to their maximum speed.
» The agents sequentially try to reach their destination cell.

The rules for the selection of a destination cell are quite complex, while the rules of movement are rather simple. Former ones are probabilistic. Most important for the decision process is the higher probability to select a cell as destination if it lies closer to the exit (probability $p \propto exp(k_S(S_{max} - S))$), with coupling strength k_S and distance S to exit). But also herding behavior, inertia, and the distance towards other agents as well as walls can play a role. In many aspects this part of the model is a higher speeds extension of the model described in Refs. [1, 2].

The rules of actual motion are deterministic, however the sequence in which the agents carry out their steps is chosen randomly. Each agent moves within a Moore neighborhood to that cell that lies closest to his destination cell. If no cell is available that is closer to the destination cell than his current position he remains where he is. A once used cell remains blocked for the rest of the round (see Ref. [3]).

3.   Testing the symmetry and the discretization artifacts

3.1.   Walking speeds and travel times of single agents

To test the benet of the considerations above for the equality of directions several simulations were carried out, where one agent moved a distance of 325 (the number < 1000 with the most solutions of Pythagoras: $325^2 = A^2+B^2$) cells into eight dierent directions with two dierent speeds. Each simulation was carried out 100 times. k_S has been set to 10.0 to make the simulation nearly deterministic.

Δx	253	260	280	300	312	315	323	325
Δy	204	195	165	125	91	80	36	0
$\rightarrow$ angle	38.9	36.9	30.5	22.6	16.3	14.3	6.4	0
$<T_{v=1}>$	274.2	276.2	285.8	303.8	313.8	316.5	324.1	326.0
$\pm$ St:D:	3.7	3.3	1.8	1.4	0.9	0.7	0.2	0.1
$<T_{v=5}>$	67.5	67.0	66.0	64.9	65.0	65.2	66.0	66.0
$\pm$ St:D:	0.5	0.2	0.2	0.4	0.4	0.4	0.0	0.0

So the overall average evacuation time for $v = 1$ was 302.6 rounds $\pm$ 7.00 rounds (2.30%), while for $v = 5$ it was 65.9 rounds $\pm$ 0.30 rounds (0.46%). This means that standarddeviation of the overall average is roughly by the same factor (5) smaller as the speed is larger. If one wants to interpret the agents moving in the two examples with 2 m/sec for $v = 1$ one round has to be interpreted as 0.2 seconds and for $v = 5$ one round would be one second. Then for $v = 1$ the time to move as far as 130 m would vary with the orientation of the discretization axis by more than 10 seconds ((326.0-275.2)*0.2), while for $v = 5$ it would be only 2.5 seconds (67.4-64.9).

3.2. A radially moving crowd

1948 agents were spread over 194812 cells of a circle area (radius 249 cells). With four exit cells in the center of the circle the agents started to move at once towards the center of the circle. The calculation was done twice: At first all agents had a maximum speed 1, during the second run, they had a maximum speed 5. See Fig.s 6 for a comparison of how the initially rotationally symmetric spatial distribution of agents evolves with time in the two cases.

Figure 6: Comparison of two simulations with a crowd (black) moving to the center of a circle. The left image shows $v=1$ agents after 180, the right one $v=5$ agents after 36 rounds.

As a last test we compared the simulated walking times of the two alternative routes (called A: Start $\rightarrow 2 \rightarrow 4 \rightarrow$ Exit and B: Start $\rightarrow 1 \rightarrow 3 \rightarrow 5 \rightarrow$ Exit) shown in Fig. 7. In reality route B is $\sqrt{2}$ times as long as route A and so should the walking times be for pedestrians with identical speeds. So this is a specic comparison of motion into the two directions 0 and 45 degree.

These are the average (ten simulations) walking times for agents with a certain speed:
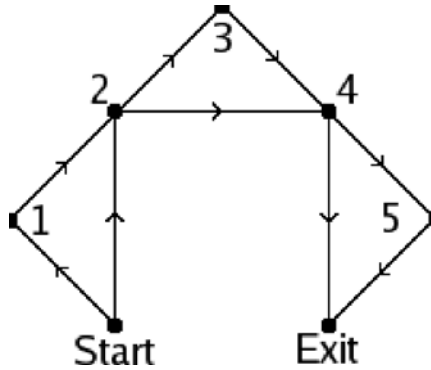
Figure 7: Two routes: Route A contains horizontal and vertical, route B diagonal parts.

	T_A	T_B	T_B/T_A	$T_B/(\sqrt{2}T_A)$
$v = 1$	291.1	328.4	1.13	0.80
$v = 2$	147.0	202.4	1.38	0.98
$v = 3$	98.6	155.2	1.57	1.11
$v = 4$	74.2	102.9	1.39	0.98
$v = 5$	59.4	86.7	1.46	1.03

The deviations from 1 in the last column are due to the integer valuedness of the static floor field which leads to probabilistic path-choosing-behavior even in the deterministic limt $k_S \rightarrow \infty$. For a real valued static floor field the last column would contain only 1.00s.

4.   Conclusions

In means of minimizing artifacts of discretization, we presented two criteria to identify the best neighborhoods for speeds larger one. We presented the results of simulations which compared motion in Moore neighborhood steps with motion in steps within the best neighborhood for $v = 5$. Depending on the observable the results showed the reduc-

tion of discretization artifacts by a factor of four or even five for the latter neighborhood. This becomes specially interesting in case of finer discretizations, where a subsequent execution of steps within Moore or von Neumann neighborhoods would lead to the same dependence of evacuation times on the orientation of the axis of discretization, yet on smaller space-scales. **«**

References

1.   K. Nishinari, A. Kirchner, A. Namazi, and A. Schadschneider: *Extended Floor Field CA model for Evacuation Dynamics*, cond-mat/0306262, December 2003 (2003).
2.   A. Kirchner, K. Nishinari, and A. Schadschneider: *Friction Effects and Clogging in a Cellular Automaton Model for Pedestrian Dynamics*, In: Phys.Rev. E, 67:056122, 2003, cond-mat/0209383 (2003).
3.   H. Klüpfel: *A Cellular Automaton Model for Crowd Movement and Egress Simulation*, PhD Thesis, Universität Duisburg-Essen, http://www.ub.uni-duisburg. de/ETD-db/theses/available/duett-08012003-092540/ (2003).

The RiMEA Project –
Development of a new Regulation

T. Meyer-König[1], N. Waldau[2], and H. Klüpfel[1]

The guideline MSC/Circ.1033, developed by the International Maritime Organisation in 2002 is the only regulation worldwide, which defines a minimum standard for simulation tools and how they have to be applied in order to perform an evacuation analysis. Its application is mandatory for RoPax vessels, ferries carrying rolling cargo as well as passengers.

However, for the use of evacuation simulations in land based applications like buildings, no precise regulation existed. Authorities having to assess evaluations based on simulations had to rely on the seriousness of the person or company performing the simulations. The following paper introduces the RiMEA project which was among others initiated by TraffGo HT. Based on the uniquely organized work of about forty participants (fire safety engineers, simulation developers and authorities) from Switzerland, Austria and Germany a new guideline for the building industry is developed. It will reach its second level of completion when PED2005 is taking place.

1.   Approval of Evacuation Concepts

There are basically three ways to ensure compliance of escape routes (lengths, exit widths) with the relevant regulations:

» material requirements according to the federal or state laws (regulations for places of convention) and the accompanying technical recommendations,

» approval according to generally accepted technological rules (DIN, ISO, EN) and

» approval according to the state of the art based on scientific and engineering methods.

Scientific and engineering methods are the application of approaches, principles, and methods that are based on scientific knowledge and comprise theoretical as well as practical (empirical) aspects.

2.   Programmes for the simulation of pedestrian streams

Programmes for the simulation of pedestrian streams are a scientific method which is used to assess and optimise the safety and evacuation concepts for building structures. Especially for special buildings which are not covered by the general building codes and are usually occupied by a large number of persons, such simulations are the tool of

---

[1]TraffGo HT GmbH, Flensburg/Germany

[2]Waldau Engineering, Vienna/Austria

choice. Furthermore, they fit nicely into a holistic and proactive safety concept.

Simulations are based on models which represent every individual and the floor plan in detail. Additionally, the interaction between the persons and between each person and her environment is taken into account.

Due to the complexity of many structures and having in mind the large scale events like the football world championships 2006 in Germany and European championships 2008 in Austria and Switzerland the required levels of safety and comfort can much more easily be achieved by applying such methods. This does not only comprise the football stadiums and public viewing areas but also infrastructure facilities like railway stations and airports.

For the scenarios most relevant in this context, computer based simulations are necessary. They are able to simulate the relevant scenarios and specific cases. The results are straightforward and understandable. Therefore, it becomes possible to predict congestion that might occur during an evacuation due to normal and emergency movement along the escape routes. This enables to assess structural or operational procedures to mitigate such congestion.

3.   Reliability, Validity, and Validation of Software Programmes

However, the application of such simulation based methods poses new challenges to administrations and authorities. In line of these considerations and especially with respect to the assumptions concerning parameters and scenarios standardized criteria are required. The same holds for the assessment of the reliability and validity of software programmes.

In Germany, Austria, and Switzerland there are currently no distinctive laws or regulations for this purpose. Authorities and engineering consultancies therefore usually have to rely on the reputation of software developers.
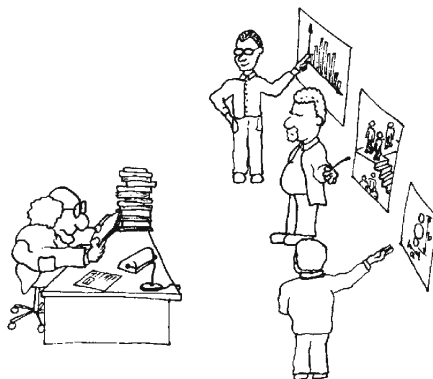
Figure 1: Without standardization, authorities have to rely on the reputation of software developers.

3.1. Goals of the RiMEA – Project

In order to improve the situation just described and to provide a reference for all those involved to assess the results of evacuation simulations a group of experts from Austria, Germany, and Switzerland founded the RiMEA Project early 2004. It is the aim of this project to establish guidelines for the performance of evacuation analyses for buildings. These guidelines are partially modelled after the International Maritime Organizations (IMO) Marine Safety Committees (MSC) circular on "Interim Guidelines on Evacuation Analyses for New and Existing Passenger Ships".
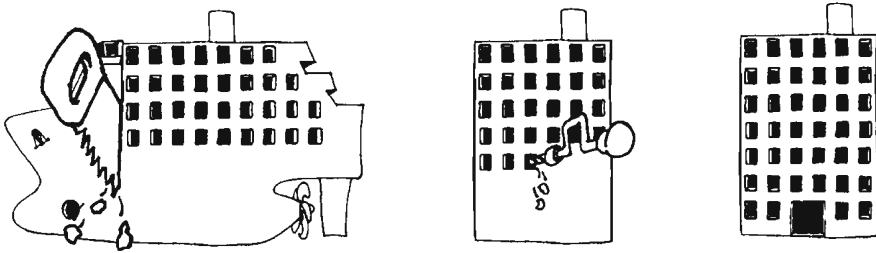
Figure 2: The basic RiMEA guideline was derived from the maritime guideline for evacuation analyses of passenger ships.

Especially architects, approval and regulatory authorities, fire safety engineers and operators of buildings are invited to participate. In order to achieve this broad participation, an open approach has been implemented based on the projects website (www.rimea.de).

4.   Procedural and Organizational Aspects

Within the first year, a first version of the RiMEA guideline was developed. This allowed all the members to prepare and submit contributions. The following iteration steps are scheduled every two months. Submissions will be edited and revised by the organizers in cooperation with the participants. This process is aimed at being as transparent as possible.

5.   Outlook

After having completed the guideline it is intended to establish a connection or incorporation into the relevant official (i.e. governmental) regulations. However, the project will be continued and the guidelines will be revised and improved as an ongoing project. The website is established as a platform for information and exchange on evacuation analyses and simulations.

6.   The Organizers

Ministerialrat Dipl.-Ing. Peter Gattermann
Member of the Austrian Committee for Standards, delegate in the European Committee for Standards, director of the Austrian Institute for the Construction of Schools and Sportsgrounds (www.oeiss.org), Vienna, Austria.

Dipl.-Ing. Tim Meyer-König
Member of the German Delegation in the Fire Protection Sub-Committee of the Marine Safety Committee of the International Maritime Organization, head of Pedestrian Division of TraffGo HT GmbH (www.traffgo.com), Flensburg, Germany.

Architect Christian Moroge,
Member of CEN/TC Committee „315 Spectator facilities" of the European Committee on Standardization and Norms, Architect Office Bayer Partner AG (www.football.ch), St.Gallen, Switzerland.

Prof. Dr. Michael Schreckenberg,
Head of the Group Physics of Transport and Traffic, University Duisburg-Essen (www.traffic.uni-duisburg.de), Duisburg, Germany.

Architect Martin Schwendimann,
Federal Office for Sport – Division Sports Facilities (www.baspo.admin.ch), Magglingen, Switzerland.

Dipl.-Ing. Nathalie Waldau
Consultant of the Austrian Institute for the Construction of Schools and Sportsgrounds (OEISS), Vienna, Austria.

7.   Structure of the Guidelines

The guideline is structured as follows:

1.   **General**
2.   **Aims**
3.   **Range of Application**
4.   **Definitions**
    » Convention facilities
    » Evacuation
    » Egress
    » Capacity
    » Awareness time

- » Individual reaction time
- » Individual walking time
- » Individual egress time
- » Minimum evacuation duration
- » Maximum evacuation duration
- » Mean evacuation duration

5. **Characteristics of Simulation Models**
   - » Population Characteristics
   - » Reaction time
   - » Unhindered walking speed on flat terrain
   - » Unhindered walking speed on stairs
   - » Exit flow rate

6. **Evacuation Analysis**
   - » Scenarios
   - » Initial distribution of persons
   - » Layout of escape routes
   - » Basic case of evacuation
   - » Flexibility of escape route arrangement
   - » Additional cases
   - » Calculation of maximum occupancy
   - » Calculation of overall egress time
   - » Identification of congestion

7. **Corrective Action**
8. **Appendix**
   Interim Guide for Validation / Verification of Simulation Programmes
   - » Component Testing
   - » Functional Verification
   - » Qualitative Verification
   - » Quantitative Verification

Football Stadium Simulation –
A microscopic simulation of the pedestrian access

H. Moldovan[1], M. Gilman[1], P. Knoblauch[1], and S. Woloj[1]

In this work we will present a set of results from the simulation of the input process of a football stadium. The results were obtained with Smartcrowd. This simulation software considers each pedestrian individually and calculates the real physical forces acting over him/her. With Smartcrowd it is possible to introduce behavioral patterns for representing collective behavior. The results were compared with observations made in the real system. We will also introduce the methodology used for extracting very useful information from the real system. The considered problem is highly complex as it involves thousands of persons, different activities and a simulation surface of about 10.000 m².

1. Introduction

In this work we will present the application of a pedestrian simulation system, Smartcrowd, for solving a highly complex real pedestrian problem. We performed the simulation of a Football Stadium in Buenos Aires. We focused on the input process simulating the stadium access areas and the adjacent streets. The aim of this work was to ensure the security conditions during this process by finding the high density areas.

Smartcrowd implements a microscopic algorithm considering that flow is made of discrete self-driven particles. The model uses molecular dynamics concepts and takes into account forces (contact, desired and social) as described by Dirk Helbing [1, 2]. Each particle is represented as an agent with its own behavior. Inspired in biological systems, our behavioral model allows each agent to have multiple behaviors. For each simulated pedestrian, the navigation mechanism builds a trajectory from the multiple available paths in the navigation space. This mechanism was implemented using DNF (M. Gilman et. al. [3]). Additional mechanisms such as collision avoidance are also used.

Data from the real system was collected in several ways. Particularly, for the present work, we focused on the data obtained by videotape recording. The video images allow measuring the density of passengers as a function of time in some selected areas.

Several cameras were located in the environs of the stadium and used to register the most critic areas defined by their complex flows and high densities. From the images, mean density values were determined for the critic areas. This work was carried out for two qualitatively different matches: a maximal affluence match (>60,000 spectators) and a mean affluence match (about 30,000 spectators).

These cases not only differ in the number of spectators but also in the geometry, access plan, number of policemen involved and number of opened ticket offices.

Simulation models for each match were built to fit and reproduce the observations. From the simulations it was possible to determine measures such as transit time for

---

each pedestrian, number of persons in the critic areas, etc. The relevance of these results resides in the difficulty or impossibility of obtaining them from the real system. With Smartcrow this is possible because the complete history of each individual is recorded into a database for further processing.

Additionally, we proof the predictive power of the built model for other performed matches. Being able to simulate real and complex situations (see also H. Moldovan et. al. [4] and D. R. Parisi et. al. [5]) is fundamental not only for validating the built model but also for verifying its scalability in space and number of simulated persons.

2.   Real System

Our real system is the River Plate Football Stadium in Buenos Aires. This is one of the most important football stadiums of the world with a capacity for about 65,000 supporters.
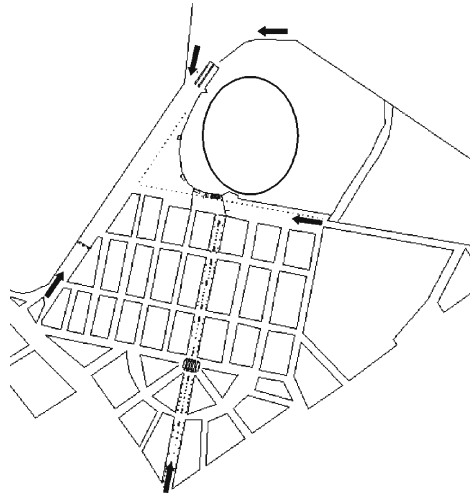
Figure 1: Map of the vicinity of the stadium. The main available access roads are identified.

In this case the pedestrian flow is characterized by 2 distinct flows: locals and visitors. The supporters arrive to the stadiums during the 3 hours before the beginning of the match. They usually arrive by train, bus or car. Clusters of people are typically formed. The average pedestrian will walk up to 4 blocks before arriving to the stadium.

Accesses to the stadium are defined for each match as part of a specific security plan. The plan involves fences for delimiting accesses and separating different flows (local and visitant). Supporters must typically walk several blocks pass through several police check points before arriving to the entrance of the stadium.

Check points are subprocesses that generate crowds of peoples in the adjacent area right before them and constitute a typical source of delays.

In these areas high densities of pedestrians are produced (above 3 pax/m^2). This is one of the main causes for further conflicts. In this system, improving the security conditions requires reducing these densities by introducing the proper modifications into the environment.

3.   Data

Based on intensive field work, the main properties of the spectators were determined for both matches. The pedestrians' properties and behaviors were characterized in the vicinities and accesses to the stadium.

Figure 2: Images obtained from the cameras located in the souroundings of the stadium.

Special attention was paid to the characterization of the different involved subprocesses (security control, pre security control, tickets control, turnstiles, ticket offices, etc.) and to the pedestrian flow patterns.

For the execution of this characterization work we used data from turnstiles and cameras provided by the Club Atlético River Plate. This material was complemented with in-situ observations and photographs. We measured times and flow rates in place and from the films.

By means of the films it was also possible to determine mean values for densities of crowds especially for the selected areas. This information was further used for contrasting and adjusting some parameters of the system.

4.   Simulations

A model considering the geometry of the stadium and the environs was built. The inputs of the simulations were taken from the real system using all the available information described in the last section.

The discrete flow was simulated by implementing a model of the real system using SmartCrowd. The problem was divided into three independent subproblems P1, P2 and P3 depicted in Figure 3. In this work we will show the results for the first subproblem P1. Figures 4, 5 and 6 show some obtained results for the match of maximal affluence.
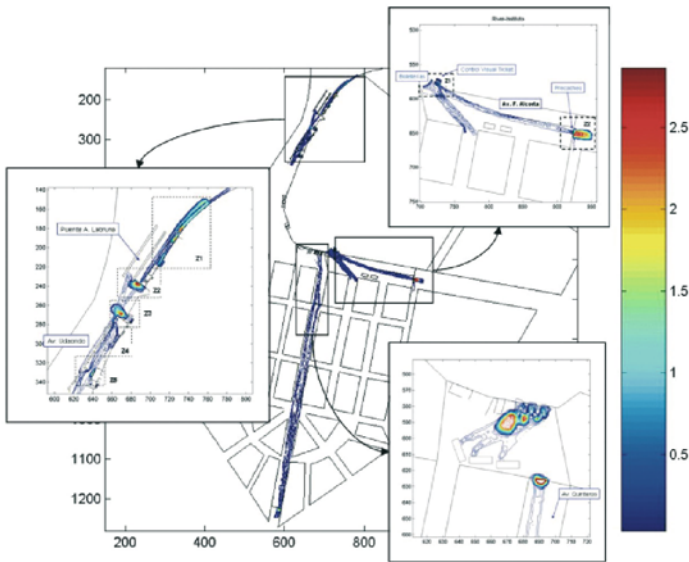
Figure 3: Mean density maps belonging to a simulation. Density is expressed in ped/m². The three amplified figures belong to the three identified subproblems.

These results are mean values of the density calculated during the half hour before the beginning of the match. This time interval is the period of maximal flow rate.

This information allows having a fast idea of the most utilized access roads and determining the most crowded areas (maximal density). These results are crucial to our main objective: to find these areas and quantify the level of accumulation that can be obtained.

Large densities can be observed in Figure 4, mainly at the beginning of the queue in the stadium's access; right before the security control. From this figure, it is clear that for this configuration and flow rates it would be necessary to augment the number of policemen involved.
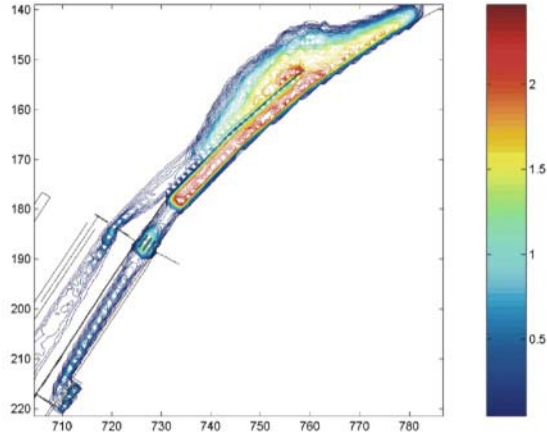
Figure 4: Detail of the area identified as Z1 in Figure 3.
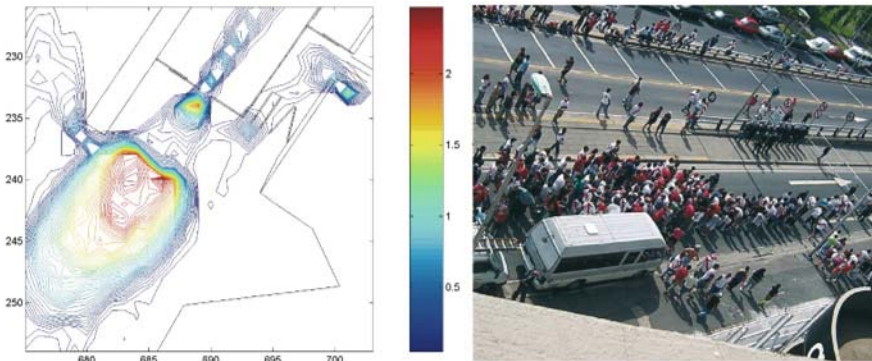
Figure 5: Detail of the area identified as Z2 in Figure 3 and its comparison with the real system.

Figure 5 shows the mean density map for the simulated and the real pre-security control process. It is important to notice that while the picture captures a time instant, the density was calculated for a time interval (approximately 10 min.).

In Figure 6 it can be observed a detail of areas Z3 and Z4. In these areas it can be easily observed the sectors with largest densities as well as the mostly selected paths and trajectories.
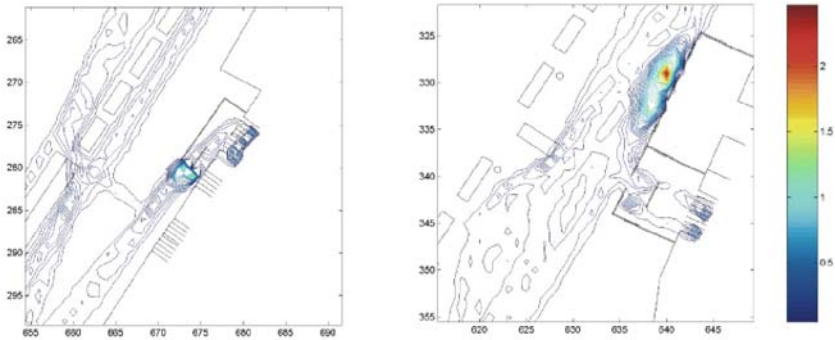
Figure 6: Details of the areas identified as Z3 and Z5 in Figure 3.

5.   Conclusion

In this work we have briefly described the methodology used for the validation of the pedestrian simulation software Smartcrowd in a real situation. This methodology was conceived to ensure that the macroscopic results obtained with the simulator were quantitatively similar to the observed in the real system. Additionally, the results show the scalability of the system for large problems.

This paper offers some insight into the usage of a simulation tool like Smartcrowd to generate important information for properly managing and planning the security of large scale events.

6.   Acknowledgment

Authors whish to acknowledge to Club Atlético River Plate. (Argentina) for their collaboration and contributed data. «

References

1.   D. Helbing and P. Molnár: *Social Force Model for Pedestrian Dynamics*, In: Physical Review E, 51, (5), pp. 4282-4286 (1995).
2.   D. Helbing, I. Farkas, and T. Vicsek: *Simulating Dynamical Features of Escape Panic*, In: Nature 407, pp. 487-490 (2000).
3.   M. Gilman, H. Moldovan, and M. Tencer: *Dynamic Navigational Field: A local and On-Demand Family of Algorithms for Wayfinding*, In: these Proceedings, Springer (2005).
4.   H. Moldovan, D. R. Parisi, and M. Gilman: *Pedestrian Pulse Dispersion in an Underground Station*, Traffic and Granular Flow 03, pp. 411-415, Springer (2005).
5.   D. Parisi, H. Moldovan, and M. Gilman: *Population and Distance Criteria for Pedestrian Decisions*, Traffic and Granular Flow 03, pp. 417-421, Springer (2005).

Instability of pedestrian flow in two-dimensional optimal velocity model

A. Nakayama[1], Y. Sugiyama[2], and K. Hasebe[3]

A two dimensional optimal velocity model was proposed for the study of pedestrian flow. We investigate the stability of homogeneous flow in the linear approximation and show the phase diagram of the model. We also investigate the behavior of pedestrian flow by numerical simulation in the cases of unidirectional and counter flow. From these results, we present a unified understanding of the properties of pedestrian flow and other related systems.

1.   Introduction

In the past decade, traffic and some related systems are investigated from the physical viewpoint of many-particle systems[1-6]. Pedestrian flow is one of such systems and presents interesting phenomena such as lane formation or blocking[7,8]. The behavior of pedestrians has been investigated not only in physics but also in engineering, and various models are proposed to reproduce the phenomena[9-18]. However, these models are tuned to reproduce the behavior of each phenomenon, and the general study of pedestrian flow itself has not been done. Dynamical models for pedestrian flow are useful for such studies, especially for analytical studies, because the motion of pedestrians is described by the dynamical equation of motion.

It is well-known that there is a similarity among pedestrian flow, traffic flow and granular flow through a pipe. A jam or a similar phenomenon is commonly observed independent of the dimensionality; one-dimensional traffic flow, two-dimensional pedestrian flow and three-dimensional granular flow. When they have a common property, we expect that the property can be explained by the same mechanism. As a candidate for the model which can explain those phenomena in a unified framework, we adopt the optimal velocity (OV) model[19-21] as follows. The property of one-dimensional traffic flow is well understood by the OV model and the traffic congestion is interpreted as a phase transition. A density wave similar to traffic congestion is observed in granular flow in liquid through a vertical pipe. In this case, the system can be reduced to quasi one-dimensional one, which is expressed by a similar equation to the OV model[22,23]. Then we expect that the behavior of pedestrians can be explained in the framework of the OV model or its two-dimensional extension.

We have proposed a two-dimensional OV model for pedestrians and granular flow[24-27]. The OV model for traffic flow is based on a simple concept: A driver maintains his optimal velocity depending on the distance to other vehicles. The two dimensional OV model is constructed along the same concept. Pedestrians are treated as identical particles moving in the two-dimensional space, and each particle decides its optimal velocity

[1]Department of Physics and Earth sciences, University of the Ryukyus, Nishihara, Okinawa 903-0213, Japan

[2]Department of Complex Systems Science, Graduate School of Information Science, Nagoya University, Nagoya, 464-8601, Japan

[3]Faculty of Business Administration, Aichi University, Miyoshi, Aichi 470-0296, Japan

depending on distances to other particles. In this paper, we show that the model gives a unified understanding of the phenomena in pedestrian flow and in one-dimensional traffic flow. We investigate the linear stability of the homogeneous flow solution. It is shown that the homogeneous flow is unstable if the density exceeds a certain critical value. In this case, the homogeneous flow is broken, and a density wave emerges spontaneously. Some typical stationary patterns are finally formed depending on the values of parameters. This is the same phenomena as traffic congestion. We also show the existence of a new phase which does not exist in a one-dimensional system. Typical profile of flow in each phase can be obtained by use of numerical simulations.

2.   Two-dimensional OV model

The one-dimensional OV is expressed by the equation of motion[19]

$$\frac{d^2}{dt^2} x_n(t) = a\left[V(\Delta x_n(t)) - \frac{d}{dt} x_n(t) \right],$$
$$V(\Delta x) = \alpha[\tanh\beta\,(\Delta x - b) + c], \tag{1}$$

where x_n and Δx_n are the position and the headway of the n-th vehicle. a is „sensitivity", which represents the strength of reaction of each driver. $V(\Delta x)$ is „OV function", which indicates an optimal velocity depending on his headway.

This model has a trivial homogeneous flow solution $x_n = hn + V(h)t + $const., where all vehicles run with the same velocity $V(h)$ and the same headway h. We can find the stability condition of the solution by the linear analysis. The stability condition for the mode solution $y_n(t) = \exp[in\theta - i\omega(\theta)t]$ is given by

$$a > V'(h)(1 + \cos\theta). \tag{2}$$

If the condition is not satisfied, the homogeneous flow is unstable for the mode θ and the flow transits to a congested flow with jam clusters.

The two-dimensional OV model for pedestrian flow is a natural extension of the one-dimensional model[24]. The equation of motion for a particle with the index j is

$$\frac{d^2}{dt^2} \mathbf{x}_j(t) = a\left[\left\{ \mathbf{V}_0 + \sum_k \mathbf{F}(\mathbf{x}_k(t) - \mathbf{x}_j(t)) \right\} - \frac{d}{dt} \mathbf{x}_j(t) \right], \tag{3}$$

where bold symbols are two-dimensional vectors. $\mathbf{x}_j = (x_j, y_j)$ and $\mathbf{x}_k = (x_k, y_k)$ are the positions of j-th and k-th particles, respectively. $\mathbf{V}_0$ is a constant vector which expresses „desired velocity". A particle moves with the desired velocity, if it is alone. $\mathbf{F}$ expresses the interaction between particles and we choose the following form.

$$\mathbf{F}(\mathbf{x}_k - \mathbf{x}_j) = f(r_{kj})(1 + \cos\varphi)\mathbf{n}_{kj},$$
$$f(r_{kj}) = \alpha[\tanh\beta(r_{kj} - b) + c],$$

$$(4)$$

where $r_{kj} = |\mathbf{x}_k\text{-}\mathbf{x}_j|$, $\cos\varphi = (x_k\text{-}x_j)/r_{kj}$ and $\mathbf{n}_{kj} = (\mathbf{x}_k\text{-}\mathbf{x}_j)/r_{kj}$. The interaction is determined by the distance r_{kj} between j-th and k-th particles and the angle φ between $\mathbf{x}_k\text{-}\mathbf{x}_j$ and V_0. The factor $(1+\cos\varphi)$ indicates that a particle is more sensitive to particles in front than those behind.

For convenience, we set $V_0 = (V_0, 0)$, which means that particles are supposed to move in the positive direction of the x-axis. We also set $c = -1$, that is, $f < 0$, which means that the interaction is repulsive[28]. This is a natural assumption for the interaction between pedestrians. The parameter α is set to $1/4$ for simplicity.

3.   Linear analysis

Before the linear analysis of homogeneous flow, we simplify the Eq.(3) by the replacement $t \to t/a$, $V_0 \to aV_0$ and $F \to aF$ as follows.

$$\frac{d^2}{dt^2}\mathbf{x}_j(t) = \mathbf{V}_0 + \sum_k \mathbf{F}(\mathbf{x}_k(t) - \mathbf{x}_j(t)) - \frac{d}{dt}\mathbf{x}_j(t).$$

$$(5)$$

Numerical simulations show that the homogeneous flow is realized at low density (see Fig.1).[24]. This homogeneous flow is expressed by the solution $\mathbf{x}_j = \mathbf{X}_j + \mathbf{v}t$. Here $\mathbf{X}_j = (X_j, Y_j)$ is a constant vector which represents a site on a triangular lattice, and $\mathbf{v} = (v_x, v_y) = \mathbf{V}_0 + \sum_k \mathbf{F}(\mathbf{X}_k - \mathbf{X}_j)$ is a constant velocity at which all particles move. The distances between any nearest-neighbor pairs are the same, and we use the distance as a parameter instead of the density.
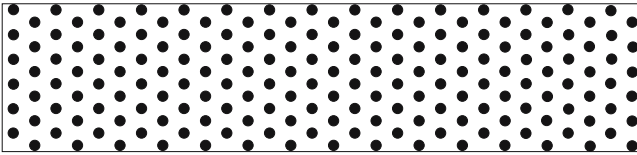
Figure 1: A snapshot of the homogeneous flow. A triangular structure is observed in a numerical simulation with periodic boundary condition. All particles represented by black disks are moving rightward.

We consider a perturbation

$$x_j \to X_j + v_x t + x_j,$$
$$y_j \to Y_j + v_y t + y_j.$$

$$(6)$$

The new x_j and y_j represent x- and y-component of the small deviation from the position (X_j, Y_j).

From Eqs.(3) and (4), we can write the linearized equations

$$\frac{d^2}{dt^2} x_j = \sum_k [A_{kj}(x_k - x_j) + B_{kj}(x_k - x_j)] - \frac{d}{dt} x_j,$$

(7)

$$\frac{d^2}{dt^2} y_j = \sum_k [C_{kj}(x_k - x_j) + D_{kj}(x_k - x_j)] - \frac{d}{dt} y_j.$$

(8)

The parameters A_{kj}, B_{kj}, C_{kj}, D_{kj} are defined by[32]

$$A_{kj} = \partial_x F_x(x, y)|_{x=X_k-X_j, y=Y_k-Y_j}, \qquad B_{kj} = \partial_y F_x(x, y)|_{x=X_k-X_j, y=Y_k-Y_j},$$

$$C_{kj} = \partial_x F_y(x, y)|_{x=X_k-X_j, y=Y_k-Y_j}, \qquad D_{kj} = \partial_y F_y(x, y)|_{x=X_k-X_j, y=Y_k-Y_j},$$

(9)

where $\boldsymbol{F} = (F_x, F_y)$.

Consider a mode which propagates at the angle φ with the x-axis. Then the wave vector is $\boldsymbol{k} = (k_x, k_y) = (k_x, pk_x)$ where $p = \tan\varphi$. The two-dimensional wave is classified into two types of modes; longitudinal modes and transverse modes.

The longitudinal modes in the φ-direction are written by

$$x_j = \exp[i\omega t + i\boldsymbol{k} \cdot \mathbf{x}] = \exp[i\omega t + i\theta(X_j + pY_j)],$$

$$y_j = px_j,$$

(10)

where $\theta = k_x$. The linearized equations (7) and (8) are rewritten as

$$\frac{d^2}{dt^2} x_j = \sum_k (A_{kj} + pB_{kj})(x_k - x_j) - \frac{d}{dt} x_j,$$

(11)

$$0 = \sum_k (A_{kj} + pB_{kj} - \frac{1}{p}C_{kj} - D_{kj})(x_k - x_j),$$

(12)

where the second equation is obtained by subtracting Eq.(8) from Eq.(7). We can find similar equations for the transverse modes by replacing $\theta = k_x \to \theta = k_y$ and $p \to 1/p$. Because the interaction with the nearest-neighbors is dominant, we neglect the interaction with further particles. The summation for k is taken over six particles around j-th one. Then we can solve Eq.(11) under the constraint (12), and can find the condition that ω does not have negative imaginary part[32].

Obviously, two special cases $\varphi = 0$ $(p = 0)$ and $\varphi = \pi/2$ $(p = \infty)$ should be investigated separately from the general case. Therefore we find six stability conditions in total: three directions of propagation (i) x-axis $(\varphi = 0)$, (ii) y-axis $(\varphi = \pi/2)$ and (iii) other direction

(0< φ < π/2) for each of two polarizations (a) longitudinal modes and (b) transverse modes. The results are shown as follows.

For the modes along the x-axis, the constraint (12) is automatically satisfied and we can easily find the stability condition. The condition for the longitudinal mode along the t-axis is

$$a > \frac{3[3f'+2(f/r)]^2}{2[3f'+(f/r)]},$$
(13)

where r is the distance between two nearest-neighbor particles and f is the function (4) and f' is its derivative. In the similar way, we can find the stability condition for the transverse mode along the x-axis.

$$a > \frac{3[f'+2(f/r)]^2}{2[f'+3(f/r)]}.$$
(14)

Here we note that the condition is quite similar to that in the extended OV model for one-dimensional system, and the instability arises first from the longest wavelength mode for both cases[29-31].

For off-x-axis modes, there exist three remarkable points. First, the constraint (12) is satisfied only in the directions $\varphi = n\pi/6$ (n=1,2,3,4,5,7,8,9,10,11), that is, no mode solutions exist in other directions. Second, only the shortest wavelength mode is allowed in each direction and for each polarization. Third, the stability condition is decided only by the distance r independent of sensitivity a.

Consider the case of $\varphi = \pi/2$ (y-axis) as an example. Particles exist at intervals of the length u in the direction of the y-axis. The constraint (12) is satisfied only for the mode $\theta = \pi/u$. This is the largest wave number of the wave which propagates along the y-axis. By solving Eq.(11) with the above results, we find the stability condition for the mode. For the longitudinal mode in the direction $\varphi = \pi/2$ (y-axis), the condition results in

$$\frac{1}{2}f'+\frac{3f'}{2r} > 0.$$
(15)

The stability condition for this mode does not depend on sensitivity a and depends only on the distance r. Similar results are obtained in the directions $\varphi = \pi/6, \pi/3$[32].

In Table 1, we show all the stability conditions in a typical case where the parameters are chosen as $\alpha = 1/4$, $\beta = 2.5$, $b = 1.0$, $c = -1.0$ of the OV function (4). We note that two critical values of distance $r = 0.59$ and $r = 1.05$ are common for various modes. These values also appear as the singularity of stability condition for the modes along the x-axis: Equation (13) is singular at $r = 0.59$ and Eq.(14) is singular at $r = 1.05$. The reason why the critical values for various modes coincide is not clear.

φ	longitudinal mode	transverse mode
0 (*x*-axis)	Eq.(13)	Eq.(14)
$\pi/6$	$r > 1.05$	$r > 0.59$
$\pi/3$	$r > 0.59$	$r > 1.05$
$\pi/2$ (*y*-axis)	$r > 1.05$	$r > 0.94$

Table 1: Stability conditions for all modes. Numerical values are calculated for the parameters $\alpha = 1/4$, $\beta = 2.5$, b = 1.0, c = -1.0.

We can draw the phase diagram from these results. In Fig.2, solid and dashed curves represent two critical curves defined by Eqs.(13) and (14). The longitudinal and transverse modes along the x-axis become unstable in the region below the solid and dashed curve, respectively. Three critical lines $r = 1.05$, $r = 0.94$ and $r = 0.59$ correspond to the stability condition in the off-*x* directions. Each mode in the off-*x* direction is unstable in the left region of corresponding dotted line. Therefore the homogeneous flow is stable in the region *A*. In the region *B*, only the transverse modes along the *x*-axis are unstable. In the region *C*, only the longitudinal modes along the *x*-axis are unstable. The region *C* corresponds to the unstable region of the homogeneous flow in the one-dimensional system. However in the region *D*, several modes become unstable simultaneously and it is unpredictable how the flow breaks. It is not clear whether dotted curve or lines in the region *D* are boundaries of phases or not.
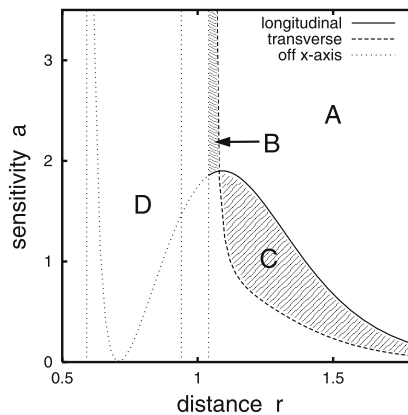
Figure 2: The phase diagram obtained by the linear analysis. Solid and dashed curves represent the critical curves given by Eqs.(13) and (14), respectively. Dotted lines represent the critical lines $r = 1.05$, $r = 0.94$ and $r = 0.59$.

4.   Numerical simulations

In this section, we show a typical behavior in each phase by numerical simulations. We adopt the periodic boundary condition in both directions of x- and y-axis for simplicity. The parameters are chosen the same values as those in Section 3. Control parameters are sensitivity and the distance among particles (see Fig.3). The point P_1 is in the phase B, and P_2 and P_7 are in the phase C. P_5 and P_6 are in the phase A, and P_3, P_4 and P_8 are in the phase D.
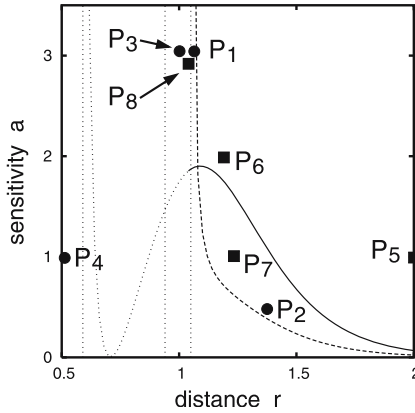
Figure 3: Black disks P1-P4 and black squares P5-P8 represent parameters used in simulations for unidirectional flow and for counter flow, respectively.

First we show the results for unidirectional flow. Figure 4 shows snapshots in the case of distance $r = 1.06$ and sensitivity $a = 3.0$ (P_1 in Fig.3). The simulation starts from the homogeneous flow (Fig.4a), and after sufficient large time we observe the transverse wave (Fig.4b).
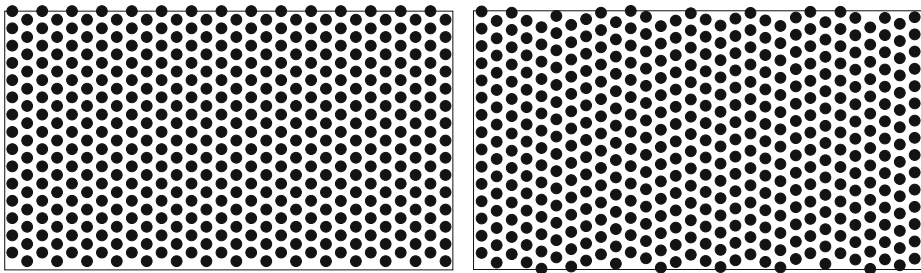
Figure 4: A typical pattern of the flow at the point P1 in the phase B. Sensitivity a is set to 3.0, and the distance among particles r is 1.06. The initial state is the homogeneous flow (a) and the transverse wave is observed after relaxation (b).

Figures 5 shows snapshots for $r = 1.3$ and $a = 0.5$ (P_2). The simulation starts from the initial state shown in Fig.4a. Figure 5a shows the early stage where the longitudinal wave is amplified. The state after relaxation is shown in Fig.5b, where we can see clear density wave.
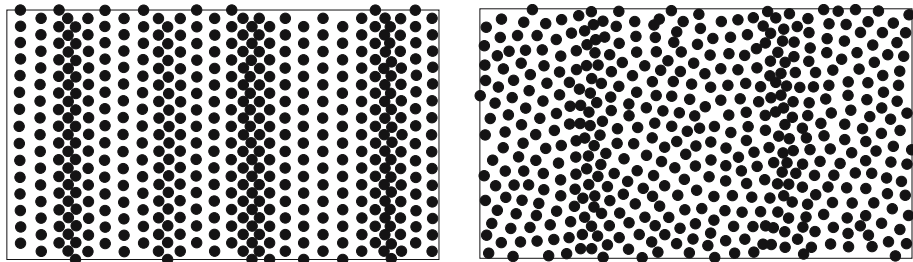
Figure 5: A typical pattern of the flow at the early stage (a) and the flow after relaxation (b) at the point P_2 ($a = 0.5$, $r = 1.3$) in the phase C.

Figures 6 is snapshots of the states after relaxation for $r = 1.0$, $a = 3.0$ (P_3) and $r = 0.5$, $a = 1.0$ (P_4), respectively. The states in Figs.5b, 6a and 6b (P_2, P_3, P_4) transit to each other continuously by the change of parameters r and a. It is difficult to find clear borders among them. In the result, we can clearly distinguish the behaviors in the phases A, B and C: the homogeneous flow in phase A, the transverse wave in phase B and the longitudinal wave in phase C. However, the border between phases C and D is not clear from the results of simulations.
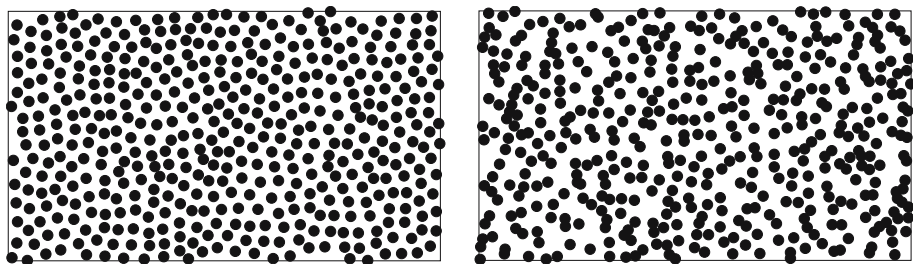
Figure 6: Snapshots of the flow after relaxation. (a) $a = 3.0$ and $r = 1.0$ (P_3). Particles move randomly but a triangular structure emerges partly. (b) $a = 1.0$ and $r = 0.5$ (P_4). Particles move randomly and no structure is observed.

Here we suggest a mechanism for a blocking phenomenon observed in counter flow based on our analysis. Figure 7 shows two snapshots of counter flow at large r (low density) after sufficient relaxation time. White or black particles are moving leftward and rightward, respectively. We set that a half number of particles move in the opposite direction, $V_0 = (-V_0, 0)$. In Fig.7a, we choose parameters as $r = 2.0$ and $a = 1.0$ (P_5 in Fig.3), and in Fig.7b, we choose $r = 1.2$ and $a = 2.0$ (P_6). Clear lanes are formed, where particles are moving in the opposite directions. Each lane can be considered as unidirec-

tional flow, and the stability condition is roughly the same as that obtained for unidirectional flow. Therefore the formed lanes are stable, since the unidirectional homogeneous flow is stable at the points P_5 and P_6.
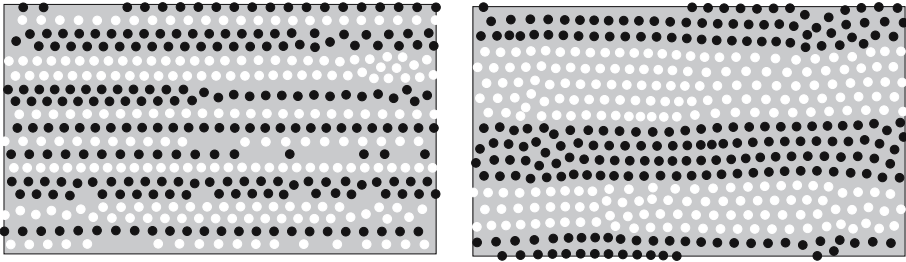
Figure 7: Typical stationary patterns of counter flow at the points (a) P_5 ($a = 1.0$, $r = 2.0$) and (b) P_6 ($a = 2.0$, $r = 1.2$) in the region A. White or black disks represent particles moving leftward and rightward, respectively. Boundary conditions are periodic in both x- and y-directions.

When the distance among particles is a little smaller than the critical value obtained by the analysis of unidirectional flow, the temporal lane formation is observed but these lanes are unstable. The final states in such cases are shown in Fig.8. These are blocking states. At shorter distance ($r < 1$), no temporal lane formation is observed, and the blocking state emerges immediately. The blocking state in our model is not completely frozen[8], because we treat pedestrians as point-particles for simplicity. Particles move windingly in the crowd and pass through a tiny space between particles, and finally escape to the opposite side of the crowd.

The simulations in Fig.8 are performed at the point P_7 ($a = 1.0$ and $r = 1.24$) in the region C and the point P_8 ($r = 1.04$ and $a = 3.0$) in the region D in Fig.3. From these results, we conclude that the lane formation occurs in the region A where the homogeneous flow is stable, and the blocking occurs in the region where the homogeneous flow is unstable. A rough sketch of the phase diagram for counter flow is as follows. There are two phases; in one phase the lane formation occurs, and in the other phase the blocking occurs. The boundary between above two phases exists near the boundary between the region A and B (C) in Fig.3.
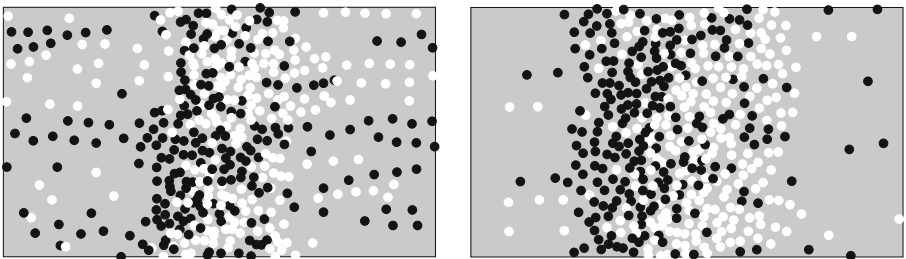
Figure 8: Typical blocking states of counter flow at the points (a) P_7 ($a = 1.0$, $r = 1.24$) and (b) P_8 ($a = 3.0$, $r = 1.04$).

5.   Summary and Discussion

We investigated the linear stability of the homogeneous flow solution in the two-dimensional OV model[24-27,32]. There are two types of instability of mode solutions. One is the instability of modes propagating in the direction of the x-axis (desired velocity). The stability conditions of these modes depend on the sensitivity a and the distance r. The other is the instability of modes which propagate in the off-x-axis direction. Such modes exist only in the directions with the angle $\varphi = n\pi/6$ ($n=1,2,3,4,5,7,8,9,10,11$). Moreover, only the shortest wavelength mode is allowed in each direction and for each polarization. The stability conditions for off-x-axis modes depend only on the distance r and not on the sensitivity a. These properties are remarkable differences from those of the modes along the x-axis.

We can draw the phase diagram from the results of the linear analysis. There exist roughly four phases: phase A (the region A in Fig.2) where the homogeneous flow is stable, phase B where the transverse modes along the x-axis are unstable, phase C where the longitudinal modes along the x-axis are unstable and phase D where several modes are unstable. We carried out numerical simulation to investigate the behavior of flow in each phase. The behaviors in the phases A, B and C can be distinguished clearly, but the behaviors in the phases C and D seem to transit each other continuously.

We also perform numerical simulations of counter flow. The lane formation occurs at a large distance (low density) and the blocking occurs at a small distance (high density). The border between these two states exists near the critical curve of the stability condition for the unidirectional flow. By use of the results of linear analysis for unidirectional flow, the results of simulations in counter flow can be understood as follows. When the lanes are formed, each lane can be considered as unidirectional flow and is stable at the density where the homogeneous flow is stable (phase A in Fig.2). If the density is a little higher (phase B and phase C), lanes are formed temporally. Each lane cannot be maintained due to the unstable modes in the x direction and the blocking phenomenon occurs finally. At much higher density, several modes in the off-x direction are unstable simultaneously, and the blocking state emerges immediately. Therefore we conclude that the two-dimensional OV model can present a unified understanding of these phenomena in pedestrian flow.

References

1.   D.E. Wolf, M. Schreckenberg, and A. Bachem (Eds.): *Workshop on Traffic and Granular Flow*, World Scientific, Singapore (1996).
2.   M. Schreckenberg and D.E. Wolf (Eds.): *Workshop on Traffic and Granular Flow* ,97, Springer-Verlag, Singapore (1998).
3.   D. Helbing, H.J. Herrmann, M. Schreckenberg, and D.E. Wolf (Eds.): *Traffic and Granular Flow* ,99, Springer-Verlag, Berlin (2000).

4.   M. Fukui, Y. Sugiyama, M. Schreckenberg, and D.E. Wolf (Eds.): *Traffic and Granular Flow* ,01, Springer, Berlin, Heidelberg (2003).

5.   D. Chowdhury, L. Santen, and A. Schadschneider: *Statistical Physics of Vehicular Traffic and Some Related Systems*, In: Physics Reports, 329, pp. 199 (2000).

6.   D. Helbing: *Traffic and Related Self-Driven Many-Particle Systems*, Rev. Mod. Phys., 73, pp. 1067 (2001).

7.   D. Helbing: *Pedestrian Dynamics and Trail Formation*, In: M. Schreckenberg and D.E. Wolf (Eds.), Traffic and Granular Flow ,97, pp. 21. Springer, Singapore (1998).

8.   D. Helbing, I. J. Frakas, and T. Vicsek: *Freezing by Heating in a Pedestrian Model*, In: D. Helbing, H.J. Herrmann, M. Schreckenberg, and D.E. Wolf (Eds.), Traffic and Granular Flow ,99, pp. 245, Springer, Berlin, Heidelberg (2000).

9.   L.F. Henderson: *On the Fluid Mechanics of Human Crowd Motion*, Transp. Res., 8, pp. 509 (1974).

10.   P.G. Gipps and B. Marksjö: *A Micro-Simulation Model for Pedestrian Flows*, Math. Comp. Simul., 27, pp.95 (1985).

11.   D. Helbing and P. Molnar: *Social Force Model for Pedestrian Dynamics*, Phys. Rev. E, 51, pp. 4282 (1995).

12.   R.L. Hughes: *The Flow of Large Crowds of Pedestrians*, Math. Comp. Simul., 53, pp. 367 (2000).

13.   C. Burstedde, K. Klauck, A. Schadschneider, and J. Zittartz: *Simulation of Pedestrian Dynamics using a Two-Dimensional Cellular Automaton*, Physica A, 295, pp. 507 (2001).

14.   A. Kirchner and A. Schadschneider: *Simulation of Evacuation Processes using a Bionics-Inspired Cellular Automaton Model for Pedestrian Dynamics*, Physica A, 312, pp. 260 (2002).

15.   A. Kirchner, H. Klüpfel, K. Nishinari, A. Schadschneider, and M. Schreckenberg: *Simulation of Competitive Egress Behavior, Comparison with Aircraft Evacuation Data*, Physica A, 324, pp. 689 (2003).

16.   A. Kirchner, K. Nishinari, and A. Schadschneider: *Friction Effects and Clogging in a Cellular Automaton Model for Pedestrian Dynamics*, Phys. Rev. E, 67, 056122 (2003).

17.   M. Schreckenberg and S. D. Sharma (Eds.), *Proceedings of the International Conference on Pedestrian and Evacuation Dynamics*, Springer, Berlin, Heidelberg, (2002).

18.   E.R. Galea (Ed.), P*roceedings of the 2nd International Conference on Pedestrian and Evacuation Dynamics*, CMS Press, University of Greenwich, London (2003).

19.   M. Bando, K. Hasebe, A. Nakayama, A. Shibata, and Y. Sugiyama: *Dynamical Model of Traffic Congestion and Numerical Simulation*, Phys. Rev. E, 51, pp. 1035 (1995).

20. M. Bando, K. Hasebe, A. Nakayama, A. Shibata, and Y. Sugiyama: *Structure Stability of Congestion in Traffic Dynamics*, Japan. J. Indust. Appl. Math., 11, pp. 203 (1994).

21. M. Bando, K. Hasebe, K. Nakanishi, A. Nakayama, A. Shibata, and Y. Sugiyama: *Phenomenological Study of Dynamical Model of Traffic Flow*, J. Phys. I France, 5, pp. 1389 (1995).

22. S. Horikawa, A. Nakahara, T. Nakayama, and M. Matsushita: *Self-Organized Critical Density Waves of Granular Material Flowing hrough a Pipe*, J. Phys. Soc. Jpn., 64, pp. 1870 (1995).

23. O. Moriyama, N. Kuroiwa, M. Matsushita, and H. Hayakawa, Phys. Rev. Lett., 80, pp. 2833 (1998).

24. Y. Sugiyama, A. Nakayama, and K. Hasebe: *2-Dimensional Optimal Velocity Models for Granular Flow and Pedestrian Dynamics*, In: M. Schreckenberg and S.D. Sharma (Eds.), Proceedings of the International Conference on Pedestrian and Evacuation Dynamics, pp. 155, Springer, Berlin, Heidelberg (2002).

25. Y. Sugiyama, A. Nakayama, and K. Hasebe: *Modeling Pedestrians and Granular Flow in 2-Dimensional Optimal Velocity Models*, In: M. Fukui, Y. Sugiyama, M. Schreckenberg, and D.E. Wolf (Eds.), Traffic and Granular Flow ,01, pp. 537, Springer, Berlin, Heidelberg (2003).

26. A. Nakayama, K. Hasebe, and Y. Sugiyama: *Optimal Velocity Model and its Applications*, In: M. Fukui, Y. Sugiyama, M. Schreckenberg, and D.E. Wolf (Eds.), Traffic and Granular Flow ,01, pp. 127, Springer, Berlin, Heidelberg (2003).

27. A. Nakayama and Y. Sugiyama: *Behavior of Pedestrian Flow based on 2 Dimensional Optimal Velocity Model*, In: E.R. Galea (Ed.), Proceedings of the International Conference on Pedestrian and Evacuation Dynamics, pp. 409, CMS Press, University of Greenwich, London (2003).

28. A. Nakayama and Y. Sugiyama, *2 dimensional optimal velocity moldel for pedestrians and biological motion*, In: P. L. Garrido and J. Marro (Eds.), Modeling of Complex Systems Seventh Granada Lectures, pp. 107, American Institute of Physics, Melville, New York, (2003).

29. A. Nakayama, Y. Sugiyama, and K. Hasebe: *Effect of Looking at the Car that Follows in an Optimal Velocity Model of Traffic Flow*, Phys. Rev. E, 65, 016112 (2001).

30. K. Hasebe, A. Nakayama, and Y. Sugiyama: *Widely Extended Optimal Velocity Model of Traffic Flow and their Linear Stability*, In: M. Fukui, Y. Sugiyama, M. Schreckenberg, and D.E. Wolf (Eds.), Traffic and Granular Flow ,01, pp. 221, Springer, Berlin, Heidelberg (2003).

31. K. Hasebe, A. Nakayama, and Y. Sugiyama: *A Dynamical Model of Cooperative Driving System for Freeway Traffic*, Phys. Rev. E, 68, 026102 (2003).

32. A. Nakayama, K. Hasebe and Y. Sugiyama: *Instability of Pedestrian Flow and Phase Structure in Two-Dimensional Optimal Velocity Model*, Phys. Rev. E71, 036121 (2005).

Evacuation Simulation at Linz Central Station – Usefulness during design, approval and start-up

C. Neumann[1] and R.J. Neunteufel[2]

For the design and the permit application procedure at the Linz Central Station, an evacuation simulation was carried out, which allowed questions of the individual parties involved about the evacuation of persons from the complex building to be answered. The large streams of people created by passengers changing trains called for specific regulations regarding passenger flows and evacuation scenarios.

1. Linz Central Station– Project Description

The central station of Linz is part of a local transportation hub uniting rail, tram and bus traffic in one node. Level -1 grants passengers access to the different transportation modes and accommodates customer centres as well as shops and restaurant facilities.

Figure 1: Linz Central Station– Overview Sketch

During rush hour, up to four tramways can stop at the tramway station on Level –2. At the same time several passenger trains may arrive or depart on different platforms.
In the course of the permit application design in compliance with railway law, an evacuation simulation using the buildingEXODUS 3.0 software (Fire Safety Engineering Group, University of Greenwich, UK, 2000) was carried out. The simulation study was further extended prior to the train station opening.

2. Questions Raised in Connection with Evacuation Simulation

The evacuation simulation for the central station in Linz was performed complementary to the existing design regulations for escape routes and emergency exits to do justice to the complexity of the building including the escape routes.

---

[1]ILF Beratende Ingenieure, Harrachstraße 26, A-4020 Linz
[2]ÖBB-Infrastruktur Bau AG, GB Projekte, Wienerstrasse 2c, A-4021 Linz

The questions, which are rather contradictory, depending on the perspectives of the parties involved, may be summarized as follows:

Design
» Where are the decisive structural elements (bottlenecks)?
» Which escape routes ought to be increased in dimension or can be optimised?
» Which requirements are to be met with respect to route marking and route guidance?

Experts involved in the permit application procedure
» Is there an adequate security level in the entire building?
» For which building sectors and for which administrative processes will additional requirements have to be established?

Future users
» Which findings shall find entrance into the alarm plan and emergency response plan?
» In which zones can areas be used accepting restrictions with respect to operating quality yet not with respect to evacuation efficiency?

3. Model Assumptions / Influencing Parameters

3.1. Section Limits

For the evacuation simulation, only one model section, representing one part of the entire building, was considered.
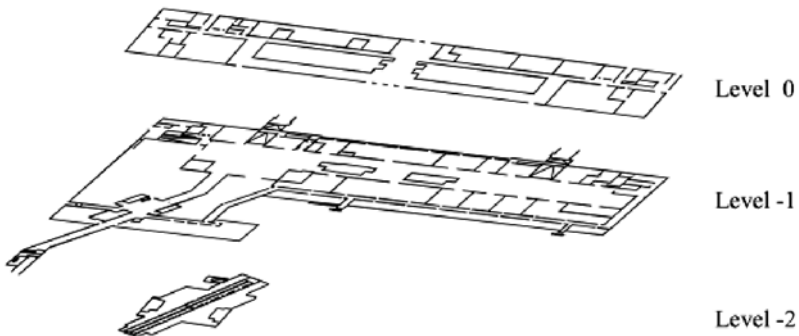
Figure 2: Line Drawing of Model Section

Train platforms and their exits were not analyzed in detail. Instead only the platform tunnel was used as simulation basis, assuming a realistic influx of passengers.

3.2. Definition of Station Occupancy

In coordination with the experts involved in the permit application procedure it was agreed to define the number of passengers based upon the figures projected for passengers changing trains and the figures anticipated for customers visiting the station shops.
And finally, a passenger census was conducted allowing the age structure of the clients to be determined.

Passenger flows at peak periods

The highest passenger rates at the station occur during the morning peak period from 7 am to 8 am and during the afternoon peak period from 5 pm to 6 pm. On the basis of passenger census figures and possible train arrival scenarios, the peak-10-minutes value was determined to serve as forecast value for the year 2015. Considering the average stay time and the actual walk time of a person in the station, a station occupancy of 50% of the peak-10-minutes was assumed for the evacuation simulation.

Customer occupancy in shops and restaurants
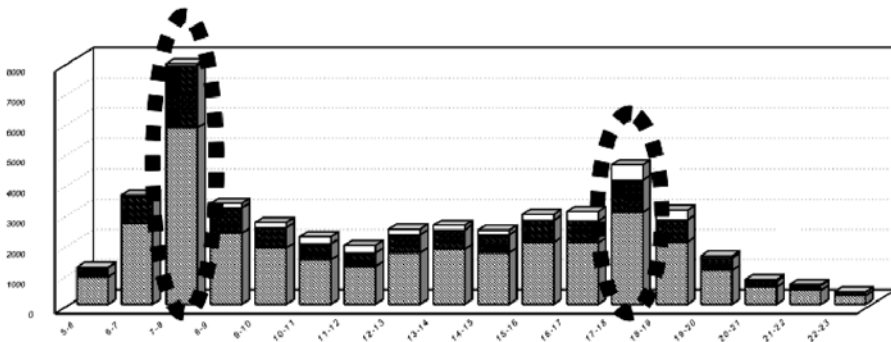
Figure 3: Daily Passenger Flow Pattern

The customers in shops and restaurants include:

»   New Customers
»   Traditional Passengers
»   Regular station Staff

Depending on the intended use of the building areas in question, a realistic number of persons was assumed for the simulation.

Passenger occupancy at underground tramway station

Under normal operating conditions only some passengers get off the tramway at the station, but in an emergency situation all passengers have to be evacuated. Hence for the evacuation simulation, the worst case scenario of four crowded tramways was assumed. By the use of this scenario, the future expansion of the tramway system has already been considered, although the present operation only allows one tramway to stop at the station.

4.   Evacuation Simulation

4.1. Definition of Scenarios

As basic scenarios, the following events were determined:

Scenario	Evacuation Assumptions
Emergency on Level -2 / Tramway station	Evacuation of four tramways and the entire railway station
Emergency on Level -1 / Passenger distribution hall	Tramways escape to the surface / evacuation of the entire railway station
Emergency on Level 00 / Exit hall	Tramways escape to the surface / evacuation of the entire railway station

Table 1: Basic scenarios

To determine the station occupancy, the morning peak period and the less busy afternoon peak period were taken into consideration.
By defining the scenarios in coordination with the experts involved in the permit application procedure, a range of basic scenarios could be analyzed offering an overview of the individual evacuation times under various boundary conditions.

4.2. Sensitivity Analyses

In addition to the basic scenarios, various sensitivity cases were investigated:

Sensitivity case	Combination with basic scenarios
One staircase on Level -2 is not available	Emergency on Level -2
Two staircases on Level -2 are not available	Emergency on Level -2
Main staircases from Level -1 to Level 00 are not available	Emergency on Level -2
Access tunnels to platforms are used / not used as escape route	With all basic scenarios

Table 2: Sensitivity Analyses for Evacuation Simulation

4.3. Temporary Use of Circulation Area

On Level -1 and 00, the circulation areas for pedestrians (passenger transfer) were not only dimensioned in line with minimum space requirements, but also in line with convenience criteria.
The station operator plans on temporarily using parts of this area for exhibitions, product presentations or restaurant facilities.

In the course of the permit application procedure, the evacuation simulation was used to check whether the evacuation efficiency is impaired by the use of certain areas.
The following procedures were adopted:

» Specification of potential areas for temporary use
» Choice of relevant basic scenarios
» Checking of impact on overall escape time
» Qualitative analysis in connection with escape flows

5. Results / Findings

5.1. Results of Evacuation Simulation

For the permitting procedure by the authorities it was agreed to document the results of the evacuation simulation by several comprehensible values to enable the experts to perform their own evaluation.
For every basic scenario and every sensitivity analysis, an evaluation sheet was prepared, specifying the respective escape routes.
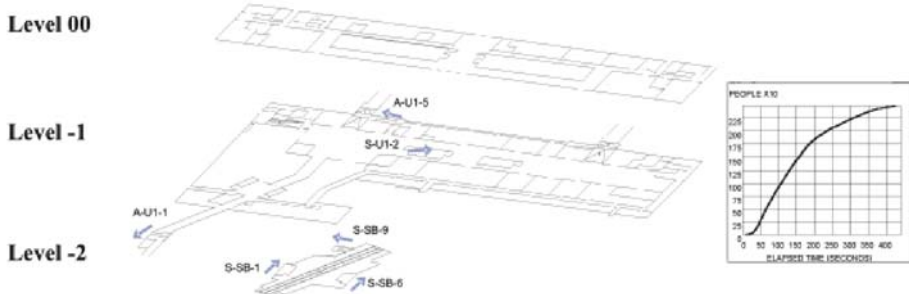
Figure 4: Main Escape Areas and Evacuation Diagram - Scenario A

An analysis of the results revealed that the evacuation time for all scenarios is decisively influenced by the staircase sector and its capacity.

As the staircase model, which is integrated in the evacuation software, reflects a rather cautious approach in comparison to the staircase capacity values rated for normal operation, the experts involved in the permit application procedure requested that calculations with higher capacity values should be performed and documented.

Example – Basic scenario A	Stairway capacity acc. to model software	High stairway capacity
Evacuation Level -2 / Tramway	03:44 min	03:04 min
Evacuation Level -1 / Passenger distribution hall	05:26 min	03:57 min
Entire building	07:32 min	05:03 min

Table 3: Evacuation Simulation Results / Example – Basic Scenario A

As the definition of those areas, which are to be considered as safe, was intensely discussed due to the wide-open space of the central station, the results of the evacuation simulation were related to defined boundaries on the corresponding level.

5.2. Contradictory Demands Made on Transfer Routes During Normal Operation and Emergency Evacuation

The dimensioning of transfer routes in line with passenger flows (changing of means of transport) stands in contrast to the demands imposed by evacuation events. Figure 5 illustrates the different demands made on the transfer routes at the central staircases.
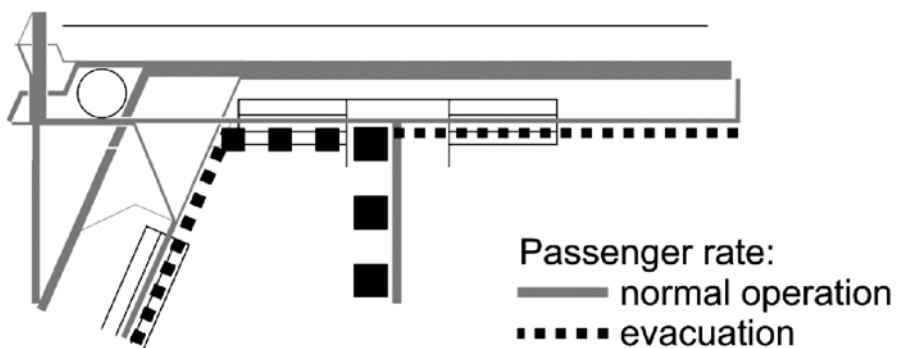
Figure 5: Detail Level -1 / Passenger Distribution Hall – Demands Made on Transfer Routes

5.3. Findings for Design, Approval and Start-Up

By simulating a number of evacuation scenarios, several building sectors, which are of relevance in case of an emergency evacuation, could be optimised.

By involving the experts in the process of defining the investigation framework and the boundary conditions, an adequate database could be made available to the authorities, paving the way for a fast and unproblematic permit application procedure.

The findings of the evacuation simulation provided a solid basis for the preparation of alarm plans and emergency response plans as well as for the decision whether the circulation area could temporarily be used for other purposes without compromising the evacuation needs. «

Why „Faster is Slower" in Evacuation Process

D.R. Parisi[1] and C.O. Dorso[1]

In the present work we studied the room evacuation problem using the social force model introduced by Helbing and coworkers. The ‚faster is slower' effect induced by increasing desired velocities was analyzed. A steady state version of the problem was implemented by reinserting outgoing pedestrians into the room. It shows that, from a macroscopic point of view, the optimal evacuation efficiency correspond to the state at which the difference between the average system desire force minus the average system granular force is maximum.

1.   Introduction

The problem of evacuation of pedestrians from a room under panic conditions is of obvious importance in common life. In last years, several computer models that simulate pedestrian dynamics were developed [1]. These codes do not take into account the effect of panic on the pedestrian behavior.

Pedestrian flow through a bottleneck [2] and clogging in a T-shape channel [3] have been studied previously using the lattice-gas model of biased random walkers. More general self driven particle systems with simple interactions were studied by Vicsek [4], Albano [5] and Czirók [6]. Phase transitions were found for these systems.

The evacuation through a narrow door during an emergency is a complex problem not well understood yet, that can cause very dramatic blocking effects. The understanding of the evacuation dynamics will allow the design of more comfortable and safe pedestrian facilities.

A model that takes into account panic is the so called ‚Social Force Model' proposed by Helbing et al. [7]. This model postulate that each pedestrian are influence by three types of forces: Granular or contact forces (dissipative interaction), Social forces (conservative and long range interaction) and Desire forces (which makes pedestrians self driven). Besides, this model considers the discrete nature of the ‚pedestrian fluid' allowing to fix the physical parameters of each individual (mass, shoulder width, desired velocity, target, etc.). Real scale interaction forces can be calculated, in particular the contact forces which may cause high pressures capable of pushing down a wall of bricks or to asphyxiate people in the crowd. The above characteristics can not be properly taken into account with cellular automata approaches or traditional models using continuous fluid approximations.

Considering the room evacuation of 200 pedestrian through a narrow door, Helbing et al. have shown [7] that the evacuation time (t_e) is a function of the desired velocity v_d. This function has a minimum at the desired velocity threshold (v_{dt}) such that below it, t_e is a decreasing function of v_d while above the tendency is reversed. It means that the evacuation process is optimum at moderated v_d. This behavior is called the „Faster is slower effect".

---

[1]Departamento de Física, Facultad de Ciencias Exactas y Naturales, Universidad de Buenos Aires. Pabellón 1, Ciudad Universitaria, (1428) Buenos Aires, Argentina.

In a previous work [8] we analyze this ‚faster is slower' effect induced by increasing desired velocities. From a microscopic point of view, it could be explained in terms of increasing clogging delays which shows a strong correlation with arch-like structures that we call ‚blocking clusters'. It must be noted that the evacuation process is non stationary, as the number of pedestrians inside the room is a function of time as well as the pressure and other dynamical properties of the system.

In the present work we focus on a stationary version of the problem. Under this condition, the state of maximum jamming is maintained along the time by reinserting outgoing particles into the room. This stationary situation allows to study some features that cannot be revealed in the non stationary case.

The numerical model used in order to perform the simulations are described in [8] which was inspired by (and it is slightly different to) the model proposed by Helbing et al. [7].

2.   Numerical Simulations

In order to explore the room evacuation dynamics, we have performed a series of numerical simulations varying v_d.

The geometry of the room was a 20 m by 20 m square with an exit door of width $L = 1.2$ m. Pedestrian shoulder width were uniformly distributed between 0.54 ± 0.04 m and their mass were 80 ± 10 kg. In all the simulations we have fixed the size of the crowd to be 200 individuals.

2.1. Stationary Simulations

It is quite intuitive that the rate at which the room is evacuated is somehow related to the pedestrian jamming in the inner neighborhood of the exit door. This effect, which we fully describe below, is difficult to study in the non stationary case because it lasts for a short time. In view of this difficulty we have implemented a stationary case in which the jamming effects remain constant in time. This has been accomplished by reinserting particles that have left the room, back inside of it. Outgoing pedestrians that have reached 3 m away from the door are instantaneously placed inside the room at a random position not closer than 1.5 m from any other pedestrian. Steady state simulations were performed for the following values of v_d: 0.8, 1.0, 1.125, 1.25, 1.375, 1.5, 1.75, 2.0, 2.25, 2.5, 3.0, 4.0, 6.0 and 8.0 m/s. The simulation time, in all cases, was 1000 seconds.

3.   Results and Analysis

3.1. Flow Rate versus Desired Velocity

Under steady state conditions the discharge curves have constant slope so the flow rate (number of particles leaving the room per unit time) is well defined and is the most relevant observable characterizing the evacuation performance of the system.

The state of the system which corresponds to most efficient evacuation is characterized by the v_d which maximizes the flow rate of the system.

As expected, the flow rate curve vs. v$_d$ has the same qualitative behavior than the evacuation time in the non stationary case, displaying an extreme at an intermediate value of v_d. However, the value of v_{dt} is quantitatively different. In the stationary problem $v_{dt} = 1.375$ m/s as can be observed in Fig. 1 (in the non stationary case, $v_{dt} = 2.0$ m/s).
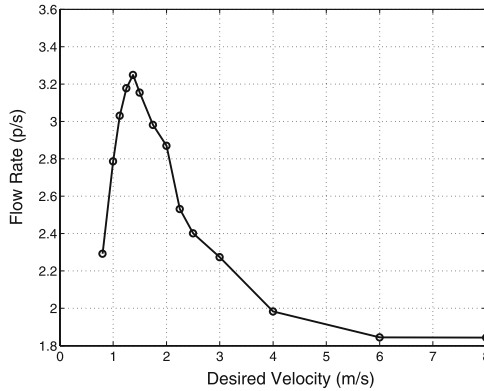
Figure 1: Flow rate of the evacuation system as a function of v_d.

3.2. Granular Cluster Analysis

In [8], a „granular cluster" (C_g) was defined in the following way: given a particle p_i of radius R_i and a cluster C_g:

$$p_i \; \varepsilon \; C_g \; \Leftrightarrow \; \exists \, p_j \; \varepsilon \; C_g \, / \, r_{ij} < \left(R_i + R_j \right)$$

where r_{ij} is the distance between particles centers of mass. This means that C_g is a set of particles that interact not only with social and desire forces, but also with granular forces.

Using the above definition we study the morphology of the system inside the room.

First, the cluster size distribution is analyzed for various values of v_d. In Fig. 2a we show such distributions for $v_d = 1.375$, 2.25, 2.5 and 3.0 m/s.

It can be seen that the shape of the distributions change from exponential (at low v_d) to U-shaped (for high v_d). In between a power law one can be found. This suggests that a phase transition might be taking place.

Looking at the second moment of the distribution without the maximum cluster, (see Fig. 2 b), we see that it displays a sharp maximum at $v_d = 2.25$ m/s , value at which the shape of the cluster size distribution is close to a power law one.

We then see that the value of v_{dt} at which the change of behavior of the flow rate takes
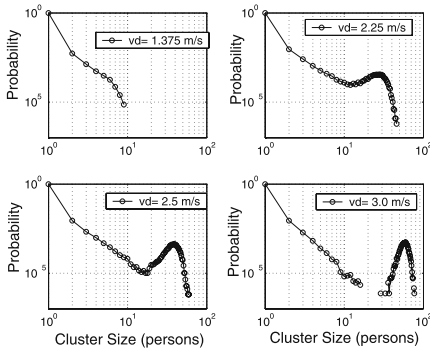
Figure 2a: Cluster size distributions for v_d = 1.375, 2.25, 2.5 and 3.0 m/s.
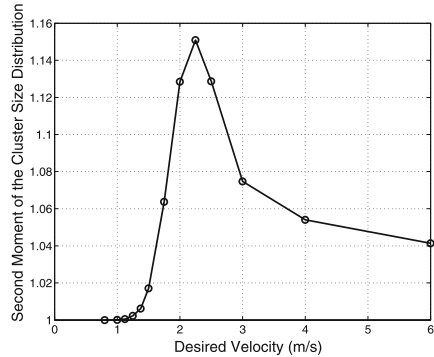
Figure 2b: 2nd moment of the cluster size distribution without the maximum cluster.

place (the flow rate change its tendency at v_{dt} = 1.375 m/s) corresponds to cluster size distribution well inside the exponentially decaying region. In the next section we explore the possible causes of the existence of an optimum v_d for evacuating the room.

3.3. Total System Forces Analysis

The probability of appearance of a blocking cluster as a function of v_d has the same tendency as in the non stationary case. This probability begins to be non negligible for values of v_d above v_{dt} = 1.375 m/s. And as in the non stationary case, it is clear that blocking clusters are responsible for the „faster is slower" effect above v_{dt}.

More information can be obtained if we analyze the total system forces.

Each particles has an unique desire force so the total desire force of the system at a given instant is

$$F_D^{Sys} = \sum_{i=1}^{N_p} \left| \mathbf{F}_{D\,i} \right|$$

For the granular interacting forces the corresponding instant total system force are given by the following equations:

$$F_G^{Sys} = \sum_{i=1}^{N_p} \sum_{j=1,\,j\neq i}^{N_p} \left| \mathbf{F}_{G\,ij}^{nor} \right| + \left| \mathbf{F}_{G\,ij}^{tan} \right|$$

In Fig. 3 the variations of the average granular and desire system forces over the region of low values of v_d can be observed.

This curves show two interesting points. The first one is the crossing point where the mean granular system force begins to be greater than the mean desired system force. This occurs near v_d = 2.25 m/s, the critical point from the granular cluster point of view (see section 3.2).

The second interesting point can be better seen if we calculate the difference between the mean desire force $<F_D^{Sys}>$ minus the mean granular force $<F_G^{Sys}>$ (Fig. 3 b).

It can be seen that this difference has a maximum at the v_{dt} where the system reaches its maximum flow rate.

This suggests that the optimum evacuation for the stationary case corresponds to a state in which a delicate relation between average desire force and average granular force is attained.

Taking into account that as the desired velocity is increased the granular force increases and that this last term does not behave linearly, the optimum evacuation is attained when the system reaches the maximal desired velocity that generates the minimal relative average granular force.
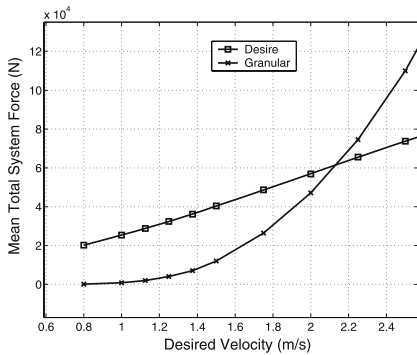
Figure 3a: Average system desire ($<F_D^{Sys}>$) and granular ($<F_G^{Sys}>$) forces versus v_d.
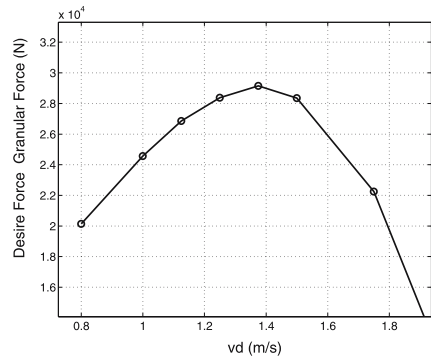
Figure 3b: Difference $<F_D^{Sys}>$ - $<F_G^{Sys}>$, shown in the previous figure. The v_d that maximizes this difference is v_{dt} (maximum evacuation efficiency).

4.   Conclusion

In this work we have performed simulations of a steady state version of the room evacuation problem. Under this condition the flow rate is well defined and it is the main observable of the system.

As in the stationary case shown by Helbing et al. we have found that there exists an optimum value of v_d at which the flow rate is maximized.

This optimum evacuation is attained when the difference between the average desire force and the average granular force is maximal.

This suggests the following explanation of the change in the flow rate curve: Being the average desire force related to the capacity of displacement of the particles and the average granular force related to the capability of particles forming clusters, this would indicate that the optimal evacuation corresponds to the situation in which particles move as fast as they can producing a minimum number of clusters. This is a preliminary result that should be further investigated.

Acknowledgments

References

1.   S. Gwynne, E.R. Galea, M. Owen, P.J. Lawrence, and L. Filippidis: *A review of the Methodologies used in the Computer Simulation of Evacuation from the Built Environment*, Building and Environment 34, pp. 741 (1999).
2.   Y. Tajima, K. Takimoto, and T. Nagatani: *Scaling of Pedestrian Channel Flow with a Bottleneck*, In: Physica A, 294, pp. 257 (2001).
3.   Y. Tajima and T. Nagatani: *Clogging Transition of Pedestrian Flow in T-Shaped Channel*, In: Physica A 303, pp. 239 (2002).
4.   T. Vicsek, A. Czirók, E. Ben-Jacob, I. Cohen, and O. Shochet: *Novel Type of Phase Transition in a System of Self-Driven Particles*, In: Physical Review Letters 75, pp. 1226 (1995).
5.   E.V. Albano: *Self Organized Collective Displacements of Self Driven Individuals*, In: Physical Review Letters 77, pp. 2129 (1996).
6.   A. Czirók, A.-L. Barabási, and T. Vicsek: *Collective Motion of Self-Propelled Particles: Kinetic Phase Transition in One Dimension*, In: Physical Review Letters 82, pp. 209 (1999).
7.   D. Helbing, I. Farkas, and T. Vicsek: *Simulating Dynamical Features of Escape Panic*, Nature 407, pp. 487-490 (2000).
8.   D.R. Parisi and C.O. Dorso: *Microscopic Dynamics of Pedestrian Evacuation*, In: Physica A 354, pp. 606 (2005).

Development of an Agent-based Behavior Module for Evacuation Models – Focused on the Behaviors in the Dark

J.H. Park[1], H. Kim[1], H. Whang[1], J. Park[1], and D. Lee[1]

In the occurrence of an emergency such as a fire, we must be able to come out of the structure we are staying at before its collapsing or fire spreading over it to save our lives. We can estimate the required safe egression time (RSET) for people to evacuate from structures such as a building and a passenger ship with Evacuation Model (EM). Although there are many EM's currently available, most of them can not simulate evacuation behaviors in the dark. This is fatal to the credibility of simulation by evacuation models. This paper describes a behavior module for evacuation models that can simulate evacuation behaviors in the dark, which is based on Intelligent Agent (IA) technology, to generate more a credible RSET. The module can generate (virtual) evacuees' key movements in the dark: (1) moving toward a wall, (2) following the wall to come out of the structure, and (3) reducing their travel speed to avoid collisions.

1. Introduction

Nowadays, there are many large and complex structures around us such as a department store, a metro station, an exhibition hall, and a passenger ship. If there is a fire in a structure of this kind, we may see that many people are killed by their lateness in escaping from the structure due to "risk factors" such as darkness, smoke, narrow stairways, complex internal configuration, and panic behaviour of evacuees.

In fact, more than two hundreds of people have lost their lives in the metro station fire in Daegu, the third largest city of Korea, 18 February 2003. Moreover, the terrorists' attack on WTC in 2001 killed more than two thousands of people.

To avoid such catastrophic results, many researchers and engineers have tried to get rid of risk factors such as narrow corridor in the early stage of design. For this, removing risk factors, the Performance-based Design (PBD) methodology has been introduced in 1990's [1].

Using PBD for safety design needs some tools that can calculate the Required Safe Egression Time (RSET) and the Available Safe Egression Time (ASET). With architectural engineering tools such as a structural strength analysis model, we can calculate the ASET of a building. For the RSET, we use an evacuation model (EM). Therefore to get a reliable result from the PBD, we must use reliable tools for RSET and ASET [2].

People's behaviour in the fire is different from their behaviour in normal situation. But most EM's do not mimic abnormal behaviour such as looking for a wall and then fol-

---

[1]Korea Ocean Research and Development Institute (KORDI)

lowing the wall. In this paper, we describe a behaviour module to make a more reliable EM focusing on human behaviour in fire.

This paper is organized as follows. In section 2, human behaviour in fire, PBD for safer design, and EM are briefly introduced for better understanding of readers. In section 3, previous work on behaviour module in EM is described. Section 4 describes a new approach to model human behaviour in fire using agent-based system (ABS) and section 5 shows some experiment results. Finally, we conclude our work and suggest future work in section 6.

2. Background

2.1. Human Behaviour in the Dark

In a daily life, we can easily identify some interesting characteristics of human, especially pedestrian, behaviours. First, pedestrians prefer the left to the right when they move on a street, a corridor, and so on. Second, if they must change their direction suddenly, they usually change their direction to the left. Third, they do not

Wall	Foregoing Evacuee	Handle	Nothing	Others
51	21	3	18	7

Table 1: Objects fumbled by survivors from the Daegu metro station fire (%)

Fast walkers	2.0
Slow walkers	1.0
Normal walkers	1.3
Crawlers (with hands and knees)	0.5
Evacuees familiar with the structure (in the darkness)	0.7
Evacuees unfamiliar with the structure (in the darkness)	0.3
Crowd	1.0
Fastest walker	3.0

Table 2: Evacuee's traveling speed in various conditions (m/s)

want to detour the path if there is nothing special on the longer path. They prefer shortcuts. Finally, they stick to the way of their coming in when they come out the structure.

For evacuation from a building, people show somewhat different behaviour: (1) they select the path they are accustomed at as their evacuation route, (2) they go forward a

place in the light, and (3) they catch up with persons ahead. Moreover, if evacuees are interfered by smoke and darkness due to the fire and blackout, they show additional different behaviour. First, they fumble for a wall to guide themselves. Second, after finding a wall, they use the wall or handles on it as guidance. Finally, they seriously reduce their travel speed due to smoke.

For example, during the evacuation process of the metro station fire in Daegu, about the half of survivors fumbled for walls to find their ways in the dark and smoke (Table 1) [3]. The travel speed of evacuees is also different from case to case (Table 2) [4][5]. This shows the importance of modelling human behaviours in the dark to develop a reliable EM.

2.2. Performance-based Design (PBD) for Safety

Generally everything that is considered during a design process can be characterized with the word of "performance." We can find out the proper number of elevators in a building in the design stage. For the safety aspect of a "structure" such as a building or a ship, we regard the RSET and the ASET's as the safety performance indices of the structure.

The RSET of a structure is the time needed for all the people in it to come out safely in an emergency. The ASET is the time during which the structure remains safe and can have many values. For example, the ASET for structural safety of a structure is the required time for it to collapse. Comparing the RSET and all the ASET's, we can decide whether a structure is safe or not in emergency such as a fire of a building and a sinking of a ship. With PBD methodology, we can decide the proper width of corridors to reduce the RSET, and modify the internal configuration of structures to increase the ASET.
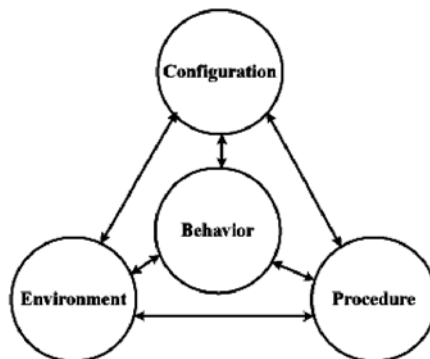
Figure 1: The Relationship between behavioural influences [7]

2.3. Evacuation Model (EM)

To calculate RSET, we use an EM that is a system or methodology to simulate and evaluate the effect of evacuation factors [6]. Evacuation factors are categorized into the internal configuration of structure, the environment during evacuation, the procedures to help evacuees, and the behaviour of evacuee [7].

As shown in Figure 1, which shows the relationship between evacuation factors, the behaviours of evacuees integrate all influences of other factors. Human behaviour is the result and expression of complicated decision-making which is based on his or her experience, knowledge, prediction, and intuition therefore it is not easy to find a satisfactory mechanism to model it. Some research teams used simplified methods and some tried more sophisticated mechanisms to achieve the goal, "modelling the behaviour of evacuee as real as reasonable."

3.   Previous Work

Currently, EM's are widely used for evaluating the evacuation capacity of all kinds of complex structures which accommodate many people in relatively small region. As EM expands its application area, many research teams have developed and are developing their own EM's. Most of EM's have their own behaviour module to mimic the people's behaviour during evacuation. In the earlier stage of EM development, there are several categories that means big difference of technical background of EM's. However, modern EM's do not have such a clear cut for classifying them based on their behaviour model because most of them use IA paradigm. By this reason, we classify EM's into three categories based on their geometry model: (1) continuous model, (2) discrete model, and (3) hybrid model.

Firstly, continuous model deals with all object including evacuees in the EM on the basis of continuous space. All the interactions between objects are calculated numerically by using physical and mathematical equations that represents evacuees' physical and psychological behaviours. This category includes Helbing's social force model [8] and Simulex [9].

Secondly, discrete model uses cell-like geometry. All walls and obstacles are transformed to discrete space and they occupy some cells on the space. Evacuees' behaviour is determined by using other cell's information such as occupation by other evacuee. During modeling the geometry information, the connections between cells can be defined either explicitly or implicitly. The former approach is called node-arc model, which has EXODUS [7] and EvacuShips [10] as its representative EM. The later is called grid-square model and PedGo [11] and Cellular Automata (CA) based EM are included in this kind of model.
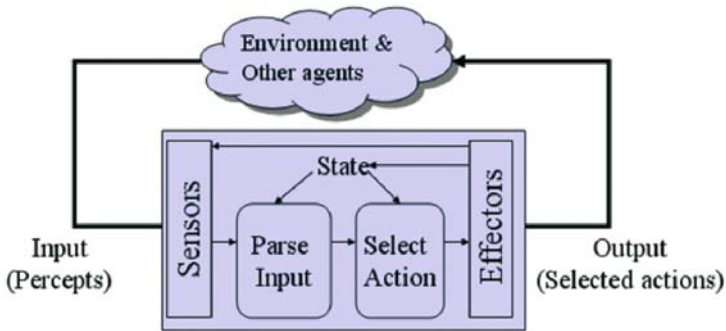
Figure 2: Conceptual diagram of Agent-Based System (ABS)

Finally, hybrid model uses continuous geometry basically but makes practical application of discrete model to reduce computation time. For example, although collision detection or prediction has O(N2) time complexity, where N is the number of all objects in the space, it can be dramatically reduced if only the neighboring objects, which can be easily determined in discrete geometry, are considered. In addition to the computing resource aspects, discrete model has advantage in cooperating with fire model that generates the most important ASET value. By these reasons, most recently developed EM's such as AENEAS [12], Evi [13], SESAMO [14], ASERI [15], and IMEX [16] use hybrid model.

Although some EM's model several special behaviours such as communication between evacuees and interaction between evacuees and evacuation helping staffs, most of currently used EM's can not correctly simulate human behaviours in the dark and smoke. They usually concentrate on collision prediction and avoidance. Human behaviours in the dark can not be same as those in the light and the moving speed will be different also. To get more accurate RSET, we need give more effort to model human behaviour in the dark in more detail, but most of EM's only reduce evacuees' travel speed for that.

4. Agent-based Behavior Module for EM

In this paper, Intelligent Agent (IA) concept is used to overcome the problems of behaviour modules of currently used EM's. IA concept enables us to model more naturally complicated behaviour such as interaction between evacuees during evacuation, communication, group behaviour, and physical interaction with force.

4.1. IA System

IA is an autonomous entity that can interact with its environment adaptively. IA has three required properties: autonomy, interactivity, and adaptiveness [17]. Using IA, we can build an Agent-Based System (ABS) which consists of agent, environment, and

coupling between them (Figure 2). IA consists of state, input, output, and process. Environment in ABS also has its state and process. Coupling is standardized interfaces for input and output between agent and environment.

EM can be an example of ABS. By applying IA technology to the development of an EM, we can describe each evacuee's behaviour in detail and in precision. IA-based behaviour module collects information from evacuation environment, processes it, and then generates proper behaviours in certain environmental condition such as darkness

4.2. Behavior Modeling

If we use IA concept for the development of an EM, we can separate behaviour module from the overall structure of the EM. This means that the complexity of behaviour that can be modeled by EM can increase with relatively small effort compared to traditional approaches. Because we use IA paradigm, evacuees' behaviours are modeled through three phases: sensing, parsing, and action selection.

In the first phase, our behaviour model, the IA, collects two dimensional visual data and its visual field is determined using its current heading. We use 180 degree as the range of evacuee's visual angle. Until now it can collect neither of three dimensional visual data and audio data, which will be implemented in the future.
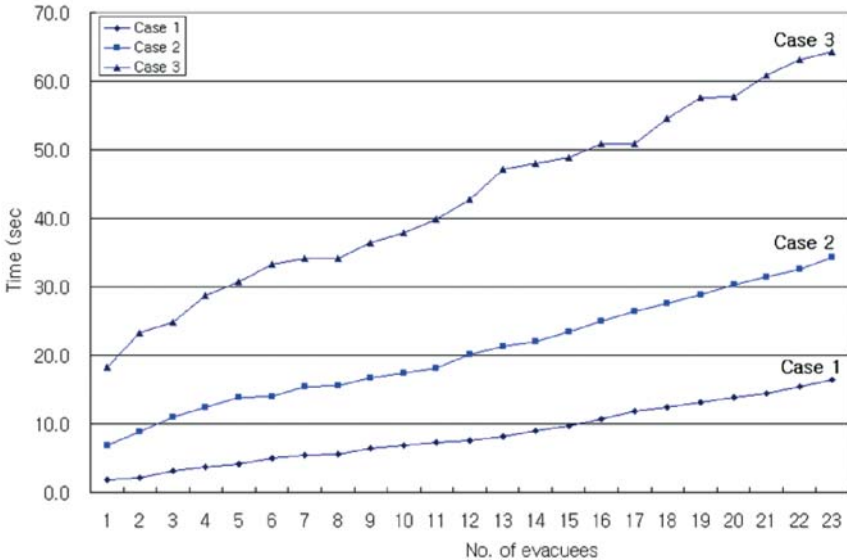
Figure 3: Cumulative evacuation time of each scenario
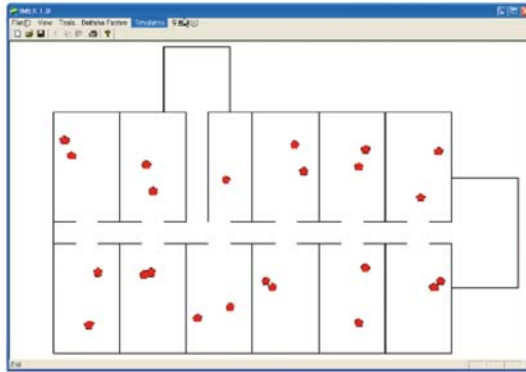
(a) After 0 second: ready for fumbling
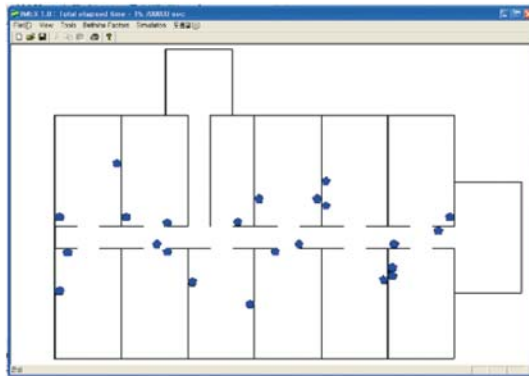
(b) After 15 seconds: wall-following
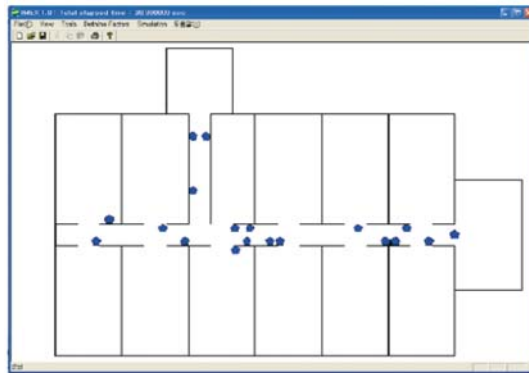
(c) After 30 seconds: wall-following

Figure 4: Screen images of fumbling and wall-following behaviour

In the parsing phase, the IA classifies recognized object into two categories, moving objects and fixed objects, and then collision to each object is predicted.

In the action selection phase, navigational activities are performed. The navigational activities include path-finding, collision avoidance based on collision prediction information, and queuing behavior. In addition to the data from outside the IA that are recognized in the earlier phase, internal attributes of several kinds are used in this phase. Those attributes represent physical status, emotional status, cognitive attribute, and social status of evacuees [18].

For the modeling of human behaviors in the dark, we make evacuees select their heading and then fumble until they reach a wall. Moving direction for fumbling is randomly determined and the travel speed is in the range 0.3 m/sec and 0.7 m/sec.

After reaching a wall, evacuees use the wall as its guidance to exits. When an evacuee is in a room and contact with a door, it passes through the door. But the evacuee treats a door as a wall if he or she is outside a room. For routing, no structural information is used. The only routing scheme is following walls and no overtaking occurs.

5.   Experiment Result

The IMO test case 10 in MSC/CIRC. 1033 ANNEX 3, "Interim Guidance On Validation/Verification of Evacuation Simulation Tools" deals with the most complex configuration among the test cases thus the simulation result is vulnerable to the assumption of the dark [19].

We simulated the system using the test case 10 with three scenarios and compared resuts: (1) evacuation with optimal routing and maximum speed, (2) evacuation with optimal routing and reduced speed, and (3) evacuation with wall-following routing and reduced speed.

For the first scenario, the shortest path routing scheme is used and evacuees moves in the speed range of 2.0 m/sec and 3.0 m/sec. From the simulation, we get an RSET around 15 seconds. For the second scenario, evacuees moves in the speed range of 0.3 m/sec and 0.7 m/sec with the same routing scheme. The simulation generates RSET around 35 seconds. The final scenario generates RSET around 65 seconds.
Figure 3 is cummulative evacuation time graph and the result shows that the evacuation in the dark requires much more time. In the first two scenarios, the RSET's are propotional to evacuees' travel speed but the RSET from last scenario is not. This is because the differnce of total travel distance. The last scenario does not assume shortest path routing and it make evacuees just follow the wall. This results in detours in routing. During the simulation, the evacuees showed fumbling, wall-follwing, and speed reduction behaviour (Figure 4).

6.   Conclusion and Future Work

In this paper, IA-based evacuee behaviour module is developed that can mimic human behaviour during evacuation in the dark. The module shows the behaviour of: (1) moving forward to find a wall, (2) following the wall to come out of the structure, and (3) reducing traveling speed. This module can more precisely estimate RSET of structures considering the effect of the dark and smoke.

To model evacuees' behaviour more correctly, we are implementing the communication between evacuees and group behaviour. These two behaviours play important role in escaping from dark space. Evacuees can not see each other and thus they will try to communicate with voice and after confronting each other, they will determine to escape together or individually. This process can be modeled only after implementing communication and group behaviour.

7.   Acknowledgements

References

1.   V. Brannigan and A. Kilpatrick: *Engineering Human Behaviour: The Human Factor in Performance Based Regulations*, Proceedings of the 3rd International Symposium on Human Behavior in Fire, pp. 463 (2004).

2.   D.A. Purser: *Behaviour and Travel Interactions in Emergency Simulations and Data Needs for Engineering Design*, In: E.R. Galea (Ed.), Proceedings of the 2nd International Conference on Pedestrian and Evacuation Dynamics, pp. 355 (2003).

3.   S. Blake et al.: *An Analysis of Human Behaviour During the WTC Disaster of 9/11 Based on Published Survivor Accounts*, Proceedings of the 3rd International Symposium on Human Behaviour in Fire, pp. 181 (2004).

4.   G.Y. Jeon and W.H. Hong: *The Research and Analysis of Fire at the Daegu Subway: A Study in Human Behavior Pattern and its Application to the Design of Escape Routes*, Proceedings of Korea Architect Society Conference, Vol. 23, No. 2, pp. 885 (2004).

5.   H. Frantzich and D. Nilsson: E*vacuation Experiments in a Smoke Filled Tunnel*, Proceedings of the 3rd International Symposium on Human Behavior in Fire, pp. 229 (2004).

6.   J.H. Park et al.: *Simulation-Based Evacuation Analysis on a High Speed Coastal Passenger Ship*, Proceedings of the Seoul International Simulation Conference, pp. 444 (2001).

7.   S. Gwynne and E.R. Galea: *Escape as a Social Behaviour*, CMS Press, Paper No. 97/IM/21 (1997).

8.   D. Helbing et al.: *Simulating Dynamical Features of Escape Panic*, Nature, Vol. 407, pp. 487-490 (2000).

9.   P. Thompson, et al.: Simulex: *Analysis and Changes for IMO Compliance*, In: E.R. Galea (Ed.), Proceedings of the 2nd International Conference on Pedestrian and Evacuation Dynamics, CMS Press, University of Greenwich, London, pp. 173 (2003).

10. L.J. Carroll, L.L. Koss, and A.T. Brumley: *EvacuShip Analysis Based on IMO Test Cases and Other Benchmark Comparisons*, In: E.R. Galea (Ed.), Proceedings of the 2nd International Conference on Pedestrian and Evacuation Dynamics, CMS Press, University of Greenwich, London, pp. 185 (2003).

11. H. Klüpfel and T. Meyer-König: *Characteristics of the PedGo Software for Crowd Movement and Egress Simulation*, In: E.R. Galea (Ed.), Proceedings of the 2nd International Conference on Pedestrian and Evacuation Dynamics, CMS Press, University of Greenwich, London, pp. 331 (2003).

12. U. Petersen, et al.: *Ship Evacuation Modelling*, In: E.R. Galea (Ed.), Proceedings of the 2nd International Conference on Pedestrian and Evacuation Dynamics, CMS Press, University of Greenwich, London, pp. 209 (2003).

13. D. Vassalos, et al.: *Advanced Evacuation Analysis – Testing the Ground on Ships*, In: E.R. Galea (Ed.), Proceedings of the 2nd International Conference on Pedestrian and Evacuation Dynamics, CMS Press, University of Greenwich, London, pp. 147 (2003).

14. A. López and F. Pérez: *Ship Evacuation Optimisation – Tools for Master and Designer Aid*, In: E.R. Galea (Ed.), Proceedings of the 2nd International Conference on Pedestrian and Evacuation Dynamics, CMS Press, University of Greenwich, London, pp. 221 (2003).

15. V. Schneider: *Simulating the Evacuation of Large Assembly Occupancies*, In: E.R. Galea (Ed.), Proceedings of the 2nd International Conference on Pedestrian and Evacuation Dynamics, CMS Press, University of Greenwich, London, pp. 319 (2003).

16. J. H. Park, H. Kim, and D. Lee, *Development of an Intelligent Agent for Evacuation Model*, In: E.R. Galea (Ed.), Proceedings of the 2nd International Conference on Pedestrian and Evacuation Dynamics, CMS Press, University of Greenwich, London, pp. 383 (2003).

17. Agent Platform Special Interest Group, Agent Technology Green Paper (2000).

18. B. Schmidt: *The Modeling of Human Behavior*, SCS (2000).

19. IMO: *Interim Guidelines for Evacuation Analysis for New and Existing Passenger Ships*, MSC/Circ. 1033 (2002)

Comparative Investigation of the Dynamic Simulation of Foot Traffic Flow

C. Rogsch[1], A. Seyfried[2], and W. Klingsch[1]

Evaluation and optimization of emergency route systems can be accomplished with different engineering methods. These methods are based on two different principles: the macroscopic and the microscopic approach. Both allow forecasting of evacuation times for various settings. In the work presented simple settings are investigated, consisting of rooms, corridor and stairs with regard to evacuation times. These calculations use current computer simulation programs, based on microscopic models, and the macroscopic method of Predtechenskii and Milinskii [1]. For the computer simulation we used ASERI 3.4c, buildingEXODUS V4.0 Level 2, PedGo Version 2.1.1 and Simulex 11.1.3. The comparison of the results shows that even for the simplest systems evacuation times vary considerably for different simulation programs and deviate from experimental results. Furthermore we investigated effects of geometric boundary conditions on the evacuation time.

1. Introduction

Already in the past investigations were performed, to verify computer simulation programs [2] and the hand-calculating-method of Predtechenskii and Milinskii [3]. For these examinations the evacuation time of complete buildings was calculated and compared with real measurements. However, this investigations did not guarantee that, these models describe the pedestrian flow in details through corridors, doors or stairs of building correctly. To exclude compensation effects one has to verify the models for each pedestrian facility separately. To compare results of the computer simulation programs among each other as well as with those of the hand-calculating-method of Predtechenskii and Milinskii we performed investigations at very simple geometries (scenarios).

1.1. Settings

In order to ensure a comparability of the results, no external steerings (e.g. speed-decreases or flow-limitations at exits) are used. The input-parameters for the characterisation of the pedestrians differ among the programs. We have chosen these parameters carefully to ensure the following values:

» unimpeded walking velocity: 1.35m/s +/- 0.2 m/s
» velocity upstairs: 50% of unimpeded walking velocity

[1]Institute for Building Material Technology & Fire Safety Science, University of Wuppertal, Pauluskirchstrasse 7, 42285 Wuppertal, Germany
[2]Central Institute for Applied Mathematics, Research Centre Jülich, 52425 Jülich, Germany

For the hand-calculating-method of Predtechenskii and Milinskii, the following groups of persons were used:

» people in winter-dress, normal conditions
» people in summer-dress, emergency conditions

2.   Investigated Scenarios

The presented results describe five different scenarios. Scenario 1 and 2 correspond to a 50 m long corridor. To exclude effects from passing the width of corridor at Scenario 1 is narrow. At Scenario 2 passing manoeuvre are possible and intended. Scenario 3 represents a simple room. At these three scenarios the investigations are performed with standard boundary conditions (persons are removed after reaching time measurement) and with improved boundary conditions (persons are not removed after time measurement) respectively. Scenario 4 consists of a room with a corridor, and for Scenario 5 a stair directed upward is added. Scenario 4 and 5 are only examined with standard boundary conditions. To investigate the relation between evacuation time and density we increased the number of persons in the scenarios and measured the time in which the last person left the facility.

2.1. Scenario 1 and 2

At Scenario 1 the corridor-width is chosen such that pedestrians move along a line, at Scenario 2 the corridor-width is 2 m i.e. passing is possible. Results for the improved boundary conditions are labelled with „extra-floor" (see Figure 2 and 3). As follows from Figure 2, most programs show longer evacuation times with increasing density. That this relationship holds also for a movement of pedestrians along a line is shown in [4]. Results of Scenario 2 (Figure 3) illustrate increase of evacuation time with increase of density for all programs. The visual analyses of animations from the program buildingEXODUS suggest that in this case the decrease of the velocity is realized by passing. Because of the length of the corridor, improved boundary conditions (extra-floor) probably do not have substantial influence on the evacuation time.
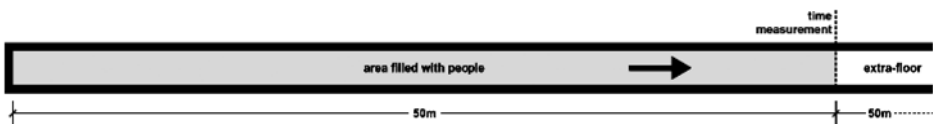
Figure 1: Scenario 1 and 2
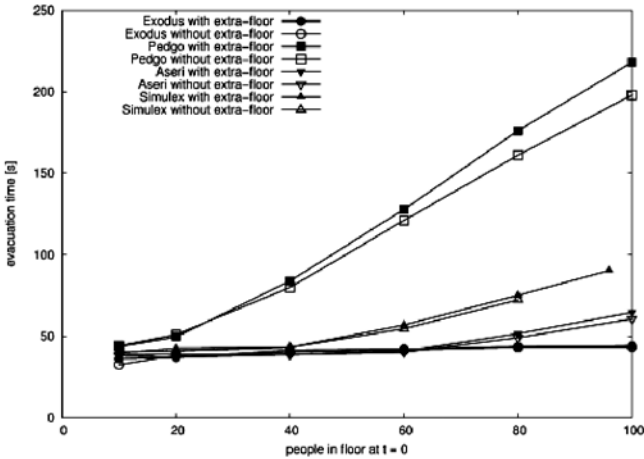
Figure 2: Scenario 1: influence of an extra-floor on evacuation time (linear movement)
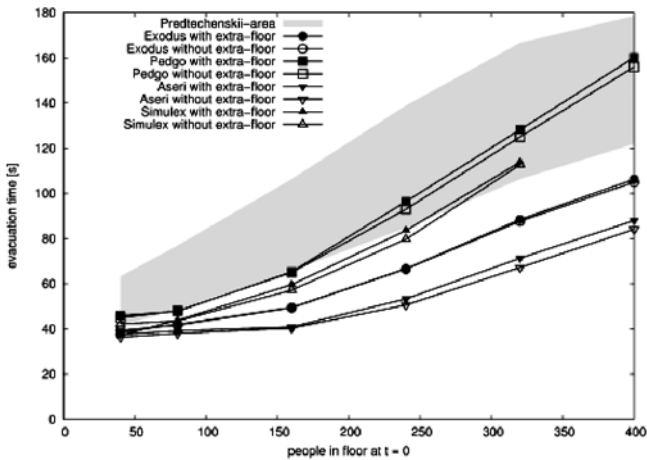
Figure 3: Scenario 2: influence of an extra-floor on evacuation time (planar movement)

2.2.   Scenario 3

The influence of the boundary conditions (extra-room) becomes apparent at this scenario. Preceding persons have an influence on the movement of the following persons. By removing persons after reaching the exit this influence is neglected and leads to an underestimation of the evacuation times. The large differences of evacuation times for different boundary conditions with the program Simulex indicates that influence between following persons is correctly implemented.
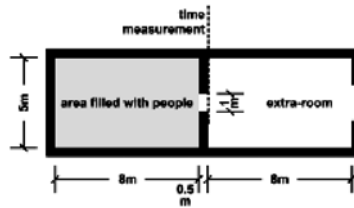
Figure 4: Scenario 3
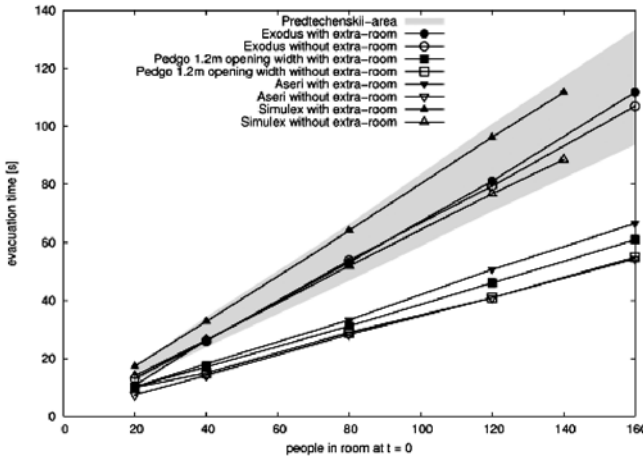
Figure 5: Scenario 3: influence of an extra-room on evacuation time

2.3.   Scenario 4

From results of Scenario 4 it is remarkably that some programs achieve only with flow-limitations (with door) the range determined by Predtechenskii and Milinskii, without flow-limitation the resulting evacuation times are smaller.
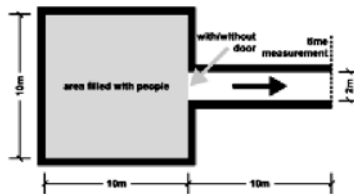
Figure 6: Scenario 4
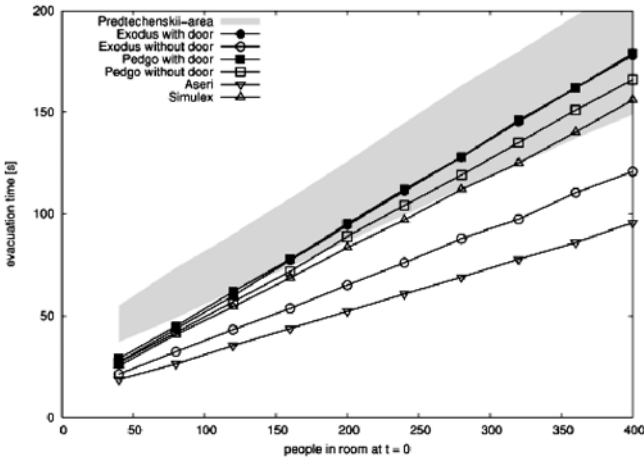
Figure 7: Scenario 4: evacuation time vs. number of people

2.4.   Scenario 5

Spread of results between the programs is remarkable wide. Compared with the range determined by Predtechenskii and Milinskii all computed results are higher or lower.
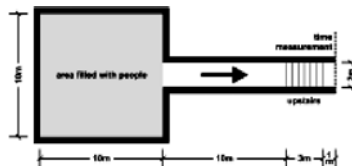
Figure 8: : Scenario 5

3.   Conclusions

Our investigation shows the large spread in the calculated evacuation times when different programs are used. For a simple room the results differ up to 100%, for the linear movement on a narrow corridor even up to 300%. Partially they fail to reproduce the experimentally relationship between raising density and longer evacuation time. The investigations showed that computer simulation programs tend to predict smaller evacuation times than the method of Predtechenskii and Milinskii. Stapelfeldt assessed even the results of Predtechenskii and Milinskii as very theoretical and fast [5]. Tendency of spread is not constant however. By that for more complex geometries differences between programs and the method of Predtechenskii and Milinskii may decrease.
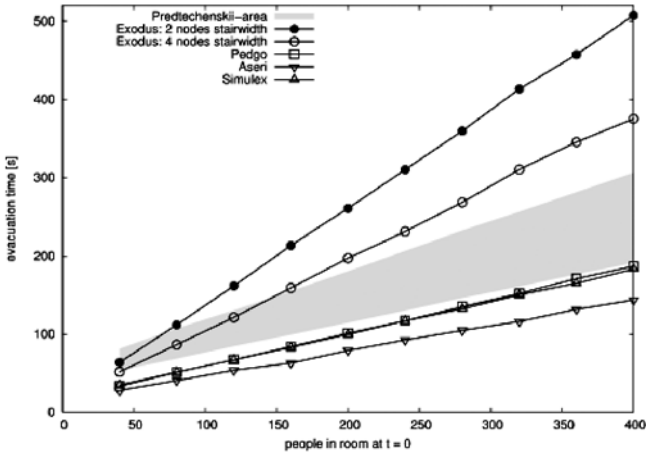
Figure 9: Scenario 5: evacuation time vs. number of people

Acknowledgments

References

1.   W.M. Predtetschenski and A.I. Milinski: *Personenströme in Gebäuden - Berechnungsmethoden für die Projektierung*, Verlagsgesellschaft Rudolf Müller (1971).
2.   L.S. Weckman and S. Mannikkö: *Evacuation of a Theatre: Exercise vs Calculations*, Fire and Materials 23, pp. 357-361 (1999).
3.   Bundesminister für Raumordnung, Bauwesen und Städtebau: *Untersuchung der Räumungsabläufe in Gebäuden als Grundlage für die Ausbildung von Rettungswegen, Teil III: Reale Räumungsversuche*, IRB-Verlag (1979).
4.   A. Seyfried et al.: *The Fundamental Diagram of Pedestrian Movement Revisted*, Journal of Statistical Mechanics, P10002 (2005).
5.   J. Stapelfeldt: P*ersonenströme durch Ausgangstüren - Beobachtungen und Versuchsergebnisse*, Brandschutz/Deutsche Feuerwehrzeitung 1 pp. 12-16 (1976).

Evacuation from underground railway stations – Available and required safe egress time for different station types and general evaluation criteria

R. Könnecke[1] and V. Schneider[1]

Safe egress in case of a fire emergency is a major challenge for all parties responsible for the design and operation of underground railway stations. Since empirical data on egress behaviour, evacuation efficiency and smoke spread is scarce, numerical simulations are an important tool in order to determine available and required safe egress time. Egress times for different types of stations and various occupant distributions are calculated using the microscopic evacuation model ASERI. Required egress times are related to corresponding available egress times obtained from CFD smoke spread simulations by applying evaluation criteria included in the German vfdb Guideline "Methods of Fire Safety Engineering". These investigations were part of a larger project including the local fire authorities to develop methods and criteria for fire safety concepts of existing and new subway stations in the city of Frankfurt.

1. Introduction

In 2001, a work group was constituted in Frankfurt am Main, Germany, including members of the local building authorities and fire brigades, scientists and fire engineers. The task of this group was the development of methods and criteria to create and analyse fire safety concepts for existing and new subway stations in the city of Frankfurt. To achieve this, methods of performance based fire engineering – including numerical simulation of fire and smoke spread and egress movement – were applied on new and existing stations. This paper is focused on the numerical simulations of egress movement and on the conclusions drawn from these results. Evaluation is done by applying the methods outlined in chapter 8 (Occupant safety) and chapter 9 (Egress analysis) of the recently published German vfdb-Guideline "Methods of Fire Safety Engineering"[1].

2. Available safe egress time in subway stations

A number of design fire scenarios differing with respect to fire size and fire location were investigated by numerical smoke spread simulations using the CFD model KOBRA-3D. A fire starting inside the passenger section of a subway train has been identified to be the worst case scenario. In order to obtain accurate dynamic rate of heat release input data it was decided to perform a series of fire tests and detailed combustion analysis for the motor coach of this type of train. It occurred that starting a fire inside this wagon requires an initial fire of substantial size. So the actual design fire scenario for the type of underground coaches used in Frankfurt assumes a buggy loaded with shopping

---

[1]I.S.T. Integrierte Sicherheits-Technik GmbH, Frankfurt am Main, Germany

goods inside the coach as initial fire source to start fire spread inside the wagon. The rate of heat release increases continuously within the first 30 minutes reaching a peak at 5.6 MW[2]. Together with corresponding yields of combustion products, mass optical density and heat of combustion this rate of heat release was used to determine the available safe egress time for the underground stations to be analysed.

In order to obtain the available safe egress time for a specific scenario, the results of the smoke spread calculations were analysed using the life safety criteria summarized in table 1. These values are considered to be thresholds for an acceptable exposure and are thus below corresponding tenability limits.

Life safety criteria	30 min exposure	15 min exposure	5 min exposure
CO concentration	100 ppm	200 ppm	500 ppm
CO_2 concentration	1 Vol.-%	2 Vol.-%	3 Vol.-%
HCN concentration	30 ppm	40 ppm	55 ppm
heat radiation	1,7 kW/m^2	2,0 kW/m^2	< 2,5 kW/m^2
smoke temperature	50 °C	50 °C	60 °C
optical density	0,1 m^{-1} – 0,2 m^{-1}	0,1 m^{-1} – 0,2 m^{-1}	0,1 m^{-1} – 0,2 m^{-1}
visibility	20 m – 10 m	20 m – 10 m	20 m – 10 m

Table 1: Limiting values for acceptable exposure[1]

Figures 1 and 2 give an example of the kind of simulations performed to obtain the available safe egress time for the underground railway stations under investigation. The optical smoke density per path length D is depicted in figure 2. The domes are used for natural smoke venting. Two smoke barriers are located above the stairway exits. Smoke spill below the barriers occurs after 3 minutes (right hand side) and 8 minutes (left hand side) respectively limiting the available safe egress time for the respective exits.

For existing stations, based on the smoke spread simulations measures were proposed to enlarge the available safe egress time. In most cases, smoke barriers or enclosures were proposed. In some cases supplemented by smoke vents. Two stations that were built during this period were designed according to the concepts developed in this work group.
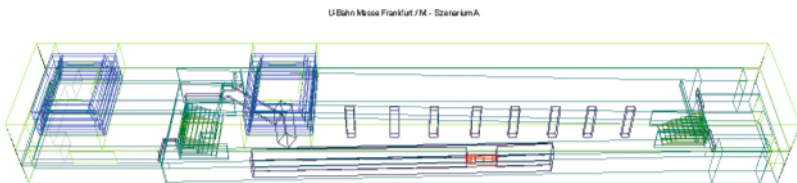

U-Bahn Messe Frankfurt /M - Szenarium A

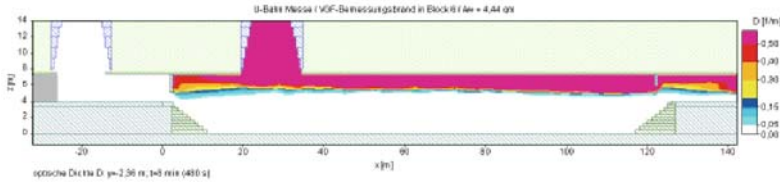**Figure 1**: Subway station with skylight domes

Figure 2: Smoke spread after 8 minutes

3.   Required safe egress time in subway stations

The bi-lingual (German-English) handbook "Fire Protection in Vehicles and Tunnels for Public Transport" 3 includes detailed descriptions of scenarios and methods to be used to evaluate self-rescue from stations. According to this guideline, egress times should be determined based on validated methods like NFPA 130 "Standard for Fixed Guideway Transit Systems", the calculation method described by Predtetschenski and Milinski or advanced microscopic evacuation models such as SIMULEX, STEPS or ASERI.

The number of people involved in an evacuation can be determined either by the procedure adopted in NFPA 130 or by the so-called EBA guidelines. As an alternative, it is possible to use firm figures from passenger counts or calculated forecasts, but not mere estimates. In the EBA guidelines, the maximum number of people to be taken into account is ascertained by the relation[3]

$P_{max} = n \times (P_1 + P_2) + P_3$

n is the number of tracks by the platform, P_1 is the seating capacity of the longest train units, P_2 is the number of permissible spaces for standing passengers and P_3 is the number of people waiting on the platform. This value is to be set to 30 % of the sum of P_1 and P_2.

For a number of stations, a detailed egress analysis was performed using the computer model ASERI. ASERI is a microscopic evacuation model simulating the individual movement of evacuees inside a complex three-dimensional environment[4].

The stations types investigated include low stations (height less than 4 m) with stairs on opposite side of platform or only in middle section of platform, high stations enclosing a large volume with stairs on opposite side of platform and crossing stations (in some cases including adjacent shopping areas).

Figures 3 and 4 illustrate the egress behaviour of people inside a complex four-level underground station. Figure 3 depicts the path of evacuees coming from the platform level into the concourse level and there taking the shortest path to the exit level.
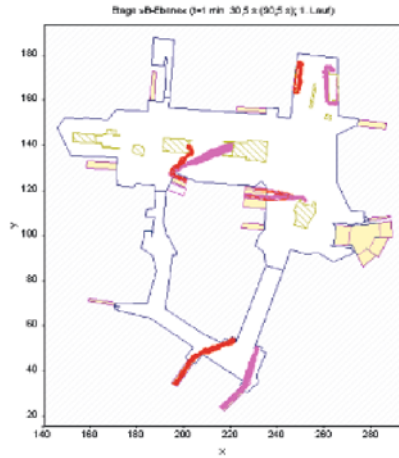
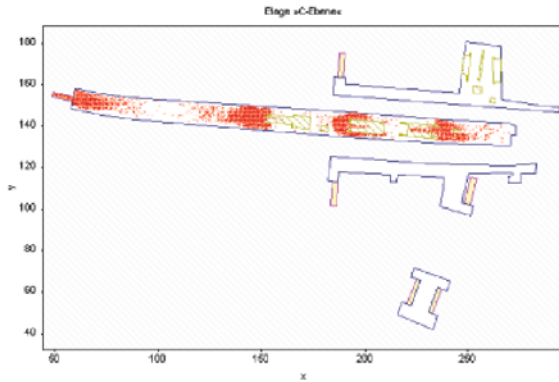**Figure 3**: Concourse level and shopping area of a complex underground station

Figure 4: Upper platform level of a complex underground station

Figure 4 shows cue formation at the four exit stairs at platform level half a minute after the start of egress movement. While balanced exit use can be assumed for most stations with simple structure and only one or two platforms, egress route choice behaviour is a decisive factor in determining the required safe egress time in complex underground stations.

Empirical and numerical studies on pedestrian flow during rush hour in Frankfurt subway stations[5] indicated total egress times of 5 to 7 minutes. Figure 5 illustrates the movement of passengers to and from the subway trains, stairs and escalators. The distribution is derived for a 30 minute interval during rush hour. The red lines represent passengers leaving the incoming trains, the blue and green lines indicate the paths of passengers to their respective wait positions before entering outgoing trains.

Numerical simulations of worst-case scenarios with respect to the number of evacuees
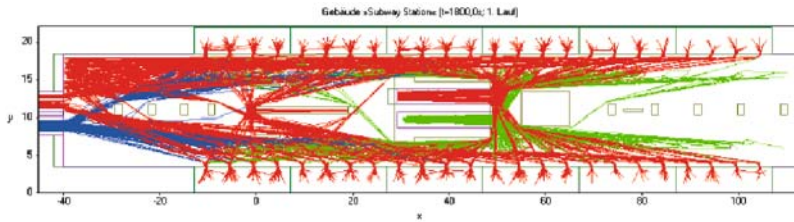
Figure 5: Track map of passenger movement on platform

resulted in travel and passage times of up to 7 minutes. To achieve a total egress time below 10 minutes (a limit required by the building authorities) the pre-movement time has to be less than 3 minutes, requiring an appropriate alarm system and fire safety management.

4.   Conclusion

Based on the expertise of the members of the work group and the analysis of numerical simulations for smoke spread and egress movement a general concept was laid down based on risk categories for the specific station and the type of train:

Risk identification:	station type
	maximum occupant load
	train type
	train travel time between stations
Risk assessment:	required safe egress time (evacuation modelling)
	available safe egress time (smoke spread modelling)
	classification (hazard levels)
Priority classification:	
Risk management:	Specific performance-based fire safety concepts
Hazard levels (train):	
Z1	wagons with low fire severity
Z2	wagons with high fire severity
Hazard levels (station):	
Type A	low station (height less than 4 m), stairs on opposite side of platform
Type B	low station (height less than 4 m), stairs in middle of platform
Type C	high stations, stairs on opposite side of platform
Type D	crossing stations (individual special cases)

At least one egress path has to be kept available for a period of ten minutes by means of an appropriate smoke management system (smoke vents, shafts or barriers). This ten minute time interval requires a high-class alarm and information system, including well-trained staff. **«**

References

1. D. Hosser (Ed.): *vfdb-Leitfaden Ingenieurmethoden des Brandschutzes*, iBMB Braunschweig), Entwurf Juni 2005 (2005).
2. E. Wilk: *Bericht zur Bestimmung eines Bemessungsbrandes für Triebfahrzeuge der U-Bahn / Frankfurt a. M.,* Anlage 8, Brandschutz Consult Ingenieur-gesell-schaft mbH, Leipzig, November 2002 (2002).
3. F. Blennemann and G. Girnau (Eds.): *Fire Protection in Vehicles and* T*unnels for Public Transport,* Research Association for Underground Transportation Facili-ties, Cologne, Mai 2005 (2005).
4. V. Schneider and R. Könnecke: *Simulating Evacuation Processes with ASERI*, In: M.Schreckenberg and S.D. Sharma (Eds.), Proceedings of the International Conference on Pedestrian and Evacuation Dynamics, Springer, Berlin (2002).
5. H.-J. Fischer, R. Könnecke, and C. Ordon: *ET: Neue Zugangsbarrieren durch Chipkarten¬lesegeräte? – Grundlagenuntersuchung im Hauptbahnhof Frankfurt am Main*, Der Nahverkehr 6/2001, pp. 34 – 38 (2001).

A discrete microscopic model for pedestrian dynamics to manage emergency situations in airport terminals

M. Schultz[1], S. Lehmann[1], and H. Fricke[1]

Airport terminals have to cope with both safety and security aspects. A terminal is divided into public and non-public areas which have different security levels and require several ways to control passengers (EU 2320/2002). The developed model must consider the mix of screened and unscreened passengers, the ever-changing traffic volume, the use of emerging technologies, and the changes made to legal requirements. Inside the terminal heterogeneous groups of people are located with different personal profiles. The discrete microscopic simulation model for passenger motion behavior presented here is based on an enhanced cellular automata model. This model considers repulsion potentials, friction effects, and path finding/guidance algorithms. To control the evacuation process, the route choice approach can be used to integrate different evacuation strategies. The model reacts fast to changes in the surrounding area and provides multiple simulation runs with an altering parameter set in a short time. To ensure a reliable result a multi-level diagnostic of the evacuation process is necessary for considering the overall evacuation time, the identification of potential bottlenecks, the analysis of the critical path through the airport terminal, guidance system influences on pedestrian dynamics, and the effects of adjusted structural measures.

1. Introduction

An airport terminal is primarily a processing building, an intermodal interchange, and an ever increasing world of excitement and diversity. There are a lot of small and medium facilities with special interests and constraints. Also, the use of wide-bodied aircrafts (e.g. A380) will lead to non-predictable higher concentrations of human beings in public and non-public areas inside an airport terminal that have not been analyzed thus far. Naturally, these crowded areas have a hazardous potential even when not considering cases of emergency.

The proposed methodology to demonstrate pedestrian dynamics [1, 2] is based on the common approach of the cellular automaton simulation model [3, 4], necessary enhancements and the social-force-based repulsion forces [5].

Inside the airport terminal heterogeneous groups of people (employees, passengers, well wishers, and visitors) are located with different personal profiles. These profiles are fundamentally categorized by citizenship, language, knowledge of the environment, culture attitudes, assertiveness and the general physique of each person.

Airport terminals as a transport interchange have to be safe from a security perspective as well. Interferences of the normal airport operations (emergencies) can lead to an inappropriate mix of screened and unscreened as well as domestic and international passengers / baggage flow [6].

---

[1]Institute of Aviation, Faculty of Transport and Traffic Sciences „Friedrich List", Dresden University of Technology, D-01062 Dresden, Germany

2.   Model

The model of the cellular automaton is a microscopic simulation model, that is both spatial and time discrete. The simulation environment is parted in square cells with an area of 0.4 m x 0.4 m, considering the minimal requirements of space of a single person [7]. A cell possesses two different states - the ground state „free" and the state „occupied" if a person or an obstacle is on it. A person can move to all surrounding cells (Figure 1a). The motion to other cells depends upon the transition probability stored in the preference matrix $M_{q,p}$ (Figure 1b).
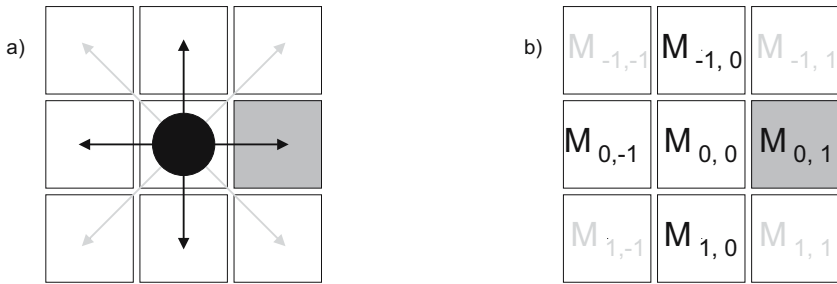
Figure 1: cell neighborhood and preference matrix.

If one assumes the independence of the longitudinal (p) and the transverse (q) components of the passengers velocity, the movement to $M_{0,1}$ ($M^{hori.}$) is determined by the common transition probability h calculated by the variance σ^2 and the expected value μ [3].

$$h_{-1} = \frac{1}{2}(\sigma^2 + \mu^2 - \mu) \qquad \mu_q = 0 \qquad\qquad 0 \leq \mu_p \leq 1 \tag{1}$$

$$h_0 = 1 - (\sigma^2 + \mu^2) \qquad 0 \leq \sigma_q^2 \leq 1 \tag{2}$$

$$h_{+1} = \frac{1}{2}(\sigma^2 + \mu^2 + \mu) \qquad \frac{1}{4}\left(|\mu_p| - \frac{1}{2}\right)^2 \leq \sigma_p^2 \leq 1 - |\mu_p|^2 \tag{3}$$

A direction dependent movement can be developed by the superposition of $M^{hori.}$ and $M^{diag.}$, which is a copy of $M^{hori.}$ turned by 45°, to consider the special case of diagonal movement (further details in [3]).

$$M_{q,p} = [1-\lambda]M_{q,p}^{hori.} + \lambda M_{q,p}^{diag.} \qquad \lambda = \tan\alpha \qquad 0° \leq \alpha \leq 45° \tag{4}$$

3.   Results

Distance

The periodic lattice structure composed of square cells has the negative side effect that there is not the same distance from one cell to every surrounding cell (seen from the center of each cell). At cells connected just via their corners, the distance is sized by a factor of approx. 1.41. To compensate this disadvantage compared to continuous simulation models, a stop-and-go algorithm is proposed. This algorithm minimizes the distance error (considering aftereffects). If a person stops once after a certain amount of diagonal steps, e.g. after every second step, the distance error will be scaling down; 3 horizontal steps approximate 2 diagonal steps (error -6%). The appropriate algorithm notation is 3/2 while the behavior is described by 2-2-2-2-2 („-" read as stop).

algorithm	steps	error E	
		after 12 steps	after 32 steps
3 / 2	2-2-2-2-2	$-6\% < E < +3\%$	$-6\% < E < -2.5\%$
4 / 3	2-3-3-3-3	$+3\% < E < +9\%$	$+5\% < E < +7\%$
7 / 5	2-3-2-3-2	$-1\% < E < +6\%$	$-0.5\% < E < +3\%$
17 / 12	2-2-3-2-3	$-2\% < E < +6\%$	$-1\% < E < +1.5\%$

Table 1: stop-and-go algorithm

Furthermore, the 17/12 algorithm will be used, because variations of the distance error in positive and negative directions are in small bands of $\pm 1.5\%$.

System immanent variance

The transition probability for every adjacent cell can be determined by the specification of a set of movement parameters $\{\mu_p, \sigma_p^2, \sigma_q^2, \alpha\}$. Figure 2 shows the preference matrix M for the set of parameters a) $\{1, 0, 0, 0°\}$ and b) $\{1, 0, 0, 26.5°\}$.
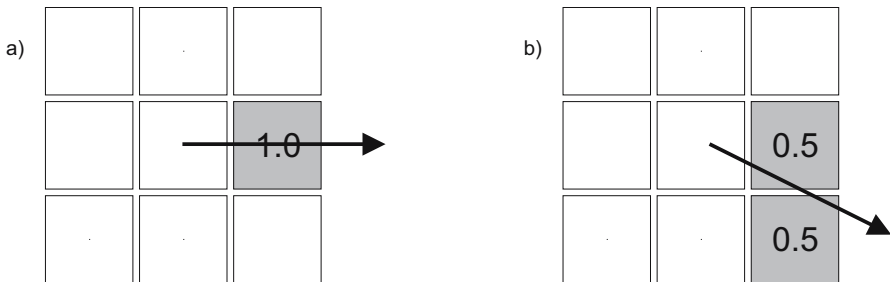

Figure 1: cell neighborhood and preference matrix.

Even though the set of movement parameters a) and b) specify no transverse variance σ_q^2, the model generates a system immanent variance σ^2, based on the regular lattice. In the case that the motion angle is a multiple of $45°$ only one cell can be chosen, otherwise a selection of two cells will be generated. The influence of σ^2 is made smaller by variations of the horizontal/vertical motion direction [σ^2 ($\alpha = 0°$, $\sigma_q^2 = 0.5$) = 5.0], than by variations of the diagonal motion direction [σ^2 ($\alpha = 45°$, $\sigma_q^2 = 0.5$) = 3.8]. Figure 3 shows the characteristics of σ^2 depending on the motion angle. Each curve represents one variation of the transverse σ_q^2 variance; generated by a test case, in which one person moves untroubled for 100 cells in the direction of each motion angle [$0°$, $45°$] with 100000 simulation runs.
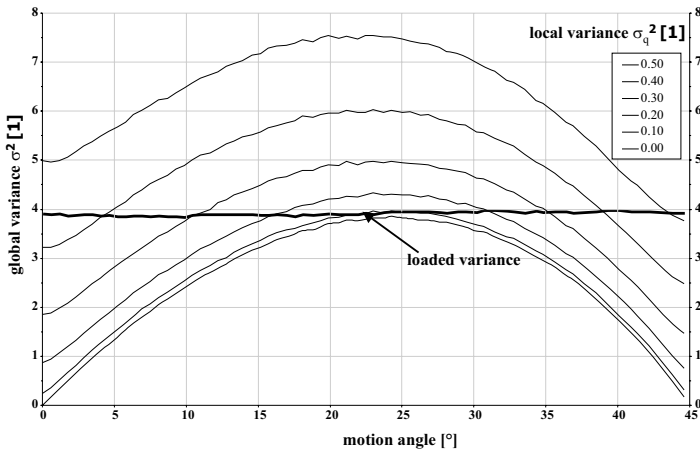
Figure 3: transverse variance σ_q^2 vs. system immanent variance σ^2

To compensate the effect of the system immanent variance σ^2, the model will be calibrated by a weighting function σ^2 (α, σ_q^2) ≈ 3.95, which leads to the loaded variance shown in figure 3.

Repulsion forces

To implement the interaction between the simulated persons (social forces - maximum range 2 m [8]) the cellular automaton model will be extended by a potential field Φ (x, y) approach, where x represents the longitudinal component and y represents the transverse component of the person's velocity.

$$\Phi = a\, e^{\frac{w_{x1}}{w_{x2}}\left(1-e^{-\frac{x}{w_{x1}}}\right)-\frac{x}{w_{x2}}-\frac{y^2}{w_y}} \qquad x < 0\left\{\; w_{x1} = \hat{w}_{x1}\;;\; w_{x2} = \hat{w}_{x2}\;\right\} \tag{5}$$

In equation (5) *a* is the amplitude and *w* represents the set of shape parameters for the potential field. There are two different sets of parameters, one for x > 0 (*w*), the other for x < 0 ($\hat{w}$). Figure 4 shows the standardized function and an adapted function with $\{ w_{x1} = 1; w_{x2} = 2; \hat{w}_{x1} = 2; \hat{w}_{x2} = 3 \}$.
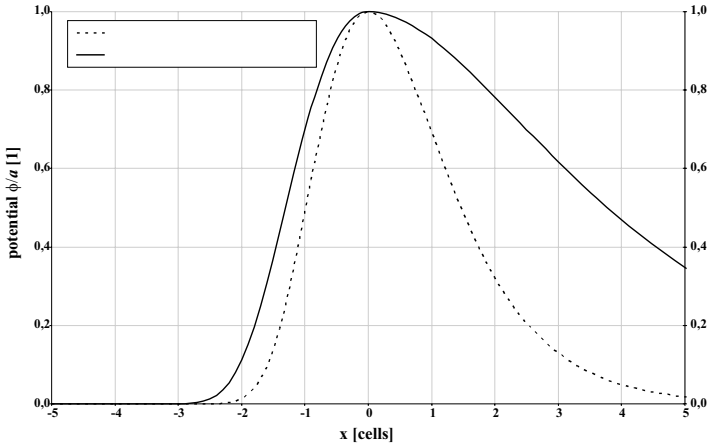

Figure 4: potential $\Phi(x, y = 0)$.

Route choice

To determine the person's path through complex building structures, the distance to the nearest exit is stored in every cell while taking into account all insurmountable obstacles. This algorithm yields artifacts in the movements of the persons [4], so this approach has to be extended. After the shortest distance for each cell has been specified, the created distance matrix can determine how far any person can move directly (the shortest path) to the destination in the horizontal (vertical) and diagonal direction. This procedure yields the actually visible final cell, which is not masked by another static object.

4.   Emergency cases

The person's profiles contain additional attributes which are mapped to the set of motion parameters. In the simulation environment, emergency cases are determined in three different ways: the lack of orientation information, the modification of the motion parameters, and the changing of the person's surrounding area (e.g. blocked exits).

It takes only one small incident to initiate a chain of subsequent events leading to an emergency situation in a complex airport terminal. To simulate emergency cases, it is necessary to determine the terminal areas which are affected by the incident and the arising consequences. The temporal expansion of the so called consequence area de-

pends on the character and the dimension of the emergency and on the conditions of the surrounding environment [9].

Even in crowded situations the emergency guidance system has to provide optical and acoustic information (aware of international differences) at an early stage, to alert people about possible dangers. These situations highlight the limits of an automatic/static system, because the system can not ensure that all persons escape using a protected route. With a managed guidance system, airport operators are able to analyze the emergency and start a successive evacuation (rerouting) regarding the character of the emergency and the terminal area classifications, e.g. security / safety zones, operational/public zones and international/domestic zones.

5.   Conclusion

The proposed discrete microscopic model allows a fast identification of potential weak points by the simulating a significant amount of airport specific scenarios. In consideration of the exceptional position of an airport terminal as an intermodal interchange, these weak points can be eliminated beforehand by means of technical, operational and architectural instruments. **«**

References

1.   M. Schultz, S. Lehmann, and H. Fricke: *Modellbildung und Parametrisierung eines zellulären Automaten zur Simulation von Notfall-/Evakuierungsszenarien in einem Flughafenterminal*, Deutsche Gesellschaft für Luft- und Raumfahrt Jahrbuch (2004).

2.   *M. Schultz, S. Lehmann, and H. Fricke: Development of a Computer-Aided Model for Reliable Terminal Evacuation Simulation - A Statistical Approach to Handle Unpredictable Passenger Behaviour, In: Pro*ceedings of the International Conference on Research in Airport Transportation (2004).

3.   C. Burstedde: *Simulation von Fußgängerverhalten mittels zweidimensionaler zellulärer Automaten*, Diploma Thesis, Institute for Theoretical Physics, University of Cologne (2001).

4.   H. Klüpfel: *A Cellular Automaton Model for Crowd Movement and Egress Simulation*, PhD Thesis, Faculty 4 – Natural Science, University Duisburg-Essen (2003).

5.   D. Helbing, L. Buzna, A. Johansson, and T. Werner: *Self-Organized Pedestrian Crowd Dynamics: Experiments, Simulations, and Design Solutions*, Transportation Science 39(1), pp. 1-24 (2005).

6.   S. Lehmann, M. Schultz, and H. Fric*ke: Bewertung von Sicherheit und Notfallmanagement an Verkehrsflughäfen*, Deutsche Gesellschaft für Luft- und Raumfahrt Jahrbuch (2004).

7.   U. Weidmann: *Transporttechnik der Fußgänger*, Schriftenreihe des IVT, 90, Zürich (1992).

8.   A. Johansson: *Pedestrian Simulations with the Social Force Model*, Master Thesis, Dresden, Göteborg (2004).

9.   S. Theiss: *Systematische Beschreibung von Notfallszenarien in einem Flughafenterminal durch den Einsatz standardisierter Methodik des Requirement Engineering*, Diploma Thesis, Institute of Aviation, Faculty of Transport and Traffic Sciences „Friedrich List", Dresden University of Technology (2004).

Steps Toward the Fundamental Diagram –
Empirical Results and Modelling

A. Seyfried[1], B. Steffen[1], W. Klingsch[2], T. Lippert[1], and M. Boltes[1]

The empirical relation between density and velocity (fundamental diagram) of pedestrian movement is not completely analyzed, particularly with regard to the `microscopic' causes which determine the relation at medium and high densities. The simplest system for the investigation of this dependency is the single-file movement. We present experimental results for this system and discuss the following observations. The data show a linear relation between the velocity and the inverse of the density, which can be regarded as the required length of one pedestrian to move. Furthermore we compare the results for the single-lane movement with literature data for the movement in a plane. This comparison shows an unexpected conformance between the fundamental diagrams, indicating that lateral interference has negligible influence on the velocity-density relation.

For the modelling we treat pedestrians as self-driven objects moving in a continuous space. On the basis of a modified social force model we analyze qualitatively the influence of various approaches for the interactions of pedestrians on the resulting velocity-density relation. The one-dimensional system allows focusing on the role of the required length and remote force. We found that the reproduction of the typical form of the fundamental diagram is possible if the model increases the required length of a person with increasing current velocity. Furthermore we demonstrate the influence of a remote force on the velocity-density relation.

1.   Introduction

Pedestrian dynamics has a multitude of practical applications, like the evaluation of escape routes or the design of pedestrian facilities, along with some more theoretical questions [1, 2, 3, 4, 5]. Empirical studies of pedestrian streams can be traced back to the year 1937 [5]. To this day a central problem is the relation between density and flow or velocity. This dependency is termed the fundamental diagram and has been the subject of many investigations from the very beginning, see references in [6, 7]. It quantifies the capacity of pedestrian facilities and thus allows e.g. the rating of escape routes. One simple system is the uni-directional movement of pedestrians in a plane without bottlenecks. In this context the fundamental diagram of Weidmann [6] is frequently cited. It is a part of a review work and the author summarized 25 different investigations for the determination of the fundamental diagram. Apart from the fact, that with growing density the velocity decreases, the relation shows a non-trivial form. Weidmann notes that different authors choose different approaches to fit their data, indicating that the dependency is not completely analyzed. A multitude of possible effects can be considered which may influence the dependency. For instance we refer to passing maneuvers, internal friction, self-organization phenomena like marching in steps [8] or ordering phenomena like the `zipper' effect [9]. A reduction of the degrees of freedom helps to

---

[1]Central Institute for Applied Mathematics, Research Centre Jülich GmbH, 52425 Jülich, Germany

[2]Institute for Building Material Technology and Fire Safety Science, University of Wuppertal, Pauluskirchstrasse 7, 42285 Wuppertal, Germany

restrict possible effects and allows an improved insight to the problem. Thus we choose a one-dimensional system for this investigation.

Furthermore, the fundamental diagram is used for the evaluation of microscopic models for pedestrian movement [10, 11, 12, 13]. The models can be classified in two categories: the cellular automata models [14, 15, 16, 17, 18] and models in a continuous space [19, 20, 21, 22]. We focus on models continuous in space, which differ substantially with respect to the `interaction' between the pedestrians and thus to the update algorithms as well. The social force model for example assumes, among other things, a repulsive force with remote action between the pedestrians [19, 23, 24, 25, 26]. Other models treat pedestrians by implementing a minimum inter-person distance, which can be interpreted as the radius of a hard body [21, 22]. For a one-dimensional system we introduce different approaches for the interaction between the pedestrians to investigate the influence of the required space and the remote action on the velocity-density relation.

This contribution summarizes parts of two articles. The reader may consult [7, 27] for more detailed discussions and additional results.

2. Experiment

2.1. Description

Our target is the measurement of the relation between density and velocity for the single-file movement of pedestrians. To facilitate this with a limited amount of test persons also for high densities and without boundary effects, we choose an experimental set-up similar to the set-up in [28].

The corridor, see Figure 1, is build up with chairs and ropes. The width of the passageway in the measurement section is 0.8 m. Thus passing is prevented and the single-file
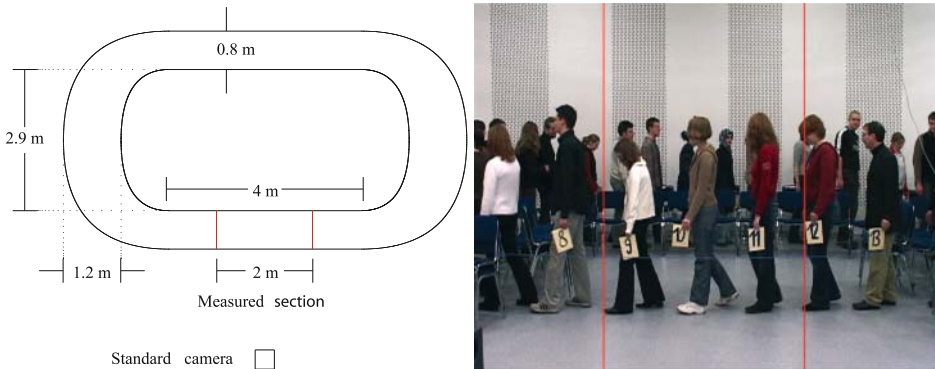

Figure 1: Left: Experimental set-up for the measurement of the velocity-density relation for the single-file movement. Right: One frame of the cycle with $N = 30$. The two vertical lines mark the measured section.

movement is enforced. The circular guiding of the passageway gives periodic boundary conditions. To reduce the effects of the curves on the measurement, we broaden the corridor in the curve and choose the position of the measured section in the center of the straight part of the passageway. The length of the measured section is $l_m = 2$ m and the whole corridor $l_p = 17.3$ m. The experiment is located in the auditorium `Rotunde' at the Central Institute for Applied Mathematics (ZAM) of the Research Centre Jülich. The group of test persons is composed of students of Technomathematics and staff of ZAM. The test persons are instructed to omit passing and not to hurry. These results in a rather relaxed conduct, i.e. the resulting free velocities are rather low. To enable measurements at different densities we execute six cycles with $N = 1, 15, 20, 25, 30, 34$ numbers of test persons in the passageway. For the cycle with $N = 1$ every person passes alone through the corridor. For the other cycles we first distribute the persons uniformly in the corridor. After the instruction to get going, every person passes the passageway two to three times. At the end we open the passageway and let the test persons get out.

2.2. Measurement set-up and data analysis

The measurement of the flow characteristics is based on video recordings with a DV camera (PAL format, 25 fps) of the measured section. These recordings were analyzed frame-wise, see Figure 1. For every person i we collect the entrance time (of the ear) in the measured section t_i^{in} and the exit time t_i^{out}. To ease the assignment of times the test persons carry numbers. These two times allow the calculation of the individual velocities $v_i^{man} = l_m/(t_i^{out}-t_i^{in})$ and the momentary number $n(t)$ of persons at time t in the measured section. The concept of a momentary `density' in the measurement region is problematic because of the small (1-5) number of persons involved. $\rho^{man}(t) = n(t)/l_m$ jumps between discrete values. For a better definition we choose $\rho^{man}(t) = \sum_{i=1}^{N} \Theta_i(t)/l_m$ where $\Theta_i(t)$ gives the `fraction' to which the person i is inside.

$$\Theta_i(t) = \begin{cases} \dfrac{t-t_i^{in}}{t_{i+1}^{in}-t_i^{in}} & : \ t \in \left[t_i^{in}, t_{i+1}^{in} \right] \\[2mm] 1 & : \ t \in \left[t_{i+1}^{in}, t_i^{out} \right] \\[2mm] \dfrac{t_{i+1}^{out}-t}{t_{i+1}^{out}-t_i^{out}} & : \ t \in \left[t_i^{out}, t_{i+1}^{out} \right] \\[2mm] 0 & : \ otherwise \end{cases}$$

$$\tag{1}$$

We regard a crossing of an individual pedestrian with velocity v_i^{man} as one statistical event, which is associated to the density ρ_i^{man}. While ρ_i^{man} is the mean value of the density during the time-slice $[t_i^{in}, t_i^{out}]$. For a more detailed discussion and an example for the development in time of ρ we refer to [7].

Figure 2 shows the distribution of the events (v_i^{man}, ρ_i^{man}) of the cycles with $N = 15$, 20, 25, 30 and 34. We exclude the data where the influence of the starting phase and
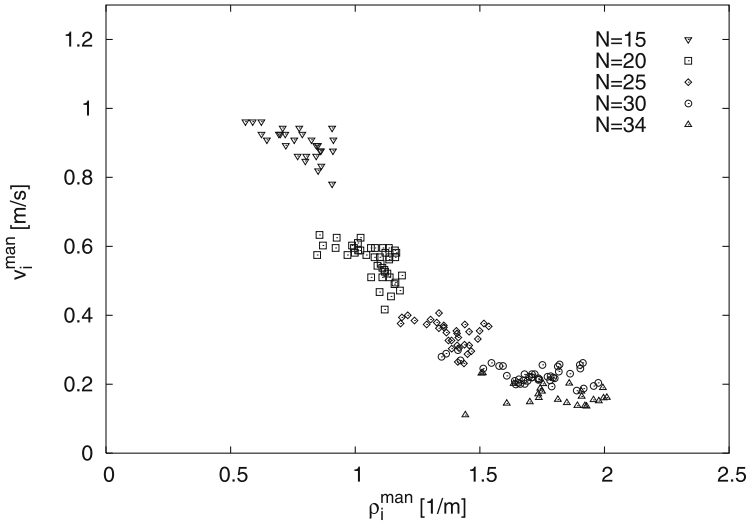
Figure 2: Dependency between the individual velocity and density for the single-file movement.

opening of the passageway are apparent. The run with $N = 1$ results in a mean value of $v_{free}^{man} = 1.24(\pm0.15)$ m/s. The deviation from the literature value 1.34 m/s according to Weidmann, can be explained by the instruction to the test persons not to hurry.

2.3. Empirical results

To compare the relation between velocity and density of the single-file movement (1d) with the movement in a plane (2d), we have to transform the line-density to an area-density.

$$\rho_{1d\rightarrow2d} = \rho^2_{1d} + C(\rho) \tag{2}$$

The correction term $C(\rho)$ is introduced to take into account that the ordering of the pedestrians in two dimensions does not occur in a square lattice. To estimate the correction term at high densities we calculate the difference between the maximal possible density in a square lattice ρ_{max}^{sq} and a hexagonal lattice ρ_{max}^{hex}. For this estimation we assume that the projection of the human body is circular. According to Weidmann the maximum density is $\rho_{max}^{hex} = 5.4$ m^{-2} which corresponds to $r = 0.23$ m. Thus one gets $\rho_{max}^{sq} = 4.7$m^{-2} and a correction term $C(\rho_{max}) = 0.7$m^{-2}.

The comparison of the relation of velocity and density for the single-file movement with the movement in a plane according to Weidmann shows a surprising conformity, see Figure 3. The correspondence at high densities was expected because of the estimation of $C(\rho)$. For smaller densities one expects larger velocities for a movement with an additional degree of freedom. But this did not occur for densities larger than one person per square meter. The qualitative agreement indicates that two-dimensional specific proper-
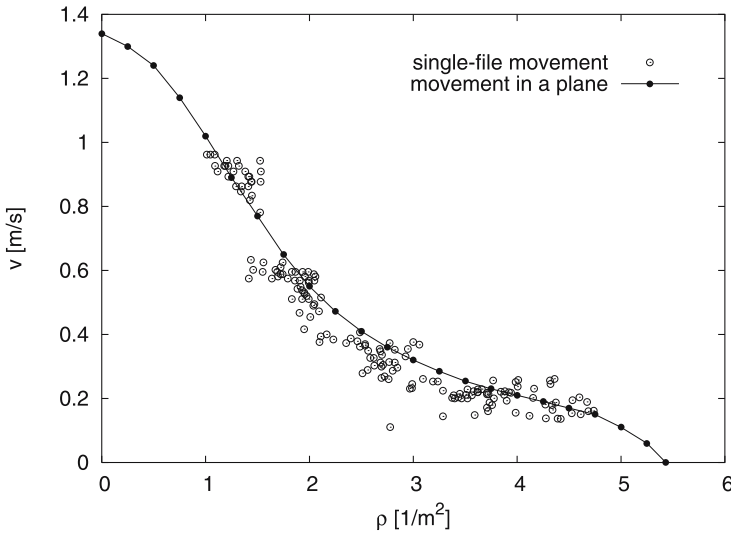
Figure 3: Comparison of the velocity-density relation for the single-lane movement with the movement in a plane according to Weidmann [6]. For the scaling of the line-density we choose a constant correction term $C(\rho) = 0.7\text{m}^{-2}$, see Equation 2.

ties, like internal friction and other lateral interferences, have no strong influence on the fundamental diagram at least at the density domains considered.

Instead, the visual analysis of the video recordings suggests that the following `microscopic' properties of pedestrian movement determine the relation between velocity and density. At intermediate densities and velocities the distance to the pedestrian in front is related to the step length as well as to the safety margin to avoid contacts with the pedestrian in front. Both, step length and safety margin are connected with the velocity. At high densities and small velocities we observed that groups pass into marching in step, see Figure 1. Furthermore the utilization of the available place is optimized. This is achieved by some persons setting their feet far right and left of the line of movement, giving some overlap in the space occupied with the pedestrian in front. While at intermediate densities and relative high velocities the pedestrians are concentrated on their movement, this concentration is reduced at smaller velocities and leads to a delayed reaction on the movement of the pedestrian in front.

In the following we focus on the correlation with the distance between the pedestrians and velocity. The sum of step length and safety margin is the distance to the next close-by pedestrian. This distance can be regarded as the required length d of one pedestrian to move with velocity v. Considering that in a one-dimensional system the harmonic average of this quantity is the inverse of the density, $d = 1/\rho$, one can investigate the relation between required length and velocity by means of the velocity-density relation for the single-file movement.

Figure 4 shows the dependency between required length and velocity. We tested several approaches for the function $d = d(v)$ and found that a linear relationship with
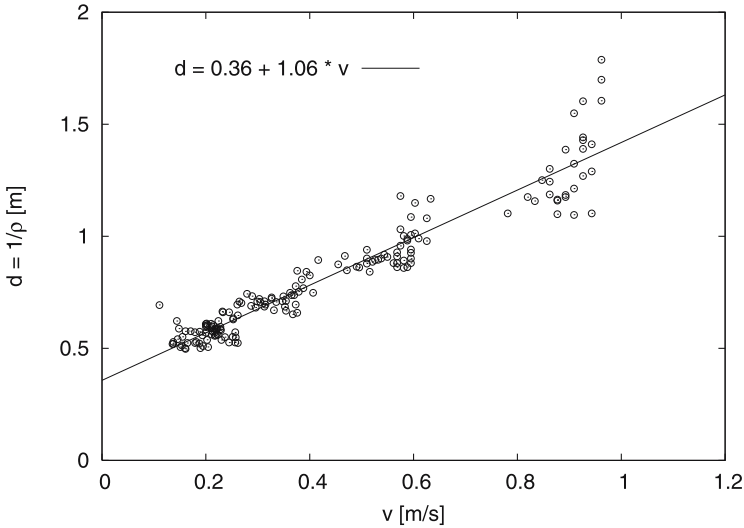
Figure 4: Dependency between required length and velocity according to the data from the cy-
cles with $N = 15, 20, 25, 30$ and 34. A linear relationship gives the best fit to the data.

$d = 0.36+1.06\ v$ gives the best fit to the data. According to [6] the step length is a linear
function of the velocity and the walking-velocity has a lower bound of $v \approx 0.5$ m/s[1].
Thus it is surprising, that the linearity for the sum of step-length and safety margin holds
even and persists for velocities smaller than 0.5 m/s. Possible explanations are the mar-
ching in steps and the optimized utilization of the available space, which compensate
the slower step frequency.

3   Modelling

3.1   Modification of the Social Force Model

The social force model was introduced by [19]. It models the one-dimensional move-
ment of a pedestrian i at position $x_i(t)$ with velocity $v_i(t)$ and mass m_i by the equation
of motions

$$\frac{dx_i}{dt} = v_i \qquad m_i \frac{dv_i}{dt} = F_i = \sum_{j \neq i} F_{ij}(x_j, x_i, v_i)$$

$$(3)$$

The summation over j accounts for the interaction with other pedestrians. We assume
that friction at the boundaries and random fluctuations can be neglected and thus the
forces are reducible to a driving and a repulsive term $F_i = F_i^{drv} + F_i^{rep}$. According to the
formulation in [24] we choose

---

[1]Lower average velocities arise from a lower step frequency.

$$F_i^{drv} = m_i \frac{v_i^0 - v_i}{\tau_i} \qquad \text{and} \qquad F_i^{rep} = \sum_{j \neq i} -\nabla A_i (\|x_j - x_i\| - d_i)^{-B_i} \qquad (4)$$

Where v_i^0 is the intended speed and τ_i controls the acceleration. The hard core d_i reflects the size of the pedestrian i acting with a remote force to other pedestrians. Without other constraints a repulsive force which is symmetric in space can lead to velocities which are in opposite direction to the intended speed. Furthermore, it is possible that the velocity of a pedestrian can exceed the intended speed through the impact of the forces of other pedestrians. In a two-dimensional system this effect can be avoided through the introduction of additional forces like a lateral friction, together with an appropriate choice of the interaction parameters. In a one-dimensional system, where lateral interferences are excluded, a loophole is the direct limitation of the velocities to a certain interval [19, 23]. Another important aspect is the dependency between the space requirement d_i and the current velocity v_i. In [10, 11] it was observed, that in cellular automata model's the consideration, that a pedestrian occupied all cells passed in one time-step, has a large impact on the velocity-density relation. And as suggested from other authors the space requirement or step length is correlated with the speed [19, 21, 29]. In Chapter 2 we quantify empirically the relation between the required length d for one pedestrian to move with velocity v. Summing up, for the modelling of regular motions of pedestrians we modify the reduced one-dimensional social force model in order to meet the following properties: the force is always pointing in the direction of the intended velocity v_i^0; the movement of a pedestrian is only influenced by effects which are directly positioned in front; the required length d of a pedestrian to move with velocity v is $d = a + b\ v$. For detailed discussion we refer to [27]. To investigate the influence of the remote action both a force which treats pedestrians as simple hard bodies and a force according to Equation 4, where a remote action is present, will be introduced. For simplicity we set $v_i^0 \geq 0$, $x_{i+1} > x_i$ and the mass of a pedestrian to $m_i = 1$.

Hard bodies without remote action

$$F_i(t) = \begin{cases} \dfrac{v_i^0 - v_i(t)}{\tau_i} & : \quad x_{i+1}(t) - x_i(t) > d_i(t) \\ -\delta(t)v_i(t) & : \quad x_{i+1}(t) - x_i(t) \leq d_i(t) \end{cases} \qquad \text{with } d_i(t) = a_i + b_i v_i(t) \qquad (5)$$

The force which acts on pedestrian i depends only on the position, its velocity, and the position of the pedestrian $i + 1$ in front. As long as the distance between the pedestrians is larger than the required length d_i, the movement of a pedestrian is only influenced by the driving term. If the required length at a given current velocity is larger than the distance the pedestrian stops (i.e. the velocity becomes zero). This ensures that the velocity of a pedestrian is restricted to the interval $v_i = [0, v_i^0]$ and that the movement is only influenced by the pedestrian in front. The definition of d_i is such that the required length increases with growing velocity.

Hard bodies with remote action

$$F_i(t) = \begin{cases} G_i(t) & : \quad v_i(t) > 0 \\ \max(0, G_i(t)) & : \quad v_i(t) \leq 0 \end{cases} \tag{6}$$

with

$$G_i(t) = \frac{v_i^0 - v_i(t)}{\tau_i} - e_i \left(\frac{1}{x_{i+1}(t) - x_i(t) - d_i(t)} \right)^{f_i} \qquad \text{and } d_i(t) = a_i + b_i v_i(t).$$

Again the force is only influenced by actions in front of the pedestrian. By means of the required length, d_i, the range of the interaction is a function of the velocity v_i. Two additional parameters, e_i and f_i, have to be introduced to fix the range and the strength of the force. Due to the remote action one has to change the condition for setting the velocity to zero. The above definition assures that the pedestrian i stops if the force would lead to a negative velocity. With the proper choice of e_i and f_i and sufficiently small time steps this condition gets active mainly during the relaxation phase. Without remote action this becomes important. The pedestrian can proceed when the influence of the driving term is large enough to get positive velocities.

This different formulation of the forces requires different update algorithms, which will be introduced in the next section. A special problem stems from the periodic boundary conditions enforced for the tests of the fundamental diagram, as these destroy the ordering by causality, which otherwise could avoid blocking situations.

3.2. Time stepping algorithm

The social force model gives a fairly large system of second order ordinary differential equations. For the hard body model with remote action, where the right hand side of the ODE's is continuous along the solution, an explicit Euler method with a time step of $\Delta t = 0.001$ s was tested and found sufficient. Within that time, the distance between two persons does not change enough to make the explicit scheme inaccurate.

The situation for the hard body model without remote force is more complicated. Here the right hand side is a distribution, and the position of the Dirac spikes is not known a priory. Hence the perfect treatment is an adaptive procedure, where each global time step is restricted to the interval up to the next contact. Unfortunately, this is a complicated and time consuming process. For a simple time step we choose the following procedure: Each person is advanced one step ($\Delta t = 0.001$ s) according to the local forces. If after this step the distance to the person in front is smaller than the required length, the velocity is set to zero and the position to the old position. Additionally, the step of the next following person is reexamined. If it is still possible, the update is completed. Otherwise, again the velocity is set to zero and the position is set to the old position, and

so on. This is an approximation to the exact parallel update. It is not completely correct, however. To test its independence from the ordering of persons, computations using different orders were performed. The differences were minute and not more than expected from reordering of arithmetic operations.

3.3. Model results

To enable a comparison with the empirical fundamental diagram from Chapter 2 we choose a system with periodic boundary conditions and a length of $L = 17.3$m. For both interactions we proofed that for system-sizes of $L = 17.3$, 20.0, 50.0m finite size effects have no notable influence on the results. The values for the intended speed v_i^0 are distributed according to a normal-distribution with a mean value of $\mu = 1.24$ m/s and $\sigma = 0.05$ m/s. In a one-dimensional system the influence of the pedestrian with the smallest intended speed masks jamming effects which are not determined by individual properties. Thus we choose a σ which is smaller than the empirical value and verified with $\sigma = 0.05$, 0.1, 0.2 m/s, that a greater variation has no influence to the mean velocities at larger densities. For the parameters τ, a, b, e and f we choose identical values for all pedestrians (for a discussion see [27]). According to [26], $\tau = 0.61$ s is a reliable value. The following figures present the dependency between mean velocity and density for different approaches to the interaction introduced in section 3.1. To demonstrate the influence of a required length dependent on velocity we choose different values for the parameter b. With $b = 0$ one get simple hard bodies. Figure 5 shows the relation between the mean
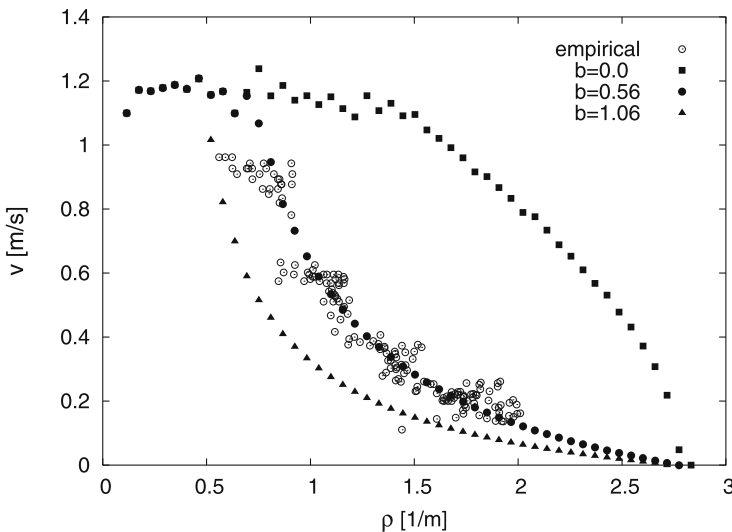
Figure 5: Velocity-density relation for hard bodies without remote action according to Equation 5 in comparison with the empirical data. The filled squares result from simple hard bodies with $a = 0.36$m and $b = 0$. The introduction of a required length leads to a good agreement with the empirical data for $b = 0.56$ s.
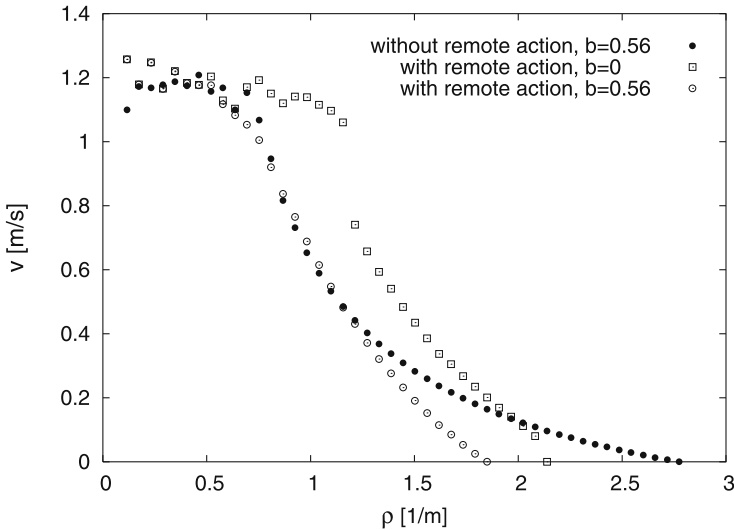
Figure 6: Velocity-density relation for hard bodies with remote action according to Equation 6 in comparison with hard bodies without a remote action (filled circles). Again we choose $a = 0.36$m. The parameter $e = 0.51N$ and $f = 2$ determine the remote force. With $b = 0$ one gets a qualitative different fundamental diagram and a gap for the resulting velocities.

values of walking speed and density for hard bodies without remote action, according to the interaction introduced in Equation 5. If the required length is independent of the velocity, one gets a negative curvature of the function $v = v(\rho)$. The velocity-dependence controls the curvature and $b = 0.56$ s results in a good agreement with the empirical data. With $b = 1.06$ s we found a difference between the velocity-density relation predicted by the model and the empirical fundamental diagram. The reason for this discrepancy is that the interaction and equation of motion do not describe the individual movement of pedestrian correctly. To illustrate the influence of the remote force, we fix the parameter $a = 0.36$ m; $b = 0.56$ s and set the values which determine the remote force to $e = 0.51N$ and $f = 2$.

The fundamental diagram for the interaction with remote action according to Equation 6 is presented in Figure 6. The influence is small if one considers the velocity-dependence of the required length. But with $b = 0$ one gets a qualitative different fundamental diagram. The increase of the velocity can be expected due to the effective reduction of the required length. The gap at $\rho \approx 1.2$m^{-1} is surprising. It is generated through the development of distinct density waves, see Figure 7, as are well known from highways. From experimental view we have so far no hints to the development of strong density waves for pedestrians, see Chapter 2. The width of the gap can be changed by variation of the parameter f which controls the range of the remote force. Near the gap the occurrence of the density waves depends on the distribution of the individual velocities, too.
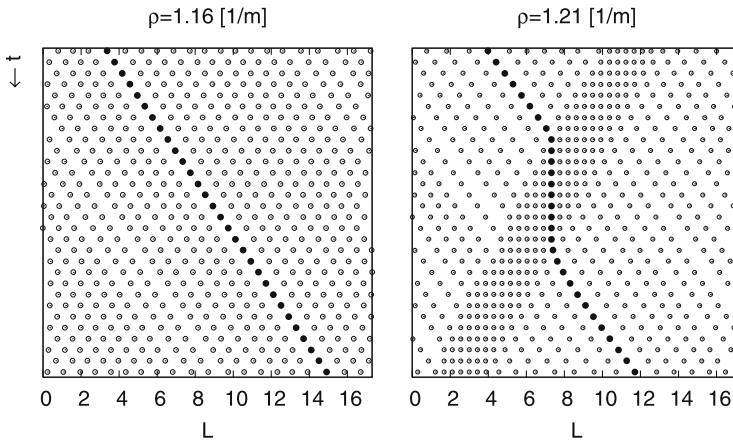
Figure 7:   Time-development of the positions for densities near the velocity-gap, see Figure 6. For ρ > 1.2m⁻¹ density waves are observable. Some individuals leave much larger than average gaps in front.

4.   Summary and outlook

In the investigation presented we determine the empirical relation between velocity and density for the single-file movement of pedestrians. The comparison of this fundamental diagram with the literature data for the movement in a plane shows a surprising agreement. The conformance indicates that the internal friction and other lateral interferences, which are excluded in the single-file movement, have no influence on the relation at the density domains considered. The visual analysis of the video recording give hints to possible effects, like the self-organization through marching in step, the optimized utilization of the available space at low velocities and the velocity dependence of step-length and safety margin. The data show a linear relation between the velocity and the inverse of the density, which can be regarded as the required length of one pedestrian to move. For the modelling we investigate the influence of the required length and remote action on the resulting velocity-density relation. We have introduced a modified one-dimensional social force model, which takes into account that the required length for moving with a certain velocity is a function of the current velocity. The model-parameter can be adjusted to yield a good agreement with the empirical fundamental diagram. This holds for hard bodies with and without remote action. The remote action has a sizeable influence on the resulting velocity-density relation only if the required length is independent of the velocity. In this case one observes distinct density waves, which lead to a velocity gap in the fundamental diagram. For the model parameter b which correlates

the required length with the current velocity, we have found that without remote action the value $b = 0.56$ s results in a velocity-density relation which is in a good agreement with the empirical fundamental diagram. However, from the same empirical fundamental diagram one determines $b = 1.06$ s. We conclude that a model which reproduces the right macroscopic dependency between density and velocity does not necessarily describe correctly the microscopic situation, and the space requirement of a person at average speed is much less than the average space requirement. This discrepancy may be explained by the 'short-sightedness' of the model. Actually, pedestrians adapt their speed not only to the person immediately in front, but to the situation further ahead, too. This gives a much smoother movement than the model predicts.

The above considerations refer to the simplest system in equilibrium and with periodic boundary conditions. In a real life scenario like a building evacuation, where one is interested in estimates of the time needed for the clearance of a building and the development of the densities in front of bottlenecks, one is confronted with open boundaries and conditions far from equilibrium. We assume that a consistency on a microscopic level needs to be achieved before one can accurately describe real life scenario. The investigation presented provides a basis for a careful extension of the modified social force model and an upgrade to two dimensions including further interactions. **«**

References

1. M. Schreckenberg and S.D. Sharma (Eds.): *Proceedings of the International Conference on Pedestrian and Evacuation Dynamics*, Springer, Berlin (2002).
2. E.R. Galea (Ed.): Proceedings of the 2nd International Conference on Pedestrian and Evacuation Dynamics, CMS Press, London (2003).
3. D. Oeding: *Verkehrsbelastung und Dimensionierung von Gehwegen und anderen Anlagen des Fußgängerverkehrs*, In: Straßenbau und Straßenverkehrstechnik, Heft 22, Bundesministerium für Verkehr, Abt. Straßenbau, Bonn (1963).
4. J.J. Fruin: *Pedestrian Planning and Design*, Elevator World, New York (1971).
5. W.M. Predtetschenski and A.I. Milinski: *Personenströme in Gebäuden - Berechnungsmethoden für die Projektierung*, Verlagsgesellschaft Rudolf Müller, Köln-Braunsfeld (1971).
6. U. Weidmann: *Transporttechnik der Fußgänger*, Schriftenreihe des IVT Nr. 90, zweite ergänzte Auflage, ETH Zürich (1993).
7. A. Seyfried, B. Steffen, W. Klingsch, and M. Boltes: *The Fundamental Diagram of Pedestrian Movement Revisited*, J.Stat. Mech., P10002 (2005).
8. P.D. Navin and R.J. Wheeler: *Pedestrian Flow Characteristics*, Traf. Engin. 39, pp. 31-36 (1969).
9. S.P. Hoogendoorn and W. Daamen: *Pedestrian Behavior at Bottlenecks*, Transp. Sci. 39/2, pp. 0147-0159 (2005).
10. T. Meyer-König, H. Klüpfel, and M. Schreckenberg: *Assessment and Analysis of Evacuation Processes on Passenger Ships by Microscopic Simulation*, In: M. Schreckenberg and S.D. Sharma (Eds.): Proceedings of the International Con-

ference on Pedestrian and Evacuation Dynamics, Springer, Berlin, pp. 297-302 (2002).

11. A. Kirchner, H. Klüpfel, K. Nishinari, A. Schadschneider and M. Schreckenberg: *Discretization Effects and the Influence of Walking Speed in Cellular Automata Models for Pedestrian Dynamics*, J. Stat. Mech. P10011 (2004).

12. S.P. Hoogendoorn, P.H.L. Bovy, and W. Daamen: *Microscopic Pedestrian Way-finding and Dynamics Modelling*, In: M. Schreckenberg and S.D. Sharma (Eds.): Proceedings of the International Conference on Pedestrian and Evacuation Dynamics, Springer, Berlin, pp. 123-154 (2002).

13. www.rimea.de

14. M. Muramatsu, T. Irie, and T. Nagatani: *Jamming Transition in Pedestrian Counter Flow*, Physica A 267, pp. 487-498 (1999).

15. V.J. Blue and J.L. Adler: *Cellular Automata Microsimulation of Bi-Directional Pedestrian Flows*, J. Transp. Res. Board 1678, pp. 135-141 (2000);

16. C. Burstedde, K. Klauck, A. Schadschneider, and J. Zittartz: *Simulation of Pedestrian Dynamics using a Two-Dimensional Cellular Automaton*, Physica A 295, pp. 507-525 (2001).

17. K. Takimoto and T. Nagatani: *Spatio-Temporal Distribution of Escape Time in Evacuation Process*, Physica A 320, pp. 611-621 (2003).

18. A. Keßel, H. Klüpfel, J. Wahle, and M. Schreckenberg: *Microscopic Simulation of Pedestrian Crowd Motion*, In: M. Schreckenberg and S.D. Sharma (Eds.): Proceedings of the International Conference on Pedestrian and Evacuation Dynamics, Springer, Berlin, pp. 193-200 (2002).

19. D. Helbing and P. Molnár: *Social Force Model for Pedestrian Dynamics*, Phys. Rev. E 51, pp. 4282-4286 (1995).

20. S.P. Hoogendoorn and P.H.L. Bovy: *Gas-Kinetic Modeling and Simulation of Pedestrian Flows*, Transp. Res. Rec. 1710, pp. 28-36 (2000).

21. P. Thompson and E. Marchant: *A Computer Model for the Evacuation of Large Building Populations*, Fire Safety Journal 24, pp. 131 (1995).

22. V. Schneider and R. Könnecke: *Simulating Evacuation Processes with ASERI*, In: M. Schreckenberg and S.D. Sharma (Eds.): Proceedings of the International Conference on Pedestrian and Evacuation Dynamics, Springer, Berlin, pp. 303-313 (2002).

23. P. Molnár: *Modellierung und Simulation der Dynamik von Fußgängerströmen*, Shaker, Aachen (1996).

24. D. Helbing, I. Farkas, and T. Vicsek: *Freezing by Heating in a Driven Mesoscopic System*, Phys. Rev. Let. 84, pp. 1240-1243 (2000).

25. D. Helbing, I. Farkas, and T. Vicsek: *Simulating Dynamical Features of Escape Panic*, Nature 407, pp. 487-490 (2000).

26. T. Werner and D. Helbing: *The Social Force Pedestrian Model Applied to Real Life Scenarios*, In: E.R. Galea (Ed.), Proceedings of the 2nd International Conference on Pedestrian and Evacuation Dynamics, CMS Press, London, pp. 17-26 (2002).

27.   A. Seyfried, Bernhard Steffen and Thomas Lippert, Basics of Modelling the Pedestrian Flow, Physica A 368, 232-238 (2006).
28.   B. D. Hankin and R. A. Wright, Passenger flow in subways, Operational Research Quarterly 9, 81-88 (1958);
29.   J. L. Pauls, Suggestions on evacuation models and research questions, Conference Proceedings of the 3rd International Symposium on Human Behaviour in Fire (2004).

Model for Office Building Usage Simulation

V. Tabak[1], B. de Vries[1], and J. Dijkstra[1]

This paper presents a model for office building usage simulation which is part of the research project "User Simulation of Space Utilisation". The aim of this project is to develop a model for the simulation of human movement to predict space utilisation in office buildings.

The underlying model takes two main types of input: firstly the workflow of the organisation and secondly the design of the building in which the organisation is (or will be) housed. The latter refers to the spatial conditions. The model generates data about the activity the members of the organisation perform and their location in the building space for the specific time interval of the simulation run. Proceeding from these data, performance indicators can be deduced, like average/maximum walking distance per individual, time occupied per space and number of persons per space. These indicators can be used to analyse the performance of a design or can act as input for other engineering methods and models.

1. Introduction

Many different building simulation tools have been developed, for example in the field of building energy systems, building physics, building services and air/smoke dispersion. There is an urgent need for these tools due to the growing complexity of buildings and the growing emphasis on performance aspects, for example in the quest for sustainable buildings [11].

Increasing computer power, better algorithms and better calibrated models make it possible to simulate physical processes at more detailed building level in shorter periods of time [8]. Yet, these models rely on assumptions referring to the behaviour of occupants of buildings. In the field of building usage simulation, research is poor on the complexity of human behaviour and the space utilisation in buildings. We think a model for building usage simulation that produces data about the activity of the members of an organisation can improve the relevance and performance of the building simulation tools. This is relevant for engineering domains as well as for architects to analyse and evaluate the performance of a building design.

For the research project "User Simulation of Space Utilisation" we develop a model for a system that is needed to simulate representative, real human behaviour and space utilisation in a building; the focus is on office buildings. In our approach we build upon two existing methods for modelling the different kinds of activities found in an organisation, namely workflow modelling and activity based modelling. These methods have to be tailored and extended for applying them into the context of building usage simulation.

In this paper we present the specifications of the simulation model. First, the two methods for predicting the activities will be detailed. Next, we will describe the integration of these two methods into one user simulation model. Before going in depth into a

---

[1]Eindhoven University of Technology, Faculty of Architecture, Building, and Planning, Design Systems group

description of our system, we first point out the current stage in related research areas. Next the relevance and critical points of our system will be highlighted in a short description of a test case. We will clarify our system by a case study and finally future steps will be discussed.

2.   Related research

The research project has common ground to topics in the research area of pedestrian and evacuation dynamics as well as to topics in the areas of activity based modelling and workflow modelling. Activity based modelling is of interest due to treating the travel and activity forecasting processes as a group decision making process introducing interaction between individuals. Workflow modelling is of interest for modelling activities that occur within an organisation.

2.1. Pedestrian and evacuation dynamics

Models developed in this research area can be divided in three categories, namely:
»   Cellular automata (CA) models
    CA models are used to model dynamic processes that are discrete in space and time, e.g. transportation systems. They have been successfully applied for pedestrian and evacuation dynamics; for example the Bypass project [12] for simulating evacuation behaviour on cruise ships.
»   Agent-based models
    Agent-based systems are currently developed for simulating virtual human behaviour in a variety of disciplines; agents represent virtual humans, e.g. pedestrians. The PEDFLOW model [10] is an example of an agent-based evolutionary system that allows modelling of pedestrian behaviour.
»   Social force models.
    Human behaviour is modelled through so-called social force fields, which determine the amount of behavioural change as reaction to forces exerted by the environment. Simulating traveller behaviour in railway stations is an example of that approach [6].

2.2. Interaction in activity based modelling

Activity models are used to predict the effect of policy measures on the possibilities of individuals to participate in activities and on the resulting travel demand [5].
Most existing approaches to model activity schedules assume an individual-based decision making process. These models do not take into account the interaction between individuals; at best only implicitly through the inclusion of explanatory variables related to household composition. According to [14, 15] there is a need for incorporating interaction between household members to develop sound forecasting models. Recently, there is a noticeable growing interest in modelling intra-household interaction in the

field of transportation research. According to [16] modelling interaction approaches can be grouped in three categories, namely:

» Structural equation models.
These models are used to explore the relationships between activities such as performed by male and female household-heads [7].

» Models that explicitly consider the intra-household interaction mechanism.
These models are based on a joint decision making process. The activity schedule of the household is the result of a negotiation process in which the interests of the individuals are weighted against those of the group [17].

» Models that represent a choice between individual and joint activity c.q. travel.
These models are based on a discrete number of activities episodes c.q. trips rather than continuous activity durations. Scott [14] has developed such a model in which the daily number of non-work, out-of-home activity episodes are modelled for household heads.

In most of the recently developed models the group decision-making process is limited to (two) household heads.

2.3. Workflow modelling

Business process modelling is a method that has been widely applied in business management to gain more insight and control over business processes. Aalst [2] suggests a workflow modelling method from an organisational point of view, based upon Petri-net theory. This is just one of the theories available in the field of workflow modelling. A lot of different workflow tools and specifications have been developed based on different paradigms. This is largely due to the lack of an universal workflow formalism [3]. According to the same authors a workflow specification can be understood from a number of different perspectives, namely:

» Control-flow perspective
Describes the workflow in terms of tasks and the way in which the order of the tasks is controlled.

» Data perspective
This perspective is ordered on top of the control-flow perspectives and deals with the data that flow through the processes.

» Resource perspective
Details how activities are allocated to resources, which are basically human or facility roles.

» Operational perspective
This perspective describes the actual execution of activities in the workflow by data manipulation (within applications).

Due to the nature of our project the resource perspective is especially of interest.

The "What, how and by whom?" approach by [1] describes three important stages in designing a business process. Following these steps guarantees that we end up with a complete model, which describes in detail the type of activities, their order and who is

responsible for an activity. However, the location of an activity is not part of a workflow modelling. To our knowledge there are no workflow tools that take the location of an activity into account.

3.   Preliminary study: simulating the usage of office spaces

Simulating the space utilisation and behaviour of occupants is relevant and important in designing layouts for office spaces. A layout which matches with its workflow is typically what an organisation wants. In practice, designing office spaces is still a traditional discipline, with little attention to the actual usage of offices spaces when it is constructed. As a result, discrepancies between theory and practice are signalised. Simulating the actual usage of designed layout before its construction can bridge the gap between theory and practice. In this way the layout can be evaluated and adjusted to better match the workflow of the organisation.

A test system was developed based on a probabilistic generation process of activity agendas for certain categories of office employees. In the generation process activities are linked to available spatial resources. Using the generated agendas human movement is simulated based on the shortest path algorithm.

Figure 1: Visualisation of movement patterns in an office layout.

After the development and evaluation of this test system, we derived a list of shortcomings:

» Interaction between persons
   Although a person often executes activities alone, without the need for any other person (e.g. preparing a presentation), many activities require some form of interaction between persons (e.g. giving a presentation). This has impact on the scheduling process (the same activity has to be inserted in the schedules of all people involved) and on the location finding process, e.g. the activity location should be able to accommodate the size of the group of employees concerned.

»   Combination of activities
    The test system was evaluated in an experiment in which people were observed in an existing office space (see Figure 1). During this experiment unexpected human behaviour was observed, namely people tend to combine several activities in one action, especially in the case of the so-called unplanned activities (see section 4.4). For example: someone will combine the activity 'walking to the printer' with the activity 'getting a cup of coffee', because he/she was already walking.

»   Timescale
    In the test case a time slot of 10 minutes was used to plan activities. This tends to be inaccurate, especially with regard to the unplanned activities.

»   Variable start and end time of employees
    In the prototype all employees had the same start and end time. This does not apply for the real world.

4. Model structure

We realized that a more elaborate model is needed to simulate human movement with a high reliability. Two critical aspects in this model are the interaction between the building occupants while performing their activities and the way to model these activities in space.

The structure of our model consists of a number of sub-models (see Figure 2). Each sub-model is interrelated with each other and takes care of one aspect in the total structure of the model for office building usage simulation.
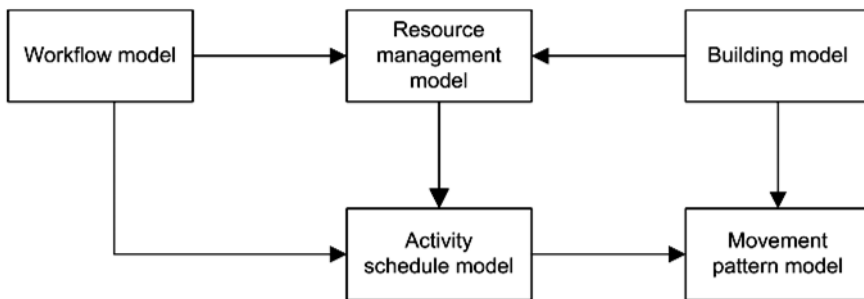
Figure 2: The model structure.

The workflow and building model depends on user-input. The resource management model and activity schedule model are user-independent and provide the necessary information for the movement pattern model. The movement pattern model takes care of producing the desired output of the system, namely a movement pattern which not only describes which activities are performed at which location, but also the route to follow between the activities.

4.1. Workflow model

In our system we distinguish two types of activities, namely skeleton and intermediate activities. The workflow model is responsible for modelling the skeleton activities. The intermediate activities are modelled with an activity-based model, which is implemented in the activity schedule model (see section 4.4).

The skeleton activities are the main activities in our system. These activities directly follow from the workflow of the organisation. The skeleton activities are responsible for highly structuring someone's schedule. Examples of these activities are: having a meeting, doing research or sending a letter. Because the skeleton activities depend on the workflow of the organisation, the user has to specify the structure of the organisation in detail as input for the system.

An organisation consists of a number of roles (e.g. secretary or manager) and a number of organisational units (e.g. the sales or complaints department). A unit usually consists of more than one role and a role can belong to more than one unit. The role is the link with the resource "person" in the resource management model (see section 4.3). A role can be fulfilled by a person.

Each organisation has its own specific workflow. Not only will the workflow strongly differ between organisation-types (an insurance company has a completely different workflow than a consultancy firm), but also in an organisation-type itself the workflow can vary (not every insurance company has the same workflow). A workflow consists of a limited number of processes. For example processes can be: handle incoming complaints or advertise products. As mentioned in the introduction and in section 3, our model must provide some means of interaction between individuals. Therefore we introduce the concept of task-type in the workflow model. A task-type is a logical unit of work, which is carried out by one resource [2]. A task-type belongs to a certain organisational unit. Some task-types (e.g. having a meeting or a presentation) require linkages between individuals that belong to the same unit. Each task-type is considered to be a skeleton activity for which one role is responsible. The roll of the skeleton activity in the activity schedule model will be discussed in section 4.4.

4.2. Building model

The building model describes the way in which we deal with the spatial conditions in which activities take place. A node object is the central point in our building model. The node object forms the link with the resource management model and the movement pattern model. All resources (e.g. workplaces or printers) are located at a node and nodes form a part of a movement pattern. All nodes are linked with each other by edges.

Each activity occurs at a certain location. These locations are called abstract-spaces and are the second type of resources. An abstract-space has no dimensions. It forms the abstraction c.q. generalisation of real spaces in buildings. In fact, an abstract-space is a collection of end-nodes. The size of this collection specifies the capacity of the abstract-space, for a meeting room this means the number of available seats.

A building consists of a number of spaces, like office rooms, meeting rooms or hallways. Each space in a building can be abstracted to an abstract-space. An abstract-space itself can consist of one or more abstract-spaces. For example an office room is an abstract-space, but it can contain two (or more) workplaces; each workspace also is an abstract-space. Or it can contain a workspace and a meeting space (both are again abstract-spaces).

An abstract-space can also contain one or more facilities, like a printer or a coffee machine. Facilities are the third and last type of resources.

4.3. Resource management model

The resource management model is a significant part in our system. It provides the interface for the schedule model with the workflow and building model. It contains and keeps track of all the information related to the recourses available either in the organisation as well as in the building. Three different types of recourses can be distinguished:

» Persons
  This type of resource is divided in two sub-types. The most important sub-type is the employee. The employee provides the link with the workflow model as well as the link with the schedule model. Each employee has a schedule with activities. The second sub-type is the guest, which plays a special role in the schedule model.
» Abstract-spaces
  All activities are performed at a certain abstract-space. This recourse is linked with the building model.
» Facilities
  This recourse provides certain facilities for the organisation to perform their duties.

4.4. Activity schedule model

For simulating the usage of office buildings it is essential to know which activities are performed by the employees in the organisation. Therefore each employee has an activity schedule. This schedule consists of an in time ordered set of activities. Each activity has a location (the abstract-space) and can involve, depending on the type of activity, one or more persons or facilities.

For modelling real human behaviour and space utilisation, workflow depended activities as well as activities that are the result of human nature are necessary. The latter activities are called intermediate activities. An activity schedule can consist of skeleton activities, intermediate activities or a combination of both activities.

The intermediate activities strongly depend on the psychological or social needs and wishes of an employee. In our model the intermediate activities are limited to the following types:

» Getting a drink
» Going to the toilet
» Receiving a guest (link with the guest resource subtype)
» Having a small break (chatting with someone)
» Having lunch.
» Smoking
» Going to the printer/copier

For determining the occurrence of intermediate activities we apply a S-shaped function [9]. This curve determines the growth of the utility of an intermediate activity as a function of the time elapsed since the previous occurrence of this activity (see Figure 3). In our approach we use the S-shape function to determine the timing of the activities and not the duration of activities. This approach deviates from most other S-shaped curve models, which describe the utility as a function of the duration of the activity. The duration of the types of activities and the parameters of the S-shaped function will be estimated with data collected of real human activity behaviour.

An intermediate activity may only occur when the utility of this activity reaches a certain value. This value is called the threshold value. The value of the threshold value is among other things affected by time pressure and by the skeleton activity that the intermediate activity is going to interrupt. For example: when our manager is in a formal meeting he is less likely to get a cup of coffee than when he is sitting behind his desk writing a letter; the more formal a skeleton activity is, the higher the utility of an intermediate activity needs to be before it is going to be executed. In the case of time pressure you are more focused on fulfilling your role and less on your social needs and/or wishes.

This activity based model is a deterministic model. The S-shaped function in conjunction with the threshold value determines the occurrence of activities. However, this does not imply that there is no variation in the outcome of this model. In the real world the intermediate activity schedule of an employee will differ from day to day in terms of types of activities, their order and timing. In our model this is guaranteed by stochastic variation in the parameters of the utility function and in the threshold.
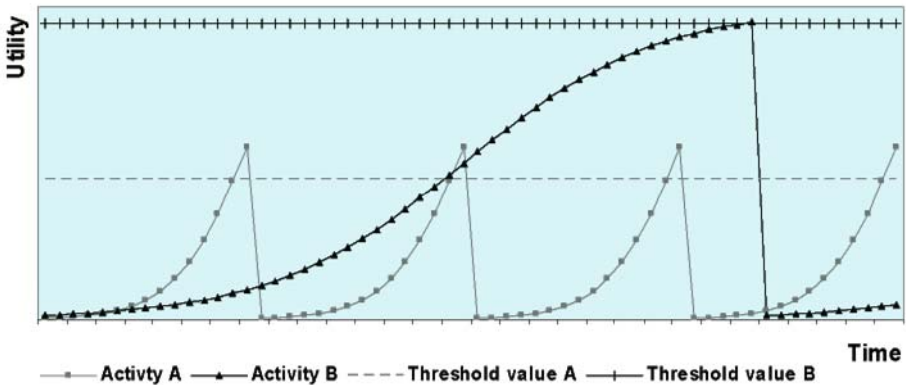
Figure 3: The S-curve and threshold value for two intermediate activities.

4.5. Movement pattern model

The schedule in the activity schedule model describes for each employee the order of activities for a certain period. It reveals the needed travel demand as derived demand from the activities. With the schedule the system knows the location of each activity for an employee, but not yet which route he or she should follow to get from one activity to another. In the movement pattern model the information about an activity in the schedule is supplied with route information to get from the location of this activity to the next activity location. A movement pattern is a combination of the activity schedule and a set of routes. The movement pattern model is linked with the network of nodes and edges in the building model. A route is an ordered set of edges.

5.   Case study: a mock-up

To demonstrate the concept of our simulation model, we discuss the subsequent process steps for a simple case of employees working in the same floor in an office building for one working day. The data has been collected in the Faculty of Architecture, Building, and Planning at the Eindhoven University of Technology for three employees, namely a manager, a secretary and a PhD.

5.1. Step 1: Determine skeleton activity schedule

The first step in predicting the space utilisation of an organisation is to determine which skeleton activities have to be performed in a certain period by our three employees.

Step 1A: Formulate the spatial workflow model
In this step we provide the data needed to describe the workflow of the organisation and the spatial conditions in which the workflow occurs. We have to create a so-called spatial workflow model, which specifies which skeleton activities need to be executed, what the order is of these activities, who is participating in the activities and at what location the activity takes place.
For our case study we input among other things the three roles, their task-types (e.g. have a PhD meeting, attend a presentation, write a conference paper) and the spatial layout of the building in which they are housed (like their workspaces and the network of nodes plus edges). The outcome of this step is a spatial workflow model which specifies in details the workflow of each employee: who does what, where and when. In other words we have specified the data for the workflow model, the resource allocation model and the building model.

Step 1B: Determine the skeleton activities
After formulating the workflow model is formulated, the next step is to run this model for a particular period (in this case one working day). This results in a skeleton activity schedule for each employee that details his or her skeleton activities for this period.

5.2.   Step 2: Determine intermediate activity schedule

After determining the skeleton activities for our three employees in question, the intermediate activities for them will be determined. With the activity based model the system predicts which intermediate activities occur during the workday (see section 4.4). Outcome of this step is per employee a schedule that describes his or her intermediate activities and their attributes (e.g. the location of an activity).

Determining the intermediate activity schedule is an iterative process. Goal of this process is to find possible combinations of intermediate activities in the schedule of one person (e.g. someone will combine walking to the printer with getting a cup of coffee, because he/she was already walking) or to find interactions between the schedules of people (e.g. an unexpected informal meeting at the coffee machine). The system will try to find combinations by checking the intermediate activity schedule of each employee with the utilities of his/her remaining, not yet added intermediate activities and by comparing his/her intermediate activity schedule with the schedules of the other two employees.

After each run in this step the schedule will be evaluated. This evaluation is based on criteria, like the utilities of the intermediate activities that are not yet implemented and the available time for intermediate activities. If no more changes to the schedule are possible or needed the process will be stopped, otherwise the step will be repeated.

5.3.   Step 3: Combine skeleton and intermediate activity schedules

With the skeleton activity schedule and the intermediate activity schedule we have the elements to build a complete activity schedule for the three employees. This activity schedule combines both schedules into one activity schedule for each employee.

5.4.   Step 4: Create movement pattern

Based on the activity schedule formulated in the previous step and the spatial layout (the network of edges in the building model) the system can now generate movement patterns. Usually there is more than one route which leads from the location of an activity to the location of the next activity. The system chooses one of those routes using a shortest path algorithm.

5.5.   Step 5: Analyze space utilisation

The movement patterns describe the space utilisation of each employee for the period in question, in this case one working day. Now we are able to analyse and evaluate the space utilisation of the building occupied by the three employees.

We need to run the movement patterns in conjunction with steering behaviour algorithms for deducing some of these indicators (e.g. walking distance). A movement pattern is a static route along the network of edges and nodes. In order to analyze the space

utilisation in more close detail (and to deduce all of the performance indicators) we need to determine the human behaviour while they are following this route. To model this behaviour we need algorithms like path following and unaligned collision avoidance [13]. These indicators can be used to evaluate the building. Table 1 shows examples of performance indicators for our case study.

Employee	Maximum walking distance (m)	Usage printer	Usage coffee machine
Manager	575	3	2
Secretary	308	0	2
PhD	697	3	4

Table 1: Performance indicators of our case study.

Another possibility is to visualize the usage of the building in for example a virtual reality environment, like the desk-CAVE [4]. By this facility a person can walk though the building and experience it while it is in use.

Future work

We are now ready to implement our model in a prototype. The implementation will be done in Java. However, before we are able to use this system and generate movement patterns, the parameters of the S-shaped function in the intermediate activity model have to be calibrated. For this purpose we will collect data about human activity behaviour in the real world. These data is organisation and building independent and need to be collected only once. For the data collection we will use an internet based questionnaire. This approach suits very well for this kind of data collection due to the magnitude of the target group. After the implementation and the data collection we will report the first test results of our system.

For a complete evaluation of the system we will perform an experiment for assessing its predictive quality in the context of a real building, organisation and actual human behaviour. We will capture the real space utilisation by using RFID (radio frequency identification) technology. This technology is used by some Dutch organisations to regulate their access control and as means of time registration. Currently, we examine the data collected by those organisations as a reliable source of data to capture space utilisation. Then the data can be used to validate our simulation model.

Acknowledgements

References

1. W.M.P. van der Aalst and K.M. van Hee: *Business Process Redesign: A Petri-Net-Based Approach*, Computers in Industry 29, pp. 15 (1996).
2. W.M.P .van der Aalst and K.M. van Hee: *Workflow Management: Models, Methods, and Systems*, MIT Press, London, UK (2002).
3. W.M.P. van der Aalst and A.H.M. ter Hofstede: *YAWL: Yet another Workflow Language*, Information Systems 30 (4), pp. 245 (2003).
4. H.H. Achten, A.J. Jessurun, and B. de Vries: *Desk-Cave - A Low-Cost Versatile Virtual Reality Design and Research Setup Between Desktop and CAVE*, In: B.Tournay and H.Tournay (Eds.), Proceedings of the 22nd International Conference on Education and Research in Computer Aided Architectural Design in Europe, pp. 142 (2004).
5. T. Arentze and H.J.P. Timmermans: *ALBATROSS, EIRASS*, Eindhoven, The Netherlands (2000).
6. W. Daamen, P.H.L. Bovy, and S.P. Hoogendoorn: *Modelling Pedestrians in Transfer Stations*, In: M. Schreckenberg and S.D. Sharma (Eds.), Proceedings of the International Confernce on Pedestrian and Evacuation Dynamics Duisburg, Springer, Berlin, pp. 59-73 (2002).
7. T.F. Golob and M.G. *McNally: A Model of Activity Participation between Household Heads*, Transportation Research Part B 31 (3), pp. 177 (1997).
8. J.L.M. Hensen: *Towards More Effective Use of Building Performance Simulation in Design*, In: J.P. van Leeuwen and H.J.P. Timmermans (Eds.), Design & Decision Support Systems in Architecture and Urban Planning, Eindhoven University of Technology, Eindhoven, The Netherlands, pp. 291 (2004).
9. C.-H. Joh: *Measuring and Predicting Adaptation in Multidimensional Activity-Travel Patterns*, Faculteit Bouwkunde, Eindhoven University of Technology, Eindhoven, The Netherlands (2004).
10. J. Kerridge, J. Hine, and M. Wigan: *Agent-Based Modelling of Pedestrian Movements - The questions that Need to be Asked and Answered*, Environment and Planning B: Planning and Design 28 (3), pp. 327 (2001).
11. K.P. Lam, N.H. Wong, and S. Chandra: *The Use of Multiple Building Performance Simulation Tools during the Design Process – A Case Study in Singapore*, Proceedings of the seventh International IBPSA Conference, pp. 815 (2001).
12. T. Meyer-König, H. Klüpfel, and M. Schreckenberg: *Assessment and Analysis of Evacuation Processes on Passenger Ships by Microscopic Simulation*, In: M. Schreckenberg and S.D. Sharma (Eds.), Proceedings of the International Confernce on Pedestrian and Evacuation Dynamics (PED), Springer-Verlag, Berlin, Germany, pp. 297-302 (2002).
13. C.W. Reynolds: *Steering Behaviors for Autonomous Characters*, The proceedings of the 1999 Game Developers Conference (1999).

14. M. Scott and P.S. Kanaroglou: *An Activity-Episode Generation Model That Captures Interactions between Household Heads: Development and Empirical Analysis*, Transportation Research Part B 36, Elsevier Science Publishers B.V., pp. 875 (2002).
15. P. Vovsha, E. Petersen, and R. Donelly: *Explicit Modeling of Joint Travel by Household Members: Statistical Evidence and Applied Approach*, 82rd annual conference of the Transportation Research Board, Washington, D.C., USA (2003).
16. P. Vovsha, E. Petersen, and R. Donelly: *Impact of Intra-Household Interaction of Individual Daily Activity-Travel Patterns*, 83rd annual conference of the Transportation Research Board, Washington, D.C., USA (2004).
17. J. Zhang, H.J.P. Timmermans, and A. Borgers: *Utility-Maximizing Model of Household Time Use for Independent, Shared, and Allocated Activities Incorporating Group Decision Mechanisms*, Transportation Research Record 1807, pp. 1 (2002).

Features of Discrete Event Simulation Systems
for Spatial Pedestrian and Evacuation Dynamics

S. M. Tauböck[1] and F. Breitenecker[1]

Discrete Event Simulation (DEVS) is a widely used approach for modelling and simulation of dynamic discrete systems. The modern object-oriented DEVS world view regards active objects (entities) passing passive objects (stations) along given path. An event mechanism updates movement of entities, being capable also of collisions and other state-dependent phenomena. Consequently; DEVS can be used for simulation of pedestrian and evacuation dynamics. Classical straightforward modelling approaches, based on abstract classical queuing systems, do not take into account the spatial distributions primarily – only for animation a spatial component is used. But modern object-oriented tools allow modelling of a spatial distribution primarily by means of topological attributes as well in active and passive objects at the modelling level. This contribution discusses the "spatial" features of DEVS simulation systems The chosen simulation tool, Enterprise Dynamics, offers a high flexibility due to its programming language 4d script that allows adding further functionality to the provided elements as well as creating completely new ones.

1.   The Scenario

The investigations regard a classical scenario: an area of defined size with a certain number of exit doors that represents a train platform, incoming doors that represent doors of an incoming train, where people enter the area and head towards the exit.
The main focus is on the movement of people through this area. Obstacles in the area may constrain this movement and may change the movement.

2.   The Simulation Tool

At present there exist a lot of software tools for modelling and simulation of discrete dynamic systems. Almost all tools are based on a modern object-oriented DEVS world view regarding active objects (entities) passing passive objects (stations) along given path. A time event mechanism updates movement of entities, being capable also of collisions and other state-dependent phenomena. Some of these tools can look back at a long tradition, now offering also any kind of object-oriented features, etc. Some of the tools are results of new research projects, starting with object-oriented approach from the first release.
All these tools are more or less similar at the basic modelling level where general entities are passing general stations. But big differences are met in application libraries: some tools have specialised for a certain application, like network modelling, offering preconfigured stations like network routers. Other tools offer different modelling levels, from a library with basic elements to high specialised modelling libraries.
In these investigations the software tool Enterprise Dynamics is used, an object-oriented

---

[1]Vienna University of Technology, Inst. for Analysis and Scientific Computing,
Research Group Mathematical Modelling and Simulation
Wiedner Hauptstrasse 8 / 101, A 1040 Vienna, Austria

dynamic analysis and control system. The system consists of a Enterprise Dynamics (e.D.)-engine® and many building blocks grouped into e.D.-Suites®. An e.D.-Suite is configured for a specific field of expertise, to assist the modeling of a specific problem, branch or area.

Animations can range from 2D flowcharts to true 3D Virtual reality models that empower imagination and creativity. Building blocks can be easily created, customized and added .

3.   Modelling Approach with Classic Elements of an DEVS

The basic Elements of a DEVS are Servers and Queues. In this first approach of modelling the movement of people through a given area toward an exit a model consisting of servers and queues is build.

Classic DEVS as Enterprise Dynamics do offer only basic routines and functions to describe the movement of elements. For usually the way of such an element is given by its passing through other elements as servers and queues.

ED offers the travelto and the moveto function to let an element (atom) move from a starting position (x_0, y_0, z_0) to a destination (x_d, y_d, z_d).

What is not taken into account when using this functions are two important things:

»   The element can not easily change its movement towards another destination
»   Several elements may take up the same position in space without causing a conflict in the system.

So when using a DEVS for this kind of simulation especially the possibility of collisions has to be taken into account.

The basic idea is now, to cover the area of interest by a "field" of servers (and queues), adding up to form the topology of the given area.

3.1. Topology

The area is cut into single places. Each place has eight adjoining places, building a structure similar to a honeycomb (Figure 1).

The places are represented by servers, the cycle time of each server gives the time the person needs to pass through and depends on the persons individual attributes as well as the position of the cell in regard to the exits. People walking through this area pass through these places, choosing the next place to go to according to implemented rules.

In principle, this modelling approach for the spatial topology is similar to modelling approaches with cellular automata, whereby a server mirrors a cell. Here, the entities are
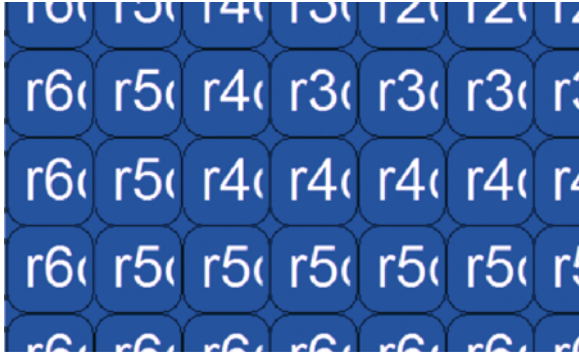
Figure 1: Places represented by servers

active objects, changing the state of a server or cell, resp., on the basis of a time event mechanism. A classical state update of cellular automata works on an equally spaced time pattern.

3.2. Movements

In DEVS time does not pass continuously but in irregular time steps depending on the event list, containing all future events. So the movements of a person can be reduced to be a sequence of events. We can identify two different events:

» entering a place
» exiting a place

Between entering and exiting will always pass a certain time, depending on the persons walking speed as each place does represent a certain walking distance, but exiting one place and entering another happens simultaneously.
These two events will be consecutively repeated until the person has reached its destination.
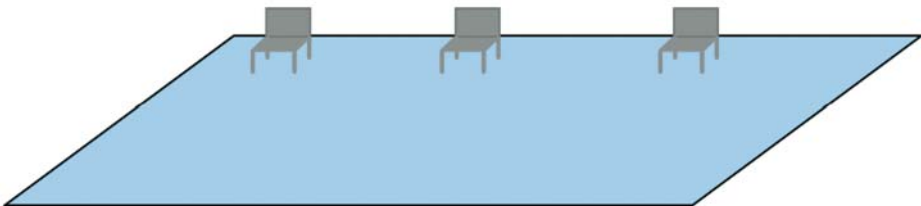
Figure 2: Area with benches

Parts of the area where people are not supposed to walk due to obstacles like benches or other reasons (Figure 2) can be easily marked. It is only necessary to set the capacity of the corresponding places to zero to ensure they can not be entered.
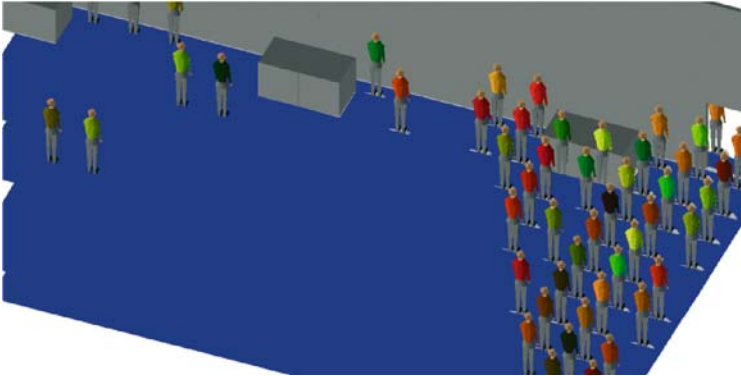
Figure 3: Pseudo-3D Visualisation of the topology shown in Figure 2.

Modern simulation tools like Enterprise Dynamics allow to generate this and other topologies automatically from databases.

3.3. People

Each person is modelled as a single element (entity) within the simulation, carrying their own attributes as size, speed, and the current spatial position.
They choose the exit they wish to use depending on the distance between their own position and the position of the exits. This decision is repeatedly done, so a change of direction might occur if the way to the chosen exit is blocked.

On this way, they are passing the (fixed) places, depending on their decisions and on the fact, which place is free. Here also elements from physical models can be used, e.g. changing speed with respect to the status in the next place, etc.

3.4. Collision

As the capacity of each single place is set to 1 and each place represents exactly one position in space it is not possible for two elements to share the same position. If the next place a person would need to pass through to continue its way towards the exit is already occupied it will enter the next free place instead, rerouting itself. If none of the adjoining places is free the person is unable to move until one is vacated.

3.5. Drawbacks of this approach

Using servers to represent each single position in the two dimensional space has one major drawback: to represent an area of even small size a huge amount of servers is needed. That slows down simulation time. In principle, the spatial distribution of a server equals the area a person needs to stand.

4.   Modelling Approach by Spatial Objects

The first approach was based on using the classic features of a DEVS. Some tools designed for creating discrete event simulation nowadays offer a lot more than these basic elements as servers and queues.

Enterprise Dynamic has its own programming language developed to offer a high flexibility in using and expanding its functionality. It is called 4d script in allusion to the fact that any element in Enterprise Dynamics has four dimensions: its coordinates in the three dimensional space and its velocity.
This language allows to create and move spatial objects, extending the capabilities of classical entities dramatically. In principle, this feature is a first step towards agent-based approaches.
The basic modelling idea is now, to model the pedestrian by such spatial objects, which are moving and allocating places.

4.1. Topology

The topology is similar to the one used in the first approach but instead of using servers to build up the walking area only the area itself is regarded now. It is once more cut into small places; once more each place has eight adjoining ones.
But now the information whether these places are free or occupied is stored in a table where each cell corresponds to one of these places.
Instead of setting capacities to zero to ensure a certain place may not be entered now it only needs to be marked as unavailable.

4.2. Movements

Movements of people are now reduced to only one reoccurring event: the next step. Time between these events once more depends on the walking speed. The continuous movement of a walking person is now broken down in jerky leaps from one position to the next.
The person no longer moves from one server into another. Instead it only changes its location, moving from its current position to the next.
The decision in what direction the next step is going to be taken is now based on the calculation of a direction vector that is calculated each time another step is taken.

Additionally it has to be checked whether the destination is already occupied by another person. In the first approach this was not necessary due to the usage of the servers – their basic functionality already covered this problem.
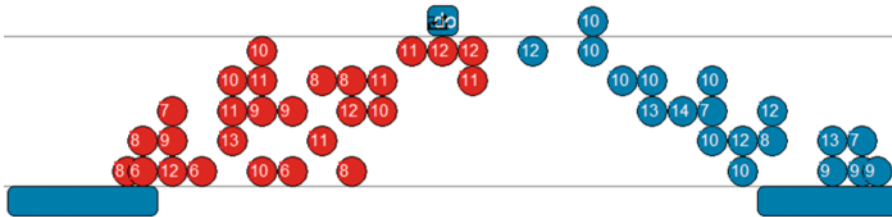

Figure 4: 2D Visualisation of Movement of Spatial Objects

4.3. Drawbacks of this approach

In the first approach, using servers to represent each single position in the two dimensional space had one major drawback: to represent an area of even small size a huge amount of servers is needed. That slows down simulation time.

In this approach, simulation time could be reduced significantly. The major drawback is, that modelling with spatial objects is a much more complex modelling technique and needs deep knowledge of the basic simulator language.

5.   Conclusion

DEVS can be used for spatial pedestrian and evacuation dynamics, if the DEVS simulation tool offers features for spatial descriptions on the modelling level, and for complex attributes for the entities or active objects.

In general, two approaches are reasonable and successful

» The first approach only uses classic features of a DEVS, trying to keep changes to them to a minimum. The result is a model where the movement restrictions are easily represented by the attributes of the servers, which cover the area under investigation

» The second approach presented reflects the ideas used in approaches based on cellular automata and agent based systems, but keeps all advantages of tested event mechanisms of DEVS systems, including collisions and individual velocities of entities. It offers a higher flexibility in implementing rules for people's movements but requires a higher amount of programming work. «

Evolving Direct Perception Models of Human Behavior in Building Systems

A. Turner[1] and A. Penn[1]

Software agents that use direct (or active) perception of the environment have recently been shown to correspond well with pedestrian movement within building and urban systems. The algorithm, based on Gibson's theory of affordances, combines random selection of destination from their field of view with reassessment of the destination every few steps. However, although the agents correlate with human movement on aggregate, as individuals they progress more erratically than people do. It might seem necessary to add higher cognitive functions in order to guide them more convincingly, but here we show that it is possible to improve their behavioral response through artificial evolution of their existing navigation rules. First we show that the destination selection method approximates stochastic direction choice by length of line-of-sight. Then we use the lines of sight to provide a set of inputs to the agents, or animats, which we evolve to fit human usage patterns within a building as best possible. We demonstrate that while agents using informational change inputs fail to evolve to fit movement patterns, an input that compares sight-line lengths improves models qualitatively, but not quantitatively, which further implies that the individual guidance mechanism may be independent of the instant spatial properties acting on direct perception.

1. Introduction

When we think of people as they navigate through the environment, it is usual to regard them as rational beings, making complex decisions based not only on the information available to them at the current time, but also on the history of their actions, and their future goals. Thus, Gibson's theory of ecological perception [1], where the occupant of the environment interacts with it directly, through the affordances it offers her or him, is usually applied to theory of insect behaviour rather than pedestrians. When it comes to people, we tend to think of how their navigation relates to a remembered view or an internal cognitive map, or at least to the cost of the activity in which they are involved. That is, if we consider a four level hierarchical framework for movement, as proposed by Trullier et al [2], with guidance at the bottom, followed by recognition-triggered response, topological navigation and metric navigation, we tend to assume that the observed actions of people — or at least their behaviorally interesting actions within geographical space — take place on the higher three levels. Guidance is usually seen as merely a device to avoid collisions and other obstacles. Therefore, while there is considerable research into how navigation is affected by place or view recognition [3, 4], spatial topology [5, 6], or the perceived metric features of the environment [7, 8], there is little to suggest how the rules of guidance may actually lead to observed 'navigational' behavior.

Nevertheless, according to Gibson, we can regard people as simple affordance-based agents using guidance to navigate. He states: 'When no constraints are put on the visual

---

[1]Bartlett School of Graduate Studies, University College London, Gower Street, London, WC1E 6BT, UK.

system, we look around, walk up to something interesting and move around it so as to see it from all sides, and go from one vista to another. That is natural vision...' [1]. To him, people simply take whatever affordance is apparent and act accordingly: perhaps to an attractive object, or simply from vista to vista. Gibson proposes that the vista itself is simply an ambient optic array of light incident on the current occupant's location. As we move through the optic array, so we cause perturbations within it, and experience optic flow, until we find ourselves at a new vista. The transfer from vista to vista we might call natural movement, as it requires no recognition of any object within it, but simply the recognition that there is environment to move through [9]. In the natural movement schema, the possibilities of the environment drive the agent through the ambient optic array from vista to vista as more possibilities open up ahead of it (see figure 1). Thus, the configuration is the determining factor of the resulting natural movement, even if different agents take different paths through it as individuals.
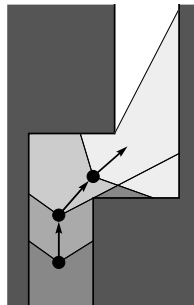
Figure 1:   As an agent moves through the environment, further vistas open up ahead of it, and it can guide itself through a configuration simply by choosing directions of further possibility, for example, by length of line-of-sight.

However, if we are to construct agents, we must consider how they recognize these environmental possibilities for movement. There is good evidence that insects use the optic flow itself to perceive the environment: honeybee dances seem to indicate the optic flow on a journey from A to B rather than landmark or other cues [10]. As the bee flies through a narrow gap, there will be fast flow of information to its sides. Humans possess radial receptors in their eyes, and so it might be thought that they too use optic flow to perceive the environment. However, the situation is more complicated: where stroke victims lose the use of these receptors, they still manage to navigate easily [11]. Further, experiments using children show they tend to use geometric as opposed to texture information to guide decisions — that is, other forms of depth-cue are being used to calculate action through basic mental manipulation [12]. From this evidence, we might assume that somehow the brain is able to construct some form of distance information to objects such as walls. While strictly speaking we should force the agent to work with the visual input directly, the use of distance data lends itself to an elegant and simple formalism,

that of the isovist. An isovist is a polygon (or polyhedron) that represents the visible area from a location. Benedikt introduces their use to architectural configurations [13], and in particular, the idea that there exist in the environment fields of isovist properties. Thus, Benedikt generates contours of equal isovist properties (for example, area or circumference) in order to try to identify areas where rapidly changing distance information takes place. He hypothesizes that such zones will form decision points for onward movement. Conroy Dalton shows that people do indeed seem to slow and make decisions at points where isovist properties change rapidly [14], and thus these informationally rich areas may be important to natural movement.

Here we attempt to test the hypothesis that changes in isovist field or distance information may be a plausible strategy to guide people through a building system. To do so, we create agents that respond to changes in the local length of line-of-sight (LoS) information by turning towards that direction if a threshold is passed (so the information is used as an affordance within a direct perception model). We compare the ability of the agents to respond to the environment in a human-like manner when given one of four different informational inputs. These are: simple length of line-of-sight in the candidate direction, the change in length of LoS between this step and the last, the length of LoS in the candidate direction as compared to the length of LoS in the current heading, and, finally, a similar comparative measure for the amount of LoS change between steps. The idea behind the two variants of LoS change inputs is that they should correspond to the agents receiving an information flow, in a similar manner to optic flow[1].

We apply the threshold agents to an art gallery situation, after original experiments using similar agents [9]. The gallery represents a situation where natural movement may well occur: most people will not know the gallery plan and thus will not use higher level navigational strategies, other than perhaps path integration; it also acts as a large area with many potential turnings, suitable for testing the agents. We evolve the receptor thresholds to fit the observed movement pattern of the people using the gallery. The methodology is obviously limited, in that it essentially evolves the model to fit a single case. However, we do find, that while agents with the comparative line-of-sight rule can attain a correlation coefficient of $R^2 = 0.84$ with observed aggregate movement patterns, those with differential field inputs only achieve at best a correlation of $R^2 = 0.56$, indicating that these receptor architectures are unlikely to be utilised in people.

2.   Background

The use of direct perception as a guidance strategy for agents is not new, with its theoretical breakthrough in Brooks's robot subsumption architecture [15]. Brooks's robots have no knowledge representation, and therefore must interact with the environment only in the ways permitted by their sensor and motor architecture. Equally, the use of ambient optic arrays (albeit in sonar form) dates back to architectures such as those introduced by Kuipers and Byun [16], where the robot is given a tripartite system of low-level sensorimotor control, topological mapping and geometric path recording. However, within software simulation of people movement, direct perception and direct

---

[1]Note that actually distance information change and optic flow may well be different.

visual control have tended to give way to higher level models of path planning. One possible reason is the high overhead of the calculation of visual information, although as we show herein, partial information still leads to good results.

As a first step to reducing calculation overhead is an exosomatic visual architecture (EVA), where the visual information is contained in the environment, rather than calculated by an individual [9]. The exosomatic visual architecture might be thought of as an ambient optic array, as visible locations waiting to be sampled from the occupant's location. We first implemented the EVA as a visibility graph of many point locations sampled on a grid [17]. This allowed the introduction of many parallel agents that choose a destination from their current field-of-view (FoV). The algorithm we used was simply to pick any destination at random from those visible on the floor ahead, and walk towards it for a number of steps, before selecting another destination, walking towards it, and so on. We applied the agents to a plan of the Tate Britain Gallery (a large art gallery in London) and adjusted the FoV and number of steps until we found the best correlation with observed room through movement for people, which occurred at a 170º FoV and with a decision after three steps, giving a correlation coefficient of $R^2 = 0.77$ [9]. Although this is extremely encouraging, there are a number of caveats. Firstly, the three step parameter is arbitrary. Would three steps hold in any other building, let alone outside? And surely a good direction might be completely overlooked if the agent were on the first or second step? Secondly, the agent paths themselves were not convincing (see figure 3 further below), involving almost constant turning. Here we try to remedy these problems. In doing so, we will introduce a line-of-sight selection rule. This loses some of the elegance of the original affordance-based rule, which picks a location from the available floor space. There is evidence to suggest that people use vision of the floor in distance perception [18]; indeed, obstacle avoidance behavior typically takes place over short ranges [19], so we may well be looking down rather than ahead while navigating. However, for overall ease, rather than using the entire visibility graph, it seems adequate to use the isovist boundary information instead, as it allows us to test a range of inputs unavailable with previous method. Furthermore, as we will show in the next section, line-of-sight and destination selection strategies correlate well with each other.

3.   Simple Line-of-Sight Agents

In this section, we demonstrate that a random selection of a floor destination point within the field-of-view (FoV) is equivalent to a stochastic choice of direction based on the length of line-of-sight (LoS) from the FoV. For both models, we sample the visual field over a grid of locations, with the field separated into 32 'bins', as shown in figure 2. We also assume that we have calculated the length of LoS in the direction of each of the 32 bins, as shown in figure 2(b). Using 15 bins to select a destination is thus equivalent to a FoV of about 170º.

For each experiment, we released 2000 of the standard destination selection agents into a plan of the Tate Britain Gallery, London, with bin information calculated every 0.75m (i.e., approximate interstep distance [9, 20]). Each agent took three steps and then rese-
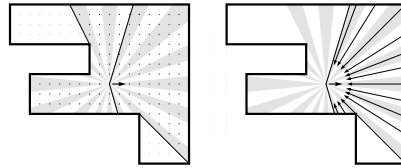
Figure 2: Using precalculated bins of information to select (a) a destination location, and (b) a line-of-sight from the current field of view.

lected its destination, and remained in the gallery for 1600 steps (about 20 minutes of simulated time). After this time it was simply removed, with no requirement to return to the entrance. Although programming return is possible, it posits a desire to leave, rather than a strict direct perception model of visual affordances; therefore we exclude it at this stage. After the experiment had been run, the number of agents entering each of 55 rooms within the gallery was recorded, and compared with observation data collected for a two day period within the actual gallery in a previous study [21]. Obtaining a correlation is somewhat difficult, as much of the movement within the gallery can simply be accounted for as diffusion from the entrance. As we leave the entrance, numbers drop off rapidly, creating a skewed data set, meaning the correlation coefficient can look artificially high. One resolution would be to use Spearman Rank Correlation; however, this loses the ability to see exactly how the model is over or underperforming. Instead, we choose a function of the data. For these experiments, we realized that a near-normal distribution of the data could be found using the cube root of the actual through movement rate. The cube root was applied to both the observation data and agent count date. The destination choice agents showed $R^2 = 0.79$, as per our previous experiments (see table 1)[2]. The line-of-sight agents were programmed to choose one of the 15 available bin directions at every third step, according to the LoS length over the total length of the 15 available bins[3]. That is, $p_i = L_i / \sum_j L_j$, where p_i is the probability of choosing direction i, L_i the length of LoS in direction i, and j are the set of 15 bins distributed evenly either side of the current heading, as shown in figure 2(b). Surprisingly, the results are very similar for both types of agents, with near one to one correlation between the two, as shown in table 1.

Although the correlation with observed movement is good both for destination selection

Correlation		Destination Selection		Line-of-Sight	
		0-step	3-step	0-step	3-step
Observed Movement		0.76	0.79	0.73	0.78
Destination Selection	0-step	—	0.94	0.93	0.88
	3-step	—	—	0.86	0.91
Line-of-Sight	0-step	—	—	—	0.93
	3-step	—	—	—	—

Table 1: Correlation coefficients (R2) of destination-selection agents and line-of-sight agents with observed movement and with each other.

[2]The number is slightly different to our earlier reported results due to the use of the cube root in this paper rather than logarithmic scales used previously.

[3]We also applied more complex functions of the line-of-sight, but none corresponded as well with observed movement as this simple linear probability function.

and LoS agents, when we compare movement traces of either method with actual people moving through the Tate Britain Gallery, there is a marked difference. Figure 3 shows the trails of 3-step LoS agents released into the gallery for 10 simulated minutes, and figure 4 the corresponding patterns of observed people movement, collected by following people surreptitiously from the entrance [21]. It is noticeable that the paths of the agents are far less linear than the people's paths. This meandering would initially seem to be due to the wide FoV, the fact that the agent may stochastically pick a wide angle, and the lack of memory of a goal. However, as we will see, neither the FoV nor the lack of memory account for this change, rather, it appears to be the lack of a default onwards forwards movement. There is also a conceptual problem with the rules of these basic agents: it is that the 'three steps' parameter is effectively an act of calibration. It seems unlikely that people really do count three steps and then make a decision; instead at some threshold, the person turns (should she or he actually be navigating through natural movement). However, if we set the number of steps taken in our model so the agent continually reassesses the situation every step (we call this a 0-step rule), the correlation with actual movement drops considerably (refer back to table 1). In addition, as might be expected, the paths become still more winding still, and all the less human-like. In order to counter these two problems, we introduce agents that continue in a straight line unless otherwise perturbed through an affordance threshold being reached. But this raises the question: how should the threshold be set? In the next section, we use a genetic algorithm can be used to evolve to a solution.
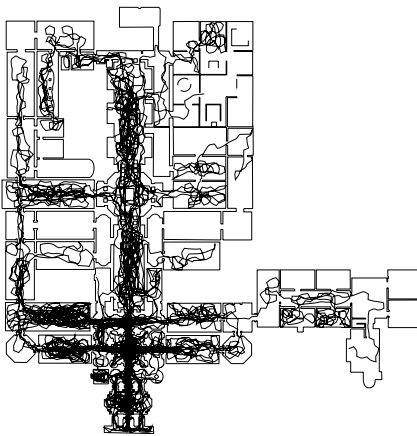
Figure 3: Trails of 20 3-step LoS agents for the first 10 minutes of their 'visit' to the Tate Britain Gallery
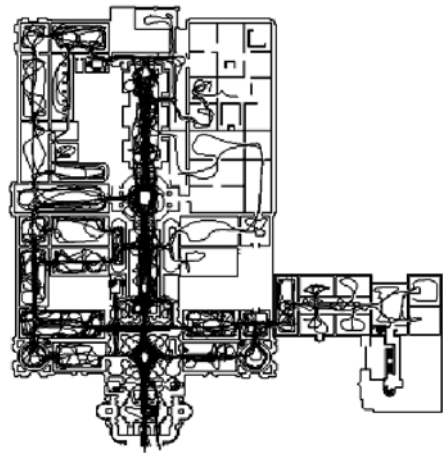
Figure 4: Trails of 19 real people followed for the first 10 minutes of their visit to the Tate Britain Gallery, reproduced from Hillier et al. (1996), p. 15 [21].

4.   Evolved Line-of-Sight Agents

In this section, we demonstrate that superior agent behaviors can be evolved to better fit human movement patterns, and that it is the visual information itself that is important, rather than the visual information flow, in natural movement guidance. In order to give the agents more appropriate response to the environment, we set them to walk forward continuously. We then give each one a set of eight paired receptors (see figure 5), one pair at each of 1 bin, 3 bins, 5 bins and 7 bins away from the current heading. The input received by the receptor itself is changed according to the experiment conducted, but in each case the basic rules of response are kept constant as follows:

» Each pair of receptors is checked in a set order, determined by a genetic algorithm gene, for example, {3,1, 2, 4}, which represents look at the third pair of receptors first (5 bins away from the current heading), then the first pair (1 bin away from the current heading), second pair and finally the fourth pair.
» The left and right inputs of the current receptor are compared to a genetically determined threshold.
» If one or other of the receptors is above the threshold, then it turns to the receptor according to a genetically determined probability. If both receptors are above the threshold, it turns to either one with the same probability.
» If the input actually triggers the turn, the remaining receptor pairs in the list are not checked and the agent makes a step.
» If no receptor pair is chosen, then the agent makes a step in the current forward facing direction.
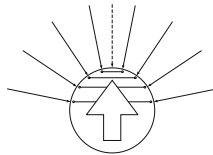
Figure 5:   Inputs to the evolutionary agents are through eight evenly-spaced inputs, reflecting properties of the ambient optic array at its current location and heading.

The aim of this set of rules is to allow the agent its own evolved choice of FoV to apply, and its own choice of which directions are most important to it. The scheme is far more simple than neural models used for other animat approaches such as evolutionary robotics, but we wanted to get to the heart of how the agent was responding to the environment, and this method allows open analysis of what control method has actually evolved. The method of evolution was a simple genetic algorithm with nine genes (one for the rule order, and eight for threshold and probability for each pair of genes). Chiasma points were placed between the genes, and the genetic algorithm used rank selection, uniform crossover and a 5% mutation rate to evolve the agents (see [22] for details of genetic algorithm operators). The parameters for the algorithm were a population size of

300 agents, evolved for a period of 3000 generations. 500 agents of each phenotype to be tested were released into the Tate Britain Gallery plan from the entrance and allowed to explore for 1600 timesteps as before. At the end of the run, the fitness was assessed as simply the correlation coefficient (R^2) between agent and observed room through movement for the 55 rooms and corridor spaces of the gallery. The experiments were programmed using UCL's Depthmap software[4] and run on a PC with an AMD Athlon 2400+ chip; each took about 2 hours to complete.

Four different types of receptor were applied. Firstly, a straight forward threshold based on distance. Each threshold was initially set to a random value between 0 and 100m. Secondly, in an attempt to see if informational flow could guide the agents better, the threshold the length of the LoS in the receptor direction divided by its length on the previous step. This threshold was given a value between 0 times as far and 5 times as far as before. Thirdly, we attempted to see if a comparison with the forward direction had an effect. This threshold was defined as the length of LoS in the receptor direction divided by the length of LoS in the forward direction. This threshold was given a value between 0 times and 10 times as far as the forward direction. Finally, we implemented a threshold which compared the informational flow in receptor and forward direction. The values used were again between 0 and 10 times the informational flow in the receptor direction as compared to the forward direction.

Table 2 shows the result of evolving the four types of agent. Note that the fitness is only a rough correlation of the agent movement with people movement, given that 500 agents were used for the sampling rather than the 2000 used to test the correlation for the basic agents. There is a clear difference between the performance of informational flow agents, which perform worse, and the length of LoS agents. The best performing agents were the comparative LoS agents, with a fitness value of 0.84. Interestingly, these agents seem to apply their first rule with probability of around 1/3 — is the 3-step rule revisiting us?

Guidance type	Directional threshold		Comparative threshold	
	Line Length	Info Flow	Line Length	Info Flow
Fitness	0.81	0.54	0.84	0.56
Rule Order	3,1,2,4	1,3,4,2	2,4,3,1	4,3,1,2
Rule 1 (Bin 1, view angle +/–10º)				
Threshold [Probability]	16.5 [0.94]	2.40 [0.01]	0.22 [0.40]	0.77 [0.00]
Rule 1 (Bin 1, view angle +/–35º)				
Threshold [Probability]	8.5 [0.67]	4.09 [0.70]	9.13 [0.04]	2.09 [0.46]
Rule 1 (Bin 1, view angle +/–55º)				
Threshold [Probability]	20.1 [0.07]	2.39 [0.18]	8.58 [0.27]	4.25 [0.85]
Rule 1 (Bin 1, view angle +/–80º)				
Threshold [Probability]	6.3 [0.86]	3.92 [0.83]	1.66 [0.27]	3.79 [0.03]

Table 2: Optimized fitness values and corresponding rulesets for best performing evolved agents

---

[4]Depthmap was written by the first author and is available free for academic use. Please see http://www.vr.ucl.ac.uk/depthmap/ for details.

We were also interested to see if the evolved agents corresponded better with observed movement. Figure 6 shows scatter plots of room through movement for the basic LoS agents and the evolved comparative LoS agents. In each case the scales have been adjusted to using cube roots, and set on a scale with a maximum of one. Although the evolved version is slightly straighter, the noticeable thing is that the outliers are all in approximately the same places. That is, it is striking that the underlying data for these two types of agents is almost identical. However, there is a quite obvious difference if we look at the patterns of paths as shown in figure 7. The evolved agents have much more realistic qualitative patterns of movement, although we have not compared the paths themselves for quantities such as mean angle of turn or frequency of major turns.
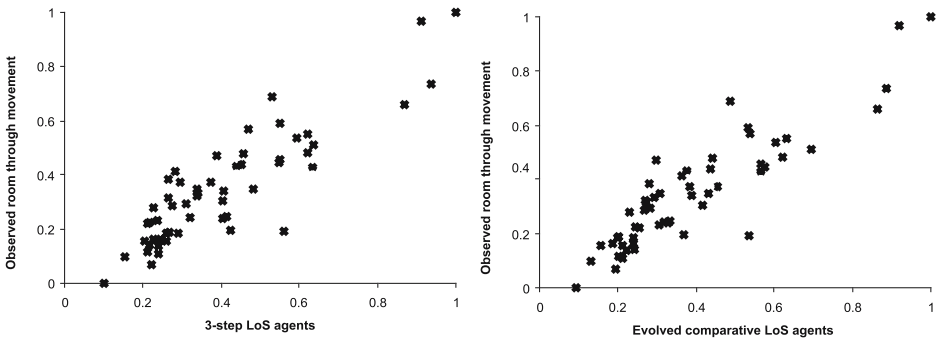
Figure 6: Scatter plots of adjusted room through movement rates for 3-step LoS and evolved comparative LoS agents against observation data for the Tate Britain Gallery.
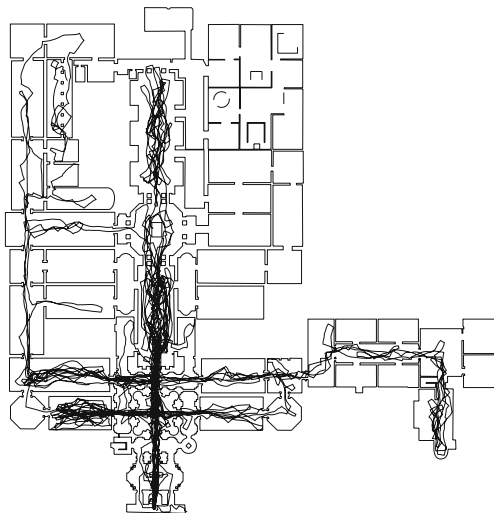
Figure 7: Trails of 20 evolved comparative LoS agents for the first 10 minutes of their 'visit' to the Tate Britain Gallery.

5.   Conclusion

In this paper, we have shown that we are able to reproduce aggregate pedestrian move-ment within buildings using extremely simple line-of-sight (LoS) based rules. Agents that use movement rules based on length of line of sight to assess the affordance of that direction for further movement correlate with $R^2 = 0.78$ with observed numbers of peo-ple walking through rooms in an art gallery environment. However, we have also shown that the individual paths of these agents do not tally with those of people, adding many more turns than would be expected. Furthermore, the agents are calibrated to correlate well with people numbers by forcing them to make a choice of destination only once every three steps. In general situations, this would lead them to miss turnings based entirely on where they are in their walk cycle. In order to overcome these problems, we programmed agents to respond to probabilisitically to thresholds of informational con-tent in the environment. We invoked Benedikt's isovist fields to suggest that picking a destination may be based on information or informational flow as we move through the environment. We evolved agents using these inputs, and found that informational flow did not lead to good correspondence. However, making a decision based on the length of LoS ahead compared to the length of LoS in a candidate direction did lead to mar-ginally improved movement models, with $R^2 = 0.84$. When we came to compare these evolved agents with the basic agents, we found that there were some striking similarities between them: the 3-step rule seemed to have been replicated in a 1/3 probability level of turn in the evolved agents, and the distribution of room through movement counts was almost identical across the two. This could indicate that there is an underlying con-stant of natural movement we are uncovering, or, of course, it could simply be that we are overfitting both types of agents to the example of the chosen art gallery. There was, however, one major difference between the two sorts of agents. Although where they go is very similar, how they go about it is quite different. The basic agents turn continually, progressing in almost circular motion of onward circles; the evolved agents, by contrast, advance in much straighter lines, similar, at least qualitatively, to those of people obser-ved within the gallery context. «

References

1.   J.J. Gibson: *The Ecological Approach to Visual Perception*, Houghton Mifflin, Boston, MA (1979).
2.   O. Trullier, S.I. Wiener, A. Berthoz, and J.A. Meyer: *Biologically Based Artificial Navigation Systems: Review and Prospects*, Progress in Neurobiology 51, pp. 483–544 (1997).
3.   R.P. Darken and J.L. Sibert: *Wayfinding Strategies and Behaviors in Large Virtual Worlds*, In: Proceedings of CHI., pp.142–149 (1996).
4.   H.A. Mallot, S. Gillner, S.D. Steck, and M.O. Franz: *Recognition-Triggered Re-sponse and the View-Graph Approach to Spatial Cognition*, In: Proceedings of COSIT, LNCS Vol. 1661, Springer, Berlin, pp. 367–380 (1999).

5. D.R. Montello: *Spatial Orientation and the Angularity of Urban Routes*, Environment and Behavior 23, pp. 47–69 (1991).
6. R. Conroy Dalton: *The Secret is to Follow your Nose: Route Path Selection and Angularity*, Environment and Behavior 35, pp. 107–131 (2003).
7. R.G. Golledge: *Path Selection and Route Preference in Human Navigation: A Progress Report*, In: A Theoretical Basis for GIS. LNCS Vol. 639, Springer, pp. 207–222 (1995).
8. D.R. Montello: *The Perception and Cognition of Environmental Distance: Direct Sources of Information*, In: Proceedings of COSIT, LNCS Vol. 1329, Springer, pp. 297–311 (1997).
9. A. Turner and A. Penn: *Encoding Natural Movement as an Agent-Based System: An Investigation into Human Pedestrian Behaviour in the Built Environment*, Environment and Planning B 29, pp. 473–490 (2002).
10. H.E., Esch, S., Zhang, M.V., Srinivasan, and J. Tautz: *Honeybee Dances Communicate Distances Measured by Optic Flow*, Nature 411, pp. 581–583 (2001).
11. L. Vaina and S. Rushton: *What Neurological Patients Tell us About the Use of Optic Flow*, International Review of Neurobiology 44, pp. 293–313 (2000).
12. L. Hermer and E.S. Spelke: *A Geometric Process for Spatial Reorientation in Young Children*, Nature 370, pp. 57–59 (1994).
13. M.L. Benedikt: To Take Hold of Space: *Isovists and Isovist Fields*, Environment and Planning B 6, pp. 47–65 (1979).
14. R.A. Conroy: *Spatial Navigation in Immersive Virtual Environments*, PhD Thesis, Bartlett School of Graduate Studies, UCL, London (2001).
15. R.A. Brooks: *Intelligence Without Representation*, Artificial Intelligence 47, pp. 139–159 (1991).
16. B.J. Kuipers and Y.T. Byun: *A Robot Exploration and Mapping Strategy Based on a Semantic Hierarchy of Patial Representations*, Journal of Robotics and Autonomous Systems 8, pp. 47–63 (1991).
17. A. Turner, M. Doxa, D. O'Sullivan, and A. Penn: *From Isovists to Visibility Graphs: A Methodology for the Analysis of Architectural Space*, Environment and Planning B 28, pp. 103–121 (2001).
18. T.L. Ooi, B. Wu, and Z.J. He: *Distance Determined by the Angular Declination Below the Horizon*, Nature 414, pp. 197–200 (2001).
19. J. Kerridge, J. Hine, and M. Wigan: *Agent-Based Modelling of Pedestrian Movements: The Questions that Need to be Asked and Answered*, Environment and Planning B 28, pp. 327–341 (2001).
20. D.H. Sutherland, K.R., Kaufman, and J.R., Moitoza: *Kinematics of Normal Human Walking*, In: Human Walking, Williams & Wilkins, Baltimore, pp. 23–44 (1994).
21. B. Hillier, M.D. Major, J. Desyllas, K. Karimi, B. Campos, and T. Stoner: *Tate Gallery, Millbank: A Study of the Existing Layout and New Masterplan Proposal*, Technical Report, Bartlett School of Graduate Studies, UCL, London (1996).

22.   D.E. Goldberg: *Genetic Algorithms in Search, Optimization and Machine Learning*, Addison-Wesley, London, UK (1989).

Fundamental diagram of a one-dimensional cellular automaton model for pedestrian flow – the ASEP with shuffled update

M. Wölki[1], A. Schadschneider[2], and M. Schreckenberg[1]

A one-dimensional cellular automaton model for pedestrian flow that describes the movement of pedestrians in a long narrow corridor is investigated. The model is equivalent to the asymmetric simple exclusion process (ASEP) with periodic boundary conditions and shuffled dynamics. In this type of update, the positions of the pedestrians are updated in a random order during one discrete time step. We derive expressions for the fundamental diagrams that are in very good agreement with simulation data. Finally we make a generalization to higher velocities and to two dimensions without lane-changing of the pedestrians.

1.   Introduction

The asymmetric simple exclusion process (ASEP) (see e.g. [1] for a review) is one of the most studied models far from equilibrium. It describes a particle system on a linear chain with hard core exclusion. Particles are only allowed to hop one cell to their right, supposed that it is empty. The usual dynamics is in continuous time: the random sequential update [1]. Moreover, discrete-time update-schemes have been studied: Ordered sequential updates, sublattice-parallel updates and fully-parallel dynamics; for an overview see [2]. Here we analyze another update scheme, that has originally been introduced in a two-dimensional cellular automaton in order to model pedestrian dynamics [3]. We briefly explain the underlying automaton. Consider a corridor, of finite width W in y-direction, divided into square cells. Each cell can either be occupied by one of the N pedestrians, or be empty. Assuming periodic boundary conditions in x-direction and impenetrable walls in y-direction implies that the density of pedestrians is constant. A pedestrian can move to neighbor cells with different transition probabilities, depending on the direction and the particular neighborhood. The preferred direction of motion is along the positive x-axis. A parallel update, in which all particles are updated simultaneously, would lead to conflicts [4] in which more than one person tries to access the same cell. Hence, another way of updating was chosen, the so-called shuffled dynamics: At the beginning of a (discrete) timestep a random permutation of the particle numbers gives the order in which the particles may move. This shuffled dynamics combines elements of discrete updates and time-continuous dynamics. It is discrete in the sense that there is a well-defined timestep during which each particle is updated exactly once. On the other hand, the order of updating the particles is not fixed. E.g. it may happen that a specific particle is updated last during a timestep and first during the next one! In order

---

[1]Theoretische Physik, Universität Duisburg-Essen, Lotharstr. 1, 47057 Duisburg, Germany
[2]Institut für Theoretische Physik, Universität zu Köln, Zülpicher Str. 77, 50937 Köln, Germany

to understand the effects introduced by this kind of updating procedure better, we investigate the simplest case first. This is the one-dimensional limit of the model with $W = 1$ in which the corridor is so small, that it is impossible for two pedestrians to move `side-by-side'. Since this yields a completely asymmetric movement to the right, the model is equivalent to the ASEP with shuffled update, explained in detail in the next section. Afterwards we investigate some simple generalizations of the model.

2.   The Model

Consider a one-dimensional lattice with L sites and periodic boundary conditions. Each site may either be occupied by one of the N pedestrians (also referred to as particles, in the following), labelled $n = 1, 2, ..., N$, or it may be empty. In each discrete timestep a random permutation $\pi(1, ..., N)$ of the particle numbers equals the update sequence. If the right neighboring cell is empty, the relevant particle moves one site to the right with probability p, if it is occupied, the particle stays on its cell. Figure 1 shows six cells and four particles from a large system with many particles, at time t (left) and $t + 1$ (right) in the deterministic case $p = 1$. The particles are numbered from the right to the left; take 4, 3, 2, 1, without loss of generality. The drawn update sequence is ..., 3, ..., 4, ...1, ..., 2, ..., where the ellipsis indicate that other particle numbers belonging to other clusters (units of neighboring persons) can be chosen inbetween (for the cluster depicted, only the relative position of the sequence are of interest). Pedestrian 3, chosen first, can not move since the cell in front is occupied by 2, and similar for pedestrian 4. Pedestrian 1 then moves deterministically and 2 moves, because it was drawn after 1. Although pedestrian 4 is drawn after 3, it can not move, since both were drawn before 1 and 2.
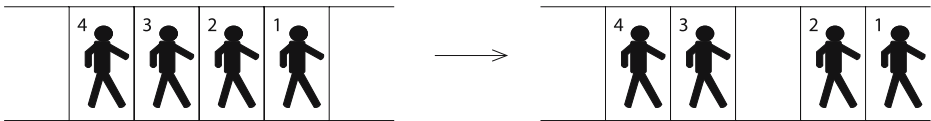
Figure 1:   Shuffled update of a cluster consisting of four particles. These are updated deterministically ($p = 1$) in the sequence 3, 4, 1, 2.

3.   Steady State Distribution and Fundamental Diagram

We assume that the probability to find a certain conguration of particles in the steady state factorizes into probabilities for interparticle distances. This is usually not exact and constitutes the so-called car-oriented mean-field (COMF) theory, successfully applied to traffic flow models [5] previously. If P_n denotes the probability to find a particle with n holes in front, the relations resulting from the master equation are:

$$P_0 = P_0 - (p - g)(1 - P_0) + p\overline{g}P_1 \quad , \tag{1}$$

$$P_1 = (p-g)(1-P_0) + (pg + (1-p)\bar{g})P_1 + p\bar{g}P_2 \quad , \tag{2}$$

$$P_n = (1-p)gP_{n-1} + (pg + (1-p)\bar{g})P_n + p\bar{g}P_{n+1} \quad , \qquad \text{for } n > 1, \tag{3}$$

in dependence on the probability $g = 1 - \bar{g}$ that the particle in front moves. As an example, we explain (3): A particle that has n holes in front had in the previous timestep either $n - 1$, n or $n + 1$ holes in front. If it had $n - 1$ holes in front the particle itself did not move (with probability $1 - p$) but the particle in front did (with probability g). The other terms can be explained similarly. The probability for a particle to have exactly $k - 1$ particles directly in front is approximated in COMF by $(1 - P_0)P_0^{k-1}$, due to the factorization in interparticle distances. Since every random sequence at a certain time t can be drawn with the same probability $(1/N!)$ one can calculate the probability with which the particle has moved at the end of the timestep. For the particle to move, at least the first k particles have to be chosen in the order from the right to the left (with probability $1/k!$ and they all have to move (with probability p^k). Therewith, the probability g is the product of the transition probability) $p^k/k!$ and $(1 - P_0)P_0^{k-1}$, summed over all possible values of k, since the particle can belong to a cluster of arbitrary length. We obtain

$$g = \sum_{k=1}^{\infty} \frac{p^k}{k!}(1-P_0)P_0^{k-1} = \begin{cases} p, & P_0 = 0, \\ \dfrac{1-P_0}{P_0}[\exp(pP_0)-1], & P_0 > 0. \end{cases} \tag{4}$$

Since g is the probability that an arbitrary particle moves it equals also the average velocity. This quantity is related to the fundamental diagram

$$J(\rho) = g\rho. \tag{5}$$

Inserting (4) in (1 - 3), an implicit expression for P_0 is obtained that has to be solved numerically, in general:

$$P_0 = \frac{p(\rho - \bar{\rho}) - (p\rho - \bar{\rho})g}{p\rho\bar{g}} \tag{6}$$

where the abbreviations $\bar{\rho} = 1 - \rho$, etc. were used. If $p = 1$ P_0 becomes explicitly $P_0 = (2\rho - 1)\theta(\rho - 1/2)/\rho$ and, using (4) the flow-density relation is explicitly

$$J(\rho, p = 1) = \begin{cases} \rho, & \rho \leq 1/2, \\ \dfrac{\rho(1-\rho)}{2\rho-1}\left[\exp\left(\dfrac{2\rho-1}{\rho}\right)-1\right], & \rho > 1/2. \end{cases} \tag{7}$$

Figure 2 shows the fundamental diagrams $J(\rho)$ for $p = 1$ and $p = 0.5$ respectively. Depicted are the results from Monte-Carlo simulations and from the above calculation in comparison. We mention here that it can be shown [6], by mapping of the ASEP with shuffled update onto generalized zero range processes that the COMF-theory applied here does not give the exact result for general choice of p and ρ. Hence, the results of this section are very good approximations, but not exact in general, which is not visible to the naked eye in Figure 2.
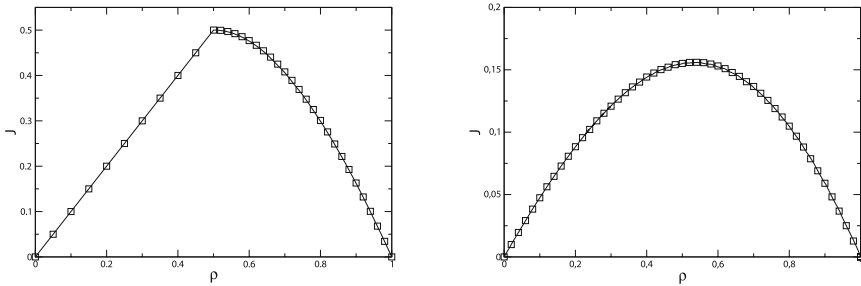
Figure 2: Fundamental diagrams for $p = 1$ (left) and $p = 0.5$ (right). Analytic and numeric results for the thermodynamic limit are depicted in comparison in both diagrams.

4.   Generalizations

In the following we consider two straightforward generalizations of the model. The next step towards a description of the whole problem of pedestrians moving under shuffled dynamics in a corridor of arbitrary width W is done by not allowing the pedestrians to change lane. Since the pedestrians are distributed stochastically on sites (and lanes) in the beginning of the time evolution, the density of pedestrians in a particular lane is fixed for all timesteps. The probability of finding i pedestrians in a particular lane is given by the hypergeometric distribution $Hyp_{N,L,L(W-1)}(i) = \begin{pmatrix} L \\ i \end{pmatrix}\begin{pmatrix} L(W-1) \\ N-i \end{pmatrix} / \begin{pmatrix} LW \\ N \end{pmatrix}$ with mean $\rho = N/(LW)$. The fundamental diagram of the model with decoupled lanes is [7]

$$\tilde{J}(\rho) = \sum_{i=0}^{L} Hyp_{\rho LW, L, L(W-1)}(i) \cdot J(i/L),$$

(8)

where $J(\rho)$ is the single-lane fundamental diagram determined in Sec. 3. Using the approximation (5), the result for a width of $W = 10$ cells and deterministic hopping ($p = 1$) in the thermodynamic limit is depicted in Figure 3 (a). One can see that the maximum is

smoother and a little bit lowered in comparison to the corresponding Figure 2 (a). Note that lane-changing, an effect that is especially relevant for high densities, would lead to a reduction of the flow. To reproduce the shift of the maximum flow to lower densities, observed in pedestrian dynamics, we introduce a larger maximum velocity v_{max}, i.e. a larger number of cells that can be passed during one timestep [8]. The simplest way is to allow a pedestrian to move the minimum of v_{max} cells and the number of empty cells in front with probability p at each timestep. In the following we again consider the case $W = 1$ and $p = 1$ only. For densities less or equal to $1/(v_{max} + 1)$ each of the pedestrians has at least v_{max} empty sites in front, i.e. the probability to find a particle in front is P_0 and the flow is determinstically given as $v_{max}\rho$. For higher densities it may happen that e.g. a pedestrian occupies a cell at time $t + 1$ that has been occupied by a different pedestrian belonging to the cluster in front at time t. However we found in computer simulations that this effect can be neglected (for relatively small v_{max}). Thus one can again describe the dynamics in the picture in which all clusters are updated in parallel. The system tries to separate the clusters by exactly v_{max} holes. The probability to have at least one hole in front is in this case $(1 - \rho)/v_{max}$ and the ratio of particles which do not have a particle in front is $(\rho - (1 - \rho)/v_{max})/\rho$. This defines the probability P_0, which can finally be written as $[(v_{max} + 1)\rho - 1]\theta(\rho - 1/(v_{max} + 1))/(v_{max}\rho)$. With the use of (7) we obtain

$$J(\rho, v_{max}, p = 1) = \begin{cases} v_{max}\,\rho, & if\ \rho \leq 1/(v_{max}+1), \\ \dfrac{v_{max}\,\rho(1-\rho)}{(1+v_{max})\rho - 1}\left[e^{\frac{(v_{max}+1)\rho-1}{v_{max}\rho}} - 1 \right], & else. \end{cases}$$

(9)
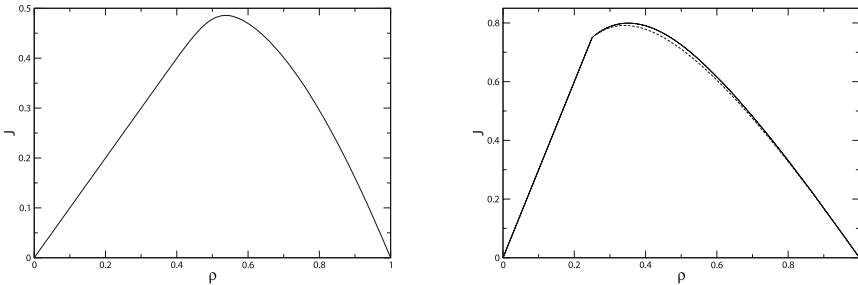
Figure 3: Fundamental diagrams for two generalized processes with $p = 1$. The left diagram shows the result for the model with decoupled lanes for $W = 10$. The right one shows the case of increased velocity $v_{max} = 3$ for $W = 1$. The dashed curve represents the analytical result, the continuous curve the result from computer simulations.

In Figure 3 (b) the resulting fundamental diagram in case of $v_{max} = 3$ and $p = 1$ is depicted. The dashed line shows the analytical in comparison to the numerical result. In opposite to the case of maximum velocity 1 , depicted in Figure 2 (b), the maximum of

the fundamental diagram and the critical point $(1/(v_{max} + 1), \rho v_{max})$ do not coincide; this is qualitatively reproduced by the analytical result. However, to recover the exact result one would have to take longer ranged correlations into account.

5.   Summary

This article studies a one-dimensional model for pedestrian flow, which is equivalent to the well known asymmetric simple exclusion process with periodic boundary conditions in case of shuffled dynamics. In this update the order in which the pedestrians are allowed to move in a timestep is determined by newly in each timestep. Steady state distribution functions are derived that are in very good agreement with Monte-Carlo data. With the knowledge of these distribution functions the fundamental diagram could be calculated approximatively, which for p = 1 has a strong asymmetry with respect to $\rho = 1/2$. This is due to the fact that for small densities all pedestrians can move independently and deterministically; for higher densities jams are formed and the probability for a pedestrian in a jam to move decreases with the number of pedestrians directly in front, due to the shuffled dynamics. Thus the flow is increased in the high density region. Furthermore we have presented generalizations of the results to a two-dimensional scenario with decoupled lanes and to higher velocities. Also in this case analytical results were presented that are in good agreement with simulations. **«**

References

1.   B. Derrida: *An Exactly Soluble Non-Equilibrium System: The Asymmetric Simple Exclusion Process*, Phys. Rep. 301, pp. 65 (1998).
2.   N. Rajewsky, L. Santen, A. Schadschneider, and M. Schreckenberg: *The Asymmetric Exclusion Process: Comparison of Update Procedures*, J. Stat. Phys. 92, pp. 151 (1998).
3.   H. Klüpfel: *A Cellular Automaton Model for Crowd Movement and Egress Simulation*, PhD thesis, Universität Duisburg-Essen (2003).
4.   A. Kirchner, K. Nishinari, and A. Schadschneider: *Friction Effects and Clogging in a Cellular Automaton Model for Pedestrian Dyna*mics, Phys. Rev. E67, 056122 (2003).
5.   A. Schadschneider: *The Nagel-Schreckenberg Model Revisited*, Eur. Phys. J. B 10 573 (1999).
6.   M. Wölki, A. Schadschneider, and M. Schreckenberg: *Asymmetric Exclusion Processes with Shuffled Dynamics*, J. Phys. A 39, pp. 33 (2006).
7.   C. Burstedde: *Simulation von Fußgängerverhalten mittels zweidimensionaler zellulärer Automaten*, Diploma thesis, Universität zu Köln (2001).
8.   A. Kirchner, H. Klüpfel, K. Nishinari, A. Schadschneider, and M. Schreckenberg: *Discretization Effects and the Influence of Walking Speed in Cellular Automata Models for Pedestrian Dynamics*, J. Stat. Mech. P10011 (2004).

Implementing Ship Motion in AENEAS –
Model Development and First Results

T. Meyer-König[1], P. Valanto[2], and D. Povel[3]

Since the first software programs for evacuation simulations were applied to ships, questions about the influence of the ship motions, and how these could be taken into account, came up. As the acceptance of simulation tools was pushed by the developments at the International Maritime Organization, research was undertaken by various institutes and the appropriate data was collected. The paper describes, how a model for the implementation of ship motions into the software AENEAS was developed and how the ship motions influence the results of the evacuation analysis. The implementation of ship motion is part of a research project, funded by the German Ministry of Transportation (BMVBW) and organised by the Hamburgische Schiffbau-Versuchsanstalt (HSVA).

1. Introduction

Since the regulation for advanced evacuation analyses for RoRo passenger ferries [1] was established, evacuation simulations are a common tool used by shipyards to demonstrate the compliance of their designs. It was the goal to establish basic rules as a first step. Over the time they will be improved, taking various parameters influencing the evacuation process into account.

Since the evacuation on ships is simulated, the most often raised question concerns the influence of the ship motion on the movement of the pedestrians onboard. To gain empirical data, there have been research projects and theoretical approaches of various institutes to find an answer to the problem. However, due to the complexity of the process and danger of injuries, full scale trials are almost impossible to conduct. Thus only tests on a small scale have been carried out. The results are summarized in this paper.

Within the scope of a research project sponsored by the BMVBW [2], the German ship model basin HSVA [3] investigates the time-dependent survival probability of damaged RoPax ferries. Therefore, the motion of a fictitious ferry in seaway under various damage conditions and sea states is calculated by the seakeeping program ROLLS. In order to assess the results, the mustering duration under the simulated conditions (ship motion) had to be determined.

Based on the literature overview, a model to influence the movement algorithms of the agents in AENEAS was developed and implemented. Thus the influence of the ship motion on the overall evacuation process can now be analysed.

2. Literature Overview

Subsequent, the results of various international research projects and publications concerning the influence of the ship motion on the pedestrian motion are listed in alphabe-

---

[1]TraffGo HT GmbH, Germany, m-k@traffgo-ht.com
[2]Hamburgische Schiffbau-Versuchsanstalt GmbH, valanto@hsva.de
[3]Germanischer Lloyd AG, pov@gl-group.com

tical order. Since the effects of dynamic ship motion were not addressed, the emphasis of the literature summary lies on the effect of static heel and trim. The evaluations sometimes address different criteria (e.g. behaviour depending on gender or age), so mean values are calculated if necessary.

2.1. BMT Fleet Technology, SHEBA

BMT Fleet Technology conducted tests with their motion simulator SHEBA [4]. It consists of a corridor mockup with stairs and a room, all equipped with handrails. The mockup can be tilted around one axis up to 22°. The test persons were of every age and gender.
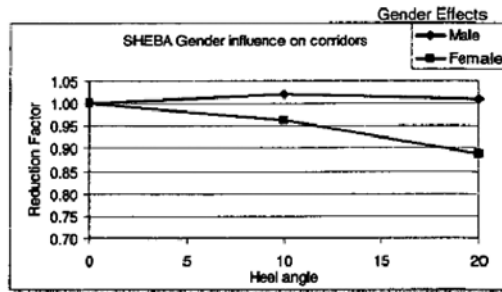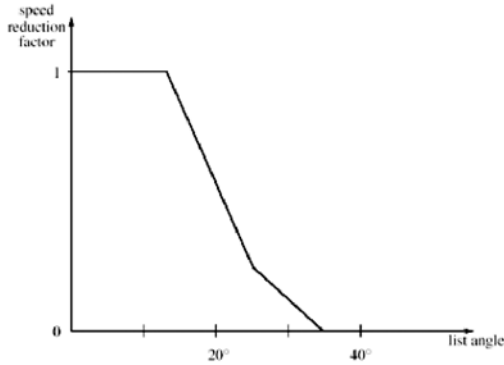

Figure 1: Reduction factor for the walking speed in a corridor depending on a transverse slope as published by BMT Fleet Technology [4].
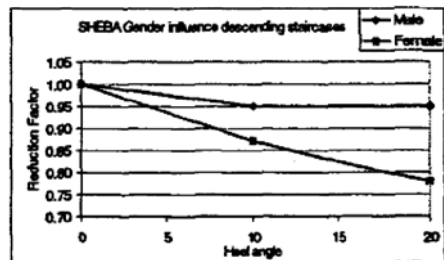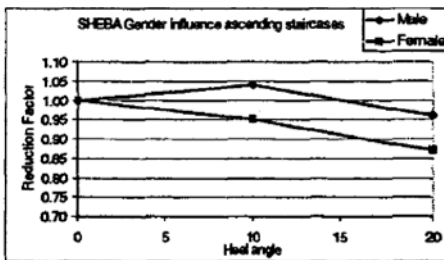
Figure 2: Reduction factors for the walking speeds on stairs depending on a transverse slope as published by BMT Fleet Technology [4].

2.2. ETH Zürich

The research of Weidmann [5] has nothing to do with the movement of persons onboard ships. He analysed the walking speed of pedestrians on longitudinal slopes. Since this case also appears onboard ships, it therefore is of interest for the model development.
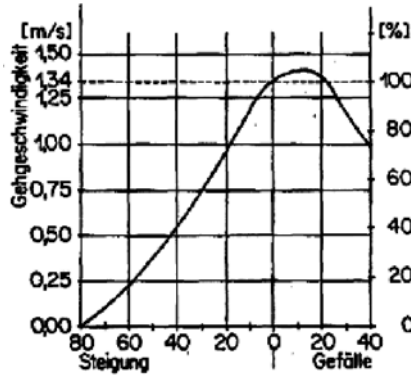
Figure 3:   Absolute walking speeds on longitudinal slopes as determined by the ETH Zürich
[5]. "Steigung" means an upward and "Gefälle" a downward slope.

2.3. KRISO

In an informal IMO paper [6] the Korean Research Institute of Ships and Ocean Engineering (KRISO) summarized their results of practical tests onboard a research ship. The test facility consisted of a corridor mockup (LxWxH: 10 x 1,2 x 1,9 m³) with handrails and a stair at its end which was mounted on the vessel. Students were used as test personal.
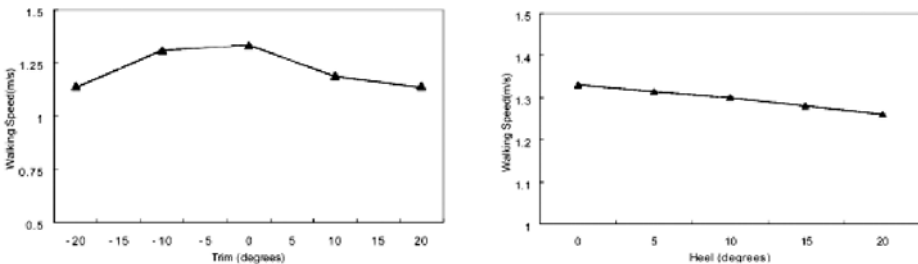
Figure 4:   Absolute walking speeds in a corridor depending on trim (left) and heel (right) angles
as determined by the Korean Research Institute of Ships and Ocean Engineering [6].

2.4. Monash University

Brumley and Koss from Monash University published the evaluation of practical tests [7]. They were performed on an open ramp, which could be tilted transversal to the walking direction. According to them, the reduction factor r_v is only depending on the "environmental moment" M_1 and the resisting moment of the pedestrian M_2.

$$r_v = \begin{cases} 1 & : M_1 \le M_2 \ (\Theta \le 15°) \\ 1-0,25 \left(\frac{M_1}{M_2}-1\right) & : M_2 \le M_1 < 4M_2 \\ 0,25 & : M_1 = 4M_2 \ (\Theta = 25°) \\ 0 & : \Theta > 35° \end{cases}$$

(1)

As a result, the graph for the reduction factor looks as follows:

Figure 5: Reduction factor for the walking speed in a corridor depending on a transverse slope as published by Brumley and Koss [7].

2.5. SSRC

In a paper published by the Ship Stability Research Centre [8] a theory for linking heel transverse to the walking direction with the walking speed was given. It is not based on any practical tests but it refers to the results of the European research project MEP-Design.

It is assumed, that the walking speed is reduced depending on the transverse angle Θ. From Θ_{max} on, the walking speed is 0. Θ_{max} is assumed to be 20°. The reduction factor is calculated by:

$$f(\Theta) = \begin{cases} \dfrac{e^{1-\left|\frac{\Theta}{\Theta_{max}}\right|}-1}{e-1} & : 0 \le \Theta \le \Theta_{max} \\ 0 & : \Theta > \Theta_{max} \end{cases}$$

(2)

Although the function looks complex, it resembles almost a linear interrelationship between the transverse slope and the reduction factor.
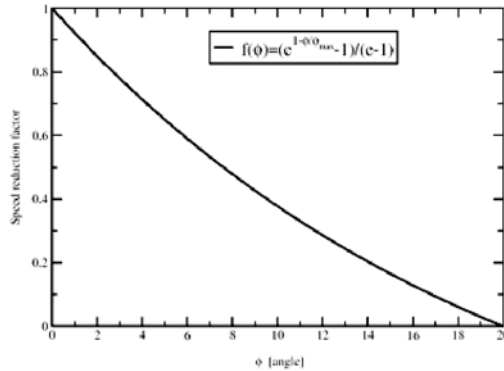
Figure 6: Reduction factor for the walking speed in a corridor depending on a transverse slope as published by the Ship Stability Research Centre [8].

2.6. TNO

Within the European research project MEP-Design, TNO conducted extensive practical tests with a completely tiltable mockup [9]. It consisted of a 20" Container with a circular corridor and stairs (width: 1,1 m). The group of test persons represented a normal population with young (18 - 40), middle aged (41 - 60) and old (61 - 83) persons.

Since the tests are well documented and also take secondary effects into account like the visual perception of stationary or vertically reference points, they are the most substantiated ones in the eyes of the authors.

The maximum tested angles were limited to 20°, since the risk of injuries with steeper slopes would significantly increase. Above 20° the ability to move was determined by the presence of handrails and only young and athletic test persons were able to move.
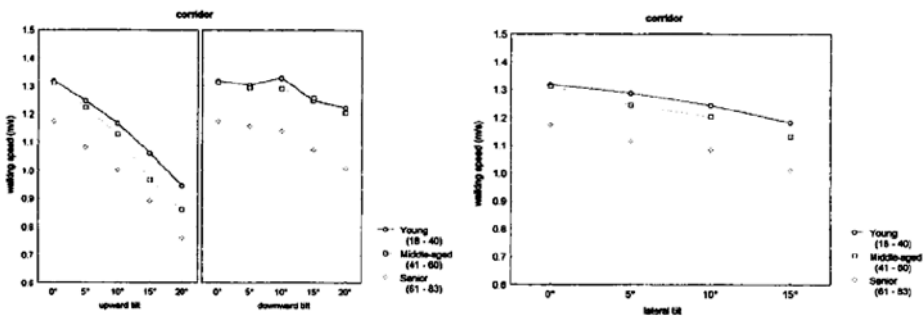
Figure 7: Absolute walking speeds in a corridor depending on longitudinal (left) and transversal (right) angles as determined by TNO [9].
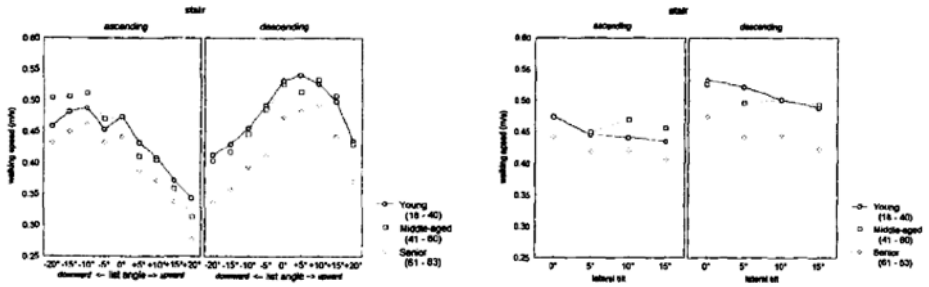
Figure 8:   Absolute walking speeds on a stair depending on longitudinal (left) and transversal
(right) angles as determined by TNO [9].

2.7. Comparison

From the cases evaluated, it becomes clear, that four scenarios have to be considered:
»   Walking on a flat surface (e.g. corridor) with a slope transversal to the walking
direction,
»   walking on a flat surface with a slope in the walking direction (longitudinal),
»   walking on stairs with a slope transversal to the walking direction, and
»   walking on stairs with a slope in the walking direction (longitudinal).
Looking at the single diagrams, the results may vary between the tests. However, when
comparing the resulting reduction factors in one diagram, the differences are in most
cases small.

Corridor, transversal slope

Comparing the various tests and the models developed by them, it becomes clear, that
the assumptions made by the SSRC [8] are extremely conservative. The practical tests
show almost equal results until about 15° heel. As pointed out by Mr. Bles of TNO [9],
no tests beyond this angle were performed due to safety reasons.
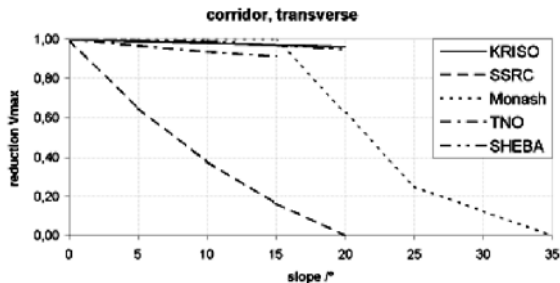
Figure 9:   Comparison of the results of various evaluations and models for a corridor with the
slope transverse to the walking direction.

Corridor, longitudinal slope

The results of the tests performed by KRISO [6] and TNO [9]are very alike. A positive slope means, that the test persons have to walk upwards.
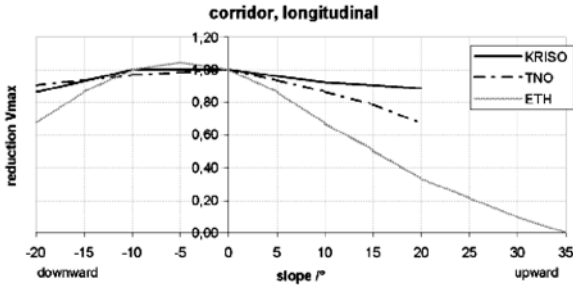

Figure 10: The results for a corridor heeling in walking direction of KRISO [6], TNO [9] and ETH [5] in comparison.

Stairs, transversal slope

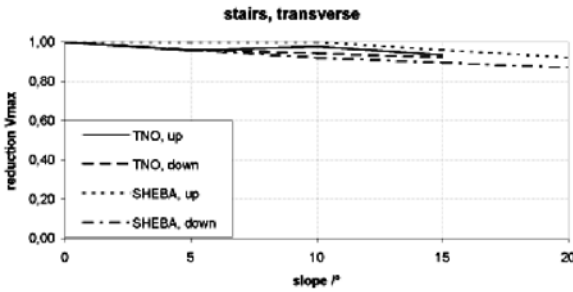The results of the tests performed by BMT [4] and TNO [9] are very alike.

Figure 11: Comparison of the results gained by TNO [9] and BMT [4] for stairs with the heel transversal to the walking direction.

Stairs, longitudinal slope

Only TNO [9] analysed the influence of stairs heeling in walking direction. A positive slope means, that the test persons are walking upwards in means of the slope.
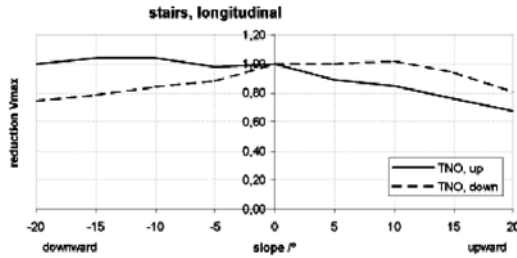
Figure 12: The results of TNO [9] showing the influence of stairs heeling in the walking direction.

3.   Modelling

The model of AENEAS was already described in the conference proceedings of the PED 2001 [10]. Since the results of tests taking roll motion into account are either poorly documented or should not be evaluated due to to few test runs, only the results of static heel are used for modelling the influence of ship motion on the pedestrian motion.

The heel mainly influences the walking speed by reducing it according to a reduction factor. Furthermore, the heel adds a drift to the movement of the agent which results in an increased required space transverse to the main heel angle.

3.1. Slope influencing the reduction factor

While it has not been analysed explicitly, it is assumed, that the normal movement of pedestrians stops when slope angles exceed 35°. Due to friction, loose material will usually start to slide if angles exceed 36-38°. This is pure mechanics, but it seems to be applicable to pedestrians on a ship. At these high angles, the geometry will also start to change significantly, which was not taken into account by the simulation, since it would consume a lot of computing time.

In order to approach the topic conservatively, AENEAS' agents will be able to move with a reduction factor of 5% between 35° and 45° and stop if angles increase even further.
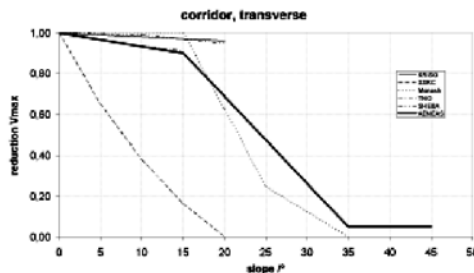
Corridor, transversal slope

Figure 13: The influence of a transversal slope on the reduction factor for a flat surface in AENEAS.
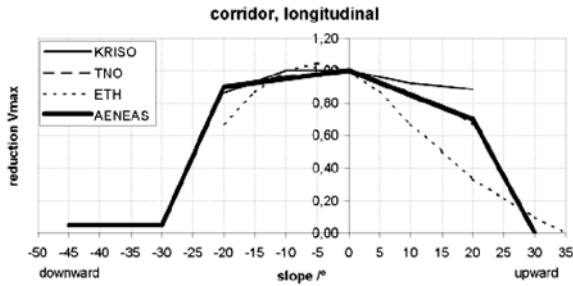
Corridor, longitudinal slope

Figure 14: The influence of a longitudinal slope on the reduction factor for a flat surface in AENEAS.
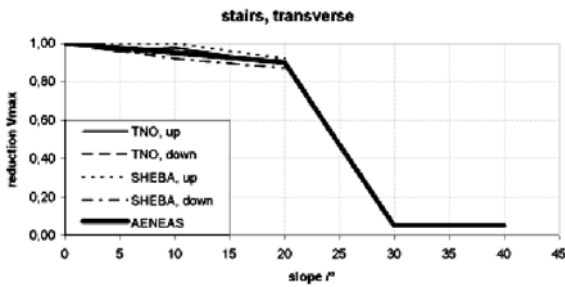
Stairs, transversal slope

Figure 15: The influence of a transversal slope on the reduction factor on a stair in AENEAS.
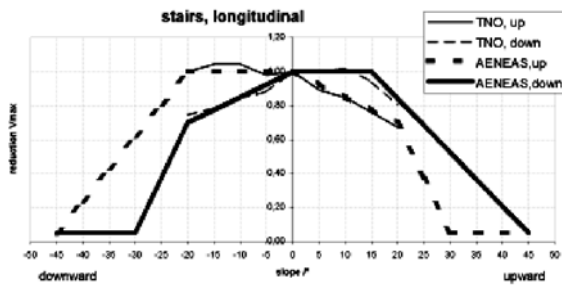
Stairs, longitudinal slope

Figure 16: The influence of a longitudinal slope on the reduction factor for a stair in AENEAS.

3.2. Reduction factor influencing the walking speed

The horizontal acceleration ($\ddot{\phi} \cdot h$) resulting from the ships motion and affecting a person is increasing or decreasing the real slope angle ϕ_{real} .

$$\phi_{feel} = \phi_{real} - \arctan \frac{\ddot{\phi} \cdot h}{g}$$

(3)

Depending on the roll angles and accelerations of the ship, the resulting, felt angles ϕ_{feel} in (ϕ_{long}) and transverse (ϕ_{trans}) to the walking direction are determined. By the felt angles, the reduction factors (r_{long} und r_{trans}) are assessed according to chapter 3.1. They affect the maximum walking speed of an agent. The overall reduction factor is determined by multiplying them:

$$r = \begin{cases} r_{long} & : & r_{long} < r_{trans} \\ r_{trans} & : & r_{trans} < r_{long} \end{cases}$$

(4)

The reduction factor is implemented by increasing the stochastic dawdle probability tr, which provides the probability that an agent stands still during a sub-update, thus reducing its walking speed.
The dawdle probability resulting from the slope (tr_ϕ) thus is calculated by:

$$tr_\phi = 1 - r$$

(5)

The overall dawdle probability resulting from the individual dawdle probability tr_i and the dawdle probability resulting from the ships movement tr_ϕ is calculated by:

$$tr = (1 - tr_i) \cdot tr_\phi + tr_i$$

(6)

3.3. Slope influencing the drift

Since a slope of the geometry results in an increase of required space, a slope dependent drift is added to each agent. Thus each agent increases its probability to move downhill

resulting in an increased demand for space in the direction of the slope.
Changing the geometry according to the heeling angles would absorb too much calculation speed, thus it is discarded.
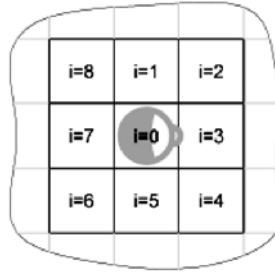

Figure 17: The indices of the cells surrounding a person.

Currently, a transition probability p_i for all neighbouring cells is calculated out of which the agent determines a walking direction [10]. For the lowest cell according to the slope and its neighbouring cells, the transition probability is changed as follows:

$$p_i = p_{i-1} = p_{i+1} = d \cdot p_{i,\max} \qquad (i < 1 \Rightarrow i = 8, \; i > 8 \Rightarrow i = 1) \tag{7}$$

d is the drift factor which is calculated as follows:

$$d = \begin{cases} 0.0333 \cdot \phi_{feel} & : \quad 0° \le \left| \phi_{feel} \right| < 30° \\ 1 & : \quad 30° \le \left| \phi_{feel} \right| \end{cases} \tag{8}$$

Example: When $\phi_{feel} = 15°$, $p_{i,max} = 0,4$ and the lowest cell is $i = 4$, the transition probabilities are set as follows: $p_3 = p_4 = p_5 = 0,2$. Next, the transition probabilities will be scaled appropriately.

4.   Example of application

The tests with the ship motion module are continuing, while this paper is written. In order to demonstrate the effect of static heel as well as dynamic roll motion, a few calculations with an exemplary RoPax design by Flensburger Schiffbau Gesellschaft (FSG RoPax 1800) were conducted.
Since the trim and pitch angles are relatively small, their effect is mostly negligible. The passenger distribution and parameters were chosen according to the IMO regulations night case [1]. Unlike the regulation, the process was modelled not only till the mustering but also to the boarding process.
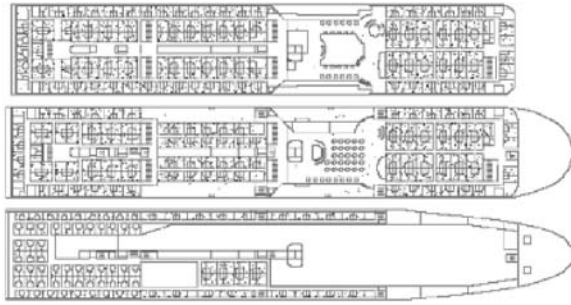
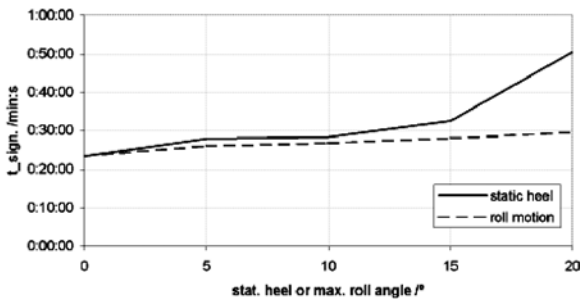**Figure 18**: The RoPax 1800 design of Flensburger Schiffbaugesellschaft.

Figure 19: The effect of static heel or periodic roll motion (T=12,5 s) for a given maximum
angle on the significant evacuation duration.

From Figure 19 it becomes clear, that small static heel angles do not cause significant problems to the passengers. When the static heel angle grows beyond 15° the evacuation duration starts to increase rapidly as the progress upwards on the inclined decks becomes increasingly difficult. Furthermore the evacuation duration distribution becomes significantly wider.

When the ship is performing a roll motion (T=12,5 s), its effect on the evacuation duration is less significant for angles up to 20°. Since the slopes which the agents have to pass change, problems of climbing up through a transverse slope become less relevant.

Further tests will be done by HSVA. They will be published in papers of the IMO. **«**

References

1.   International Maritime Organization (IMO): *Interim Guidelines for Evacuation Analyses for New and Existing Passenger Craft*, MSC/Circ. 1033 (2002).
2.   Ministry of Transportation, Building and Housing (Bundesministerium für Verkehr, Bau- und Wohnungswesen), Germany, http://www.bmvbw.de/
3.   Hamburg Ship Model Basin (Hamburgische Schiffbau-Versuchsanstalt GmbH), Germany, http://www.hsva.de

4.   I. Glen: *BMT Fleet Technology*, Conference Documentation, 1st International Conference Escape, Evacuation and Recovery, Lloyd's List (2004).

5.   U. Weidmann: *Transporttechnik der Fussgaenger*, Schriftenreihe des IVT Nr. 90, ETH Zürich (1992).

6.   IMO MSC78/INF.8: *An Experimental Study on the Walking Speed Prediction in Evacuation Analysis*, Korea Research Institute of Ships and Ocean Engineering (2004).

7.   A. Brumley and L. Koss: *The Implication of Human Behaviour on the Evacuation of Ferries and Cruise Ships*, Proceedings of AME'98, Australian Maritime Engineering, CRC Annual Post-Graduate Conference (1998).

8.   D. Vassalos, H. Kim, G. Christiansen, and J. Majunder: *A Mesoscopic Model for Passenger Evacuation*, In: M.Schreckenberg and S.D. Sharma (Eds.), Proceedings of the International Conference on Pedestrian and Evacuation Dynamics, Springer, Berlin, pp. 369-391 (2002).

9.   W. Bles, S. Novy, and L.C. Boer: *Influence of Ship Listing and Ship Motion on Walking Speed*, In: M.Schreckenberg and S.D. Sharma (Eds.), Proceedings of the International Conference on Pedestrian and Evacuation Dynamics, Springer, Berlin, pp. 437-452 (2002).

10. T. Meyer-König, H. Klüpfel, and M. Schreckenberg: *Assessement and Analysis of Evacuation Processes on Passenger Ships by Microscopic Simulation*, In: M.Schreckenberg and S.D. Sharma (Eds.), Proceedings of the International Conference on Pedestrian and Evacuation Dynamics, Springer, Berlin, pp. 297-302 (2002).

Data Collection in Support of the Modelling of Naval Vessels

S. Gwynne[1], L. Filippidis[1], E.R. Galea[1], D. Cooney[1], and P. Boxall[2]

Evacuation analysis of passenger and commercial shipping can be undertaken using computer-based simulation tools such as maritimeEXODUS. These tools emulate human shipboard behaviour during emergency scenarios; however it is largely based around the behaviour of civilian passengers and fixtures and fittings of merchant vessels. If these tools and procedures are to be applied to naval vessels there is a clear requirement to understand the behaviour of well-trained naval personnel interacting with the fixtures and fittings that are exclusive to warships.

Human factor trials using Royal Navy training facilities were recently undertaken to collect data to improve our understanding of the performance of naval personnel in warship environments. The trials were designed and conducted by staff from the Fire Safety Engineering Group (FSEG) of the University of Greenwich on behalf of the Sea Technology Group (STG), Defence Procurement Agency. The trials involved a selection of RN volunteers with sea-going experience in warships, operating and traversing structural components under different angles of heel. This paper describes the trials and some of the collected data.

1.   Introduction

In the wake of several prominent maritime disasters, there is a growing interest in the marine industry in issues regarding the evacuation of passengers[1, 2]. This interest has been mirrored in the Ministry of Defence (MOD) through the introduction of the Escape and Evacuation Naval Authority (EENA). The EENA requires that both new and current designs of MOD vessels undergo an Escape analysis prior to the issue of a Certificate of Safety – Escape and Evacuation. However it is recognised that the current analytical framework, as described in IMO MSC Circular 1033[3], is based upon commercial vessels and civilian personnel who do not necessarily have sea-going experience. Additionally the evacuation scenarios provided are not necessarily appropriate for warships because the evacuation philosophy is different from that of passenger ships. There are also differences in demographics between Royal Navy (RN) and civilian populations and compared to merchant ships, fixtures and fittings used on board MOD vessels vary considerably. It is therefore reasonable to expect that the underlying data as presented in[3] would not be representative of warships and could only be used comparatively. To improve our understanding of the performance of military personnel and to allow the development and validation of current evacuation tools, it was considered necessary to conduct trials to gather data relating to the interaction of RN personnel with components found in warships. It is anticipated that this process will eventually require large-scale trials for the overall validation. Once this data has been collated and analysed, computer tools could then be developed, bolstering our confidence in the techniques to reliably predict the overall times to escape. In turn these can then be utilised in the development of performance based standards for the EENA.

―――――――――――――

[1]Fire Safety Engineering Group, University of Greenwich, UK
[2]Sea Technology Group, Defence Procurement Agency, Ministry of Defence, UK

2.   Evacuation Process for Warships

The operating philosophy in warships differs from commercial vessels in that every effort will be made using damage control and fire-fighting techniques in order to save the ship; the intention being to avoid abandonment. In an operational situation priority will be given to the vessel over the individual, hence for military personnel evacuation would be only undertaken at the last possible moment when it is not physically possible to save the ship. The chain of events following an incident does vary slightly from peace to wartime:

Peacetime:
»   Initiating event.
»   Alarm.
»   Standing Sea Emergency Party (SSEP) tackle incident.
»   If the incident is too large for the SSEP to deal with the ship goes to Emergency Stations.[†]
»   If the incident is not contained the Ship's Commanding Officer will make the decision to abandon ship.
»   Launch and board life-rafts.
»   Clear Ship.

In wartime these chain of events differ in so much as personnel are positioned in pre-determined places known as 'Action Stations' and are accounted for on their arrival at that position. Personnel not involved in the war-fighting effort, or external battle, are positioned in Forward Repair Party Posts (FRPP), within Main Machinery Spaces and Switchboard compartments. Therefore if the ship is damaged, then personnel are pre-positioned with the appropriate equipment ready to deal with any fire or floods. If the incident is of such a scale that greater manpower is required to deal with it then the Command Priorities will change to focus on the internal battle rather than the external. The decision to abandon would again only be taken once it was ascertained that the vessel is unsalvageable:

Wartime:
»   Personnel at Action Stations.
»   Ship receives damage.
»   FRPPs tackle incident.
»   Command Priorities change to provide greater manpower to save ship.
»   If the incident is not contained the Ship's Commanding Officer will make the decision to abandon ship.
»   Launch and board life-rafts.
»   Clear Ship.

[†]At Emergency Stations personnel are accounted for and if able, collect personal life-saving equipment whilst en route. All manpower will be utilised if required to assist with the incident.

Given the differences in the scenarios that may evolve when examining an incident involving a warship as opposed civilian vessels, it is even more important that the data collected is flexible enough such that it may be applied in an appropriate manner within the simulation model being used.

Another difference between passenger ships scenarios and warships is the attributes of the population involved. UK Defence Statistics information published by the Defence Analytical Services Agency for December 2004 indicates that the current age profile of the Royal Navy for Male and Female Personnel is as shown in Figure 1. From this it can be calculated that the average age is 32 and that male personnel constitute 89.7% of the total RN population and female personnel, some 10.3%.
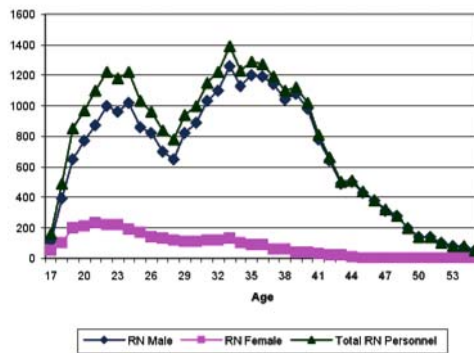

Figure 1: Age Distribution of Trained Royal Navy Personnel

It is clear to see from Table 1, that the population make-up as supplied in IMO MSC 1033[3] for the advanced evacuation analysis does not reflect that of the RN in terms of age, gender and physical attributes.

In addition to the age profiles, all personnel will have passed a fitness test and be medically fit to serve on board. They will all have been trained with at least the Basic Sea Survival Course and many will have done the Intermediate Sea Survival Training. This includes instruction on how to don survival clothing and life-jackets, along with training in Marine Evacuation Systems (MES) for those joining ships that have them fitted. Additionally damage control and fire-fighting techniques are taught. Through demonstrations, equipment familiarisation and practical experience, all personnel have the necessary knowledge, skills and experiences to enable them to safely escape from an RN vessel.

Population groups –passengers	Percentage of passengers (%)
Females younger then 30 years	7
Females 30-50 years old	7
Females older than 50 years	16
Females older than 50, mobility impaired	20
Males younger than 30 years	7
Males 30-50 years old	7
Males older than 50 years	16
Males older than 50, mobility impaired	20
Population groups – crew	Percentage of crew (%)
Crew females	50
Crew males	50

Table 1: IMO MSC/Circ.1033 Annex 2 Population's composition (age and gender)

The training does not stop when a person joins a ship and joining-routines are undertaken to ensure that personnel are familiarised with the ship layout and the safety features on board. In addition to this ship-wide training is organised and ship programmes include periods of Operational Sea Training to ensure that the personnel involved are fully prepared for any tasking which they may receive.

Finally the warship configuration is inherently more complex than that of a commercial vessel and the fixtures and fittings are very different. For instance there is a wide use of escape hatches and wire escape ladders to form secondary means of escape. Given the makeup of the population on board and their physical abilities these are considered adequate, even though they would be unacceptable on passenger ships.

3.   Previous Studies

It is acknowledged that some effort has been invested in the collection of data and the development of maritime evacuation models suitable for the warship applications[1,2,4,5]. While this work represents an initial step in the development of warship specific evacuation simulation environments, much more effort is required in order to collect data representative of naval personnel performance within the complex and varied warship environment and the implementation of this data in evacuation modelling tools. For example, while previous studies addressed a number of warship specific factors, there were a number of omissions and shortfall in the data collected. For example:

» The majority of participants in study[4] were civilian adult males and females.
» The majority of studies have taken place under conditions of normal lighting.
» The majority of studies have been conducted in calm to moderate conditions.
» No data is publicly available involving personnel wearing typical RN clothing.

» In general, studies of Escape and Evacuation (E&E) activities using experimental facilities to examine the impact of adverse and dynamic deck orientations are limited in number and scale, warship analysis has been limited only to static heel angles[5].

» Where life-jackets have been worn in trials, these have been the commercial types with rigid buoyancy, rather than MOD types as defined in Defence Standard 02-148, such as the General Service Life Jacket.

» Formal data on the use of RN life-saving appliances (e.g. life-rafts, survival suits, life jackets) have not been published. Furthermore, existing data is based on the achievement of statutory standards, rather than expected performance under a range of realistic sea-going conditions and is often not available publicly.

» The majority of available E&E data relates to the use of commercial ship passageways, stairways and doors.

» Data on the use of passageways, access ladders, hatches and watertight doors typical of RN ships is limited. Where data has been collected for these components, they have utilised similar, but not identical fittings and equipment to those found on RN vessels[5].

These knowledge and data gaps prompted the RN to embark on a series of dedicated evacuation trials designed to address the highlighted issues. Although the trials do not redress all of the issues highlighted, they initiate the process of producing a more comprehensive and detailed understanding of the performance of RN personnel when operating components found on board warships, under a number of different environmental conditions.

4.   Conduct of trials

The trials involved a selection of RN volunteers, all of whom had sea-going experience in warships and in operating and traversing a number of structural components, under different angles of heel. Whilst being restricted to those participants available for the trials, an attempt was made to get as representative a distribution of attributes (i.e. age and gender) as was possible and ideally representative of the RN sea-going population.

The trials were designed and conducted by staff from the Fire Safety Engineering Group (FSEG) of the University of Greenwich on behalf of the Sea Technology Group (STG), Defence Procurement Agency, United Kingdom MoD using the Damage Repair Instructional Unit (DRIU) at HMS EXCELLENT and on board HMS BRISTOL.

These venues were chosen in order to capture the components that might typically be found in current warship designs and the ability to simulate attitudinal changes (e.g. up to 20° of heel) using the DRUI facility. A sub-set of the components on these vessels were selected to be used during the trials according to their applicability and issues of safety.

During the week, 163 individuals took part (144 males and 19 females, with ages ranging from 17 to 52 years of age), with a minority of the participants performing tasks across more than one day. The participants were allocated to specific components and performed all of the tasks associated with each of those components (e.g. open watertight door away, close towards, traverse up, traverse down, etc.). These were completed at 0º on HMS BRISTOL and at 0º, 10º and 20º of heel on the DRIU facility. The order in which the actions were performed and in which the environmental conditions were experienced were changed throughout.

The trials primarily involved participants interacting with the components on an individual basis. However, where possible, group trials were also performed in order to provide a means of comparing the data collected and the reconstituted modular component data.

The data collected was of generic value, improving our understanding of the performance of RN personnel. The manner in which the tasks were performed will provide an invaluable data-set that could then be used for modelling purposes, which might range from simple hand calculations to complex computer simulations, performed using state-of-the-art ship evacuation modelling software such as maritimeEXODUS[1, 2, 5-11]. To ensure that this would be the case, the data collected relates to specific actions under controlled conditions, rather than event streams. For instance the time to open a watertight door at 10° was measured, rather than the overall time to perform a series of complex actions such as the time taken to progress from Point A to Point B, traversing and operating several components. Using this modular approach, the data collected can be combined and/or reassembled in any way seen fit, in order to simulate the time taken to perform a series of tasks, producing the basis for a far more flexible and powerful tool than might otherwise have been the case. The collected data is therefore component and scenario specific rather than vessel specific, allowing it to be applied in a much wider range of situations and warships.

For each of the actions measured an operational definition was produced in order to establish a consistent set of markers denoting the area of interest. It was important to establish this early on in the experimental design as it determined, to a large degree, the procedure applied during the trials. For instance, the camera positions were sensitive to these definitions, as the data collected had to enable the determination of the actions performed according to these operational definitions. For instance, in Figure 2 a deck of the DRIU facility is shown with several markings. Here, a water tight door is depicted (marked as a black filled rectangle). The movement of the participants, when using this component, is then captured through the operation of three video cameras whose positions are denoted by the "$\forall$" symbol. In addition, the storage and movement of the participants (showed as a hatched area) is also shown. By planning the trial in such detail, the movement of the participants and the data collection itself could be better choreographed.
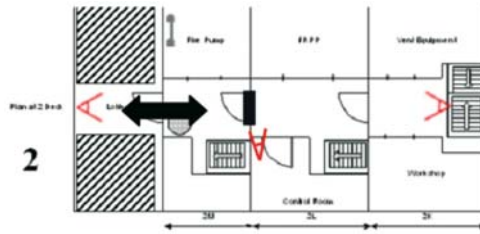
Figure 2: Depiction of one aspect of the trial procedure

Passageway (with red risk combing)‡, Water Tight Door (WTD, with 2 and 12 clips locked), Sliding Door, Watertight Hatch (WTH) with Kidney, non Watertight Door, 60° stairs (no hatch), 60° stairs (hatch present), Escape Scuttle, Wire Escape Ladder, and Kick-Out Panels. The components were tested with various combinations of opening/closing and ascending/descending operations. Care was taken to ensure that data-sets were produced that completely described the subjects during each possible operation of the component. Within the DRIU static heels of 0°, 10° and 20° were used. It is intended that further environmental conditions such as motion, flooding, darkness and smoke will be introduced in future trials. Figure 3 displays examples of 3 of the components on the DRIU facility that were examined.

The following components were examined on board HMS BRISTOL:

WTDs with 12 clips one opening on the left and one on the right, Smoke Curtain, Passageway (with and without red risk combing), Slide Door, WTH with Kidney one opening on the left and one on the right, WTD with lever one opening on the left and one on the right, Small WTD, Stable door, Airlock door, WTDs with 2 clips one opening on the left and one on the right, External 60 degrees. As with the DRIU trials the components were tested with various combinations of opening/closing and ascending/descending operations. Again, care was taken to ensure that data-sets were produced that completely described the operations performed by the subjects during each usage of the present components. Figure 4 displays examples of 3 components used in HMS BRISTOL.
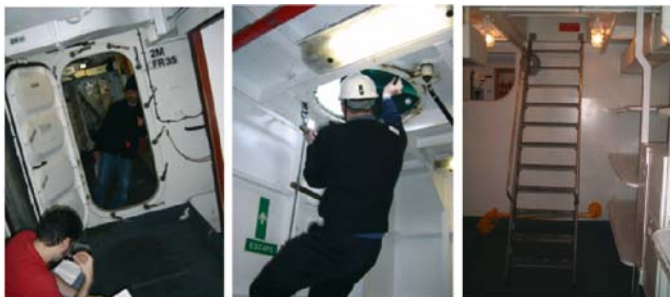

Figure 3: Components on the DRIU, a) Water Tight Door with 12 clips, b) Escape Scuttle, c) 60° degrees stair with the hatch present

---

‡The combing within the red risk zone is slightly higher than that found elsewhere in the ship owing to the probability of receiving damage in those regions.

Figure 4:   Components on HMS BRISTOL, a) WaterTight Door with lever, b) Airlock,
c) Smoke Curtain

The collected footage has been analysed in order to establish the time taken to perform each operation. A distribution of values are now available describing the expected time to perform each of the operations covered during the trials.

The analysis process has been conducted in a number of stages, relating to the re-formatting of the data and the analytical procedures applied:

» Data has been captured from the digital video tapes and transferred to digital animation files. This was performed so that no frames were dropped from the footage; i.e. maintaining the integrity of the original information collected. This has been performed for all of the footage available (i.e. all components and camera angles), associating footage that was collected from different camera positions of the operation of the same component. A large number of small animations have been produced that relate specifically to the operation of different component as collected from a number of different camera positions.

» These associated clips are to then be loaded into Adobe Premiere where they will be synchronised (i.e. the footage from several cameras is aligned) allowing judgements to be made from several positions according to the operational definitions of the actions performed by the participants (see Figure 5).

» Once the beginning and end points of a particular action (e.g. opening a WTD) have been established, markers can then be inserted onto the footage. This is particularly important as it will allow the measurements made by the analysts to be checked and cross- referenced with other measurements made. This would not have been the case if the data been analysed manually.

This method has been designed to produce as consistent a set of data as possible, that is able to be re-investigated easily and which can be validated through the examination made by different analysts. This method also allows the full use of the data collected, allowing the analysis of multiple streams of information within the same window.
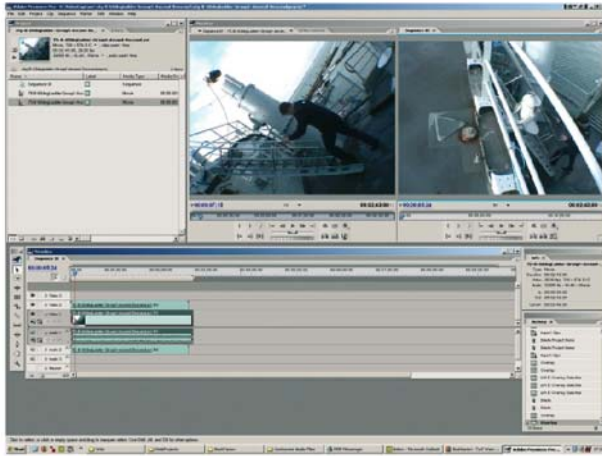
Figure 5: The loading of multiple views of the same event into Adobe Premiere.

The data collected was therefore formatted so that it would be of direct value to a number of different 'user' types. By collecting as complete a stream of information as possible and then categorising it in a modular format, the data can be reconstituted in a manner deemed fit by the user. For instance, let us assumed that the engineer wishes to examine how an individual (or group of individuals) moves along a corridor, operate a WTD and then climb a ladder at 10 degrees of heel. To understand the possible performance parameters involved here, the engineer might refer directly to the data collected during the trials (see Table 2-Table 4) or make use of an evacuation model (such as maritime-EXODUS, see Section 5) that has the data embedded within it.

WTD-left hinged-12 clips in use	
	10° of Heel
OpenTowards	20.11 [13.24-29.52]

Table 2: Data collected during the trials reflecting the use of a WTD at 10 °.

Wire Ladder Traversal	
	10° of Heel
Ascend	10.01 [6.92-17.08]

Table 3: Data collected during the trials reflecting the use of a Ladder at 10 °.

Passage Traversal	
	10° of Heel
Traversal	7.44 [5.04-10.8]

Table 4: Data collected during the trials reflecting the use of a Passage at 10 °.

The data presented in these tables can then be re-combined to represent the estmated time for an individual to perform these tasks. A more detailed, including examining the data according to individual parameters, such as Age and Gender, might also be possible. The example presented here is simply to indicate the potential, even from a relatively simple analysis of the data-set.

5.   Proposed Use of Collected Data

It is intended that the data collected will be used to update evacuation analysis techniques, in particular software analysis tools. One such software package capable of incorporating the data collected is maritimeEXODUS[1, 2, 5-13].

maritimeEXODUS is one of a group of software tools designed by the Fire Safety Engineering Group of the University of Greenwich and is capable of simulating both the emergency evacuation and normal circulation of crew (and passengers) from ships. The software allows the user to incorporate human performance and environmental factors into the analysis along with the layout and safety features.

The model currently includes several data-sets describing the interaction between personnel and egress components (e.g. those produced during the SHEBA trials by the University of Greenwich and BMT Fleet Technology[1]). This data has been incorporated into the model and directly influences the performance of the simulated evacuees when they interact with components under a variety of different conditions. The data from the SHEBA trials is derived for two different sets of trials: one involving naval personnel (where they operated watertight doors, hatches and traversed corridors, 60° and vertical ladders and corridors[5, 10]; the other involving civilian personnel who traversed corridors and standard maritime stairs[1, 10]. The civilian dataset is currently being expanded to include the impact of dynamic motion and the impact of static heel with smoke and dynamic motion with smoke as part of the EU Framework 5 project Fire-Exit[12, 13]. Both sets of trials were conducted at a variety of static heel angles. Although these data-sets have enormous value, they are not deemed to be sufficient to adequately represent naval scenarios involving RN vessels and personnel due either to nature of the participants, the components being examined and/or the environmental conditions involved.

6.   Conclusions

The main purpose of the STG trials was to collect data to improve escape analysis techniques rather than to test a particular hypothesis; they were conducted to both strengthen the basis for any future hypotheses to be made and to broaden our understanding of the behavioural factors at work. This data is being collected based on the following points:

» Human performance in E&E activities in warships differs from that on commercial and passenger ships owing to the differences in ship environments, personnel involved and operating philosophy.

» Data describing the performance of RN personnel undertaking E&E activities is required, in addition to that already existing describing the performance of civilians. This is due to differences in equipment and systems used, personnel fitness, degree and type of training and group association effects.

» The performance of RN personnel undertaking E&E activities will be influenced by individual component features and environmental attitude.

» The performance of RN personnel undertaking E&E activities will be influenced by individual personnel characteristics. These influences may include gender, anthropometric characteristics, age, sea-going experience and personality type.

» The time for a person to travel through a complex E&E route comprising a number of physical components can be represented by the sum (or some other function) of the individual times for that individual to transit each physical component of the route e.g. corridors, doors, ladders and hatches.

The trials described in this paper represent the start of an extensive series of work planned to capture a full set of data representing the performance of RN personnel interacting with all RN fixtures and fittings under a variety of environmental conditions. Finally, while difficult to obtain, it is hoped that response time data representative of RN personnel performance will also be collected. Once a full set of data is available this will be made available to enhance current software packages prior to large-scale validation of the evacuation analysis techniques.

7.   Acknowledgements

References

1.   E.R. Galea, L. Filippidis, S. Gwynne, P. Lawrence, G. Sharp, D. Blackshields: *The Development of an Advanced Ship Evacuation Simulation Software Product and Associated Large Scale Testing Facility for the Collection of Human Shipboard Behaviour Data*, In: Proceedings International Conference on Human Factors in

Ship Design and Operation, The Royal Institution of Naval Architects, London, pp. 37-50 (2002).

2. E.R. Galea, P. Lawrence, S. Gwynne, G. Sharp, N. Hurst, Z. Wang, and J. Ewer: *Integrated Fire and Evacuation in Maritime Environments*, In: Proceedings of the 2nd International Maritime Safety Conference on Design for Safety, Sakai Japan, Publisher Ship and Ocean Foundation, 27-30 Oct 2004, pp. 161-170 (2004).

3. IMO MSC Circular 1033, June 2002 (2002).

4 RN Escape and Evacuation Data Collection Trials, Quintec Associates Limited QAL/P1167/02/2.5/04/02-7

5. P.J. Lawrence, S. Gwynne, E.R. Galea, and G. Sharp: NADMAP 320: *Extending The Capabilites Of The maritimeEXODUS Ship Evacuation Model To Include Ladders, Hatches And 60 Degree Stairs*, Report prepared for the MoD Sea Technology Group, November 2002 (2002).

6. E.R. Galea, S. Gwynne, D. Blackshields, P. Lawrence, L. Filippidis: *Predicting the Evacuation Performance of Passenger Ships Using Computer Simulation*, In: Proceedings of the 9th International Fire Science Conference Interflam 2001, Interscience communications, ISBN 0953231275, Edinburgh, pp. 853-864 (2001).

7. D.A. Purser: *Toxicity Assessment of Combustion Products*, In: P.J. Dilenno, C.L. Beyer, R.L.P. Custer, W.D. Walton, J.M.W. Watts, D. Drusdale, J.R. Hall (Eds.), The SFPE Handbook of Fire Protection Engineering (2nd Edition), National Fire Protection Association, Quincy, Ma, pp. 2-85 - 2-146 (1996).

8. S. Gwynne: *The Introduction of Adaptive Social Decision-Making in the Mathematical Modelling of Egress Behaviour*, PhD. Thesis, University of Greenwich, London (2000).

9. T. Jin: *Visibility Through Fire Smoke*, Journal of Fire and Flammability, 9, pp. 135-155 (1978).

10. BMT Fleetechnology, Ottawa Canada, 2002, http://www.shebafacility.com

11. W. Bles, S. Nooy, and L.C. Boer: *Influence of Ship Listing and Ship Motion on Walking Speed*, In: M. Schreckenberg and S.D. Sharma (Eds.), Proceedings of the International Conference on Pedestrian and Evacuation Dynamics, Springer, Berlin, ISBN 3-540-42690-6, pp. 437-452 (2002).

12. F. Caldeira-Saraiva, J.Gyngell, R.Wheeler, E.R.Galea, A.Carran, R.Skjong, E.Vanem, K.Johansson, B.Rutherford, and A.J.Simoes: *Simulation of Ship Evacuation and Passenger Circulation Re*, In: Proceedings of the 2nd International Maritime Safety Conference on Design for Safety, Sakai Japan, Publisher Ship and Ocean Foundation, 27-30 Oct 2004, pp. 197-205 (2004).

13. E.R. Galea and J. Gyngell: *The European Union Fire-Exit Project, Improving Maritime Safety*, Cruise Ship Interiors International, Summer 2004, pp. 60-65 (2004).

Self-organised choice based on inter-attraction: the example of gregarious animals

J.L. Deneubourg[1], J. Halloy[1], J.-M. Amé[1,2], C. Rivault[2], and C. Detrain[1]

The spatial distribution of individuals is an important subject in many fields because it conditions the levels of interactions among individuals, and more generally the structuring as well as the organization of populations. Increase in density of individuals in a given area can be induced by environmental stimuli and/or by interactions among individuals (1-3). Thus, various definitions of aggregation have been given, ecologists privilege the importance of environmental stimuli, while others privilege existing relationships between group members.

Aggregation is one of the most widespread social phenomena and occurs at all biological levels, from bacteria to mammals including humans (4, 5). If sometimes, aggregation is associated to non-adaptive, often it is the ground on which more complex social structures are built such as synchronization or division of labour (6). However, knowledge of the mechanisms implied in the formation of aggregates remains fragmentary. The study of the proximal causes, i.e. mechanisms involved in group formation, can benefit from concepts of self-organization (5, 7). These groups find their origin and their cohesion in the inter-attraction among individuals: group members are then the source of attraction. However, in most of the situations, patterns of aggregation, resulting from individual responses to conspecifics are modulated by environmental heterogeneity (5).

Previous studies on cockroaches have already described their aggregative distribution in a natural environment where different age-classes share the resources that are present in their home range. They exhibit a strong tendency to gather during their resting period in safe shelters. Therefore, shelters are important, but also limited environmental resources for these insects.

The basic mechanisms underlying group formation is the modulation of the individual resting time as a function of the number of conspecifics on a site. In insects cuticular hydrocarbons act as a recognition signal allowing attraction between individuals (8). Cockroaches prefer their own strain odour to another strain (9). Nevertheless, when groups in tests came from two different strains, they aggregated on one site only and did not show any difference from group coming from one strain.

We used this insect as an example to show that a self-organized process leads to a diversity of optimal patterns without modification of the individual behaviours and any general knowledge of the available resources. These experimental and theoretical results point to a generic self-organized pattern-formation process independent of the level of animal sociability that should be found in other group-living organisms that present inter-attraction.

1.   A brief description of the experiments

In this case study, groups of Blattella germanica larvae were tested in an arena with p identical shelters (p = 2, 3, 4). The carrying capacity of each shelter (S) corresponds to

[1] Service d'Ecologie Sociale CP231, Université libre de Bruxelles, Av. F.D. Roosevelt, 50, B-1050 Bruxelles, Belgique.

[2] UMR CNRS 6552 Ethologie Evolution Ecologie, Université de Rennes 1, Campus de Beaulieu, 35042 Rennes, France.

the maximal number of cockroaches it can harbour (12). Thus the total carrying capacity of the set-up is pS. At the end of all tests (after 24 hours), most of the insects had settled in the shelters and only a few remained in the arena (Fig. 1).

This site selection behaviour results from the dynamics of shifts between shelters and exploration of the arena by the insects.
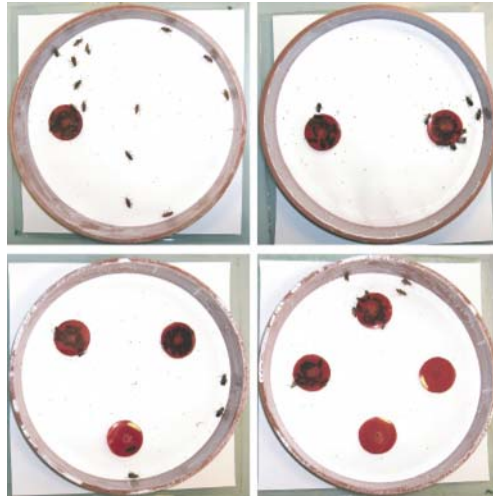

Figure 1: Example of experimental set-up. Choice tests with groups of 30 cockroach adults (Blattella germanica (L.)) and with two, three and four shelters. Groups of cock-roaches were placed in the setup and 24h after the pictures were taken. Most of the individuals are under the shelters. The carrying capacity of the shelters (S) is ≈ 25 adults

2.   Model: aggregation and crowding

Previous studies provided data to build a dynamical model of aggregation, based on the behaviour of individuals (10, 11). Each individual in shelter i has a probability Q_i (inverse of resting time) to leave it and to start to explore. Each exploring cockroach has a probability to encounter and to join the site i (R_i). Experiments show that Q_i decreases with the square of the density of individuals x_i present in the shelter i according to the following equation:

$$Q_i = \frac{\theta}{1 + (\rho \frac{x_i}{S})^n}$$

(1)

This formulates the inter-individual attraction effect. Parameter θ is the maximal probability of leaving a shelter per time unit and ρ is a reference surface ratio for estimating carrying capacities.

The probability for an exploring cockroach to join site i (R_i) decreases with the ratio between the number of individuals present in site i (x_i) and its carrying capacity (S):

$$R_i = \mu(1 - \frac{x_i}{S})$$

(2)

where μ is the maximal kinetic constant of entering the shelter. R_i decreases when the crowding effect (x_i/S) increases.

The differential equations describing the time evolution of the number of individuals on each site (x_i) can be written:

$$\frac{dx_i}{dt} = \mu x_e (1 - \frac{x_i}{S}) - \frac{\theta x_i}{1 + (\rho \frac{x_i}{S})^2} \qquad i = 1, ..., p$$

(3)

$$N = x_e + \sum_{i=1}^{p} x_i$$

(4)

where x_e is the population outside the shelters. When all the shelters are identical all the parameters characterizing the sites are equal.

In order to sort out the main effects arising from the fluctuations, we used Monte Carlo simulations where the random aspect of the process is automatically incorporated. The simulations are based on the same mechanisms defined in the differential system of equations (1-3) or (6-7, see below) (For more details see 11, 12).

The stable stationary states of this model demonstrate that for two shelters ($p=2$) with small carrying capacities ($S<N/2$) the individuals fill the two shelters up to their maximum ($x_1=x_2=S$) and the remaining individuals stay outside. Remarkably, when the carrying capacity of each shelter exceeds half the population ($S>N/2$), the shelter are no longer saturated, but equipartition of the groups between the two shelters remains ($x_1=x_2=N/2<S$) (Fig. 2, a). Experiments with two shelters and $N/2 <S<N$ show that the most frequent of all the potential distributions actually corresponds to equal numbers of cockroaches in each shelter ($x_1=x_2=N/2$) (12). Thus, the intuitively expected solution of saturating one of the shelters and then placing the remaining individuals in the second shelter is not the one expressed by gregarious insects.

When S increases and becomes markedly larger than the size of the total population ($S>N$) the new stable solution emerging is all the population in one shelter, leaving the second shelter empty and no animals staying outside. The site that receives the whole population is chosen randomly. Equipartition between the two sites still exist but is unstable. The experiments confirm that for large shelters nearly all the individuals aggregate in one of the shelters, the others remain empty.

When the number of shelters is larger ($p>2$) and the total carrying capacity of the shelters is below the size of the population ($S<N/p$), the insects tend to use the available
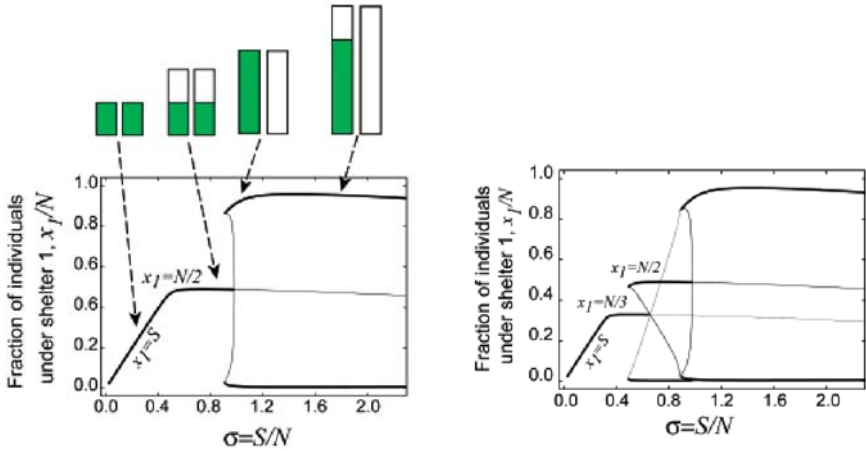
Figure 2: Bifurcation diagrams showing the number of individuals in one shelter, (x_1) in rela-
tion to the ratio σ = carrying capacity of the shelters (S)/ total number of insects N.
$\mu = 0.001\ s^{-1}$, $\theta = 0.01\ s^{-1}$, $\rho = 40.8$ for two shelters.
Panels show the case of (a) two, and (b) three shelters; thin lines indicate unstable
states and thick lines indicate stable states.
(a): for low values of σ (= S/N), the stable solution corresponds to equipartition:
$x_1 = x_2$. A bifurcation occurs around $\sigma = 0.5$ and after the system presents three steady
states. The equipartition of individuals is unstable whereas the two other solutions are
stable i.e. $x_1 \approx N$ and $x_1 \approx 0$. These branches can also be viewed as the mirror solutions
for x_2, when $x_1 = N$ then $x_2 = 0$ and vice versa. As the values of x_1 or x_2 are around N,
on average less than one individual may stay outside the shelters ($x_e \approx 0$).
(b): for low values of σ, the only stable solution is equipartition of individuals bet-
ween the three shelters ($x_1 = x_2 = x_3$). When S increases ($\sigma \approx 1/2$), this state becomes
unstable. The stable branch corresponds to solutions where the individuals are equal-
ly distributed only among two of the three shelters, the last one remaining empty.
For $S > N$ ($\sigma > 1$), two branches for x_1 are stable corresponding to the solution where
only one shelter harbours all the individuals and the two others are therefore empty
($\{x_1 \approx N, x_2 \approx x_3 \approx 0\}$; $\{x_1 \approx x_3 \approx 0, x_2 \approx N\}$; $\{x_1 \approx x_2 \approx 0, x_3 \approx N\}$). The branches
corresponding to an equal distribution between two or three shelters are unstable.

space as much as possible, saturating the sites, and the remaining insects stay outside.
When the shelter size S increases ($N/p < S < N$) a structured cascade of stable solutions
appears. When $p = 3$, the partitions correspond to respectively $N/3$ in three, $N/2$ in two
and N of the three available sites. Note that the population does not use all the available
shelters as their carrying capacity increases but among selected sites, all cockroaches
are equally partitioned. For high values of S, whatever the number of shelters present
only one shelter is selected randomly (with a frequency of $1/p$) and catches the whole
population (Fig 2,b).
When $S < N/p$, the population uses the scarce resource as much as possible. The plateau
value of N/p at which the population stops saturating the occupied shelters starts when

the total carrying capacity of the shelters is equal to the size of the population ($S=N/p$). When the resource is no longer scarce, the population can start to optimize its partitioning in the available space, taking into account the trade-off between being together and access to the shelter resource. Adaptive values of gregariousness are facilitation of pairing of adults, protection against predation, acceleration of development, reduced evaporation and increased longevity (13). Assuming that the mean benefit per individual (B) is:

$$B = \frac{1}{N} \sum_{i=1}^{p} x_i (1 + (\frac{\rho x_i}{S})^2)(1 - \frac{x_i}{S})$$

(5)

B depends on the number of conspecifics present in the shelter $(1+(\frac{\rho x_i}{S})^2)$. This term reflects the different cooperativity reducing the different stresses and is balanced by the

probability to join the group in the shelter $(1-\frac{x_i}{S})$. The cascade of stable solutions and equipartitions of the type N in one site, $N/2$ in two sites, $N/3$ in three sites or $N/4$ in four sites respectively correspond to optimal benefit associated to clustering balanced by limited resources. For $S>N$, the highest benefit value is reached when all the population aggregates in only one shelter. For $N>S>N/2$, B is maximum for the equipartion between two shelters whatever the number of shelters. For $N/2>S>N/3$, B is maximum for the partition between three shelters, again whatever the number of shelters, and so on (12).

3. Two strains

The model can be generalized for groups of individuals from several different strains. Here, we only consider groups formed by two different strains. We have used: x for strain 1 and y for strain 2. Experimental tests showed that larvae prefer their own strain odour to that of other strains (9). In this case, the probability for one individual belonging to one strain to leave is always a function of the number of individuals present on the site. The influence of individuals belonging to the same strain can be more important than that of individuals belonging to the other strain. In this case, the basic model must be completed with parameters of inter-attraction between strains i and j: β_{ij}.
x_i and y_i are respectively the number of individuals of strain 1 and 2 in this site i. We suppose that the interaction of strain 1 on strain 2 is the same that 2 on 1 and from then $\beta_{12}= \beta_{21}= \beta$. The parameters of inter-attraction inside a strain already present in the single strain model are always considered equals to 1 ($\beta_{11}= \beta_{22}= 1$). To express that an individual of one strain tends to stay more with an individual of the same strain than with individual of another strain, β is lower than 1. For $\beta = 0$, it corresponds to two independent strains.
The probability to leave the site i for a larva from x_i ($Q_{x,i}$) or from y_i ($Q_{y,i}$) are:

$$Q_{x,i} = \frac{\theta}{k + (\rho \frac{(x_i + \beta y_i)}{S})^2} \qquad Q_{y,i} = \frac{\theta}{k + (\rho \frac{(y_i + \beta x_i)}{S})^2} \tag{6}$$

We discuss here the case where the carrying capacity S is much more larger than the total population. Therefore, a simplified version of the model may be analysed: we neglect the population outside the shelters and the insects travel between the two shelters. With two strains x and y, the model equations can be now written in the form:

$$\frac{dx_i}{dt} = -Q_{x,i}x_i + Q_{x,j}x_j$$

$$\frac{dy_i}{dt} = -Q_{y,i}y_i + Q_{y,j}y_j$$

$$i = 1, j = 2 \qquad i = 2, j = 1 \tag{7}$$

With $x_1 + x_2 = N_x$, $y_1 + y_2 = N_y$.

N_x, N_y are the populations of both strains. We discuss here, the cases with an equal number ($N_x = N_y = N$) of individuals of two types of strain.

The model has nine stationary solutions.
»   The first solution, corresponds to a dispersal of individuals of both strains on both sites:

$$x_i = y_i = 0.5N, \qquad i = 1, 2 \tag{8.1}$$

This solution is unstable if

$$N^2 > \frac{4k}{(1+\beta)^2}$$

»   A group of two conjugate solutions correspond to a heterogeneous distribution of individuals. Most individuals of both strains selected the same site:
$x_i = y_i = X_\pm \quad i = 1, 2$

$$X_\pm = 0.5N \pm 0.5\sqrt{N^2 - \frac{4k}{(1+\beta)^2}} \tag{8.2}$$

These solutions correspond to the aggregation of the individuals of both strains on the same site and exist if:

$$N^2 > \frac{4k}{(1+\beta)^2}$$

» A second group of two conjugate solutions correspond to segregation between the two strains, each strain selects one of the sites:
$x_i = y_i = X_\pm$ $i = 1, j = 2$ and $i = 2, j = 1$

$$X_\pm = 0.5N \pm \sqrt{N^2 - \frac{4(k + N^2\beta^2)}{(1-\beta)^2}}$$

(8.3)

These solutions do not exist if (1) $\beta < 0.333$ and (2) if $\beta \geq 0.333$ and $N^2 > \frac{4k}{(1 - 2\beta - 3\beta^2)}$.

These solutions are stable for: $\beta < \beta_{asympt} - 2k^{0.5} N^{-2}$ with $\beta_{asympt} \approx 0.236$.

» A last group of four conjugate solutions correspond to a mixture of individuals of both strains on both sites. The solutions are always unstable (14)

To summarize, three sectors can be defined when N varies as a function of β: dispersal, aggregation plus segregation and aggregation alone. The model shows that only for small value of $\beta(< 0.25)$, and $N > 5$, the population may adopt two different patterns: both strains are aggregated on the same site or both strains are segregated (the majority of one strain is on one site, the majority of the second strain is on the second site). Monte-Carlo simulations show us the frequency of selection of the different patterns. When $\beta \geq 0.2$ more than 75% of simulations mixed groups are aggregated altogether on one site. It is only when β is very small that the frequency of segregation is large. For small N, the both strains are distributed on both site and mixed. For larger N and β, the individuals of both strains aggregate on the same site.

These theoretical results are in agreement with the experimental ones that show that individuals from the two strains aggregated on one of the sites. More than 75% of tests are characterised by more than 80% of larvae on the same site. No difference is observed between the tests with one strain and all the tests with different proportion of two strains (11).

4.   Discussion

The aggregative patterns result from the dynamics of changes between shelters and they emerge mainly due to an activation process: the larger the population in a shelter, the lower the probability to leave the shelter. This adaptive and complex dynamics changes the vision of aggregation processes that are often considered as a mere gathering of individuals and shows that they are among the keystones for collective decisions. Without global or perfect information and elaborated communication, the insects are able to assess the availability of resources and adapt the way they divide into different groups among selected sites.

This processes lead to an economy in terms of individual capacities and to epigenetic plasticity of proximate behaviour. The fitness of self-organized aggregation includes

not only solutions with optimal benefit but also a high plasticity allowing the optimal pattern to be attained easily.

In the experiments with two different strains in various proportions, they were presented a choice between two resting sites that were more than large enough to house the entire group. The fact that the tested animals came from the same strain or from two different strains did not influence the aggregation pattern although these cockroaches had the capacity to discriminate between the odours and preferred to rest in papers impregnated with their own strain odour.

In simulations, for group sizes similar to those used in the experiments, an inter-strain inter-attraction parameter, up to 10 times less than an intra-strain inter-attraction parameter lead to the formation of a single mixed aggregate similar to the one strain aggregate. The experimental and theoretical models discuss the situations where we have two shelters and one or two strains. However, analysis of the theoretical model for more than two sites and for more than two strains (not summarise in this paper) predicts similar collective response and mainly the systematic aggregation of all strains together despite a weak inter-attraction between the strains.

This study and others (5,14) reveal powerful mechanisms and may suggest that these «self-organized scripts» could be numerous despite the fact that in terms of individual or group benefits, the situations could be different. The collective choice process in fragmented environments presented here should have its equivalent in many gregarious animals including vertebrates such as fishes around fish aggregation devices (15). We predict that this basic process, modulated by specific species traits, should be generic and of a particular importance for activities in which cooperativity and spatial organization matters such as traffic regulation (16-18) .

Acknowledgements

References

1.   J.K. Parrish and W.M. Hamner: *Animal Groups in Three Dimensions*, Cambridge University Press, Cambridge (1997).
2.   J.K. Parrish and L. Edelstein-Keshet: *Complexity, Pattern, and Evolutionary Trade-Offs in Animal Aggregation*, Science, 284, pp. 99-101 (1999).
3.   J. Krause and G.D. Ruxton: *Living in Groups*, Oxford University Press, Oxford (2002).

4. M. Schreckenberg and S.D. Sharma (Eds.): *Proceedings of the International Conference on Pedestrian and Evacuation Dynamics*, Springer, Berlin (2002).

5. S. Camazine et al.: *Self-Organization in Biological Systems*, Princeton University Press, Princeton, NJ (2001).

6. J.L. Deneubourg, A. Lioni, and C. Detrain: *Dynamics of Aggregation and Emergence of Cooperation*, Biol. Bull., 202, pp. 262-267 (2002).

7. J.L. Deneubourg and S. Goss: *Collective Patterns and Decision-Making*, Ethology, Ecology & Evolution. 1, pp. 295-311 (1989).

8. L. Sreng, A. Cloarec, and C. Rivault: *Cuticular Extracts Inducing Aggregation in the German Cockroach*, In: Blattella germanica (L.), J Insect Physiol. 44, pp. 909-918 (1998).

9. C. Rivault and A. Cloarec: *Cockroach Aggregation: Discrimination between Strain Odours*, In: Blattella germanica, Anim Behav, 55, pp. 177-184 (1998).

10. R. Jeanson, C. Rivault, J.L. Deneubourg, S. Blanco, R. Fournier, C. Jost, and G. Theraulaz: *Self-Organized Aggregation in Cockroaches*, Animal Behaviour, 69, pp. 169-180 (2005).

11. J.M. Amé, C. Rivault, and J.L. Deneubourg: *Cockroach Aggregation based on Strain Odour Recognition*, Animal Behaviour, 68, pp. 793-801 (2004).

12. J.M. Amé, J. Halloy, C. Rivault, C. Detrain, and J.L. Deneubourg: *Collegial Decision Making based on Social Amplification Leads to Optimal Group Formation*, Proc. Nat. Acad Sc., 103, pp. 5835-5840 (2006).

13. M. Dambach and B. Goehlen: *Aggregation Density and Longevity Correlate with Humidity in First-Instar Nymphs of the Cockroach*, In: Blattella germanica L., Dictyoptera), J Ins Physiol. 45, pp. 423-429 (1999).

14. D.J.T. Sumpter: *The Principles of Collective Animal Behaviour*, Phil. Trans.R. Soc.B., 361, pp. 5-22 (2006).

15. C. Girard, S. Benhamou, L. Dagorn: *FAD: Fish Aggregating Device or Fish Attracting Device? A New Analysis of Yellowfin Tuna Movements Around Floating Objects*, Animal Behaviour, 67, pp. 319-326 (2004).

16. I.D. Couzin and N.R. Franks: *Self-Organized Lane Formation and Optimized Traffic Flow in Army Ants*, Proc. R. Soc. B., 270, pp. 139-146 (2003).

17. A. John, A. Schadschneider, D. Chowdhury, and K. Nishinari: *Collective Effects in Traffic on Bi-Directional Ant-Trail*, J. Theor. Biol., 231, pp. 279 (2004).

18. A. Dussutour, V. Fourcassié, D. Helbing, and J.L. Deneubourg: *Optimal Traffic Organization in Ants under Crowded Conditions*, Nature, 428, pp. 70-73 (2004).

Traffic on bi-directional ant-trails

A. John[1], A. Kunwar[2], A. Namazi[1], D. Chowdhury[2], K. Nishinari[3], and A. Schadschneider[1]

We generalize cellular automaton models for uni-directional ant-trails to bi-directional motion. Several extensions (1-lane, 2-lane with and without common pheromone trail) corresponding to different realistic situations are compared. The interactions between the ants give rise to interesting collective behavior which is reflected in the flow properties and the spatio-temporal organization of the ants along the trail.

1.   Introduction

The motion of ants along their trail system and the dynamics of pedestrians have certain similarities which have been discussed in more detail elsewhere in these proceedings [1]. There we have focused on the uni-directional motion of ants along their trails. Although many ant species exhibit predominantly uni-directional flow of workers (outbound or nestbound, depending on the time of day), also bi-directional flow is frequently observed [2]. For such situations the approach based on cellular automata models reviewed in [1] has to be extended. Here we will discuss three different generalizations to understand the possible effects of interacting streams moving in opposite directions. We especially focus on the flow properties [3] and the spatio-temporal organization of the ants on these trails which is of direct biological relevance [4].

2.   CA-models for bi-directional ant-trails

In [1] we have discussed the basic model for the uni-directional motion of ants on an existing trail and its most important properties. This cellular automaton (CA) model is an extension of the asymmetric simple exclusion process (ASEP) by including the effects of the pheromones and their dynamics. Ants move forward with a hopping rate depending on the pheromone occupation of the target cell. If pheromone is present there it moves with probability Q, whereas in the absence of pheromone it moves with q < Q. Thus the pheromone field induces particle-wise disorder in the hopping probabilities.

There are different ways of generalizing this model to the bi-directional motion of ants on a trail. All models considered here reduce to the basic uni-directional model if only ants moving in one direction are present. The generalizations correspond to various realistic situations. Sometimes more or less well-separated lanes are formed for the opposite directions (Fig. 1) which will be denoted by "left (L)" and "right (R)" in the following. Nevertheless there still can be interaction effects between the ants on different lanes, e.g. due to communication processes [5]. In other situations, like the motion along a cable shown in Fig. 2, ants moving in opposite directions follow the same trail or lane. In this case a single-lane model of bi-directional motion is more appropriate.

[1]Institut für Theoretische Physik, Universität zu Köln, 50937 Köln, Germany

[2]Physics Department, Indian Institute of Technology, Kanpur 208016, India

[3]Department of Aeronautics and Astronautics, Faculty of Engineering, University of Tokyo, Tokyo 113-8656, Japan

Figure 1: Bi-directional traffic on a trunk trail
with multiple lanes. The virtually
blind workers follow invisible phero-
mone tracks. Moving on these tracks
they are able to meet each other and
exchange information via head-on
encounters.

Figure 2: Bi-directional traffic restricted to
one single lane. Workers facing each
other in opposite direction make way
by temporally walking on the under-
side of the cable.

2.1. Bi-directional trails with one common pheromone field

The most natural extension of the uni-directional model to bi-directional traffic corre-
sponds to adding a second lattice, so that ants moving in opposite directions occupy
separate lanes [6]. If the lanes are close to each other one can assume that the ants
share a common pheromone field. Taking into account a possible hindrance effect when
oppositely moving ants meet, an additional hopping probability is introduced. If the
nearest neighbor site in opposite direction is occupied, an ant moves to an unoccupied
cell in front with probability K instead of Q (in the presence of pheromones) or q (in the
absence of pheromones).

The main feature of this model is the occurrence of a stationary and localized ant-cluster
(Fig. 3). The position of the cluster is fixed anywhere in the system and fluctuates only
slighty. As the cluster also appears for vanishing ant-pheromone coupling it can be con-
sidered a generic property of this model. In addition the particle flux roughly stays con-
stant over intermediate densities (Fig. 4). Surprisingly these plateaus occur for K < Q as
well as for K > Q. Cluster and plateau formation are both part of the same phenomenon
and can be understand in terms of induced lattice-wise 'defects', i.e. localized regions
with an effectively reduced hopping rate [6].

2.2. Bi-directional trails with separated pheromone fields

Instead of considering a two-lane model with common pheromone trail, one can also
study bi-directional traffic on two lanes with separate pheromone trails for both di-
rections. Coupling between both lanes is achieved in the same way as in Sec. 2.1 by
introducing a hopping probability depending on the presence of counterflow. For this
case of separate lanes the hindrance effect can e.g. result from communication processes
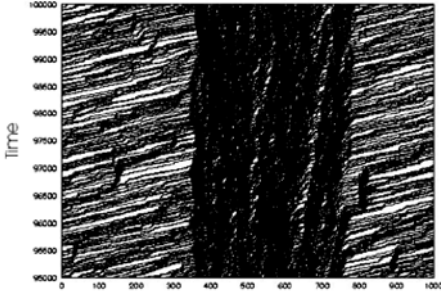
Figure 3: Space-time plot showing a localized and stationary ant-cluster. Ants passing this cluster undergo a change in hopping-probability. This effectively has the same impact as defects localized on the lattice.
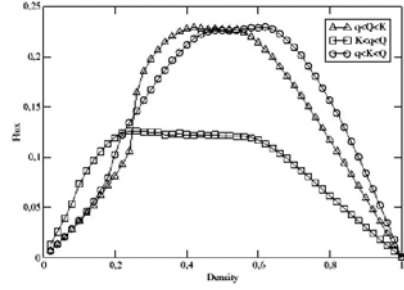

Figure 4: Fundamental diagram showing plateaus of flux vs. density. Depending on the choice of parameters, ants or empty sites in counterdirection form defects.
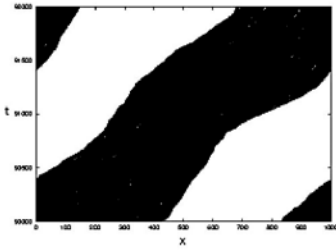

Figure 5: Space-time plot showing a moving ant-cluster varying in length. The interaction between clusters moving in opposite directions leads to a change of hopping probability and velocity.
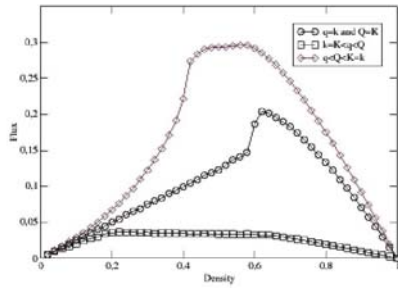

Figure 6: Fundamental diagram showing flux vs. density. The existence of a cluster leads to the linear regime. But also plateaus appear and are the dominant feature in case of extreme repulsion by ants in counterdirection.

between oppositely moving ants [5]. As each trail has its own pheromone field, for that case, two possibilities occur. If a pheromone mark is present in the associated cell of the own pheromone field the hopping probability is K and k otherwise. This model reduces to our uni-directional one not only in the absence of either right- or left-movers, but also in the limit k=q, K=Q. In the case of counterflow and vanishing coupling to pheromone marks this model turns out to be equivalent to the one already introduced in Sec. 2.1. Although the interaction between ants moving in opposite directions is achieved in the same way as in Sec. 2.1 the results are quite different. On each lattice one observes one

stationary cluster (Fig. 5) like in the model for uni-directional traffic (q<Q). Unlike in the model discussed above, the clusters are not localized, but move through the system. Since they move in opposite directions, they finally have to cross each other. During this crossing the coupling to counterflow becomes relevant and the clusters interact. In the case K<q<Q this leads to a decrease of the average velocity. Obviously this model is dominated by the effects already known from the uni-directional model. Thus the fundamental diagrams roughly look the same (Fig. 6). In addition, a small plateau region at intermediate densities can be found in the case q<Q<K. Effects of lattice-wise disorder are present, but not dominant.

2.3. Single-lane bi-directional ant trail model

In situations such as the motion along a hanging cable shown in Fig. 2 it is most natural to consider a one-lane bi-directional model which allows for the exchange of oppositely moving particles on neighboring sites [7]. This exchange of their position happens with probability K. In all the other cases the dynamics is identical to that of the uni-directional model. In the extreme case of instantaneously vanishing (f=1) or never vanishing (f=0) pheromone marks, this model becomes identical to the AHR model [8]. Note that even in the limit of very large densities a non-vanishing flow can be observed in this model through the exchange of left- and right-movers.

The space-time plot (Fig. 7) indicates that the mechanisms of cluster formation are dominant. This was to be expected because this model reduces to our uni-directional one in the absence of counterflow. However, the dynamics of the clusters is very different
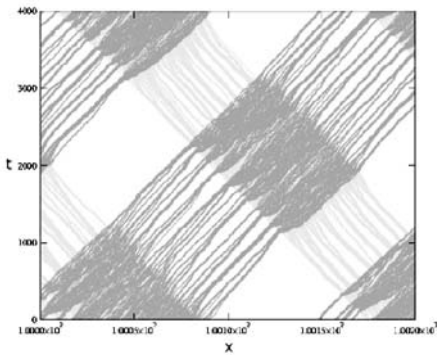

Figure 7: Space-time plot for ants moving in both directions. Due to the hard-core exclusion principle the clusters have to diffuse through each other. This leads to some kind of shredding which leaves the existence of the cluster itself unaffected.
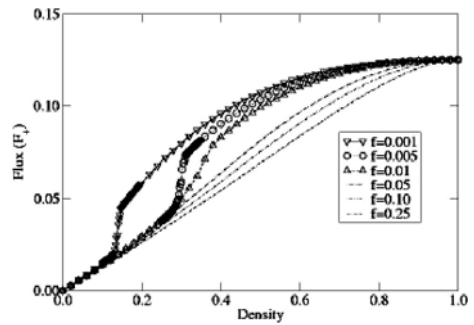
Figure 8: Fundamental diagram showing flux vs. density. Like in the models introduced above a regime with linearly increasing flux exists for small densities. Unlike in the other models the flux does not decrease to zero for maximum density.

from that in the other counterflow models. As ants move on the same lattice, the clusters which move in opposite directions have to pass through each other when they collide. This leads to a "shredding" of the clusters which can be clearly seen in Fig. 7. It competes with coarsening processes related to the pheromone-mediated interactions. The details of the shredding and coarsening depend on the system parameters, but generically the clusters will not completely be dissolved [7].

3.   Summary and Outlook

We have reviewed investigations of different possibilities for coupling flows of ants in opposite directions. In all cases the interactions give rise to an interesting spatio-temporal organization of the ants, e.g. the formation of localized or moving clusters. These properties have also a direct influence on the flux which in principle should be observable empirically.

Further investigations will have to address the question of the advantage for the flowing agents. Generally the coupling between the oppositely moving flows enables information exchange. In reality, this might be relevant for the exploitation of a food source. Workers returning to the nest can give information about quality or extend of the source to other workers. This allows establishing some kind of global flux-control by strictly local interactions.

Up to now only few experimental data for the flow properties are available and these concern mostly uni-directional motion. Recently, the influence of bottlenecks in counterflow situations has been investigated experimentally [9, 10]. Here the repulsion of counterflowing ants in a narrow corridor leads to the passing of clusters in alternating directions. The observed behavior has indeed certain similarities with that of pedestrian streams, e.g. at narrow doors.

For further results on the motion of ants and pedestrians we refer to our webpage [11]. «

References

1.   A. Schadschneider et al.: *From Ant Trails to Pedestrian Dynamics*, In: these proceedings, Springer (2006).
2.   D. Couzin and N.R. Franks: *Self-Organized Lane Formation and Optimized Traffic Flow in Army Ants*, Proc. Roy. Soc. Lond. B, 02PB0606 (2002).
3.   M. Burd, D. Archer, N. Aranwela, and D.J. Stradling: *Traffic Dynamics of the Leaf-Cutting Ant Atta Cephalotes*, American Naturalist 159, pp. 283 (2002).
4.   B. Hölldobler and E.O. Wilson: *The Ants*, Belknap, Cambridge, USA (1990).
5.   M. Burd and N. Aranwela: *Head-On Encounter Rates and Walking Speed of Foragers in Leaf-Cutting Ant Traffic*, Insectes Sociaux 50, pp. 3 (2003).

6.   A. John, A. Schadschneider, D. Chowdhury, and K. Nishinari: *Collective Effects in Traffic on Bi-Directional Ant-Trails*, J. Theor. Biol. 231, pp. 279 (2004).

7.   A. Kunwar, D. Chowdhury, A. Schadschneider, and K. Nishinari: *Competition of Coarsening and Shredding of Clusters in a Driven Diffusive Lattice Gas*, to be published.

8.   P.F. Arndt, T. Heinzel, and V. Rittenberg: *Spontaneous Breaking of Translational Invariance and Spatial Condensation in Stationary States on a Ring*, J. Stat. Phys. 97, pp. 1 (1999).

9.   A. Dussutour, V. Fourcassié, D. Helbing, and J.L. Deneubourg: *Optimal Traffic Organization Under Crowded Condition*, Nature 428, pp. 70 (2004).

10. A. Dussutour, J.L. Deneubourg, and V. Fourcassié: *Temporal Organization of Bi-Directional Traffic*, In: The Ant Lasius niger (L.), Jrl. Exp. Biol. (2005).

11. Internet resource: www.thp.uni-koeln.de/ant-traffic

Herding in Real Escape Panic

C. Saloma[1] and G.J. Perez[1]

We introduce the element of copying in an agent-based model of escape panic to describe with greater accuracy the exit behavior of mice that are escaping from a flooded two-exit chamber. Aside from the panic threshold φ (0 ≤ φ ≤ 5), our model utilizes the imitation tendency α (0 ≤ α ≤ 1) such that agents with φ = 0, are calm and tend to stay put while those that are likely to copy their neighbors are described by large α values. A high degree of copying among escaping agents favors the emergence of herding behavior. Both the Moore and the von Neumann neighborhood are tried to depict the movement of agents in a plane. Herding decreases the exit throughput Q by causing an inefficient utilization of the two available exits for escape. The dependence of Q with α and the exit door separation are highly nonlinear. The inclusion of α has significantly improved the capability of our model to explain the Q-behavior that was observed in the mice experiments. Interestingly, simulation results show that copying could promote faster room evacuation at α ≈ 0.5 and especially at high room occupancy rates (> 60%). At α ≈ 0.5, an agent is equally likely to copy or ignore the action of its neighbor.

1.   Introduction

Herding happens when ordinary people behave as a group, effectively surrendering their ability to function as individuals. In panic situations where decisions have to be made quickly under duress it is likely for individuals to lose their ability to decide on their own. Instead, these impaired individuals tend to imitate the action of their neighbors. The tendency to rely on others is a product of experience. Lessons from the past would tell individuals to value majority decisions. The likelihood to imitate is increased by lack of self-confidence or ample preparation – an inexperienced person will find it less costly to depend on the leadership of a perceived alpha individual or expert.

The severe congestion and high pressures that are induced or worsened by herding continue to exact a high cost to society in terms of infrastructure damage and loss of life and limb [1 – 3]. The role of herding in escape panic has been studied using equations of motion in the presence of interaction forces [4]. However, quantitative comparisons between model prediction and experimental result have remained scarce. The present work aims at reducing the gap between theory and experiment thereby improving our understanding of escape panic behavior.

In our experiments with mice that were escaping from a flooded two-exit chamber [5], we found that the single-parameter agent-based model of escape panic could not explain adequately the observed dependence of the exit throughput Q with door separation. Q is the average number of agents (mice) that have escaped per unit time. The predicted Q value was always larger than the experimentally measured Q for a given door separation value. The single-parameter model allowed the escape of more agents than what is actually possible in the mice experiment.

[1]National Institute of Physics, University of the Philippines Diliman, Quezon City 1101, Philippines, E-mail: csaloma@nip.upd.edu.ph

A careful examination of the video footage revealed that the mice experiments yielded lower Q values because the mice were unable to utilize efficiently the two available exits for escape. Mice were found to cluster around an exit almost totally oblivious that another one was free and available.

In this work, we present an agent-based model for escape panic that incorporates the effect of herding among agents who are trying to escape from a room. In addition to the panic threshold φ (≥ 0), the model utilizes a second independent parameter called the imitation tendency α. Agents with φ = 0, are calm and prefer to remain in their present positions. On the other hand, those with large φ values are highly ambulant. Moreover, agents that act independently are described with α = 0. While those that always follow their neighbors are given a value of α = 1 (blind copying).

We show that the two-parameter model can explain more accurately the dependence of Q on door separation that was observed in mice that were escaping from a flooded two-exit chamber. A high degree of copying among escaping agents favors the emergence of herding behavior. In a two-exit room, the attainable Q value is reduced because herding prevents the efficient utilization of all available exits for escape.

The performance of the two-parameter model was determined using the von Neumann and the Moore neighborhood to describe the movement of an agent in a plane. In a von Neumann neighborhood, an agent can move along one of four possible directions representing North, South, East and West. In a Moore neighborhood, it can choose one of eight possible directions of motion [6]. We investigate if the two neighborhoods yield the same predictions for Q and the room evacuation time T at different values of α and the room occupancy rate. It is reasonable to expect that the discrepancy in the number of degrees of freedom for the two neighborhoods can lead to diverse outcomes for Q and T depending on the density of agents in the room.

2.   Methodology

2.1. The Two-Parameter Model

An agent A_k inside a room measuring M x N cells is given a specific value for the panic threshold φ and the imitation level α where: $0 \leq \varphi \leq 5$ (an arbitrarily chosen maximum) and $0 \leq \alpha \leq 1$. At any given iteration time i, A_k occupies a particular cell except when the agent has already escaped out of the room where index i = 1, 2, …, I. Depending on the type of neighborhood, A_k is surrounded by four (von Neumann) or eight (Moore) neighboring cells.

In the next iteration time $(i + 1)$, A_k can occupy any of the vacant cells in its neighborhood. A_k moves into an available cell that it is facing if the following condition is true: $l + r < b + \varphi$, where l, r, and b are the number of occupied cells on the left, right and back of A_k respectively. Hence, an A_k with φ = 0, prefers to remain in its present location. Left alone, A_k would take the path of shortest Euclidean distance to the nearest exit. At any given time i, the room is described by an occupancy rate $R(\%) = 100K/MN$, where K is

the total number of agents inside the room. The exit door width is equal to one cell unit. All agents in the room know the locations of the two exits beforehand.

Facing more than one available neighboring cell to occupy, an A_k with $\alpha = 1$, chooses that cell which has been recently vacated by its neighbor. If there is more than one such cell then the final choice is a result of uniform random selection by A_k. On the other hand, A_k prefers to move to a cell that brings it closer to a targeted exit if its associated α value is zero. A value of α between 0 and 1 implies a probabilistic choice between the two extreme strategies.

An agent-based model for describing the dynamics of escape panic offers a number of important advantages over other approaches such as the flow model. In an agent-based model, each agent can be easily tagged with its own unique values of α and φ. Such latitude provides versatility to the model in describing a wide variety of possible cases in escape panic. Moreover, the outputs of an agent-based model are reliable even when the number of agents is not statistically large which is a crucial factor when comparing simulation results with experimental data - controlled experiments in real escape panic are difficult to perform using statistically large numbers of agents. Additional technical details about agent-based modeling in escape panic can be found in Reference 7. Here, all the K agents in the room have same values for α and φ to reduce computational complexity.

The simple rules that are employed to incorporate herding in the two-parameter model are consistent with accepted assumptions and observations about emergency evacuations. Although people prefer to leave via an exit where the queue is shorter [8-9], herding predominates when orientation and visibility are poor. Under extreme pressure, most individuals would use one and the same exit neglecting the availability of other exits [10].

Herding is also observed when people are caught in an unfamiliar situation [4-5, 11-12]. Herding can also arise from the tendency of threatened people to escape through the same door that they had previously used as entrance [4].

2.2. The Mice Experiments

The mouse experiments were conducted from January to August 2002 using albino mice of ICR stock that were originally sourced from the Research Institute of Tropical Medicine (Muntilupa, Philippines) and bred at the National Institute of Molecular Biology and Biolotechnology of the University of the Philippines. The ages of the mice varied from 6 to 12 months, and their (width) sizes ranged from 2.5 to 3.0 cm measured along the axial plane. They weighed from 25 to 35g.

The experiments were performed in a rectangular container [dimensions (in cm): 50 x 36 x 28.5 cm] that was partitioned in a wet-dry (3:1) configuration. The mice were released in a pool of water (depth = 10.5 cm, nominal water temperature = 25 deg C) and allowed to swim towards a dry platform. An exit of 3.5 cm width is located between the wet and dry areas. The set-up was designed to induce panic in main and maintain directed flow towards the exit (from wet to dry). Experiments were performed in a two-exit

configuration for different door separation values of 0 (single exit), 3.5, 7.0, 14.0 and 21.0 cm. More information about the mice experiments is available in Reference 5.

3.   Results and Discussion

3.1. Comparison between throughput predictions of two-parameter model and experimental results

Figure 1 plots the dependence of throughput Q with door separation d for different φ values at φ = 5 and R = 11.9%. Each data point represents the average of 20 trials. A value of d = 0, implies a room with a single exit of width equal to 2 cells. In a two-exit room, Q can exceed unity because it is possible for two agents to leave the room simultaneously.

Numerical simulations were carried out for both the von Neumann (Fig 1a) and Moore neighborhood (Fig 1b) using a short iteration period of I = 90. The room occupation rate R is held constant at all times by adding a new agent at a random location in the room every time an agent was able to escape.

Figure 1 shows that Q decreases with increasing α. For a given α, Q increases with d for $d \leq 2$ and stays relatively constant afterwards. A more effective utilization of the two exits is achieved by increasing the door separation thereby reducing the debilitating effect of herding on Q. These characteristics were observed for both the von Neumann and Moore neighborhood.
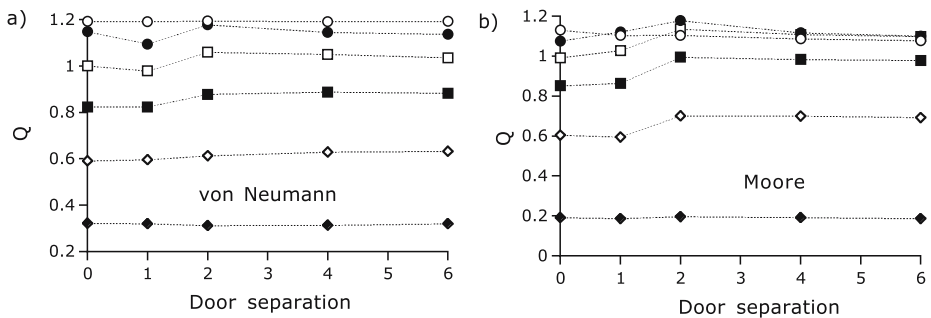

Figure 1: Exit throughput Q versus door separation in two-exit room at α = 0 (circles), 0.2 (filled circles), 0.4 (squares), 0.6 (filled squares), 0.8 (diamonds) and 1 (filled diamonds): a) von Neumann neighborhood, and b) Moore neighborhood. Other parameter values: K = 30 agents, Room size = 18 X 14, φ = 5, I = 90.

In the Moore neighborhood, Q approaches towards a common value with increasing d for α = 0, 0.2, and 0.4. The behavior sets the α-range where copying among agents could be described as low. The degeneracy in Q is caused by the larger number of allowed directions for movement in a Moore neighborhood.
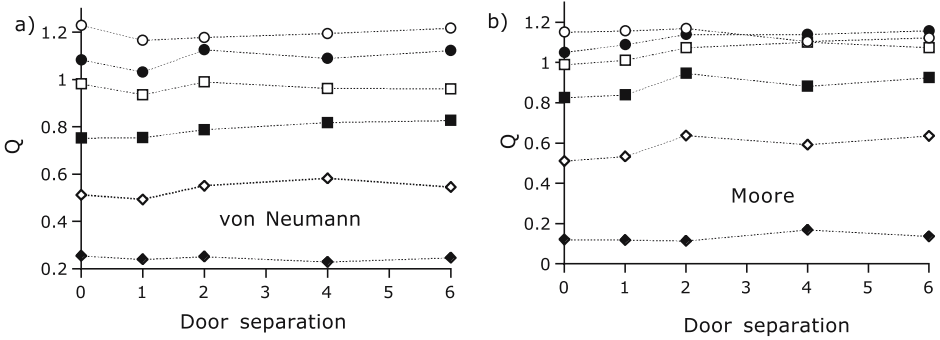
Figure 2: Throughput Q versus door separation in two-exit room at α = 0 (circles), 0.2 (filled circles), 0.4 (squares), 0.6 (filled squares), 0.8 (diamonds) and 1 (filled diamonds: a) von Neumann neighborhood, and b) Moore neighborhood. Other parameter values: $K = 30$ agents, Room size = 18 X 14, φ = 5, $I = 50,000$.
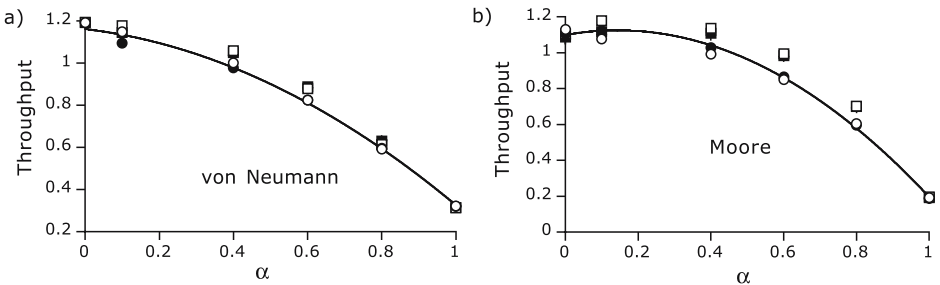

Figure 3: Throughput Q versus imitation parameter α in two-exit room with door separation d = 0 (circles), 1 (filled circles). 2 (squares). 4 (filled squares) and 6 (cross hairs) in a) von Neumann and b) Moore (filled circles) neighborhood where K = 30 agents, room size = 18 x 14 cells, φ = 5, I = 90 time units. Solid curves in a) Q = -0.628α² – 0.208α + 1.162, and in b) Q = -1.266α² – 0.363α + 1.099.

Figure 2 plots the dependence of Q with d in the case of a long iteration period $I = 50,000$. A comparison between Figures 1 and 2 reveals that the dependence of Q with d is independent of I.

Figure 3 presents the relation between Q and the imitation level α for a von Neumann (3a) and Moore (3b) neighborhood with $R = 11.9\%$ and $I = 90$. For a given d, Q decreases with α in a relation that is approximated by a second-order polynomial in α. The rate of decrease of Q with α is faster in a von Neumann neighborhood. The dependence of Q with α is quite robust against changes in the door separation distance.

We now compare our simulation results with measurements that were obtained from the mice experiments at $R = 11.9\%$. [5]. Figure 4 plots the dependence of Q with d for the mice experiments (filled circles). Simulation results are also presented from the two-parameter model with a Moore (squares, α = 0.8) and a von Neumann (filled squares,
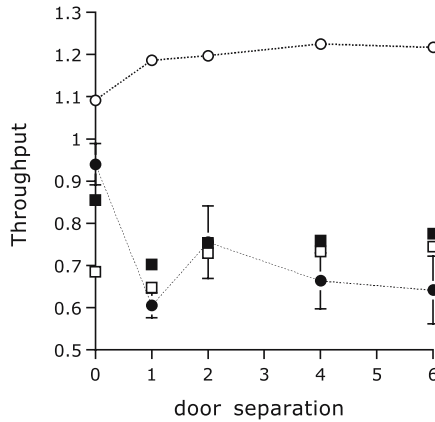
Figure 4: Comparison between simulation and experimental (filled circles) results for through-put Q as a function of door separation d with $K = 30$ agents, room size = 18 x 14 cells, $\varphi = 5$, $I = 90$ time units. Two-parameter model with Moore (squares, $\alpha = 0.8$) and von Neumann (filled squares, $\alpha = 0.7$) neighborhood. Also shown is the simulation result (circles) obtained with single-parameter model ($\alpha = 0$). Standard deviations (out of four trials) are given for the experimental results.

$\alpha = 0.7$) neighborhood. Also plotted in Fig 4 is the simulation result (circles) that is generated by a single-parameter model that neglects the possibility of copying between agents ($\alpha = 0$).

The single-parameter model predicts a Q that increases with increasing d because wider door separations reduce the possibility of interference between arcs that are formed around every exit in a two-exit room. Interference impedes the flow of escape by con-centrating a large number of agents over a small portion of the room [7].

However, the prediction of the single-parameter model was not observed in the mice ex-periments. Instead, the measurements revealed that Q became smaller with increasing d. In a given trial, most of the mice clustered around a particular exit ignoring the presence of the other available exit regardless of its distance.

Clearly, the introduction of α has improved the capability of the model to describe the experimental results. Mice exhibited herding behavior that prevented them from getting out of the water pool (and into the dry platform) in the shortest possible time.

3.2. Other predictions of the two-parameter model

We now consider the effect of herding for different number of agents inside a two-exit room (room size = 18 X 14 cells, $\varphi = 5$). Figure 5 plots the simulation results (von Neumann neighborhood) for the room evacuation time T as a function of the imitation parameter α at different initial values $R(i=0) = R_0$ of the room occupancy rate given by $R_0(\%)= 10, 20, 40, 60$ and 80. The T(α) plot is computed at various door separation value of $d = 0, 1, 2, 4,$ and 6. The data points do not include outliers – iteration was stopped when total evacuation of the room is not achieved after $I = 50,000$ iteration steps.
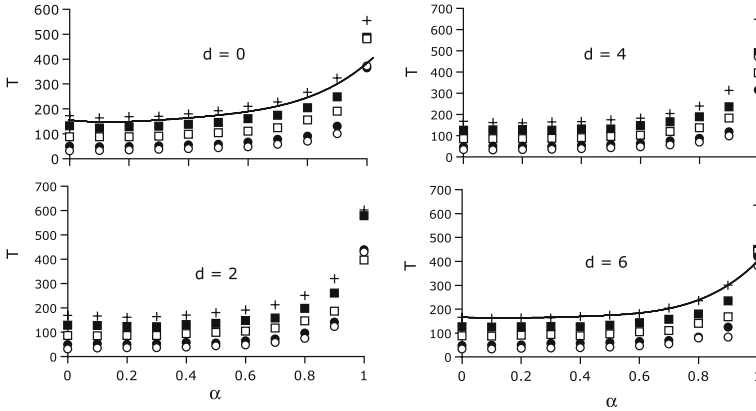
Figure 5: von Neumann neighborhood. Evacuation time T versus α at different door separation *d* and initial room occupancy $R_0(\%) = 10$ (circles), 20 (filled circles), 40 (squares), 60 (filled squares), and 80 (cross-hairs). Solid curves: $T(d = 0) = 823\alpha^4 - 1187.5\alpha^3 + 743.4\alpha^2 - 139.1\alpha + 172.6$; $T(6) = 898.9\alpha^4 - 1124\alpha^3 + 550\alpha^2 - 91.8\alpha + 166.6$.

The time that is needed to evacuate a room becomes longer at higher R_0 values. For a given R_0, evacuation time T increases with α in a highly nonlinear manner. For a given *d* value, T(α) is best approximated by a monotonically increasing 4th-order polynomial (see solid curves in Fig 5). The T(α) curve increases slowly in the range: α < 5, then ra-
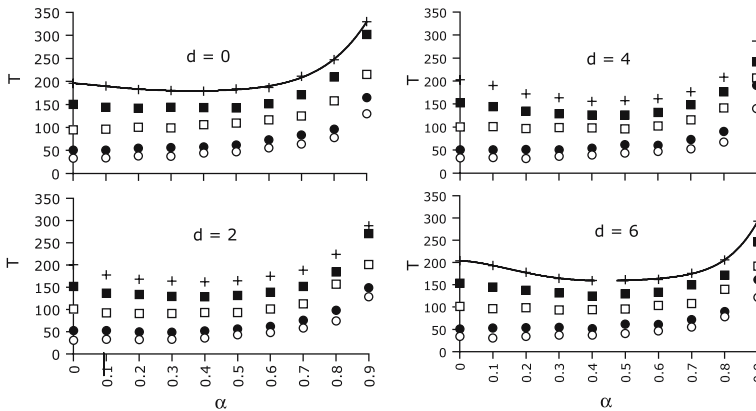

Figure 6: Moore neighborhood. Evacuation time T versus α at different door separation d and at $R_0(\%) = 10$ (circles), 20 (filled circles), 40 (squares), 60 (filled squares), and 80 (cross-hairs). Solid curves: $T(d=0) = 111.1\alpha^6 + 1328.86\alpha^5 - 2221.6\alpha^4 + 1376\alpha^3 - 259\alpha^2 - 51.2\alpha + 196$. $T(d=6) = 2357.6\alpha^6 + 1929.1\alpha^5 - 2223.2\alpha^4 + 3177.1\alpha^3 - 1056\alpha^2 - 30.1\alpha + 204.2$.

pidly at larger α values. The deleterious effect of herding during escape panic is sudden and catastrophic.

Figure 6 plots the simulation results (Moore neighborhood) for T as a function of α at $R_0(\%) = 10, 20, 40, 60$ and 80. The T(α) plot is computed for $d = 0, 1, 2, 4,$ and 6. For a given d, T(α) is best approximated by a 6th-order polynomial (see solid curves in Fig 6) that exhibits a minimum at $α \approx 0.5$ that becomes more obvious at high room occupancy rates ($R_0 > 60\%$). At $α \approx 0.5$, an agent is equally likely to follow its neighbor or to decide on its own unaffected by any external influence.

The existence of a minimum in the T(α) curve is quite interesting. It implies that herding could promote faster room evacuation when the escape strategy is not an extreme one that is founded strictly on total distrust ($α = 0$) or blind copying ($α = 1$) alone but rather on a healthy mix of actions resulting from deliberate individual decisions and copying based on available information.

4.   Summary

In this work, we have presented the performance of a new two-parameter agent-based model for describing the escape of agents that are under threat in a two-exit room. The model utilizes two independent parameters for describing the degree of panic ($φ$) and the likelihood ($α$) of an agent to imitate the action of its neighbors.

The two-parameter model could explain more accurately the exit throughput behavior that has been observed in the mice experiments under different separation distances of the two exits. The mice exhibited herding behavior while escaping from a pool of water in a two-exit flooded chamber.

The two-parameter model revealed a highly nonlinear dependence between the room evacuation time T and α. With a Moore neighborhood, the T(α) curve featured a minimum around $α = 0.5$ which indicates that the copying can enhance the evacuation speed of a room especially at high occupancy rates. This interesting prediction has not yet been observed in real escape panic.

The unexpected benefit of copying is realized in a Moore neighborhood because it offers more possible directions to choose from when moving towards a targeted exit that is known a priori to the agents in the room. Clogs are easier to decongest in the presence of more options that also favors the emergence of streamline flow towards the exit.

Acknowledgment

References

1. D. Helbing, I. Farkas, and T. Vicsek: Panic: *A Quantitative Analysis*, http://angel. elte.hu/panic/article/artic m.html (2000).
2. Official: *Chicago Club Was to Close Second Floor*, http://www.cnn.com/2003/ US/Midwest/02/17/chicago.nightclub/index.html
3. E. Zuckermann: *Death Toll Clims to 95 from Rhode Island Fire Blamed on Rock Band's Special*, http://www/signonsandiego.com/news/nation/20030221-1515-nightclubfir.html (2003).
4. D. Helbing, I. Farkas, and T. Vicsek: *Simulating Dynamical Features of Escape Panic*, Nature 407, pp. 487-490 (2000).
5. C. Saloma, G. Perez, M. Lim, G. Tapang, and C. Palmes-Saloma, Proc. Natl. Acad. Sci. USA 100, pp. 11947-11952 (2003).
6. S. Wolfram: *A New Kind of Science*, Wolfram Media, Inc., Canada (2002).
7. G. Perez, G. Tapang, M. Lim, and C. Saloma, Physica A 312, pp. 609-618 (2002).
8. D. Helbing, L. Buzna, and T. Werner: *Self-Organized Pedestrian Crowd Dynamics and Design Solutions*, DOI:trafficforum/03120401, Traffic Forum, 2003-12 (2003).
9. T. Nagatani, K. Takimoto, M. Isobe, and D. Helbing: *Evacuation Process from a Room with Two Exits*, Working paper (2003).
10. M. Isobe, D. Helbing, and T. Nagatani: *Many Particle Simulation of the Evacuation Process from a Room Without Visibility*, preprint http://arXiv.org/abs/cond-mat/0306136 (2003).
11. D. Helbing and T. Platkowski, Europhysics Lett 60, pp. 227-233 (2002).
12. D. Elliot and D. Smith, Industrial & Enviromental Crisis Quarterly 7, pp. 205-229 (2003).

From Ant Trails to Pedestrian Dynamics –
Learning from Nature

A. Schadschneider[1], D. Chowdhury[2], and K. Nishinari[3]

Many insects like, for example, ants communicate via chemical signals. This process, called chemotaxis, allows them to build large trail systems which have many similarities with human transport networks. In order to investigate the dynamics and spatio-temporal organization of ants on an existing trail system we have proposed a stochastic cellular automaton model. In contrast to the situation in highway traffic, it predicts a non-mono-tonic speed-density relation. This effect has its origin in the formation of loose clusters, i.e. space regions of enhanced, but not maximal, density. Inspired by the behaviour of ants on their trails, we have also developed a model for pedestrian dynamics. In this approach the interaction between the pedestrians is implemented as "virtual chemotaxis". In this way all interactions are strictly local and so even large crowds can be simulated very efficiently. In addition, the model is able to reproduce the empirically observed collective effects, e.g. the formation of lanes in counterflow.

1.   Introduction

Organized traffic [1,2] is not only a phenomenon restricted to human societies, but can also be observed in other biological systems. Prominent examples of self-organized motion in biology are herding, flocking and swarm formation [3-5]. In addition, insects like ants build trail systems [6,7] that have many similarities with human transport systems, like highway networks.

Essential for the formation of ant trails is a form of communication called chemotaxis [6,8,9,10]. Ants communicate with each other by dropping a chemical (generically called pheromone) on the substrate as they move forward. Although we cannot smell it, the trail pheromone sticks to the substrate long enough for the other following sniffing ants to pick up its smell and follow the trail. Ant trails may serve different purposes (trunk trails, migratory routes) and may also be used in a different way by different species [6]. Therefore, one-way trails as well as trails with counterflow of ants have been observed.

Here we will not discuss the process of trail formation itself, which has been studied extensively in the past (see e.g. [10,11] and references therein). Instead, we assume the existence of a trail network that is constantly reinforced by the ants. Since we focus on one particular trail it is natural to assume that the motion of the ants is one-dimensional.

[1]Institut für Theoretische Physik, Universität zu Köln, 50937 Köln, Germany

[2]Department of Physics, Indian Institute of Technology, Kanpur 208016, India

[3]Department of Aeronautics and Astronautics, Faculty of Engineering, University of Tokyo, Hongo, Bunkyo-ku, Tokyo 113-8656, Japan

In traffic flow interactions between the vehicles typically lead to a reduction of the average velocity v. This is obvious for braking manoeuvres to avoid crashes. Therefore $v(\rho)$ decreases with increasing density ρ. In this article we shall show a qualitatively different result for ant trails. Overtaking is very rare in ant trails, perhaps because of approximately equal speeds of the ants. Nevertheless, the presence of pheromones leads to an overall enhancement of the average speed.

The behaviour of social insects has inspired the development of efficient strategies for solving complex problems [12,13]. Problems treated thus far range from routing or search algorithms in computer science to cooperative transport of multi-agent systems in robotics. Although routing problems dealing with human agents in cars or airplanes have already been addressed, direct application to humans, e.g. as pedestrians, is still at its beginnings. Inspired by the trail laying and recruiting behaviour in ant trails we have developed a model for pedestrian dynamics. In this approach the interaction between pedestrians occurs via 'virtual chemotaxis'. However, the motion in pedestrian dynamics is essentially two-dimensional. The basic idea is implemented in a cellular automata approach since this class of models is especially well suited for large scale computer simulations on the basis of microscopic rules of interaction. This allows for an efficient simulation even of very large crowds.

Although competitive behaviour is also known, strong cooperative patterns are characteristic for social insects, as indicated by the name. Taking traffic on already existing ant trails as an example, we will discuss similarities and differences between modelling traffic on ant trails and pedestrian dynamics. One common feature of all models that will be discussed is the restriction of the agent's perception to nearest neighbour cells. As most ant species are virtually blind this obviously is reasonable. For pedestrians (except maybe in panic situations) this might not be obvious.

2.   Modelling of Ant Trails

In [14-16] we have developed a particle-hopping model, formulated in terms of a stochastic cellular automaton (CA), which may be interpreted as a model of uni-directional flow on an ant-trail. As mentioned above, we do not want to address the question of the emergence of the ant-trail, but focus on the traffic of ants on a trail which has already been formed. The model generalizes the asymmetric simple exclusion process (ASEP) [1,17] with parallel dynamics by taking into account the effect of the pheromone.

The ASEP is one of the simplest examples of a system driven far from equilibrium. Space is discretized into cells that can be occupied by at most one particle at a time. The cells are labelled by the index i ($i = 1,2,...,L$); L being the length of the lattice. The number of particles will be denoted by N. In the totally asymmetric case (TASEP) particles are allowed to move in one direction only, e.g. to the right. If the right neighbour site is empty a particle hops there with probability q. For parallel (synchronous) dynamics this

is identical to the Nagel-Schreckenberg (NaSch) model [18] with maximal velocity 1 and braking probability $p = 1 - q$.

2.1. Definition of the uni-directional ant-trail model

As mentioned in the introduction, ants communicate with each other by dropping phero-mones on the substrate as they crawl forward. In our model of uni-directional ant-traffic [14,15] the ants move according to a rule which is essentially an extension of the TASEP dynamics. In addition to the particle density a second field is introduced which models the pheromone trail (see Fig. 1). For simplicity, only the two states "pheromone present" and "no pheromone present" are distinguished. The hopping probability of the ants is now modified by the presence of pheromones; it is larger if a pheromone is present at the destination site. Furthermore, the dynamics of the pheromones has to be specified. They are created by ants at their current location and free pheromones, i.e. pheromo-nes located at sites where no ant is present, evaporate with probability f per unit time. Assuming periodic boundary conditions, the state of the system is updated at each time step in two stages (see Fig. 1). In stage I ants are allowed to move while in stage II the pheromones are allowed to evaporate. In each stage the stochastic dynamical rules are applied in parallel to all ants and pheromones, respectively.

Stage I: Motion of ants

An ant in cell i that has an empty cell in front of it moves forward to the next cell with

$$probability = \begin{cases} Q & \text{if a pheromone is present at } i+1, \\ q & \text{if no pheromone is present at } i+1. \end{cases}$$

(1)

In order to be consistent with real ant-trails, we assume $q < Q$. The value of the hopping probability represents the average velocity $\bar{v}$ of non-interacting ants. Without encoun-tering pheromone at any hop a single isolated ant moves with $\bar{v} = q$, whereas $\bar{v} = Q$ if it finds pheromone at the target site during each hop. Thus Stage I, in a simple way, represents the fact that ants move faster towards their destination if they are guided by pheromones.
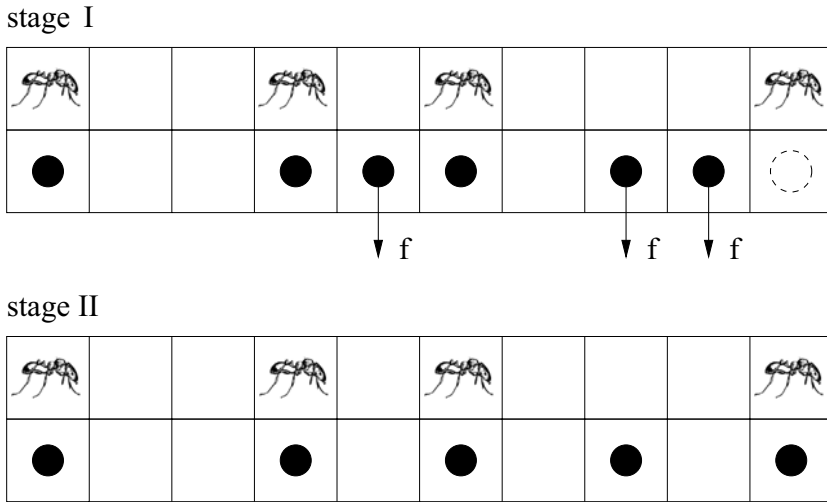
state at time t

stage I

stage II

state at time t+1
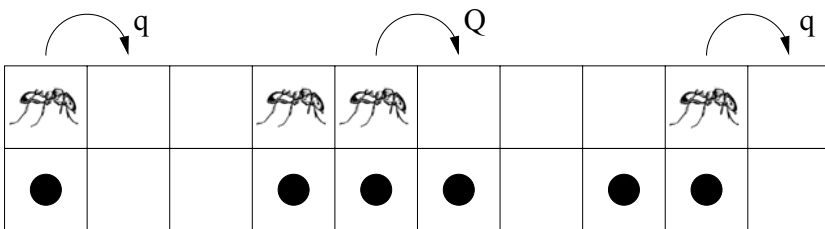
Figure 1: Schematic representation of typical configurations; it also illustrates the update pro-
cedure. Shown are the two grids for ants (upper grid) and pheromones (lower grid) at
different stages of an update step. Top: Configuration at time t, i.e. before stage I of the
update. The non-vanishing hopping probabilities of the ants are also shown explicitly.
Middle: Configuration after one possible realisation of stage I. Two ants have moved
compared to the top part of the figure. Also indicated are the pheromones that may
evaporate in stage II of the update scheme. Bottom: Configuration after one possible
realization of stage II. Two pheromones have evaporated and one pheromone has been
created due to the motion of an ant.

Stage II: Evaporation of pheromones

At each cell i occupied by an ant after Stage I a pheromone will be created. In this way,
a kind of `pheromone trace' is produced by moving ants. On the other hand, any `free'
pheromone at a site i not occupied by an ant will evaporate with the probability f per
unit time. Therefore the trace created by a moving ant will disappear after some time if
it is not renewed by other ants.

Despite its simplicity, this model contains the basics that describe the motion of ants
in a trail. The forward motion is represented by the hopping, whereas the mutual hin-
drance of ants comes from the exclusion principle that allows at most one ant per cell.
The influence of the pheromone is encoded in the hopping probabilities q and Q and,
finally, the finite lifetime of the pheromones has been taken into account through the
evaporation probability f. Of course, many subtle details have been neglected. However,
these details are not expected to be important for understanding the basic principles
underlying the process of chemotaxis.

The model can also be extended to bi-directional ant trails [16,19] where interactions between ants moving in opposite directions become important, e.g. for communication processes. This is discussed in more detail elsewhere in these proceedings [19].

The ant-trail model we propose here is closely related to the bus-route model with parallel updating [20,21]. In the bus-route model passengers arrive at a bus stop with probability f. Buses move from stop to stop and pick up all passengers if they arrive at a stop. Thus they have to slow down. This is captured by the hopping probabilities for the buses. If no passengers wait at a stop they move forward with probability Q, whereas they move with probability $q < Q$ if they have to pick up passengers. This has an obvious correspondence to the ant trail model: If one identifies the bus stops with the cells in the ant trail model, buses are the analogues of the ants and passengers of the pheromones. Just as the number of buses is conserved in the bus-route model, the number of ants is conserved in the ant trail model. Similarly, the dynamical variable representing the presence (or absence) of pheromone is not conserved in the ant trail model just as the number of passengers is not conserved by the dynamics of the bus-route model. However, there is a crucial difference: in the bus-route model buses slow down to pick up the waiting passengers whereas in the ant trail model ants speed up in the presence of pheromones. Thus absence of pheromones corresponds to the presence of passengers. After this identification, the two models are seen to be equivalent.

2.2. Fundamental diagram

In vehicular traffic, usually, the inter-vehicle interactions tend to hinder each other's motion so that the average speed $\bar{v}$ of the vehicles decreases monotonically with increasing density $\rho = N/L$. This can be seen in Fig. 2 where also the fundamental diagram, i.e. the flux-density relation, of the NaSch model with $v_{max} = 1$ (or the TASEP with parallel updating) is shown for two different hopping probabilities. This flux, which is particle-hole symmetric, is given by [22]

$$J_{NS}(q_{NS}\rho) = \frac{1}{2}\left[1 - \sqrt{1 - 4q_{NS}\rho(1-\rho)}\right]$$

(2)

where $q_{NS} = 1 - p$ with p being the braking probability. Note that flux and average density generally are related by $J(\rho) = \rho \cdot \bar{v}$.

In contrast, in the model of ant-traffic the average speed of the ants varies non-monotonically with their density over a wide range of small values of f (see Fig. 2) because of the coupling of their dynamics with that of the pheromone. This uncommon variation of the average speed gives rise to the unusual dependence of the flux on the density of the ants (Fig.2), which now exhibits an inflection point. Furthermore, the flux is no longer particle-hole symmetric.
In the limits $f = 0$ and $f = 1$ the ant trail model reduces to the NaSch model. For $f = 0$
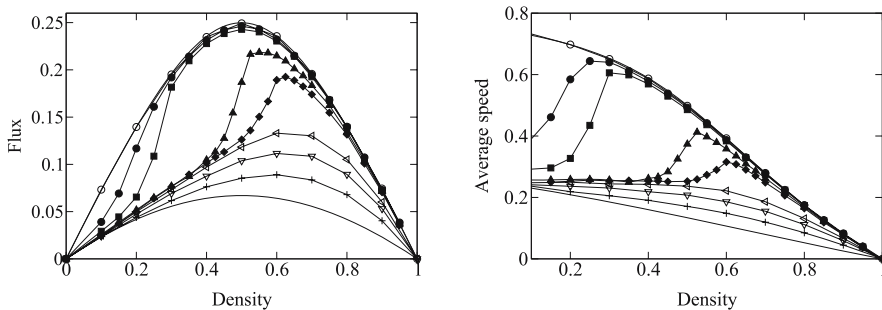
Figure 2:   Fundamental diagrams for the ant-trail model for $q = 0.25$, $Q = 0.75$ and different eva-
poration rates f. f increases from top to bottom. The symbols corresponds to the values
$f = 0.0001, 0.0005, 0.001, 0.005, 0.01, 0.05, 0.10,$ and 0.25 (from top to bottom). The
two extremal curves (without symbols) correspond to the NaSch limits $f = 0$ and $f = 1$,
respectively. Left: Density dependence of the flow. Right: Density dependence of the
average velocity. In both cases, anomalous curves are indicated by filled symbols.

pheromones can not evaporate. Therefore, in the stationary state pheromone is present
at all sites and the ants always move with probability Q. For $f = 0$, on the other hand,
the pheromone created by an ant will evaporate immediately as soon as the ants moves
forward. Therefore all ants will move with probability q. These two curves are upper
and lower bounds for the flows that are possible in the ant trail model.

In the low density limit, the distance between consecutive ants is large in general. There-
fore, if the evaporation probability f is not too small, any pheromone created by the
previous ant will have disappeared and motion occurs with probability q. Therefore the
flow and average velocity asymptotically follow the behaviour of a NaSch model with
hopping probability q. For large densities, distances between consecutive ants are very
small in general. Therefore any created pheromone has not enough time to evaporate
and ants will move generically with probability Q. Then, asymptotically the flow and
average velocity will be given by a NaSch model with hopping probability Q.

At intermediate densities we expect a crossover between these two behaviours. This
simple argument already indicates that the shapes of the fundamental diagrams can ex-
hibit a shape that differs from the one known from traffic models.

2.3. Spatio-temporal organization

How can the unusual density-dependence of the average velocity be understood? Using
mean-field-type theories that implicitly assume a homogeneous stationary state does
not allow to reproduce the simulation results in a satisfactory way [15]. This indicates
that the stationary state is characterized by some sort of clustering. This is confirmed by
considering the probabilities of finding an ant, pheromone and nothing in front of a cell
occupied by an ant. Typical results from computer simulations are shown in Fig. 3.
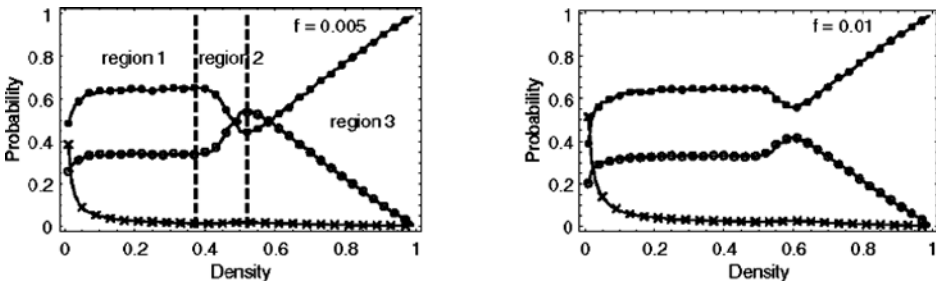
Figure 3: Numerical results for the probabilities of finding an ant ($\bullet$), pheromone but no ant ($\circ$)
and nothing ($\times$) in front of an ant are plotted against density of the ants.

One can distinguish three different regions. "Region 1" is characterized by the flat part
of the curves in Fig. 3 in the low density regime. Here, in spite of low density of the
ants, the probability of finding an ant in front of another is quite high. This implies the
fact that ants tend to form a cluster. On the other hand, cluster-size distributions ob-
tained from computer simulations show that the probability of finding isolated ants are
always higher than that of finding a cluster of ants occupying nearest-neighbour sites
[15]. These two apparently contradictory observations can be reconciled by assuming
that the ants form "loose clusters" in the region 1. The term "loose" means that there are
small gaps in between successive ants in the cluster, and the cluster looks like an usual
compact cluster if it is seen from a distance (Fig. 4). In other words, a loose cluster is just
a loose assembly of isolated ants that corresponds to a space region with density larger
than the average density ρ, but smaller than the maximal density ($\rho = 1$) of a compact
cluster.

Figure 4: (Left) Schematic explanation of the loose cluster. H is the hopping probability of ants
inside the loose cluster and h is that of the leading ant. (Right) The stationary loose
cluster. The average gap between ants becomes h/H.

Let us assume that the loose cluster becomes stationary after sufficient time has passed.
Then the hopping probability of all the ants, except the leading one, is assumed to be

H, while that of the leading one is h (see Fig. 4). The values of H and h have to be determined self-consistently. If f is small enough, then H will be close to Q because the gap between ants is quite small. On the other hand, if the density of ants is low enough, then h will be very close to q because the pheromone dropped by the leading ant would evaporate when the following ant arrives there.

The typical size of the gap between successive ants in the cluster can be estimated [15] by considering a simple time evolution beginning with a usual compact cluster (with local density $\rho = 1$). In this loose cluster approximation (LCA), the leading ant will move forward by one site over the time interval $1/h$. This hopping occurs repeatedly and in the interval of the successive hopping, the number of the following ants which will move one step is H/h. Thus, in the stationary state, strings (compact clusters) of length H/h, separated from each other by one vacant site, will produced repeatedly by the ants (see Fig. 4). Then the average gap between ants is $[(H/h-1)\cdot0+1\cdot1]/(H/h) = H/h$, independent of their density ρ. Interestingly, the density-independent average gap in the LCA is consistent with the flat part (i.e., region 1) observed in computer simulations (Fig. 3). In other words, region 1 is dominated by loose clusters.

Beyond region 1, the effect of pheromone of the last ant becomes dominant. Then the hopping probability of leading ants becomes large and the gap becomes wider, which will increase the flow. We call this region as region 2, in which "looser" clusters are formed in the stationary state. It is characterized by a negative gradient of the density dependence of the probability to find an ant in front of a cell occupied by an ant (see Fig. 3). Considering these facts, we obtain the following equations for h and H:

$$\left(\frac{h-q}{Q-q}\right)^{h} = (1-f)^{L-1}, \qquad \left(\frac{H-q}{Q-q}\right)^{H} = (1-f)^{h/H},$$

$$(3)$$

where l is the length of the cluster given by $l = \rho \cdot L + (\rho \cdot L - 1)h/H$. These equations can be applied to the region 1 and 2.

The total flux in this system is then calculated as follows. The effective density in the loose cluster is given by

$$\rho_{eff} = \frac{1}{1+h/H}$$

$$(4)$$

Therefore, considering the fact that there are no ants in the part of the length $L-l$, the total flux J can be expressed by the flux in the NaSch model (see (2)) as

$$J = \frac{l}{L} J_{NS}(H, \rho_{eff})$$

$$(5)$$

Above the density $\rho = 1/2$, ants are assumed to be uniformly distributed such that a mean-field approximation works well [15]. We call this region as region 3. Thus we have three typical regions in this model. In region 3, the relation $H = h$ holds because all the gaps have the same length, i.e. the state is homogeneous. Thus h is determined by the equation given above with the exponent L-l of the expression on the right hand side replaced by $1/\rho$-1. The flux is then given by $J_{NS}(h,\rho)$.

In region 1 we can simplify the analysis by assuming $h = q$ in the two equations (3) that determine h and H. Then the flux-density relation becomes linear. Numerical results for regions 1 and 2 can be obtained by solving these equations using the Newton method for densities $\rho \leq 1/2$. Above this value of density, the homogeneous solution can be used. Together these approximations can reproduce the results of the simulations rather well [15].

The intuitive description based on the loose cluster approximation as described above can be improved [23] by using an approximate mapping onto a so-called zero-range process (ZRP) [24,25]. The ZRP is a particle-hopping model where the hopping probabilities do not depend on the state of occupation of the target site. It has the advantage of being exactly solvable.

The mapping starts from an effective hopping probability $u = q(1-g)+Qg$, where g is the probability that there is a surviving pheromone directly in front of the ant. This depends on the time t elapsed since the previous ant left this site and can be estimated by $t = x/v$, where x is the gap and v the average velocity. This yields the hopping rate

$$u(x) = q + (Q-q)(1-f)^{x/v} \tag{6}$$

for the corresponding ZRP [23].

Using the exact solution of the ZRP with these hopping rates results for the fundamental diagram can be obtained that are in good agreement with the simulations. Note that v has to be determined self-consistently. The results also indicate that in general the different regimes are not separated by true phase transitions. Only in the limit $f \to 0$ a transition occurs at the density $\rho_c = (Q - q)/(Q - q^2)$ if the thermodynamic limit $L \to \infty$ is performed before the limit $f \to 0$.

Another phenomenon observed in the simulations is coarsening. At intermediate time usually several loose clusters are formed (Fig. 5). However, the velocity of a cluster depends on the distance to the next cluster ahead. Obviously, the probability that the pheromone created by the last ant of the previous cluster survives decreases with increasing distance. Therefore clusters with a small headway move faster than those with a large headway. This induces a coarsening process such that after long times only one loose cluster survives (Fig. 5). A similar behaviour has been observed in the bus-route model [20,21].
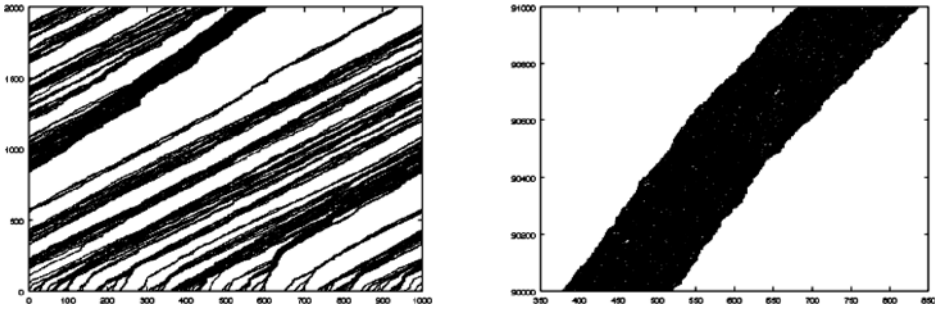
Figure 5: Space-time plots showing the coarsening process of the loose clusters. The left part shows a system of density $\rho = 0.1$ at early times. The right part corresponds to the stationary state. The evaporation probability of the pheromones is $f = 0.0005$.

So far we have only considered periodic boundary conditions. However, for ant-trails open boundary conditions are more realistic. Suppose α and β denote the probabilities of incoming and outgoing particles at the open boundaries per unit time. The phase diagram of the ASEP in the α-β-plane has been investigated exhaustively [1,17]. In [23] we have investigated the effects of varying the pheromone evaporation probability f on this phase diagram. Just as in the case of the ASEP, we found for all f three different phases (see Fig. 6). For fixed q, Q, and f, in the maximal-current phase the flux is independent of α and β. In the low- and high-density phase the flow is determined only by the inflow and outflow rate, respectively.
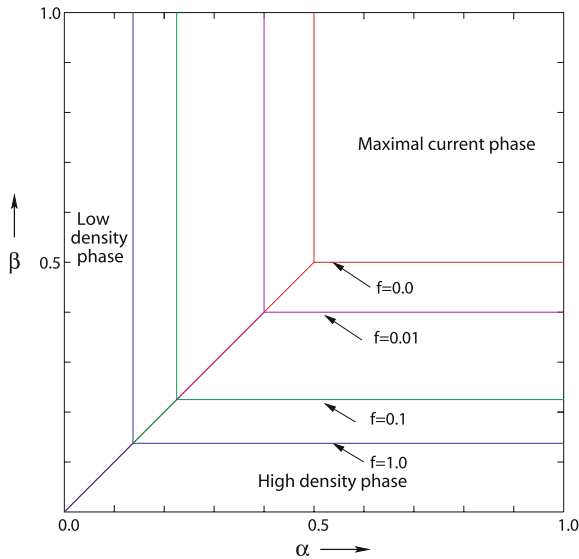

Figure 6: Phase diagram in the case of open boundary conditions for $q = 0.25$, $Q = 0.75$ and several values of the pheromone evaporation probability f.

3.   Modelling of Pedestrian Dynamics

So far various models for the simulation of pedestrian dynamics have been proposed (see e.g. [26,27] and references therein). In the following we discuss a promising new approach, the floor field model [28-34], in more detail. This model takes inspiration from the ant trail model of Sec. 2. The interaction between pedestrians is implemented as "virtual chemotaxis" which allows to translate a long-ranged spatial interaction into a local interaction with "memory". Guided by the phenomenon of chemotaxis the interactions between pedestrians are thus local and allow for computational efficiency.

3.1. Floor field cellular automaton

The model is implemented as a cellular automaton where pedestrians correspond to particles that move on a two-dimensional lattice of cells. Each cell can be occupied by at most one particle which reflects that the interactions between them are repulsive for short distances, i.e. one likes to keep a minimal distance to others in order to avoid bumping into them. Particles can move to one of the neighbouring cells based on certain transition probabilities. These are determined by three factors: (1) the desired direction of motion, e.g. the shortest connection, (2) interactions with other pedestrians, and (3) interactions with the infrastructure (walls, doors, etc.).

First of all, basic transition probabilities are determined which reflect the preferred walking direction and speed of each individual in the form of a matrix of preferences M. The entries of this matrix can be related to the preferred velocity vector and its longitudinal and transversal standard deviations [28].

Next interactions between pedestrians are taken into account. The exclusion principle models the short-range repulsion. However, for larger distances the interaction is often attractive. E.g. when walking in a crowded area it is usually advantageous to follow directly behind the predecessor. This is implemented by virtual chemotaxis. Moving particles create a „pheromone" at the cell which they leave, thus creating a kind of trace. So apart from the occupation number, each cell carries an additional quantity (field) D similar to the pheromone field in the ant trail model. It is called dynamic floor field since it has its own dynamics given by diffusion and decay [28] which leads to a dilution and finally the vanishing of the trace after some time.

For a unified description of the interactions it is advantageous to introduce another floor field, the static floor field S is constant and takes into account the interactions with the infrastructure, e.g. preferred areas, walls and other obstacles. In the case of evacuation processes, the static floor field describes the shortest distance to an exit door. S is calculated for each lattice site using some distance metric. The field value increases in the direction of the exit such that it is largest for door cells. An explicit construction of S can be found in [29,32]. Thus the static floor field can even be used to incorporate the information usually contained in the matrix of preference.

The transition probabilities given by the matrix of preference are now modified by the strengths of the floor fields D_{ij} and S_{ij} in the target cell (i,j). A motion in the direction of large fields is preferred. Schematically the transition probabilities are given by

$$p_{ij} = Z \cdot M_{ij} \cdot \exp(k_D D_{ij}) \cdot \exp(k_S S_{ij}) \cdot (1 - n_{ij}) \tag{7}$$

where k_D and k_S are coupling constants. Z is a normalization factor to ensure $\sum_{(i,j)} p_{ij} = 1$. The factor $1 - n_{ij}$, with the occupation number n_{ij}, takes into account that transitions to occupied cells are forbidden.

One important additional effect has to be considered. Due to the use of parallel dynamics it might happen that two (or more) pedestrians choose the same target cell where they try to move. Such a situation is called a conflict. Due to the hard-core exclusion, at most one of the persons can move. In order to make the model more realistic, a friction parameter μ (see [30,34] for details) is introduced. Then in a conflict, with probability μ all pedestrians remain at their site, i.e. nobody is allowed to move. With probability 1-μ one of the individuals moves to the desired cell. It is determined by a probabilistic method, e.g. by choosing one of them with equal probabilities. The effects of this friction parameter are similar to those of contact friction in granular materials. It can be interpreted as a moment of hesitation when people meet and try to avoid each other. Friction is a local effect that can have enormous influence on macroscopic quantities like flow and evacuation time [30]. Note that the kind of friction introduced here only influences interacting particles, not the average velocity of a freely moving pedestrian.

The details of the update rules can be found in [28,30,33]. There it is also shown that large pedestrian crowds of a several hundred people can be simulated 10 to 100 times faster than real time. More importantly the models allows to reproduce the empirically observed phenomena, e.g lane formation etc. [33].

3.2. Fundamental diagram

In [31] the fundamental diagram for the motion of pedestrians along a long corridor has been studied with the floor field cellular automaton. For the basic model variant it has been found that it is almost particle-hole symmetric. However, empirical studies point to a non-symmetric fundamental diagram where the maximal values of the flow occur for densities $\rho < 1/2$ [35,36]. The origin of the almost symmetric shape of the theoretical flow-density relation is the fact that pedestrians can only move forward one cell at a time. Therefore the behaviour in the corridor is well described by decoupled ASEP-type models with their symmetric fundamental diagram (see (2)). Introducing an extension of the interaction range through the implementation of a larger walking speed v_{max}, as in models for highway traffic [1,18,22], the maximum is indeed shifted to smaller densities [31]. This is related to the fact that the required space increases with increasing veloci-

ties, a fact not captured by choice $v_{max} = 1$. This effect needs also to be implemented in other models, e.g. the social-force model [37].

4. Conclusions

In this contribution we have described recent progress in understanding the dynamics of ants on their trail systems. Modifying the well-studied asymmetric simple exclusion process to account for the process of chemotaxis, an unusual behaviour of the flow-density relation for small pheromone evaporation rates is predicted. This effect is rather robust and can also be found in counterflow situations. It is related to the spatio-temporal organization of the ants on the trail which form so-called loose clusters.

So far, to our knowledge, there is only one quantitative study on the flux of ants on an existing trail [38]. From videotapes of trails build by leaf-cutting ants, values of flow, density, and velocity were extracted by hand. The fundamental diagrams obtained from this laborious procedure show a scattering of the data that is too strong to decide about possible anomalies. Very recent results under a more controlled setting indicate that the density dependence of the velocity could indeed be non-monotonous [39].

In Sec. 3 we have discussed the floor field model for pedestrian dynamics that takes its inspiration from the ant trail model. Interactions are implemented by virtual chemotaxis which keeps them local and allows for extremely efficient simulations. At the same time the model reproduces the collective effects observed in large crowds.

Although models of pedestrian dynamics are generically two-dimensional, analogies to ant trails exist. As mentioned above in both cases the observed rich spectrum of collective effects can be reproduced by models with local interactions. Using real or virtual chemotaxis effects of non-local interactions can be captured through the "memory" of the pheromone field.

Despite these similarities, differences remain. Ants are social insects and their behaviour is dominated by cooperation. As we know from everyday experience this is not necessarily the case in pedestrian dynamics. The success of the floor field model might indicate that here cooperation happens on an unconscious level. **«**

References

1. D. Chowdhury, L. Santen, and A. Schadschneider: *Statistical Physics of Vehicular Traffic and Some Related Systems*, Phys. Rep. 329, pp. 199 (2000).
2. D. Helbing: *Traffic and Related Self-Driven Many-Particle Systems*, Rev. Mod. Phys. 73, pp.1067 (2001).
3. J.K. Parrish and L Edelstein-Keshet: *Complexity, Pattern, and Evolutionary Trade-Offs in Animal Aggregation*, Science 284, pp. 99 (1999).

4. Y. Tu: *Phases and Phase Transitions in Flocking Systems*, Physica A281, 30 (2000).
5. E.M. Rauch, M.M. Millonas, and D.R. Chialvo: *Pattern Formation and Functionality in Swarm Models*, Phys. Lett. A 207, pp. 185 (1997).
6. B. Hölldobler and E.O. Wilson: *The Ants*, Belknap, Cambridge, USA (1990).
7. N.R. Franks: *Evolution of Mass Transit Systems in Ants: A Tale of Two Societies*, In: I.P. Woiwod, D.R. Reynolds, and C.D. Thomas (Eds.), Insect Movement: Mechanisms and Consequences, CAB International (2001).
8. S. Camenzine, J.L. Deneubourg, N.R. Franks, J. Sneyd, G. Theraulaz, and E. Bonabeau: *Self-Organization in Biological Systems*, Princeton University Press (2002).
9. A.S. Mikhailov and V. Calenbuhr: *From Cells to Societies*, Springer (2002).
10. E. Ben-Jacob: *From Snowflake Formation to Growth of Bacterial Colonies*, Contemp. Phys. 38, pp. 205 (1997).
11. F. Schweitzer: *Brownian Agents and Active Particles*, Springer Series in Synergetics (2003).
12. E. Bonabeau, M. Dorigo, and G. Theraulaz: *Inspiration for Optimization from Social Insect Behaviour*, Nature 400, pp. 39 (2000).
13. E. Bonabeu, M. Dorigo, and G. Theraulaz: *Swarm Intelligence*, Oxford University Press (1999).
14. D. Chowdhury, V. Guttal, K. Nishinari, and A. Schadschneider: *A Cellular-Automata Model of Flow in Ant-Trails: Non-Monotonic Variation of Speed with Density*, J. Phys. A 35, L573 (2002).
15. K. Nishinari, D. Chowdhury, and A. Schadschneider: *Cluster Formation and Anomalous Fundamental Diagram in an Ant Trail Model*, Phys. Rev. E 67, 036120 (2003).
16. A. John, A. Schadschneider, D. Chowdhury, and K. Nishinari: *Collective Effects in Traffic on Bi-Directional Ant Trails*, J. Theor. Biol. 231, pp. 279 (2004).
17. B. Derrida: *An Exactly Soluble Non-Equilibrium System: The Asymmetric Simple Exclusion Process*, Phys. Rep. 301, pp. 65 (1998).
18. K. Nagel and M. Schreckenberg: *A Cellular Automaton Model for Freeway Traffic*, J. Physique I 2, 2221 (1992).
19. A. John, A. Kunwar, A. Namazi, D. Chowdhury, K. Nishinari, and A. Schadschneider: *Traffic on Bi-Directional Ant-Trails*, In: these proceedings, Springer (2006).
20. O.J. O'Loan, M.R. Evans, and M.E. Cates: *Spontaneous Jamming in a One-Dimensional System: The Bus Route Model*, Phys. Rev. E 58, pp. 1404 (1998).
21. D. Chowdhury and R.C. Desai: *Steady-States and Kinetics of Ordering in Bus-Route Models: Connection with the Nagel-Schreckenberg Model*, Eur. Phys. J. B 15, pp. 375 (2000).
22. M. Schreckenberg, A. Schadschneider, K. Nagel, and N. Ito: *Discrete Stochastic Models for Traffic Flow*, Phys. Rev. E 51, pp. 2939 (1995).

23. A. Kunwar, A. John, K. Nishinari, A. Schadschneider, and D. Chowdhury: *Collective Traffic-Like Movement of Ants on a Trail: Dynamical Phases and Phase Transitions*, J. Phys. Soc. Jpn. 73, pp. 2979 (2004).

24. F. Spitzer: *Interaction of Markov processes*, Adv. Math. 5, pp. 246 (1970).

25. M.R. Evans and T. Hanney: *Nonequilibrium Statistical Mechanics of the Zero-Range Process and Related Models*, J. Phys. A 38, R195 (2005).

26. M. Schreckenberg and S.D. Sharma (Eds.): *Proceedings of the International Conference on Pedestrian and Evacuation Dynamics*, Springer, Berlin (2002).

27. E.R. Galea (Ed.): *Proceedings of the 2nd International Conference on Pedestrian and Evacuation Dynamics*, CMS Press, London (2003).

28. C. Burstedde, K. Klauck, A. Schadschneider, and J. Zittartz, *Simulation of Pedestrian Dynamics Using a 2-Dimensional Cellular Automaton*, Physica A 295, pp. 507 (2001).

29. A. Kirchner and A. Schadschneider: *Simulation of Evacuation Processes Using a Bionics-Inspired Cellular Automaton Model for Pedestrian Dynamics*, Physica A 312, pp. 260 (2002).

30. A. Kirchner, K. Nishinari, and A. Schadschneider: *Friction Effects and Clogging in a Cellular Automaton Model for Pedestrian Dynamics*, Phys. Rev. E 67, 056122 (2003).

31. A. Kirchner, H. Klüpfel, K. Nishinari, A. Schadschneider, and M. Schreckenberg: *Discretization Effects and the Influence of Walking Speed in Cellular Automata Models for Pedestrian Dynamics*, J. Stat. Mech. P10011 (2004).

32. K. Nishinari, A. Kirchner, A. Namazi, and A. Schadschneider: *Extended Floor Field CA Model for Evacuation Dynamics*, IEICE Trans. Inf. & Syst. E87-D, 726 (2004).

33. C. Burstedde, A. Schadschneider et al.: *Cellular Automaton Approach to Pedestrian Dynamics - Applications*, In: M. Schreckenberg and S.D. Sharma (Eds.): Proceedings of the International Conference on Pedestrian and Evacuation Dynamics, Springer, Berlin, pp. 87-97 (2002).

34. A. Schadschneider et al.: *Role of Conflict in the Field Cellular Automaton Model for Pedestrian Dynamics*, In: E.R. Galea (Ed.): Proceedings of the 2nd International Conference on Pedestrian and Evacuation Dynamics, CMS Press, London, pp. 51-62 (2003).

35. U. Weidmann: *Transporttechnik der Fußgänger*, Schriftenreihe des IVT, Vol. 90, ETH Zürich (1992).

36. Highway Capacity Manual, Special Report 209, Chapter 13, Transportation Research Board, Washington DC (1994).

37. A. Seyfried, B. Steffen, and T. Lippert: *Basics of Modelling the Pedestrian Flow*, physics/0506189.

38. M. Burd, D. Archer, N. Aranwlela, and D.J. Stradling: *Traffic Dynamics of the Leaf-Cutting Ant, Atta cephalotes*, Am. Naturalist 159, pp. 283 (2002).

39. M. Burd et al.: private communication.